THE UNIVERSITY OF PENNSYLVANIA ORTHOPAEDIC JOURNAL

VOLUME 34 JUNE 2024

Partnering with you to deliver exemplary orthopaedic care for youth.

The Division of Orthopaedics at Children's Hospital of Philadelphia is one of the largest and most active pediatric orthopaedic centers in the world. We've been repeatedly recognized by *U.S. News & World Report's* rankings of Best Children's Hospitals in the nation; and were ranked No. 1 for orthopaedics two of the past three years.

We offer breakthrough treatments for any condition that can affect a youth's growing bones and muscles. Our team has special expertise in:

- Hip preservation
- Limb differences
- Bone tumors
- Spine disorders
- Brachial plexus injuries
- Orthopaedic trauma
- Sports injuries
- Thoracic insufficiency syndrome

Children's Hospital of Philadelphia®
Division of Orthopaedics

CONNECT WITH US
To discuss a referral, schedule a comprehensive evaluation or seek a second opinion, call our Provider Priority Line at **800-TRY-CHOP** and press 2, or visit **chop.edu/ortho-professionals.**

U·P·O·J

The University of Pennsylvania Orthopaedic Journal

Volume 34 June 2024

Editorial Board

U·P·O·J

The University of Pennsylvania Orthopaedic Journal

Volume 34, June 2024

Table of Contents

Research Articles

Basic Science Section

Letter from the Editors

Mohammed Abdullah, MD and Eric Schweppe, MD

Mohammed Abdullah, MD

Eric Schweppe, MD

It is our distinct pleasure to present to you the 34th edition of the University of Pennsylvania Orthopaedic Journal (UPOJ). Begun in 1986 under the guidance of Dr. Carl T. Brighton, the UPOJ remains a testament to the Department's commitment to basic science and clinical research—always striving to gain new insights and seek better understanding of the musculoskeletal system, with the ultimate goal of providing the best possible care for our patients.

We dedicate this 34th edition of the UPOJ to Dr. Eric Hume, a consummate surgeon, educator, and leader for our residency program. In the wake of ongoing growth and change in the residency program, Dr. Hume's virtues of kindness, grit, and good-humor serve as beacons to strive towards. Read more about this cornerstone of the residency in Dr. Joseph Bernstein's article on page 7.

This year saw the change of command of Penn Orthopaedics from Dr. L. Scott Levin to Dr. Benjamin "Kyle" Potter. The department's tremendous accomplishments in the last fifteen-years are highlighted in Dr. Levin's final letter as chairman (see page 2). His rock-ribbed style of servant leadership risks understating his signal impact on our program, not the least of which are the articles on this very page. His dedication to the UPOJ and its authors will echo in the annals of orthopaedic surgery for generations.

We are additionally grateful support of the journal's advisor, Dr. Samir Mehta. We also would like to thank our section editors. As a fully resident-run publication, the UPOJ would not be possible without their contributions: Erin Hale (Shoulder and Elbow), Alyssa Thorman (Bone and Cartilage), Chinedu Okafor (Tendon and Ligament), Emily Eiel (Foot and Ankle), Bradley Osemwengie (Spine), Rachel Flaugh (Pediatrics), Jaret "Mac" Karnuta (Arthroplasty), Lisa Friedman (Trauma), Ellis Berns (Hand), Maxwell Cardwell (Oncology), and Caroline Granruth (Sports).

The UPOJ has been financially independent from the Department of Orthopaedic Surgery since 1997, thanks to generous financial support from our advertisers. And so on behalf of the Department, we thank them again for their generosity in supporting the educational and research missions of Penn Orthopaedics.

The journal is viewable for free online and on all mobile devices at www.upoj.org. Keep updated with a digital subscription database at www.upoj.org/subscribe. It has been our honor to serve as editors for the 34th edition of the UPOJ. On behalf of all contributors, we hope you find this edition informative, enriching, and inspiring.

Letter from the Chair: Building on a Legacy of Excellence

L. Scott Levin, MD, FACS, FAOA

This year's Chairman's letter will be the last time I share my perspective as the leader of the Department of Orthopedic Surgery at Penn Medicine. On June 24, 2024, I will hand over the command of the department to Dr. Benjamin Kyle Potter, MD, FACS (Colonel, US Army Retired). I could not be prouder to have Dr. Potter succeed me. As a West Point graduate and distinguished surgeon scientist, he has served our country with distinction, leading on the battlefield, in the classroom, the research laboratory, and as Chairman of Surgery at Walter Reed National Naval Medical Center in Bethesda. As an accomplished and innovative Orthopedic Oncologist, he has dedicated his career to limb salvage, extremity reconstruction, and amputee care. I want to recognize Dr. Greg Farwell, who served as Chair of the Penn Search Committee. Dr. Farwell stewarded the search process with grace and skill. Andrew Duncan and I have already been working with Dr. Potter to assure an orderly transition in departmental leadership.

Before writing this, I compiled the previous 14 years of UPOJ Chair letters that I have written and read each one of them. It seems like yesterday that I arrived at Penn on July 1, 2009, at 0600. I remember meeting that first day with our residents and reviewing with them my expectations—"Levin's rules" as they are known: teamwork, communication, strong work ethic, and professionalism. These themes have not changed in 15 years. That day at 6pm, I held my first faculty meeting. I remember saying to the faculty, "I work for you; you do not work for me. We will work together to create success across our missions. My job is to help you succeed in your career by providing guidance, resources, and support to allow you to realize your goals." The measure of our team's success over the last 15 years has been the development, first and foremost, of people. They collectively have led to our success as a department. Recruiting and retaining the right people were essential to establish the programs that we've developed. These include new procedures and innovations in clinical care, expansion of educational opportunities for our medical students, residents, fellows, and faculty and most critically the advancement of musculoskeletal science that remains for our department a necessity and not a luxury.

During my recruitment in the spring of 2009, I requested space and resources to establish the Penn Human Tissue Laboratory. Completed in 2011, the HTL has supported each of our missions by providing a platform to develop new surgical procedures, serving as a valuable resource for our trainees, and functioning as a research laboratory focused on anatomy. The HTL has benefited those from the Penn community as well as visiting anatomy research scholars from around the world, such as China, Israel, and Italy.

In parallel to the construction and opening of the Human Tissue Laboratory, Penn Medicine supported the development of a Vascularized Composite Allotransplantation (VCA) program. Penn is one of the few centers in the world that has performed upper extremity transplantation. Building on the success of the upper extremity VCA program in adults and children, a world-class uterus transplantation program was established by Katherine O'Neill and Nawar Latif from the Department of Obstetrics and Gynecology.

The Orthoplastic approach to extremity reconstruction in the domains of trauma, tumor, and infection was introduced upon my arrival and has been promoted as a multidisciplinary enterprise that treats patients from around the world. Penn Presbyterian Medical Center is the home of the Penn Orthoplastic Limb Salvage Center. The center attracts patients who are told that the only treatment for a compromised limb is amputation. Using our skills and collaborative spirit, we salvage extremities heavily based on the principles and practices of reconstructive microsurgery. Doctors Samir Mehta, Stephen Kovach, and I have led these efforts. I could not be prouder of this clinical program.

In 2009, I arrived at Penn Medicine with a clinical skill set that has been shared with my colleagues and, most importantly, with patients to enhance their quality of life. These include programs that address sternal instability following heart surgery the use of vascularized fibula grafts for the treatment of avascular necrosis of the hip (See youtube), the Orthoplastic approach to limb salvage, the use of medial femoral condyle microsurgical transplantation for foot and ankle reconstruction, establishing the 3C pediatric protocol at Children's Hospital for extremity vascular injuries, and the living donor liver transplant program using the operating microscope for hepatic artery anastomosis.

Basic science research includes co-stimulatory blockade to optimize tolerance of vascularized composite allografts, ex vivo limb preservation funded by foundations, and DOD-funded patient-reported outcome studies in hand transplantation. Educational advances include establishing

the Orthoplastic Fellowship. The Division of Sports Medicine established the Penn Cartilage Pr0ogram, led by Jim Carrey, Brian Sennett, and Rob Mauck. We recently established the Penn Nerve Center, a collaborative effort among plastic surgeons, orthopedic surgeons, and neurosurgeons, co-directed by Dr. Zarina Ali and myself. We have established a fully Penn Integrated Hand Service that, in my opinion, is the foremost academic hand service in the United States. We have expanded several research platforms, including the VA hospital, which recently led to an $8.25 million grant by Robert Mauck and colleagues, which included many stakeholders from the MSK community.

Renovations of the Mackay Labs in the Stemmler building, expansion of the VA laboratory space (Translational Musculoskeletal Research Consortium), building the Penn Medicine University City (PMUC) Musculoskeletal Institute, and garnering funds for the Biedermann Biomechanics Lab are examples of physical plant expansions that have benefited Penn Orthopedics. We raised six endowed chairs, including the Abramson Family Foundation Sarcoma Chair, the Abramson Family Foundation Fund for Adult Reconstruction, the Ralston Chair, the WW Smith Endowed Chair, the Hans Jorg Wyss Fund for Immunology and VCA Research, and the Wyss Lorich Orthopedic Trauma Educational Fund.

New educational programs were established for our residents, including the Michael Kelly Wharton School of Business Leadership Program and the Medical Education Track created by Dr. Cara Cipriano. We also established an exchange with Monaco for the shoulder and elbow fellow with Tristan Lascar, MD, which provides an international experience for shoulder education. We established new named lectureships that include the Heppenstall Lecture, the Sam Bal Lecture, the Nakos Lecture, the June Wapner Lecture, and the Vincent Arlet Lecture.

Affiliate partnerships with the Granview Orthopedic Group, Princeton Orthopedics, and Bayhealth were created, expanding our presence in our region. Working with the health system, we developed a community orthopedic arm at Chester County Hospital. We established a Women's Health Initiative within the Division of Sports Medicine and in partnership with the Department of Family Medicine. Other firsts include the development of the Musculoskeletal and Rheumatology Service Line and the Penn Spine Center. We established a relationship with Shriners Hospital for Crippled Children in hand and microsurgery, spine, and oncology. We created an Advisory Council for Orthopedics to facilitate development and highlight the advances of the department. Diversity was increased in terms of women in orthopedics as well as underrepresented minorities at the resident, fellow, and faculty levels.

Penn Orthopedics was rated the number one department in the country three years ago with regard to NIH funding, and for the last two years has been ranked number two. We have partnered with the health system to provide care for the Philadelphia Flyers, Philadelphia 76ers, as well as US Squash, and the Philadelphia Union soccer team. We established annual courses in microvascular surgery (the Penn Flap Course) that attract attendees from around the world. We have expanded fellowship positions in adult reconstruction, spine surgery, and Orthoplastic Surgery. The expansion of advanced practice providers has been exponential. Fifteen years ago, there was one nurse practitioner in the department. Today, we currently have over 45 physician assistants. The growth of the faculty has been exponential, as well as the doubling of the budget in the Mackay Laboratory. Tenure-track research faculty that have been hired all have been successful with regard to peer-reviewed funding from the NIH and other granting agencies.

In summary, things look quite different today than they did 15 years ago. Each of our achievements has been a team effort. I embrace the acronym "T.E.A.M." This stands for: "Together Everyone Achieves More." As a team, we have achieved a lot. However, our work is never done. We always must keep our eyes on the horizon and look ahead to new frontiers to conquer. It is easy to be sidetracked by turbulent waters, stormy seas, and clouds that obscure our path going forward. I have questioned myself several times as the leader of this great department and asked several times, "What can I do better? Where am I ineffective? What must I do to improve our department over time?" Each leader has a style and a personality, strengths, and weaknesses. I hope that my strengths have advantaged the department. In cases where I have shortcomings, I know that other members of our team have stepped forward and provided support and direction in areas where I've been less effective. I am most grateful for that support.

The state of the Department of Orthopaedic Surgery at Penn Medicine is strong. We will get stronger and have more impact in the years ahead. Our new leadership, faculty skill and expertise, and dedication to our missions will be directed to new horizons. I have been honored to serve as the chairman for the last 15 years. It is time to step aside and facilitate the continued success of our great department.

With gratitude and respect for all,

LSL

Letter from the Program Director

Daniel C. Farber, MD

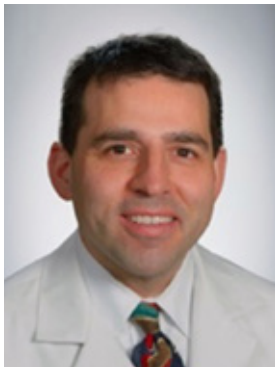

It has been another busy year for the residency program and finally one where there have not been any significant COVID related disruptions. Under the guidance of our Academic Chief Residents (Lucas Myerson, Steven Zhang, and Kesey Young), we initiated several new projects aimed at maximizing the residents' educational experience. There have been numerous successful labs and sawbones events for the residents to further their training.

The housestaff at Penn voted to unionize in the late spring of 2023. To date, we have not seen the effects of this as negotiations are ongoing between the union and PennMedicine. Despite this, we continue to look at ways to enhance our residents' experience. We have spent time this year revamping the format of the residency budget and are excited to launch a new budget system that will formalize many of the Orthopaedic benefits we provide for the residents such as lead, loupes, and funds for courses and conferences.

We welcomed our new class of interns, a varied bunch who brought much to the Penn environment and to the residency. The Okafor twins (not really), Chiel (Penn) and Chinedu (Duke), Maxwell Cardwell (Wisconsin), Tyler Murphy (Hofstra), Brett Croen (Drexel), Jiwon Park (Michigan), Sarah Rapaport (Hopkins) and Tensae Assefa (NYU). However, 2 of our interns came to the realization of their true calling partway through the intern year. We will bid farewell to Jiwon Park who will be switching to the Physical Medicine and Rehabilitation program at University of Michigan as well as Sarah Rapaport who will be entering the Emergency Medicine program at MGH this coming July. So this coming year, we will welcome Shivani Pandya and Pushpak Pondugula who will be joining us as new PGY 2s. We also wish Sam Oduwole PGY2 well as he transitions to the Physical Medicine and Rehabilitation program at Penn and we welcome Nnaemeka Okorie who will join the incoming PGY3 class as a transfer from the Howard University program. Lastly, Sand Mastrangelo has switched gears as well and will be starting Psychiatry at MGH this next academic year, leaving us at the end of their PGY3 year. While we are at it, congratulations to the PGY5 class of 7 who will move on to their fellowships: Stephen Barchick (Spine at Emory), Sachin Gupta (Spine at Leatherman), Lucas Myerson (Shoulder/Elbow at NYU), Richard Kim (Shoulder/Elbow at Kerlin-Jobe), Matthew Stein (Joints at Duke), Kelsey Young (Hand at NYU), and Steven Zhang (Spine at Wash U).

We thank all our faculty for their dedication to the residency program but there are a few that have made some notable contributions. Dr. Cara Cipriano continues her role as Director of the Undergraduate Medical education providing us with a fantastic pipeline of medical students ripe for learning the benefits of an orthopaedic career or at least learning some crucial anatomy and basic MSK care. Lorraine Boakye and Tim Costales have taken on shepherding the intern skills month and we are already seeing some great enhancements to that experience. Samir Mehta, trauma faculty and expert educator, took 2 of our chiefs (Sachin and Steve Zhang) to the Dominican Republic this year where they truly learned orthopaedics in an austere environment unlike the smooth running technologically advanced operating rooms at Penn. We also welcomed Liane Miller, MD back to Penn as faculty this year in the Sports Division, another great resident who has come back to the nest to share their expertise, research and wisdom with the next generation of residents.

In the quest to keep Penn at the top of its educational game, we formed a group of faculty and residents to take a deep dive into the format of our education program and examine whether changing up the format of conferences and rotations might enhance the resident experience. We also welcome a number of new resources that we expect will give residents more time in the clinics and ORs including additional advanced practice provider support, planned renovations of "the bunker," and more.

We can never thank Dr. L. Scott Levin enough for his steadfast support over the past 14 years and for what he has done to grow this department and raise the resident experience to new heights. A number of other thank you's are always in order every year. First, kudos to Dr. Stephen Liu, our Associate Program Director, who is an invaluable asset to the program and to me. Angela Nieves, our primary residency program coordinator, and Abbi Goldman, who assists with the residency, numerous fellowships, and the med students, are key and crucial components of the education mission at Penn Ortho and we appreciate their efforts to support the residents and fellows.

On a bittersweet note, this will be my last update as program director. With new leadership on the way comes opportunity for change and I will be stepping down from this role to make way for that change. Dr. Andrew Sobel will assume responsibility for the residency as Interim Program Director and Steve Liu will continue as Associate Program Director. I will work closely with them to transition the program as smoothly as possible. I want

to thank all the faculty, residents, alumni and staff at Penn for their partnership over the past 5 years. It has truly been an honor to serve in this position. I want to especially thank Scott Levin for providing me this opportunity and entrusting me with this most important mission.

Everyone at Penn Orthopaedics will continue to wake up every morning looking for ways to continue to improve the educational mission! If you remember your days as a resident or fellow and want to support this mission, please donate to the Penn Orthopaedic Education Fund. All donations directly benefit the residents and support everything from educational resources, resident instructional courses, and academic travel to the occasional resident happy hour that helps boost morale. Please contact Allyse Orsini at aorsini@upenn.edu or 267-788-0975. Also check out our Instagram page at Penn.Ortho!

Wishing everyone a happy and healthy and productive 2024-5 Academic year!

A Letter of Gratitude and Anticipation: Welcoming Dr. B. Kyle Potter as Our New Chairman

Jean-Claude G. D'Alleyrand, MD

Benjamin "Kyle" Potter, MD

We have all benefited from Dr. Levin's sacrifices and leadership as he built our Department into an Academia powerhouse, filled with world-class clinicians, researchers and educators. As this academic year draws to a close, so too does his tenure as our Department leader and Chair. While it saddens me to bid farewell to him in his capacity as Chair, I am grateful for the year that I have spent working alongside him, collaborating with him clinically and learning from him as a leader. I am also profoundly grateful that he will pass the torch to B. Kyle Potter, MD, a colleague I have known for almost 15 years. That is a lengthy time, more than enough to gauge his character, leadership ability and clinical acumen.

Dr. Potter began his internship at Walter Reed in 2001, ten weeks before the terrorist attacks of 9/11. When American Airlines Flight 77 struck the Pentagon that morning, many of the injured patients were evacuated to Walter Reed, beginning a flow of casualties that would not stop for twenty years. During large offensives, such as the Battles of Fallujah, the casualty flow would reach staggering proportions, with plane after plane arriving filled with injuries that fortunately few surgeons will ever encounter. Treating untold numbers of catastrophic wounds would drive most surgeons into any specialty that would protect them from experiencing those injuries again, but Dr. Potter chose a different path. Seeing an opportunity to ease the suffering of our combat casualties, he pursued an Oncology fellowship so that he could lead Walter Reed's Amputee programs and make a maximal impact on our Nation's wounded heroes. In the years we served together, he always led by example, taking on the hardest cases, building a giant research machine and holding himself to the same standards to which he held others at every stage of his career. Selfless service is in his nature, and it continues to guide him as he grasps the baton to continue our Department's upward progression in the domains of patient care, education and research.

Dr. Potter's CV is impressive by any standard, reflecting a prolific research portfolio and numerous scientific contributions while leading at the highest levels of Army Orthopaedics. While these accomplishments are to be expected for an incoming Chair of a prestigious Department like ours, it is his intangible qualities that will benefit Penn Orthopaedics the most. His moral compass, his sense of Duty, his sense of "others before self" … these are the qualities that have guided him in the years I have known him and they will continue to do so as he makes the decisions that will most benefit our Department. While transitions can sometimes be difficult, his efforts will take Penn Orthopaedics into another era of excellence, and I ask all my beloved colleagues and the esteemed alumni of this Department to give him their full support, as I have mine. If we stand united behind our common goals of clinical excellence and world-class patient care, there is no limit to what we can accomplish: for each other, for Penn and for the deserving patients in our care.

In friendship,

Jean-Claude G. D'Alleyrand, MD

Dedication: Dr. Eric Hume, MD

Joseph Bernstein, MD

I met Eric Hume briefly on a visit to Jefferson in 1989, but my first meaningful interaction was on a Tuesday in February, 2011, his first day as a staff surgeon at the VA.

We were sitting in the "Chief of Orthopaedics" office waiting for the first patients to roll back when one of the residents came by to ask about a consult from the Emergency Room.

The ER doctors had suspected an ankle fracture, we were told, so they got films. The ankle was fine. Yet on the lateral, there was a small line through the calcaneus. The resident proposed a boot and non-weight-bearing status. I said "Sure, it looks innocent enough."

To that, Eric said, "I can see why you think it looks innocent, but maybe we should get a CT scan first. The x-ray probably understates the severity of the injury. The fracture might be unstable, if it's not stable it might displace and if it displaces the patient will be sad. So we might want to fix this."

Not recalling that Eric had been doing trauma for years at Cooper and at Jefferson before that, I asked him "Do you mind if I crosscheck on that?"

"Sure," Eric replied.

I texted the trauma chief the x-ray and clinical history, and, as we have come to expect, got a helpful reply at once: I can see why you think this fracture looks innocent, but get a CT scan first. The x-ray probably understates the severity of the injury. The fracture might be unstable. If it's not stable it might displace. And if it displaces the patient will be sad. So you might want to fix this. See Essex-Lopresti British Journal of Surgery 39.157 (1952): 395-419.

———— ✧ ————

I did not fully appreciate it at the time, but that little encounter in so many ways encapsulates the Hume approach. It was knowing. It was modest. It was a gentle nudge. And perhaps needless to say, it was about improving patient care.

———— ✧ ————

Dr. Hume was hired at Penn to be an arthroplasty specialist. We had four joints on the schedule that very day I met him, in fact. I could be forgiven for assuming that maybe Trauma was not his world. Yet, as I came to learn, living in multiple environments, at home in all of them, is something Eric does particularly well (see Figure 1).

———— ✧ ————

Eric, it turned out, found a great niche in the arthroplasty world: everybody's friend. For some reason, joint surgeons enjoy a good feud. It seems that there is nothing like an argument over aspirin vs heparin or the merits of various infection-detecting methodologies to leave a room looking like a slaughterhouse. In this environment, Eric's respect for other people's ideas –and the people themselves – allowed him to see the merits of all sides to a question, and to disagree, if he must, without being disagreeable.

I particularly enjoyed listening to Eric debate a resident who was defending, say, kinematic alignment for total knee replacement, especially since Eric's performance, challenging a different resident who favored mechanical alignment the previous week, was fresh in my mind.

———— ✧ ————

After a few months of sharing the VA office every Tuesday, I also came to discover Eric's great fund of knowledge outside of orthopaedic surgery as well. In those pre-CHAT days, when one of our children would ask me "Why did that airliner crash?" or "How does a toilet work?" or, "Which is better, A/C or D/C current?" I would always propose getting back to them after work on Tuesday. I always was smarter after work on Tuesdays…

———— ✧ ————

Eric's good humor has to be acknowledged. If I can break the clubhouse omertà just a bit, I must confess that any whining or complaining you may have heard coming from behind the closed doors of the Chief's Office was me. Eric was—and is!—so darn cheerful!

And he'd be forgiven if he weren't cheerful, I should add. Medicine has changed so much since Eric graduated from medical school in 1978, and to the extent that these changes made healthcare delivery safer or more effective (and some certainly have), hardly any have made surgical practice more pleasant. Consider: our "Chief of Orthopaedics" office is 4 desks crammed into 89.2 square feet of windowless space, not that I am counting. And yet, despite this, despite malpractice insurance premiums going moonward while surgical reimbursements have dropped by 90% in real terms, despite every challenge, Eric is always whistling while he works.

———— ✧ ————

In the annals of orthopaedics, there is no Hume procedure and no Hume classification. Our city is unlikely to have a Hume Institute any time soon. Nonetheless, Eric Hume's legacy eclipses such monuments: his true legacy is the cascade of positive actions and good works undertaken by the more than 1000 students, residents, fellows, and colleagues he has inspired over a 40-year career.

When we go to work with gusto; when we make sure we are knowledgeable and apply that knowledge for our patients' benefit; when we consider our rivals' arguments in the best possible light; and when we respond to some knuckleheaded administrative fiat with a chuckle or wry smile, we are placing yet one more stone on the living Hume Tribute. In embodying these virtues, we not only honor Dr. Hume's legacy but perpetuate it. Hence, it is

with immense gratitude that the residency class dedicates this issue of the Journal to him and it is with immense respect that I lift a glass to toast him: Here's to Dr. Eric Hume—a true giant in our field—whose legacy is measured by the indelible impact he has left on our hearts and minds.

Figure 1A – 1C. Traditionally, the superhero is characterized by many costumes and modes of transportation. (Photographs courtesy Lenora Hume).

Fostering Excellence: The UPOJ's Impact on Orthopaedic Editors Through the Years

Mohammed Abdullah, MD and Eric Schweppe, MD
Co-Editors-in-Chief, 2024

The University of Pennsylvania Orthopaedic Journal (UPOJ) has long been an essential part of the Penn residency experience, shaping the professional development of many of its past editors. Roshan Shah describes it as a "formative part of my training," emphasizing the comprehensive learning in fundraising, marketing, and academic publishing. This hands-on involvement not only honed his skills but also ingrained a deep appreciation for the journal's historical significance and the dedication of faculty advisors. The impact of such experiences is profound, leaving lasting memories and connections that extend beyond the residency years.

For Penn Orthopaedics, the UPOJ serves as a beacon of the department's commitment to excellence and innovation. Pramod B. Voleti highlights the journal's role in the residency program, describing it as a "stimulus for original research and a landing spot for peer-reviewed articles." The meticulous process of producing each edition, from soliciting articles to securing funding and distributing the journal, provides residents with invaluable insights into the academic and practical aspects of medical publishing. This not only elevates the residency experience but also reinforces the department's reputation for producing high-quality scientific work.

The greater orthopedic community benefits immensely from the UPOJ's contributions. Andrew H. Milby reflects on the pride of bringing complex projects to fruition, a sentiment echoed by other past editors-in-chief like Tyler Morris and Alexander Neuwirth. They appreciate the journal's unique combination of current research, departmental news, and personal insights, which fosters a sense of continuity and progress within the field. The UPOJ stands out as a publication that not only documents significant advancements but also nurtures the professional growth of its contributors, ensuring a lasting legacy for the orthopedic community. Under Dr. Levin's leadership, the UPOJ has fostered the growth and development of 30 editors-in-chief (**Fig 1**). Dr. Shah still proudly wears his UPOJ fleece jacket, finding it handy for those late-night research sessions as an attending, proving that the journal's influence—and his dedication—never fade.

Roshan Shah, MD
Editor-in-Chief, 2010
Columbia University

"Co-Editing UPOJ with Jason Hsu was a formative part of my training. We developed the 20th anniversary issue, a hardcover special edition. It commemorated Dr. Richard Lackman's successful tenure as chair and heralded the legendary force and impact of Dr. L. Scott Levin's leadership at the helm. I learned about fundraising, marketing, and academic publishing, about the history of Penn Ortho, and about our alumni's commitment to this department. I bore witness to our faculty advisors pouring themselves into the journal, as they did all aspects of our education. The impact of this experience will be long lasting. Indeed, I am wearing my UPOJ fleece jacket as I write."

Pramod B. Voleti, MD
Editor-in-Chief, 2012
Montefiore Einstein

"Serving as an editor-in-chief for the University of Pennsylvania Orthopaedic Journal was a tremendous honor and a transformative experience for me. Through this undertaking, I acquired insight into the painstaking steps required to produce a high-quality scientific publication, including soliciting articles, editing manuscripts, coordinating peer review, securing funding, designing print and online layouts, and distributing printed journals. I also gained a newfound respect for the editorial and peer-review process. I still consider my involvement in the UPOJ as one of the highlights of my residency experience at Penn. The journal brings tremendous value to the residency program and to the department, serving as a stimulus for original research and a landing spot for peer-reviewed articles. Through its 34 editions, it has had a lasting impact on countless orthopedic residents. It brings me joy to see that the UPOJ is still going strong and will continue its legacy into the future."

Andrew Milby, MD
Editor-in-Chief, 2013
Emory University

"As I reflect on my time spent on the UPOJ, I take immense pride in having brought a complex project to fruition. I gained an appreciation for the steps involved in fundraising, solicitation of content, peer review, copy editing, formatting, and printing. In contrast to the commercial journals published by many other orthopaedic departments, I am especially proud to know that the UPOJ rests squarely on the shoulders of two motivated and industrious residents each year. Our issue would not have materialized without a team effort, and I remain grateful for all of Sarah Yannascoli's hard work during our year in the trenches."

Tyler Morris, MD
Editor-in-Chief, 2015
Clarksville, TN

"As a prior editor-in-chief of the UPOJ, I understand the hard work that goes into creating each annual edition. It is a unique combination of current research and events, news relevant to alumni of the program, and personal letters from personnel in the department. I know of no other periodical like it in the country. Since graduating from the program, I look forward to the new edition every year to see what is happening in the program and the direction the department is moving."

Alexander Neuwirth, MD
Editor-in-Chief, 2015
Columbia University

"Serving as Editor in Chief of UPOJ was a tremendous honor and privilege, and it was an instrumental part of my academic development. The process was deeply educational in many different ways. It allowed me to develop a profound appreciation for the journal editing and printing process, from requesting, identifying and selecting articles to fine tuning them to fulfil the journal's criteria. Furthermore, the process taught me how to raise funding from a variety of partners to allow for the publication at high volume of the journal while managing a budget closely to ensure future viability. Lastly, on a more personal note, I found the opportunity to leave a lasting, printed, legacy at Penn immensely gratifying, and to this day, it is one of the professional achievements I am most proud of. I very much look forward to reading the 2024 "

Year	Dedication	Editors-in-Chief
2010	Richard Lackman, MD	Jason Hsu, MD and Roshan Shah, MD
2011	Zachary B. Friedenberg, MD	Chancellor F. Gray, MD and Mara L. Schenker, MD
2012	Mary Ann Keenan, MD	Tae Won B. Kim, MD and Pramod B. Voleti, MD
2013	Bruce Heppenstall, MD	Andrew H. Milby, MD and Sarah M.Yannascoli, MD
2014	Ernest Gentchos, MD	Vishal Saxena, MD and Joshua A. Gordon, MD
2015	John Esterhai, MD	Alexander Neuwirth, MD and Tyler Morris, MD
2016	Gerald Williams, MD	James Friedman, MD and Cody Hillin, MD
2017	Malcom Ecker, MD	Blair Ashely, MD and Dan Gittings, MD
2018	Marvin Steinberg, MD	Mike Ebbe, MD and Adnan Cheema, MD
2019	Paul Lotke, MD	Liane Miller, MD and Matthew Counihan, MD
2020	William George DeLong, MD	George Fryhofer, MD and Kelsey Bonilla, MD
2021	Craig Israelite, MD	Sachin Gupta, MD and Matt Stein, MD
2022	G. Russel Huffman, MD	Kendall Masada, MD and Jordan Cohen, MD
2023	L. Scott Levin, MD	Bijan Dehghani MD and Mitch Hallman, MD
2024	Eric Hume, MD	Mohammed Abdullah, MD and Eric Schweppe, MD

Figure 1: Prior UPOJ Dedications and Editors-in-Chief under the leadership of Dr. L. Scott Levin.

Spine Division

Amrit Khalsa, MD

Spine Faculty


Harvey Smith, MD


Vincent Arlet, MD


Amrit Khalsa, MD


David Casper, MD


J. Rush Fisher, MD

The Orthopaedic Spine Division continues to charge ahead. The division continues to provide comprehensive state-of-the-art patient care ranging from cutting-edge endoscopic spinal surgery to the most complex revision scoliosis procedures. From spinal tumor to Level 1 spine trauma, the division provides a wide breadth of care.

It is with the sincerest gratitude and appreciation that the Spine Division recognizes Dr. Vincent Arlet's retirement this year. Dr. Arlet's legacy at both Penn Orthopaedics and national and international level will continue to live on through the multitude of residents and fellows he has trained throughout his illustrious career.

The division welcomes Dr. Sherif Sherif as he transitions his practice to Pennsylvania Hospital to pick up where Dr. Arlet left off taking on the most complex adult spinal scoliosis procedures.

From an educational standpoint, the Spine Division continues to thrive. In addition to supporting a rotating PGY 3 and PGY 4 resident, 3 of the matriculating chief residents are attending elite spine fellowships across the country next year. Under the leadership of the Penn Orthopaedic Spine Fellowship Co-Directors, Drs. David Casper and Amrit Khalsa, an additional clinical fellow was added in conjunction with collaboration with the Shriner's Hospital of Philadelphia and Virtua Health System in New Jersey. The Penn Orthopaedic Spine Fellowship continues to blossom into one of the premier spine fellowships in the country.

Dr. Harvey Smith continues to advance translational research surrounding biologic spinal disc-replacement with several recent landmark peer-reviewed publications in collaboration with Dr. Robert Mauck and other McKay Laboratory researchers. Dr. Smith succeeds in sustaining a busy clinical practice while remaining an international thought-leader in the field.

Dr. Rush Fisher continues to advance the field of spinal arthroplasty as he transitions his high-volume practice to Penn-affiliate Chester County Hospital.

The Spine Division is supported by an illustrious host of advanced practice providers and administrative assistants that continue to elevate the division as we grow both clinically and academically.

Hand Division

David Bozentka, MD

Hand Surgery Faculty

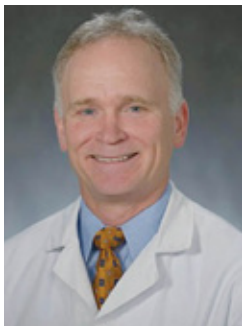
David Bozentka, MD


David Steinberg, MD


L. Scott Levin, MD, FACS


Hannah Lee, MD, PhD


Andrew Sobel, MD


Robert Carrigan, MD


Apurva Shah, MD, MBA


Stephen Liu, MD

Once again, the Hand and Upper Extremity Service within the Department of Orthopaedic Surgery has excelled. This year, we've bolstered our team with additional skilled clinical staff, enhancing the quality of care we provide. Moreover, we've ensured an outstanding educational journey for our residents and fellows. Additionally, our dedication to research has grown, with a multitude of studies underway within our team.

Under the guidance of David Steinberg, MD, and Ines Lin, MD, the Hand, Upper Extremity and Microsurgery Fellowship at the University of Pennsylvania has continued to flourish. The two current fellows have had a successful and enriching year, making significant strides in their clinical and academic pursuits. Due to the continued expansion in both clinical and academic activities, the program has applied for an increase to three hand surgical fellows. Thanks to the Chan Family Surgery Education Fund, established by the generous contributions of Peter SH Chan MD and Karen Postick Chan MD, our fellows have had the opportunity to attend the flap dissection course as well as the annual meetings of the American Society for Surgery of the Hand and American Association of Hand Surgeons. In addition, our weekly didactic fellow-run hand surgery conference has continued to thrive, with topics ranging from joint radiology conferences to pediatric conferences, journal clubs, and case reviews.

Our current fellows Drs. Vinay Rao and Kurt Mohty have performed exceptionally well over the past year. Dr. Rao will enter a six month pediatric hand surgery fellowship at the Shriner's Hospital of Philadlephia under the tutelage of Drs. Scott Kozen and Daniel Zltotolow. Dr. Kurt Mohty is finalizing plans to return home in Arizona for a hand surgical practice.

In February, we interviewed twenty-five candidates from over one hundred applicants for the two current Hand Fellowship positions. The incoming fellows for next year include Dr. Julian Klosowiak, MD and Caroline McLaughlin, MD, who are currently completing thier plastic surgery residency at Northwestern University and Penn State Health Milton S. Hershey Medical Center respectively.

Our section has seen great advancements in our research productivity. Dr. Hannah Lee has earned a VA Career Development grant of over $2M to study a novel neural scaffold with temporal and spatial regulation of neurogenic factors. Her accomplishments as a clinician-scientist have been nothing short of amazing with multiple posters and podium presentations, issuance of a patent, and other grants that support her nerve research. Dr. Levin,

working with our former hand fellow Chris Jehle and orthoplastics fellow Dominik Kaiser, has started to present his data on an ex-vivo model for limb perfusion that can have substantial translational applications to those with limb amputations. Dr. Sobel was awarded the McCabe Fund Grant this year and has delivered podium presentations on various clinical studies at the last three large national hand surgery and orthopedic meetings (ASSH, AAHS, AAOS). The section will be working with Auxillium to test a new nerve repair device and is finalizing other industry work related to Dupuytren's and a tendon adhesion barrier.

To keep you informed of our developments, Penn Hand Surgery is found on social media. Under the leadership of Mylinh Nguyen, the service has a robust social media site showcasing interesting cases, hand-section staff, presentations, and awards. We encourage group members and alums to send suggestions for the site. In addition, stay updated with the program by following us on Instagram @ Pennhandsurgery.

For over 20 years, Penn Orthopedics has honored the memory of Dr. Leo Leung, a promising young surgeon who passed away suddenly during his chief year of residency in 2002. The Leo Leung Memorial Fund was created to fund an annual visiting professorship, where we honor Leo and invite guest lecturers from around the world to share their work and advance the educational experience for our residents and trainees. Through the generosity of friends, and family of Leo, the Leo Leung lectureship has been funded in perpetuity as an endowed lectureship.

The hand transplant team has successfully performed bilateral upper extremity allotransplantation on four patients with quadra-membral amputations, resulting in remarkable outcomes that have transformed their lives. The team has continued to meet regularly, rehearsing in the human tissue lab with cadavers, fine-tuning the procedure checklists in preparation for the fifth bilateral upper extremity allotransplantation.

The hand and upper extremity service could not function without the outstanding support from our superb advanced practice providers, nurses, and administrative assistants. With this exceptional support and collaboration, the future looks bright for the hand surgery section.

Shoulder and Elbow Division

David Glaser, MD

Shoulder & Elbow Faculty

David Glaser, MD

Andrew Kuntz, MD

Gabe Horneff, MD

In FY24, the group performed over 10,000 visits and performed over 900 surgical cases with anatomic and revision shoulder arthroplasty showing the greatest increase. The section's tertiary referral network has remained strong, along with the complexity of cases. Gabe Horneff's practice has achieved steady state, with a strong balance of primary and revision surgery. Our virtual indications conference has continued and includes a nationwide group of our past fellows, our therapy team, and regional shoulder and elbow providers. Jeff Abrams has been a welcome addition to our educational mission. Through a virtual platform, the group of talented sub-specialists re-unite monthly to discuss complex cases, and opportunities for research

After over three years of tireless effort, Andy Kuntz has launched PatientIQ within our Division and continues to shepherd its expansion to the rest of our department. A robust database system, automating patient reported data collection with analytical functionality and data sharing. Within the first 9 months of our pilot, greater than 4,600 patients were enrolled with ~41,500 outcomes measured. Most impressively, these numbers were achieved without additional effort from our staff. It has already provided some interesting insight into significant difference in task completion rates when stratified by patient demographic variables (age range, gender, ethnicity, and marital status). Andy Kuntz continues to lead our research effort, setting a high standard for both scientific methods and clinical outcomes. To parallel his research interests in anatomy, functionality and mechanisms of injury of the rotator cuff and outcomes of arthroplasty, he has decided to focus his clinical practice towards the treatment of glenohumeral arthritis. We would like to recognize Andy for his continued focus as a clinician-scientist, providing world class clinical care, while contributing to all aspects of our research mission- clinical, translational and basic science. Alongside Andy, Gabe has helped expanded our clinical research program, mentoring several medical students and residents with their academic endeavors.

The fellowship has continued to thrive, attracting the most competitive candidates. This year's candidate pool was as competitive as prior years. Our program is unique in that the fellow has exposure to four different surgeons, with complementary philosophies, who use an extreme range of devices and approaches. John Kelly has added an additional opportunity to fellows interested in creative arthroscopic approaches to manage complex shoulder and elbow pathology. Additionally, now in its seventh year, and in collaboration with our French colleagues, we offer our fellow an opportunity to visit world leaders in shoulder surgery. Mike Livesey (F'24) will return from Monaco and France to join Mohit Goholta (F'14) at the University of Maryland. Holt Cutler (F'23) joined Howard Harris and others at the well known Carrell Clinic in Dallas. Brandon Romero (F'22) joined University of Nevada Las Vegas. Past fellows who enjoyed the European experience included Christy Piper (F'21), Greg Gomez (F'19), Josh Rogozinski (F'18), and Chad Myeroff (F'17) who spent between two to three weeks visiting academic centers in Europe. We will continue to leverage our internal cohesiveness, therapy partners (superstars Brian Leggin, Joseph Kearns, and Marty Kelly) and recent collaborations with non-Penn shoulder and elbow providers, to bring success to our division.

Adult Reconstruction Division

Charles Nelson, MD

Arthroplasty Faculty


Charles Nelson, MD


Craig Israelite, MD


T. David Tarity, MD.


Christopher Anthony, MD


Neil Sheth, MD

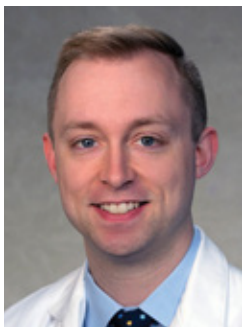
Christopher Travers, MD


Emmanuel Gibon, MD, PhD


Timothy Costales, MD

This past academic year has been marked by significant strides and accomplishments within the Penn Orthopaedics Adult Reconstruction Division. We've maintained our commitment to delivering exceptional care, catering to both healthy and high-risk patients with innovative approaches aimed at minimizing complications and enhancing outcomes. Our dedication to clinical excellence is paralleled by our active engagement in scientific endeavors and clinical education, both nationally and abroad. Moreover, our faculty members have continued to assume leadership roles and contribute their expertise to various esteemed national orthopaedic organizations, including the American Academy of Orthopaedic Surgeons, The Hip Society, The Knee Society, the International Hip Society, the American Association of Hip and Knee Surgeons, the American Orthopaedic Association, and the American Board of Orthopaedic Surgeons.

Throughout the year, our faculty have made noteworthy contributions to the field through numerous peer-reviewed publications, scientific presentations, and invited lectures. Notably, Neil Sheth's paper on "Inferior Screw Fixation Decreases Acetabular Component Failure following Revision Total Hip Arthroplasty" earned him the prestigious Surgical Techniques and Technology Award from the American Association of Hip and Knee Surgeons. Similarly, Emmanuel Gibon's research on "Randomized Clinical Trial of Cementless vs. Cemented Tibial Components: Durable and Reliable at 10 Years" was recognized with the John Insall Award from the Knee Society.

In addition to our academic achievements, our division remains actively involved in clinical research, with substantial support from federal and industry sources. Our Adult Reconstruction faculty comprises esteemed individuals, including Professor Charles L. Nelson, MD, Associate Professors Eric Hume, MD, Craig Israelite, MD, and Neil Sheth, MD, as well as Assistant Professors Christopher Travers, MD, Christopher Anthony, MD, T. David Tarity, MD, Emmanuel Gibon, MD, PhD, and Timothy Costales, MD.

We are proud of the progress made this year and remain dedicated to advancing orthopaedic care through excellence in patient care, research, and education.

Foot and Ankle Division

Casey Humbyrd, MD

Foot & Ankle Faculty

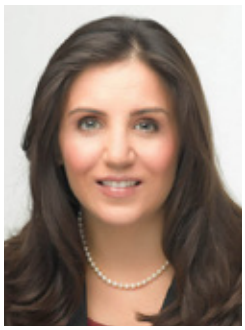

Casey Humbyrd, MD

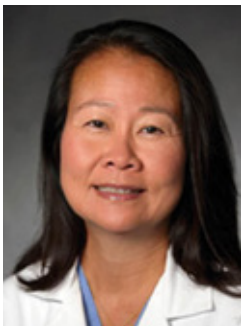

Wen Chao, MD

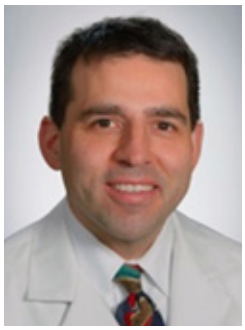

Daniel Farber, MD

Anthony "Bobby" Ndu, MD

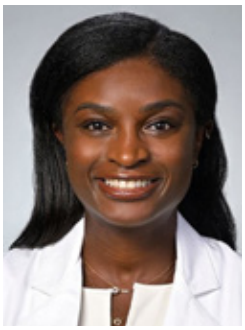

Lorraine Boakye, MD

2023 was a dynamic and transitional year for the Foot and Ankle Division.

After starting his academic career at the University of Pennsylvania in 1973 as a Penn Undergraduate, Dr. Keith Wapner ended his academic and clinical practice at Penn June 30, 2023. Dr. Wapner's 37 years in practice were celebrated with a department-wide celebration. Despite his retirement, he continues to routinely join weekly conferences to add insight and humor. His presence at Penn also lives on both with the Keith Wapner Academic Scholarship and the June Wapner Annual Lectureship.

Dr. Wen Chao has been on staff as an Orthopaedic Foot and Ankle surgeon at Pennsylvania Hospital since March of 2001. She continues as the Orthopaedic Foot and Ankle Consultant to the Philadelphia Ballet since 2001. Because of this affiliation, she takes care of the professional dancers from Philadelphia Ballet, professional dancers from other dance companies, students from the School of Philadelphia Ballet, Rock Ballet School, and other students who aspire to become an elite dancer. She also treats many high school, collegiate and professional athletes. She is a member of AAOS, AOFAS, AOA and the Orthopaedic Foot Club (OFC). She was nominated to AOA and became a member in 2006. She was also nominated to OFC and became a member in 2002. She serves as a member on the Public Education Committee for the AOFAS. She is a reviewer for Foot and Ankle International/Foot and Ankle Orthopaedics. Dr. Chao has two IRB approved projects that are still ongoing. They are "Staple fixation compared to compression plate and screws fixation for tarsometatarsal joint arthrodesis: Radiographic comparison study" and "Magnetic resonance imaging and dynamic ultrasonography findings and intra-operative correlations of peroneal tendon pathology."

As Vice Chair for Education and Residency Program Director, Dr. Daniel Farber continues to lead the educational mission of the department while maintaining a busy clinical practice. He serves on the education committee of AOFAS as well as service as Chair of the AAOS Resolutions committee. In December, he completed the inaugural European Foot and Ankle Society / AOFAS traveling fellow program visiting centers and sharing ideas and surgical techniques in Germany, France, and Spain. He serves as a reviewer for Foot and Ankle International/Foot and Ankle Orthopaedics as well as the American Journal of Sports Medicine. Finally, he continues collaborations with Lou Soslowsky, PhD and the McKay lab and Josh Baxter, PhD of the Human performance lab on his K01 and R01 awards exploring Achilles pathology as well as his role on the recent P50 grant.

Dr. Anthony "Bobby" Ndu is finishing his third year in clinical practice since his return to PENN. He serves as a member of the AOFAS DEI committee. He recently spearheaded a very successful orthopedic early exposure program for regional undergraduate and preclinical medical students in conjunction with Nth dimensions and the AOFAS. He continues to expand his minimally invasive clinical practice. Dr. Ndu is interested in MIS surgical outcomes beyond bunions and for more expansive applications. He recently helped organize a multicenter research group focused on MIS surgical outcomes with collaborators from across the country. His recent publication in Techniques of Foot and Ankle Surgery on Multimodal Utilization of Intraoperative Antibiosis in Complex Foot and Ankle Infection was selected as the CME article for the publication. He remains dedicated to education teaching at multiple MIS courses in the coming academic year. He also continues to work with and mentor undergraduate and junior medical students interested in a career in orthopedics.

Dr. Lorraine Boakye has made strides in growing her clinical practice and has loved working with trainees. She continues to serve as the Director of Research for the Foot and Ankle Division. She has been successful in securing grant funding both internally—through the McCabe Fund

and University Research Foundation, and externally—through the American Orthopaedic Foot and Ankle Society (AOFAS). She continues to collaborate with Dr. Josh Baxter on Achilles tendinopathy and rupture projects, as well as clinicians and researchers at NYU and Brigham and Women's Hospital on research regarding sustainability in surgery. She was selected as an inaugural Michael P. Kelly Senior Leadership Fellow by the Orthopaedic Research Education Fund. Dr. Boakye serves as a reviewer the Journal of the American Academy of Orthopaedic Surgeons, and Clinical Orthopaedics and Related Research, and was recently invited to review for the Journal of Bone and Joint Surgery. She serves in leadership roles with the AAOS Diversity Advisory Board, the Ruth Jackson Orthopaedic Society, the J. Robert Gladden Orthopaedic Society, the International Orthopaedic Diversity Alliance, AOFAS, the Arthroscopy Association of North America and the Medical Student Orthopedic Society. Dr. Boakye maintains an active role in mentorship, including her involvement in a formal longitudinal mentorship program for local medical students sponsored by CHOP.

Dr. Casey Humbyrd is starting her fourth year leading the Foot and Ankle Division at Penn. She has continued her research work in collaboration with the McKay laboratory, serving as the Associate Director of the Penn Achilles Tendinopathy Center for Translation Research. She has also built her relationship with Josh Baxter and the Gait Lab, with ongoing funded research and planned additional NIH support in the coming year. Her work has focused on optimizing Achilles tendon rupture rehabilitation as well as gait changes in pregnancy. She continues to serve as the chair of the Conflict-of-Interest Committee for the AOFAS as well as serving as a delegate to the American Medical Association on behalf of the American Academy of Orthopaedic Surgeons. She also continues to be a question writer for the American Board of Orthopaedic Surgeons as well as a reviewer for multiple medical journals. Dr. Humbyrd continues her clinical and academic work in medical ethics, serving as chair of the Pennsylvania Hospital Ethics Committee, as well as a columnist on ethical issues for Clinical Orthopaedics and Related Research. She continues to maintain a busy clinical practice, including the care of collegiate athletes at Penn as well as professional relationships including the 76ers, Flyers, and Union.

The division's primary research focus remained the P50 research grant funded work on Achilles Tendinopathy (see details in "Health Systems Update").

Orthopaedic Oncology Division

Cara Cipriano, MD, MSc

Orthopaedic Oncology Faculty

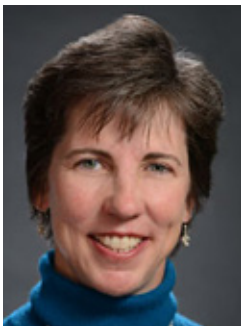

Kristy Weber, MD, FACS

Cara Cipriano, MD, MSc

Benjamin "Kyle" Potter, MD

It has been another full year for the Orthopaedic Oncology service at Penn. Highlights include the addition of new team members, the 10th annual Steps to Cure Sarcoma Walk/Run, the first annual Penn Resident Tumor Review Course, and the opportunity to deliver quality, multidisciplinary care to our patients.

Dr. Cara Cipriano is beginning her fourth year as Chief of the Orthopaedic Oncology division. Her practice includes musculoskeletal oncology as well as primary and revision joint replacement, with clinics at PCAM, Radnor, and the Farm Journal Building at Pennsylvania Hospital. She also devotes a large portion of her time to education, particularly in her role as the Director of Undergraduate Medical Education for the department and leader of the Resident Medical Education Track for the residency.

Dr. Kristy Weber continues to serve as a leader, both in the department as Vice Chair of Faculty Affairs and at the Abramson Cancer Center as Director of the Sarcoma Program. She practices musculoskeletal oncology at HUP, PCAM, and CHOP, and actively engages in resident education. Additionally, she remains dedicated to supporting women and sexual/gender minorities in the field of Orthopaedic Surgery. In the past year, she has organized multiple events, including dinners for residents and the Perry Initiative, an inspiring program that exposes women high school and medical students to careers in orthopaedic surgery and engineering.

The Orthopaedic Oncology team is currently at its strongest. Kate Barrie, PA, is increasing her independent clinics as well as her leadership in education. She has presented lectures for APPs both regionally and nationally and is involved in organizing the APP program for the Musculoskeletal Tumor Society annual meeting. Nicole Koffke, RN, has been with the team for over a year and is taking excellent care of patients while obtaining her Masters degree at Drexel University. Allyson Woodley joined the team as our Surgical Coordinator in 2023, bringing organization and incredible crafting talent to the group. The team works together to provide high-level care that is knowledgeable, efficient, and kind. Outside of work, all three enjoy spending time with their pets (Odin, Roger, and Britney, respectively), as well as their significant others.

We are thrilled that Dr. Benjamin Kyle Potter will be joining Penn, not only as the Chair of the Department, but as a member of the tumor division. In addition to expertise in musculoskeletal oncology care, Dr. Potter is a leader in osseointegration, an evolving technology that is dramatically improving function and quality of life for amputees. His unique skill and knowledge will broaden the range of services we can provide for our patients at Penn.

Our basic and translational science teams at Penn Medicine, Penn Veterinary Medicine, and the Children's Hospital of Philadelphia (CHOP) continue to push the envelope of modulating the immune environment in soft tissue and bone sarcoma. We are actively searching to add a sarcoma scientist to our team in the year ahead. Dr. Malay Haldar's work has garnered additional grants and high impact papers. Dr. Irfan Asangani has made new and exciting discoveries in Ewing sarcoma. Dr. Karin Eisinger has started a new company to identify targets to prevent sarcoma metastasis. Dr. Nicola Mason's dog trials using a vaccine for osteosarcoma has progressed to national trials in children. She is building a team with a focus on sarcoma at Penn Vet. Overall, the portfolio of available clinical trials for patients with bone and soft tissue sarcomas as well as aggressive benign conditions has continued an upward trajectory over the past year at Penn.

In the clinical research arena, our multidisciplinary group is studying local control of metastatic bone disease in the extremities and spine, with the ultimate goal of

relieving pain and improving function in these patients. We are also investigating the factors that contribute to decisions patients make regarding surgery, and how they feel about them postoperatively. Understanding these various aspects of will help us to take the best possible care of our patients.

We celebrated a decade of Steps to Cure Sarcoma with our 10th Annual Walk/Run on May 19, 2024 (www.stepstocuresarcoma.com). The event, which is tirelessly organized by our patient/family advocacy group, raises awareness as well as funds for sarcoma translational and clinical research. Many thanks, as always, for your continued support of our work and our patients!

Additionally, this year our team held the first annual Penn Resident Tumor Review Course (https://www.med.upenn.edu/msktumor2024/). Funded by a generous donation from the Altman family, the course provided a comprehensive overview of musculoskeletal oncology that was engaging as well as educational. The one-day program was designed and taught by Dr. Cipriano and Dr. Weber, together with Dr. Alexandre Arkader from CHOP and Dr. John Wojcik from Pathology. The content focused on the diagnosis and treatment of various sarcomas, ensuring that these rare tumors will be recognized and appropriately managed by future orthopaedic surgeons. It was attended by residents from several regional programs, including Jefferson, Temple, Cooper, Penn State, St Luke's, and Monmouth. We look forward to building on this new tradition in future years!

Orthoplastic Limb Salvage Division

Benjamin Gundlach, MD and L. Scott Levin, MD, FACS

Orthoplastic Limb Salvage Faculty

Stephen Kovach III, MD

L. Scott Levin, MD, FACS

Samir Mehta, MD

Jean-Claude G. D'Alleyrand, MD, MSE

We started the academic year by welcoming Jean-Claude Gregoire D'Alleyrand, MD, to Penn Orthopaedics. Dr. D'Alleyrand joins us after a distinguished career in the military - having practiced at Walter Reed National Military Medical Center and Landstuhl Regional Medical Center – following orthopedic traumatology fellowship training at Shock Trauma. He has immense experience with limb salvage in the war-wounded population, deformity correction and bone transport for complex non-unions. He has quickly become a vital member of the Limb Salvage and Orthoplastic Center at Penn.

Many of the orthoplastic and limb salvage faculty continue to support the men and women of Ukraine via weekly teleconference calls, helping to assist with their in-country war wounded. Penn has also welcomed several Ukraine soldiers to Philadelphia to receive complex care for their extremity injuries and amputation care. Drs. Steve Kovach and Andrew Bauder (prior Penn plastic surgery resident) traveled to Ukraine twice in 2023 and are planning to return again in April 2024. While there, they will work out of military hospitals in Uzhhorod to provide microvascular free-flap coverage and reconstruction of mangled extremities.

The orthoplastic surgery fellowship continues to grow and attract new trainees. In May 2023 we bid farewell to Dominik Kaiser as he returned to Switzerland with his family to being practice, where he is applying the orthoplastic experience to orthopedic oncology, arthroplasty, and trauma patients. Benjamin Gundlach, MD, joined the fellowship in April 2023, having completed Orthopedic Surgery residency at The University of Michigan, followed by hand and pediatric hand fellowship at Thomas Jefferson University and The Shriner's Hospital for Children respectively. During his fellowship year, Dr. Gundlach has participated in over 80 upper and lower limb microsurgical procedures. Peter Qi, MD, will be joining as the next orthoplastic surgery fellow in July 2024. Peter is currently a hand fellow at Wellspan in York, PA, and trained in plastic surgery at University of Toronto.

The hand transplant team has been actively working to prepare and rehearse for a hopeful bilateral hand transplant to occur in the first half of 2024. Dr. Levin and Chrissy McAndrew – among the many other vital members of the transplant team – have been working diligently to gain the support and approval for a Swiss citizen to travel to Philadelphia for the life-changing operation.

Vascularized composite allotransplantation (VCA) research at Penn also continues to progress. Previous orthoplastic fellow Alexander Govshievich's work in creating an ex-vivo limb perfusion system is now being used experimentally to perfuse limbs that have been surgically amputated. Working under Dr. Levin and Mourkioti; Dr. Gundlach and Kevin Cobbol, MS, procured the forelimbs of pigs, which were then connected to the perfusion apparatus and actively perfused for 72 hours. Muscle biopsies have demonstrated improved preservation of muscle fiber size and architecture compared to cold-storage controls. The research group is excited to take this data and apply for further NIH and/or SBIR grant funding in 2024, with an ultimate goal of creating a system that can actively perfuse limbs and allow for safe transport during transplant procurement, or to trauma centers in the case of dysvascular limb trauma.

The Penn Orthoplastic and Limb Salvage Surgery Center continues to grow in clinical volume and evolve in services provided with each passing year. We are very privileged to be one of the only centers in the US to provide such complex, yet unified and collaborative care with such an incredible group of staff and faculty.

Children's Hospital of Philadelphia

Jack Flynn, MD, Ryan Quinn, MHA, and Divya Talwar, PhD, MPH

Pediatric Faculty


John Flynn, MD


Jason Anari, MD


Alexandre Arkader, MD


Keith Baldwin, MD, MPH, MSPT

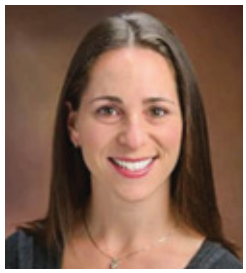
Naomi Brown, MD, FAAP, CAQSM


Patrick Cahill, MD


Robert Carrigan, MD


Benjamin Chang, MD, FACS


Richard Davidson, MD


Vincent Deeney, MD


Malcom Ecker, MD


Theodore Ganley, MD


B. David Horn, MD


J. Todd Lawrence, MD, PhD


Ines Lin, MD


Kathleen Maguire, MD


Christina Master, MD, FAAP, CAQSM, FACSM

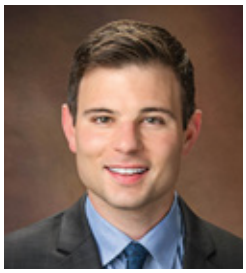
Christopher Renjilian, MD


Wudbhav Sankar, MD


Apurva Shah, MD, MBA


David Spiegel, MD


Brian Vernau, MD, FAAP, CAQSM


Kristy Weber, MD, FACS


Lawrence Wells, MD

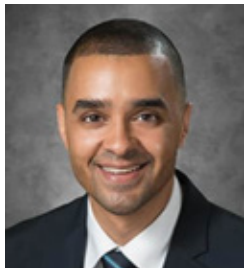
Brendan Williams, MD


Jennifer Winell, MD


Joseph Yellin, MD

Introduction

The Division of Orthopaedic Surgery at the Children's Hospital of Philadelphia (CHOP) had another successful and productive year of significant growth, accomplishment, and innovation. For the third time in four years, CHOP Orthopaedics was recognized by US News as the top pediatric orthopaedic program in the nation.

In 2023, CHOP Orthopaedics welcomed a new sports medicine orthopaedic surgeon and sports medicine pediatrician to our team, participated at national and international conferences, won awards for our research work, maintained enrollment of three FDA Phase IIIb investigational drug trials and a feasibility device trial, published ~200 articles, and obtained significant extramural funding from major funding agencies such as National Institutes of Health (NIH), Department of Defense (DoD), and National Science Foundation (NSF).

Clinical Program

Our Orthopaedic faculty continues to expand and is currently comprised of thirty members: eighteen specially trained pediatric orthopaedic surgeons (including three transition-to-adult care faculty), four non-operative physicians, six sports medicine-trained pediatricians, and two collaborating plastic surgeons. In March 2023, we welcomed Dr. Joseph Yellin (Figure 1), who joined us as an Attending Surgeon in Sports Medicine. He completed his medical degree at the University of Pennsylvania, residency at the Harvard Combined Orthopaedic Residency Program, Pediatric Orthopaedic Fellowship at CHOP and another Orthopaedic Sports Medicine Fellowship at the University of Pennsylvania. Our division also welcomed faculty member, Dr. Thomas Swaffield (Figure 2) as a new sports medicine pediatrician. He earned his medical degree at George Washington University in Washington, DC. Dr. Swaffield completed his residency at Penn State Milton S. Hershey Medical Center, then a primary care sports medicine fellow at CHOP.

Education Program

CHOP Orthopaedics currently funds four one-year clinical fellowships. The 2023-2024 clinical fellows are Stefano Cardin, MD (Figure 3); Joel Turtle, MD (Figure 4); Lee Haruno, MD (Figure 5); and Christopher DeFrancesco, MD (Figure 6). For next year, Dr. Cardin will start as an Assistant Professor at Orlando Health—Arnold Palmer Hospital for Children. Dr. Turtle will work at Spencer Fox Eccles School of Medicine at the University of Utah as an Assistant Professor. Dr. Haruno will begin his journey as Clinical Assistant Professor at Hawaii Pacific Health. Dr. DeFrancesco will complete a Sports Medicine Fellowship at Boston Children's Hospital. The 2023-24 research fellow was Dr. Akbar Syed, MD from India (Figure 7). While at CHOP, Dr. Syed focused his research efforts on clinical research related to pediatric trauma, hand, neuromuscular conditions, tumors, and sports injuries. He will stay with our division for another year.

Figure 1. Joseph Yellin, MD

Figure 2. Thomas Swaffield, MD

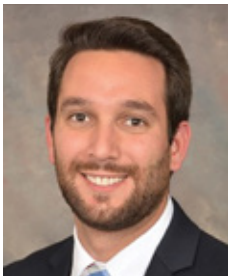

Figure 3. Stefano Cardin, MD

Figure 4. Joel Turtle, MD

Figure 5. Lee Haruno, MD

Figure 6. Joseph Yellin, MD

Figure 7. Akbar Syed, MD

To celebrate the graduation of the 2022-2023 clinical fellows, the Division hosted the Nicholson Visiting Professor Program and Fellows Graduation & Reunion in June 2023. This year's Visiting Professor was Dr. Michelle S. Caird. Dr. Caird is the Harold W. and Helen L. Gehring Professor and Chair of the Department of Orthopaedic Surgery at the University of Michigan in the Division of Pediatric Orthopaedics. Clinically, she treats multiple pediatric orthopaedic conditions including fractures, spinal deformity, and lower extremity deformity. As the director of the University of Michigan Osteogenesis Imperfecta Multidisciplinary Clinic, her areas of special expertise include treating fractures and spinal deformity in children with osteogenesis imperfecta, and in the laboratory she investigates bone healing in this disease and other pediatric low bone mass diseases with NIH grant support with her collaborators.

The 2023 Drummond Rising Star Visiting Professor was Gertrude Ying Li, MD. Dr. Li is a Clinical Associate Professor of Orthopaedic Surgery and Chief of Pediatric Orthopaedic Surgery. Dr. Li's primary clinical and research focus is on pediatric spinal deformity. She is an active member of the Pediatric Spine Study Group and serves on the Research Council. Dr. Li currently serves as the Chair of the Outcomes and Benchmarking Committee of SRS. She also has an interest in pediatric orthopaedic trauma and is a member of the FACTS and CORTICES study groups.

Research Program

Basic Science and Translational Research

This past year, the Translational Research Program in Pediatric Orthopedics (TRPPO) at CHOP, led by Dr. Maurizio Pacifici, has made impressive progress in researching rare pediatric musculoskeletal disorders. The TRPPO scientists have generated novel insights on key aspects of the mechanisms of skeletal development and growth in children and how abnormalities in these basic mechanisms occur and can cause disease. Comprised of the labs of Drs. Fanxin Long, Veronique Lefebvre, Eiki Koyama, and Maurizio Pacifici, the TRPPO has 12 NIH grants and receives additional research support from the Eagles Autism Foundation, Pediatric Orthopedic Society, Lamb-Shaffer Syndrome Organization, MHE Research Foundation, and other private organizations. Some of the disorders the TRPPO studies include Fibrodysplasia Ossificans Progressiva (FOP), Hereditary Multiple Exostoses (HME), Achondroplasia, Hjadu-Cheney syndrome, pediatric bone fragility diseases, and juvenile diabetes.

Wyss Campbell Center for Thoracic Insufficiency Syndrome (CTIS) Research Program

The Division's Center for Thoracic Insufficiency Syndrome (CTIS) continued developing innovative projects in translational research. The CTIS program strives to develop novel imaging techniques, construct new metrics for clinical outcomes, and establish reliable evidence to support innovative surgical strategies and devices through its research. These efforts are made possible by the collaboration of a multidisciplinary team of specialists from clinical research, image processing, informatics, and basic sciences/biomechanics. Currently, the CTIS Basic Science Lab is developing an animal model of TIS that will provide a platform for testing novel devices. The animal surgeries and biomechanics testing will be performed at Penn Vet's New Bolton Center. In addition, the CTIS team in collaboration with Medical Image Processing Group were awarded an NIH R01 grant to develop novel dynamic functional metrics for TIS patients by establishing a comprehensive normative database of dMRI images and anatomic and functional models and metrics, and to translate these to develop biomarkers of TIS and of its corrective-surgery outcomes.

With the generous philanthropic support, Dr. Campbell's legacy was strengthened with the continued establishment of *Wyss/Campbell Center for Thoracic Insufficiency Syndrome*, enabling CHOP to discover countless more breakthroughs in research and care for TIS children.

Genetic Research

CHOP Orthopaedics continues to work in collaboration with the Center for Applied Genomics (CAG), led by Dr. Hakon Hakonarson and Dr. Struan Grant, to compile a registry of DNA and RNA samples. These samples are obtained from patients and families with a variety of orthopaedic conditions including adolescent idiopathic scoliosis (AIS), osteochondritis dissecans (OCD) of the knee, Tibial Spine fractures (TSF) and multiple hereditary exostoses (MHE). The team is investigating further genetic characterizations of the EXT1/EXT2 mutations harbored by each exostosis and identify second hit(s) across exostoses from the same patient. This pilot project represents the first biomedical research focused on MHE and will provide novel and broadly relevant information. The goal is to translate the findings to prognostic tools based on the severity of the disease and to identify therapeutic means to counter the effects of EXT1/EXT2 plus "second hit" mutations. Dr. Ganley is collaborating with CAG to identify if patients who have experienced traumatic ACL ruptures or tibial spine fractures may also have a genetic predisposition toward these injuries. The aim of this collaboration is to perform polygenic risk assessment analyses with the more long-term goal of being able to provide individuals unique genetic risk assessment scores that would be applicable among patients with ACL injuries, tibial spine fractures, and unique cartilage conditions such as osteochondritis dissecans of the knee.

Clinical Research

The Division of Orthopaedic Surgery is currently conducting more than 236 IRB-approved clinical research projects. This includes more than 100 prospective and observational studies. CHOP Ortho faculty are also members of a number of multicenter study groups, including the Harms Study Group (HSG), the Pediatric Spine Study Group (PSSG), Research in Osteochondritis Dissecans of the Knee (ROCK), SCFE Longitudinal International Prospective Registry (SLIP), Tibial Spine Prospective Cohort (TSF-PC), The Fox Pediatric Spinal Deformity Study (Fox PSDS), Pediatric ACL: Understanding Treatment Operations (PLUTO), Medial Epicondyle Outcomes Multicenter (MEMO) study and International Hip Dysplasia Institute (IHDI), Children's Orthopedic Trauma and Infection Consortium for Evidence based Studies (CORTICES), Congenital Upper Limb Differences Registry (CoULD), Research in Osteochondritis of the Elbow (ROCKET), Sports Cohort Outcomes Registry (SCORE), and International Perthes Study Group (IPSG). Investigators within the division have been awarded funding from both

internal and external sources to conduct these studies. In 2023, the Division published over 200 articles in major orthopaedic journals, including *JAMA, JBJS, JPO*, and *CORR*. Members across our division presented more than 224 presentations at international and national conferences last year alone.

Our Benjamin Fox Research Fellowship for medical students between 3rd and 4th years welcomed Nathan Chaclas (Geisinger Commonwealth School of Medicine), David VanEenenaam (SUNY Upstate Medical University), and Vineet Desai (Harvard Medical School). (Figure 8-10).

Figure 8. Nathan Chaclas

Figure 9. David VanEenenaam

Figure 10. Vineet Desai

Recognition and Achievements

Our faculty have assumed several leadership roles within the pediatric orthopaedic community over the past year.

Jason Anari, MD served as international faculty member at the Salzburg Medical Seminar in Pediatric Orthopedics in Salzburg, Austria. Dr. Anari continued his work as PI from Pediatric Orthopaedics Society of North America (POSNA) titled, "*Managing failure to lengthen in MCGR: Best practice guidelines"*.

Alexandre Arkader, MD is the Vice Chair for the Pediatric Orthopaedic Society of North America (POSNA) Educational Course Committee. He served as a sub-committee chair for Global Courses. Dr. Arkader continues to serve as a reviewer for *Journal of American Academy of Orthopaedic Surgeons, Journal of Bone and Joint Surgery Essential Surgical Techniques, BMC Musculoskeletal Disorders, Journal of Pediatric Orthopaedics B, Journal of Children's Orthopaedics, Current Orthopaedic Practice, Clinical Orthopaedics and Related Research, and Pediatric Radiology*. He is also on the Surgical Advisory Board for Orthopediatrics. Dr Arkader continues to serve as Editor for tumors section, *JPOSNA*. He also received a Cell and Gene Therapy Seed Grant as Co-PI with Dr. Fanxin Long titled "*Wnt-based gene therapy for bone repair*." Dr. Arkader is an active member of CORTICES study group. Lastly, to continue his collaboration with our translational research program with Dr. Pacifici, Dr. Arkader was awarded a POSNA Research Grant.

Keith Baldwin, MD, MSPT, MPH is the Associate Director of Orthopaedic Trauma in the Division of Orthopedic Surgery. Dr. Baldwin is a Resident Advisory board member for the American Journal of Orthopaedics. He currently serves as a reviewer for several journals including the *BMC Medical Education, BMC Musculoskeletal Disorders, BMJ Open, Journal of Pediatric Orthopaedics, Annals of Internal Medicine, Journal of Bone and Joint Surgery—American*, *American Academy of Pediatrics, Clinical Orthopaedics and Related Research, Indian Journal of Orthopaedics, Journal of Orthopedic Trauma, International Research Journal of Medicine and Medical Sciences, PM & R Journal*. He also serves as an associate editor for Journal of Orthopedic Trauma and an editorial board member of the *American Journal of Orthopedics, Current Orthopaedic Practice* and *World Journal of Orthopedics*. He serves as a section editor for The Journal of Bone and Joint Surgery Reviews. Dr. Baldwin is an active member of CORTICES Study Group and CORTICES Research Committee. He continued his research work supported by the prestigious *Standard Research Grant* from Scoliosis Research Society.

Patrick Cahill, MD started his term as Board of Director for Pediatric Cervical Spine Study Group. He serves as Chair for Health Policy Committee and a member of the Governance Council, Pediatric Device Task Force, and Program Committee at Scoliosis Research Society. He is also a member of POSNA's Quality, Safety, Value Initiative Committee and Advocacy Committee. He continues to serve as an Associate Editor for *Spine Deformity Journal* and as a reviewer for the *Journal of Bone and Joint Surgery – American* and the Thrasher Research Fund. Dr. Cahill is an active member in the Harms Study Group, Pediatric Spine Study Group, and Fox Pediatric Spine Deformity study group, which are multi-center groups prospectively researching care improvements for complex pediatric spine deformities. Dr. Cahill continues to serve as co-PI from Scoliosis Research Society titled, "*New Strategies for Pulmonary Assessment in Spinal and Chest Wall Deformity*". He is the Director for *Wyss/Campbell Center for Thoracic Insufficiency Syndrome*.

Robert Carrigan, MD continues to serve on the ASSH Fellows Conference Committee, AAOS Appropriate Use Committee, and POSNA Resident Newsletter Committee. He also serves as a reviewer for *Journal of Hand Surgery* and *Clinical Orthopaedics and Related Research*.

Richard Davidson, MD has continued to serve as an associate editor for Foot & Ankle, International. He also serves as a reviewer for *Clinical Orthopedics and Related Research*. Dr. Davidson serves on the editorial board for, Children's Doctor, a publication of the Doctors of The Children's Hospital of Philadelphia.

B. David Horn, MD continues to serve as a reviewer for journals, such as *Clinical Orthopaedics and Related Research (CORR), Pediatric Emergency Medicine, and Pediatrics*.

Jack Flynn, MD, Chief of the Division of Orthopaedics, continues to serve as a Director on the American Board of Orthopaedic Surgery and continued his term as the President of the Pediatric Spine Study Group/Pediatric Spine Foundation. He continued to serve on the JBJS Board of Trustees. Dr. Flynn is a co-editor of *Lovell and Winter's Pediatric Orthopaedics, Rockwood's Fractures in*

Children, Operative Techniques in Pediatric Orthopaedics. Dr Flynn serves on the Editorial Board of *Journal of Spinal Deformity*. He was the invited lecturer for Hawaii Orthopaedic Association, the residency graduation speaker at Wake Forest University and in 2023 served as Visiting Professor at Texas Children's Hospital, Montefiore Medical Center and Columbia University.

Theodore Ganley, MD is the Sports Medicine Director at CHOP, was the second VP of the Pediatric Research in Sports Medicine (PRISM) group, co-founder and executive board member as well as President for the Research in Osteochondritis Dissecans of the Knee (ROCK) group, executive committee member for the American Academy of Pediatrics, advisory board member for the International Pediatric Orthopaedic Symposium, and program chair for the Philadelphia Orthopaedic Society. Along with his leadership roles, he continues to be actively involved in biomechanical studies utilizing cadaver specimens in collaboration with the *Biedermann Lab for Orthopaedic Research* and *Human Motion Lab*. He is leading a nationwide initiative on Tibial Spine prospective study group with 14 sites currently participating and it was funded by *Arthur H. Huene Memorial Award* from POSNA. Additionally, he is the site leader for the FDA clinical trial for studying the efficacy and safety of autologous cultured chondrocytes on porcine collagen membrane (MACI). Dr. Ganley also serves as the site PI for recently NIH funded grant "*IMPACCT: Infrastructure for Musculoskeletal Pediatric Acute Care Clinical Trials*".

Chrissy Goodbody, MD is one of our new faculty members continuing her work at Limb Extremity Deformities. She currently serves as a peer reviewer for the *Journal of Bone and Joint Surgery* and table instructor for Baltimore Limb Deformity Course. Dr. Goodbody is also a member of Limb Lengthening and Reconstructive Society and Philadelphia Orthopaedic Society.

John Todd Lawrence, MD, PhD continued his collaborative work with Dr. Leo Han at Drexel University. Funded by the National Science Foundation, the project focused on conducting in vitro studies for a novel cartilage repair strategy. Dr. Lawrence is an active member of sports medicine multicenter research groups such as PLUTO and he leads a 12-site study group MEMO, which is the largest group studying medial epicondyle fractures and injuries. He continues to serve as a reviewer for the *American Journal of Sports Medicine (AJSM)*, *Journal of Shoulder and Elbow Surgery (JSES), Journal of Children's Orthopaedics (JCO), Journal of Bone and Joint Surgery (JBJS), and Clinical Orthopaedics and Related Research (CORR)*. Dr. Lawrence continues to serve as a co-PI from NIH titled "*A Low-Cost, Collaborative Tool for the Tracking of Youth Activities to Reduce Risk of Physical Injury*" and site Co-PI for recently NIH funded grant "*IMPACCT: Infrastructure for Musculoskeletal Pediatric Acute Care Clinical Trials*".

Kathleen Maguire, MD is an active member of AAOS Emerging Leaders Program, POSNA, American Orthopaedic Society for Sports Medicine, American College of Sports Medicine, Arthroscopy Association of North America and the American Medical Association. Dr. Maguire serves as a reviewer for the *American Journal of Sports Medicine*.

Wudbhav Sankar, MD is the Director of the Young Adult Hip Preservation Program at CHOP. Dr. Sankar currently serves as Secretary for the Pediatric Orthopaedic Society of North America (POSNA) and co-director of the International Hip Dysplasia Institute. He remains active in several study groups including Academic Network of Conservational Hip Outcomes Research (ANCHOR), SCFE Longitudinal International Prospective Registry (SLIP) and International Perthes Study Group (IPSG). Also, he serves as co-director for the International Hip Dysplasia Institute (IHDI) Medical Advisory Board. Dr. Sankar is currently a reviewer for the *Journal of Bone and Joint Surgery, Journal of Pediatric Orthopaedics, Clinical Orthopaedics and Related Research, Journal of Pediatric Orthopaedics*. Dr. Sankar also serves as an Editorial Board Reviewer for *Techniques in Orthopaedics and Journal of Children's Orthopaedics*.

Apurva Shah, MD, MBA continues his tenure as the Director of Clinical Research. He continued to serve as co-PI on the grant from Orthopaedic Trauma Association titled, "*Opioid utilization after rotational ankle fractures*". Dr. Shah is currently a reviewer for the *Journal of Bone and Joint Surgery* and *Journal of Pediatric Orthopaedics*. Dr. Shah is also serving as the PI for Angela S.M. Kuo Memorial Award from POSNA for his research project "*Opioid vs. Non-Opioid Analgesia in Pediatric Supracondylar Humerus Fractures*." He also serves as the site Co-PI for recently NIH funded grant "*IMPACCT: Infrastructure for Musculoskeletal Pediatric Acute Care Clinical Trials*". He received a research grant from UPenn Center for Human Appearance and POSNA Microgrant to continue his research work on Brachial Plexus injuries.

David Spiegel, MD continued his work with the Children's Hospital of Philadelphia Global Health Pilot Grant. He currently is the chair for the International Scholars Program at AAOS. Dr. Spiegel continued to be active academically internationally, giving lectures in Iraq, Nepal, and Pakistan.

Lawrence Wells, MD is the Associate Director of the Sports Medicine Performance Center at CHOP. Dr. Wells currently serves as the President of Board of Directors for the Philadelphia Orthopaedic Society and as Vice Chair for Inclusion, Diversity and Equity at the Perelman School of Medicine.

Brendan Williams, MD continued his work at our Sports Medicine Performance Center. Dr. Williams serves on AAOS Emerging Leaders Program and a member of American Academy of Orthopaedic Surgeons, American Academy of Pediatrics, POSNA, Pediatric Research in Sports Medicine, and PRISM. He continued his tenure as Board of Directors for Children Beyond Our Borders. Dr. Williams serves as an ad hoc reviewer for *Pediatrics, The Journal of Bone and Joint Surgery—Case Connector, and The American Journal of Sports Medicine*.

Corporal Michael J. Crescenz Philadelphia VA Medical Center

Jean-Claude G. D'Alleyrand, MD, MSE


Joseph Bernstein, MD


L. Scott Levin, MD


Eric Hume, MD


Andrew Kuntz, MD


Hannah Lee, MD, PhD


Harvey Smith, MD


David Steinberg, MD


Timothy Costales, MD


Jean-Claude G. D'Alleyrand, MD, MSE


Sherif Sherif, MD

This past academic year has been one of growth and change for the Orthopaedic team at the Corporal Michael J. Crescenz VA Medical Center (CMCVAMC). In August 2023, David Steinberg, MD stepped down after graciously serving as Interim Chief for the preceding two years. Dr. Steinberg helped keep the Orthopaedic ship afloat during that time, in addition to managing his busy Hand Surgery practice and extensive research activities. Dr. Steinberg has been succeeded by Jean-Claude G. D'Alleyrand, MD, a retired Army Traumatologist who came to us from Landstuhl Germany. Bringing his own perspective as a Veteran patient, Dr. D'Alleyrand has been focused on increasing the delivery of high-quality surgical care to as many Veterans as possible.

In addition to changes in our leadership, CMCVAMC has also gained a new Sports surgeon, Liane Miller, MD, who brings capabilities to our section that are particularly advantageous for our younger patients, such as hip arthroscopy and cartilage restoration. She also has a great interest in shoulder instability, including recurrent dislocations. Her dedication will augment the existing shoulder practice of Andrew Kuntz, MD, who, in addition to being a passionate researcher and surgeon for rotator cuff pathology, is the only VA surgeon in our region performing shoulder arthroplasty. We've also grown our Spine Surgery service with the addition of Sherif Sherif, MD, augmenting the practice of long-time VA Spine surgeon, Harvey Smith, MD. In addition to treating the full complement of degenerative and compressive spinal disorders, Dr. Sherif also brings additional capabilities and extensive training in complex spine and spinal deformity correction. Penn Orthopaedics now covers 100% of the spine pathology here at CMCVAMC, and we could not do so without the tireless efforts of Jennifer Sheehan, CRNP and Samantha McDevitt, PA-C. The tireless patient advocacy and professionalism they showed during the transition from a joint Neuro-Ortho Spine effort to a completely Orthopaedic one has been nothing short of inspirational.

During this period of transition, our Veteran patients have benefited from increased surgical access, with the Ortho team boosting surgical case volume by roughly 40% over the last five months compared to previous years. This increase is primarily due to a 50% increase in arthroplasty cases, an initiative spearheaded by Drs. Eric Hume and Timothy Costales in December. Their arthroplasty efforts have been augmented by Drs. Joseph Bernstein and Andrew Kuntz. As a result, CMCVAMC Orthopaedics is on pace to provide the most arthroplasty surgery in the region by next year.

In addition to delivering quality surgical care to our patients and educating our next generation of Orthopaedic

Figure 1. VA Secretary Denis McDonough, VA researchers, and local Veterans gather to celebrate the opening of the new CReATE Motion Research Center at the Philadelphia VA Medical Center on March 27, 2024

Surgeons, our team has also been extremely productive on the research front in partnership with the McKay Orthopaedic Laboratory and the CMCVAMC Translational Musculoskeletal Research Center. Dr. Steinberg continues his Merit grant-funded research and was selected to be the Orthopaedic co-investigator for the CMCVAMC Cartilage Regeneration using Advanced Technologies to Enable Motion (CReATE Motion) Center, in partnership with investigators at the Atlanta VA This research enterprise, with over $6M of direct research funding over a 5-year period, supports research innovations in cartilage regeneration and ways to restore joint function. The Center is such an important effort that the Secretary of Veterans Affairs attended the ribbon-cutting ceremony (Figure 1).[1] Hannah Lee, MD has been awarded a prestigious five-year Career Development Award (CDA), an important milestone in her already storied research career. Dr. Miller has recently received her first VA grant, a two-year SPiRE grant, a pilot grant that is a steppingstone to what will assuredly be a stellar research career. Drs. Kuntz and Smith have both been repeatedly funded by VA Merit grants and continue to be so, with Dr. Smith publishing a cover article in *Science Translational Medicine,* a preeminent journal with incredibly stringent publication criteria. Dr. Bernstein is currently applying for his second Merit grant and continues to investigate and publish on a number of conditions that are important for the Veteran patient population while also serving as a Deputy Editor for *Clinical Orthopaedics and Related Research*. He also recently published *Orthopaedia*, a free peer-reviewed textbook for students and practitioners, helping to deliver quality Orthopaedic care worldwide, independent of cost.

While our colleagues' research efforts are impressive and will help future generations of Veteran patients, we could not treat our current patients without the devotion and professionalism of our Advanced Practice Providers and skilled Orthopaedic Nurses. Chip Staska, PA-C has been at CMCVAMC for a great many years, a constant force of calm professionalism in the face of high staff and resident turnover. We have been quite fortunate to have Eric Drennan, PA-C, a Navy Veteran himself, join our ranks and bring his love of his fellow Servicemembers to our team. Our superb Orthopaedic Nurses, Alex David, RN and John Yohannan, RN are instrumental to the care navigation and preoperative coordination that our complex patients require. Without their help and that of Ms. Sheehan and

Ms. McDeVitt, we could not deliver the care that our noble patients deserve. We, and our patients, are truly grateful for all they do.

There are very few easy military careers and most of our patients continue to carry heavy burdens, physically and emotionally, many years after taking off their uniforms for the last time. Regardless of their reasons for serving or what they did while in uniform, our Nation is a better place for their sacrifices. The Orthopaedic team of CMCVAMC takes great pride in serving these patients as they have served us, and we will continue to fulfill our mandate to provide them with world-class care, ease their suffering through musculoskeletal research, and educate our Nation's next generation of surgeons.

References

1. Sprey E. VA opens new research center to seek novel arthritis treatments. *VA Res Curr.* 1 April 2024. https://www.research.va.gov/currents/0424-VA-opens-new-research-center-to-seek-novel-arthritis-treatments.cfm.

Pennsylvania Hospital

Neil Sheth, MD

Pennsylvania Hospital (PAH) has a rich history in Philadelphia as the nation's first hospital. Founded in 1751 by Benjamin Franklin and Dr. Thomas Bond, the hospital was intended as a safe haven for the care of the "sick-poor and insane of Philadelphia." Located in the heart of South Philadelphia, its brand name draws thousands of patients annually to receive their care at the corner of 8th and Spruce Streets.

Education is at the forefront of our focus at PAH. Residents are typically in the operating room three to four days per week, with dedicated clinic time in multiple sub-specialties. Video conferencing continues for conferences historically held at PMUC, sub-specialty specific conferences for spine, foot and ankle, and arhroplasty continue to be coordinated virtually.

The administration at Pennsylvania hospital continues to be extremely supportive of the expanded presence of orthopaedic faculty and residents. The hospital system has further increased the number of physician extenders, doubled the OR block time for the department, and increased physical space for clinical work and administrative duties. Their continued support is critical as the orthopaedic volume continues to grow and additional attendings are added to the faculty. These efforts have allowed PAH to maintain its reputation in the region as a first-class hospital.

The Department of Orthopaedic Surgery at the University of Pennsylvania now staffs over 20 attending surgeons and non-operative providers from various sub-specialties to populate the orthopaedic clinic in the Cathcart Building and the Farm-Journal Building. Among the sub-specialties represented are adult hip and knee reconstruction, foot and ankle, hand/plastic surgery, neuro-orthopaedics, shoulder and elbow, spine/deformity, sports medicine, and trauma. Notable Dr. Boakye (foot and ankle surgery) has been the newest addition to the roster at Pennsylvania Hospital.

With the continued increase in operative volume, PAH continues to be staffed by a PGY-1, PGY-2, PGY-4 and complemented by a team of advanced practice providers and physician extenders that assist with patient clinical care and floor work. The Orthopaedic Intern spends a portion of the week in the operating room or across various outpatient clinics and also assists the PAH team with patient care issues on the floor.

With the continually changing healthcare environment, we continue to grow the outpatient total joint arthroplasty program which started six years ago. We have implemented and continue to refine the dedicated rapid recovery program—the 9th floor extended stay unit opened in October 2019 and now services nearly 60%+ of the orthopaedic patient volume coming through PAH. In addition, new robotic and technological platforms are being offered at Pennsylvania Hospital. Pennsylvania Hospital is poised to be successful in the region as we continue to evolve.

Penn Center for Musculoskeletal Disorders

Louis J. Soslowsky, PhD

Founding Director of the Penn Center for Musculoskeletal Disorders

The Penn Center for Musculoskeletal Disorders (PCMD) was initiated in 2004 with a goal to bring musculoskeletal researchers across campus together at the University of Pennsylvania. In 2006, the National Institute of Arthritis and Musculoskeletal Skin Diseases of the NIH funded our center grant proposal at which time we became one of five such NIH-recognized Centers in the country (www.med.upenn.edu/pcmd). In 2011, this Center grant was renewed for another five years and was the only one of the three up for renewal that was re-funded that year. Through the review by the NIH, Penn scored a perfect "ten" and was hailed as "exceptional" by the review panel! In 2016, we received another "exceptional" score, highest ranked in the country, by the NIH review panel and were renewed for another five years. We were pleased that in 2021, we were renewed again for five more years. We remain the longest running such center in the country.

The overall goal of this Center is to promote cooperative interactions among investigators, accelerate and enrich the effectiveness and efficiency of ongoing research, foster new collaborations and new research, and ultimately, translate our research efforts into better and new therapies for musculoskeletal disorders. The central theme of the Center continues to be "Musculoskeletal Tissue Injury and Repair". This theme is broad (as it includes all musculoskeletal tissue types, such as bone, cartilage, disc, ligament, meniscus, muscle, and tendon), focused (as takes advantage of commonalities in approaches across tissue types), and clinically significant (as it fosters development of assays, procedures and knowledge in pre-clinical animal and human models of translational relevance). It is important to note that our PCMD is not a "bone center" nor is it a "muscle center". Rather, it is truly a "musculoskeletal center" and has emerged as the recognized home for musculoskeletal research across the Penn campus and as a technical and intellectual resource for the broader Philadelphia musculoskeletal research community. Thus, the primary overall aims of this Center are to enhance and advance the research productivity of investigators in musculoskeletal tissue injury and repair by: 1) Providing innovation within critical resource core facilities in areas that cross disciplines, length scales, and hierarchies. These core facilities are mCT Imaging, Biomechanics, and Histology, 2) Developing a pilot and feasibility grant program for investigators, with direct mentorship, whereby new approaches, ideas, and collaborations can be developed prior to seeking extramural funding, 3) Developing educational and research enrichment programs spanning tissue types, research approaches, and paradigms, through which members can learn from national leaders and from each other, and 4) Initiating a new mechanism to allow our Affiliate members access to our Cores with a focus on less resource-rich institutions and those that serve more diverse communities. High quality musculoskeletal research is currently being conducted by many groups at Penn. While many bring sophisticated approaches to bear on musculoskeletal problems, few groups have the required expertise and facilities to perform high quality and specialized assays in their own labs. Furthermore, most investigators are not aware of approaches utilized, and results obtained, in other tissues that may have direct relevance on their research questions. Ultimately, close cooperation, communication, and collaboration among researchers across musculoskeletal tissue types and from a wide variety of disciplines will significantly enhance the research of our members. The Center will provide opportunities to integrate multi-disciplinary techniques to determine mechanisms for tissue function, injury, degeneration, repair, and regeneration, with the ultimate goal of advancing the diagnosis, treatment, and prevention of diseases and injuries of the musculoskeletal system.

The Center currently has a membership of more than 180 faculty across five schools at Penn (Perelman School of Medicine, School of Engineering and Applied Science, School of Veterinary Medicine, School of Dental Medicine, and School of Arts and Sciences). We also now have 70 affiliate faculty members for more than 20 institutions regionally as we expand the reach and impact of our Center. For more information on the PCMD, please visit our website at www.med.upenn.edu/pcmd.

Clinical Research

Annamarie D. Horan, MPA, PhD

Featured Topic: Penn Clinical Research Management System (CRMS)

The Penn CRMS is an enterprise-wide Velos, Inc. based 21 CFR Part 11 compliant system that incorporates capabilities that enable full audit trails and wherein security is supported by individual user accounts requiring specific training and permissions. The Penn CRMS can be utilized by Penn as a data capture system for local or multisite trials. Permissions within the system can be configured for local users as well as users from external sites, and for view only by monitors, and sponsors. The Penn CRMS facilitates study operations and reduces costs by enabling remote monitoring and/or virtual signatures. Existing Electronic Case Report Forms (eCRFs) can be imported into Penn CRMS from other systems such as REDCap. Notifications and alerts can be generated as emails from within the system to appropriate parties. Robust financial features are also available for budget building, milestone tracking, automated invoicing and payment reconciliation. The system can also be used to generate Institutional, Departmental, PI and study level metrics.

Important Perelman School of Medicine (PSOM) Standard Operating Procedures (SOPs) for Clinical Research can be found at https://www.med.upenn.edu/clinicalresearch/policies-procedures-and-guidance.html#OperationalResearchTechnologySOPs8. PSOM requires registration in and use of Penn CRMS for all applicable studies per SOP 400 "CRMS Requirements". In addition to protocol registration in Penn CRMS, patient level research association in Penn CRMS is also required for applicable studies. In the Department of Orthopaedic Surgery, the Clinical Research Team completes the Penn CRMS registration on behalf of the surgeon PI as part of our routine services. For studies that are set up with a workflow that engages Penn Chart, patient registration in Penn CRMS is seamless as the two systems are linked. Many studies do not require use of Penn Chart in their workflow. In these cases, the Orthopaedic Surgery CRC or McKay Lab Teams complete direct patient level research association. It is therefore critical that all surgeon PIs ensure that at least one Orthopaedic Surgery CRC are designated as Study Contacts in the Penn IRB system and that the OS CRC is appropriately engaged in all aspects of the research including exempt studies.

As of this writing, Penn Orthopaedics has 77 studies with an Active/Pre-Active Status out of the 214 studies registered in the Penn CRMS (Table 1). There are 75 studies with an active status and 2 studies ready to launch.

Since Penn CRMS initiation, the Orthopaedic Surgery CRCs and the McKay Laboratory Teams have completed the association of 16,826 patients to our portfolio of 214 studies according to 21 different enrollment categories as shown in Table 2. It is important to note that enrollment criteria for any study must be obeyed and just over 60% of patients pre-screened for study participation (10,247) are not or are not yet enrolled due to the following dispositions: active decline of participation (1534), incomplete participation status (169 (identified, interested, in pre-screening activities)) or not meeting full eligibility criteria (8543).

Table 1 Penn CRMS Utilization for Penn Orthopaedic Surgery

Penn Ortho (by Responsible Org)	Count
4607 - CC-Cancer Center	1
4373 - OS-Clinical Research	202
4374 - OS-McKay Laboratories	11
Studies Registered	**214**
Registered Closed Studies (all Orgs)	**137**
4607 - CC-Cancer Center	0
4373 - OS-Clinical Research	34
4374 - OS-McKay Laboratories	7
Open/Recruiting (Active)	**41**
4607 - CC-Cancer Center	0
4373 - OS-Clinical Research	34
4374 - OS-McKay Laboratories	0
Closed to Accrual (Still Active)	**34**
4607 - CC-Cancer Center	0
4373 - OS-Clinical Research	2
4374 - OS-McKay Laboratories	0
Pre-Open (Pending Active)	**2**
Total Active/Pre-Active Studies	**77**

Among those patients who do enroll (6,579), 5,471 individuals have achieved a "completed" status either through actually completing all protocol milestones (4,988) or for any 1 of 11 dispositions related to study withdrawal/discontinuation (483). The remaining 1,108 patients have 1 of 4 Active Statuses (Active Follow-Up, Active on Study, Consented/Enrolled, and Long-term Follow-up). Orthopaedic Surgery CRCs and the McKay Laboratory Teams continue to ensure the performance of visit scheduling, study procedures, data capture, research billing review, and Adverse Event monitoring. As most of the Orthopaedic Surgery studies require multi-year commitments from the participants, completion of all study activities can take as long as 5 to 10 years after the last participant is enrolled. The study commitment duration is a critical consideration in the development of study budgets and logistical planning for any new study both for the success of that study and in relation to the overall study burden on the Department. At this writing, Penn Orthopaedics is ranked among the Top 5 Departments in PSOM with respect to applicable study registration in Penn CRMS (100%) and for patient research association in those applicable studies (~88% of studies have patient registrations).

Table 2. Subject Enrollment into Penn Orthopaedics Clinical Research Studies by Responsible Org

Participant Enrollment Status	4372-OS-Orthopaedic Surgery	4373-OS-Clinical Research	4374-OS-McKay Laboratories	Grand Total
Declined	14	1,520		1,534
Identified		155		155
Ineligible	17	8,526		8,543
Interested		13		13
Pre-Consent Screening		2		2
Subtotal Disqualified/Pre-Enrolled Subjects	**31**	**10,216**	**0**	**10,247**
Off Study/Withdrawn-Complete Protocol	8	4,939	41	4,988
Off Study/Withdrawn-Disease Progression		3		3
Off Study/Withdrawn-Failed Post-consent Screening	3	98	1	102
Off Study/Withdrawn-Lost to Follow-Up	6	84	5	95
Off Study/Withdrawn-Never Treated	7	92	2	101
Off Study/Withdrawn-PI Decision		28		28
Off Study/Withdrawn-SAE/AE	2	16		18
Off Study/Withdrawn-Subject Decision	4	115	3	122
Off Study/Withdrawn-Subject Relocated		10	2	12
Off Treatment-Failed Post-consent Screening		1		1
Off Treatment-SAE/AE		1		1
Subtotal Inactive Subjects	**30**	**5,387**	**54**	**5,471**
Active Follow-Up	3	289	18	310
Active on Study	12	94	9	115
Consented/Enrolled	3	598	2	603
Long-term Follow-up		73		73
Post-Consent Screening		7		7
Subtotal Active Subjects	**18**	**1,061**	**29**	**1,108**
Grand Total	**79**	**16,664**	**83**	**16,826**

Penn Orthopaedics Update 2024

As shown in Table 3, the Department carries a slightly lower protocol burden from FY22 with 117 open protocols of which 21 are extramurally funded. The funding sources include Industry, Federal, non-Federal, and private.

Adult Reconstruction remains highly productive with 18 open studies, 7 of which are extramurally funded. The myMobility study (NCT03737149) led by Dr. Israelite has completed global enrollment and is proceeding toward closeout. Our site did very well on this project, and we look forward to seeing the results. Dr. Israelite is also pending closure of the Persona Total Knee Arthroplasty Outcomes Study (NCT02255383) which started in 2014. Penn has contributed 55 patients to this study and 37 patients remain in active follow-up.

Dr. Nelson's PCORI funded PEPPER Study (NCT02810704) is in its 8th performance year and has just been renewed. This is a large pragmatic clinical trial to inform patient choice and balance risk tolerances of individuals who face decisions about different drugs and strategies for deep vein thrombosis (DVT) and pulmonary embolism (PE) prevention after total hip (THA) and knee (TKA) replacement. The targeted multi-site enrollment is 24,000 participants. To date we have contributed 193 patients, to this study with 95 completed and 15 remain in active follow up for this study and enrollment is still open. The Rush University Medical Center Consortium Study "Dexamethasone in Total Knee Arthroplasty: What Dose Should We Be Giving Patients Intraoperatively?" (NCT05018091) is designed to determine the most efficacious and safest dexamethasone dose given intraoperatively during TKA that reduces post-operative opioid consumption and pain, improves postoperative nausea and vomiting, and minimizes post-operative complications. Enrollment is now closed, and 19 patients have been enrolled from our site. Dr. Nelson has successfully completed all site activities for the DePuy Ceramic on Ceramic Hip study (NCT02096211) after 11 years (original PI Dr. Hume) with 29 patients completed. Lastly for Dr. Nelson, Congratulations that the "Autogenous Bone Marrow Aspirate Concentrate for the Treatment of Osteonecrosis of the Femoral Head" study (Johns Hopkins, Primary Site, Lynne Jones, PhD PI) has been awarded by NIH! Site setup is in progress.

Dr. Costales has ushered the Smith & Nephew R3 Delta Ceramic Acetabular System PAS U.S. (R3-PAS) protocol (NCT03056534) through closeout after 8 years (Original PI Dr. Lee). Our site contributed 26 patients to this protocol. We thank Dr. Tarity who is completing the Post Approval Study of the Commercially Available U-Motion II+ Acetabular System and UTF Reduced Stem (U-Move) (NCT02761499) (Original PI Dr. Lee). Dr. Sheth continues work on "Analysis of a Tapered Porous Coated Stem and a Cementless Hemispherical Acetabular Component" (NCT03168750) sponsored by Medacta USA.

Foot & Ankle continues to feature Dr. Farber's Treace Medical Concepts, Inc.'s "Early Weight-Bearing After the Lapiplasty Mini-Incision Procedure (Mini3D)" study (NCT05082012). We anticipate that additional updates for the Foot & Ankle Division will be submitted elsewhere in this edition of the UPOJ by colleagues Dr. Josh Baxter and Dr. Casey Humbyrd.

Hand Surgery Dr. Levin's DOD-funded Hand Transplantation Qualitative Research Study (W81XWH1820067) has been successfully completed. A second related study "Assessing the Benefits of Hand Transplant Compared

Table 3. Open vs Funded Protocols by Sub-Specialty Division		
Division	**Total Open Protocols**	**Funded**
Adult Recon	18	7
Foot & Ankle	14	2
Hand	17	2
Oncology	10	0
Shoulder & Elbow	6	3
Spine	7	2
Sports Medicine	19	2
Trauma	18	3
Grand Total	**117**	**21**

with Other Treatments" continues the collaboration among Penn, the University of Delaware, and Walter Reed National Military Medical Center as well as additional sites.

Shoulder & Elbow remains a strong and stable Division in Clinical Research under Dr. Kuntz's leadership. We are in the process of completing closeout activities for the 3 remaining industry-sponsored studies in this Division and look forward to new activities.

Spine Dr. Casper now leads the COMPaSS™ Observational Registry (Clinical Outcome Measures in Personalized aprevo® **Spine Surgery)** funded by Carlsmed Inc. Dr. Smith continues to lead the STRUCTURE study (NCT04294004), a Phase II study enrolling patients undergoing single level transforaminal lumbar interbody fusion.

Sports Medicine Dr. Carey continues in his role as the Local and Global PI on the Vericel sponsored PEAK study (NCT03588975) and the Osteochondritis Dissecans of Knee Prospective Cohort (NCT02771496) under the ROCK Consortium. This registry study is now in its 10th year.

Ortho Trauma Dr. Samir Mehta with Resident Bijan Dehghani, MD received 2 foundation awards this year to investigate whether Next-Gen Sequencing (NGS) will more accurately, and reliably identify potential sources of infection after fracture when compared to standard microbiological cultures. The OREF award ($71,568) focuses on general open fractures and the FOT award ($51,766) concentrates on gunshot related fractures. Also, the study "Novel Topical Antibiotic Therapy to Reduce Infection After Operative Treatment of Fractures at High Risk of Infection: A Multicenter RCT (TOBRA)" funded through the University of Maryland (NCT04597008) has been awarded after 3 years of contract negotiations. The Ortho Trauma team is excited to move forward with the TOBRA study. Additional pre-proposals from the Division of Ortho Trauma for other studies are pending responses from the funders.

Financial Report

Table 4 shows the Total Costs (Direct Costs + Indirect Costs) expended during the periods shown for all categories (Personnel and Non-Personnel Costs). The revenue sources for these expenditures include both current sources and previously earned revenues that remain available from completed projects. Unless projects are grant-funded, revenue supporting Clinical Research is received in a reimbursement method and therefore lags behind the performance period due to the invoicing and payment process.

Table 4. Clinical Research Expenditures FY 21 - FY23				
Division	**FY21**	**FY22**	**FY23**	**Sum FY21 - FY23**
Adult Reconstruction	$120,360	$278,474	$264,879	$663,713
Foot & Ankle	$42,857	$55,406	$10,549	$108,812
Hand	$78,357	$175,873	$88,556	$342,786
Shoulder & Elbow	$131,376	$149,603	$86,586	$367,565
Spine	$21,234	$54,646	$5,958	$81,838
Sports	$44,540	$93,926	$134,812	$273,278
Trauma	$3,007	$106,238	$398	$109,643
Grand Total	**$441,731**	**$914,166**	**$591,738**	**$1,947,635**

Helena Moses
Adult Reconstruction

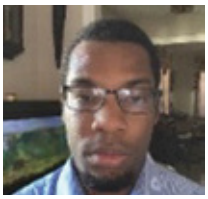

Warren Harding
Adult Reconstruction

Mounika Ponakala
Sports Medicine

Ellen Stinger
Spine, F&A, Hand

Artsiom Meliukh
Adult Reconstruction

Samir Mehta, MD
Chief, Division of Orthopaedic Trauma, Medical Director of Clinical Research
Associate Professor of Orthopaedic Surgery

Annamarie Horan, MPA, PhD
Director of Clinical Research
Orthopaedic Surgery and Anesthesiology & Critical Care

Penn Achilles Tendinopathy Center of Research Translation

Louis J. Soslowsky, PhD

Founding Director of the Penn Achilles Tendinopathy Center of Research Translation

The Penn Achilles Tendinopathy Center of Research Translation (PAT-CORT) was initiated in 2023 with a goal to foster fundamental discovery research to guide translation, as well as employ and develop translational resources, models and technologies, to address the highly significant research and unmet clinical challenge of Achilles tendinopathy. The Center's research will discover fundamental physiologic processes to guide translation. It will also as serve as a test bed for defining the role, as well as the scientific and translational rigor, of a repetitive use Achilles tendinopathy animal model through implementation of an exciting series of in vivo longitudinal assays to be conducted in parallel in both animal and human subjects. At the University of Pennsylvania, we are uniquely positioned with a critical mass of multidisciplinary scientists and clinicians with strong interest and expertise in these and related areas. In 2023, the National Institute of Arthritis and Musculoskeletal Skin Diseases of the NIH funded our center proposal with an $8M grant P50 AR080581.

The overall goal of the PAT-CORT is to develop new insight and technologies that uncover the mechanobiologic basis of Achilles tendinopathy across length scales, from the nucleus, to the cell, to the tissue microenvironment, to pre-clinical animal models, to patients. We will assess these critical elements during disease onset and progression, informed by both animal models that replicate disease processes and source material and real-world loading data from living human subjects. The PAT-CORT (see Figure) is comprised of four independent and yet interactive elements, including an Administrative Core to oversee and guide interactions and primary Research Projects focused on the transfer of information from the external tendon cell microenvironment through the cytoskeleton (Project 1) and on chromatin remodeling and mechano-epigenetic regulation of tendon cell phenotype (Project 2). Using cells, tissue, and loading information derived from both human and animal tendinopathic models (Tissue Core), these research projects will advance our knowledge of the origins of tendinopathic disease and define new avenues for therapeutic intervention. Together, our highly interdisciplinary team, innovative tools, and outstanding and interactive Research Projects and Cores will dramatically advance knowledge, develop innovative tools and insight, and provide new directions for translation of novel therapies to treat Achilles tendinopathy

For more information on the PAT-CORT, please visit our website at www.med.upenn.edu/patcort/.

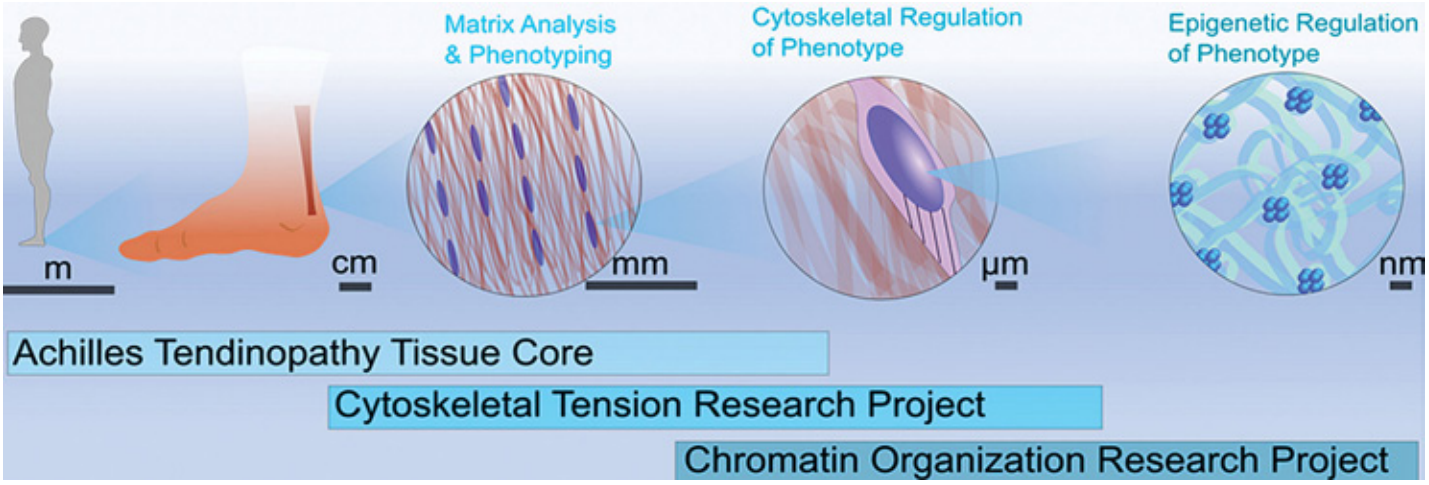

Current Residents

Clinical Year 5 Resident Spotlight

Stephen Barchick, MD
Fellowship:
Medical School: Duke University
Undergraduate: Harvard University

Sachin Gupta, MD*
Fellowship:
Medical School: George Washington University
Undergraduate: George Washington University

Joung (Richard) Kim, MD
Fellowship:
Medical School: Icahn School of Medicine at Mount Sinai
Undergraduate: University of Rochester

Charles Lucas Myerson, MD
Fellowship:
Medical School: Tulane University
Undergraduate: University of Southern California

Matthew Stein, MD, MS*
Fellowship:
Medical School: Georgetown University
Undergraduate: Univ. of Maryland

Kelsey Young, MD
Fellowship:
Medical School: Cornell University
Undergraduate: Cornell University

Steven Zhang, MD
Fellowship:
Medical School: Stanford University
Undergraduate: Cornell University

*Indicates Resident is in the 6-year Research Track

Clinical Year 4 Residents

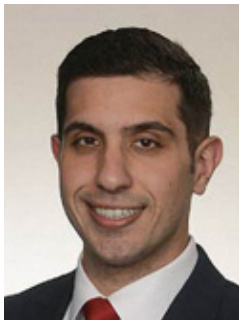

Aymen Alqazzaz, MD

Undergraduate:
University of Maryland

Medical School:
University of Maryland

Ashleigh Bush, MD

Undergraduate:
Indiana University

Medical School:
Indiana University

Jordan Cohen, MD*

Undergraduate:
University of Maryland

Medical School:
George Washington University

Kathleen Collins, MD

Undergraduate:
Morehouse School of Medicine

Medical School:
Virginia Polytechnic Institute and State University

Cody Hansen, MD

Undergraduate:
University of California San Diego

Medical School:
University of Denver

Kendall Masada, MD*

Undergraduate:
University of Texas

Medical School:
University of Texas Health Science Center

Brian Velasco, MD

Undergraduate:
Geisinger Commonwealth School of Medicine

Medical School:
Franklin & Marshall College

Dainn Woo, MD

Undergraduate:
New York University

Medical School:
The City College of New York

*Indicates Resident is in the 6-year Research Track

Clinical Year 3 Residents

Jordan Cohen, MD*

Undergraduate:
University of Maryland

Medical School:
George Washington University

Bijan Dehghani, MD*

Undergraduate:
Albany Medical College

Medical School:
Boston University

Caroline Granruth, MD

Medical School:
Tulane University

Undergraduate:
University of Virginia

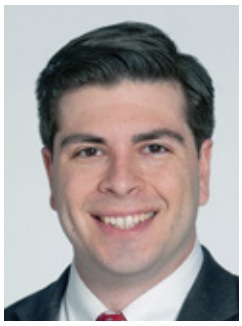

Jaret (Mac) Karnuta, MD, MS

Medical School:
Case Western Reserve

Undergraduate:
Duke University

Erin Kelly, MD

Medical School:
Wake Forest School of Medicine

Undergraduate:
Wake Forest University

Sand Mastrangelo, MD

Medical School:
Dartmouth

Undergraduate:
Brown University

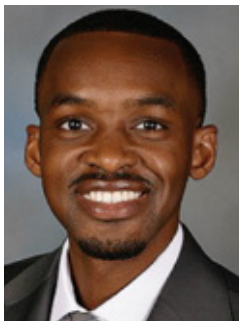

Bradley Osemwengie, MD

Medical School:
Texas Tech

Undergraduate:
University of North Texas

Weston Smith, MD

Medical School:
University of Utah

Undergraduate:
Brigham Young University

Research Year

Mohammed Abdullah, MD*

Medical School:
The University of Texas Medical Branch

Undergraduate:
The University of Houston

Eric Schweppe, MD*

Medical School:
Columbia University

Undergraduate:
United States Military Academy

*Indicates Resident is in the 6-year Research Track

Clinical Year 2 Residents

Ellis Berns, MD

Medical School:
Brown University
Undergraduate:
Brown University

Anna Blaeser, MD

Medical School:
Albany Medical College
Undergraduate:
University of Minnesota

Emily Eiel, MD

Medical School:
University of Massachusetts
Undergraduate:
Colgate University

Rachel Flaugh, MD*

Medical School:
Harvard Medical School
Undergraduate:
University of Nebraska

Lisa Friedman, MD*
Medical School:
Case Western Reserve University
Undergraduate:
Carleton College

Emily Eiel, MD
Medical School:
Quinnipiac University

Undergraduate:
La Salle University

Alyssa Thorman, MD
Medical School:
University of Utah

Undergraduate:
University of Utah

Thompson Zhuang, MD
Medical School:
Stanford University

Undergraduate:
Princeton University

*Indicates Resident is in the 6-year Research Track

Clinical Year 1 Residents

Tensae Assefa, MD

Medical School:
New York University Grossman School of Medicine
Undergraduate:
Rice University

Maxwell Cardwell, MD

Medical School:
Medical College of Wisconsin

Undergraduate:
Washington University

Brett Croen, MD

Medical School:
Drexel University College of Medicine

Undergraduate:
University of Michigan

Tyler Humphrey, MD

Medical School:
Donald and Barbara Zucker School of Medicine at Hofstra/Northwell
Undergraduate:
University of San Diego

Chielozor Okafor, MD

Medical School:
Perelman School of Medicine at the University of Pennsylvania
Undergraduate:
Rutgers University

*Indicates Resident is in the 6-year Research Track

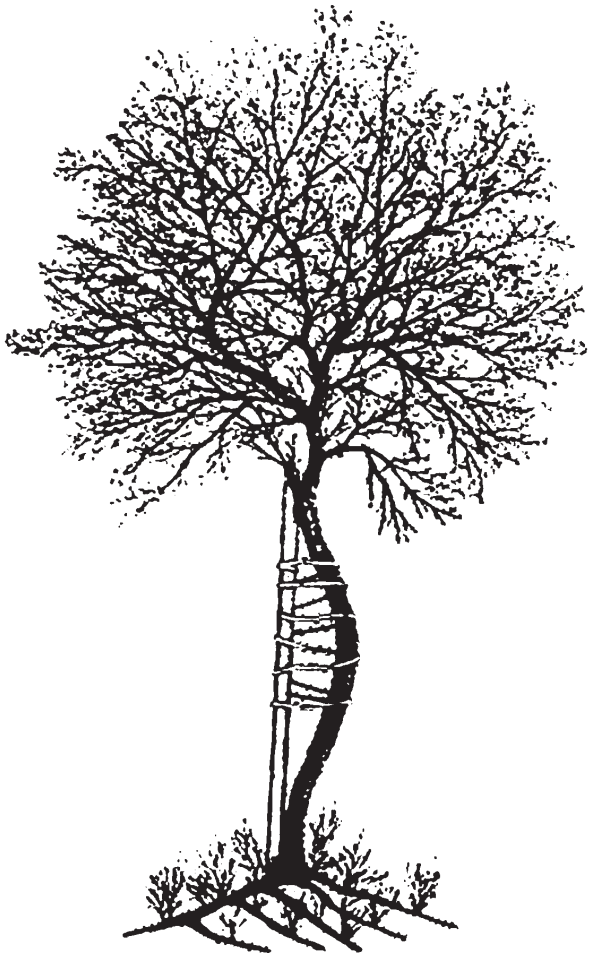

University of Pennsylvania Orthopaedic Journal

2023-2024 Clinical and Basic Science Research

The following sections highlight clinical and basic science research conducted at the University of Pennsylvania in the field of Orthopedics, including work from the Department of Orthopaedic Surgery, The McKay Laboratory for Orthopaedic Research, Children's Hospital of Philadelphia, and the Philadelphia Veterans Affairs Translational Musculoskeletal Research Center. In addition to research, each clinical section is preceded with a "Tips & Tricks" article highlighting case reports or surgical techniques for education and to display the breadth of musculoskeletal disease seen and treated in our hospital system.

Clinical Research Sections:

Trauma

Spine

Sports

Hand

Shoulder and Elbow

Adult Reconstruction

Foot and Ankle

Oncology

Orthoplastics

Arthroplasty

Pediatrics

Basic Science Research Sections:

Bone & Development

Cartilage, Meniscus & Disc

Muscle, Tendon, & Ligament

Trauma

U·P·O·J

Tips and Tricks: Utilization of an Articulated Tensioning Device to Treat a Humeral Shaft Nonunion: Technical Considerations and Case Example

Lisa G. M. Friedman, MD, MA
Stephen Barchick, MD
Chielozor Okafor, MD
Bradley Osemwengie, MD
Samir Mehta, MD

Department of Orthopaedic Surgery, University of Pennsylvania

Introduction

Humeral shaft fractures compromise approximately 3% of fractures and can be treated both operatively and non-operatively with good success.[1,2] However, some studies cite a nonunion rate as high as 33% when these injuries are treated non-operatively and up to 10% when treated operatively.[3] The risk factors for non-union are numerous, including patient factors, the fracture morphology, and the biologic environment. Before surgery for a non-union, metabolic factors, such as endocrine abnormalities, must be addressed. Patients who smoke should be counseled about quitting. In addition, it is imperative to ensure there is no infection contributing to the lack of bone healing by performing a laboratory work-up consisting of white blood cell count, erythrocyte sedimentation rate and C-reactive protein. If there is concern for infected nonunion, a biopsy may be indicated.[4] Non-unions can be classified as atrophic, with a paucity of callus formation due to inadequate local biology; hypertrophic, with abundant callus formation but with lack of union at the fracture site owing to a lack of stability; or oligotrophic, with minimal callus at the fracture site due to significant displacement.4 Non-unions can further by classified as septic or aseptic based on the presence of infection at the fracture site.[5]

While non-operative treatment is appropriate for most patients sustaining a humeral shaft fracture, anatomic factors such as transverse fracture pattern or concomitant glenohumeral arthritis and patient factors such as Vitamin D deficiency or use of certain medications can increase the risk of developing a non-union.[3,5] Non-operative treatment is typically by way of functional brace, once swelling subsides, to provide compression of the soft tissue at the fracture site to maintain alignment, and the fractures must be radiographically surveilled to ensure the fracture heals. According to Driesman et al., mobility at a humeral fracture site at 6 weeks is 99% specific for predicting future fracture non-union.[6]

There are a variety of techniques described for operative fixation of humeral shaft fractures. Intramedullary nailing, bridge fixation, and compression plating, through open and minimally invasive techniques have been described, as well as external fixation in damage control situations. Open reduction internal fixation with a 4.5mm compression plate has the benefit of visualizing an anatomic reduction as well as the ability to find and protect the radial nerve, pending the approach and extent of dissection. Open reduction also provides access to augment the fracture site with autogenous bone graft or biologic augmentation. An intramedullary device can minimize periosteal stripping as well as provide for secondary healing in comminuted fractures in which an anatomic reduction would be challenging. Non-union rates are similar between the two techniques, but intramedullary nailing is associated with a higher overall complication rate and shoulder pain, while plating is associated with faster functional recovery, faster time to union, improved shoulder range of motion, though a higher rate of radial nerve palsy.[7-10]

In the case of humeral shaft non-union, the gold standard for treatment is compression plating. In a systematic review, Peters et al. found a 98% union rate for humeral non-unions treated with plate fixation with autologous bone grafting, with a complication rate of 12%.[11] As with acute fractures, the benefits of this technique are that it allows for compression at the fracture site, correction of malignment, and access to the fracture site to incorporate various types of osteoconductive, osteoinductive, and osteogenic substances.[12,13] In particular, the purpose of compression is to minimize motion between the fracture fragment, thereby eliminating strain and optimizing primary bone healing.

The amount of compression across a fracture site is important with regards to minimizing strain and optimizing the healing environment. In a study by Lucas et al., compression was measured across a fracture site created in composite sawbone models

utilizing various techniques. They found that the use of an articulating tensioning device created more compression across the fracture site than utilizing a Verbrugge clamp with a push-pull screw located outside of the plate. Both techniques provided more compression than a standard dynamic compression technique.[14]

Case Example

A 48-year-old, right-hand dominant male presented to an outside hospital two days after a fall onto his arm. He was diagnosed with a closed, transverse midshaft humerus fracture and temporized with a coaptation splint. Of note, the patient had a significant history of seizure disorder, smoking, and hypertension. Approximately 1 week later, he was seen in the outside clinic and was fitted with a Sarmiento brace. Approximately 2 weeks after the injury, he presented again with an ill-fitting Sarmiento that was applied more proximally. Imaging showed minimal callus formation at that time and no significant changes in alignment. This was also the case when he followed up 4 weeks after the injury. The patient was given a bone stimulator and continued in the Sarmiento brace. He was seen again 9 weeks after the injury with similar findings. He was seen 14.5 weeks after his injury after sustaining two seizures and hitting his injured arm. Images were unchanged. The patient's smoking increased his risk for non-union by causing vasoconstriction and reducing capacity to carry oxygen to tissues.[15] The patient was also at increased risk of fracture both due to his seizure disorder as well as the anti-epileptic medications used to treated it.[16] His seizures were treated with phenobarbital and valproate acid, increasing his risk for non-union by decreasing bone mineral density.[17]

The patient was referred to our outpatient trauma clinic for evaluation of his humerus, now sixteen weeks after his initial presentation. The patient was neurovascularly intact, including the radial nerve, and had tenderness at the fracture site. Radiographs showed no interval callus formation (Figure 1). The patient was scheduled for surgery two weeks after he was seen in clinic, 18 weeks after his injury.

The patient was taken to the operating room and placed supine on a reversed radiolucent bed with a radiolucent board to hold the operative extremity in appropriate position for surgical exposure and utilization of fluoroscopy. Antibiotics were administered, the arm was prepped and draped in sterile fashion. An anterolateral approach to the humeral shaft was utilized. The fascia was incised, and the biceps was taken medially. The brachialis was identified and split in the interval between the two innervating nerves (musculocutaneous medially and radial nerve laterally), revealing a fibrous nonunion. The non-union was debrided until bleeding bone edges were identified. With bleeding bone edges, the edges were approximated under direct visualization.

For reduction, a 2.5mm drill bit was utilized to drill unicortical holes on each side of the nonunion to place a modified point-to-point clamp to both reduce and initially compress across the fracture site (Figure 2). A second modified point-to-point was applied in similar fashion to hold the reduction in compression on the opposite side to prevent eccentric reduction and far-side gapping. Biplanar

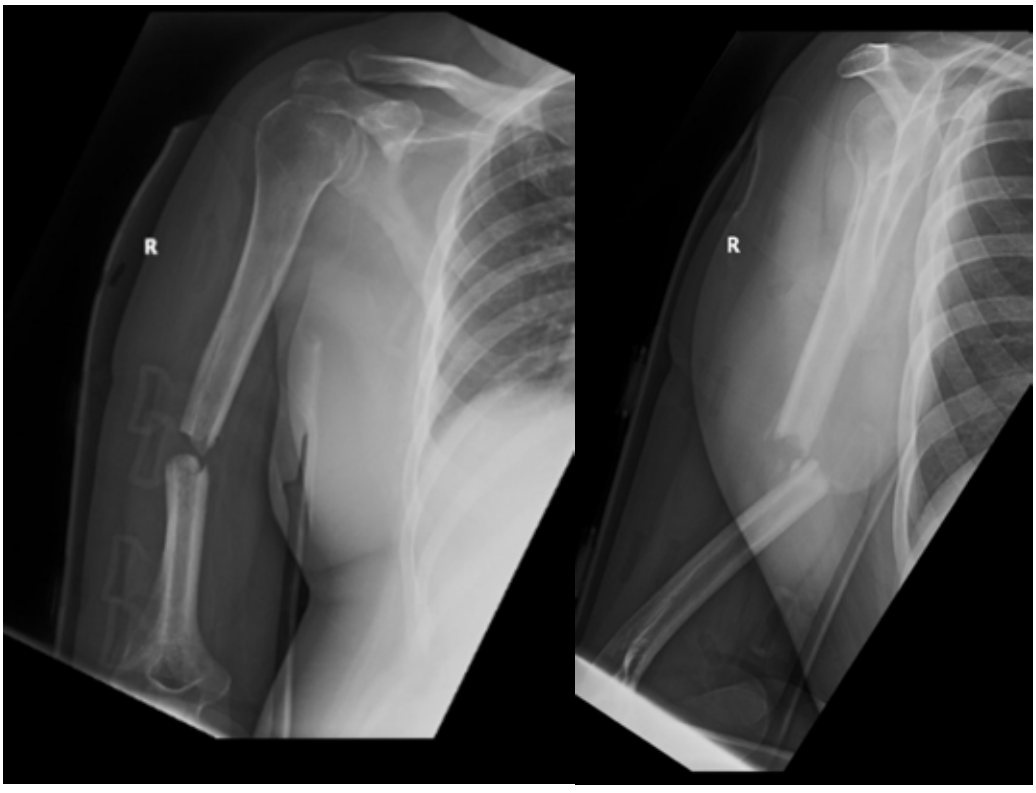

Figure 1. AP and Lateral of the humerus demonstrates a transverse mid-diaphyseal humeral shaft fracture non-union 16 weeks after initial injury.

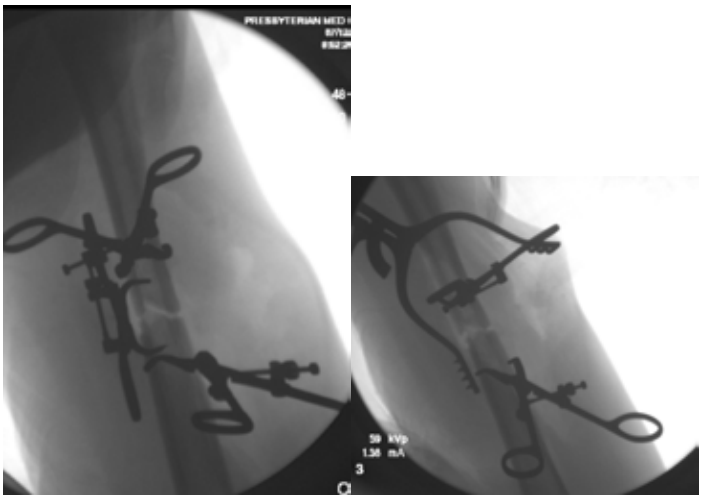

Figure 2. Intraoperative fluoroscopic images demonstrating a debrided non-union site and a reduced fracture held together by a single modified point-to-point exhibiting increased fracture gap on the far side. This is addressed by a second modified point-to-point to clamp on the far side to prevent eccentric compression.

fluoroscopy was utilized to ensure appropriate alignment and cortical width matching on bone ends of the fracture.

A 9-hole, 4.5mm LC-DCP implant was utilized and placed with the central hole over the fracture site. The plate was contoured slightly to prevent gapping of the far cortex when applied to bone in compression mode. The plate was applied to the bone and pinned on both sides (Figure 3). The first screw was placed distal to the fracture site to create a distal bone-plate construct. The second screw placed in the bone was proximal to the plate to utilize the articulated tensioning device (ATD). With appropriate spacing between the proximal edge of the plate, the screw and the ATD, the ATD was utilized to compress across the fracture site and a screw was placed eccentrically in the proximal end of the plate, proximal to the fracture site. The strain gauge on the device utilizes a color-coding system: green to yellow to red to indicate when appropriate tension has been applied (Figure 4).[18] The device was tensioned through the red section, providing compression across the fracture site. (Figure 5). The third screw was placed centrally in a hole distal to the fracture site, followed by the fourth screw which was placed eccentrically in the proximal end of an oblong hole on the proximal end of the fracture to achieve additional compression of the nonunion site.

Multiple screws were placed on either side of the fracture site utilizing a compression technique to further provide more compression. It is recommended that one obtains six to eight cortices of fixation proximal and distal to the fracture site.[2,19] Non-locking screws were placed proximally and distally and the articulating tensioning device was removed. The fracture was reduced and hardware was appropriately placed (Figure 6). Local autogenous bone

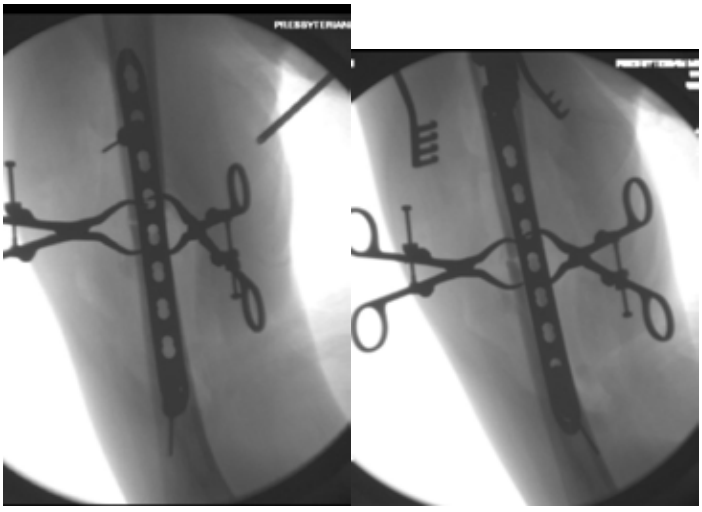

Figure 3. Intraoperative fluoroscopic images demonstrating a 9-hole, over-contoured anterolateral plate was utilized and pinned on both sides with two clamps reducing and symmetrically compressing the nonunion.

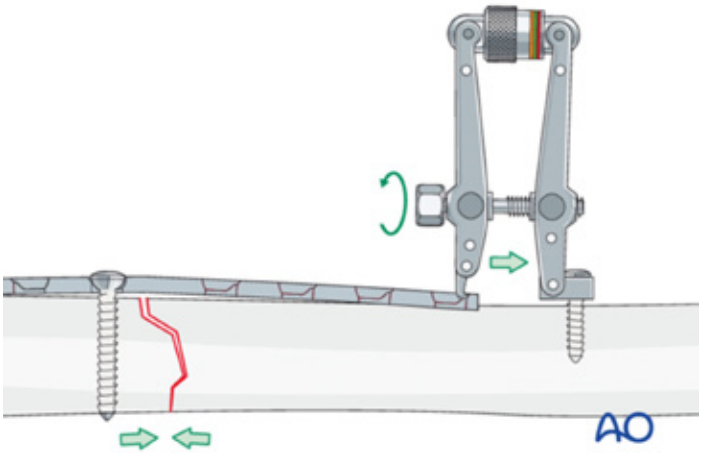

Figure 4. Schematic diagram demonstrating the use of an articulated tensioning device.[20]

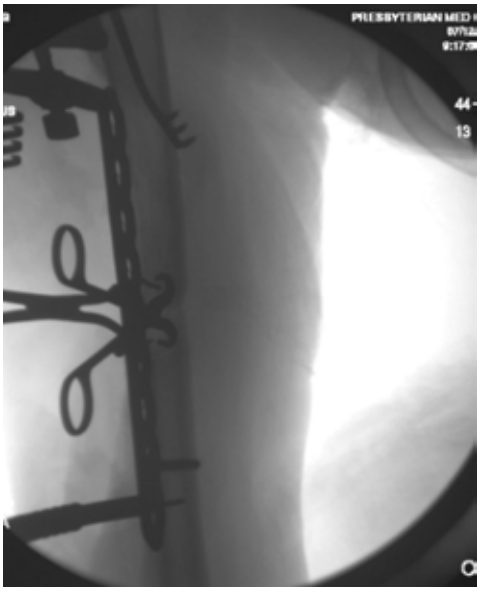

Figure 5. Intraoperative fluoroscopic image demonstrating an articulated tensioning device that was placed proximally and utilized to provide compression through the fracture site.

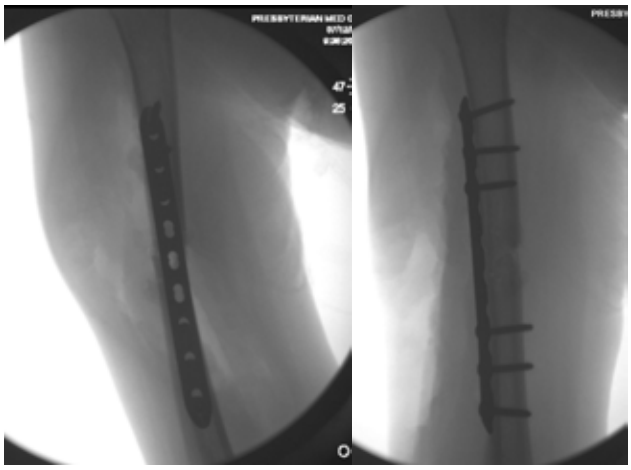

Figure 6. Fluoroscopic images demonstrate the final construct with a reduced, compression fracture site and hardware in appropriate position.

as well as Vivigen (DePuy Synthes, Raynham, MA (frozen corticocancellous bone matrix, demineralized bone, and bone cells) were applied. The wound was closed with a multilayer closure using 2-0 vicyrl, 3-0 vicryl and staples. The patient recovered uneventfully in the post-anesthesia care unit and was discharged home the same day (Figure 7). The patient was made weight bearing as tolerated on the injured extremity and was give 325 mg of aspirin twice daily for venous thrombosis prophylaxis and a short course of oral antibiotics for infection prophylaxis.

The patient followed-up at two-weeks for an incision check and staple removal at which time he began physical therapy. He remained neurovascularly intact. At six-weeks postoperatively, radiographs demonstrated interval healing at the fracture site with hardware in appropriate position (Figure 8). The patient weaned out of his sling in the weeks following surgery and he continued with physical therapy. He was discharged from the practice six weeks after surgery to follow up on as add-needed basis given his successful outcome.

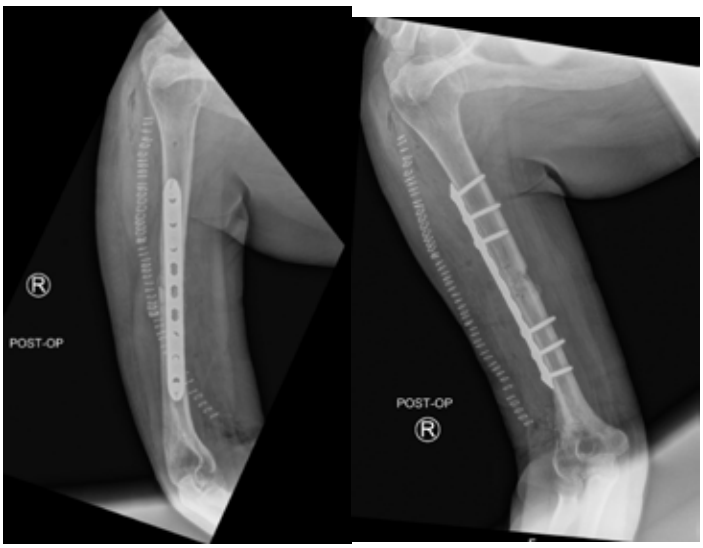

Figure 7. AP and lateral radiographs of the humerus were taken in the post-anesthesia care unit demonstrating the final construct.

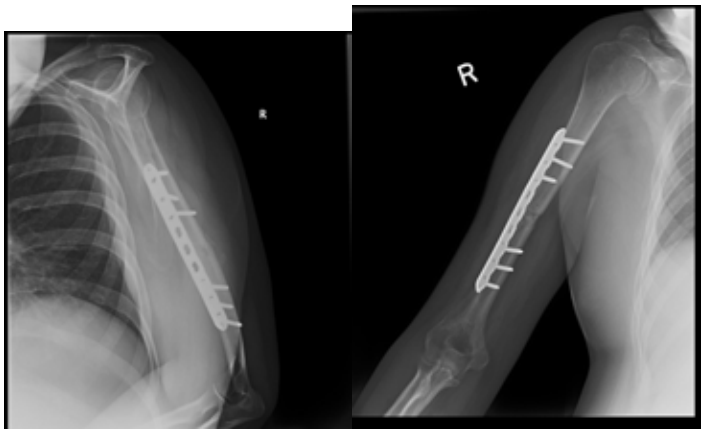

Figure 8. AP and lateral radiographs of the humerus at six-week follow up demonstrates interval healing of the fracture site and appropriately aligned hardware.

Conclusion

This case demonstrates the use of an articulated tensioning device to treat humeral shaft non-unions. By augmenting compression across the fracture site, thereby eliminating strain, this technique can enhance healing. While non-union is a common outcome in non-operatively treated humeral shaft fractures, an articulated tensioning device is a valuable tool, providing more compression than other methods, thereby enhancing bone healing.

References

1. Volgas DA, Stannard JP, and Alonso JE. Nonunions of the humerus. *Clin Orthop Relat* Res. 2004;(419):46-50.

2. Walker M, Palumbo B, Badman B, *et al.* Humeral shaft fractures: A review. *J Shoulder Elbow Surg.* 2011;20(5):833-844.

3. Oliver WM, Searle HKC, Ng ZH, *et al.* Factors associated with humeral shaft nonunion. *J Shoulder Elbow Surg.* 2021;30(10):2283-2295.

4. Hak DJ, Fitzpatrick D, Bishop JA, *et al.* Delayed union and nonunions: Epidemiology, clinical issues, and financial aspects. *Injury.* 2014;45 Suppl 2:3

5. Naclerio EH and McKee MD. Approach to humeral shaft nonunion: Evaluation and surgical techniques. J *Am Acad Orthop Surg.* 2022;30(2):50-59.

6. Driesman AS, Fisher N, Karia R, Konda S, *et al.* Fracture site mobility at 6 weeks after humeral shaft fracture predicts nonunion without surgery. *J Orthop Trauma.* 2017;31(12):657-662

7. Heineman DJ, Bhandari M, Poolman RW. Plate fixation or intramedullary fixation of humeral shaft fractures--an update. *Acta Orthop.* 2012;83(3):317-318.

8. Den Hartog D, Mahabier KC, Van Bergen SH, *et al.* Functional and clinical outcomes after plate osteosynthesis versus intramedullary nailing of a humeral shaft fracture: The results of the HUMMER multicenter, prospective cohort study. *J Bone Joint Surg Am.* 2023;105(14):1101-1111.

9. Ouyang H, Xiong J, Xiang P, *et al.* Plate versus intramedullary nail fixation in the treatment of humeral shaft fractures: An updated meta-analysis. *J Shoulder Elbow Surg.* 2013;22(3):387-395.

10. Amer KM, Kurland AM, Smith B, *et al.* Intramedullary nailing versus plate fixation for humeral shaft fractures: A systematic review and meta-analysis. *Arch Bone Jt Surg.* 2022;10(8):661-667.

11. Peters RM, Claessen FMAP, Doornberg JN, *et al.* Union rate after operative treatment of humeral shaft nonunion--A systematic review. *Injury.* 2015;46(12):2314-2324.

12. Padhye KP, Kulkarni VS, Kulkarni GS, *et al.* Plating, nailing, external fixation, and fibular strut grafting for non-union of humeral shaft fractures. *J Orthop Surg* (Hong Kong). 2013;21(3):327-331.

13. Li Y, Wang C, Wang M, Huang L, *et al.* Postoperative malrotation of humeral shaft fracture after plating compared with intramedullary nailing. *J Shoulder Elbow Surg.* 2011;20(6):947-954. doi: 10.1016/j.jse.2010.12.016.

14. Lucas JF, Lee MA, and Eastman JG. Optimizing compression: Comparing eccentric plate holes and external tensioning devices. *Injury.* 2016;47(7):1461-1465.

15. Copuroglu C, Calori GM, and Giannoudis PV. Fracture non-union: Who is at risk? *Injury*. 2013;44(11):1379-1382.

16. Pack AM, Morrell MJ. Epilepsy and bone health in adults. *Epilepsy Behav*. 2004;5 Suppl 2:24.

17. Svalheim S, Roste LS, Nakken KO, *et al.* Bone health in adults with epilepsy. *Acta Neurol Scand Suppl*. 2011;(191):89-95.

18. Depuy Synthes. 4.5 mm LCP proximal femur plates: surgical technique. http://synthes.vo.llnwd.net/o16/LLNWMB8/US%20Mobile/Synthes%20North%20America/Product%20Support%20Materials/Technique%20Guides/DSUSTRM09161039%20Rev%20B.pdf. Website. Updated 2021.

19. Mistry MR, Tat J, Husain R, *et al.*, Inadequate proximal screw fixation increases risk of failure following plate fixation of diaphyseal humerus fractures. *J Orthop Surg Res*. 2023;18(1):142-2.

20. Camuso M, and White R. AO surgery reference. ORIF - compression plating. https://surgeryreference.aofoundation.org/orthopedic-trauma/adult-trauma/tibial-shaft/simple-fracture-transverse/orif-compression-plating#fixation Website. Updated 2012.

Management of a Multiply-Injured Patient with a Diaphyseal Tibial Fracture: Case Report and Technical Tips for Traveling Traction

Chielozor I. Okafor, MD
Bradley O. Osemwengie, MD
Lisa G.M. Friedman, MD, MA
Jordan S. Cohen, MD
Stephen R. Barchick, MD
Derek J. Donegan, MD, MBA

Department of Orthopaedic Surgery, University of Pennsylvania

Introduction

Diaphyseal tibia fractures are the most common long bone fracture of which 24% are open injuries.[1] Because these injuries are associated with increased risk of wound complications and infection due to the degree of soft tissue injury, initial management is vital to set a good foundation for healing. For a variety of factors, some patients may not be clinically stable enough to undergo definitive fixation immediately. In those situations, the surgeon may employ principles of damage control orthopedics (DCO) and stabilize the fracture with external fixation and defer open reduction and internal fixation (ORIF) to a later time.[2]

Most diaphyseal tibia fractures are treated with intramedullary nailing. However, for those treated initially with external fixation, one technique is the transfixion pin distractor technique or "traveling traction" (Figure 1).[3] This external fixation provides relative stability at the fracture site by providing adequate length, alignment, and rotation. Traveling traction use began in the 1990s to help with obtaining fracture reduction prior to intramedullary nail insertion.[4] Traveling traction in the tibia is performed by placing a Schanz pin in the proximal tibia and in the distal portion of the tibia or the posterior portion calcaneus in a bicortical fashion so that the pin is accessible on both the medial and lateral sides of the limb. Both Schanz pins are clamped on either end and are connected to each other with bars placed medially and laterally. Manual reduction can be obtained and then the clamps are tightened to hold the fracture out to length. Since this external fixator is parallel to the tibia, it is easy to manage from a nursing care standpoint. Proper placement can also facilitate future instrumentation of the tibia with nailing when the Schanz pin is placed out of the way of the planned path of the nail. Once the tibia is locked proximally and distally, the external fixator can be removed. This case report describes the use of traveling traction as a temporizing measure and reduction tool with a plan for future definitive fixation.

Case Presentation

The patient is a 33-year-old-male who was brought in by police drop-off after sustaining multiple gunshot wounds (GSWs). Initial survey in the trauma bay revealed GSWs to the left upper back, right lower back, right buttock, and right groin. His overall injury burden included a left hemopneumothorax, left hemidiaphragm, high-grade renal and splenic lacerations, right femoral vein injury as well as multiple lumbar spinous process, transverse process fractures, and rib fractures. A chest tube was placed immediately upon arrival in the trauma bay, and the vascular injury required reconstruction by vascular surgery. Transfusion protocol was initiated upon arrival due to hypotension. The patient was taken to the OR emergently for cavitary triage. During the surgical procedure, he was found to have an open right tibia fracture (Figure 2). Vascular surgery performed femoral vein reconstruction. Trauma surgery

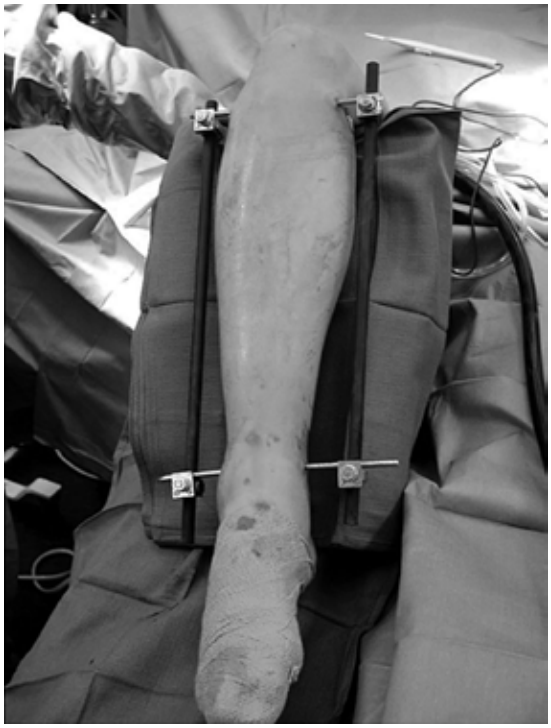

Figure 1. An example of the tibial transfixion pin distractor technique (aka 'traveling traction').

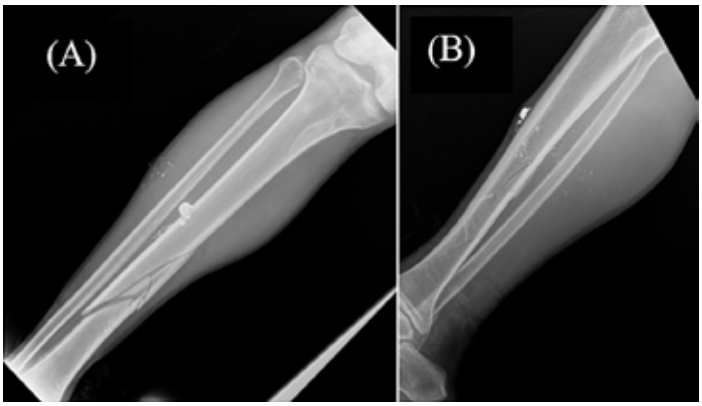

Figure 2. (A) AP and **(B)** lateral x-ray of the right tibia and fibula demonstrating a comminuted midshaft tibia fracture.

performed fasciotomies of the right lower leg. Orthopedic surgery was consulted intra-operatively for management of the open fracture. Due to the unstable nature of the patient, the decision was made to perform tibial fracture stabilization with damage control orthopedics and the utilization of traveling traction.

The Procedure

Traveling Traction

After vascular reconstruction of the femoral vein and right lower leg fasciotomies, the orthopaedic team assumed surgical care of the patient for surgical management of the tibia fracture. The right lower extremity was addressed first by irrigating the fasciotomy wounds and the open fracture site.

The procedure begins with obtaining a perfect lateral of the knee and foot to obtain an appropriate starting point for 5.0mm Schanz pin. An appropriately sized drill bit was placed medially on the posteroinferior quadrant of calcaneus under fluoroscopic guidance as described by Tornetta. A path was drilled through the near and far cortex in the axial plane from a medial to lateral trajectory. This technique allows the surgeon to minimize the risk of iatrogenic damage to the neurovascular bundle medially.[5]

After this, a centrally threaded 5.0mm Schanz pin was placed so the threads were within the bony calcaneus (Figure 3). Attention was then turned to the proximal tibia. Under fluoroscopic guidance with a perfect lateral of the knee, the appropriate starting point for the proximal tibia pin was identified. This is at the lateral surface of the tibia, just anterior to the proximal aspect of the fibular head (Figure 4). A bicortical path was drilled followed by placement of a centrally threaded 5.0mm Schanz pin so the pin would be parallel to the articular surface of the tibial plateau and the pin in the calcaneus. Importantly, the proximal fixator pin is placed posterior in the tibia to allow for uninhibited placement of an intramedullary nail should that be the selected option for definitive treatment.

Next, clamps were placed on both ends of the proximal and distal Schanz pins into which two bars were placed. The clamps were placed on the inside of each pin to allow for more stable distraction. A closed reduction of the tibia was performed and the frame was locked in place. Postoperative radiographs of the external fixator were obtained (Figure 5). The fasciotomy incisions were left open. The right lower leg skin incisions were then loosely closed with staples and a vessel loop using the roman sandal technique to allow for soft tissue swelling (Figure 6). A dry dressing was applied to the overlying

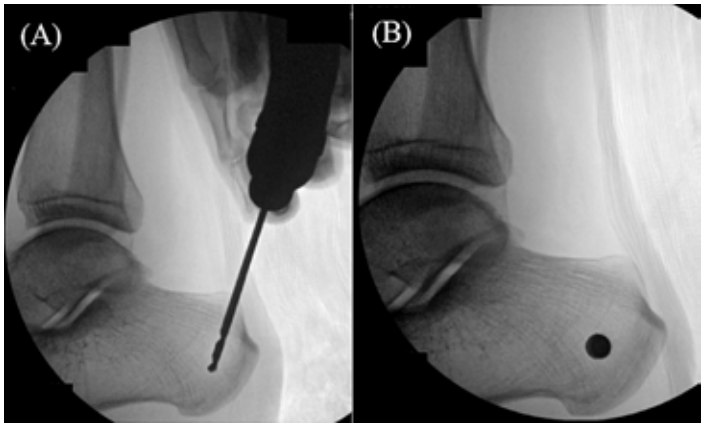

Figure 3. Intraoperative fluoroscopic imaging demonstrating **(A)** Placement of drill bit in posteroinferior quadrant of calcaneus; **(B)** Bicortical Schanz pin placed in posterior quadrant of calcaneus.

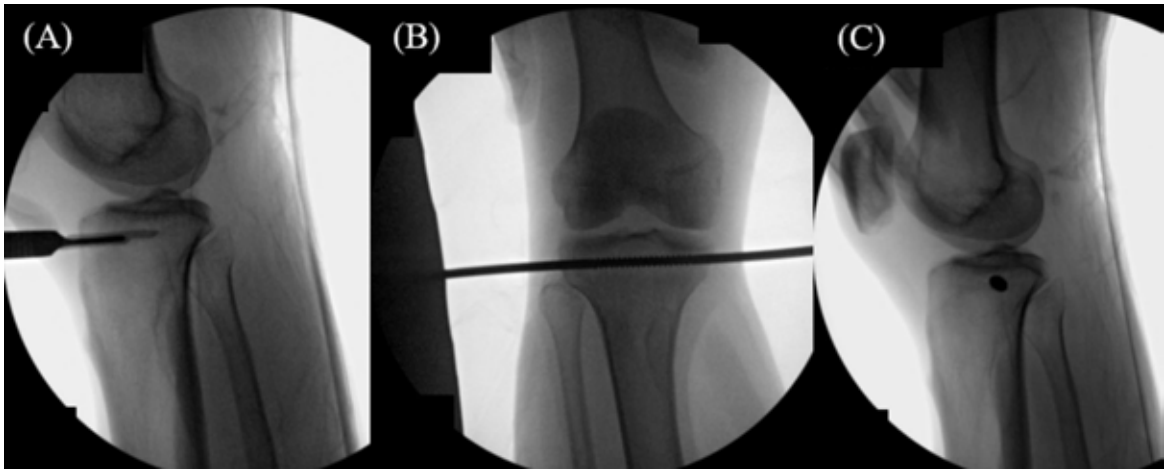

Figure 4. Intraoperative fluoroscopic imaging demonstrating **(A)** Lateral of proximal tibia localizing starting point for drill bit (just anterior to the proximal fibular head); **(B)** AP and (C) lateral of the proximal tibia showing Schanz pin placement.

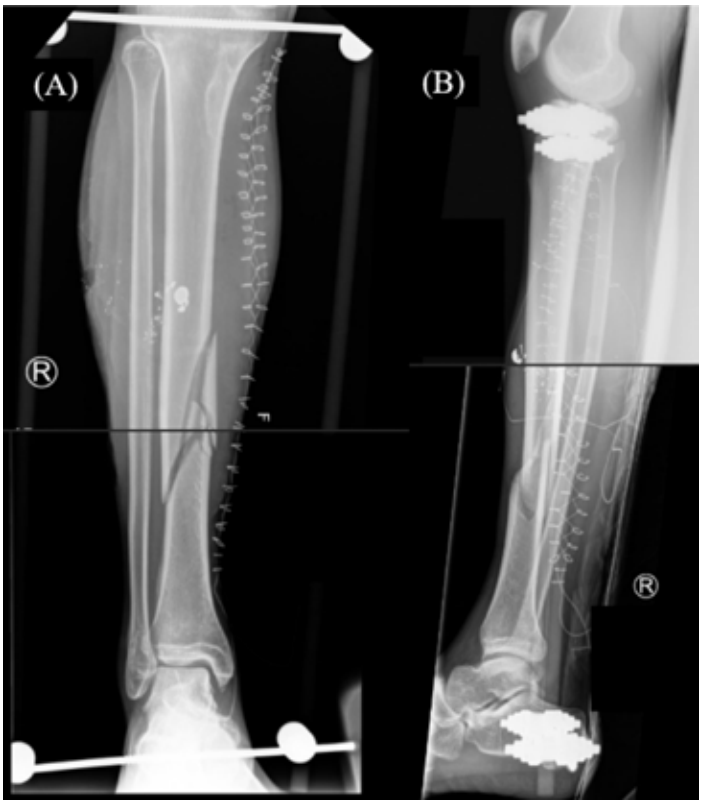

Figure 5. Postoperative **(A)** AP and **(B)** lateral radiographs of the right tibia and fibula status post application of traveling traction external fixation demonstrating adequate length, alignment, and rotation.

exposed subcutaneous tissue. The general trauma surgeon team resumed care of the patient intra-operatively. The orthopaedic plan included continuous first-generation cephalosporin antibiotics until the patient could be definitely closed.

Intramedullary Nail (IMN)

The patient was taken back to the OR for definitive fixation of his tibia. The right lower extremity was prepped and draped with the external fixator on and irrigation and debridement was performed at the fracture site. The fasciotomy wounds were evaluated, hematoma was evacuated, and any necrotic muscle was excised in all four compartments. Attention was then turned to fixing the tibia.

Our institution's preferred technique is placement of a tibial nail through a suprapatellar approach. With the patient's operative extremity on a bone foam extremity holder, a small incision proximal to the patella was utilized sharply centered over the quadriceps tendon. Under subcutaneous tissue, the medial and lateral edges of the tendon were identified following by sharp dissection centered on the tendon through bone to allow access to the knee. With a threaded guide wire, the starting point was obtained just medial to the lateral tibial spine and on the most anterior aspect of the tibial plateau. The guide wire was then taken into proximal tibia in appropriate trajectory. The proximal tibia was opened with an opening reamer and the ball-tip guide wire was then taken into the proximal tibia across the fracture into the distal tibia.

Before reaming was begun, care was taken to assure the reduction of the shaft component was maintained thorough the open traumatic wound with a pointed reduction clamp (Figure 7). The tibia was reamed to 1.5mm (11.5mm diameter) above the size of the anticipated nail. A 10mm nail of appropriate length was placed while the external fixator was still in place (Figure 8).

Our standard technique is to bury blunt guide wire tip into the subchondral bone above the tibial plafond, measure the length and down size by 1-2cm for appropriate nail placement. With fluoroscopy appropriate placement of the ball tip guide wire was conformed centered on both the AP and lateral radiographs of the tibial plafond. The nail was then secured with two interlocking screws proximally through the jig and two interlocking screws distally through the perfect circle technique. The external fixator

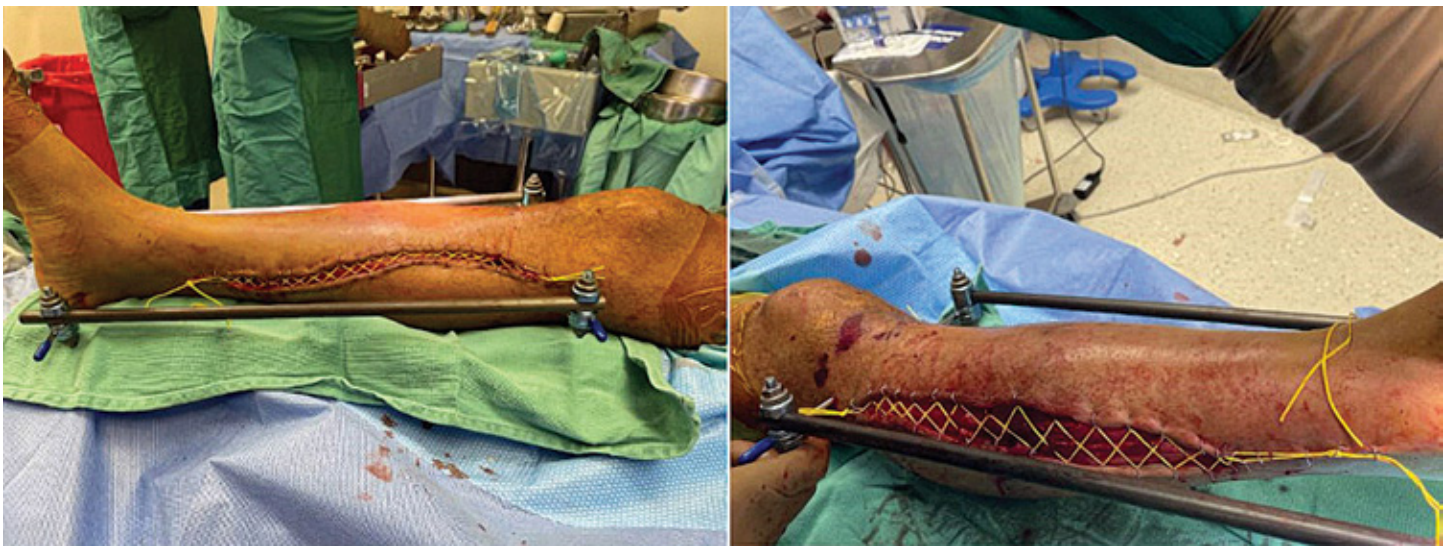

Figure 6. Intraoperative photograph demonstrating the lower extremity immediately after placement of tibial traction. The skin incisions over the sites of fasciotomies were closed with staples and vessel loops using the Roman sandal technique to allow for swelling of the compartments.

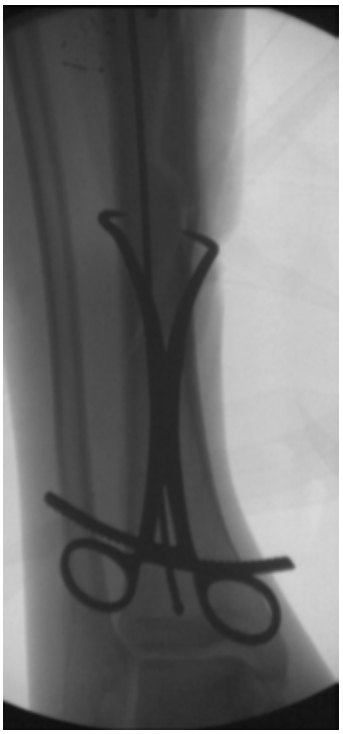

Figure 7. Intraoperative fluoroscopic imaging demonstrates application of point of reduction clamp at the fracture site with guide wire in place but prior to reaming during definitive fixation with an intramedullary nail.

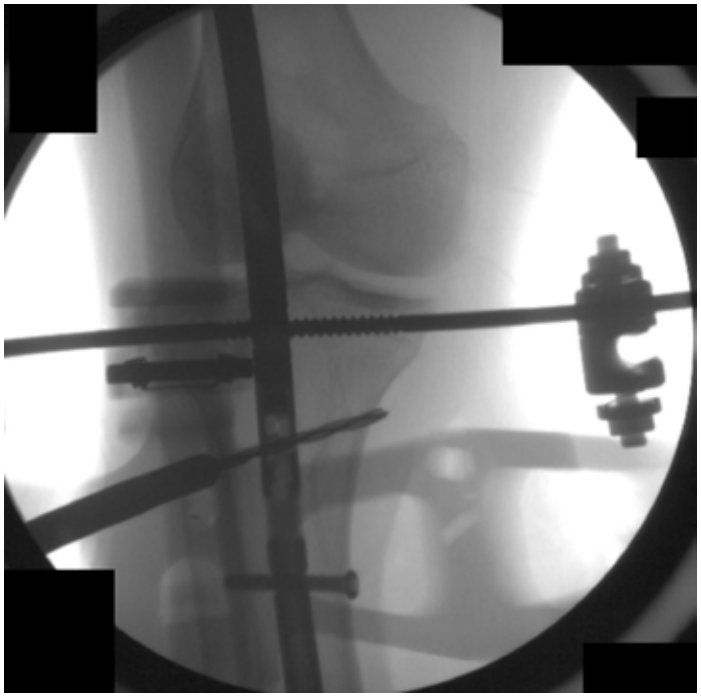

Figure 8. Intraoperative fluoroscopic imaging demonstrating tibia intramedullary nail insertion while the external fixator is still in place.

was removed once the tibia IMN was locked proximally and distally. The wound was then irrigated thoroughly, hemostasis achieved, vancomycin powder was placed in the medial and lateral fasciotomy wounds to reduce the risk of infection with this open fracture.[6] The wounds were then closed in a complex fashion with multiple retention sutures using #3-0 nylon. The rest of the surgical incisions were closed in a layered fashion with #1 Vicryl, #2-0 Vicryl, and #3-0 nylon. An incisional vac and sterile dressing were placed. Postoperative imaging of the final construct was obtained (Figure 9).

The patient was eventually extubated and an exam was able to be performed two days after tibia nail placement. He was found to have a right lower extremity foot drop at that time. The patient was eventually discharged home. At two months postop, the skin incisions were healed (Figure 10). At that time, he was ambulating with a walker

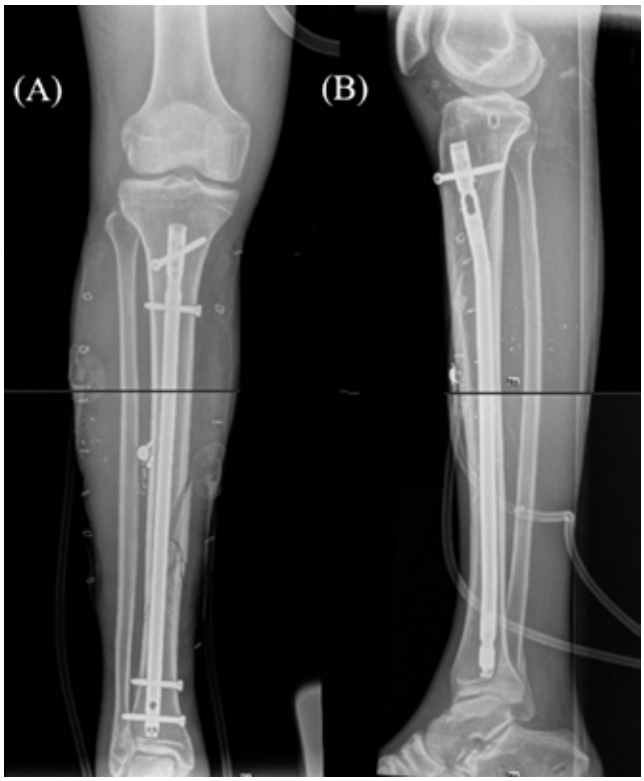

Figure 9. Immediate postoperative **(A)** AP and **(B)** lateral radiographs of the tibia IMN showing adequate length, alignment, and rotation at the fracture site. Traveling tibia traction has been removed.

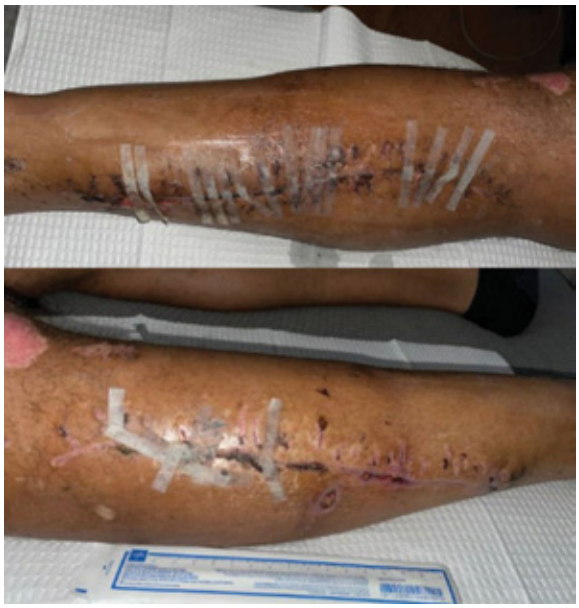

Figure 10. Clinical photograph of **(A)** medial and **(B)** lateral right leg six-weeks postop. Skin incisions almost fully healed.

with a persistent foot drop. Interval callous formation was noted at the fracture site with stable hardware (Figure 11). He was prescribed a molded ankle foot orthosis (MAFO) for his foot drop and prescribed physical therapy. At two months post op, his skin incisions were fully healed (Figure 12).

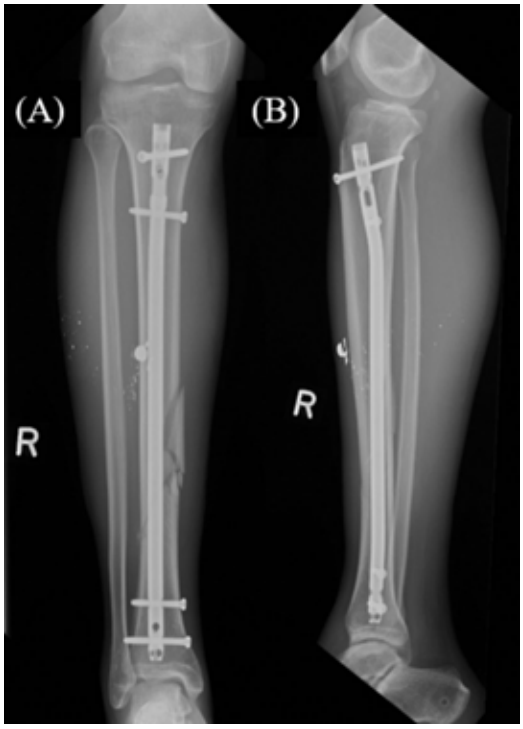

Figure 11. Six-week postoperative **(A)** AP and **(B)** lateral radiographs that show the tibia IMN in good position and interval callus formation at the fracture site.

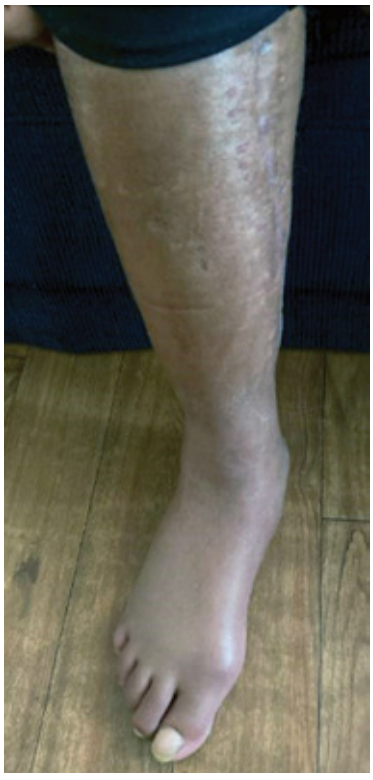

Figure 12. Clinical photograph of the right lower extremity two months postop. Incisions well healed.

Discussion

Tibia shaft fractures are often treated surgically utilizing an intramedullary nail. However, patients who are not clinically stable enough for IMN placement require DCO and may require temporization via external fixation. In delaying the physiologic stress that may arise from IMN placement, the surgeon significantly decreases the risk of the patient experiencing a two-hit phenomenon. As such, the risk of iatrogenic morbidity and mortality decreases.[2] Additionally, in this case where a patient is undergoing surgery for emergent care to save life or limb, the senior author prefers to utilize the least invasive surgery necessary to manage the patient's injury.

Traveling traction utilizes principles of external fixation while facilitating attainment of length, alignment, and rotation for planned definitive fixation. Some authors have found that fractures reduced with a combination of traveling traction and percutaneous clamps had significantly better postoperative coronal alignment than manual reduction alone and percutaneous clamping alone.[7] This supports the use of traveling traction as a reduction tool for tibia IMN especially in challenging fractures of the proximal and distal tibia. It is also important to consider the time between initial temporization with external fixation and definitive fixation with IMN due to the risk of infection. Melvin et al. advocate for conversion from external to internal fixation as soon as the patient can tolerate and adequate soft tissue coverage can be attained to reduce the risk of infection.[8]

The orthopaedic surgery team was engaged via an intraoperative consultation. Although it would have been ideal to obtain informed consent from the patient himself or next-of-kin, neither were feasible at the time. The patient's other traumatic injuries were being managed surgically, thus he could not give informed consent for the surgical management of his tibia fracture. Moreover, his identity was unknown, so contacting a family member could not be done in a timely manner. The high risk of serious disability without emergent treatment of the fracture made this an appropriate case for the orthopaedic surgery team to operate under implied consent.[9] Despite the unplanned nature of the encounter, the physician is ethically obligated to weigh the benefits and burdens of their planned intervention and act in a way that does not cause harm to the patient.[10] Compared to options such as a delta frame external fixator or an IMN, the traveling traction technique allowed for the most minimally invasive intervention to preserve his injured limb and prevent serious disability.

Conclusion

Traveling traction is a viable option for external fixation of the tibia in clinically unstable trauma patients requiring temporary fixation. It is also a valuable reduction tool for preliminary reduction with other adjuncts like point of reduction clamps while the tibial IMN is inserted. By

utilizing this technique, the surgeon can temporize the fractured limb in an unstable patient and may also obtain excellent reduction of the tibia fracture during definitive fixation without the need for additional equipment or personnel.

References

1. Melvin SJ, Dombroski DG, Torbert JT, *et al.* Open Tibial Shaft Fractures: I. Evaluation and Initial Wound Management. *American Academy of Orthopaedic Surgeon* 2010. 18(1): 10-19.

2. D'Alleyrand JC, O'Toole RV. The evolution of damage control orthopedics: current evidence and practical applications of early appropriate care. *Orthop Clin North Am* 2013; 44(4): 499-507.

3. Wysocki RW, Kapotas JS, Virkus WW. Intramedullary Nailing of Proximal and Distal One-Third Tibial Shaft Fractures with Intraoperative Two-Pin External Fixation. *The Journal of Trauma: Injury, Infection, and Critical Care* 2009. 66(4): 1135-1139.

4. Moed BR, Watson JT. Intramedullary nailing of the tibia without a fracture table: the transfixion pin distractor technique. *J Orthop Trauma* 1994. 8(3):195-202.

5. Casey D, McConnell T, Parekh S, Tornetta P 3rd. Percutaneous pin placement in the medial calcaneus: is anywhere safe?. *J Orthop Trauma* 2002. 16(1):26-29.

6. O'Toole RV, Joshi M, Carlini AR, *et al.* Effect of Intrawound Vancomycin Powder in Operatively Treated High-risk Tibia Fractures: A Randomized Clinical Trial. *JAMA Surg* 2021. 156(5):e207259.

7. Behlmer RJ, Whiting PS, Kliethermes SA, *et al.* Reduction techniques for intramedullary nailing of tibial shaft fractures: a comparative study. *OTA Int* 2021. 4(1): 095.

8. Melvin JS, Dombroski DG, Torbert JT, *et al.* Open tibial shaft fractures: II. Definitive management and limb salvage. *J Am Acad Orthop Surg* 2010.18(2):108-17.

9. Cocanour CS. Informed consent- It's more than a signature on a piece of paper. *Am J Surg* 2017. 214(6): 993-997.

10. Kumar S, Tatarian T, Palazzo F. A surgeon's framework for the unplanned intraoperative consultation. *Langenbecks Arch Surg* 2023. 408(42).

Spine

U·P·O·J

Tips and Tricks: Lumbar Spinal Peri-implant Lucency with Spontaneous Resolution- A Decision to Stay the Course

Bradley Osemwengie, MD[1]
Tensae Assefa, MD[1]
Chinedu Okafor, MD[1]
Jennifer X. Hong, BA[1]
Harvey Smith, MD[1]

[1]Department of Orthopaedic Surgery
University of Pennsylvania

Introduction

Pedicle screws are threaded implants inserted through the vertebral pedicles in the spine. They are widely used to achieve rigid, tri-columnar fixation of the spine during posterior spinal instrumentation surgery.[1] With appropriate technique, they have been shown to increase fusion rates and therefore provide better outcomes in patients suffering from compressive pathologies.[2,3]

One of the complications of pedicle screw placement is screw loosening. This can occur due to bony remodeling secondary to decreased load going through the fixed bone (stress shielding), intraoperative microfractures caused by screw placement, or the presence of osteoporotic bone which precludes adequate fixation of the screw.[4,5] Screw loosening frequently presents as worsening back pain and can result in pseudoarthrosis and increased patient morbidity. Motion at the sites of instrumentation can also cause neurologic symptoms by compressing on the neural elements. This can cause a recurrence of the symptomatology that was supposed to be alleviated by the index spinal procedure. A reliable method of identifying screw loosening is evaluating for radiographic lucencies on CT imaging.[6] Although MRI is the usual test of choice in the setting of spinal pathology, CT scans are also heavily utilized in order delineate osseous architecture especially in the setting of prior instrumentation. CT imaging is also helpful to assess for evidence of hardware failure and relative amounts of peri-implant osteopenia.

Treatment for pedicular screw loosening varies based on clinical significance and presence of pseudoarthrosis. Patients with minimal back pain and evidence of successful spinal fusion can pursue nonoperative management. However, evidence of pseudoarthrosis, hardware malposition that can threaten neural elements, worsening back pain, and progressive neurological deficits may require revision spinal surgery.[7] We present a case of posterior spinal decompression and fusion with postoperative screw lucency that not only resolved with nonoperative treatment, but also had a disappearance of the peri-implant lucency.

Case presentation

A 73-year-old female presented to the office on July 2014 with low back and bilateral leg pain that had been present for 2-3 years. The pain radiated laterally down the leg to the foot with numbness in the buttocks and leg, and her left leg pain radiated posteriorly to the knee with associated numbness. Conservative treatment with physical therapy, epidural injections, and anti-inflammatories provided only minimal relief. On exam, she had normal range of motion to the lumbar spine with no point tenderness. She was neurovascularly intact except for decreased sensation to light touch in the left lower extremity.

A lumbar spine x-ray demonstrated mild lumbar scoliosis and L3-L4, L4-L5 spondylolisthesis (Figure 1). Lumbar spine MRI revealed multilevel lumbar disc degeneration, disc bulges, facet arthropathy, and spinal stenosis, most pronounced L3/L4 and L4/L5 (Figure 2).

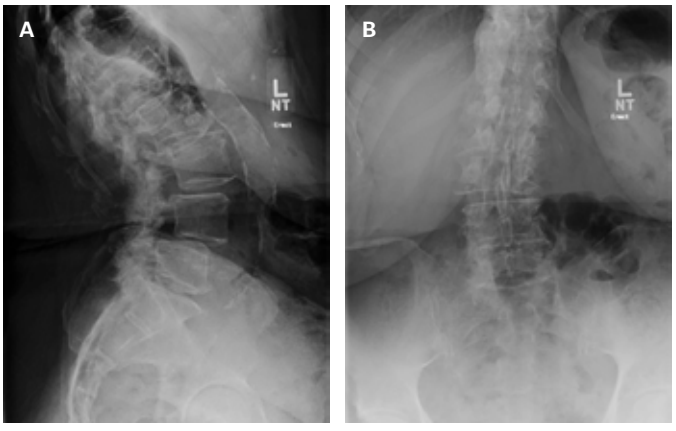

Figure 1. Lumbar spine x-ray. **(A)** Lateral x-ray showing L3/L4, L4/L5 spondylolisthesis; **(B)** AP x-ray showing mild lumbar scoliosis.

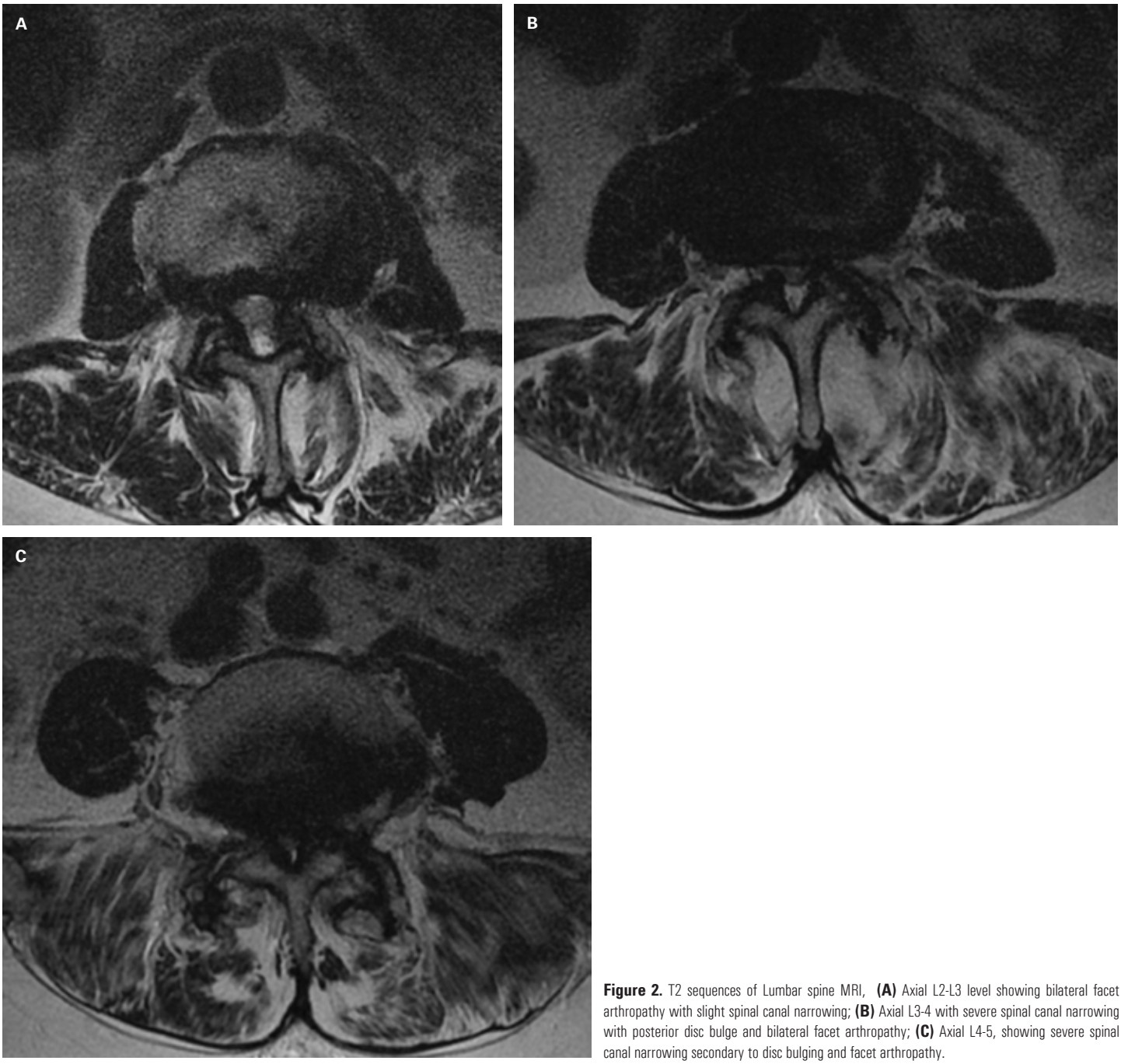

Figure 2. T2 sequences of Lumbar spine MRI, **(A)** Axial L2-L3 level showing bilateral facet arthropathy with slight spinal canal narrowing; **(B)** Axial L3-4 with severe spinal canal narrowing with posterior disc bulge and bilateral facet arthropathy; **(C)** Axial L4-5, showing severe spinal canal narrowing secondary to disc bulging and facet arthropathy.

Based on imaging findings and clinical presentation, the patient was diagnosed degenerative spondylolisthesis with multilevel lumbar stenosis. Given the failure of nonoperative treatment in alleviating symptoms, the patient decided to proceed with elective surgery. The patient underwent L2-L3, L3-L4, L4-L5 posterior lumbar decompression and fusion on September 2014. There were no complications during the postoperative hospital course and the patient was discharged on post op day 3.

At 2- and 6-weeks follow-up, the patient's sensation in the lower limbs normalized and X-rays revealed stable hardware in adequate position. (Figure 3).

At seven months follow-up, the patient reported increased back pain and right lateral hip pain impeding activities of daily living. Aquatic physical therapy was recommended and provided moderate symptom improvement. At one year follow-up, the patient reported continued back pain and a CT scan was obtained to evaluate for hardware positioning (Figure 4). Images revealed lucencies adjacent to the bilateral pedicle screws at L2 and L5, suggestive of hardware loosening. There was a fusion mass present.

Given the imaging findings suggestive of hardware loosening, the option of a revision fusion procedure was discussed with the patient. After a risk versus benefits

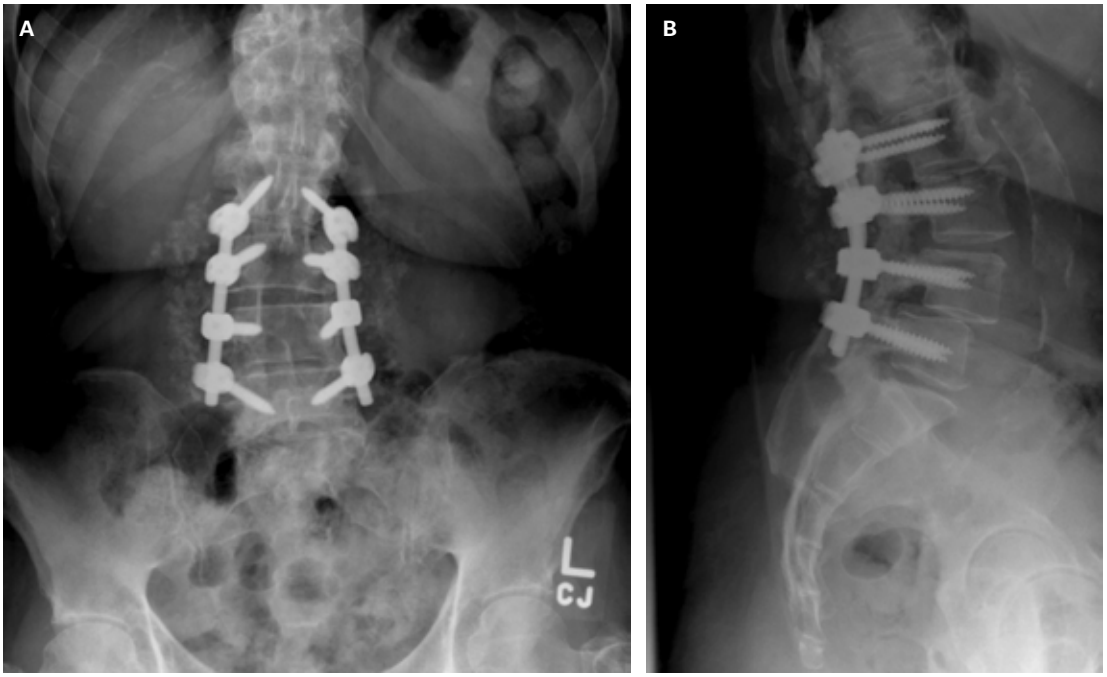

Figure 3. (A) AP and **(B)** lateral x-rays of the lumbar spine at 6 week follow up showing L2-L5 posterior spinal fusion in adequate position.

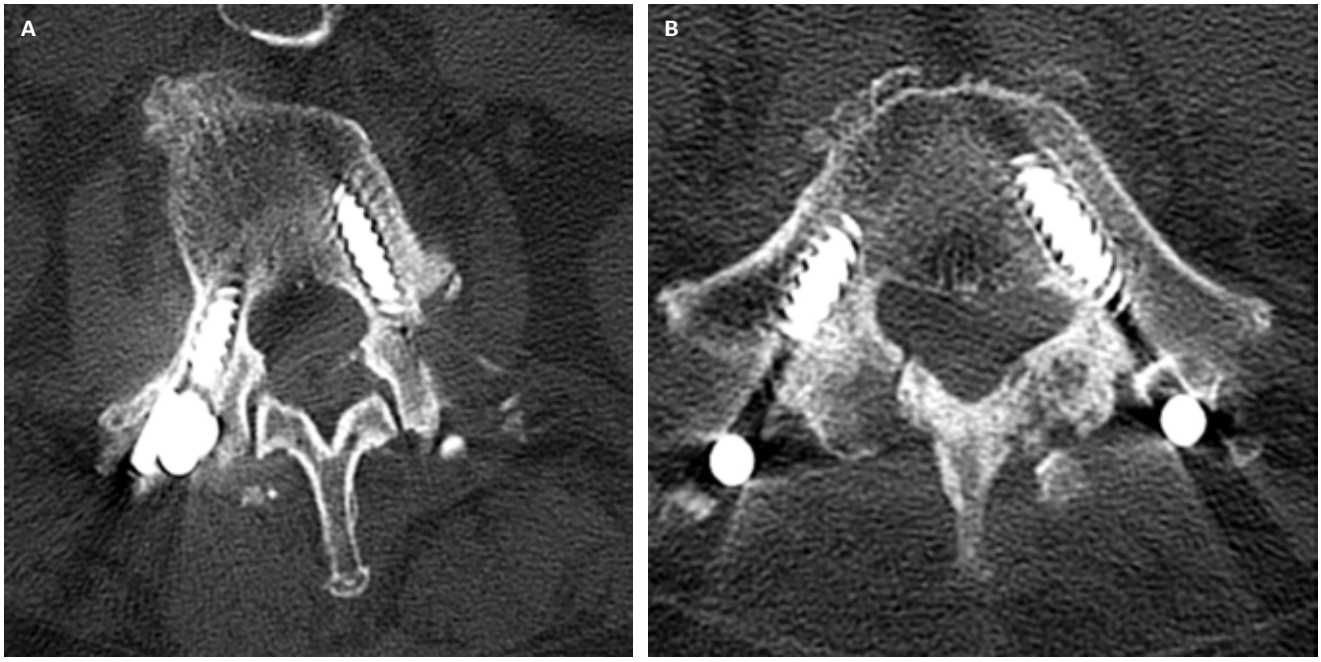

Figure 4. 1-year post-op Axial CT images highlighting bilateral pedicle screw lucencies at (A) L2 and (B) L5.

discussion, the patient elected to proceed with conservative treatment options and was referred to a pain management specialist for symptom management.

At three years postoperative follow up, the patient had improved functionality and was no longer complaining of back pain. A repeat CT scan was obtained to characterize hardware positioning. Images revealed no lucencies about the pedicle screws at L2 and L5 (Figure 5). There was successful osseous fusion across L2-L5 with no evidence of hardware malposition.

Discussion

Pedicle screws can be used reliably to achieve spinal fixation in deformity correction surgery. Possible complications include screw loosening, which can present with post-operative back pain that is refractory to medications and physical therapy. Assessing for peri-hardware radiolucent zones, indicating osteolysis, is a reliable way to track screw loosening.[8]

Historically, persistent back pain in the setting of hardware loosening has been viewed as an indication

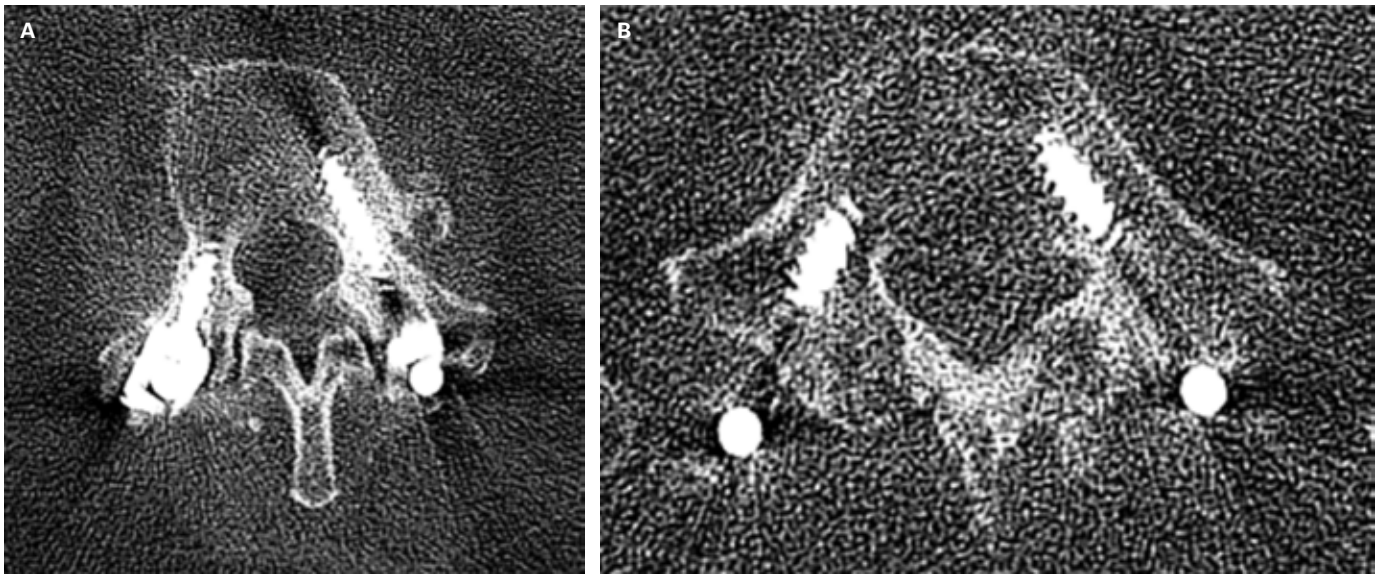

Figure 5. 3-year post-op Axial CT images at **(A)** L2 and **(B)** L5 highlighting stable pedicle screws in the lumbar spine. There appears to be resolution of the bilateral pedicle screw lucencies compared to two years prior.

for revision surgery. It may be a marker of ongoing pseudoarthrosis which can increase the risk for patient disability. We present a case of postoperative screw loosening treated nonoperatively with subsequent resolution of peri-implant lucency.

There is limited literature on nonoperative treatment of screw loosening, so the mechanism for resolution of peri-screw osteolysis in this case report remains unclear. Some authors track screw loosening differently by assessing for screw pull out (either partial or complete). Studies have shown that screw loosening rates may be more than four times higher when defined by radiolucent zones as compared to implant pullout.8 This may indicate that in patients with a higher risk for screw loosening, such as osteoporosis, implant pullout assessment should be used to supplement radiolucent findings on imaging.

Conclusion

Radiolucent zones around pedicle screws are a marker of osteolysis and ongoing screw loosening. Osteoporotic patients are at higher risk for osteolysis and need careful assessment of spinal implant positioning. Radiolucent zones may represent false positivity as concerns screw loosening in such patients. Implant pullout should always be assessed prior to surgical consideration. Consideration of the patient symptomatology and desires for further surgical intervention should be explored as well. More literature is needed to track long term outcomes in such patients.

References

1. Jain, N.S., Hah, R.J. (2021). Pedicle Screw Fixation. In: Cheng, B.C. (eds) H*andbook of Spine Technology*. Springer, Cham.

2. Ghogawala Z, Dziura J, Butler WE, *et al.* Laminectomy plus Fusion versus Laminectomy Alone for Lumbar Spondylolisthesis. *N Engl J Med*. 2016 Apr 14;374(15):1424-34.

3. Lorenz M, Zindrick M, Schwaegler P, *et al.* A comparison of single-level fusions with and without hardware. *Spine* (Phila Pa 1976). 1991 Aug;16(8 Suppl):S455-8

4. Rosinski AA, Mittal A, Odeh K, *et al.* Alternatives to Traditional Pedicle Screws for Posterior Fixation of the Degenerative Lumbar Spine. *JBJS Rev*. 2021 Jul 28;9(7).

5. Rometsch E, Spruit M, Zigler JE, *et al.* Screw-Related Complications After Instrumentation of the Osteoporotic Spine: A Systematic Literature Review With Meta-Analysis. *Global Spine J*. 2020 Feb;10(1):69-88.

6. Sandén B, Olerud C, Petrén-Mallmin M, *et al.* The significance of radiolucent zones surrounding pedicle screws. Definition of screw loosening in spinal instrumentation. *J Bone Joint Surg Br*. 2004 Apr;86(3):457-61.

7. Ponnusamy KE, Iyer S, Gupta G, *et al.* Instrumentation of the osteoporotic spine: biomechanical and clinical considerations. *Spine J*. 2011 Jan;11(1):54-63.

8. Marie-Hardy L, Pascal-Moussellard H, Barnaba A, *et al.* Screw Loosening in Posterior Spine Fusion: Prevalence and Risk Factors. *Global Spine J*. 2020 Aug;10(5):598-602.

Recurrent Delayed Surgical Site Infections in Adolescent Idiopathic Scoliosis

Bradley Osemwengie, MD
Caroline Granruth, MD
Tensae Assefa, MD
Amrit Khalsa, MD

Department of Orthopaedic Surgery
University of Pennsylvania

Introduction

Adolescent idiopathic scoliosis (AIS) is a deformity of the spine characterized by lateral deflection and rotation of the vertebral bodies.[1] It is the most common type of scoliosis in children of age 10 to 18 years, and typically presents between 10-12 years of age. It occurs more frequently in females, with a 10:1 female-to-male ratio. Diagnosis is made by a measured Cobb angle of > 10 degrees on a standing AP radiograph. The most common presenting pattern of deformity is a right convex curvature of the thoracic spine, which causes forward rotation and protrusion of the right shoulder.[1,2]

Nonoperative treatment is aimed at preventing curve progression and primarily consists of bracing. Studies have shown that for Cobb angles of 25-45 degrees, consistent bracing for >13 hours/day can significantly decrease curve progression to < 50 degrees.[2] Although various kinds of bracing designs exist, there is no evidence that one brace is superior in preventing curve progression.[3] Surgical indications for AIS include Cobb angle > 50 degrees and sequela such as restrictive pulmonary function. Posterior spinal fusion (PSF) has become the mainstay of surgical treatment for severe AIS to correct and prevent further progression of spinal deformity.[4]

Delayed infection after PSF for AIS is an uncommon complication but is one of the leading causes of late revision surgery. It is defined as the development of a surgical site infection (SSI) > 1 year after primary spinal surgery. Mechanisms include late activation of bacteria implanted at the time of index surgery or hematogenous seeding.[5] Studies have described different treatment modalities for delayed infection after PSF including implant removal, implant exchange, implant retention, and/or long-term antibiotics.[6] We present the case of one AIS patient with two instances of delayed infection after PSF treated with both implant retention and ultimately implant removal.

Patient Presentation

An otherwise healthy 7-year-old girl was observed to have asymmetric shoulder height. After a thorough evaluation, she was diagnosed with idiopathic scoliosis. Nonoperative treatment was initiated with back bracing to prevent curve progression. By the age of twelve, despite compliance with bracing up to 13 hours/day, there was persistent curve progression (Cobb angle 41 degrees) as well as worsening pulmonary function with new onset asthma (Figure 1). Surgical treatment was indicated for curve correction, and the

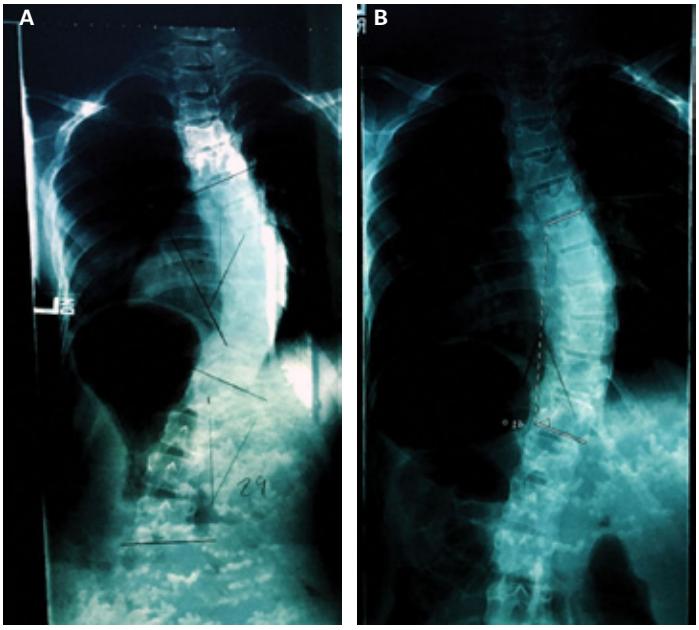

Figure 1. Preoperative thoracolumbar x-rays. **(A)** PA x-ray showing scoliosis of the thoracic spine; **(B)** PA of thoracolumbar spine showing a Cobb angle of 41 degrees.

patient underwent a T2-L3 posterior spinal fusion (PSF) on January 2007 by a fellowship-trained pediatric orthopedic spine surgeon. The case was prolonged (>8 hours), requiring intra-operative transfusion, and the patient remained intubated in the ICU for comfort until post-op day 1. The patient was also noted to have new onset right sided Horner's syndrome post-operatively (ptosis and miosis). Her hospital course was otherwise uncomplicated, and the patient was discharged home on post-op day five. She completed three months of physical therapy and had a full recovery with asthma resolution. Postoperative x-rays demonstrated appropriate hardware alignment (Figure 2).

At eighteen months postoperatively, the patient was noted to have an erythematous area of fluctuance on her lower back, at the distal aspect of her surgical incision. She had no systemic symptoms, but an infectious workup revealed elevated ESR and WBC, consistent with a surgical site infection. She underwent surgical incision and drainage of her infection on August 2008 with implant retention. Intra-operatively, it was apparent that the infection extended both proximally and distally with several pockets of purulent material deep to fascia and surrounding bone. After thorough debridement of soft tissue, bone, and hardware, the proximal half of the wound was primarily closed in layers. The distal half of the incision was left open down to bone, and a negative pressure wound therapy (NPWT) vac was placed to fill the defect. Culture specimens obtained in the operating room grew Staphylococcus epidermidis. The patient continued NPWT for two months postoperatively until the wound granulated and healed completely by secondary intention. She also completed a six-week course of IV levofloxacin. She continued to have a full recovery at her post-operative visits through ten years of follow-up without evidence of recurrent infection or pseudoarthrosis.

On April 2023, sixteen years after her index spinal fusion surgery, she began experiencing new onset mid back pain. She was found to have an area of fluctuance at the distal aspect of her incision and presented to the outpatient office for an evaluation the next day. On exam, the patient was neurovascularly intact. There was a 3 cm fluid collection at the distal aspect of her surgical incision that was tender to palpation with purulent drainage. A bedside culture was performed with minor sterile debridement, which later grew few Staphylococcus hominis, and few anaerobic gram-positive rods. X-rays at the time showed intact hardware. MRI of the entire spine revealed two thoracolumbar abscesses, measuring 2 x 3.7 x 6.5cm on the left side, and 1 x 2.3 x 3.8 cm on the right side (Figure 3). A CT was obtained and demonstrated complete fusion without concern for pseudarthrosis (Figure 4). The patient proceeded with surgical intervention in the form of irrigation and debridement with removal of hardware.

Hospital Course

The patient went to the operating room on April 2023 for irrigation and debridement with T2-L3 removal of hardware and NPWT placement. Gross purulence was noted intraoperatively, as well as complete bony fusion

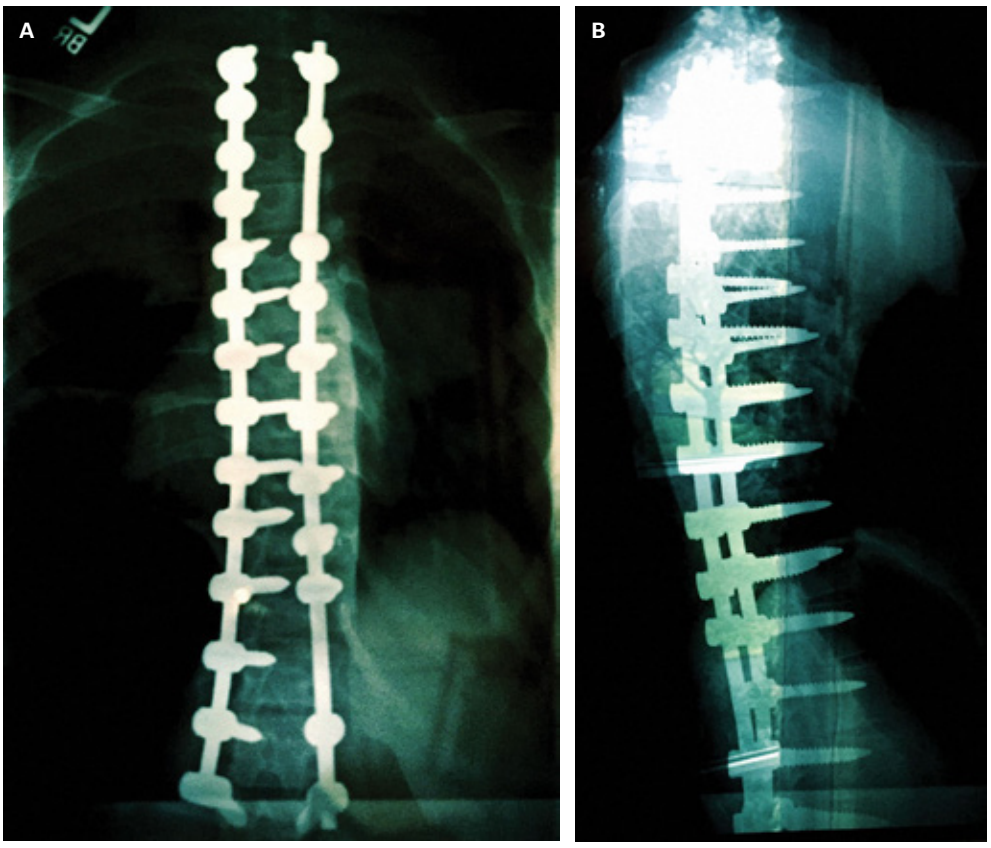

Figure 2. Postoperative thoracolumbar x-rays. **(A)** PA x-ray showing T2-L3 posterior spinal fusion; **(B)** Lateral x-ray of thoracolumbar spine showing T2-L3 (PSF).

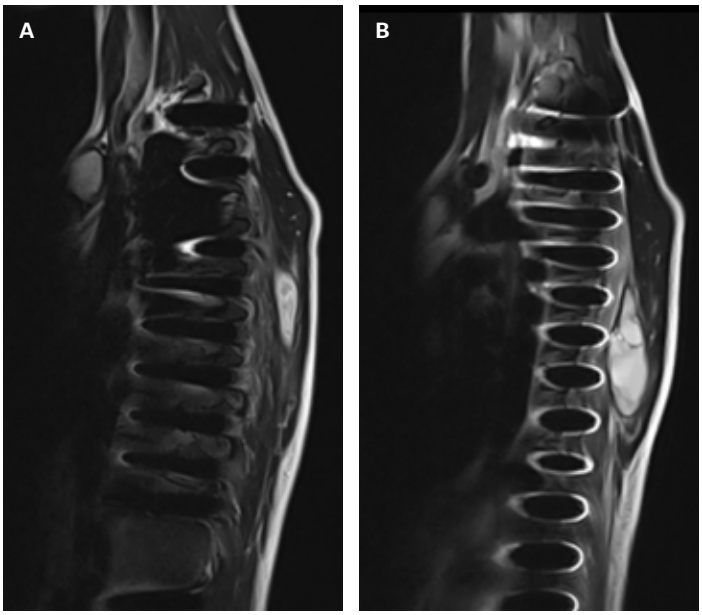

Figure 3. (A,B) Sagittal T2 MRI images of thoracolumbar spine showing two abscesses in the thoracic region.

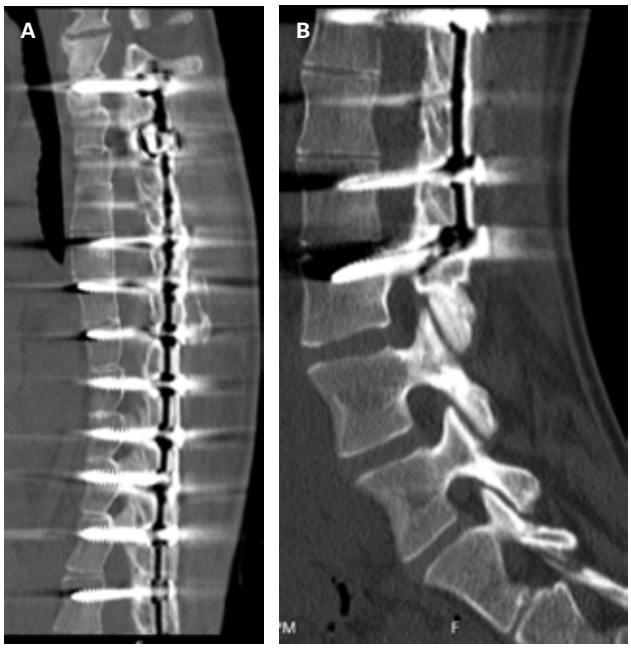

Figure 4. CT sagittal scan of **(A)** thoracic and **(B)** lumbar spine showing no evidence of hardware loosening or fracture.

from T2-L3. All hardware was removed, and non-viable tissue was extensively debrided. Following this, plastic surgery performed a complex wound closure using rotational myocutaneous flaps. An incisional vac was placed along with 3 drains.

The patient was started on empiric vancomycin and cefepime postoperatively, which was narrowed to daptomycin pending culture growth. Culture specimens obtained in the operating room grew Cutibacterium acnes. Her hospital course was complicated by acute blood loss anemia requiring blood transfusion. She was stable for discharge home on post-op day seven. She completed a six-week course of IV antibiotics. Following this, she completed a six-week course of oral doxycycline. The patient was closely followed by infectious diseases (ID), plastic surgery, and orthopedic surgery during this time, and was progressing appropriately. Thoracolumbar x-rays were obtained during each postoperative office visit, most recently on June 2024, showing interval removal of spinal hardware with stable bony alignment (Figure 5).

Discussion

We report a case of recurrent, delayed surgical site infection in a patient with AIS. Multiple studies have analyzed the rates of infection after scoliosis surgery, with infection rates ranging from 1% - 5% for AIS.7 Risk factors for infection after scoliosis surgery include non-idiopathic pathology, revision surgery, and utilizing growing constructs.8-9 The most isolated pathogens include Staph aureus, Staph epidermidis, and Cutibacterium acnes (C. acnes).10

C. acnes is a gram-positive anaerobic bacillus located in pilosebaceous glands, usually responsible for late postoperative surgical site infections (SSI) due to its indolent nature.11 Prior studies have described the prevalence of C. acnes in delayed infection after AIS.12, 13 A 2018 case control study was unable to identify any significant risk factors for the development of this infection.14

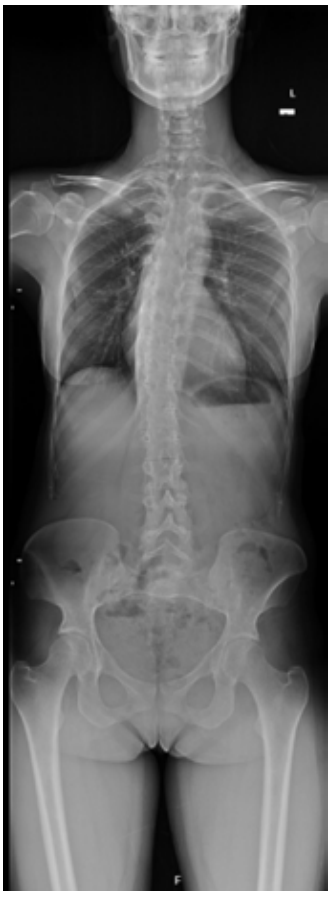

Figure 5. Standing thoracolumbar x-rays obtained two months postoperatively after removal of hardware.

Conclusion

This is a case report denoting the presence of two delayed surgical site infections in a patient that underwent thoracolumbar fusion for adolescent idiopathic scoliosis. Although this is a rare complication for this procedure, vigilance must be maintained on the part of the patient and providers to detect any changes in skin, pain, or neurological status in this patient population as delayed infection is always a possibility. Due to the indolent nature of the infectious process, a high clinical suspicion should be maintained to prevent the long-term sequelae of a missed deep SSI.

References

1. Parent S, Newton PO, Wenger DR. Adolescent idiopathic scoliosis: etiology, anatomy, natural history, and bracing. *Instr Course Lect.* 2005;54:529-36.

2. Gomez JA, Hresko MT, Glotzbecker MP. Nonsurgical Management of Adolescent Idiopathic Scoliosis. J *Am Acad Orthop Surg.* 2016;24(8):555-64.

3. Weinstein SL, Dolan LA, Wright JG, et al. Effects of bracing in adolescents with idiopathic scoliosis. N *Engl J Med.* 2013;369(16):1512-21.

4. Von Heideken J, Iversen MD, Gerdhem P. Rapidly increasing incidence in scoliosis surgery over 14 years in a nationwide sample. *Eur Spine J.* 2018;27(2):286-292.

5. Clark CE, Shufflebarger HL. Late-developing infection in instrumented idiopathic scoliosis. *Spine (Phila Pa* 1976). 1999;24(18):1909-12.

6. Smith JS, Shaffrey CI, Sansur CA, *et al.* Scoliosis Research Society Morbidity and Mortality Committee. Rates of infection after spine surgery based on 108,419 procedures: a report from the Scoliosis Research Society Morbidity and Mortality Committee. *Spine* (Phila Pa 1976). 2011;36(7):556-63.

7. Warner SJ, Uppstrom TJ, Miller AO, *et al.* Epidemiology of Deep Surgical Site Infections After Pediatric Spinal Fusion Surgery. *Spine* (Phila Pa 1976). 2017;42(3):E163-E168.

8. Cahill PJ, Warnick DE, Lee MJ, *et al.* Infection after spinal fusion for pediatric spinal deformity: thirty years of experience at a single institution. *Spine* (Phila Pa 1976). 2010; 35(12):1211-7.

9. Aleissa S, Parsons D, Grant J, *et al.* Deep wound infection following pediatric scoliosis surgery: incidence and analysis of risk factors. *Can J Surg.* 2011; 54(4):263-9.

10. Mackenzie, W.G. Stuart BS, MA1; Matsumoto, Hiroko MA1; Williams, Brendan A. BA1 *et. al.* Surgical Site Infection Following Spinal Instrumentation for Scoliosis: A Multicenter Analysis of Rates, Risk Factors, and Pathogens. *The Journal of Bone & Joint Surgery* 2013; 95(9):p 800-806

11. Kardile MP, Bains SS, Kuo CC, *et al.* Is Propionibacterium acnes becoming the most common bacteria in delayed infections following adolescent idiopathic scoliosis surgery? *Spine Deform.* 2021;9(3):757-767.

12. Gelderman SJ, Faber C, Kampinga GA, *et al.* A high prevalence of Cutibacterium acnes infections in scoliosis revision surgery, a diagnostic and therapeutic dilemma. *Spine Deform.* 2023. (2):319-327.

13. Hahn F, Zbinden R, Min K. Late implant infections caused by Propionibacterium acnes in scoliosis surgery. *Eur Spine J.* 2005; (8):783-8.

14. Swarup I, Gruskay J, Price M, *et al.* Propionibacterium acnes infections in patients with idiopathic scoliosis: a case-control study and review of the literature. *J Child Orthop.* 2018;12(2):173-180.

Trans-endplate Diffusion Across the Spectrum of Human Disc Degeneration

Brianna S. Orozco, BS[1,2]
Sarah E. Gullbrand, PhD[1,2]

[1]University of Pennsylvania, Philadelphia, PA

[2]Corporal Michael J. Crescenz VA Medical Center, Philadelphia, PA

Introduction

The intervertebral discs are the largest avascular structures in the body and depend primarily on diffusion via the vertebral endplates to receive nutrients and expel waste products.[1] Due to the avascularity of the intervertebral discs, it has been suggested that reduced disc nutrition is a significant contributor to the degenerative process.[1] Studies have shown that the reduction of disc nutrients can occur due to the calcification of the endplate that impairs diffusion to the disc.[2] However, alterations in trans-endplate transport across the spectrum of spinal degeneration and the relative contributions of pathology in the bone and cartilage endplate remain poorly understood. In this study, human cadaveric endplate samples were used to assess and correlate trans-endplate diffusion with the structure, composition, and mechanical function of the bone and cartilage endplate to determine factors affecting trans-endplate transport across the spectrum of disc degeneration.

Methods

Four lumbar spines (1 male, 3 female; age range: 50-70 years) were obtained from human cadavers (Science Care). T2-weighted MRIs were obtained for disc Pfirrmann grading and T2 mapping was used quantify nucleus pulposus (NP) T2 relaxation times.[3] Spinal motion segments (n = 20) were dissected. From each disc, tissue samples of nucleus pulposus and annulus fibrosus were obtained from each motion segment and underwent biochemical assays including DMMB to quantify GAG concentration, PicoGreen to quantify DNA, and hydroxyproline for collagen quantification. From these segments, two cylindrical cores (n = 18) with a diameter of 10 mm and an average thickness of 2.50 mm were obtained that included endplate-cartilage interface with trabecular bone. One core was used for passive diffusion experiments using a custom diffusion chamber (**Figure 1A**). The upstream chamber was loaded with 1.1 mg/mL of sodium fluorescein (MW = 367.27), and triplicates of the downstream chamber were collected every hour for six hours. Fluorescence was read via a microplate reader, and the concentration of the downstream chamber calculated based on a fluorescein standard curve. Total diffusion was quantified by calculating the area under the curve (AUC). Endplate cores were then fixed and μCT scanned with a resolution of 7.40 μm to evaluate bone endplate morphometry and cartilage thickness following repeated μCT after staining the cores overnight with Lugol's solution.

Results

Diffusion experiments demonstrated significant variability in trans-endplate diffusion across donors and spinal levels within the same donor (**Figure 1B**). Correlations between NP T2 and diffusion revealed a bimodal relationship between diffusion and disc health. When discs were stratified further by Pfirrmann Grade, there was a significant positive linear correlation between NP T2 and diffusion for Pfirrmann Grade 2 discs. There was, however, a trend towards increasing diffusion with decreasing NP T2 relaxation time in Pfirrmann Grade 3 discs (**Figure 2A**). Comparison of NP GAG content between samples with low

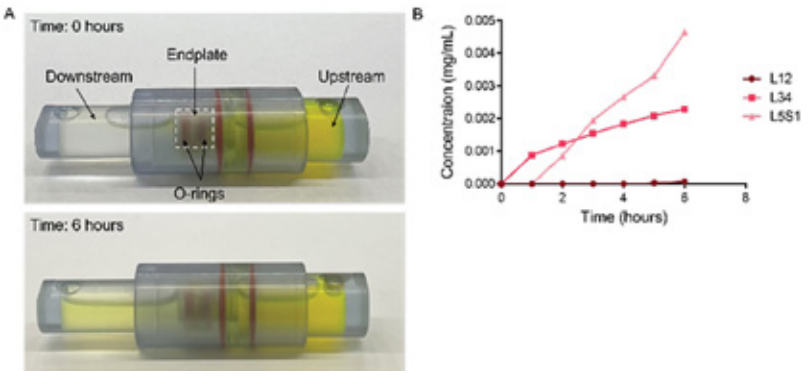

Figure 1. (A) The passive diffusion chamber utilized; **(B)** Example concentration vs time curves for three levels from a single donor.

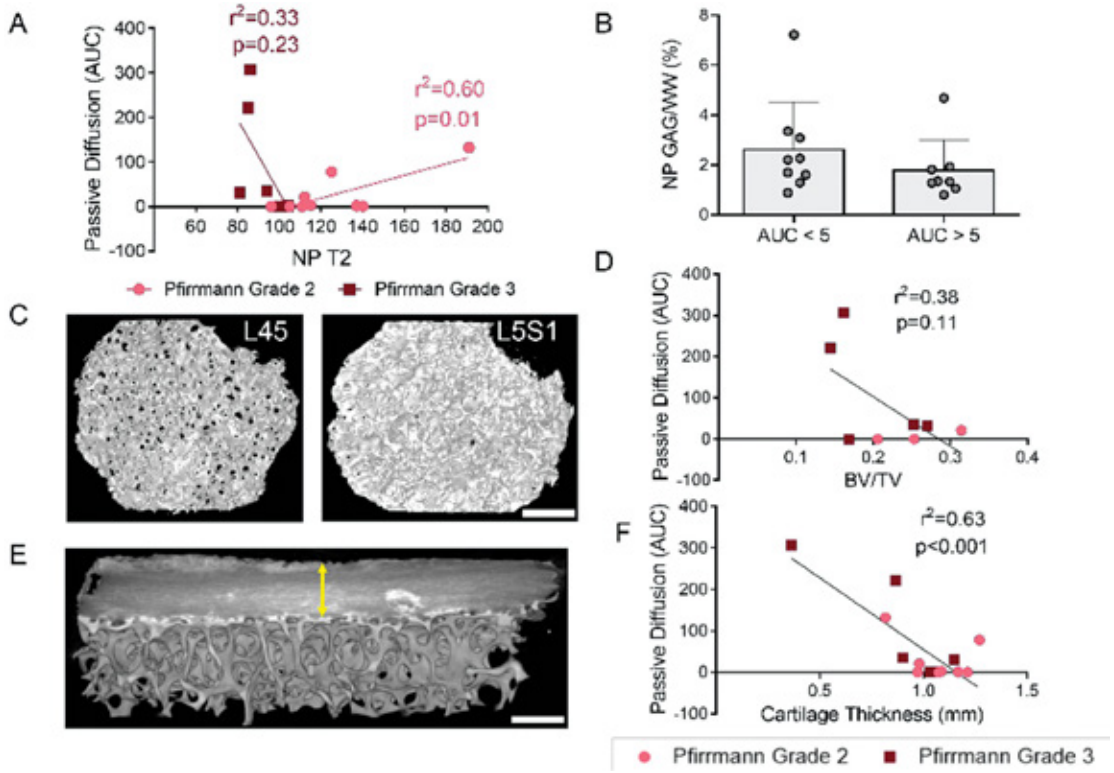

Figure 2. (A) Passive Diffusion quantified by area under the curve (AUC) vs. NP T2; **(B)** Nucleus Pulpous GAG Content compared to AUC; **(C)** Images of μCT that show porosity of samples among the same donor; **(D)** Passive Diffusion (AUC) not correlated with BV/T; **(E)** Image of a endplate cross-section showing stained cartilage endplate (indicated by the arrow) with Lugol's Solution; **(F)** Passive Diffusion (AUC) correlated with cartilage thickness. Scale = 0.5 mm.

(AUC < 5) and high (AUC > 5) diffusion demonstrated that NP GAG content trended lower in samples with high diffusion (**Figure 2B**). 3D µCT reconstructions demonstrated substantial variability in bone endplate porosity across levels even from the same donor, which could affect passive diffusion (**Figure 2C**). However, no significant correlation was found between endplate bone volume fraction (BV/TV) and passive diffusion (**Figure 2D**). Cartilage endplate thickness measured from Lugol's enhanced µCT (**Figure 2E**) was found to significantly inversely correlate with passive diffusion, demonstrating that as cartilage endplate thickness increases, passive diffusion decreases (**Figure 2F**).

Discussion

Our results suggest that trans-endplate diffusion is not altered in a linear fashion across the spectrum of disc degeneration, as both healthy (high NP T2) and degenerative (low NP T2) discs exhibited high trans-endplate diffusion—a trend also observed in prior human MRI studies of diffusion into the disc.[4] A limitation of the current study is that our sample set contained primarily moderately degenerative discs. Therefore, we are currently expanding our sample set to include more healthy and severely degenerative discs to more rigorously quantify the spectrum of disease. Our data also suggests that cartilage endplate thickness is the main structural factor affecting solute transport under passive diffusion. Prior studies have demonstrated the effect of cartilage endplate composition on diffusion. This is currently being investigated in our ongoing work in addition to cartilage endplate mechanical properties.[5] Interestingly, only weak correlations between diffusion and bony endplate density were observed, in contrast to our prior work in a rabbit disc degeneration model.[6] It is possible that the bony endplate may have a greater impact on disc nutrition during convective transport. It has shown that dynamic loading induced convective flow can augment transport into the disc, and future work will focus on understanding the endplate structure-function properties conducive to enhanced transport under convective flow.[7]

References

1. Maroudas A, Stockwell R, Nachemson A, Urban J. 1975. Factors involved in the nutrition of the human lumbar intervertebral disc: cellularity and diffusion of glucose in vitro. *Journal of Anatomy*. 120:113–130.

2. Benneker LM, Heini PF, Alini M, *et al.* 2005. 2004 Young Investigator Award Winner: vertebral endplate marrow contact channel occlusions and intervertebral disc degeneration. *Spine* (Phila. Pa. 1976). 30:167–73

3. Ashinsky, B. G., Gullbrand, S. E., Wang, C., *et al.* (2021). Degeneration alters structure-function relationships at multiple length-scales and across interfaces in human intervertebral discs. *Journal of Anatomy*, 238(4), 986-998.

4. Rajasekaran, S., Babu, J. N., Arun, R., *et al.* (2004). ISSLS prize winner: a study of diffusion in human lumbar discs: a serial magnetic resonance imaging study documenting the influence of the endplate on diffusion in normal and degenerate discs. *Spine*, 29(23), 2654-2667.

5. Dolor, A., Sampson, S. L., Lazar, A. A., *et al.* (2019). Matrix modification for enhancing the transport properties of the human cartilage endplate to improve disc nutrition. *PloS one*, 14(4), e0215218.

6. Ashinsky, B. G., Bonnevie, E. D., Mandalapu, S. A., *et al.* (2020). Intervertebral disc degeneration is associated with aberrant endplate remodeling and reduced small molecule transport. *Journal of Bone and Mineral Research*, 35(8), 1572-1581.

7. Sampson, S. L., Sylvia, M., & Fields, A. J. (2019). Effects of dynamic loading on solute transport through the human cartilage endplate. *Journal of biomechanics*, 83, 273-279.

U·P·O·J

Dropped Head Syndrome: A Case of Post-Surgical Distal Junctional Kyphosis and Chronic Infection

Bradley Osemwengie, MD[1]
Jennifer X. Hong, BA[2]
Tensae Assefa, MD[1]
Chinedu Okafor, MD[1]
Amrit Khalsa, MD[1]

1Department of Orthopaedic Surgery University of Pennsylvania

2Perelman School of Medicine at the University of Pennsylvania

Introduction

As the adage goes in spine surgery, 'Either you are creating deformity or correcting it.' Post-surgical deformity is a complication of spinal surgery. One of these complications is proximal junctional kyphosis, where segments of the spine proximal to a fusion construct begin to develop a kyphotic deformity.[1] Another less frequent complication is distal junctional kyphosis (DJK), where the spinal kyphotic deformity develops distal to the fusion construct. DJK is defined as the development of a kyphotic angle over 10 degrees below a fusion construct.[2] A risk factor to developing DJK is malalignment of the cervical spine. This can be preoperatively measured by an increased value of the C2-7 sagittal vertical axis (SVA).[3,4] The C2-7 Sagittal Vertical Axis (SVA) is calculated by measuring the horizontal distance between the posterosuperior corner of the C7 vertebral body and a plumb line drawn from the center of the C2 vertebral body. Normal values should be less than four centimeters. Another risk factor for developing DJK is the exclusion of the sagittal stable vertebra in the fusion construct.[2] The sagittal stable vertebra is defined as the first vertebra touched by the posterior sacral vertical line (PSVL).

Infection can also accentuate this deformity because the osseous elements of the spine lose their structural integrity, thereby exacerbating the kyphotic collapse. Large angular corrections of sagittal deformity can occur with the use of posterior spinal osteotomies.[5] These procedures resect a portion of bone from the spine, and the resultant defect is 'closed down' and fixed into place with hardware, thereby restoring the sagittal axis of the spine. A concern with instrumented osteotomies in the setting of infection is with placing fresh spinal hardware into a contaminated surgical field. Another concern is with the adequacy of fixation after deformity correction due to the poor quality of infected bone. We present a case of patient with 'Dropped Head Syndrome' deformity correction in the setting of distal junctional kyphosis after multiple spinal procedures in the setting of chronic infection.

Case Presentation

A 73-year-old female patient presented to an outside surgeon with one year of progressive neck pain that radiated to her left head, eye, shoulder, and left arm. She reported weakness in holding her head up and needing to lay back in the afternoon to get relief. Physical therapy provided no relief and epidural injections provided relief for only a few weeks. The patient had a past surgical history of C5-6 cervical fusion performed in 1990.

Physical exam revealed bilateral deltoid weakness and very limited range of motion of the cervical spine. The patient could attain ten degrees of flexion and essentially had no extension or lateral flexion. A cervical MRI revealed large facet changes at C4-5 and C6-7 with associated degenerative disk disease, and the patient was diagnosed with cervical radiculopathy (Figure 1). On July 2021, the patient underwent left hemilaminectomies and posterior instrumented fusion (PSF) of C4-7 (Figure 2).

Two weeks later, the patient began experiencing pain over the surgical incision site. After suture removal, she developed severe swelling, redness, and tenderness at the site. Physical exam revealed fluctuance at the inferior portion of the incision, which ruptured and drained greenish/yellowish fluid the following day. Two days later, the patient underwent incision and drainage. No purulence was found intra-operatively. Operative cultures grew methicillin-sensitive Staphylococcus aureus (MSSA). Patient was prescribed a six-week course of IV cefazolin.

At 6 months postop from the index laminectomy and fusion, the patient had improved clinically but was still experienced persisting issues. She reported daily worsening neck pain that began mid-afternoon with associated headaches that limited her physical activity. She also noted a sensation of prominent hardware and diarrhea due to her suppressive antibiotics. The patient then underwent removal of posterior surgical instrumentation. Upon exploration, the previously instrumented regions appeared fused.

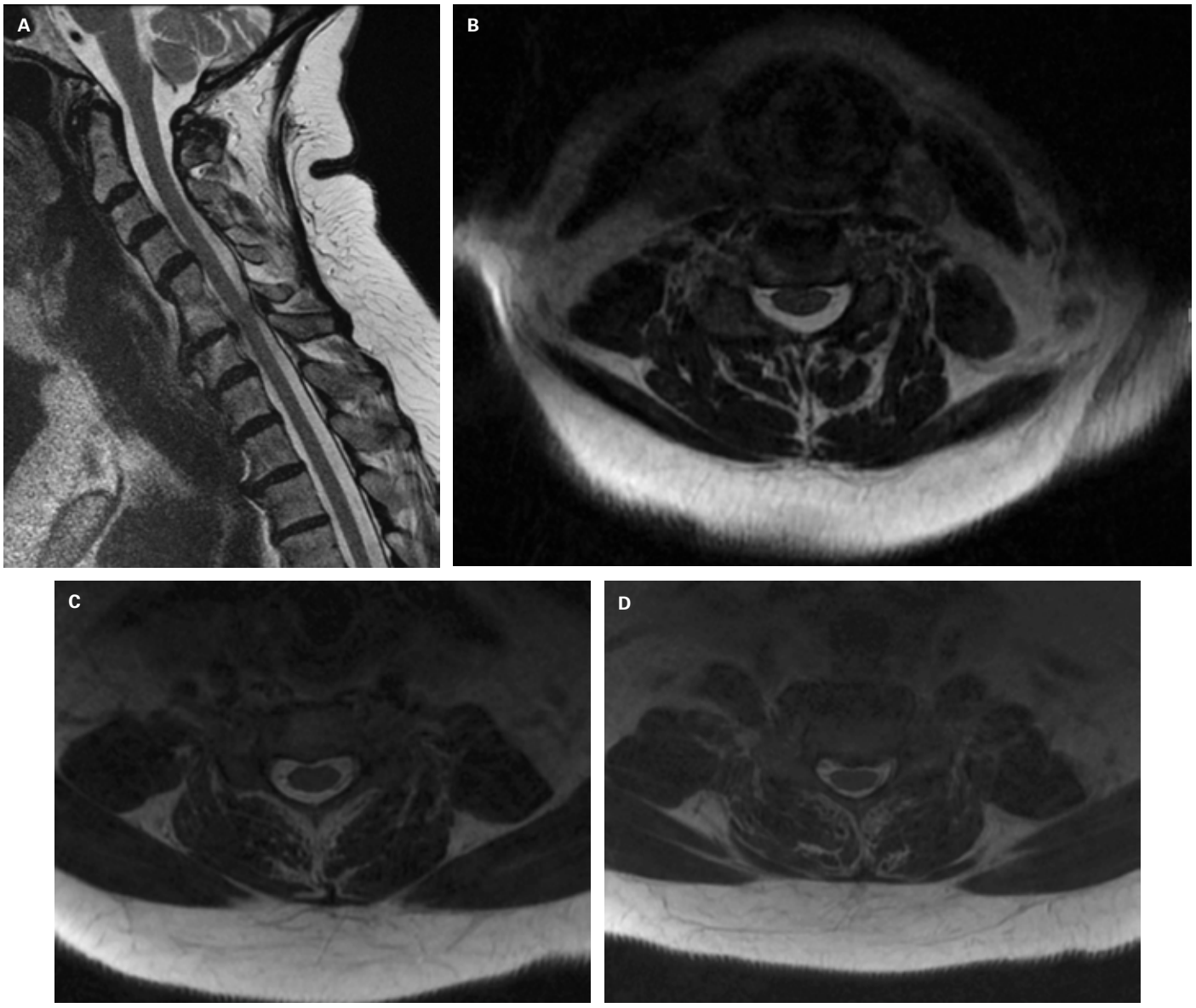

Figure 1. MRI of the cervical spine. **(A)** T2 sagittal MRI of the cervical spine showing evidence of spinal canal narrowing at C5/6 and C6/7. C 5/6 appear to be auto fused; **(B)** Axial cut at C4/5 level showing patent spinal canal; **(C)** Axial cut at C5/6 showing mild posterior disc bulge with mild spinal canal narrowing; **(D)** Axial cut at C6/C7 showing moderate disc bulge with moderate spinal canal narrowing.

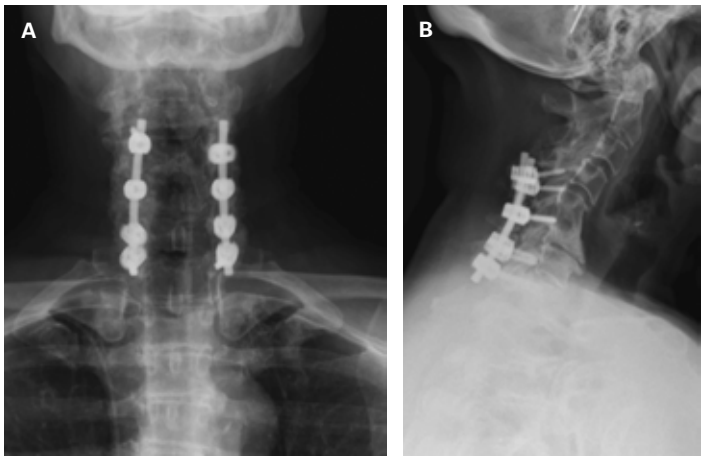

Figure 2. (A) AP and **(B)** lateral of the cervical spine showing C4-C7 posterior spinal fusion with hardware in adequate position.

One year postop from the removal of hardware, the patient presented again with worsening neck pain radiating into the left arm, left thumb, and right shoulder. She reported associated headaches and the need to support her head with her hand suggesting ongoing cervical instability. The pain worsened throughout physical therapy and was not relieved by a soft cervical collar. Reclining helped to alleviate her pain. Cervical x-rays revealed a fixed kyphotic deformity at C4-5 (Figure 3). Two years after the index C4-C7 PSF, the patient underwent surgery. The plan for surgery was to perform facetectomies to increase the mobility of the cervical spine. The patient would then undergo and anterior fusion with an extended posterior instrumented fusion. Intraoperatively, however, the C3 through T1 vertebrae were found to be completely fused, and the surgeon determined that deconstructing the

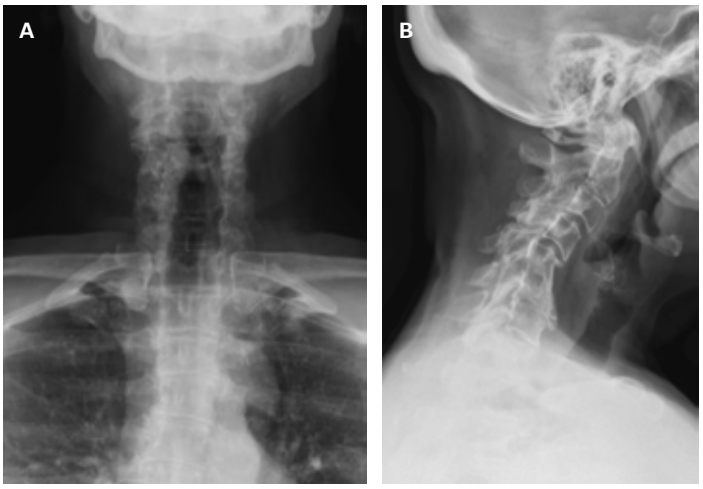

Figure 3. (A) AP and **(B)** lateral of the cervical spine showing removal of PSF. There is a fixed kyphotic deformity at C4-5.

existing fusion would create unnecessary risk. Instead, the patient underwent C2-T3 posterior spinal fusion (PSF) with C2/3 and T2/3 posterior column osteotomies (Figure 4).

Five weeks after the revision fusion procedure, the patient developed debilitating interscapular stabbing pain radiating to her armpits and diaphragm and a progressive head drop. Physical exam revealed two small subcutaneous fluid collections. Cervical X-rays a new kyphotic deformity distal to her cervicothoracic instrumentation and pullout of the T2 and T3 pedicle screws.(Figure 5). MRI revealed fluid adjacent to T2 and T3 vertebral bodies concerning for discitis, osteomyelitis, and epidural abscess (Figure 6). With these findings, the patient underwent posterior cervical irrigation and debridement. Purulence was encountered deep to the fascia. Operative cultures grew MSSA and the patient was placed on six weeks of IV cefazolin.

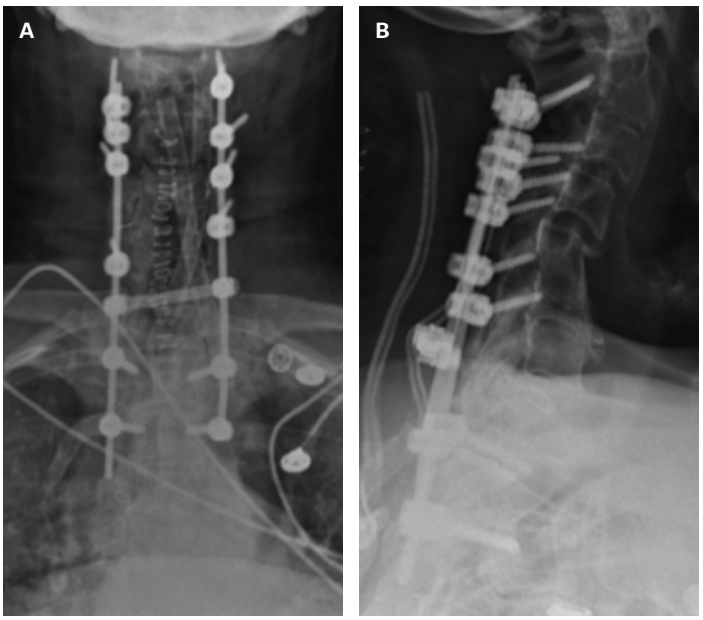

Figure 4. (A) AP and **(B)** lateral of the cervical spine showing a PSF extending from C2-T3.

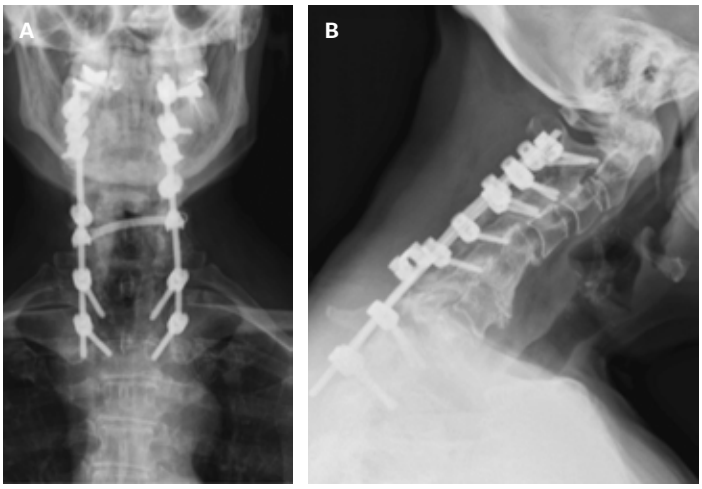

Figure 5. (A) AP and **(B)** lateral of the cervical spine showing a PSF extending from C2-T3 with a new kyphotic deformity distal to the instrumentation. Pullout of the T2 and T3 pedicle screws is also noted.

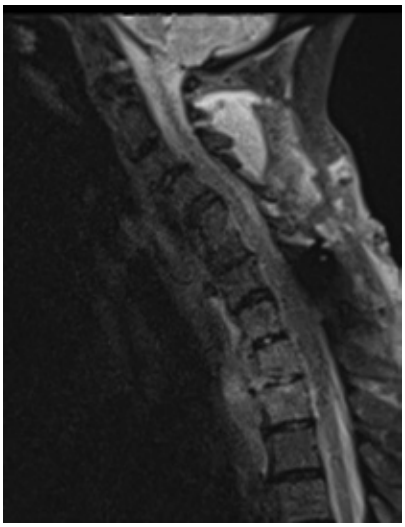

Figure 6. STIR sagittal MRI of the cervical spine showing increase in signal intensity in the vertebral bodies and discs of T2 and T3 as well as a fluid collection concerning for osteomyelitis, discitis, and epidural abscess.

Two months after the posterior cervical irrigation and debridement, the patient reported continued persistent debilitating neck pain and was referred to the orthopaedic surgery department. The neck pain radiated into her lower back and limited her upward and horizontal gaze, which impeded her activities of daily living as she was unable to remain upright for more than twenty minutes at a time before needing to recline due to pain. Cervical X-rays showed multilevel degenerative changes with post-surgical changes spanning C2-T3 with interval osteolysis, screw pull-out at T2-T3, and 70 degrees of kyphosis spanning C2-T4 (Figure 7). CT of the cervical and upper thoracic spine also displays a kyphotic deformity, osteolysis of the vertebral bodies, as well as pedicle screw cutout in the osteolytic bone (Figure 8).

The decision was made to pursue surgical management in the form of C2-T10 posterior spinal fusion, lower cervical and thoracic osteotomies, and a T3 pedicle subtraction osteotomy. Prior to positioning, neuro-monitoring ran baseline sensory and motor evoked potentials which showed baseline deficits. Posterior column osteotomies

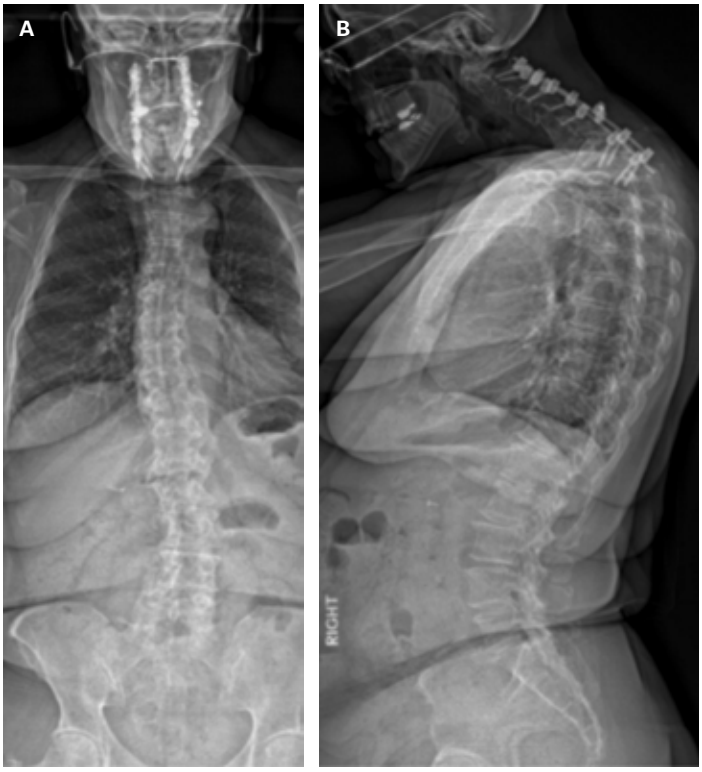

Figure 7. (A) AP and **(B)** lateral of the entire spine showing the C2-T3 PSF with 70 degrees of kyphosis spanning from C2-T4.

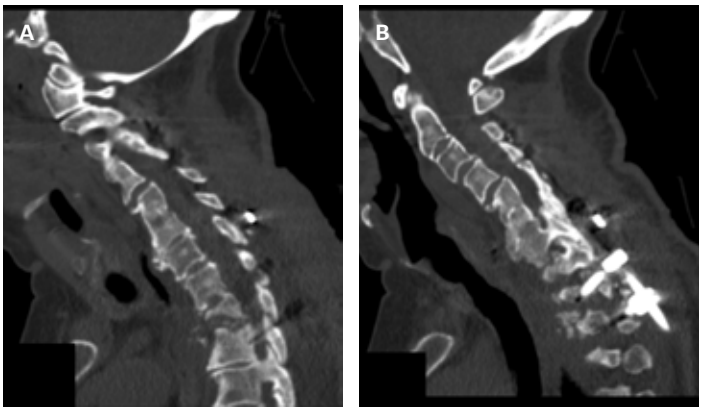

Figure 8. CT of the cervical and upper thoracic spine. **(A)** Mid-sagittal view showing kyphotic deformity and osteolysis of the vertebral bodies; **(B)** Parasagittal view showing pedicle screw cutout in the osteolytic bone.

were performed at every segment spanning C7 to T10. Next, the previous C2-T3 hardware was identified. Pedicle screws were placed at T1 and T4-10. The prior cervical rods and the loosened bilateral T2 and T3 screws were removed. The bilateral C2 screws and cervical lateral mass screws were all well-fixated and left in place. The T3 pedicle subtraction osteotomy was the next step. The bilateral T3 pedicles were resected. The spinal cord and bilateral T2 and T3 nerve roots were visualized directly and shown to be free of compression during this step. Two transition rods were then placed and a compression reduction maneuver was performed across the T3 region. Neuromonitoring was stable, and then screws were locked into place. The C5 to T10 facet joints and lamina were decorticated and bone graft was placed to help with the fusion. Vancomycin powder was applied into the surgical bed. Plastic surgery then performed a layered closure and the incision was closed with an incisional vacuum.

At 6 weeks follow-up, the patient reported improving post-operative pain and numbness to the occiput and surrounding the incision. Physical exam revealed a well-healing incision with no drainage, erythema, or warmth. X-ray of cervical and thoracic spine revealed spinal hardware in adequate position with no evidence of loosening or failure (Figure 9). The patient was placed on chronic suppressive doxycycline by the infectious disease team.

Discussion

Distal junctional kyphosis can be a complication of spinal surgery in the setting of infection as well as fusion constructs that do not extend far enough distally. Dropped head syndrome can ensue if the kyphotic deformity progresses further leading to significant patient morbidity. Dropped head syndrome occurs when there is a severe kyphotic deformity in the cervicothoracic spine.6 Risks and benefits should be weighed as far as correcting deformity and inserting instrumentation in the setting of infection due to concerns of seeding hardware.

A variety of posterior spinal osteotomies exist for the correction of spinal deformity. Ponte or Smith-Peterson osteotomies are used for minor corrections of sagittal imbalance and can be used at multiple spinal levels for roughly ten degrees of correction per level.7 Pedicle subtraction osteotomies at the apex of the kyphosis provide a reliable way to achieve sagittal plane deformity correction

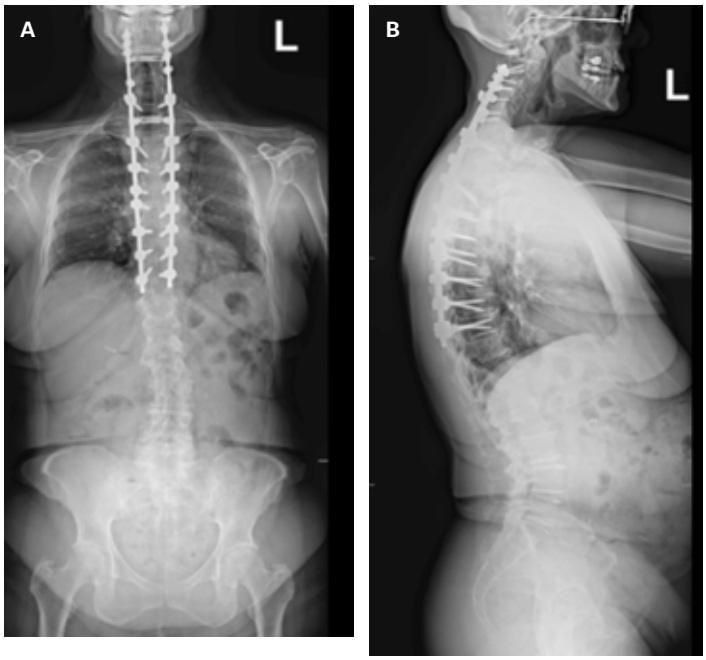

Figure 9. (A) AP and **(B)** lateral of the entire spine showing the C2-T10 PSF showing hardware in appropriate placement and a marked improvement of kyphosis.

of up to forty degrees at a singular level.8 Care must be taken to ensure pedicle screws provide adequate purchase in bone that may be compromised due to osteoporosis or infection.

Consideration should also go into whether the osteotomies and instrumentation should occur in one stage versus two stages in the setting of infection. Performing the entire corrective surgery in one stage limits operating room exposure and is less of a physiologic insult to the patient. However, a one stage operation risks seeding hardware. A two-stage procedure would give the patient more time to clear the infection in between procedures but risks a period of spinal instability in the interim. In the case of a severe kyphotic deformity and infected vertebral osseous structures, there is a concern that the bone integrity after removal of instrumentation would not support physiological demands. This could lead to further progression of deformity and neurological complications from cord or nerve root compression. The provider should also pay special attention to neuromonitoring signals as corrections of chronic deformities can precipitate neurologic damage. Finally, adequate postoperative antibiotic coverage in the setting of infection should be administered to minimize the chance of seeding hardware.

Conclusion

In the setting of a multiply-revised posterior spinal construct in the setting of chronic infection and significant distal junctional kyphotic spinal deformity, a thoughtful approach should be used to ensure adequate spinal stability and deformity correction while preventing neurological deficits in the process. This case illustrates the complex decision-making that goes into providing adequate care to a patient with significant spinal pathology, deformity, and infection to prevent deformity progression and give her the best chance at improved quality of life.

References

1. Dubousset J, Diebo BG. Proximal Junctional Kyphosis in Modern Spine Surgery: Why Is it So Common?. *Spine Surg Relat Res*. 2022;7(2):120-128. Published 2022 Jun 28.

2. Sawada Y, Takahashi S, Terai H, *et al.* Short-Term Risk Factors for Distal Junctional Kyphosis after Spinal Reconstruction Surgery in Patients with Osteoporotic Vertebrae. *Asian Spine J*. 2024;18(1):101-109.

3. Lee JJ, Park JH, Oh YG, *et al.* Change in the Alignment and Distal Junctional Kyphosis Development after Posterior Cervical Spinal Fusion Surgery for Cervical Spondylotic Myelopathy - Risk Factor Analysis. *J Korean Neurosurg Soc*. 2022;65(4):549-557.

4. Passias PG, Horn SR, Lafage V, *et al.* Effect of age-adjusted alignment goals and distal inclination angle on the fate of distal junctional kyphosis in cervical deformity surgery. *J Craniovertebr Junction Spine*. 2021;12(1):65-71.

5. Kose KC, Bozduman O, Yenigul AE, *et al.* Spinal osteotomies: indications, limits, and pitfalls. *EFORT Open Rev*. 2017;2(3):73-82. Published 2017 Apr 27.

6. Martin AR, Reddy R, Fehlings MG. Dropped head syndrome: diagnosis and management. *Evid Based Spine Care J*. 2011;2(2):41-47.

7. Hyun SJ, Kim YJ, Rhim SC. Spinal pedicle subtraction osteotomy for fixed sagittal imbalance patients. World *J Clin Cases*. 2013;1(8):242-248.

8. Gupta MC, Gupta S, Kelly MP, *et al.* Pedicle Subtraction Osteotomy. *JBJS Essent Surg Tech*. 2020;10(1):e0028.1-11. Published 2020 Feb 3.

Sports

U·P·O·J

Tips & Tricks: Tips and Tricks: Use of a Spinal Needle for Partial Meniscectomy of a Bucket Handle Meniscus Tear

Caroline Granruth, MD MPH
Heather Kellett, MD
Sand Mastrangelo, MD
Brian Sennett, MD

Department of Orthopaedic Surgery
University of Pennsylvania

Background

Meniscal tears are common intraarticular injuries resulting from forceful twisting or hyperflexion of the knee. Bucket handle tears, in particular, account for 10-19% of these injuries and frequently occur with a concomitant ACL injury. Most bucket handle meniscus tears involve the medial meniscus.[8]

In addition to the pain and mechanical symptoms associated with other, more common meniscal injuries, bucket handle tears can cause intermittent episodes of locking of the knee joint secondary to displacement of the torn fragment into the intercondylar notch. This fragment can also flip back into its anatomic position, which provides transient unlocking of the joint.

MRI is both a sensitive and specific modality for detecting bucket handle meniscus tears. These injuries typically consist of a vertical or oblique tear involving the posterior horn of the meniscus that extends longitudinally through the body and anterior horn. As a result, the inner meniscal fragment can be seen displaced into the intercondylar notch. Several signs on MRI are useful in detecting bucket handle meniscus tears including the "absent bow tie sign" in the coronal plane and the "double PCL sign" in the sagittal plane.[4]

Whenever possible, meniscal repair is the operative treatment of choice for meniscus tears. This is especially true for bucket handle tears which typically involve a large portion of the meniscus.[3] However, certain characteristics make some of these bucket handle tears more suitable to partial meniscectomy rather than repair. These include a tear occurring in the avascular zone, a tear associated with underlying degenerative changes, inability to anatomically reduce the displaced fragment during attempted repair, and significant deformation of the torn fragment.[1,9]

Arthroscopic partial meniscectomy and resection of the bucket handle tear is a commonly performed, yet often challenging, procedure. Various techniques have been described for the resection and removal of the bucket handle tear which occasionally require an accessory, posteromedial portal to optimize visualization.1 Other described techniques require additional equipment not typically utilized during a standard partial meniscectomy such as a beaver blade or suture punch.[2,6,7]

The use of a spinal needle—an inexpensive, readily available instrument used in standard diagnostic arthroscopy - was first described in 2002.[5] This technique guide seeks to expand on the originally described technique with use of intra-operative images for guided understanding.

Surgical Technique

The patient is positioned supine on a regular OR table with a lateral post located 2-3 finger breadths proximal to the knee flexion crease. The extremity is prepped and draped in usual sterile fashion. The knee is injected with local anesthetic. Portal sites are marked using the lateral tibial plateau, lateral edge of the patellar tendon, and inferior border of patella as landmarks for the lateral portal. The medial portal is marked directly across from the lateral portal. Local anesthetic is injected at the portal sites. The lateral portal is incised, dilated with a hemostat, and the arthroscope is placed into the knee joint. A spinal needle is used to localize the height and trajectory of the medial portal just superior to the medial meniscus. The medial portal is incised, dilated with a hemostat, and the probe is inserted. A diagnostic arthroscopy of the knee is first performed to identify and characterize the tear (Figure 1A-B) as well as any additional intra-articular pathology.

Once the decision has been made to proceed with partial meniscectomy rather than repair, the first step is to detach the "handle" from its attachment site on the anterior horn using a "predator" (Figure 1C). This creates a flap which allows the tear to be better grasped. The arthroscope is then switched from the lateral portal to the medial portal to improve visualization of the posterior horn. A "wolf" grabber is then inserted in the ipsilateral portal with the tooth near the end of the anterior horn to control the flap. Maintaining a firm grasp on the flap, the grabber is twisted

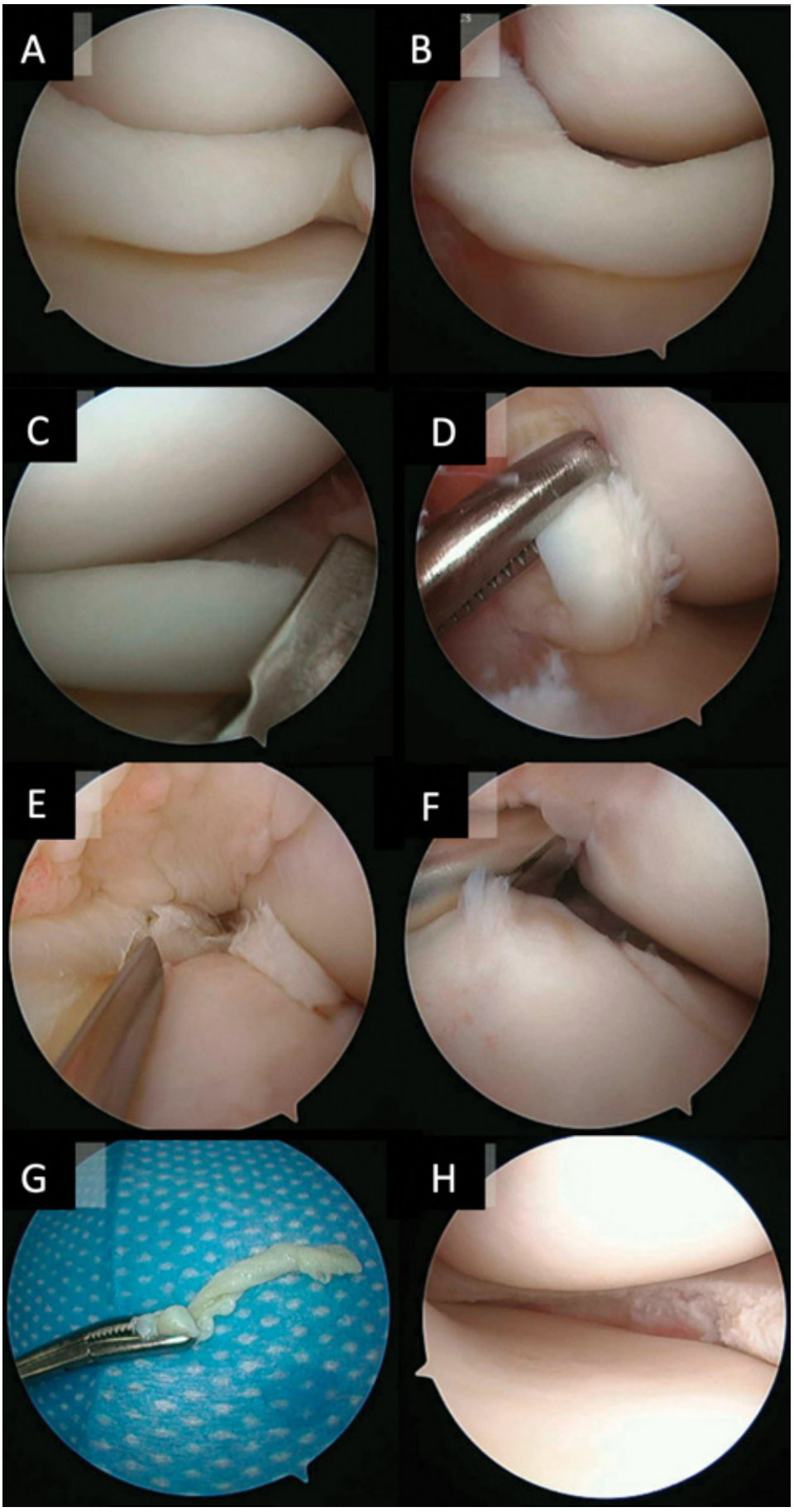

Figure 1. Arthroscopic partial meniscectomy of bucket handle meniscus tear. **(A-B)** Bucket handle meniscus tear on diagnostic arthroscopy; **(C)** Using "preadtor" to detach the "handle" from its attachment site on the anterior horn; **(D)** Using the "wolf" grabber to twist the flap away from the posterior horn; **(E-F)** Repeatedly passing spinal needle into flap of meniscus at its posterior attachment site until fully release; **(G)** Removal of the torn meniscus through the medial portal; **(H)** Using curved shaver to contour the remaining meniscus.

either clockwise or counterclockwise in order to twist the flap of meniscus away from the posterior horn (Figure 1D). This is continued until a condensed shape of meniscal tissue is formed at the base of the posterior horn that can be easily removed.

Under arthroscopic visualization, the same 18-gauge spinal needle is inserted on the ipsilateral side, one-third of the way from the medial border of the patella to the medial portal, and one centimeter higher than the medial portal. The beveled tip of the spinal needle is repeatedly passed into the condensed flap of meniscus at its posterior attachment site while continuing to twist the flap with the wolf grabber until it is released (Figure 1E-F). The flap of tissue can be removed from the joint through the medial portal with the "wolf" grabber (Figure 1G). To complete the partial meniscectomy, a curved shaver is used to contour and smooth the remaining meniscus (Figure 1H).

Conclusion

This technique uses portals that have already been established, and instruments that have been opened for the diagnostic arthroscopy. The meniscal flap is twisted into a tight, condensed shape, allowing for controlled detachment with the spinal needle. Removing the tear in one piece rather than dividing it not only improves efficiency as there are no small fragments to retrieve, but also minimizes the formation of postoperative loose bodies. This technique is an inexpensive, effective, and reliable method for resection of a bucket handle meniscus tear.

References

1. Ahn JH, Oh I. Arthroscopic partial meniscectomy of a medial meniscus bucket-handle tear using the posteromedial portal. *Arthroscopy*. 2004;20(7):e75-e77.

2. Binnet MS, Gürkan I, Cetin C. Arthroscopic resection of bucket-handle tears with the help of a suture punch: a simple technique to shorten operating time. *Arthroscopy*. 2000;16(6):665-669.

3. Costa GG, Grassi A, Zocco G, *et al.* What Is the Failure Rate After Arthroscopic Repair of Bucket-Handle Meniscal Tears? A Systematic Review and Meta-analysis. *Am J Sports Med*. 2022;50(6):1742-1752.

4. Dorsay, T.A., Helms, C.A. Bucket-handle meniscal tears of the knee: sensitivity and specificity of MRI signs. *Skeletal Radiol*. 2003; 32:266-272.

5. Lehman CR, Meyers JF. Needle-assisted arthroscopic meniscal debridement. *Arthroscopy*. 2002;18(8):948-949.

6. Mullins RC, Drez DJ Jr. Resection of bucket-handle meniscus tears: a simple technique using a Beaver blade. *Arthroscopy*. 1992;8(2):267-268.

7. Paksima N, Ceccarelli B, Vitols A. A new technique for arthroscopic resection of a bucket handle tear. *Arthroscopy*. 1998;14(5):537-539.

8. Shakespeare DT, Rigby HS. The bucket-handle tear of the meniscus: a clinical and arthrographic study. *J Bone Joint Surg Br*. 1983; 65:383–387.

9. Weiss CB, Lundberg M, Hamberg P, *et al.* Non-operative treatment of meniscal tears. *J Bone Joint Surg Am*. 1989;71(6):811-822.

Motion Analysis and Biomechanical Evaluation Following Anterior Cruciate Ligament Reconstruction

Kevin M. Landrum, BS[1]
David P. VanEenenaam, BS[1]
Elliot Greenberg, PT, DPT, PhD[2]
Valentina Graci, PhD[3,4]
Theodore J. Ganley, MD[1]

[1]Division of Orthopaedics, Children's Hospital of Philadelphia, Philadelphia, PA

[2]Department of Physical Therapy, Specialty Care and Surgery Center, Bucks County, The Children's Hospital of Philadelphia, Chalfont, Pennsylvania

[3]Center for Injury Research and Prevention, The Children's Hospital of Philadelphia, 2716 South Street, Philadelphia, PA

[4]School of Biomedical Engineering, Science and Health Systems, Drexel University, Philadelphia, PA

Introduction

Annually, it is estimated over 3.5 million young athletes in the U.S. sustain sports-related injuries.[1,2] The knee is the second most common site of injury in athletes aged 15-25, resulting a substantial surgical and economic burden on both patients and healthcare systems.[2,3] Anterior cruciate ligament (ACL) ruptures, many of which occur via a non-contact mechanism, make up over 25% of knee injuries in high school athletes and require surgical intervention and prolonged postoperative rehabilitation before return to sport.[4] Motion analysis of biomechanical risk factors for primary, or repeat ACL injuries have been a topic of extensive research within sports medicine, given the opportunity to mitigate further injury and improve recovery.[5] This paper aims to detail recent progress and established views (2020-2024) regarding biomechanical evaluations and motion analysis post-ACL reconstruction (ACLR), while highlighting necessary points for future investigation.

Return to Sport Analysis and Longitudinal Investigation

Assessments at Return-To-Sport Time Point

Return to sport clearance (RTS), or the clearance granted to begin progression back to pre-injury activities, gradually introduces high-intensity stress on the new ACL graft, which may cause limb movement pattern asymmetry. Losciale et al. found that subjects post-ACLR, regardless of meeting RTS criteria, defined as achieving satisfactory strength and functional performance, did not show normalized landing mechanics on double-leg landing, and some achieved limb symmetry more by unloading the uninjured leg rather than loading the injured leg to the same standard of their uninjured limb.[6] Vij et al. evaluated sex-specific biomechanical changes post-ACLR, showing females exhibited smaller hip adduction moments and larger average knee joint extension moments, potentially increasing risk factors for reinjury.[7]

There have been recent efforts in validating 2D motion analysis systems, which are generally simpler to clinically implement and operate than 3D motion analysis systems.[8,9] A 2022 study performed by Di Paolo et al. validated a 2D scoring system for single leg hop tests that effectively identified stiffer landing patterns which have been correlated with increased injury and reinjury risk.[8] This system offers an adjunct to limb symmetry performance metrics that incorporates movement quality assessments at the time of RTS decision making.

Despite passing limb symmetry based RTS criteria, athletes may still exhibit abnormal landing mechanics. Developing accurate 2D motion analysis metrics can enhance movement quality assessment, complement existing outcome metrics, and potentially improve ACLR rehab outcomes.

Asymmetry at Longer Term Follow Up

Recent efforts have been made to evaluate kinematics at follow up time points beyond the point of RTS. Ithurburn et al. evaluated quadriceps strength, measured at time of RTS, against 3D biomechanical performance during the drop-vertical jump test two years post-ACLR.[10] They found those with low quadriceps strength at RTS testing had greater asymmetry during landing for knee flexion excursion and peak vertical ground reaction force two years postoperatively.[10] Webster et al. assessed landing biomechanics at one and three years post ACLR and found that differences between limbs existed for most biomechanical variables, with minimal variation observed throughout the study's duration.[11] These results suggest asymmetries persist beyond RTS and symmetrical biomechanics are not organically reacquired through sports participation, potentially heightening the risk of reinjury.

Larson et al. performed 3D motion analysis of college aged female athletes, 1-3 years after ACLR, during crossover hop testing and found that roughly half of subjects landed with an "extended knee," indicating a potential quadriceps avoidance pattern and a subsequent increased reinjury risk.[12] One study by Naili et al. studied an athlete pre- and post-ACLR, finding persistent asymmetry at 29

months postoperatively, eventually corrected by adjusting strength in the uninjured limb to achieve limb symmetry.[13] These studies reveal that biomechanical asymmetries, can persist years after ACLR, and may be more prevalent in those with quadriceps weakness.

Gait analysis

Two recent studies have evaluated that gait of young patients following ACL injury.[14,15] Ursei et al. evaluated compensatory movements using 3D motion analysis in children who had suffered ACL injuries, but not yet undergone treatment.[14] The subjects were found to exhibit increased plantar flexion at initial contact and decreased dorsiflexion during the stance period.[14] These findings are not only the first regarding compensation patterns in ACL-deficient children, but also are different from those reported in adults. Knurr et al., performed a longitudinal study comparing running biomechanics in collegiate athletes prior to ACL injury and again at months four, six, eight, and twelve, postoperatively.[15] By the one-year postoperative time point, the surgical limb had not yet recovered its pre-injury biomechanics, suggesting that deficits in mechanics likely persist beyond the typical RTS timeframe.[15] These findings illustrate that postoperative biomechanical asymmetries likely exist in nearly all aspects of sport, not only in landing, cutting, and jumping.

Future research and Lateral Extraarticular Tenodesis

Recent research in the pediatric population has suggested biomechanical benefits in terms of decreased residual rotatory instability, and clinical benefits of decreased reinjury from performing a lateral extraarticular tenodesis (LET).[16–18] During this procedure, concomitant with the ACLR, an additional soft tissue structure is constructed on the lateral portion of the knee with the intention of introducing additional stability. However, a common concern regarding LET procedures is potential over constraint and alteration of native knee biomechanics from the introduction of an additional stabilizing structure.[19–21]

Currently, no literature exists within the pediatric population regarding in vivo kinematic motion analysis for patients who underwent combined ACLR-LET. Future investigations should look to evaluate knee kinematics for patients following ACLR-LET to better understand the effects this procedure has in comparison to both native knee kinematics and those of patients receiving ACLR only.

Conclusion

Current research around motion analysis following ACLR reveals significant and persistent biomechanical between-limb asymmetries and compensatory movement strategies that develop postoperatively. Clinically, motion analysis offers the ability to monitor these movement patterns, identify biomechanical changes for each patient, and ultimately personalize treatment to acquire optimal kinematics to minimize reinjury risk. It may also be used as an adjunct evaluation tool at time of RTS testing. Future research should expand to assess differences among surgical techniques like LET and continue the current lines of investigation with larger sample sizes and higher level of evidence.

References

1. Ferguson RW, Green A, Hansen LM. Game Changers: Stats, Stories and What Communities Are Doing to Protect Young Athletes. Washington, DC: Safe Kids Worldwide, August 2013.

2. Edison BR, Pandya N, Patel NM, *et al.* Sex and Gender Differences in Pediatric Knee Injuries. *Clin Sports Med* 2022;41(4): 769-787.

3. Ingram JG, Fields SK, Yard EE, *et al.* Epidemiology of Knee Injuries among Boys and Girls in US High School Athletics. *Am J Sports Med* 2008;36(6): 1116-1122.

4. Swenson DM, Collins CL, Best TM, *et al.* Epidemiology of knee injuries among U.S. high school athletes, 2005/2006-2010/2011. *Med Sci Sports Exerc* 2013;45(3): 462-469.

5. Bates NA and Hewett TE. Motion Analysis and the ACL: Classification of Injury Risk. *J Knee Surg* 2016;29(2): 117-125.

6. Losciale JM, Ithurburn MP, Paterno MV, *et al.* Passing return-to-sport criteria and landing biomechanics in young athletes following anterior cruciate ligament reconstruction. *J Orthop Res Off Publ Orthop Res Soc* 2022;40(1): 208-218.

7. Vij N, Tummala S, Vaughn J, *et al.* Biomechanical Gender Differences in the Uninjured Extremity After Anterior Cruciate Ligament Reconstruction in Adolescent Athletes: A Retrospective Motion Analysis Study. *Cureus* 15(2): e35596.

8. Di Paolo S, Zaffagnini S, Tosarelli F, *et al.* Beyond Distance: A Simple Qualitative Assessment of the Single-Leg Hop Test in Return-to-Play Testing. *Sports Health* 2022;14(6): 906-911.

9. Straub RK and Powers CM. Utility of 2D Video Analysis for Assessing Frontal Plane Trunk and Pelvis Motion during Stepping, Landing, and Change in Direction Tasks: A Validity Study. *Int J Sports Phys Ther* 2022;17(2): 139-147. Published 2022 Feb 1.

10. Ithurburn MP, Thomas S, Paterno MV, *et al.* Young athletes after ACL reconstruction with asymmetric quadriceps strength at the time of return-to-sport clearance demonstrate drop-landing asymmetries two years later. *The Knee* 2021;29: 520-529.

11. Webster KE, Ristanis S, Feller JA. A longitudinal investigation of landing biomechanics following anterior cruciate ligament reconstruction. *Phys Ther Sport* 2021;50: 36-41.

12. Larson D, Nathan Vannatta C, Rutherford D, *et al.* Kinetic changes associated with extended knee landings following anterior cruciate ligament reconstruction in females. *Phys Ther Sport* 2021;52: 180-188.

13. Naili JE, Markström JL, Häger CK. A Longitudinal Case-Control Study of a Female Athlete Preinjury and After ACL Reconstruction: Hop Performance, Knee Muscle Strength, and Knee Landing Mechanics. *Sports Health* 2023;15(3): 357-360.

14. Ursei ME, Accadbled F, Scandella M, *et al.* Foot and ankle compensation for anterior cruciate ligament deficiency during gait in children. *Orthop Traumatol Surg Res* OTS. 2020;106(1): 179-183.

15. Knurr KA, Kliethermes SA, Stiffler-Joachim MR, *et al.* Running Biomechanics Before Injury and 1 Year After Anterior Cruciate Ligament Reconstruction in Division I Collegiate Athletes. *Am J Sports Med* 2021;49(10): 2607-2614.

16. Perelli S, Costa GG, Terron VM, *et al.* Combined Anterior Cruciate Ligament Reconstruction and Modified Lemaire Lateral Extra-articular Tenodesis Better Restores Knee Stability and Reduces Failure Rates Than Isolated Anterior Cruciate Ligament Reconstruction in Skeletally Immature Patients. *Am J Sports Med* 2022;50(14): 3778-3785.

17. Green DW, Hidalgo Perea S, Brusalis CM, *et al.* A Modified Lemaire Lateral Extra-articular Tenodesis in High-Risk Adolescents Undergoing Anterior Cruciate Ligament Reconstruction With Quadriceps Tendon Autograft: 2-Year Clinical Outcomes. *Am J Sports Med* 2023;51(6): 1441-1446.

18. Carrozzo A, Monaco E, Saithna A, *et al.* Clinical Outcomes of Combined Anterior Cruciate Ligament Reconstruction and Lateral Extra-articular Tenodesis Procedures in Skeletally Immature Patients: A Systematic Review From the SANTI Study Group. *J Pediatr Orthop* 2023;43(1): 24-30.

19. Madhan AS, Ganley TJ, McKay SD, *et al.* Trends in Anterolateral Ligament Reconstruction and Lateral Extra-articular Tenodesis With ACL Reconstruction in Children and Adolescents. *Orthop J Sports Med* 2022;10(4).

20. Devitt BM, Lord BR, Williams A, *et al.* Biomechanical Assessment of a Distally Fixed Lateral Extra-articular Augmentation Procedure in the Treatment of Anterolateral Rotational Laxity of the Knee. *Am J Sports Med* 2019;47(9): 2102-2109.

21. Wytrykowski K, Swider P, Reina N, *et al.* Cadaveric Study Comparing the Biomechanical Properties of Grafts Used for Knee Anterolateral Ligament Reconstruction. *Arthroscopy*. 2016;32(11): 2288-2294.

Is writing style associated with peer reviewer recommendations?

George E. Sayegh, BS
Amelia E. Mercado, BSA
Jacob E. Thomas, MA
David Ring, MD, PhD
Tom J. Crijns MD

Department of Surgery and Perioperative Care, Dell Medical School, The University of Texas at Austin, Austin, Texas, USA

Introduction

Background

Peer review is the evaluation of scientific work by peer experts in one's discipline prior to release of the work to the public. In theory, a study with good reason, rigor, and reproducibility will pass peer review. However, other factors may influence the peer review process, including reviewer-level variables or article-level variables such as writing style. In one cross-disciplinary analysis of 5,094 journals, acceptance rates varied by journal discipline and correlated with the age of the journal, the impact factor of the journal, number of reviewers for each paper, and their editor's country of residence.[1] There is also evidence that studies with a prospective randomized controlled study design, appropriate statistical analysis, positive paper titles, and statistically significant study findings are associated with acceptance.[2–7]

Rationale

Our research teams and colleagues have often debated the potential advantages and potential drawbacks of a promotional writing style. We are interested in the influence, if any, of writing style on peer reviewer recommendation to accept.

Study Questions

In a randomized simulation-based experiment, we asked: (1) Are specific writing styles associated with recommendation for acceptance of a musculoskeletal experiment? And (2) Is the recommendation to accept a musculoskeletal experiment associated with peer reviewer ratings of the importance of specific manuscript characteristics?

Methods

Study design and setting

This study was approved by our Institutional Review Board. Members of the Science of Variation Group (SOVG) were invited to participate in this randomize simulation-based experiment, and 125 musculoskeletal surgeons completed the online experiment. The SOVG is an international collaborative of orthopedic, plastic, and general surgeons who treat musculoskeletal pathophysiology and participate in monthly experiments that investigate reliability and variation in care. We welcome diversity and all surgeons who perform musculoskeletal procedures are invited to join the SOVG (https://www.surveymonkey.com/r/SOVG_FB).

Description of experiment, treatment, or surgery

Ten manuscripts published in the Journal of Bone & Joint Surgery (JBJS) were selected. For each of the ten manuscripts, researchers rewrote the four different versions of an abstract with a different writing style: technical, scientific, promotional, and dispassionate.

Variables, outcome measures, data sources, and bias

The simulation-based experiment first measured participant familiarity with the peer review process. Participants with no peer-reviewing experience were excluded. Each participant was randomly shown one version of each of the 10 abstracts. Participants rated each according to the peer review scoring system used by the Journal of Bone and Joint Surgery.

Statistical analysis, study size

We conducted descriptive statistics to summarize the characteristics of study participants (Table 1). Multilevel logistic regression was used to analyze the relationship between the dichotomized rating of accept or reject and the ratings of the importance of various aspects of peer review and abstract writing style. We evaluated Odds Ratios for each variable. For level-2 effects, we calculated a Variance Partition Coefficient (VPC) and plotted probability of recommendation to accept with 95% confidence intervals for each writing style (Figure 1).

Table 1. Peer reviewer survey responses (N = 125)

Discrete Variables	Value % (number)
Re-written Abstract Ratings	
Acceptable	16% (201)
Valuable but Incomplete	30% (373)
Interesting but has Serious Concerns	28% (350)
Not Suitable	26% (326)
Gender	
Men	92% (115)
Women	8.0% (10)
Practice location	
United States	49% (61)
Europe	31% (39)
Other	20% (25)
Years in practice	
0-5	28% (35)
6-10	19% (24)
11-20	31% (39)
21-30	22% (27)
Subspecialty	
Fracture surgery	34% (43)
Hand and wrist	31% (39)
Shoulder and elbow	18% (23)
Other	16% (20)
Supervising trainees	89% (111)

Continuous Variables	Median (IQR)
Experience (years)	10 (8-15)
Average time to review manuscript (hours)	2 (1-3)
Most important manuscript characteristics (ranked, 1 - 8)	
Methodology	1 (1-2)
Originality	2 (1-3)
Organization	4 (3-5)
Statistical analysis	4 (3-5)
Clarity of tables/figures	5 (4-6)
Grammar and spelling	6 (5-7)
Quality of references	6 (5-7)
Number of references	8 (7-8)

Discrete variables as percentage (number); Continuous variables as median (interquartile range).

Results

Are specific writing styles associated with recommendation for publication?

Writing style accounted for 2.7% of variance in recommendation to accept. Technical style was the most favorable, followed by dispassionate, then scientific; and promotional style was the least favorable (Table 2, Figure 1). Using multilevel logistic regression, abstract acceptance was also associated with the reviewer factors self-reported greater time spent reviewing a paper (OR: 1.10; 95% CI 1.02-1.19) and fewer years of peer reviewing experience (OR: 0.98, 95% CI: 0.96-0.99).

Is the recommendation to accept a musculoskeletal experiment associated with peer reviewer ratings of the importance of specific manuscript characteristics?

Using multilevel logistic regression, abstract acceptance was associated with lower ratings of the importance of methodology and number of references (OR: 1.29, 95% CI: 1.12-1.50; OR: 1.34, 95% CI: 1.14-1.57 respectively; Table 2).

Discussion

The peer-review process for scientific publications is subject to conscious and unconscious human bias.[8] In a simulation-based experiment that varied writing style of scientific abstracts and asked surgeon scholars for their peer review determinations, we found that personal characteristics of peer reviewers, including a modest susceptibility to jargon, may influence the peer review process.

Limitations

The results of this study should be interpreted in light of the following limitations. Our experiment was performed with an international group of respondents, some of whom speak English as a second language, which might influence the interpretation of writing style.

Are specific writing styles associated with recommendation for acceptance of a musculoskeletal experiment?

The observation that a technical writing style was modestly associated with recommendation to accept suggests that reviewers may be swayed by jargon and suggests that self-promotion is not an effective strategy. The observation that less experience and efficiency of peer reviewers is associated with recommendation to accept is inconsistent with a study where two non-authentic, but realistic, manuscripts with a number of common methodological flaws were reviewed by 156 Scandinavian family medicine, internal medicine, and general surgery peer reviewers and an association was found between younger peer reviewers and stricter manuscript assessments as assessed on a 5-point rating scale.[9]

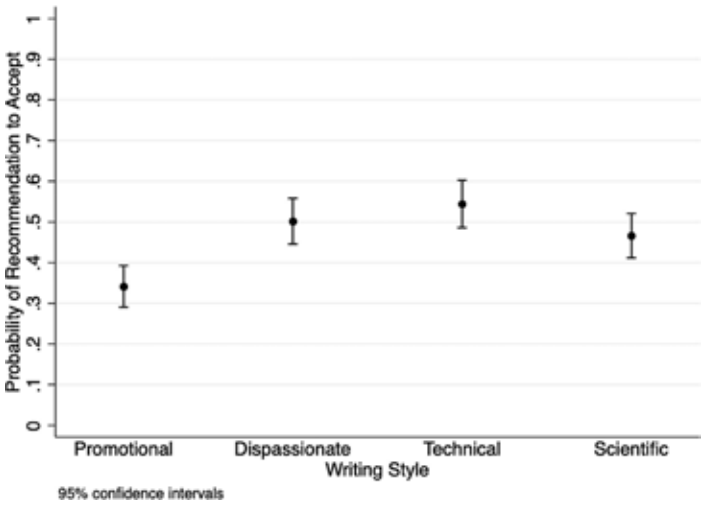

Figure 1. The probabilities of a recommendation to accept for 4 different writing styles.

Table 2. Multilevel Logistic Regression Model Parameter Estimates for abstracts receiving a Recommendation to Accept rating in JBJS Peer Review (n=1,250)

Variable	Estimate	95% C.I.
Fixed Effects	*Odds Ratio*	
Hours spent peer reviewing a paper (1-10)	**1.10**	**1.02, 1.19**
Years experience peer reviewing	**0.98**	**0.96, 0.99**
Importance of the following characteristics of a scientific paper [1 (the most important) – 7 (not important at all)]		
Originality	1.06	0.95, 1.20
Organization	0.96	0.86, 1.07
Statistics	1.01	0.89, 1.14
Methodology	**1.29**	**1.12, 1.50**
Grammar	0.96	0.86, 1.07
Number of References	**1.34**	**1.14, 1.57**
Quality of References	0.97	0.86, 1.10
Random Effects	*Variance*	
Writing Style	**0.09**	**0.02, 0.44**
VPC For Abstract Type (%)	2.7	

Bold indicates statistical significance ($p<0.05$)

VPC = Variance Partition Coefficient

Is the recommendation to accept a musculoskeletal experiment associated with peer reviewer ratings of the importance of specific manuscript characteristics?

The finding that recommendation for manuscript acceptance is associated with lower ratings on the importance of methodology and number of references are discordant with prior research and might be specific to musculoskeletal surgeons. For instance, a prospective cohort study of 1,107 manuscripts submitted to the *British Medical Journal*, *Lancet*, and *Annals of Internal Medicine* which found that submitted manuscripts are more likely to be published if they are rated as having high methodological quality.[10] Another study of 445 reviews of 196 papers by 335 peer reviewers with ratings of rhetoric, structure, science, and import also found an association between manuscript acceptance and higher peer reviewer ratings of scientific content and structure.[11]

Conclusions

Our findings confirm that the personal reviewer factors, including a modest influence of writing style, are associated with recommendations to publish, and that a promotional writing style is not effective. Editors and editorial staff can be attentive to the human element of manuscript evaluation.

References

1. Sugimoto CR, Larivière V, Ni C, *et al.* Journal acceptance rates: A cross-disciplinary analysis of variability and relationships with journal measures. *J Informetr* 2013; 7: 897–906.

2. Basilious A, Benavides Vargas AM, Buys YM. Publication rate of abstracts presented at the 2010 Canadian Ophthalmological Society Annual Meeting. *Canadian Journal of Ophthalmology* 2017; 52: 343–348.

3. Easterbrook PJ, Gopalan R, Berlin JA, *et al.* Publication bias in clinical research. *The Lancet* 1991; 337: 867–872.

4. Ha TH, Yoon DY, Goo DH, *et al.* Publication Rates for Abstracts Presented by Korean Investigators at Major Radiology Meetings. *Korean J Radiol* 2008; 9: 303.

5. Muffly TM, Webster K, Conageski C, *et al.* Predictors of Manuscript Publication. *Female Pelvic Med Reconstr Surg* 2016; 22: 83–87.

6. Treanor L, Frank RA, Cherpak LA, *et al*. Publication bias in diagnostic imaging: conference abstracts with positive conclusions are more likely to be published. *Eur Radiol* 2020; 30: 2964–2972.

7. Winnik S, Raptis DA, Walker JH, *et al.* From abstract to impact in cardiovascular research: factors predicting publication and citation. *Eur Heart J* 2012; 33: 3034–3045.

8. McKenzie ND, Liu R, Chiu A V., *et al.* Exploring Bias in Scientific Peer Review: An ASCO Initiative. *JCO Oncol Pract* 2022; 18: 791–799.

9. Nylenna M. Multiple Blinded Reviews of the Same Two Manuscripts. *JAMA* 1994; 272: 149.

10. Lee KP, Boyd EA, Holroyd-Leduc JM, *et al.* Predictors of publication: characteristics of submitted manuscripts associated with acceptance at major biomedical journals. *Medical Journal of Australia* 2006; 184: 621–626.

11. Kliewer MA, DeLong DM, Freed K, *et al.* Peer Review at the American Journal of Roentgenology: How Reviewer and Manuscript Characteristics Affected Editorial Decisions on 196 Major Papers. *American Journal of Roentgenology* 2004; 183: 1545–1550.

Hand

Tips & Tricks: Closed Reduction of Pediatric Distal Radius Fractures in the Emergency Department

Ellis Berns, MD[1]
Thompson Zhuang, MD MBA[1]
Apurva Shah, MD MBA[2]

[1]Department of Orthopaedic Surgery
University of Pennsylvania

[2]Department of Orthopaedic Surgery
Children's Hospital of Pennsylvania

Introduction

Distal radius fractures are the most common type of fracture encountered in patients below the age of sixteen.[1] As such, they are frequently encountered in the emergency room setting by the orthopaedic physician on call.

Although no universally accepted standardized treatment protocol for the treatment of pediatric distal radius fractures exists, the principal of restoring functional alignment dictates management. The distal radius has immense remodeling potential, as the distal radial physis contributes 75% to the longitudinal growth of the radius. However, remodeling potential is inversely correlated with age; therefore, there is a lower tolerance for incompletely reduced distal radii in older children.[2] Malalignment can lead to a loss of range of motion and in turn a loss of function. For example, while angulation of greater than 10 degrees in the distal third of the forearm results in loss of 20 degrees of pronation-supination range of motion, angulation less than 10 degrees cause minimal limitation on range of motion.[3] (Figure 1)

Guided by acceptable restoration of function, general radiographic parameters have been described that constitute an acceptable reduction. In younger patients (e.g., less than 10 years), 20-25 degrees of sagittal plane angulation and 10 degrees of coronal plane angulation can be expected to remodel. In patients greater than 10 years, less than 15 degrees of residual angulation can be accepted. Deformity is typically better tolerated in the plane of motion of the wrist joint (i.e., sagittal). By this same principle, rotational deformities are poorly tolerated and cannot be expected to significantly remodel.[4] However, while rotational malalignment can ultimately limit range of motion, this may not lead to functional limitations.

Minimal bayonet apposition, or overriding of the major fracture fragments, can be accepted in patients under 10 as this is not likely to limit range of motion or function and may remodel.[5] Ultimately, as children approach skeletal maturity, treating fractures with bayonet apposition using closed reduction can pose a significant challenge given the deforming forces and narrow margin of acceptable radiographic parameters. In practice, there remains high variation between surgeons in terms of tolerance of residual deformity, especially in older children.[3,6]

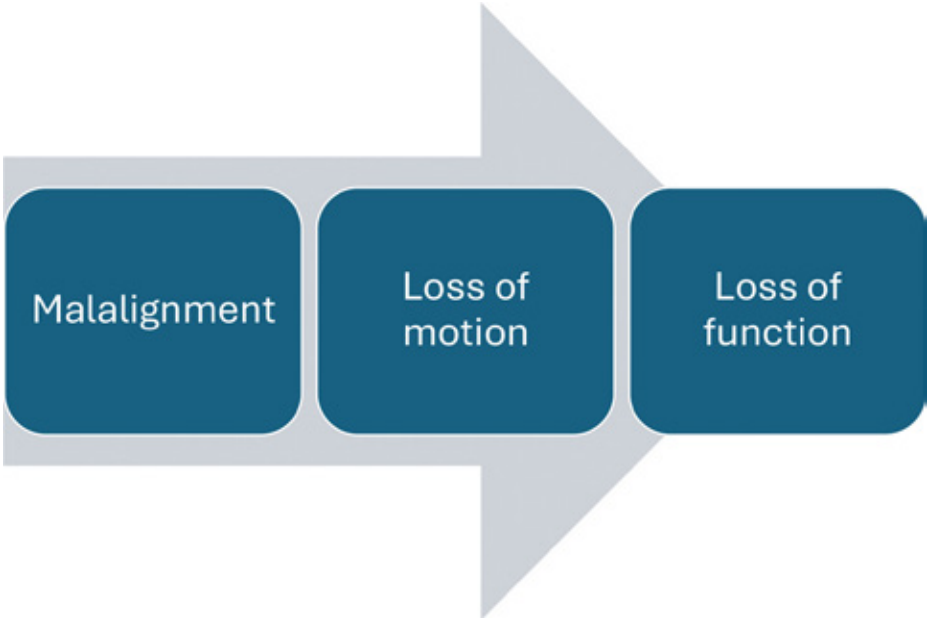

Figure 1. Downstream effects of malaligned distal radius fractures on patient outcomes.

Treating distal radius fractures successfully via closed reduction saves healthcare costs, risks of anesthesia, and risks of operative management, and is frequently definitive treatment of the injury.[7] Given their frequency, there is significant interest in guidance on closed management of these injuries.[8] Successful nonoperative management relies on precise closed reduction, a well-molded cast, and frequent observation in clinic. Ideal closed reduction maneuvers are simple, easily reproducible, and effective for both new and more experienced practitioners. In this paper, we aimed to describe a series of tips and tricks to aid in closed reduction and management of pediatric distal radius fractures.

Tips and Tricks

#1 Let It Hang!

The most significant deforming force on the distal radius is the brachioradialis, a muscle originating from the lateral distal humerus and inserting on the radial styloid. It aids in elbow flexion but, following a distal radius fracture, retracts the distal fragment proximally, which can result in a bayonet deformity.[9]

Prior to attempting closed reduction for shortened fractures, encircle the index and middle finger with a role of gauze or finger traps and securely attach to a ceiling fixture. Place a counterweight around the elbow, typically created using bags of saline and stockinette. This setup counteracts the shortening and radial deviation caused by the brachioradialis before fracture manipulation and fatigues the muscle. Leave the patient in this position for five to fifteen minutes to maximize the effect. Patients should be counseled that their fingers may discolor due to tourniquet constriction, which will quickly resolve once this reduction aid is removed.

#2 Help Yourself!

Two maneuvers can accomplish self-provided counter-force for reduction when an assistant is unavailable:

- A bedsheet can be folded lengthwise and draped over the upper arm with the elbow flexed at 90 degrees. Counter traction is applied by anchoring on the sheet by standing on it while applying axial traction distal to the fracture side.
- The physician's leg is placed over the patients arm so that the physician can flex their knee and capture the patients' upper arm. When axial traction is applied distal to the fracture site, the physician has precise control of the proximal arm to provide counter traction. This method has been shown to provide a significant force of countertraction and allows for close positioning for more precise direction of the distal fracture fragment in the axial, coronal, and sagittal planes,[10] (Figure 2)

Figure 2. Demonstration of the lower extremity assisted counter-traction method for distal radius reduction. The lower extremity provides axial counterforce as the distal fragment is manipulated. This position allows for precise control of the distal fragment and strong counter-traction, ideal for fractures with bayonet deformity.

#3 Its More Than You Think!

Due to periosteal entrapment within the fracture site, the reduction requires recreation of deformity at the fracture site to free the soft tissues. In addition, bayonetted forearm fractures require significant deformity recreation to angle the opposed cortex of the distal fracture and allow for axial traction to bring the distal segment "up and over" the proximal segment. A short course of live fluoroscopy can reveal the degree of recreation required to free the cortex of the fracture fragment. This technique should be used with caution to not expose the patient to excess radiation. The distal fracture may need to be "walked" over the proximal fragment with several small reduction maneuvers to achieve an adequate final position.

If an incomplete ulna fracture prevents deformity recreation, completion of the fracture may be required

to achieve acceptable reduction of the distal radius. This should be discussed as a potential outcome with the parents prior to beginning the reduction attempt. Although the idea of completing a fracture seems oppositional to orthopaedic principles, restoring length to the radius is required for the principle of restoring functional outcomes.

#4 Know When to Hold'Em

After adequate closed reduction has been obtained, a fiberglass cast is then applied. Significant care must be taken while the undercast padding and then the cast is applied to not lose the reduction. For dorsally displaced fractures, wrist flexion can help hold the reduction during the cast application process. The reduction can also be held by an assistant holding the child's index and middle fingers to apply ulnar deviation with the child's elbow flexed to 90 degrees. Holding and molding in a position of stability may prevent re-displacement of the fracture in the cast.[11]

#5 Proper Molding, Take a Seat!

After the cast is applied, the critical step of molding is performed. A well-placed mold is critical for preventing fracture re-displacement.

Studies have validated radiographic parameters to evaluate cast applications, the most frequently used being the cast index, or the measurement of the cast in the sagittal plane divided by the measurement in the coronal plane at the fracture site. A ratio $<.80$ is predictive of maintaining reduction in the cast.[12] A three-point mold prevents re-displacement by buttressing the fracture in the plane of original displacement.

One method is for the physician to sit on a stool adjacent to the patient. The knee should be placed at the apex side of the deformity, just proximal to the fracture site. The palms are placed on either side of the knee on the opposite side of the cast to create the three-point mold. Alternate this position with oppositional force in the sagittal plane at the fracture site to optimize the cast index. (Figure 3)

Another method is to first establish the cast index by performing an interosseous mold along the entire cast. Then, the physician places their thenar eminence just proximal to the fracture site on the apex side of the deformity and the other thenar eminence on the opposite side over the distal fragment. This counteracts the deforming force. The hand on the non-apex side of the cast alternates between the distal fragment and a point proximal to the apex-sided hand to create the three-point mold.

#6 Beat the Heat, Circle Back

An exam should always be performed after closed reduction and after the patient has recovered from sedation. The degree of swelling should be assessed, as well as any signs of nerve compression (e.g., median neuropathy) that may occur.

Figure 3. Demonstration of a three-point mold for a dorsally displaced fracture. The knee is placed on the apex side of the deformity in the sagittal plane, just proximal to the fracture site. The distal palm is used to buttress the fracture from re-displacing. The proximal palm completes the three-point mold. This position should be alternated with direct compression at the fracture site to optimize the cast index.

In patients with significant swelling before or after reduction, bivalving the cast can allow more room for soft tissue expansion. The risk of bivalving includes a loss of reduction as the patient's swelling decreases. A compressive wrap or another layer of cast material can be applied after the cast is loosened.

Preventing cast burns when bivalving or removing casts is paramount. Risk factors for cast saw burns include inexperienced physicians, conscious sedation, and casts over the wrist.[13] The utmost caution must be taken when using a cast saw in a patient who is still under sedation and cannot report feeling the heat of the blade. If the cast needs to be bivalaved, wait until the patient has recovered from sedation to allow for their feedback during removal. Commercially available safety strips can be slid between layers of the cast padding provide an additional layer of protection.

#7 See You Again

Because re-displacement can occur in over 20% of pediatric distal forearm fractures,[14] children who undergo

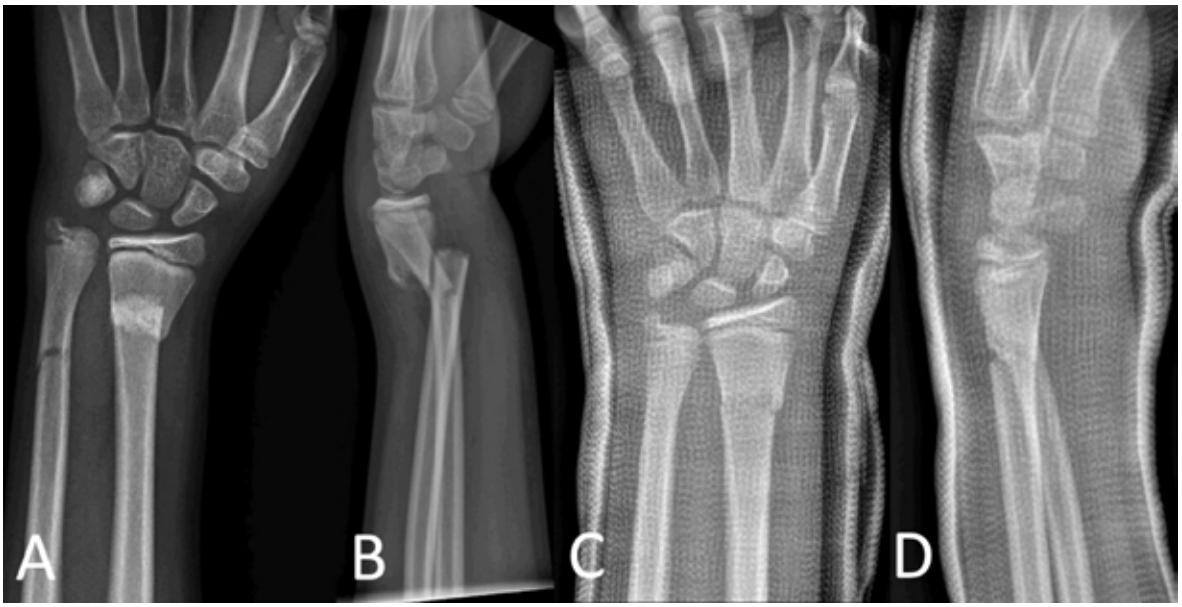

Figure 4. Posteroanterior (A) and lateral (B) radiographs of a 13-year-old male who sustained a left dorsally displaced distal radius metadiaphyseal fracture with bayonet apposition and distal ulnar diaphysis and ulnar styloid fractures after a basketball injury. The fracture was reduced under conscious sedation in the emergency department and placed in a short arm fiberglass cast using many of the tips and tricks described. PA (C) and lateral (D) demonstrate maintenance of the reduction at 1 week follow up. Cast index is 0.70.

closed reduction of these fractures should follow up in fracture clinic in a week for a fracture alignment check.

#8 Bailout - Wedge It

Fractures in even the most well-molded casts can re-displace. When fractures re-displace along one plane, the cast can be wedged to correct this malalignment.

The opening wedge is most used, in which the cast is cut in the concavity of the deformity and cast is then wedged open on that side to correct the angular deformity.[15]

While several methods have been described to calculate the amount of wedging required to correct a given angular deformity, a simple method without the need for mathematical calculations exists. A piece of paper is overlaid on a radiograph of the fracture and the long axes of the proximal and distal fracture segments are traced with a pen. The paper is then cut along the traced line, creating a template of the fracture deformity. The paper is then placed on the cast and the angular deformity is traced with a marker. The cast is then cut at the concavity of the fracture deformity, leaving a hinge at the point of maximal convexity. The cast can then be wedged open until the fracture lines that were traced on the cast beforehand are made straight.

Conclusion

Displaced pediatric distal radius fractures can provide a significant challenge to treat using closed reduction. Reduction of these fractures is critical to restore functional outcomes of the upper extremity. Application of these tips and tricks during each step of the reduction process can aid in closed management of pediatric distal radius fractures in the emergency department by the physician on call.

References

1. Randsborg P-H, Gulbrandsen P, Šaltyte Benth J. *et al.* Fractures in Children: Epidemiology and Activity-Specific Fracture Rates. JBJS. 2013;95(7):e42.

2. Jeroense KTV, America T, Witbreuk MMEH, *et al.* Malunion of distal radius fractures in children: Remodeling speed in 33 children with angular malunions of ≥ 15 degrees. Acta Orthopaedica. 2015;86(2):233–237.

3. Greig D, Silva M. Management of Distal Radius Fractures in Adolescent Patients. Journal of Pediatric Orthopaedics. 2021;41:S1.

4. Ray S, Manske MC. Pediatric Forearm Malunions. *Hand Clinics*. 2024;40(1):35–48.

5. Crawford SN, Lee LSK, Izuka BH. Closed treatment of overriding distal radial fractures without reduction in children. The Journal of Bone and Joint Surgery. *American Volume*. 2012;94(3):246–252.

6. Bernthal NM, Mitchell S, Bales JG, *et al.* Variation in practice habits in the treatment of pediatric distal radius fractures. *Journal of Pediatric Orthopaedics B*. 2015;24(5):400.

7. Godfrey JM, Little KJ, Cornwall R, *et al.* A Bundled Payment Model for Pediatric Distal Radius Fractures: Defining an Episode of Care. *Journal of Pediatric Orthopedics*. 2019;39(3):e216–e221.

8. Hennrikus WL, Mehlman CT. The Community Orthopedic Surgeon Taking Trauma Call: Pediatric Distal Radius and Ulna Fracture Pearls and Pitfalls. *Journal of Orthopaedic Trauma*. 2019;33 Suppl 8:S6–S11.

9. Koh S, Andersen CR, Buford WL, *et al.* Anatomy of the distal brachioradialis and its potential relationship to distal radius fracture. *The Journal of Hand Surgery*. 2006;31(1):2–8.

10. Eichinger JK, Agochukwu U, Franklin J, *et al.* A New Reduction Technique for Completely Displaced Forearm and Wrist Fractures in Children: A Biomechanical Assessment and 4-year Clinical Evaluation. *Journal of Pediatric Orthopaedics*. 2011;31(7):e73.

11. Kralj R, Pešorda D, Keretić D, *et al.* Secondary displacement in distal forearm fractures in children: adequate positioning of the wrist in the cast is more important than cast index. *Journal of Pediatric Orthopedics. Part B*. 2023;32(2):145–151.

12. Kamat AS, Pierse N, Devane P, *et al.* Redefining the Cast Index: The Optimum Technique to Reduce Redisplacement in Pediatric Distal Forearm Fractures. *Journal of Pediatric Orthopaedics*. 2012;32(8):787.

13. Larson JE, Nicolay RW. Cast Saw Burn Prevention: An Evidence-Based Review. *JAAOS–Journal of the American Academy of Orthopaedic Surgeons*. 2021;29(9):380.

14. McQuinn AG, Jaarsma RL. Risk Factors for Redisplacement of Pediatric Distal Forearm and Distal Radius Fractures. *Journal of Pediatric Orthopaedics*. 2012;32(7):687.

15. Samora JB, Klingele KE, Beebe AC, *et al.* Is there still a place for cast wedging in pediatric forearm fractures? *Journal of Pediatric Orthopedics*. 2014;34(3):246–252.

Subcondylar Fossa Reconstruction: Outcomes in Pediatric Patients following Malunion of Proximal Phalanx Fractures

David P. VanEenenaam Jr., BS[1]
Sarah L. Struble, BS[2]
Eliza Buttrick, BA[1]
Benjamin Chang, MD[1,2]
Apurva S. Shah, MD MBA[1]

[1]Children's Hospital of Philadelphia Division of Orthopaedics

[2]Children's Hospital of Philadelphia Division of Plastic, Reconstructive, and Oral Surgery

Introduction

Phalangeal neck fractures usually occur as a result of crush injuries and are seen almost exclusively in the pediatric population.1 For displaced morphologies, the distal fragment can angulate dorsally, causing palmar angulation of the proximal fragment, sometimes more than 90 degrees, that can be underestimated if a lateral radiograph of the fracture is not obtained.[1] Natural realignment is less likely to occur due to the lack of distal growth plate, which may result in a bony block and malunion. Malunion of proximal phalanx fractures require surgical intervention, and corrective osteotomy is technically challenging in this area as the distal bony fragment is often too small for stable internal fixation. Current literature describes multiple techniques with varying complexity to address this injury and there is no consensus on the ideal operation to manage this condition.[2,3] The subcondylar fossa reconstruction first proposed by Simmons et. al in 1987 is a simple and safe surgical technique that removes the offending bony block to recreate the subcondylar fossa without complex fixation.1 Since its initial description, there have been no updates on outcomes within the pediatric population in the current literature, with the exception of a single case report in one adult from 2014.[4] The goal of this study was to provide an update on outcomes following subcondylar fossa reconstruction in a larger cohort of patients.

Methods

We identified four patients who underwent a subcondylar fossa reconstruction at a large tertiary-care pediatric hospital between 2012-2022. Patient age, sex, mechanism of injury, injury location and initial treatment, pre- and post-operative flexion, angular deformity, and complications were recorded. A palmar zigzag (Brunner approach) incision or lateral mid-axial incision centered over the proximal interphalangeal (PIP) joint is made, separating the overlying subcutaneous tissues in the digital neurovascular bundles in the flexor tendon sheath. A small opening in the flexor tendon sheath is made between the A2 and A4 pulleys by lifting a rectangular flap. The flexor digitorum superficialis (FDS) and flexor digitorum profundus (FDP) are then retracted to expose the volar aspect of the PIP joint. The volar plate is incised along its proximal and lateral margins, elevated off the phalangeal neck, and the digit is flexed to identify the malunion and bony block. The prominent phalangeal neck is excised with a rongeur or a motorized burr, confirming excision with fluoroscopy. Intraoperative flexion is performed to confirm adequate motion. Removing a significant quantity of bone may be necessary, though care should be taken to preserve the integrity of the dorsal cortex. The palmar plate and flexor sheath are then repaired with interrupting sutures. The patient may be discharged home on the same day, with dressings removed 48 to 72 hours following the procedure. At that time, self-directed range of motion exercises can be initiated, with occupational therapy providing aggressive active and passive range of motion the week following surgery.

Results

Case 1.

IA, a 16-year-old male, sustained a fall while playing football, resulting in a fracture of the right proximal phalanx of his small finger. This was treated with NSAIDS and tape by his athletic trainer and not formally evaluated by a physician until five months later due to prolonged range of motion (ROM) deficit. He was found to have a proximal phalanx long oblique fracture malunion with translation and ulnar deviation. There was hypertrophic bony remodeling noted along the radial aspect of the proximal phalanx on radiographs. His PIP flexion was limited to 30 degrees. A subcondylar fossa reconstruction was performed, achieving 95 degrees of flexion in the operating room, and maintained postoperatively. At 4 months following surgery, the patient had PIP flexion to 90 degrees, with acceptable alignment and no new bony callous formation on radiographs.

Case 2.

CH, a 9-year-old male, sustained a fall while playing football, resulting in a fracture of the right index finger proximal phalanx. He was treated in an ulnar gutter short arm cast, which healed with abundant callous formation at the proximal phalanx, restricting ROM to 40 degrees of flexion. A subcondylar fossa reconstruction was performed, and the patient obtained 90 degrees of PIP flexion at 4 months postoperatively, with no evidence of residual deformity.

Case 3.

CH, an 11-year-old male jammed his left small finger playing basketball, resulting in a proximal phalangeal fracture treated initially with closed reduction and percutaneous pinning that healed with a volar bony block of the PIP joint, restricting flexion to 45 degrees (Figure 1). A subcondylar fossa reconstruction was performed using a mid-lateral incision (Figure 2), and the patient obtained 95 degrees of PIP flexion at 3 months postoperatively (Figure 3), and no evidence of residual callous formation.

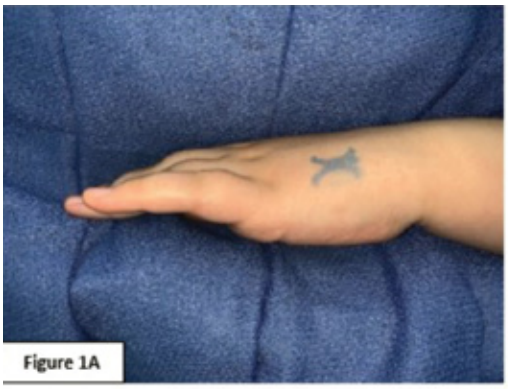

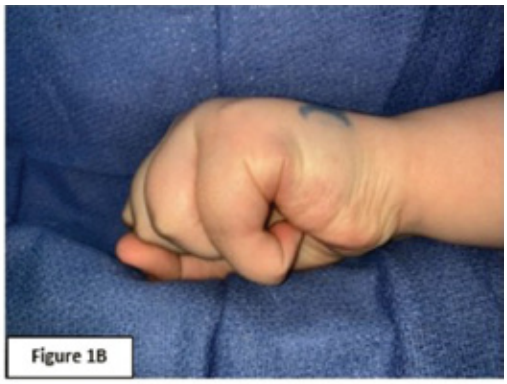

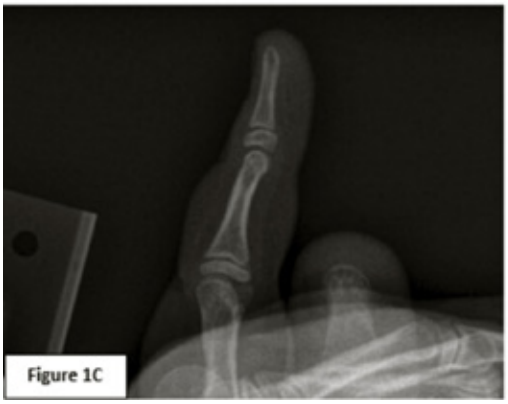

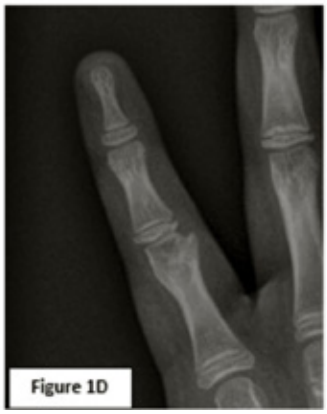

Figure 1. Clinical photographs of an 11-year-old male with **(A)** volar bony block at the PIP joint of the left small finger, fully extended and; **(B)** with restricted flection to 55°; **(C)** Lateral radiographic view of the patient's bony block on the volar aspect of the PIP joint of the left small finger.;**(D)** PA view of bony malunion at the volar aspect of the PIP joint of the left small finger.

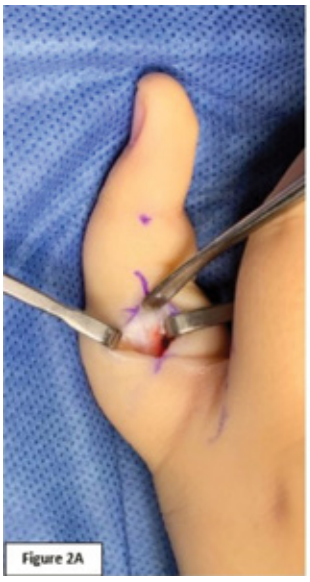

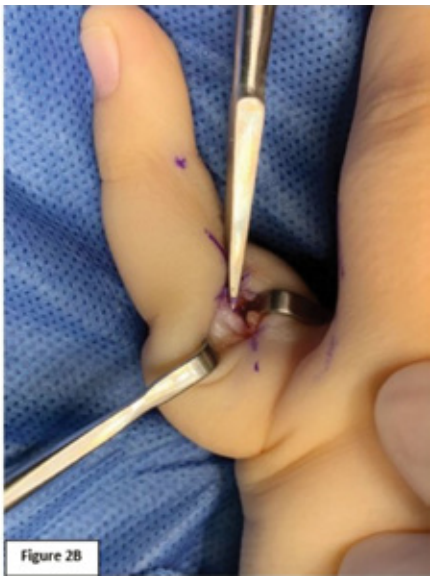

Figure 2. (A) Subcondylar fossa reconstruction on the left small finger of an 11-year-old male using a mid-lateral approach, incising the flexor tendon sheath between the A2 and A4 pulleys; **(B)** Exposure of the phalangeal neck of the proximal phalanx of the left small finger of the same patient using a hand osteotome to recreate recess under fluoroscopic guidance.

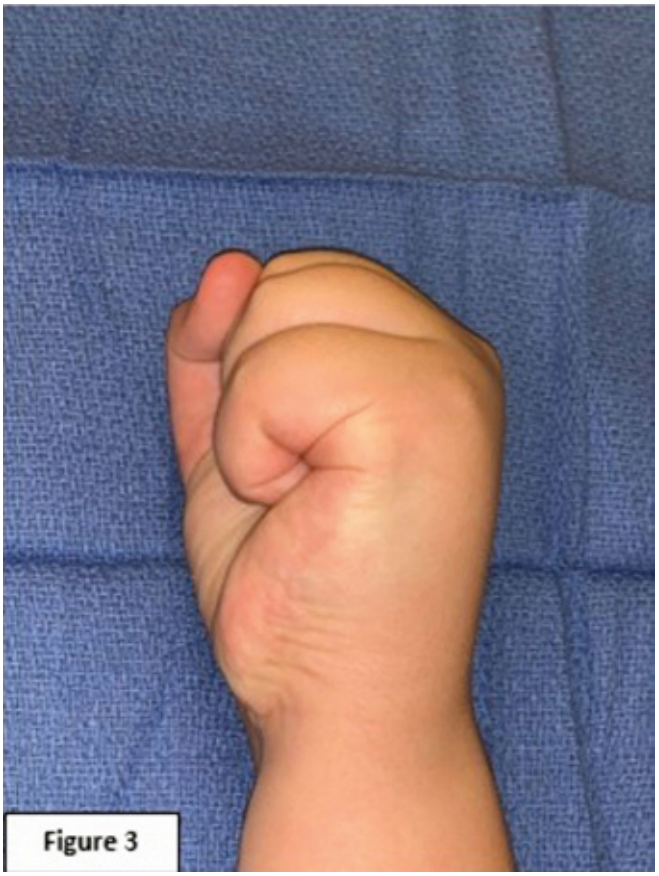

Figure 3. 11-year-old male post subcondylar fossa reconstruction, demonstrating full flexion of the left small finger PIP joint.

Case 4.

DP, a 15-year-old female crashed into a parked car while riding her bike and sustained a proximal phalangeal neck fracture of the right small finger that was not immobilized or evaluated until 3 months post injury due to persistent ROM deficit. She was found to have a displaced proximal phalangeal neck fracture healing in an extended, shortened pattern, with PIP flexion limited to 55 degrees. She underwent a subcondylar fossa reconstruction and achieved 95 degrees of flexion with no evidence of deformity.

Conclusion

Subcondylar fossa reconstruction provides a safe and effective solution for the surgical correction of malunion in proximal phalanx fractures among pediatric patients. This study contributes valuable data on its outcomes, advocating for its consideration as a preferred technique in appropriate cases.

References

1.Simmons BP and Peters TT. Subcondylar fossa reconstruction for malunion of fractures of the proximal phalanx in children. J Hand Surg. 1987;12(6):1079-1082.

2.Teoh LC, Yong FC, Chong KC. Condylar advancement osteotomy for correcting condylar malunion of the finger. *J Hand Surg Edinb Scotl*. 2002;27(1):31-35.

3.Kang HJ, Sung SY, Ha JW, *et al.* Operative treatment for proximal phalangeal neck fractures of the finger in children. *Yonsei Med J*. 2005;46(4):491-495.

4.Kang YC and Tan PL. Simple Surgery to Improve Flexion Deficit Resulting from Mal-Union of Fracture Neck of the Proximal Phalanx–a Case Report: Hand Surgery. *Hand Surg*. 2014;19(1):123-125.

Shoulder and Elbow

Tips & Tricks: Arthroscopic Shoulder Arthrodesis in Young Patients with Brachial Plexus Injuries: Restoration of Shoulder Stability for Hand Positioning

Erin A. Hale, MD[1]
Brett J. Croen, MD[1]
L. Scott Levin, MD[1]
David L. Glaser, MD[1]

[1]Department of Orthopaedic Surgery
University of Pennsylvania

Introduction

Shoulder arthrodesis is a surgical procedure involving fusion of the glenohumeral joint and possible supplemental acromiohumeral fusion. The procedure was traditionally indicated in cases of significant trauma including brachial plexus injuries and massive irreparable rotator cuff tears with insufficient deltoid compensation, as well as cases of substantial bone loss following infection, tumor resection, or failed glenohumeral arthroplasty.[1] With the continuing evolution of shoulder arthroplasty and arthroscopy to address complex shoulder pathology, the indications for shoulder arthrodesis are diminishing. However, for the brachial plexopathy patient with retained or restored elbow and hand function without a stable shoulder, shoulder arthrodesis can be a life-changing procedure.[2]

Brachial plexopathies present a multi-disciplinary issue which often requires the involvement of microsurgeons, neurosurgeons, hand surgeons, and shoulder and elbow surgeons. Patients with upper or complete brachial plexus injuries suffer from loss of shoulder abduction, shoulder external rotation, and elbow flexion due to injury to the C5 and C6 nerve roots supplying the suprascapular, subscapular, axillary, and musculocutaneous nerves.[3] Up to 29% of brachial plexopathy patients present with isolated upper trunk injuries. The degree to which elbow flexion is affected is variable. However, the two most important goals of surgery are restoration of elbow flexion followed by shoulder stability.[3] Without intact elbow flexion, a patient with a surgically stabilized shoulder will still not be able to reach their head for feeding and personal hygiene. Prior to consideration of shoulder arthrodesis, microsurgery to repair the suprascapular and axillary nerves is often considered. Muscle or nerve transfers can also be used to improve shoulder abduction and external rotation.[2] Free functional muscle transfers such as a functional gracilis transfer for restoration of elbow flexion and rudimentary grasping have also been described when local and rotational muscle transfers have not adequately restored function.[4,5]

Shoulder arthrodesis is often indicated for shoulder stabilization in cases with retained elbow flexion or in conjunction with free functional muscle transfer or bipolar latissimus transfer in cases with loss of elbow flexion. The goal of shoulder arthrodesis is to stabilize the glenohumeral joint to allow for range of motion through the scapulothoracic joint and to position the elbow in space in such a way that the patient will be able to reach their hand to the mouth and to the perineum for hygiene. Successful shoulder arthrodesis requires intact periscapular musculature including a functional trapezius, levator scapulae, latissimus dorsi, serratus anterior, and rhomboid muscles to allow for motion through the scapulothoracic joint after arthrodesis.[6] The improvement in function provided by shoulder arthrodesis allows patients to independently complete activities of daily living.

Case Presentation

We present the cases of two young male patients who presented after sustaining brachial plexus injuries in motorcycle collisions. Patient A sustained his injury at age 20, two years prior to presentation. At the time of his injury, he also sustained a subdural hematoma and numerous orthopaedic injuries. EMG confirmed a left upper and middle truck brachial plexus injury with lower truck involvement to a lesser degree. He underwent brachial plexus exploration and lateral cord neurolysis with left phrenic nerve to musculocutaneous nerve transfer using sural nerve graft. Two months later he underwent a median nerve fascicular transfer to the brachialis branch of the musculocutaneous nerve (modified Oberlin procedure). At the time of presentation to our team, he had severe atrophy of the left upper extremity with some elbow flexion and some active

finger flexion. However, he was unable to reach his mouth with his left hand. Given the patient's lack of meaningful function of the left upper extremity the decision was made to proceed with arthroscopic shoulder arthrodesis twenty months after the initial injury (Figure 1).

Patient B sustained his injury at age 43, three years prior to presentation. In addition to his right brachial plexus injury, he also suffered numerous orthopaedic injuries and cervical spine fractures. Following the injury, Patient B was unable to abduct, adduct, flex, or extend his right shoulder. EMG confirmed a severe right upper and middle trunk brachial plexopathy. Patient B underwent right supraclavicular brachial plexus exploration, neurolysis, and nerve graft repair from C5 to the suprascapular nerve and upper trunk, and right ulnar nerve fascicular transfer to the biceps branch of the musculocutaneous nerve. He later underwent right radial to axillary nerve transfer. Fifteen months after initial injury the patient continued to have significantly limited right upper extremity function despite multiple surgical interventions and consistent physical therapy participation (Figure 2). The decision was then made to proceed with right arthroscopic shoulder arthrodesis.

Procedure

Both patients underwent the same positioning and approach. The patients were placed in the beach-chair position. The glenohumeral joint was visualized through a posterior portal. An anterior portal was then established. A shaver was used to debride the labrum circumferentially. A high-speed burr was then utilized to remove cartilage from both the humeral and glenoid articular surfaces. Special attention was paid to ensuring adequate cartilage removal from the areas of joint surfaces which correlated with the ideal fusion position given each patient's unique needs. The quality of the debridement was assessed by camera through both the anterior and posterior portals. A microfracture kit was employed to fenestrate the cortices under fluoroscopic guidance.

Attention was turned to proper alignment of the glenohumeral joint for functional arthrodesis. The glenohumeral joint was placed in approximately 30 degrees each of forward flexion, abduction, and internal rotation with minor adjustments made to accommodate for the patients' thin frames. Elbow range of motion was assessed to assure the patient would be able to bring the hand up to the head and down to the thigh. Patient A

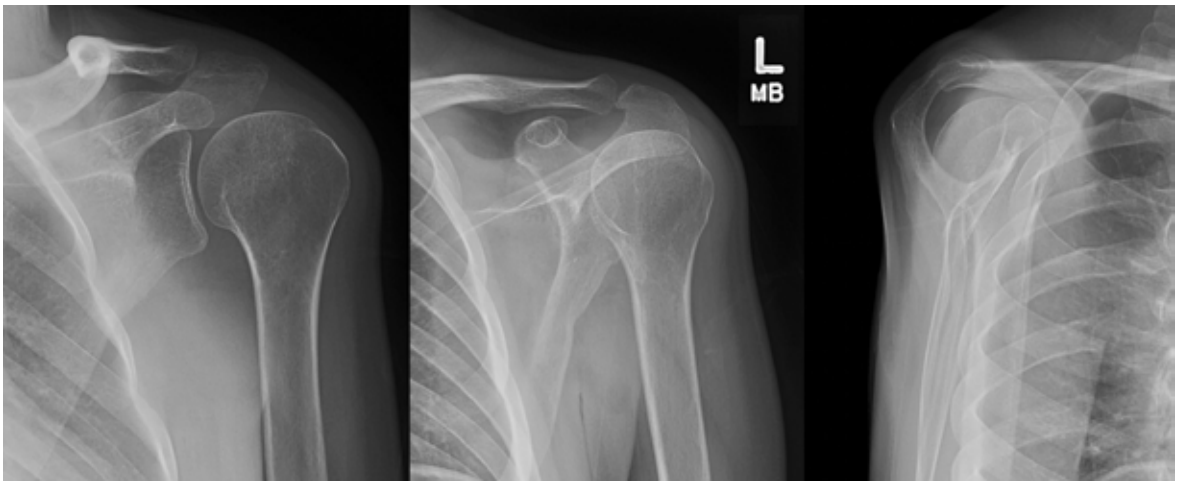

Figure 1. Pre-operative imaging of the left shoulder of Patient A demonstrating reduced humeral head without fracture.

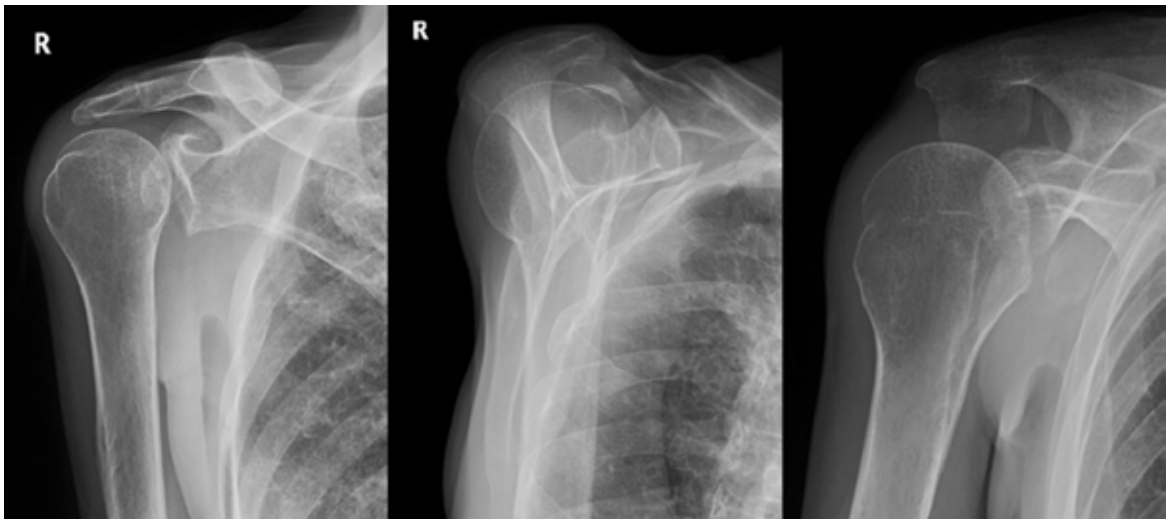

Figure 2. Pre-operative imaging of the right shoulder of Patient B demonstrating high-riding humeral head and right clavicle malunion.

required less internal rotation and more abduction than typical to allow for elbow flexion to meet the mouth given his significant motor deficits.

Fluoroscopy was utilized to template the starting point and trajectory of the screws that would be placed across the glenohumeral joint. Once the appropriate starting point was determined, an incision was made over the lateral humerus to allow for screws to be placed across the glenohumeral joint. For both patients a drill-tip guidewire and reverse drilling in between cortices were utilized which allowed for increased tactile feedback as each cortex was passed. Screw length was measured off the guidewire. Patient A was noted to have poor bone quality at the humeral head and had four screws placed across the glenohumeral joint. Three 6.5mm self-drilling, self-tapping, partially-threaded screws were placed with washers: one down the inferior angle of the scapula, one straight across the joint, and one through the upper portion of the joint. An additional 4.5mm screw was placed across the joint for reinforcement. Finally, a fully-threaded 6.5mm screw was placed from the acromion through the humeral head to the calcar.

Patient B also had placement of three 6.5mm self-drilling, self-tapping, partially-threaded screws with washers. However, given higher bone quality he did not require placement of a 4.5mm reinforcement screw across the glenohumeral joint. The first, more inferior, screw was placed just behind the bicipital groove along the greater tuberosity with 30 degrees retroversion. A second, more superior screw was then placed parallel to the first in the same fashion. A third screw was placed at the top of the greater tuberosity through the inferior angle of the scapula. To achieve rotational stability, a final fully-threaded 6.5mm screw was placed from the middle of the acromion to the calcar of the humerus.

The arthroscopic portals and screw incisions were then closed. Sterile dressings were applied. Patient A was placed in a bulky splint post-operatively. Patient B was placed in a sling. Both patients were awoken and transferred to the post-operative area without complication. Imaging obtained on the day of surgery demonstrated screw fixation of the glenohumeral joint with appropriate alignment (Figures 3 and 4).

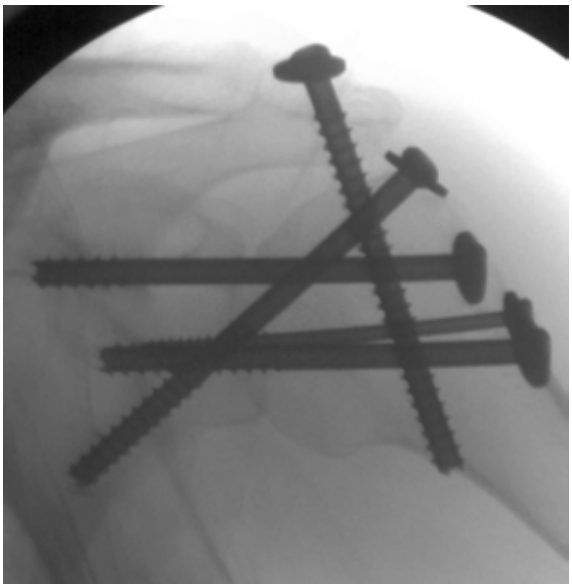

Figure 3. Day of surgery intra-operative imagining of the left shoulder demonstrating shoulder arthrodesis with screw fixation.

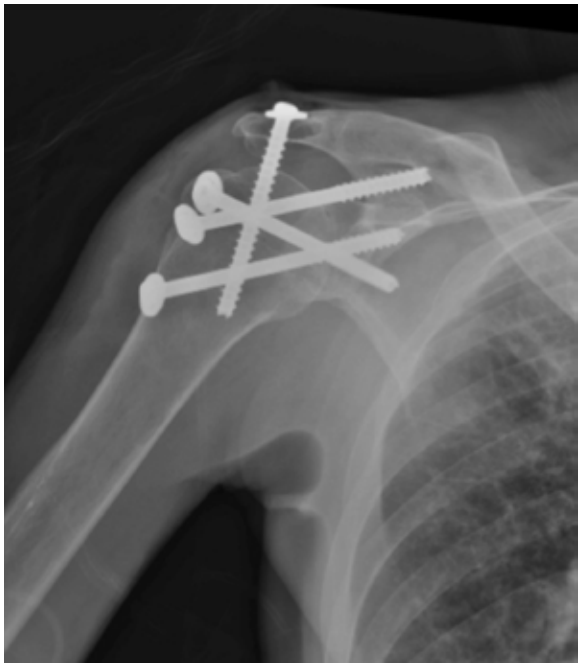

Figure 4. Day of surgery post-operative imagining of the right shoulder demonstrating shoulder arthrodesis with screw fixation.

Follow-up

Patient A had an uncomplicated post-operative course. His incisions healed well without any prominent hardware. Six weeks post-operatively the patient was able to reach his mouth with his hand. In the two years following arthroscopic shoulder arthrodesis the patient underwent wrist arthrodesis and multiple tendon transfers at the wrist and hand which further improved hand positioning and function. Imaging obtained 2.5 years after shoulder arthrodesis confirmed complete fusion of the glenohumeral joint with hardware retained in the appropriate position without evidence of failure (Figure 5).

At six-week follow-up Patient B was doing well and satisfied with his progress. His surgical incisions were well-healed. He was instructed to discontinue use of the sling and to continue to focus on elbow range of motion and strengthening. Imaging obtained at follow-up demonstrated appropriately aligned glenohumeral joint with evidence of early fusion. Hardware was well-fixed without out evidence of lucency or displacement (Figures 6). With consistent physical therapy the patient was able to flex the elbow to reach his mouth two months post-operatively.

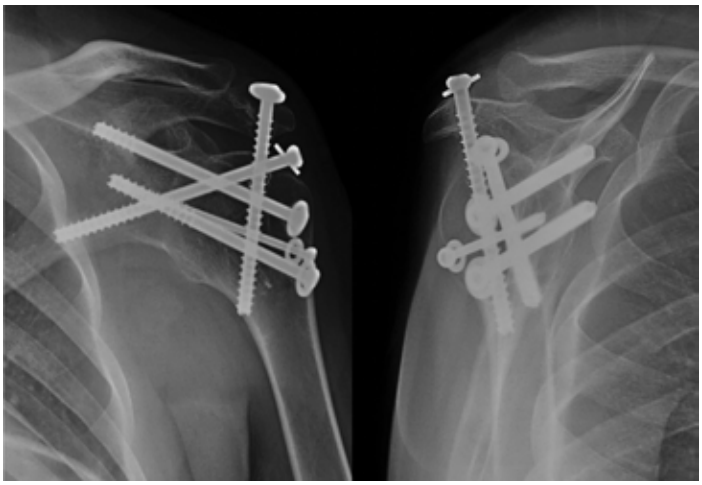

Figure 5. 2.5-year post-operative imaging of the left shoulder of Patient A demonstrating well-aligned glenohumeral arthrodesis with complete fusion of the glenohumeral joint.

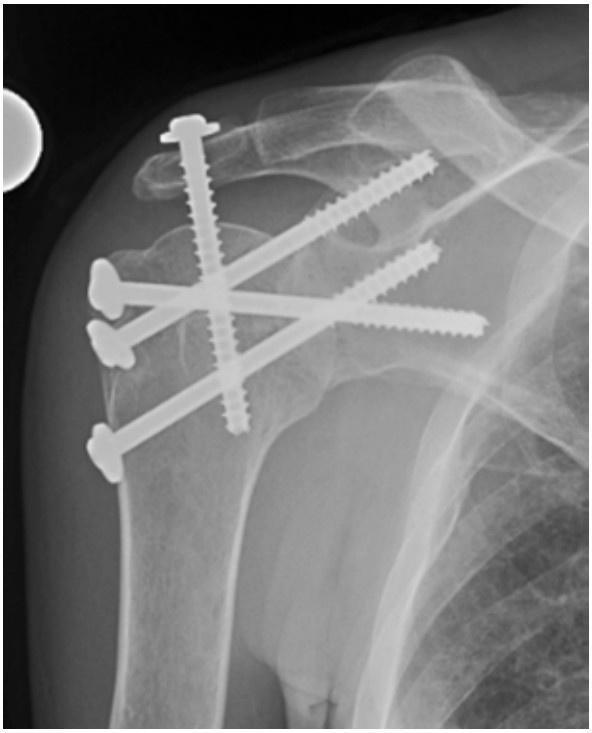

Figure 6. One-month post-operative imaging of the right shoulder demonstrating well-aligned glenohumeral arthrodesis with hardware in place.

Discussion

Traditionally, shoulder arthrodesis has been completed as an open procedure with utilization of a nonlocking plate over the humerus and scapular spine followed by an extended period of upper extremity immobilization.[6,7] Alternatively, shoulder arthrodesis has been performed arthroscopically with percutaneous screw placement across the glenohumeral joint with the addition of an external fixation device for added support while the fusion heals. We present the use of arthroscopic shoulder arthrodesis without the addition of external fixation in the setting of a traumatic upper brachial plexus injury.

Arthroscopic Arthrodesis

Arthroscopic arthrodesis is a minimally invasive alternative to the traditional open shoulder arthrodesis with lower likelihood of prominent hardware, risk of infection, elbow stiffness from prolonged immobilization, and post-operative humerus fracture caused by the stress riser at the distal end of a scapulohumeral plate, which have all been seen in other shoulder arthrodesis techniques.[1,7] Particularly for the young population most commonly affected by traumatic brachial plexopathy, arthroscopic surgery offers a cosmetic advantage over open arthrodesis. Additionally, these young patients generally have a biologic advantage which supports fusion following arthroscopic joint preparation without the necessity of open exposure of the joint.

There is a paucity of literature assessing the outcomes of arthroscopic shoulder arthrodesis compared to open shoulder arthrodesis; the literature that does exist is in the format of individual case studies or small case series.[1,8,9] The first case report of arthroscopic-assisted glenohumeral arthrodesis was published in 1992.[10] This case involved a 39-year-old woman with axillary nerve palsy, global left shoulder pain, and multidirectional instability following a traumatic shoulder dislocation seven years earlier. In this case the glenohumeral joint was visualized through a posterior portal and a curette was utilized through the anterior portal to debride hyaline cartilage from the joint surface. Next a motorized abrader was used to take the joint surface down to bleeding bone. The arm was positioned in 25 degrees of abduction, 30 degrees of forward flexion and 50 degrees of internal rotation as recommended by Rowe in 1983.[11] Two 6.5mm cannulated cancellous lag screws were placed across the glenohumeral joint, and a third screw was then placed from the acromion through the humeral head and neck. Screw placement was confirmed with fluoroscopy, portals were closed with suture, and the patient was placed in a foam abduction pillow. The arm was immobilized for four weeks at which point active range-of-motion exercises were initiated. At six weeks post-operatively the patient was able to reach her mouth and perineal area. Imaging at ten-weeks post-operatively confirmed glenohumeral fusion.

Other case reports have followed a similar operative technique. In 2008, Syal et al published a report of two cases of arthroscopic shoulder arthrodesis.[8] Their paper focused on cases of global shoulder instability which had failed numerous muscle and tendon transfers prior to consideration of shoulder arthrodesis. In this study the patients were placed in the beach chair position, and the standard posterior arthroscopic portal was used for visualization of the glenohumeral joint. The anterior portal was used to prepare the joint for fusion. The arm was positioned in 30 degrees flexion, 30 degrees abduction, and 30 degrees internal rotation. An anterior cruciate ligament (ACL) guide was utilized for placement of two guidewires across the glenohumeral joint. Two 6.5mm cannulated

screws were then placed over the guidewires. A third 6.5mm cannulated screw was placed from the acromion into the humeral head as was also demonstrated in our case. Screw position was confirmed with fluoroscopy. Post-operatively the patients were each placed in an abduction pillow for three months and they both went on to fusion.

Arthroscopic Arthrodesis with External Fixation

Alternative surgical options include arthroscopic joint preparation with placement of external fixation device as described by Lenoir et al.[9] In their case series they placed three external fixation pins in the scapular spine and three pins in the humeral shaft. They prepared the glenohumeral joint for arthrodesis, keeping in mind the ideal glenohumeral joint position of 30 degrees forward flexion, 30 degrees abduction, 30 degrees internal rotation for arthrodesis. All eight of the patients in their case series had two parallel 6.5mm screws placed across the glenohumeral joint. Two of the patients had an additional screw placed from the acromion to the humeral head due to concern for poor bone quality. The post-operative protocol included immobilization with an abduction pillow for 4 weeks followed by mobilization with physical therapy for the scapulothoracic joint. External fixation was removed after 2 months for all patients in the study. All patients in the study went on to fusion of the glenohumeral joint and had statistically significant improvements in the American Shoulder and Elbow Surgeons (ASES) index, Disabilities of the Arm, Shoulder and Hand (DASH) score, and the Simple Shoulder Test. When compared to casting or bracing, external fixation allows for scapulothoracic and elbow range of motion while selectively blocking scapulohumeral movement. However, an external fixation device can be uncomfortable for patients, require surgical removal, and adds the risk of pin loosening, pin track infection, and fracture at the pin sites.[7,8]

Open Arthrodesis

Traditional open glenohumeral arthrodesis can be performed in the beach chair position of lateral decubitus position based on the surgeon's preference.[6] The glenohumeral joint is accessed via a longitudinal incision beginning proximally at the glenoid fossa or scapular spine and extending distally past the acromion and continuing along to axis of the humerus. The deltoid is reflected to expose the scapula, acromion, and proximal humerus. Care is taken to preserve the axillary nerve when still functional. The rotator cuff and joint capsule are then reflected to expose the joint. The glenohumeral joint surfaces and inferior acromion are prepped with a combination of reamers and burrs. Controversy exists regarding the appropriate position of glenohumeral joint for optimal function, though the majority of sources agree it is most important that the arm be placed in a position which allows the patient to reach both the mouth and perineal area.[6,12,13] The preferred position of the humerus on the glenoid involves a combination of intra-articular and extra-articular positioning with the humerus aligned with the superior aspect of the glenoid and the inferior aspect of the acromion allowing for increased bone-to-bone contact.[6,13] A reconstruction, dynamic, or locked plate, screws across the glenohumeral joint, or external fixation device, or any combination of those fixation techniques is then used to secure the shoulder joint in the preferred position.[6]

While open glenohumeral arthrodesis has been the most common technique for shoulder fusion, there have been many documented complications. Plate fixation with open arthrodesis has been shown to cause skin irritation often necessitating hardware removal.[14] Nonunion rates of open glenohumeral arthrodesis are reported as high as 24%.[7,12] Additionally, Wagner et al reported a 21% humeral shaft fracture rate just distal to the plate used in open arthrodesis due to the stress riser created by the construct.[7] This leads to further immobilization and possible revision surgery. Infection following open glenohumeral arthrodesis has been noted in 4% to 12% of cases often necessitating additional surgery.[7,13-15] Three studies looking at shoulder arthrodesis complications found that 10% of patients required a revision surgery to perform a humeral osteotomy for correction of glenohumeral malpositioning which significantly delayed return to activity and limited functional recovery.[13,16,17]

Conclusion

Glenohumeral arthrodesis is a well-established procedure which can provide substantial improvement in upper extremity range of motion and function in patients for whom nerve and muscle transfers have failed to restore shoulder stability and function. Traditional open glenohumeral arthrodesis has shown success in restoring function and decreasing pain when appropriately indicated. However, open arthrodesis has consistently demonstrated high complication rates which often necessitate additional surgical procedures. Arthroscopic glenohumeral arthrodesis offers the benefits of open arthrodesis with a significantly less invasive procedure, less prominent hardware, and lower potential for infection or fracture. Arthroscopic shoulder arthrodesis can be utilized for restoration of shoulder stability as part of a multi-disciplinary approach to improve function of the upper extremity following brachial plexus injury.

References

1. Jiménez-Martín A, Pérez-Hidalgo S. Arthroscopic arthrodesis of the shoulder: Fourteen-year follow-up. *Int J Shoulder Surg.* 2011 Apr;5(2):54-9.

2. Górecki M, Czarnecki P. The influence of shoulder arthrodesis on the function of the upper limb in adult patients after a brachial plexus injury: a systematic literature review with elements of meta-analysis. *EFORT Open Rev.* 2021 Sep 14;6(9):797-807.

3. Wu KY, Spinner RJ, Shin AY. Traumatic brachial plexus injury: diagnosis and treatment. *Curr Opin Neurol.* 2022 Dec 1;35(6):708-717.

4. Graf A, Ojemakinde A, Gupta S, *et al.* Form and Function: Technique for Free Functional Gracilis Harvest With Greater Saphenous Vein for Large Skin Paddle. *Tech Hand Up Extrem Surg.* 2023 Sep 1;27(3):194-198.

5. Fischer JP, Elliott RM, Kozin SH, *et al.* Free function muscle transfers for upper extremity reconstruction: a review of indications, techniques, and outcomes. *J Hand Surg Am*. 2013 Dec;38(12):2485-90.

6. Michael A. Del Core, Holt S. Cutler, *et al.* Glenohumeral arthrodesis. *JSES Reviews, Reports, and Techniques*. 2021;1(4) 367-372.

7. Atlan F, Durand S, Fox M, *et al.* Functional outcome of glenohumeral fusion in brachial plexus palsy: a report of 54 cases. *J Hand Surg Am*. 2012 Apr;37(4):683-8.

8. Porcellini G, Savoie FH III, Campi F, *et al.* Arthroscopically assisted shoulder arthrodesis: is it an effective technique? *Arthroscopy*. 2014 Dec;30(12):1550-6.

9. Lenoir H, Williams T, Griffart A, *et al.* Arthroscopic arthrodesis of the shoulder in brachial plexus palsy. *J Shoulder Elbow Surg*. 2017 May;26(5):e115-e121.

10. Morgan CD, Casscells CD. Arthroscopic-assisted glenohumeral arthrodesis. *Arthroscopy*. 1992;8(2):262-6.

11. Rowe CR. Arthrodesis of the shoulder used in treating painful conditions. *Clin Orthop Relat Res*. 1983 Mar;(173):92-6.

12. Wagner ER, McLaughlin R, Sarfani S, *et al.* Long-term outcomes of glenohumeral arthrodesis. *J Bone Joint Surg Am*. 2018;100:598-604.

13. Sousa R, Pereira A, Massada M, *et al.* Shoulder arthrodesis in adult brachial plexus injury: what is the optimal position? *J Hand Surg Eur* Vol 2011;36:541-7. https://doi.org/10.1177/ 1753193411405742.

14. Ruhmann O, Schmolke S, Bohnsack M, *et al.* Shoulder arthrodesis: indications, technique, results, and complications. *J Shoulder Elbow Surg* 2005;14:38-50.

15. Chammas M, Goubier JN, Coulet B, *et al.* Glenohumeral arthrodesis in upper and total brachial plexus palsy. A comparison of functional results. *J Bone Joint Surg Br* 2004;86:692-5.

16. Irlenbusch U, Rott O, Irlenbusch L. Indication, technique and long-term results after shoulder arthrodesis performed with plate fixation. Z Orthop Unfall 2018;156:53-61.

17. Miller BS, Harper WP, Gillies RM, *et al.* Biomechanical analysis of five fixation techniques used in glenohumeral arthrodesis. *ANZ J Surg* 2003;73:1015-7.

Use of Internal Joint Stabilizer after Transradial Amputation and Elbow Instability: A Case Report

Madison Craft, MD[1]
Brian Chenoweth, MD[1]

[1]University of Oklahoma Health Science Center Department of Orthopedic Surgery and Rehabilitation

Introduction

Transradial amputations are most commonly indicated after a severe traumatic injury to the wrist or hand. Concomitant elbow injuries such as fractures and/or dislocations resulting in joint instability complicate forearm amputations because elbow function is crucial to recovery time, limb functionality, and potential prosthetic use. We report a case of a traumatic mangled upper extremity requiring transradial amputation with concomitant elbow instability treated with application of internal joint stabilizer and ligament repair. Informed consent was obtained from patient.

Case

This patient is a 75-year-old female with past medical history of schizophrenia who was involved in a motor vehicle accident and sustained a severe left upper extremity injury with significant degloving and a dysvascular hand. (Figure 1A&B) Upon arrival, a CT angiography of the left upper extremity showed no flow of the radial or ulnar arteries distal to the fracture site concerning for arterial injury. The patient was taken emergently to the OR for limb salvage versus amputation. Upon intraoperative exam, there was significant degloving to 80% of the circumference of the distal forearm with complex disruption of the radial and ulnar arteries as well as significant tendon and bony destruction. The left hand showed poor capillary refill and no waveform on any digits with pulse oximetry. A transradial amputation was performed and a negative pressure wound therapy device was applied. The patient was also found to have an ipsilateral elbow dislocation which was closed reduced intraoperatively. Following reduction, the elbow remained grossly unstable. The patient was taken back to the operative room two days later for repeat debridement and negative pressure wound therapy exchange. Due to the patient's age and previous psychiatric history of schizophrenia, the use of an elbow internal joint stabilizer was recommended to facilitate return of range of motion and protected functional use in the setting of loss of the hand. The patient agreed and was taken to the operating room three days later for definitive reconstruction. (Figure 1C) Intraoperatively, proximal avulsion of the lateral ulnar collateral ligament (LUCL) was identified and primarily repaired with a suture anchor. The hinged internal fixator was applied. (Figure 1D) It is the authors technique to place the center axis pin first utilizing the set guides. This is followed by placement of a suture anchor just anterior to the center axis of rotation and axis pin location. Once the fixator position was finalized, the elbow was taken through full range of motion with satisfactory stability achieved. Finally, the transradial amputation was formalized with primary tension free closure. A brief period of immobilization was performed for pain control and then gentle range of motion was initiated. Discharge direct to home under care of family was performed at 7 days following the last surgery.

At 2 weeks post-operative clinic visit, the patient's stitches were removed. She achieved elbow range of motion from 20 degrees to 60 degrees. We recommended she continue to work on range of motion and begin gentle functional use of the arm. At the 6 weeks post-operative clinic visit, the patient reported mild phantom limb pain, but it did not interfere with her daily living. The surgical incision was well-healed, and range of motion was observed from 20 degrees to 110 degrees. X-rays showed stable alignment of the internal joint stabilizer and concentric reduction of the elbow joint (Figure 1E). At the 12-week post-operative clinic visit, the patient reported reduced pain and significant improvements in functional use. Her range of motion had improved with extension to 0 degrees. She was noted to have some difficulty with pronation and supination. At 8 months post-operative, the patient had been fitted for a prosthetic and showed promise with her initial prosthesis training as well as ongoing occupational and physical therapy sessions. She was provided a conventional transradial prosthesis with myoelectric controlled terminal device in order to achieve her functional goals and bimanual tasks.

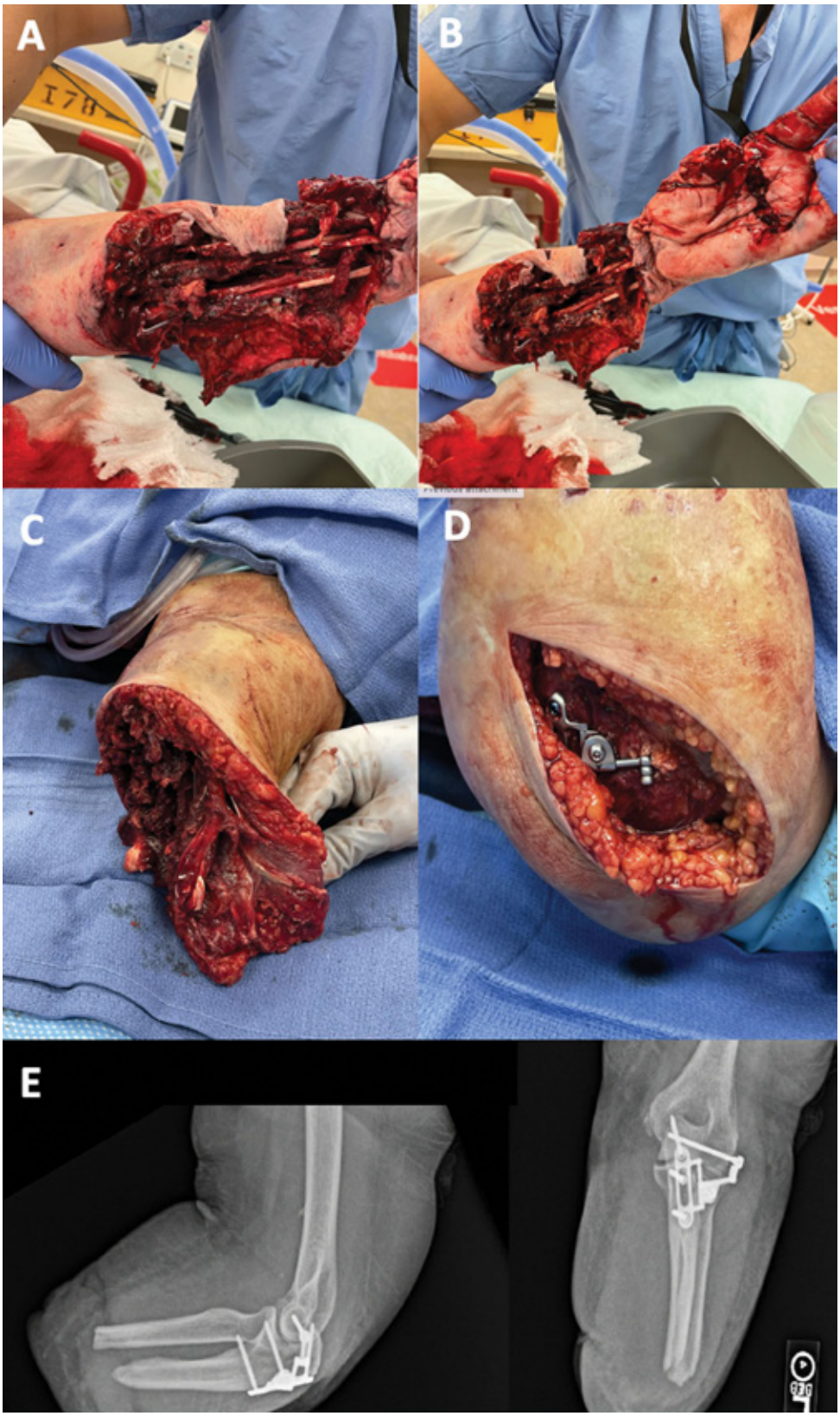

Figure 1. (A&B) Significant degloving injury to the left upper extremity upon presentation to the trauma center; **(C)** Our patient's extremity after debridement and application of negative pressure wound vacuum; **(D)** Placement of internal joint stabilizer in the left elbow; **(E)** Six-week postoperative x-rays demonstrate stable alignment of the internal joint stabilizer and concentric reduction of the elbow joint.

At the 20 months post-operative clinic visit, the patient was wearing the prosthesis at least two hours a day. She was continuing to wear it more and was getting more proficient with it. Occupational therapy was also continued to help improve function.

Discussion

This patient's unique injury combination prompts the discussion of outcomes between transradial amputation and elbow disarticulation. Previous studies favor transradial amputation, specifically distal transradial amputation, over

elbow disarticulation with benefits including increased pronation and supination and a more stable lever arm.[14,18] Free vascularized tissue transfers have even been used to preserve upper extremity amputation level and have resulted in improved residual limb function.[1] When an injury warrants a proximal transradial amputation, only 5 cm of residual ulna is needed for use of a non-hinge prosthesis and retention of elbow flexion.[3] This should be a goal when a proximal transradial amputation must be performed. Conversely, an elbow disarticulation loses native elbow flexion which decreases functionality for activities of daily living.[6] Another major concern is cosmetic appearance due to the more distal position of the prosthetic elbow. Because the humerus remains at full length, the center of rotation of the prosthetic elbow must move distally creating an inequality compared to the contralateral side.[20]

The rate of prosthetic acceptance has many attributing factors, some include weight of prosthesis, ease of use, stump-socket discomfort, time between injury and obtaining prosthesis, cosmetic appearance, ipsilateral hand dominance, and shoulder stiffness.[22] With recent technological advancements such as use of myoelectric protheses, 3D printed prostheses, and osseointegration techniques, some of these issues have decreased significantly.[2,19,20] This is crucial as patients that are more satisfied with their prosthesis have higher perceived functionality of the limb and lower rates of prosthesis abandonment.[24] Other factors to consider are hand dominance as patients are more likely to use a prosthesis on their dominant side; and time between injury and obtaining the prosthesis as a prolonged period of time increases abandonment.[14,16,24] Prosthesis training with occupational or physical therapy also has an impact on prosthesis rejection suggesting individualized training is also important.[13]

Most of the literature on elbow disarticulations includes it with other types of upper extremity amputations making it difficult to solely compare elbow disarticulations with transradial amputations. One of the few studies was by Dudkiewicz et al who found that 50% of patients with elbow disarticulations used a prosthesis.[5] Conversely, a review by Tintle et al reported a rate of transradial prosthesis use of 80% to 94%.[21] This high rate of prosthetic use has been mirrored in other studies as well.[10,16,18,22] This is likely due to the more mechanically advantageous lever arm that allows for generation of greater torque in a transradial amputation.14

Phantom limb pain is a complex phenomenon and is a major reason for prosthetic rejection in elbow disarticulations and transradial amputations.[5,21] However, this chronic pain did not seem to impair functional prosthesis wear or the ability to return to work for transradial amputees as they have the highest percentage in return to work when compared with elbow disarticulations or transhumerual amputations.[6,20-22] There is a wide range of mechanisms that have been described attempting to explain the pathophysiology, but there is still no clear explanation to the cause of phantom limb pain.[7] Despite our patient reporting mild symptoms related to phantom limb pain, this did not interfere with prosthesis application.

The schizophrenic population is known to have an increased risk of postoperative complications and lower functional outcomes after a surgical procedure in general.[4,9,11] Mental health plays a crucial role in outcomes after orthopedic injuries specifically affecting progress with physical therapy mentally and physically in order to achieve good functional results.[8,23] This aspect of our patient's past medical history in addition to her advanced age facilitated our decision to proceed with a transradial amputation and use of an internal joint stabilizer over an elbow disarticulation. The use of a hinged internal fixator to stabilize the elbow joint by maintaining concentric reduction during elbow motion allowed for more protection during early range of motion exercises decreasing time spent in a splint.[12,15,17] Our patient was able to perform early elbow motion and began using the residual limb sooner than if alternative treatments had been pursued. This advantage contributes to the early functional use of the residual limb as well as potential fitting and use of a prosthesis.

Conclusion

Thus, we describe a viable option for treatment of traumatic upper extremity injury requiring amputation with associated elbow instability. We utilized a technique that maintained as much length of the residual extremity as possible while using an internal joint stabilizer to promote early elbow range of motion and functionality. In the setting of advanced age and psychiatric illness, this may have decreased chances for complications and increased her likelihood of functional use.

References

1. Baccarani A, Follmar KE, De Santis GA, *et al.* Free vascularized tissue transfer to preserve upper extremity amputation levels. *Plast Reconstr Surg.* 2007;120(4):971-81.

2. Bates TJ, Fergason JR, Pierrie SN. Technological Advances in Prosthesis Design and Rehabilitation Following Upper Extremity Limb Loss. *Curr Rev Musculoskelet Med.* 2020;13(4):485-93.

3. Bukowski EL. Atlas of Amputations and Limb Deficiencies: Surgical, Prosthetic, and Rehabilitation Principles. DG Smith JM, JH Bowker, editor. Rosemont, IL American Academy of Orthopaedic Surgeons; 2004 1 April 2006.

4. Daumit GL, Pronovost PJ, Anthony CB, *et al.* Adverse events during medical and surgical hospitalizations for persons with schizophrenia. *Arch Gen Psychiatry.* 2006;63(3):267-72.

5. Dudkiewicz I, Gabrielov R, Seiv-Ner I, *et al.* Evaluation of prosthetic usage in upper limb amputees. *Disabil Rehabil.* 2004;26(1):60-3.

6. Fitzgibbons P, Medvedev G. Functional and Clinical Outcomes of Upper Extremity Amputation. *J Am Acad Orthop Surg.* 2015;23(12):751-60.

7. Hanyu-Deutmeyer AA, Cascella M, Varacallo M. Phantom Limb Pain. StatPearls. Treasure Island (FL)2022.

8. Kugelman D, Qatu A, Haglin J, *et al.* Impact of Psychiatric Illness on Outcomes After Operatively Managed Tibial Plateau Fractures (OTA-41). *J Orthop Trauma.* 2018;32(6):e221-e5.

9. Liao CC, Shen WW, Chang CC, *et al.* Surgical adverse outcomes in patients with schizophrenia: a population-based study. *Ann Surg.* 2013;257(3):433-8.

10. Millstein SG, Heger H, Hunter GA. Prosthetic use in adult upper limb amputees: a comparison of the body powered and electrically powered prostheses. *Prosthet Orthot Int.* 1986;10(1):27-34.

11. Ng JPH, Ho SWL, Yam MGJ, *et al.* Functional Outcomes of Patients with Schizophrenia After Hip Fracture Surgery: A 1-Year Follow-up from an Institutional Hip Fracture Registry. *J Bone Joint Surg Am*. 2021;103(9):786-94.

12. Orbay JL, Ring D, Kachooei AR, *et al.* Multicenter trial of an internal joint stabilizer for the elbow. *J Shoulder Elbow Surg*. 2017;26(1):125-32.

13. Ostlie K, Lesjo IM, Franklin RJ, *et al.* Prosthesis rejection in acquired major upper-limb amputees: a population-based survey. *Disabil Rehabil Assist Technol*. 2012;7(4):294-303.

14. Ovadia SA, Askari M. Upper extremity amputations and prosthetics. *Semin Plast Surg*. 2015;29(1):55-61.

15. Pasternack JB, Ciminero ML, Choueka J, *et al.* Patient outcomes for the Internal Joint Stabilizer of the Elbow (IJS-E). *J Shoulder Elbow Surg*. 2020;29(6):e238-e44.

16. Pinzur MS, Angelats J, Light TR, *et al.* Functional outcome following traumatic upper limb amputation and prosthetic limb fitting. *J Hand Surg Am*. 1994;19(5):836-9.

17. Sochol KM, Andelman SM, Koehler SM, *et al.* Treatment of Traumatic Elbow Instability With an Internal Joint Stabilizer. *J Hand Surg Am*. 2019;44(2):161 e1- e7.

18. Sturup J, Thyregod HC, Jensen JS, *et al.* Traumatic amputation of the upper limb: the use of body-powered prostheses and employment consequences. *Prosthet Orthot Int*. 1988;12(1):50-2.

19. Taylor CE, Drew AJ, Zhang Y, *et al.* Upper extremity prosthetic selection influences loading of transhumeral osseointegrated systems. *PLoS One*. 2020;15(8):e0237179.

20. Tintle SM, Baechler MF, Nanos GP, *et al.* Traumatic and trauma-related amputations: Part II: Upper extremity and future directions. *J Bone Joint Surg Am*. 2010;92(18):2934-45.

21. Tintle SM, Baechler MF, Nanos GP, *et al.* Reoperations following combat-related upper-extremity amputations. *J Bone Joint Surg Am*. 2012;94(16):e1191-6.

22. Wright TW, Hagen AD, Wood MB. Prosthetic usage in major upper extremity amputations. *J Hand Surg Am*. 1995;20(4):619-22.

23. You DZ, Leighton JL, Schneider PS. Current Concepts in Rehabilitation Protocols to Optimize Patient Function Following Musculoskeletal Trauma. *Injury*. 2020;51 Suppl 2:S5-S9.

24. Zhang X, Baun KS, Trent L, *et al.* Factors influencing perceived function in the upper limb prosthesis user population. *PMR*. 2021.

Foot and Ankle

Tips and Tricks: Minimally Invasive Surgery with Transverse Osteotomy for Hallux Valgus Correction

Emily S. Eiel, MD
Lorraine A. T. Boakye, MD

Department of Orthopaedic Surgery, University of Pennsylvania, Philadelphia, PA

Minimally invasive bunionectomy techniques have emerged as a promising alternative to traditional open surgery for the correction of hallux valgus deformities. Minimally invasive bunionectomy offers several potential advantages, including reduced soft tissue trauma, faster recovery times, improved cosmesis, and comparable correction of deformity without significant difference in complication rate. However, challenges such as surgeon experience and learning curve, patient selection, and long-term outcomes remain important considerations. By addressing these topics, this article aims to assist orthopaedic surgeons in making informed decisions regarding the adoption and optimization of minimally invasive techniques for hallux valgus correction.

Background

Over 150 procedures have been described in the orthopaedic literature for treatment of hallux valgus deformity. Minimally invasive techniques have become increasingly popular, especially within the past 10 years. Minimally invasive surgery (MIS) techniques for bunionectomy broadly fall into three categories: first generation is the Isham procedure, a medial closing wedge osteotomy without fixation;[1] second generation is the Bösch procedure or modified Hohmann osteotomy;[2] and third generation, which includes minimally invasive chevron and akin osteotomies (MICA) with headless compression screws.[3]

There has been an increasing number of prospective cohort studies, randomized controlled trials (RCTs), and meta-analyses performed to determine the differences in outcomes between open and MIS procedures. Almost all of these studies focus on three categories of interest: radiographic outcomes, including hallux valgus angle (HVA), first intermetatarsal angle (IMA), and distal metatarsal articular angle (DMAA); clinical outcomes, including American Orthopaedic Foot and Ankle Society (AOFAS) functional score, visual analog scale (VAS) pain score, patient satisfaction, and complication rate (i.e. infection, recurrence, nonunion, screw irritation); and health systems considerations, including operative time, length of stay and cost.

While earlier RCTs only included patients with mild to moderate hallux valgus deformities,[4] more recent trials have included patients severe deformity,[5,6] and all of these trials found no difference in radiographic correction or functional outcomes. Studies did find a significant advantage of MIS in various patient satisfaction measures including cosmesis,[4] post-operative pain,[5] or overall satisfaction with surgery.[6] Two recent meta-analyses by Singh et al. and Ji et al. reviewed 9 and 22 studies respectively, and each found no overall differences in radiographic outcomes between MIS and open techniques.[7,8] When comparing subgroups of MIS generation to open, third generation MICA procedure had significantly lower HVA and second generation Bösch procedure had significantly lower IMA.8 Additionally, sesamoid position correction was significantly greater with MIS techniques.8 While Singh et al. concluded functional outcomes were higher in open procedures, more recent literature, including Ji et al, concluded that functional outcomes were higher in MIS procedures and pain scores were significantly lower in the immediate post-operative period, although no different from open procedures by the time of final follow up. There was significantly higher patient satisfaction after MIS procedures and no difference in rate of complications. Both meta-analyses concluded operative time was significantly shorter in MIS as well, although few details about surgeon experience and training were provided or included in the analysis.

Hochheuser discusses the differences in complications between open and MIS bunionectomy, concluding there is overall no difference in possible complications or outcomes between the two (Table 1).[9] The comprehensive review notes decreased infection rate given the decreased size of incisions, delayed radiographic union but no difference in overall nonunion rate or

Table 1. Benefits and Drawbacks of MIS bunionectomy compared to open surgery

Benefits	Drawbacks	No difference
Increased patient satisfaction	Potentially more difficult to correct severe deformity or address joint instability	Radiographic correction of HVA, IMA, DMAA
Decreased operative time*	Increased use of radiation[3]	AOFAS functionality score**
Lower pain score in immediate post-op period	Delayed radiographic union (noting no difference in overall nonunion rate or symptoms)[9]	Pain score at final follow up appointment
Decreased infection rate	Increased rate of transient post-op paresthesias[9]	Overall complication rate and need for revision
Improved cosmesis		

*Meta-analysis data indicates decreased time, but more recent prospective cohort study found no difference although does not account for differences in surgeon familiarity with techniques.
**Meta-analysis data indicated no difference, while some studies report increased scores for MIS and others report increased scores for open.

symptomatic nonunion, and comparable rates of avascular necrosis and stiffness. Their data suggest that even for less experienced surgeons, there is low to no risk of neurovascular or tendon injury.

Most recently, Balesar et al. conducted a prospective cohort study in which two-thirds of patients underwent MICA osteotomies and one third underwent open Chevron osteotomy, and they found no differences in radiographic hallux valgus correction, functional outcomes, pain, patient satisfaction, or operative time.[10] It is worth noting that the differential in number of patients in the MIS vs open groups is likely multifactorial but may be due to increasing patient awareness of and desire to undergo MIS procedures, as well as increasing surgeon familiarity with MIS indications and techniques.

While MIS bunionectomy is rapidly gaining popularity, surgeon inexperience with minimally invasive techniques is often cited as an argument for open bunionectomy. Palmanovich et al. sought to define the learning curve of the third generation MIS bunionectomy technique and found the learning curve plateaued at 21 cases, fluoroscopic time plateaued at 27 cases, and mean operative time decreased by more than half over the first 50 cases.[11] While there is no better preparation than prior experience and repetition, the tips and tricks in this article may aid in jumpstarting the learning curve and perceived barrier for surgeons interested in incorporating MIS bunionectomy procedures into their practice.

Redfern and Vernois have previously detailed surgical techniques and troubleshooting for MICA osteotomies,[12] whereas this article provides tips and tricks for using a transverse osteotomy and external guide system. One benefit of this technique is the relative ease and speed with which a transverse osteotomy can be completed compared to a Chevron osteotomy. Another benefit is the ability to use the guide to translate and position the distal fragment rather than requiring the surgeon to manually lever and maintain its position while placing guidewires.

Tips and Tricks for MIS Bunionectomy with Transverse Osteotomy

Pick Your Patient

There are a number of considerations to keep in mind when deciding whether minimally invasive techniques may be appropriate for your patient.

- **Severity of deformity**: MIS techniques may be less difficult in patients with mild to moderate deformity. While MIS bunionectomy can be performed in patients with severe deformity, it should be considered only once the surgeon is well versed in the technique. It is worth noting that MIS technique will not allow for stabilization of an unstable joint, in which case an open procedure may be required.
- **Comorbidities**: Patients with medical comorbidities that put them at increased risk for wound healing complications such as diabetics or smokers may be good candidates for MIS bunionectomy given the smaller incisions and decreased soft tissue injury. The prospective cohort study by Balesar et al. had more smokers in the MIS group than open and found no increased rate of wound healing complications or nonunion.
- **Prior surgery**: Patients who have undergone prior surgery likely have altered anatomy or scar tissue that may make MIS more difficult, in which case open procedure should be considered. However, MIS may actually become a more viable option if prior incisions and concerns regarding inadequate skin bridge make a dorsal or medial incision less likely to heal.

Guide, Don't Guess

There is a variety of surgical equipment that can be used to perform minimally invasive bunionectomy. The most commonly used system at this institution includes a capital fragment guidewire and shifting device, trajectory guide, K-wire guides, and parallel guides. The procedure can be broken down into a few key steps:

- **Osteotomy**: Make the transverse osteotomy with a burr through a medial stab incision at the distal metadiaphysis of the first metatarsal (Figure 1a).
- **Guide placement**: Place the hook of the shifting guide through the stab incision and into the intramedullary canal of the first metatarsal. Ensure careful and accurate guide placement of the device where the capital fragment shifter contacts the metatarsal head (Figure 1b).
- **Correction**: Derotate the toe, advance the capital fragment guidewire through the shifter to the lateral cortex, and turn the shifter clockwise to shift the fragment laterally about 50-75% and confirm under fluoroscopy. (Figure 2a).
- **Pinning**: Attach the aiming arm with K-wire positioning knob to the capital fragment guidewire in line with the first metatarsal, making a stab incision to ensure the guide is seated flush on the medial surface of the metatarsal. Advance a K-wire through two cortices of the proximal metatarsal and one of the distal fragment, then place a second K-wire parallel and distal to the first using the parallel guide (Figure 1c). It is sometimes helpful to place K-wires in the proximal segment prior to capital fragment translation when utilizing a free-hand technique.
- **Fixation**: Drill over the first K-wire, measure, and place cannulated screws prior to K-wire removal (Figure 2b). It is helpful to place the first screw prior to drilling for the second to ensure no loss of fixation. You may either drill through the drill sleeves of the guide or remove the guide to drill and place screws over the K-wires. Confirm screw placement on fluoroscopy (Figure 1d) and close your 3-4 stab incisions.

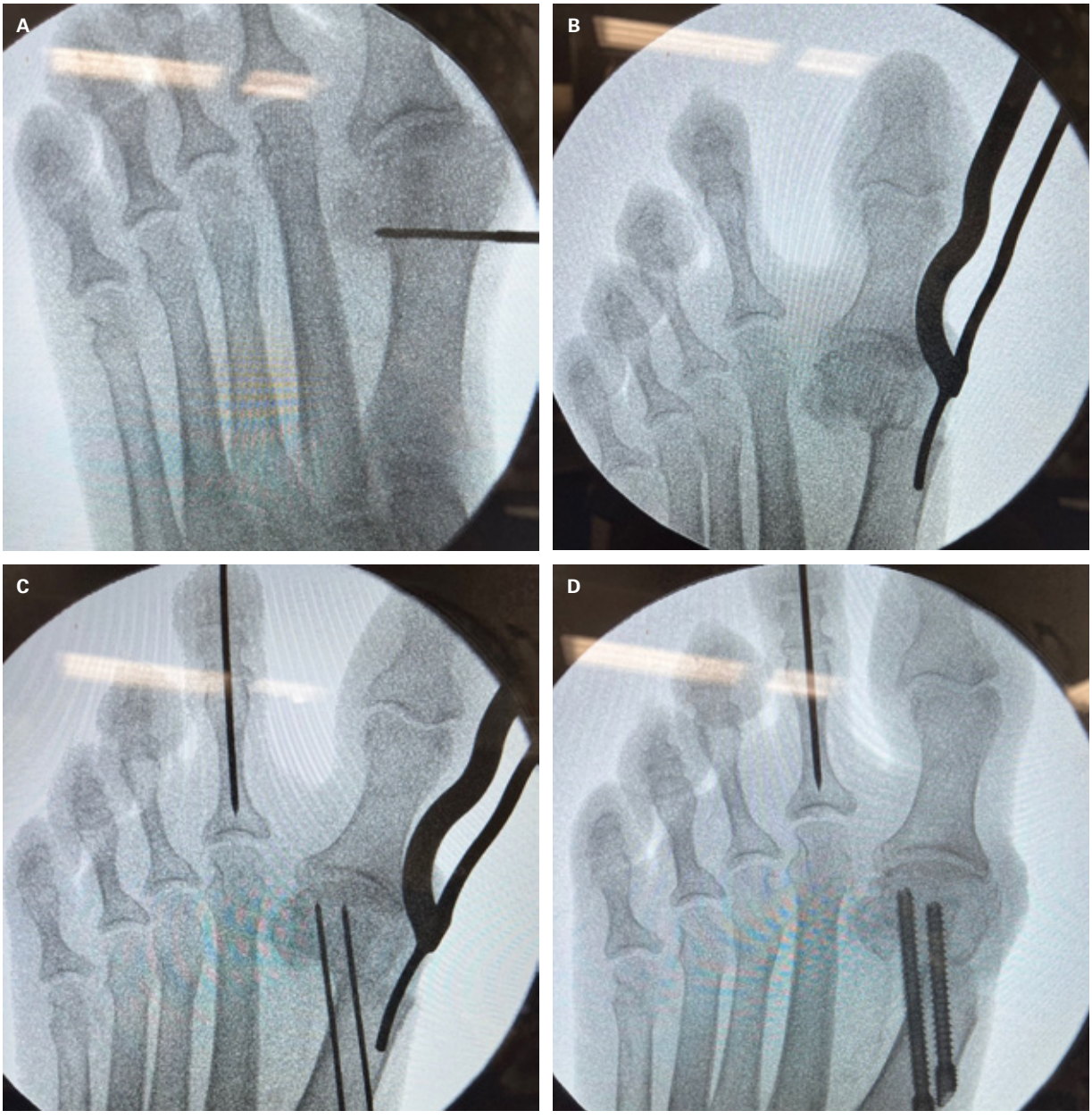

Figure 1. Intraoperative fluoroscopy showing **(A)** transverse osteotomy at the first metatarsal distal metadiaphysis; **(B)** insertion of the shifting guide into the intramedullary canal; **(C)** parallel K-wire placement through two cortices of the metatarsal and into the capital fragment; **(D)** headless canulated screw placement and K-wire removal.

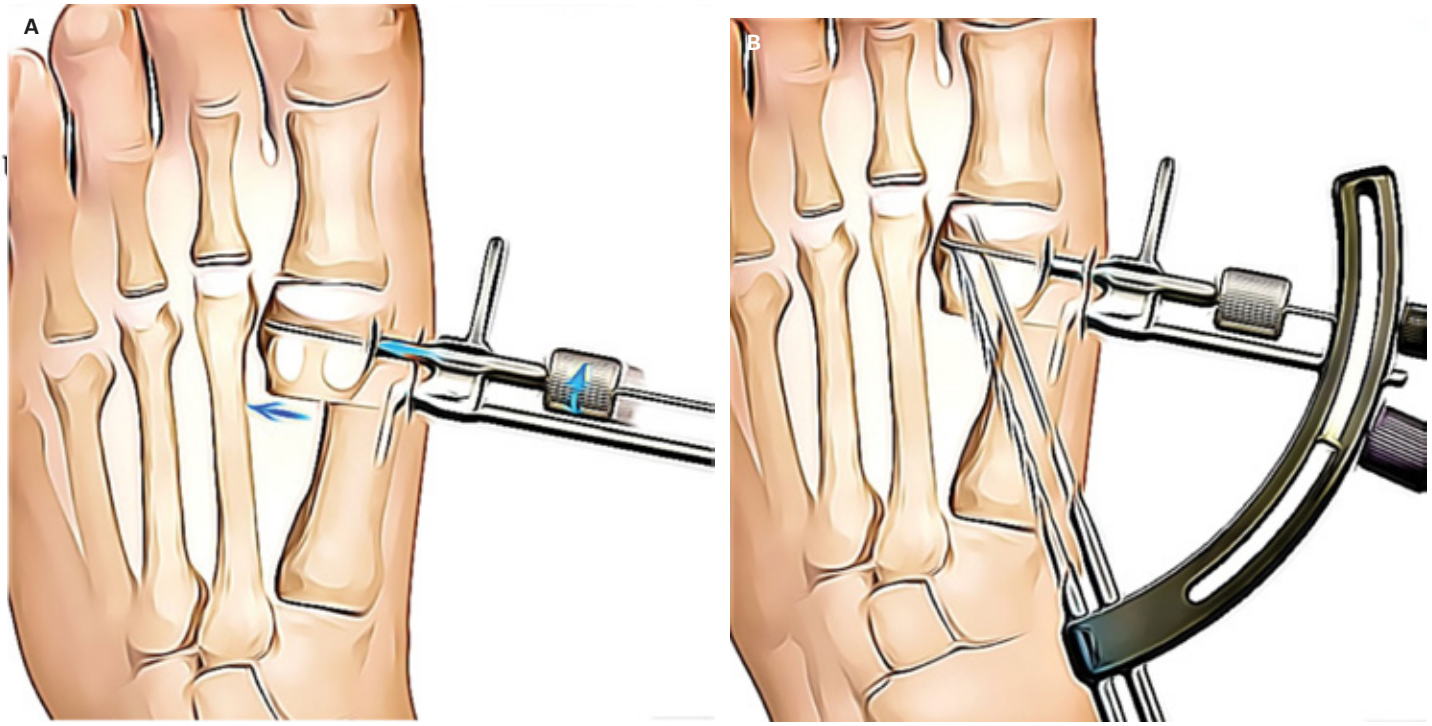

Figure 2. Stylized depictions of external guide system used at this institution showing **(A)** shifting guide with hook in first metatarsal intramedullary canal and capital fragment shifter on metatarsal head with capital fragment guidewire in place. Clockwise turn of shifter results in lateral movement of capital fragment, and **(B)** trajectory guide attached to shifting guide to aid in appropriate parallel K-wire placement, drilling, and eventually screw placement.

Post-operative Protocol

As for any surgery, post-operative care is integral to the success of a surgery both short and long term. In our experience, patients have the best clinical outcomes after MIS bunionectomy when adhering to the following postoperative protocol:

- **Weeks 0-2**: NWB in post-op shoe or CAM boot, sutures out at 2-week appointment.
    - It is helpful to place a spica/bunion dressing for ongoing management of soft tissue tension.
- **Weeks 2-6**: WBAT in post-**op shoe vs** CAM boot, XR at 6-week appointment
- **Weeks 6-8**: WBAT in post-op shoe vs sneaker

This differs from typical open bunionectomy post-operative protocols in that patients are allowed to commence weightbearing more quickly (2 vs 6 weeks) and are able to resume regular shoe wear earlier (6-8 vs 12 weeks).

Conclusion

Minimally invasive procedures for addressing hallux valgus deformities have emerged as a promising alternative to traditional open surgery for addressing hallux valgus deformities. With comparable radiographic outcomes, improved patient reported outcomes, and decreased time and healthcare dollar expenditures, a minimally invasive technique for hallux valgus correction is a great option for the appropriate patient. Given often cited challenges such as surgeon expertise, patient selection criteria, and long-term outcomes, these tips and tricks for the use of a transverse osteotomy and external guide may provide insights to facilitate informed decision-making regarding the adoption and optimization of minimally invasive procedures for hallux valgus correction.

References

1. Isham SA. The Reverdin-Isham procedure for the correction of hallux abducto valgus. A distal metatarsal osteotomy procedure. *Clin Podiatr Med Surg.* 1991 Jan;8(1):81-94.

2. Bösch P, Wanke S, Legenstein R. Hallux valgus correction by the method of Bösch: a new technique with a seven-to-ten-year follow-up. *Foot Ankle Clin.* 2000 Sep;5(3):485-98, v-vi.

3. Altenberger S, Kriegelstein S, Gottschalk O, *et al.* The minimally invasive Chevron and Akin osteotomy (MICA). *Oper Orthop Traumatol.* 2018;30(3):148-160.

4. Radwan YA, Mansour AM. Percutaneous distal metatarsal osteotomy versus distal chevron osteotomy for correction of mild-to-moderate hallux valgus deformity. *Arch Orthop Trauma Surg.* 2012;132(11):1539-1546.

5. Lee M, Walsh J, Smith MM, *et al.* Hallux Valgus Correction Comparing Percutaneous Chevron/Akin (PECA) and Open Scarf/Akin Osteotomies. *Foot Ankle Int.* 2017;38(8):838-846.

5. Kaufmann G, Dammerer D, Heyenbrock F, *et al.* Minimally invasive versus open chevron osteotomy for hallux valgus correction: a randomized controlled trial. *Int Orthop.* 2019;43(2):343-350.

7. Singh MS, Khurana A, Kapoor D, *et al.* Minimally invasive vs open distal metatarsal osteotomy for hallux valgus - A systematic review and meta-analysis. *J Clin Orthop Trauma.* 2020;11(3):348-356.

8. Ji L, Wang K, Ding S, *et al.* Minimally Invasive vs. Open Surgery for Hallux Valgus: A Meta-Analysis. *Front Surg.* 2022;9:843410.

9. Hochheuser G. Complications of Minimally Invasive Surgery for Hallux Valgus and How to Deal with Them. *Foot Ankle Clin.* 2020;25(3):399-406.

10. Balesar VV, Bruin LL, van Liebergen M, *et al.* MICA Procedure vs Open Chevron Osteotomy for Hallux Valgus Correction: A Prospective Cohort Study. *Foot Ankle Orthop.* 2024 Jan 28;9(1):24730114231224725.

11. Palmanovich E, Ohana N, Atzmon R, *et al.* MICA: A Learning Curve. *J Foot Ankle Surg.* 2020;59(4):781-783.

12. Redfern D, Vernois J. Minimally Invasive Chevron Akin (MICA) for Correction of Hallux Valgus. *Tech Foot Ankle Surg.* 2016;15(1):1.

Don't Forget to Evaluate the Ankle—Tips and Tricks for Operative Treatment of Distal Third Tibia Fractures

Bradley O. Osemwengie, MD
Chielozor I. Okafor, MD
Lisa G.M. Friedman, MD, MA
Stephen R. Barchick, MD
Samir Mehta, MD

Department of Orthopaedic Surgery, University of Pennsylvania

Introduction

Tibial shaft fractures are commonly managed with open reduction and internal fixation (ORIF) using an intramedullary nail (IMN). Tibia Fractures are the most common open fracture with approximately 24% of tibial diaphysis fractures being open.[1] Intramedullary nailing provides excellent rates of union in cases of open tibial shaft fractures.[2] In addition, reamed intramedullary nails have lower rates of reoperation compared to unreamed tibial nails.[3]

Combined tibia and fibula fractures usually occur after high energy mechanisms such as motor vehicle accidents.[4] There are numerous considerations for operative versus non-operative management of fibula fractures in patients with a concomitant tibia fracture. Surgeons who favor fixation may cite improved ability to restore tibial length, alignment, and rotation. Those favoring non-operative management of associated fibula fractures cite its possibility to decrease cyclic loading of the tibial fracture site, thereby risking delayed union or nonunion.[5]

Distal third tibia shaft fractures may be associated with occult posterior malleolus fractures in about 30% of patients that may be displaced iatrogenically during IMN of the tibia shaft fracture.[6] As such, it is vital to identify associated posterior malleolus fractures to prevent further articular surface damage during ORIF. As a matter of practice, our institution orders advanced imaging in the form a CT scan for any distal third tibia fracture to assess for this highly associated injury as it may affect surgical decision-making.

The posterior malleolus and syndesmosis are connected via the posteroinferior tibiofibular ligament (PITFL). Fixing posterior malleolus fractures and fibular fractures can confer stability to the syndesmosis which may obviate the need to surgically fix the syndesmosis.[7]

In cases of syndesmotic instability, transyndesmotic fixation can be achieved using suture buttons, screws, or a combination of the two constructs.[8] This is typically performed after the other fractured components are addressed. The syndesmotic integrity is then determined after a stress exam as to whether it needs to be stabilized surgically.

The selected staging of multiple different surgical steps is important with the increasing complexity of fractures. We present the case of a patient with an open distal third tibia fracture, posterior malleolus fracture, distal fibula fracture, and an additional unstable syndesmosis after a motorcycle collision. The sequence of fixation as well as meticulous wound closure are of importance in this case. A successful surgical outcome requires a thorough preoperative plan so that each step assists with creating of an overall appropriate construct to stabilize the injury—and in the case of an open fracture—also prevent infection.

Case Presentation

The patient is a 31-year-old male who presented with a Gustilo-Anderson Type 3A (GA3) open left distal-third spiral tibia and fibula fracture. The patient was temporized in the trauma bay, the wound was washed with saline and betadine and he was placed into a splint. Antibiotics (Ceftriaxone for GA3 injuries) and tetanus were administered upon arrival. Advanced imaging was obtained which revealed an intra-articular extension of the tibial shaft fracture with a posterior malleolus fracture (Figure 1,2). The patient was admitted and administered standing antibiotics. His injured leg was elevated on a ramp and serial compartment checks were performed.

Surgical Technique

Given the concern for his soft tissue envelope, he underwent surgical debridement and irrigation and temporizing external fixation of the left leg one day after presentation. The traumatic wound was extended both proximally and distally at the apices. A The fractured ends of the tibia were exposed and debrided. Any loose fragments of diaphyseal bone and debris were removed. The wound was then irrigated with 6 liters of normal saline. The deep tissue was closed

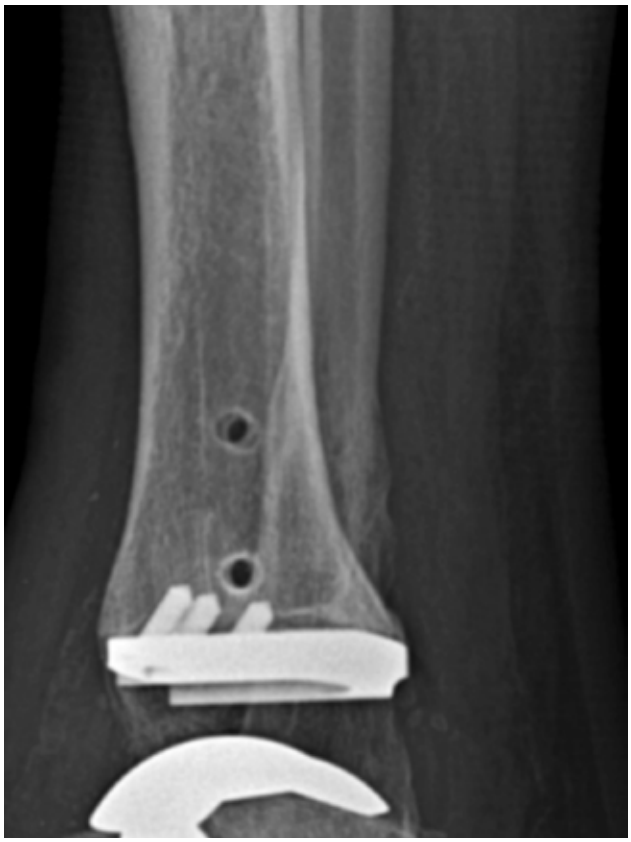

Figure 1. Initial patient evaluation in the trauma bay showing an open tibia fracture with bone extruding through the skin.

with Vicryl. The skin was closed primarily with #3-0 nylon in an Allgöwer-Donati fashion. The external fixator was then applied. One Schanz pin was placed trans-calcaneal and one in the proximal tibia in an anterior to posterior direction. The delta frame was then constructed, the tibia fracture and trimalleolar ankle fracture was closed reduced, and the construct was locked. An out of plane pin in the tibia was placed to enhance the multiplanar construct.

Six days after his injury, definitive fixation was performed. The patient was positioned supine on a radiolucent table with a hip bump. The operative leg was elevated on a leg ramp to aid with intraoperative fluoroscopic acquisition. The left leg was prepped and draped. The fibula was first addressed. The external fixator remained in place to help maintain fibular length. An incision was made over the distal tip of the fibula after identification of an appropriate starting point was identified on both AP and lateral fluoroscopic images. A 3.5 mm drill hole was made at the tip of the fibula followed by a 2.5 mm drill bit to ream the canal distally. A humeral guidewire was inserted into the entry site created in the fibula distally (Figure 3). Next, an incision was made over the fibular shaft fracture. A small lobster clamp was used to manipulate and reduce the fracture fragments (Figure 4). After reduction, the humeral

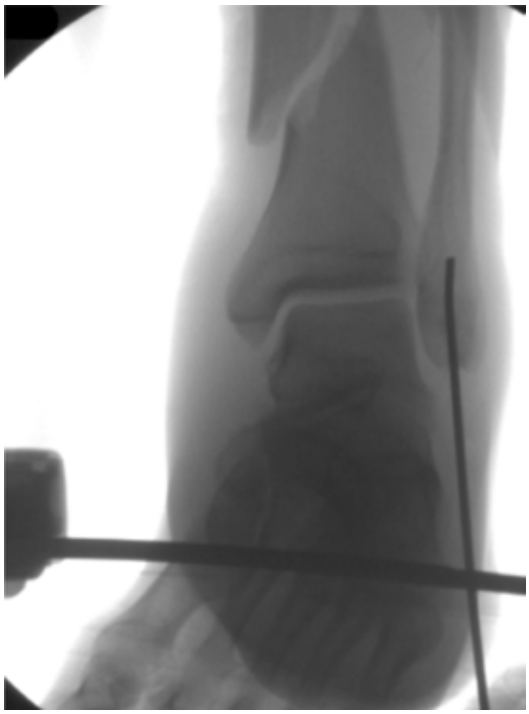

Figure 3. Intraoperative mortise x-ray of the ankle showing humeral guidewire insertion into the distal aspect of the fibula.

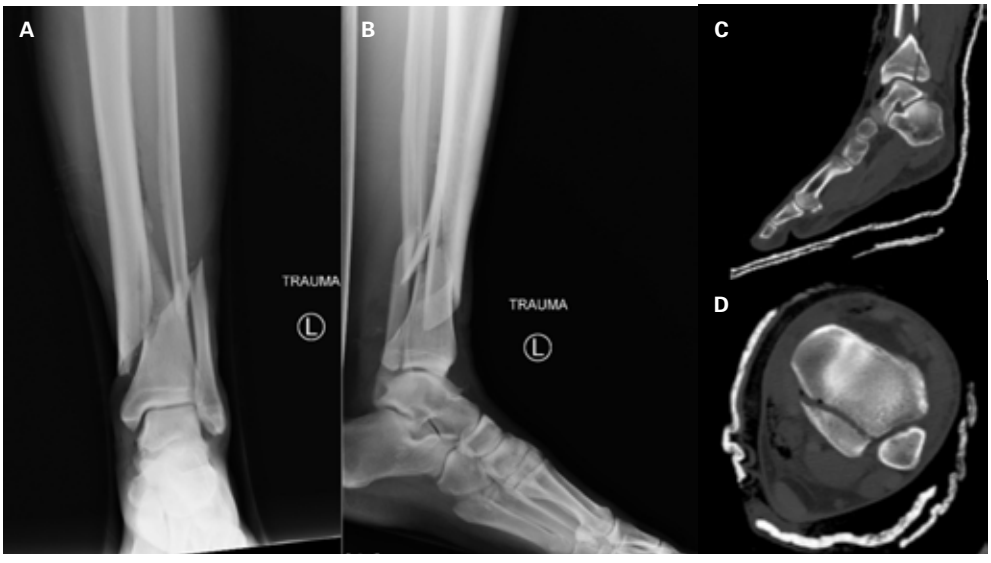

Figure 2. (A) Anteroposterior and **(B)** lateral radiographs of the left distal tibia showing spiral distal third tibia and fibula fractures and posterior malleolus fracture; **(C)** Sagittal and **(D)** axial CT slices further characterizing the non-displaced posterior malleolus fracture.

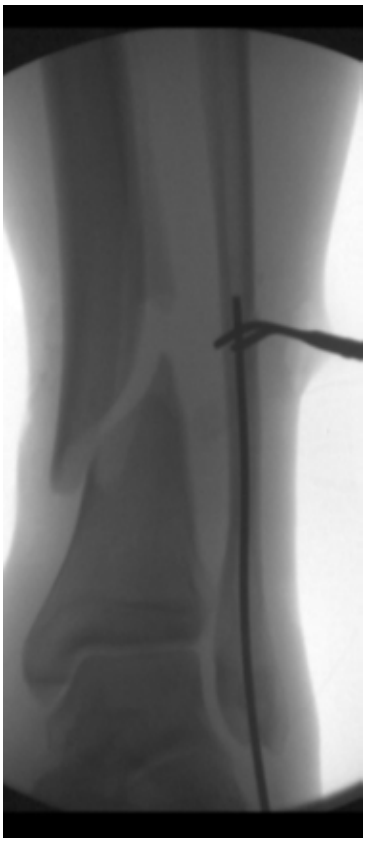

Figure 4. Intraoperative fluoroscopy image of the left distal tibia/fibula showing reduction of the fibula fracture with a lobster claw reduction clamp. Humeral guide wire has now been passed proximal to the fracture site in the fibula.

guidewire was advance just short of the fibular head, thereby stabilizing the fibular shaft fracture. The fibular guide wire was then cut and advanced so the entire wire could be buried within the fibula to avoid prominence.

With the fibula now stabilized, the posterior malleolus was addressed. Percutaneous incisions were made over the distal tibia followed by blunt dissection down to the level of the tibial plafond. This technique was selected to protect the anterior compartment tendons and neurovascular structures. The posterior malleolus was fixed by inserting two screws via a lag by technique approach to compress the posterior malleolus. This was done by drilling the outer diameter (3.5mm) of the screw up to the fracture site. The drill was then switched to a 2.5mm drill bit to match the inner diameter of the screw. This was drilled through the far cortex. A depth gauge was inserted to measure appropriate length screw. A 3.5mm fully threaded screw with a washer was then placed at the level of the plafond. This step was repeated for a second plafond screw (Figure 5). Because of the nondisplaced nature of this fracture, no reduction aids were required. As there was now adequate reduction/compression of the articular surface, the last fracture to be addressed was the tibial shaft.

The 17-centimeter traumatic wound on the medial side of the shin was opened. The fracture site was debrided a second time and all loose bone fragments were removed followed by irrigation with six liters of normal saline. Aided by the fixation achieved of the fibula fracture, a pointed reduction clamp was then used to reduce the tibial shaft through the open traumatic wound (Figure 6). AP and

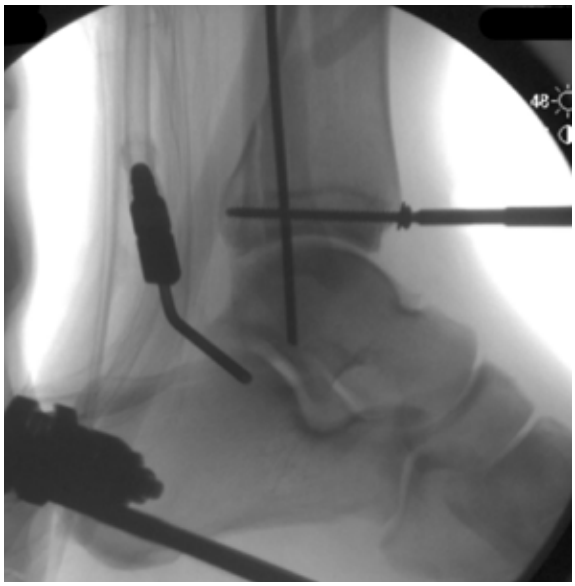

Figure 5. Intraoperative fluoroscopy of the lateral distal tibia demonstrating posterior malleolus fracture fixation via placement of anterior to posterior lag screw with washer.

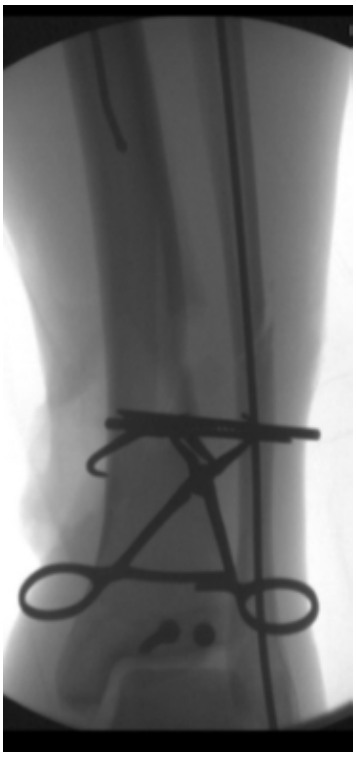

Figure 6. Intraoperative fluoroscopy of the tibia/fibula demonstrating use of reduction clamps to reduce the tibial shaft fracture.

lateral fluoroscopic images confirmed length, alignment, and rotation of the distal third tibia fracture. The external fixator tibial pins were then removed along with the bars attached to them. The calcaneal pin was left in place to pull traction if needed. The surgical team next moved to placement of a tibial nail.

The suprapatellar approach was used to gain access to the patellofemoral joint with a small incision starting a fingerbreadth above the superior pole of the patella centered over the quadriceps tendon. After dissection to the paratenon, medial and lateral edges of the quadriceps tendon were identified and the quadriceps tendon was

incised to bone sharply. The patellofemoral guide was placed into the knee. A drill tip wire was placed in the ideal starting point for an IMN on both the AP and lateral views: just medial to the lateral tibial spine and on the anterior lip of the tibial plateau.

On a lateral radiograph, the proximal tibia was reamed with utilizing fluoroscopy to confirm the posterior tibial cortex was not violated. A ball-tipped guidewire was inserted down the canal, past the fracture site which remained appropriately reduced, to the physeal scar. Sequential reaming was performed up to a size 11mm reamer. A 10mm nail was inserted over the ball-tipped guidewire. The ball-tipped guidewire was removed, and the intramedullary nail was stabilized with two screws proximally using the external targeting guide and two screws distally using the perfect circles technique. The temporizing clamp was then removed. The calcaneal Schanz pin was removed as well.

Due to the high energy mechanism of injury, the syndesmosis was assessed with an external rotation stress examination of the ankle. An appropriate mortise radiograph was obtained and with external rotation stress, syndesmotic instability was noted. As a result, while manually squeezing the tibia and fibula to maintain the syndesmotic relationship, a single 3.5mm quadricortical transyndesmotic screw was placed across the fibula and tibia to stabilize the syndesmosis (Figure 7).

All the wounds were thoroughly irrigated with saline. Vancomycin powder was then administered over the site of the prior open fracture. The regular surgical incisions were closed in staged fashion as is standard practice. The skin layer was closed with Allgöwer-Donati stitches utilizing #3-0 nylon. The patient was splinted and made non-weightbearing. Postoperative x-rays were obtained (Figure 8). The patient was admitted, with compartment checks for 24 hours after surgery, 24 hours of antibiotics,

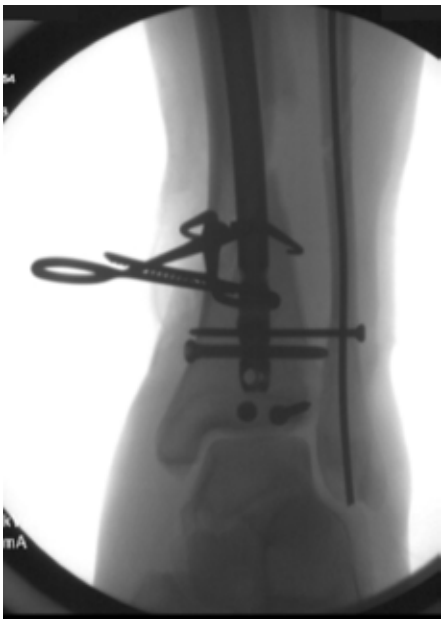

Figure 7. Intraoperative fluoroscopy of the tibia/fibula demonstrating placement of a quadricortical transyndesmotic screw across the distal tibia/fibula.

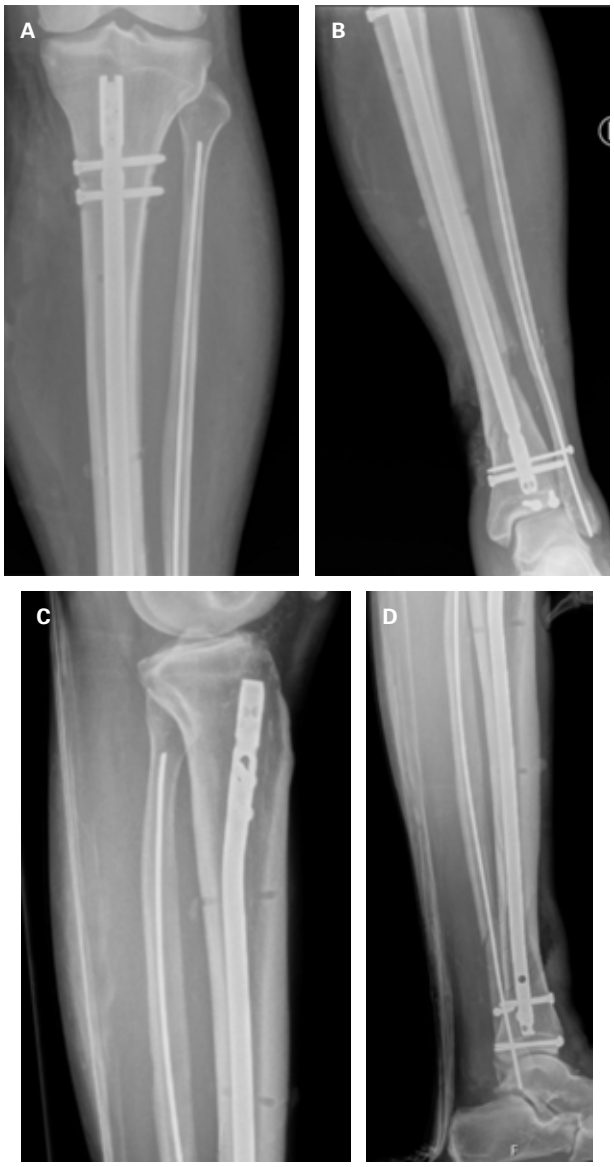

Figure 8. Immediate postoperative radiographs showing a restoration of tibia/fibula length alignment and rotation with the tibia IMN, fibular nail, plafond screws, and a transyndesmotic screw. **(A)** AP of proximal tibia/fibula; **(B)** AP of distal tibia/ fibula; **(C)** Lateral of proximal tibia/fibula; **(D)** Lateral of distal tibia/fibula.

and made non-weight-bearing in a splint for both soft tissue rest and given the intra-articular and syndesmotic injuries.

The patient followed in clinic two weeks postoperatively from definitive fixation. He was noted to have expected healing of his fractures and skin (Figure 9, 10). The sutures over the open fracture were removed twenty-nine days after definitive fixation. At two months postop, he was allowed to weight bear as tolerated. Skin incision at that time had some areas of eschar (Figure 11).

At three months postop, he was able to return to work as a mechanic. Approximately seven months postop, radiographs revealed interval healing at his fracture site. Notably, the syndesmotic screw was found to be broken at this visit, but he denied any symptoms related to this (Figure 12). A discussion was had regarding eventual

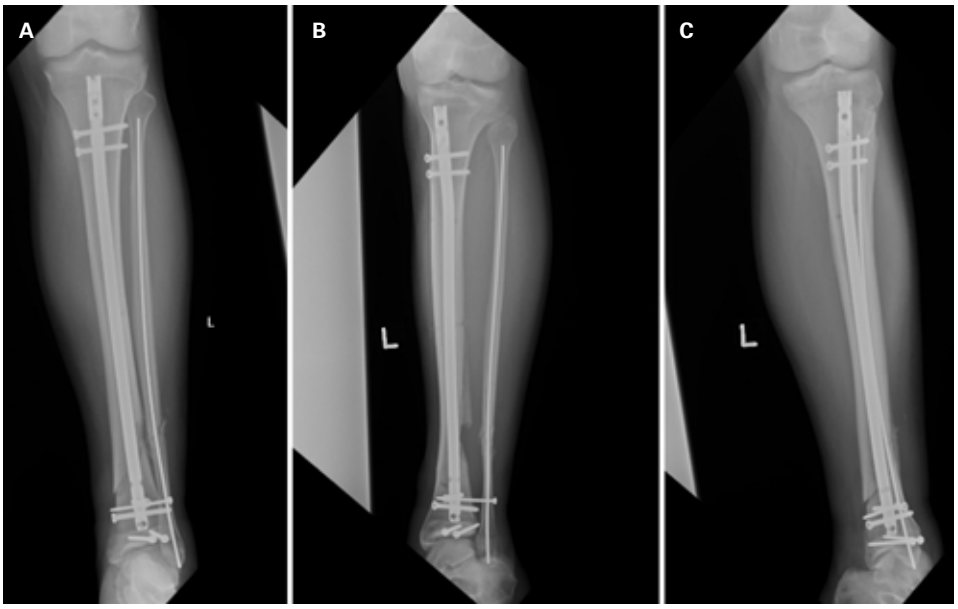

Figure 9. Anteroposterior, oblique, and lateral radiographs of the left tibia and fibula 8 weeks postoperatively demonstrating interval healing at the distal tibia and fibula fracture sites with callous formation.

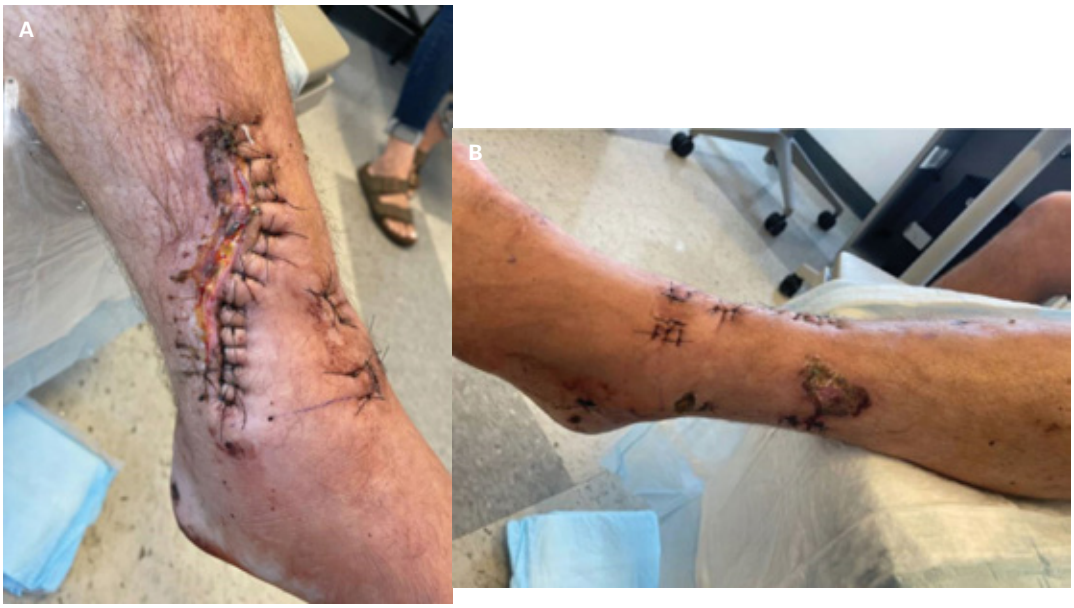

Figure 10. Clinical photographs demonstrating Allgöwer-Donati sutures of the left **(A)** medial and **(B)** lateral ankle incisions 13 days postoperatively.

removal of hardware if the patient so desired. The patient had full range of motion and strength of his left lower extremity. Clinical photos at this visit are shown in Figure 13. He was discharged from the practice and instructed to follow up as needed.

Discussion

Open tibial shaft fractures are often definitively treated with IMN. Open fractures treated with IMN demonstrate excellent rates of union. Concurrent posterior malleolus fractures should be addressed prior to inserting the IMN to avoid displacing the fracture and damaging the articular surface.[6]

There is conflicting literature on whether one should fix the fibula. Some authors suggest there is no benefit, as patients who undergo ORIF exhibit similar rates of deformity, infection, and union.[5] However, other series have advocated for ORIF of the fibula to promote soft tissue healing. Fibula fixation may also assist with achieving appropriate length, alignment, and rotation of the tibia, as was the choice for surgical management with this patient.[9] Generally, methods for ORIF of the fibula include plating and nailing. The method in this case stabilizes the fibula with a small-diameter humeral guide wire, which has been shown to facilitate tibia reduction without disturbing local soft tissues.[10] The incision for fibula humeral guide wire instrumentation with another small incision over the fibular shaft fracture site is much smaller than what would be required for fibular shaft plating.

Posterior malleolus fractures are usually fixed if the fracture involves more than 25% of the articular surface. Fractures with less than two-millimeter step-off and involving less than 25% of the articular surface can be managed non-operatively.[11] Fracture fixation methods vary

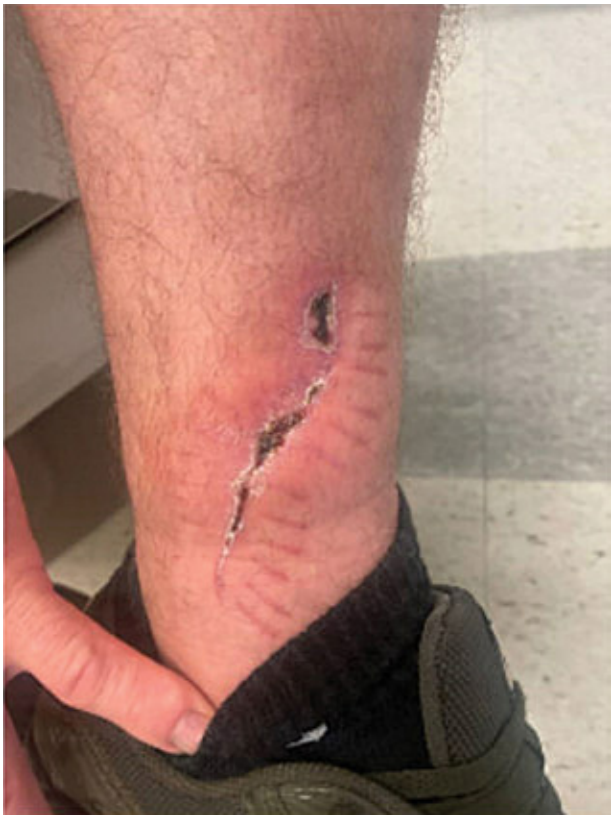

Figure 11. Clinical photograph of the left medial lower leg demonstrating interval healing of the incision eight weeks postoperatively. Areas of dry eschar are noted along the incision.

depending on the fracture type. Buttress plating, posterior to anterior lag screws, and anterior to posterior lag screws are popular options for fixation in this region of the body. Buttress plating has been shown to be biomechanically superior to lag screw fixation by minimizing vertical displacement of the fracture fragment.[12] However, plating requires a more extensive soft tissue dissection and requires modification in patient positioning to expose the fracture site. Lag screws are a useful fixation strategy in nondisplaced fractures that do not require a significant reduction. Anterior to posterior lag screws also avoids having to reposition the patient for that component of the procedure.

Transyndesmotic fixation is utilized to stabilize a disrupted syndesmosis. This can be achieved with flexible fixation by way of suture buttons or more rigid fixation by way of screws. Tricortical or quadricortical fixation can be used with no apparent difference between the two options. The goal of syndesmotic fixation is to restore the tibia/fibula interval, preserve fibular length, and maintain proper alignment of the fibula in the tibial incisura.[13]

In this case, the fibula was first reduced and fixed to help with obtaining the appropriate length of the fractured tibia. The posterior malleolus was then fixed prior to instrumentation of the tibia to prevent displacement of the articular surface. Obtaining length and stability of the fibula can reduce the posterior malleolus due to the attached soft tissue. Once the tibial shaft was fixed, the syndesmosis was stressed and deemed to be injured. A screw was placed across the tibia and fibula to stabilize the syndesmosis.

Risk of deep surgical site infection needs to be considered in the setting of open fractures. In the setting of open tibia fractures, vancomycin powder use has been shown to reduce the risk of gram-positive deep surgical site infection.[14] In addition, given the increased risk of skin complications in open fractures, meticulous soft tissue handling is imperative. The use of Allgöwer-Donati suture technique during primary closure has been associated with higher rates of primary healing and decreased rates of

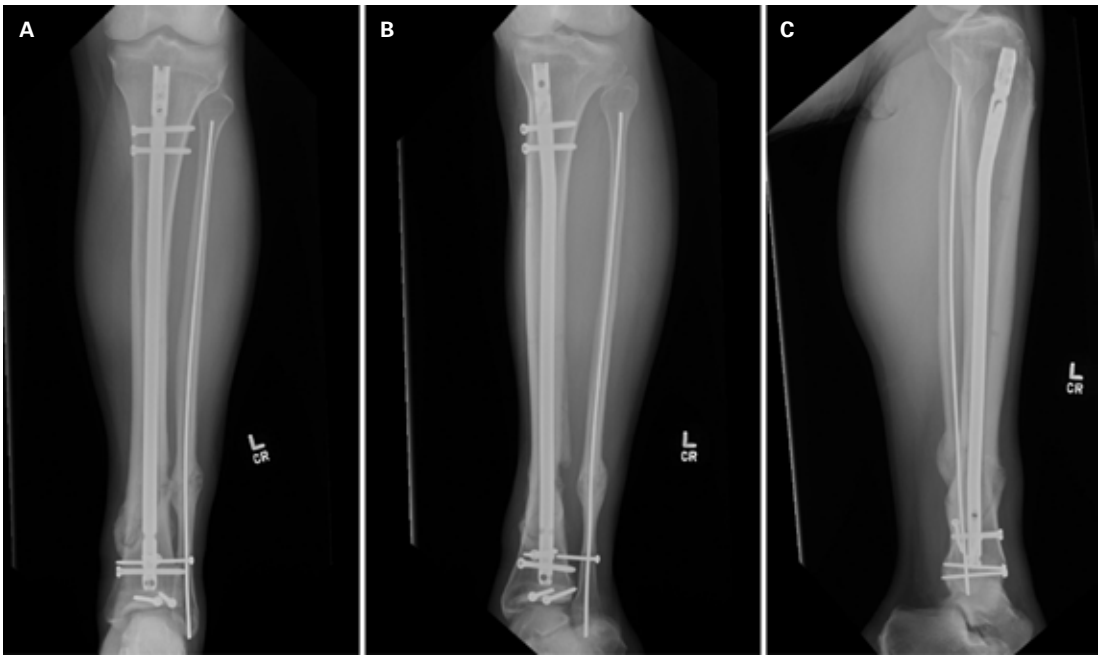

Figure 12. (A) Anteroposterior, **(B)** oblique, and **(C)** lateral radiographs of the left tibia/fibula six months postoperatively demonstrating interval healing at the distal tibia and fibula fracture sites. There is a fracture of the transyndesmotic screw noted.

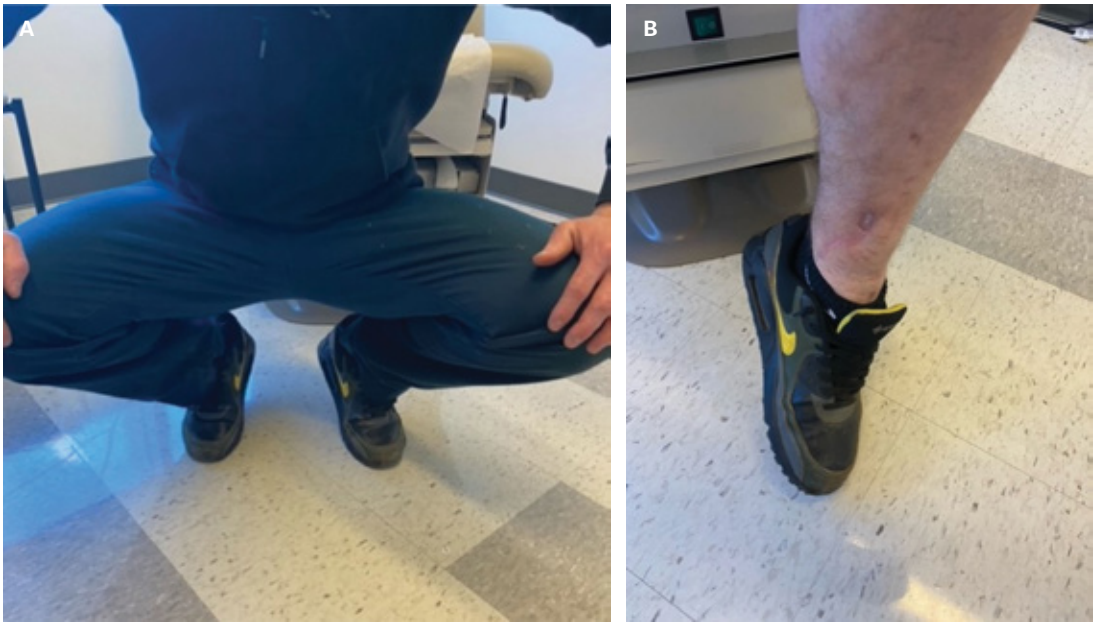

Figure 13. Clinical photographs demonstrating **(A)** a painless squat and **(B)** a healed left medial ankle incision six months postoperatively.

subsequent flap procedures.[15] The Allgöwer-Donati suture has been shown to allow for better soft tissue perfusion and less strangulation compared to the vertical mattress in a clinical trial.[16]

Conclusion

The order of fixation for each component of a complex lower extremity injury is vital when obtaining appropriate reduction and fixation. Fixation of the fibula assists with obtaining the desired length of the tibia. Fixation of the articular surface prevents additional difficulties with anatomic reduction of the articular surface before insertion of the tibia IMN. It also prevents the disruption of the articular surface during nail insertion. The syndesmosis is stressed and stabilized if needed after all other fixation is complete. Wound bed vancomycin powder helps to prevent deep surgical site infection. Lastly, skin closure using sutures in an Allgöwer-Donati fashion allows for optimal healing of complex wounds that are at high risk for complications.

References

1. Melvin JS, Dombroski DG, Torbert JT, *et al.* Open tibial shaft fractures: I. Evaluation and initial wound management. *J Am Acad Orthop Surg*. 2010; 18(1):10-9.

2. Melvin JS, Dombroski DG, Torbert JT, *et al.* Open tibial shaft fractures: II. Definitive management and limb salvage. *J Am Acad Orthop Surg*. 2010; 18(2):108-17.

3. Prospectively Evaluate Reamed Intramedullary Nails in Patients with Tibial Fractures Investigators, Bhandari M, Guyatt G, Tornetta P, *et al.* Operatively Treated High-risk Tibia Fractures: A Randomized Clinical Trial. *JAMA Surg* 2021; 156(5):e207259. Randomized trial of reamed and unreamed intramedullary nailing of tibial shaft fractures. *J Bone Joint Surg Am*. 2008; 90(12):2567-2578.

4. Torino D, Mehta S. Fibular Fixation in Distal Tibia Fractures: Reduction Aid or Nonunion Generator?. *Journal of Orthopaedic Trauma*. 2016; 30 S22-S25.

5. Li C, Li Z, Wang Q, *et al.* The Role of Fibular Fixation in Distal Tibia-Fibula Fractures: A Meta-Analysis. *Adv Orthop*. 2021; 2021:6668467.

6. Wang Z, Chen W, Zhu Y, *et al.* Incidence and missed diagnosis risk of occult posterior malleolar fractures associated with the tibial shaft fractures: a systematic review. *J Orthop Surg Res*. 2021; 16(1):355.

7. Behery OA, Narayanan R, Konda SR, *et al.* Posterior Malleolar Fixation Reduces the Incidence of Trans-Syndesmotic Fixation in Rotational Ankle Fracture Repair. *Iowa Orthop J*. 2021; 41(1):121-125.

8. Xu Y, Kang R, Li M, *et al.* The Clinical Efficacy of Suture-Button Fixation and Trans-Syndesmotic Screw Fixation in the Treatment of Ankle Fracture Combined With Distal Tibiofibular Syndesmosis Injury: A Retrospective Study. *J Foot Ankle Surg*. 2022; 61(1):143-148.

9. Huang CW, Wu WT, Yu TC, *et al.* Retrograde Intramedullary Kirschner Wire Fixation as an Alternative for Treating Distal Fibular Shaft Fractures Combined with Distal Tibial Pilon Fractures. *J Pers Med*. 2022;12(7):1124.

10. Dombroski D, Scolaro JA, Pulos N, *et al.* Fibular fracture stabilization with a guidewire as supplementary fixation in tibia fractures. *Am J Orthop* (Belle Mead NJ). 2012; 41(11):506-9.

11. De Vries JS, Wijgman AJ, Sierevelt IN. Long-term results of ankle fractures with a posterior malleolar fragment. *J Foot Ankle Surg*. 2005; 44(3):211-217.

12. Anwar A, Zhang Z, Lv D, *et al.* Biomechanical efficacy of AP, PA lag screws and posterior plating for fixation of posterior malleolar fractures: a three dimensional finite element study. *BMC Musculoskelet Disord*. 2018;19(1):73.

13. Porter DA, Jaggers RR, Barnes AF, *et al.* Optimal management of ankle syndesmosis injuries. *Open Access J Sports Med*. 2014 Aug 5;5:173-82.

14. Major Extremity Trauma Research Consortium (METRC), O'Toole RV, Joshi M, Carlini Anthony R, *et al.* Effect of Intrawound Vancomycin Powder in Operatively Treated High-risk Tibia Fractures: A Randomized Clinical Trial. *JAMA Surg*. 2021;156(5):e207259.

15. DeBaun, Malcolm R. MD, Goodnough, L. *et al.* Type III Open Tibia Fractures Treated With Single-Stage Immediate Medullary Nailing and Attempted Primary Closure Yield Low Rates of Flap Coverage. *Journal of the American Academy of Orthopaedic Surgeons*. 2021. 31(5):p 252-257,

16. Shannon, Steven F. MD, Houdek, Matthew T. MD, Wyles, Cody C. BS, *et al.* Allgöwer–Donati Versus Vertical Mattress Suture Technique Impact on Perfusion in Ankle Fracture Surgery: A Randomized Clinical Trial Using Intraoperative Angiography. *Journal of Orthopaedic Trauma* 2017. 31(2):p 97-102

Tendon Loads Measured over 2 Weeks of Daily Living are Associated with Achilles Tendinopathy Patient Outcomes

Ke Song, PhD[1]*,
Michelle P. Kwon, BS[1],
Andrew K. Smith, PT, DPT, MS[2],
Karin Grävare Silbernagel, PT, ATC, PhD, FAPTA[2]
Josh R. Baxter, PhD[1]

[1]Department of Orthopaedic Surgery
University of Pennsylvania

[2]Department of Physical Therapy
University of Delaware

Introduction

Achilles tendinopathy is a debilitating chronic condition prevalent in physically active adults.[1] Exercise rehabilitation can effectively reduce symptoms in a short term,[2] yet long-term outcomes vary greatly among patients[3] as 35–60% still experience pain and up to 50% seek alternative treatments including surgery.[4,5] A major challenge for improving rehabilitation outcomes is to determine the cumulative effects of tendon loading due to exercises and patient-specific daily living. The purpose of our study was to develop a strategy to measure cumulative tendon loads in Achilles tendinopathy patients and determine their associations with patient outcomes and characteristics including age, severity of tendinopathy, and self-reported activity level.

Methods

We enrolled 8 patients diagnosed with Achilles tendinopathy and 3 pain-free controls after informed consent in this IRB-approved study. We continuously measured loads in each patient's most painful tendon (random side for controls) over a 2-week span using an instrumented force-sensing insole (Loadsol) and a physics-based algorithm.[6] We computed cumulative tendon loads over the entire monitoring period above 2 pre-defined thresholds: "*overall*" load as $\geq$ 0.3 body weight ($\times$BW) that results from any non-trivial daily living activities,[7] and "*high*" load as $\geq$ 3.0$\times$BW which is above walking level and thus primarily due to dynamic exercises.[7] We computed cumulative loading time as the total time when tendon load is over the *overall* and *high* thresholds, and cumulative loading impulse as the integral of *overall* and *high* load over their cumulative loading time (**Figure 1, insets**). We defined *overall* cumulative loading time ($\geq$ 0.3$\times$BW) as the "Total Active Hours", and normalized the *overall* and *high* cumulative loading impulse by Total Active Hours to control for the variable total periods that participants wore the instrumented insole. We also normalized *high* loading time by Total Active Hours to represent the percentage of time when the tendon was loaded above a *high* level. To determine whether these 3 normalized metrics (*overall* and *high* loads per Active Hour; percentage of time over *high* load) are associated with patient outcomes, we calculated Pearson correlations between these metrics and participant age, self-reported severity of Achilles tendinopathy,[8] and a self-reported current Physical Activity Scale (PAS).2 We defined a correlation coefficient of $|r| \geq 0.7$ as strong, 0.4 – 0.7 as moderate, and 0.1 – 0.4 as weak.[9] We combined data from the patients and controls for these preliminary analyses (n = 11).

Results

Eleven participants (age: 43.5 $\pm$ 17.2 y/o, BMI: 30.5 $\pm$ 7.0 kg/m2) logged insole data over 10.3 $\pm$ 2.3 days (range: 6 – 13), capturing 21.4 $\pm$ 9.5 Total Active Hours (11.6 – 46.9) and cumulating 23.5 $\pm$ 11.3 $\times$BW*hours of *overall* tendon loading impulse (9.8 – 53.5). As a subset of *overall* load, participants had highly variable *high* loading time (0.9 $\pm$ 0.9 hours, 0 – 2.4) and impulse (3.2 $\pm$ 3.3 $\times$BW*hours, 0 – 9.3). Per Active Hour, participants cumulated 1.10 $\pm$ 0.17 $\times$BW of *overall* load (0.82 – 1.28) and 0.14 $\pm$ 0.12 $\times$BW of *high* load (0 – 0.38). Percentage of time over *high* load was 3.8 $\pm$ 3.1% (0 – 10.0). *Overall* load per Active Hour was weakly correlated to age ($r = -0.247$) and severity of tendinopathy ($r = 0.367$), and moderately to self-reported activity level ($r = 0.458$, (Figure 1, left). In contrast, reduced *high* load per Active Hour was strongly correlated to older age ($r = -0.733$) and a lower self-reported activity level ($r = 0.705$, (Figure 1, center), while moderately correlated to more severe tendinopathy ($r = 0.548$). Likewise, a lower percentage of time over *high* load was strongly correlated with older age (r = -0.744) and less self-reported activities ($r = 0.707$, (Figure 1, right) and moderately with disease severity ($r = 0.558$).

Discussion

Our study is the first we know to experimentally measure Achilles tendon loads

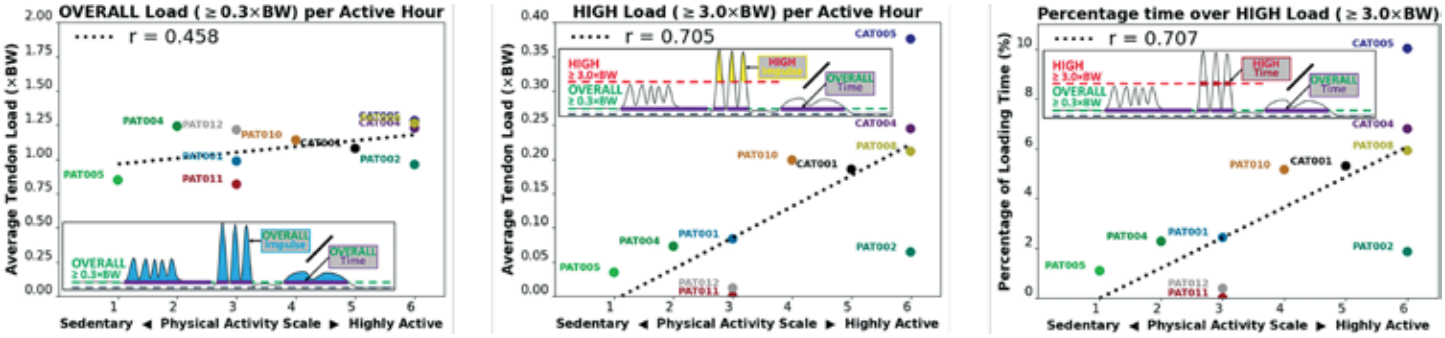

Figure 1. Self-reported activity level vs. normalized Achilles tendon loads measured over 2 weeks of force-sensing insole monitoring: (left) overall tendon load (≥ 0.3×BW) per Active Hour, (center) high load (≥ 3.0×BW) per Active Hour, and (right) percentage of time over high load. Cumulative high load showed stronger correlations ($r > 0.7$) to self-reported activity level than overall load likely because it varied more substantially among individuals due to occupations and lifestyles. Each marker represents a patient (PAT) or control (CAT). Inset diagrams depict the definitions of each normalized load metric.

during daily living over a weeks-long duration. While the cumulative loading time and impulse are confounded by the inherent variability of data amount available, they also denote the variation of real-world tendon loading profiles due to patient-specific characteristics (age), lifestyles (activity level), and tendon health (severity of tendinopathy). The associations between measured cumulative tendon loads and patient outcomes became more pronounced when loading time and impulse were normalized by Total Active Hours. We found that reduced cumulative *high* Achilles tendon loads are associated with older age, more severe tendinopathy, and more sedentary lifestyle (Figure 1, center and right). Measured cumulative tendon loads generally matched both self-reported activities and tendon health status. For example, among the 4 individuals who reported the highest current activity level (PAS = 6), the 2 patients had less cumulative *high* load than the 2 controls. Although preliminary, our data also reveal links between sensor metrics and daily living events, as the patient who cumulated more *high* load (PAT008, yellow marker) frequently self-reported running via daily text surveys, while the other patient (PAT002, teal marker) did not. Our ongoing research is recruiting a larger homogeneous patient cohort to explicitly define how cumulative tendon loads throughout patient-specific daily living influence the biological health of the Achilles tendon.

Significance

Tendon loading during daily living is a major contributor to Achilles tendinopathy. Our results confirm the clinical benefits of using self-reported activities and disease severity to guide exercise rehabilitation, while also establishing a rigorous strategy to quantify cumulative Achilles tendon loads throughout daily living. Our wearable sensing paradigm provides clinicians with a powerful tool to identify unique loading profiles that govern patient-specific outcomes, customize rehabilitation exercises, and monitor their impacts out of the clinic to promote the therapeutic effects of tendon loading.

References

1. Shaikh Z, Perry M, Morrissey D, *et al.* Achilles tendinopathy in club runners. *Int J Sports Med* 2012; 33(5): 390–4.

2. Silbernagel KG, Thomeé R, Eriksson BI, *et al.* Continued sports activity, using a pain-monitoring model, during rehabilitation in patients with Achilles tendinopathy: a randomized controlled study. *Am J Sports Med* 2007; 35(6): 897–906.

3. Woodley BL, Newsham-West RJ, Baxter GD. Chronic tendinopathy: effectiveness of eccentric exercise. *Br J Sports Med* 2007; 41(4): 188–98.

4. Silbernagel KG, Brorsson A, Lundberg M. The majority of patients with Achilles tendinopathy recover fully when treated with exercise alone: a 5-year follow-up. *Am J Sports Med* 2011; 39(3): 607–13.

5. van der Plas A, de Jonge S, de Vos RJ, *et al.* A 5-year follow-up study of Alfredson's heel-drop exercise programme in chronic midportion Achilles tendinopathy. *Br J Sports Med* 2012; 46(3): 214–8.

6. Hullfish TJ, Baxter JR. A simple instrumented insole algorithm to estimate plantar flexion moments. *Gait Posture* 2020; 79: 92–5.

7. Baxter JR, Corrigan P, Hullfish TJ, *et al.* Exercise progression to incrementally load the Achilles tendon. *Med Sci Sports Exerc* 2021; 53(1): 124–30.

8. Robinson JM, Cook JL, Purdam C, *et al.* The VISA-A questionnaire: a valid and reliable index of the clinical severity of Achilles tendinopathy. *Br J Sports Med* 2001; 35(5): 335–41.

9. Schober P, Boer C, Schwarte LA. Correlation coefficients: appropriate use and interpretation. *Anesth Analg* 2018; 126(5): 1763–8.

Evidence of a Loose Total Ankle After Tibial Intramedullary Nail Insertion

Bradley Osemwengie, MD
Tensae Assefa, MD
Casey Jo Humbyrd, MD, MBE

Department of Orthopaedic Surgery
University of Pennsylvania

Introduction

Total ankle replacements (TARs) are a reliable surgical solution for patients with arthritis of the ankle.[1] Rates of TARs are increasing as the procedure becomes more popular and patients seek to maintain range of motion of the tibiotalar joint unavailable with ankle arthrodesis.[2] With the increasing volume of total ankle arthroplasties, there has been a concomitant increase in the number of total ankle revisions.[3]

Total ankle revision procedures are usually indicated in the setting of infection, evidence of peri-implant loosening on imaging, or persistent ankle pain following a traumatic event with a prior total ankle already in place.[4] Preoperative work-up should include evaluation for potential infection prior to a revision procedure. This generally includes obtaining a CBC, ESR, and CRP. X-rays and CT scans are helpful to evaluate component positioning, evidence of cyst formation, as well as evidence of radiolucency around the implant.

During revision procedures, the tibia and the talar components can be exchanged. However, due to the bone loss associated with infection or from the act of removing the components, the components may need to be revised to a stemmed total ankle arthroplasty that incorporates a larger footprint into the distal tibia to fill in any residual voids. Even though total ankle replacements are usually performed by foot and ankle trained orthopedic surgeons, surgeons that participate in fracture care should also be aware of these implant designs due to the potential for peri-implant fractures. The following case demonstrates a complication with a total ankle replacement after an ipsilateral lower extremity fracture with subsequent intramedullary nail fixation.

Patient Presentation

The patient is a 56-year-old male with polymyalgia rheumatica (on chronic steroids) with left ankle pain. The patient has a remote history of a myocardial infarction and a liver transplant. He underwent a left total ankle replacement for post-traumatic arthritis at an outside hospital (OSH) in January 2020. The patient denied any ankle pain post-operatively. Two months post-operatively, he sustained a left tibial shaft fracture after a fall. He underwent a left tibial intramedullary nail (IMN) by a general orthopedist at the same OSH.

After the tibial nail insertion, the patient started developing worsening ankle pain as well as a feeling of a loose sensation about his ankle. The pain persisted without any improvement. The patient presented to the foot and ankle service in late 2023 and was noted to have maximal tenderness to palpation at the anterior ankle. An infection workup was obtained in the form a CBC, ESR, CRP. These lab values were within normal limits. X-rays and CT of the left tibia/fibula were obtained. X rays of the left ankle and distal tibia showed evidence of a tibial nail as well as an ipsilateral total ankle arthroplasty. The tibial nail was in close proximity to the ankle prosthesis. There was evidence of lucency around the tibial component of the total ankle replacement. Callous formation was noted over the midshaft tibia suggesting healing at the prior fracture site (Figure 1). A CT scan revealed lucency and cyst formation around the tibial component of the TAR (Figure 2). Due to the patient's persistent pain, sensation of looseness, and imaging that suggested lucency around the tibial component, the decision was made to perform a revision total ankle replacement.

Surgery

Prior to addressing the total ankle, the tibial nail was removed. Three of the four interlocking screws were removed under fluoroscopic guidance. A suprapatellar approach was then used to approach the proximal portion of the tibial nail. The end cap was removed, and a jig was inserted in the cannulated portion of the nail. The final interlocking screw was removed and the nail was removed without issue.

The total ankle replacement was then approached through the prior anterior incision. Evidence of metallosis was found

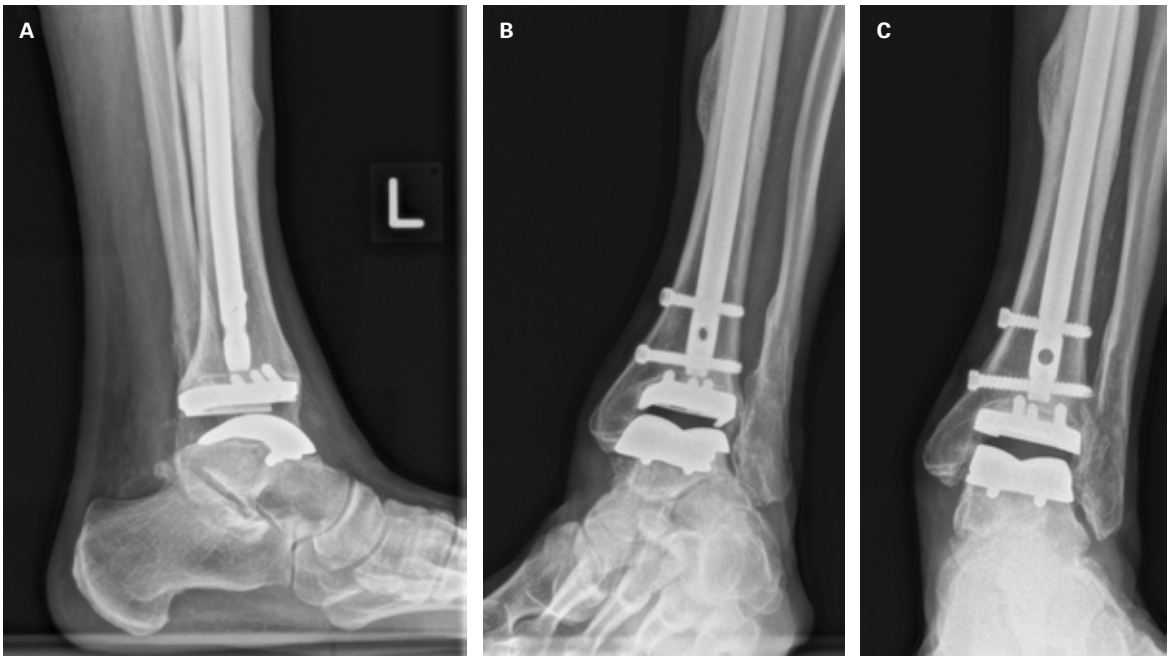

Figure 1. (A) Lateral, **(B)** mortise, and **(C)** AP x-rays of the left ankle/distal tibia. The tibial nail is in close proximity to the ankle prosthesis. There is evidence of lucency around the tibial component of the total ankle replacement. Callous formation is noted over the midshaft tibia suggesting healing at the prior fracture site.

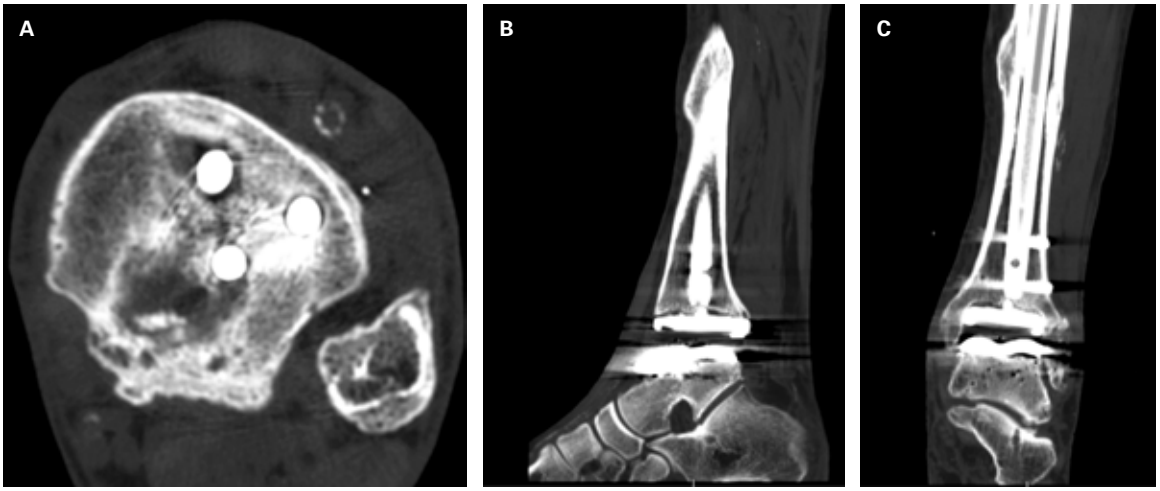

Figure 2. (A) Axial, **(B)** Lateral, and **(C)** AP CAT scan of the left distal tibia. The tibial nail is in close proximity to the ankle prosthesis. There is evidence of lucency around the tibial component of the total ankle replacement. Cyst formation is also noted around the tibial component of the TAR.

in the ankle joint. The tibial component easily dislodged with removal of the polyethylene component. There was a notable amount of cement present on the tibial component. A freer was used to probe the talar component which was also found to be loose. A cement mantle was found on the talar implant as well. A saw was used to freshen the cuts on the tibia and the talus and all the cement was removed. Deeper peg holes were created and a new tibial component was placed. The talar drill holes were re-drilled anteriorly and filled with bone graft after careful removal of surrounding bony overgrowth. A size four tibia and size four talus were implanted which were the same sizes used for the index total ankle arthroplasty. The polyethylene was upsized from a six millimeter to a ten-millimeter implant. Adequate fixation and range of motion was achieved intraoperatively.

Post-operative imaging showed the total ankle components in appropriate alignment (Figure 3). The patient was placed into a short leg splint and made non-weightbearing. On most recent follow up at six-weeks post operation, the patient was doing well. He has been working with physical therapy and denies ankle pain. He notes some pain over the plantar fascia as well as mild pain over the Achilles. X-rays obtained at that time showed early bony ingrowth surrounding the tibial component (Figure 4).

Discussion

Total ankle arthroplasties have longevity if indicated in the right patient population. According to a study analyzing rates of total ankle revisions in the short term, the mean survival rate at two years was 0.94, 0.86 at five years, 0.82 at seven years, and 0.77 at ten-year follow up. Long term survival rates were 0.66 at fifteen years and 0.62 at nineteen-year follow-up.[5] One of the most common indications for revision total ankle arthroplasty is loosening of the components.[6] It was noted in the operative report of the tibial IMN that the nail avoided the

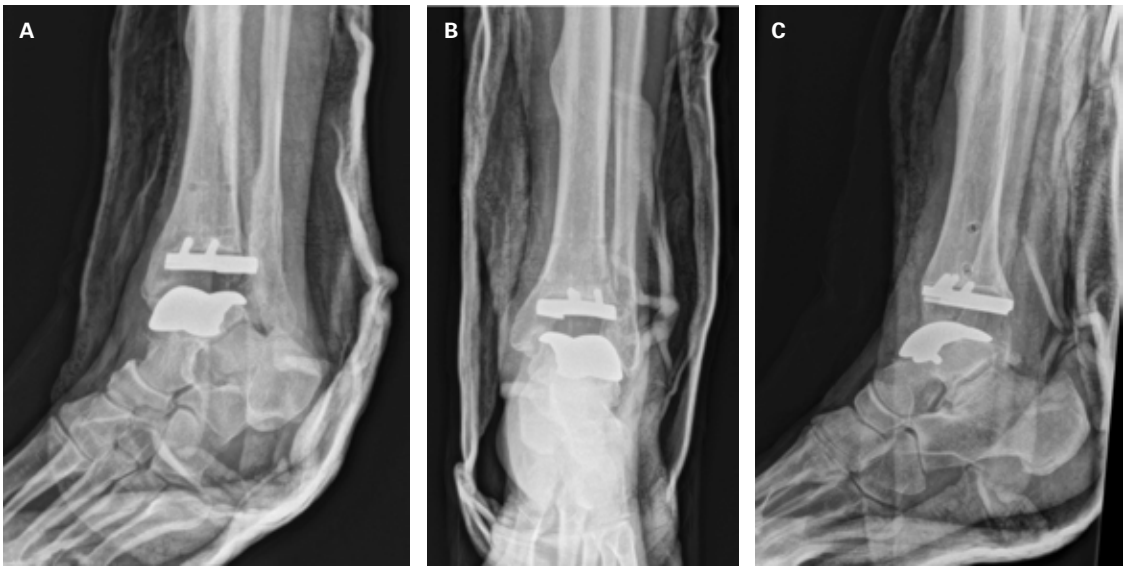

Figure 3. Postoperative **(A)** mortise, **(B)** AP, and **(C)** lateral x-rays of the left ankle. The tibial nail has been removed with residual defects in the tibia from prior interlocking screws. The revision total ankle components are in adequate position.

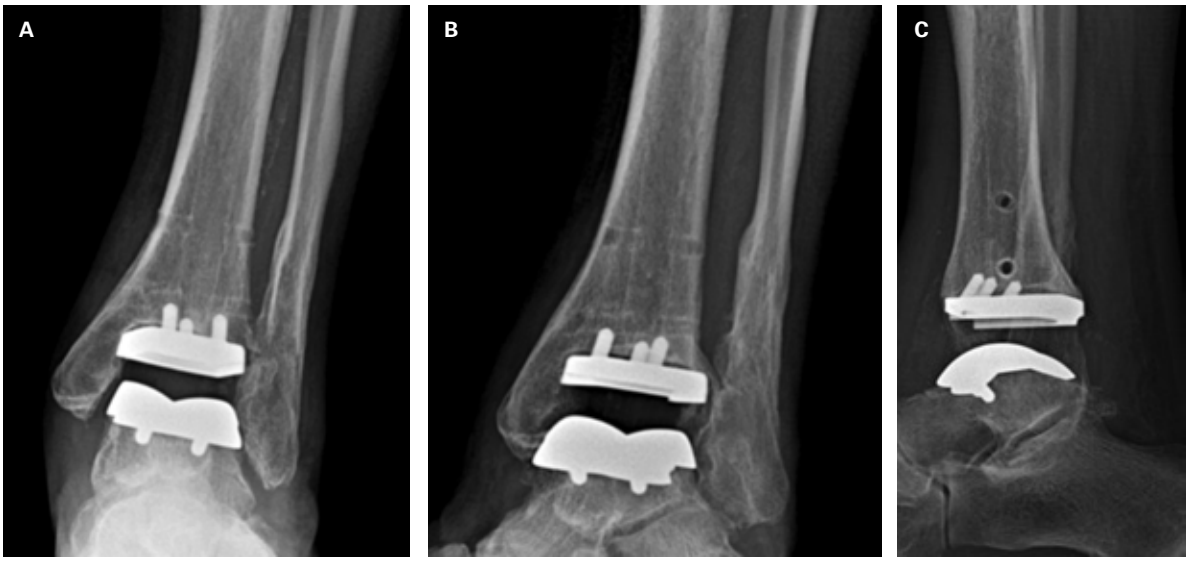

Figure 4. Six-week postoperative **(A)** AP, **(B)** mortise, and **(C)** lateral x-rays of the left ankle. Total ankle components are in adequate position. Progression of the bony ingrowth surrounding the tibial component of the TAR is best appreciated on the lateral x-ray compared to the immediate postop images in Figure 3.

total ankle prosthesis. However, on x-ray and CT imaging, the tibial nail was in close proximity to the tibial pegs of the total ankle replacement. The fact that the patient's ankle pain and feeling of looseness occurred immediately after tibial nail insertion further suggests that the implant was loosened during tibial nail insertion. Adequate intraoperative fluoroscopy must be utilized to ensure that the total ankle prosthesis is not disrupted during guidewire insertion, reaming, or final nail seating.

While nearly all TAR implants were approved for use with cement, anecdotally, most orthopaedic surgeons do not utilize cement for their TARs. Cemented arthroplasties are, however, common in total knee and total hip procedures. In knee and hip arthroplasty, the main argument for the use of cement is immediate fixation. Drawbacks include osteolysis and aseptic loosening at the bone-cement interface. Uncemented technique benefits include preserving bone stock, avoiding cement fragmentation, and reducing the risk of implant loosening via the process of bony ingrowth. The main drawback is bony ingrowth takes a longer time compared to the immediate fixation from cement.[7] This patient had a cemented ankle prosthesis that removed easily on intra-operative evaluation. It is possible that the complete separation of the cement mantle to the distal tibia seen intraoperatively may not have occurred with an uncemented approach. Postoperative physical exam with new onset pain or sensory changes should also be noted as potential consequences of iatrogenic damage to total ankle arthroplasty components.

Conclusion

This case demonstrates a loose total ankle replacement after the insertion of a tibial IMN. As the rates of total ankle replacements increase, foot and ankle surgeons and device companies should be ready for the increase in revisions as well. As no case of a loose total ankle replacement after tibial nail insertion has been reported, this report serves as

a reminder that care must be taken by orthopedists when inserting tibial IMN to avoid loosening of a total ankle prosthesis.

References

1. Barg A, Wimmer MD, Wiewiorski M, *et al.* Total ankle replacement. *Dtsch Arztebl Int*. 2015;112(11):177-84.

2. Karzon AL, Kadakia RJ, Coleman MM, *et al.* The Rise of Total Ankle Arthroplasty Use: A Database Analysis Describing Case Volumes and Incidence Trends in the United States Between 2009 and 2019. *Foot Ankle Int*. 2022;43(11):1501-1510.

3. Ratnasamy PP, Maloy GC, Oghenesume OP, *et al.* The Burden of Revision Total Ankle Replacement Has Increased From 2010 to 2020. *Foot Ankle Orthop*. 2023; 8(3):24730114231198234.

4. Richter D, Krähenbühl N, Susdorf R, Barg A, Ruiz R, *et al.* What Are the Indications for Implant Revision in Three-component Total Ankle Arthroplasty? *Clin Orthop Relat Res*. 2021; 479(3):601-609.

5. Perry TA, Silman A, Culliford D, *et al.* Survival of primary ankle replacements: data from global joint registries. *J Foot Ankle Res*. 2022;15(1):33.

6. Myerson MS, Aiyer AA, Ellington JK. Revision Total Ankle Replacement. *JBJS Essent Surg Tech*. 2015;5(2):e7.

7. Chen K, Xu J, Dai H, *et al.* Uncemented Tibial Fixation Has Comparable Prognostic Outcomes and Safety Versus Cemented Fixation in Cruciate-Retaining Total Knee Arthroplasty: A Meta-Analysis of Randomized Controlled Trials. *J Clin Med*. 2023;12(5):1961.

Oncology

Tips and Tricks: Initial Management of Unknown Soft Tissue Masses

Maxwell Cardwell, MD
Jaret Karnuta, MD, MS
Cara Cipriano, MD

Department of Orthopaedic Surgery, University of Pennsylvania, Philadelphia, PA 19104

Introduction

Soft tissue masses are common and can initially present to a variety of providers, including primary care or emergency physicians, dermatologists, plastic surgeons, general surgeons, and orthopaedic surgeons. The majority of these masses are benign processes, whether reactive, traumatic, or neoplastic. Though much more rare, 20 soft tissue malignancies are diagnosed per every 1 million individuals in the US per year.[1] The presentation of benign and malignant tumors can be similar; however, appropriate management ranges from reassurance, to simple excision, to wide resection with radiation and occasionally chemotherapy.[2] Delay in diagnosis, poor biopsy technique, or inadequate excision can complicate treatment, even leading to amputation or mortality. Therefore, it is critical that soft tissue tumors are appropriately evaluated and accurately diagnosed. The purpose of this paper is to provide an overview of the key aspects of history, exam, and imaging that help elucidate which soft tissue masses are concerning for malignancy and should be referred to an orthopaedic oncologist.

History

Key questions to ask any patient presenting with a soft tissue mass include when they first noticed the mass and if it has changed in size. Masses that have rapid growth tend to be more concerning for malignancy, while benign entities are often slow growing, fluctuating in size, or can even resolve over time. The clinician should also ask whether there is a history of trauma or radiation exposure to the area. Antecedent trauma makes the diagnosis of a hematoma or myositis ossificans more likely; conversely, without a history of trauma, the possibility of sarcoma must be strongly considered.[3] Prior radiation therapy is a known risk factor for development of soft tissue sarcoma.[4] A personal or family history of cancer should be noted but is often unrelated, as the vast majority of soft tissue tumors are sporadic. Conditions such as Li-Fraumeni, Gardner syndrome, and Neurofibromatosis are very rare but associated with high risk of osteosarcoma, desmoid tumors, and benign or malignant peripheral nerve sheath tumors, respectively. Most soft tissue sarcomas are asymptomatic; they do not cause pain until they are large enough to compress surrounding structures. This may cause patients to delay seeking evaluation of the mass. Conversely, several benign soft tissue tumors, such as schwannomas, can be quite painful, as can non-neoplastic masses such as abscesses or inflammatory processes. Finally, soft tissue sarcomas do not cause unplanned weight loss or constitutional symptoms, with a notable exception of lymphoma.

Physical Exam

On exam the mass should be fully visualized, and the contralateral extremity should be exposed for comparison. The size, depth, and consistency of the mass are critical in determining further work up. Masses that are large (>5cm), deep to fascia, nonmobile, and firm compared to surrounding tissue are most suspicious; however, any mass warrants some form of imaging prior to consideration of monitoring or removal.3 Skin changes should be noted; cutaneous ulceration is more suggestive of skin cancer, but angiosarcoma is often superficial, and other sarcomas that have grown large enough can also present as a fungating mass. Warmth, erythema, tenderness, and fluctuance are more suggestive of an abscess, especially with a history of constitutional symptoms. Lastly a diagnosis of hematoma should not be made without a history of trauma, the presence of ecchymosis on physical exam, and confirmatory imaging.[4]

Imaging

MRI is the gold standard in the work up of a soft tissue mass. T1 weighted images are best for anatomic visualization, whereas T2 weighted images are best for demonstrating water-gradients such as edema and reactive changes. The administration of gadolinium contrast allows improved differentiation of cystic and solid lesions and allows the

diagnosis of neovascularization. There is great variation in the specific sequences used, and their interpretation should be left up to the orthopaedic oncologist or experienced musculoskeletal radiologist. On MRI, soft-tissue sarcomas typically grow centrifugally and respect anatomic planes. They tend to be hypointense on T1, hyperintense on T2, demonstrate heterogeneity on both sequences, and often are solid with angiogenic contrast patterns.3 MRI is capable of definitive diagnosis of many lesions including lipomas, hemangiomas, ganglion and synovial cysts, myositis ossificans, and pigmented villonodular synovitis.[4]

Other imaging modalities have utility in soft tissue mass work-up, with the caveat that they are less sensitive than MRI. For example, ultrasound imaging is considerably less expensive and time-consuming; it can be valuable to confirm certain benign diagnoses including cysts and lipomas but has an unacceptably high misdiagnosis rate for other conditions. Doyle et al. found that of 43 patients with biopsy-proven soft tissue tumors, ultrasound imaging had a 23% rate of incorrect initial diagnosis. In their cohort, 5/43 patients suffered a delay in diagnosis as a result. Notably, the most common error was misdiagnosing a true malignant mass as a hematoma.[5] Because of this, any uncertainty on ultrasound should prompt further work-up with an MRI. CT can be useful in the diagnosis of osseous lesions but offers less value in the work up of soft-tissue masses.[6] The presence of phleboliths on either CT or XR can suggest a hemangioma, and the presence of mature appearing trabecular bone in the periphery of a soft tissue mass suggests myositis ossificans. However, this information alone is often not enough to fully exclude the diagnosis of soft tissue sarcoma and must be correlated with clinical presentation.

Biopsy

Any soft tissue mass that cannot be confidently diagnosed with the history, physical exam, and imaging studies should undergo biopsy. A mass can be biopsied via percutaneous or open methods. Percutaneous biopsy techniques include fine needle aspiration (FNA) and core needle biopsy (CNB). The key difference between fine needle aspiration and core needle biopsy is that only cytologic studies examining cell characteristics can be conducted on a FNA sample, whereas CNB samples can undergo histologic analysis examining the structural relationship of the cells to one another. Therefore, FNA is adequate for hematologic cancers, but CNB is more accurate for sarcoma.

Open biopsy is considered the most sensitive and accurate diagnostic test and may be necessary in certain scenarios, such as highly necrotic or dedifferentiated tumors. Verheijen et al. showed that in diagnosing soft tissue sarcomas open/incisional biopsy had an affirmative diagnosis of 95%, 78% after CNB, and 38% after FNA. After a FNA and a subsequent histological biopsy the sensitivity increased to 71%.[7] After a negative CNB in patients where there was a high suspicion for malignancy a subsequent open biopsy increased the sensitivity to 90%. Pohlig et al. found no difference in the diagnostic accuracy between CNB and open biopsy. However, open biopsy carries risks of increased morbidity and contamination of surrounding tissues, so CNB remains the most commonly performed type of biopsy for sarcoma.[8] If open biopsy is undertaken, an orthopaedic oncologist or surgeon who will ultimately do the resection should be involved to ensure both that the appropriate sample is collected and that future treatment will not be jeopardized by the biopsy itself.

Case Report

Patient John Doe is a 57 year-old male with no significant past medical history who initially presented to his primary care physician with one year of mild pain in his right posterior thigh and no antecedent trauma. The pain worsened with extension of his knee and was recalcitrant to a course of physical therapy. He eventually saw an outside orthopaedic surgeon who believed the mass was consistent with a hematoma but ordered an MRI for diagnosis. The MRI demonstrated a $4.5 \times 4.0 \times 10.1$ cm intramuscular mass along the myotendinous junction of the semitendinosus with a final radiology read of a hematoma (Figures 1,2). An intra-lesional removal of the mass was performed with findings of dark-colored serous fluid deep to muscle fascia. The surrounding cavity was described as “dead muscle tissue.” A sample was sent to pathology and described as “dense fibrosis, fibrin, focal hemosiderin, compatible with site of organizing hematoma/scar formation.” No evidence of malignancy was noted.

Due to continued pain around his surgical site, a repeat MRI without contrast was ordered, demonstrating

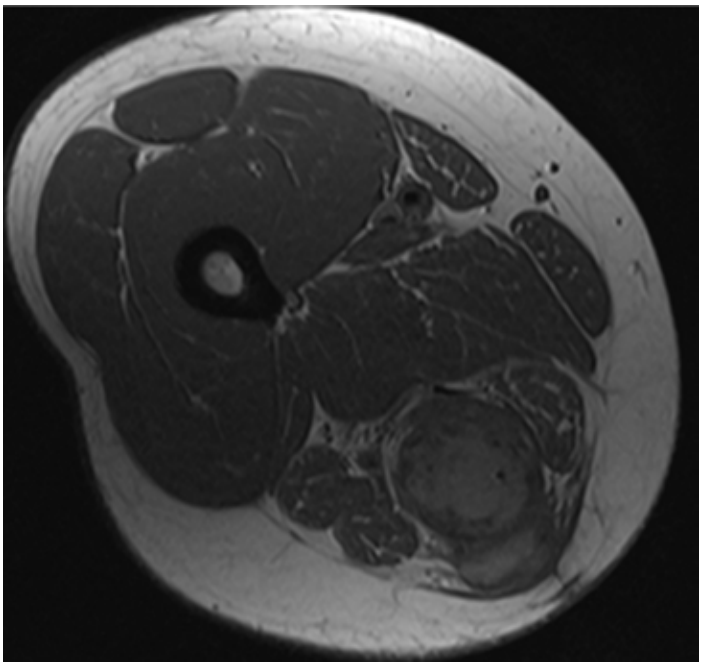

Figure 1. T1 Axial MRI at greatest cross-sectional area of tumor prior to initial biopsy and procedure demonstrates a heterogeneous mass in the posterior compartment of the thigh (4.5 x 4.0 x 10.1 cm).

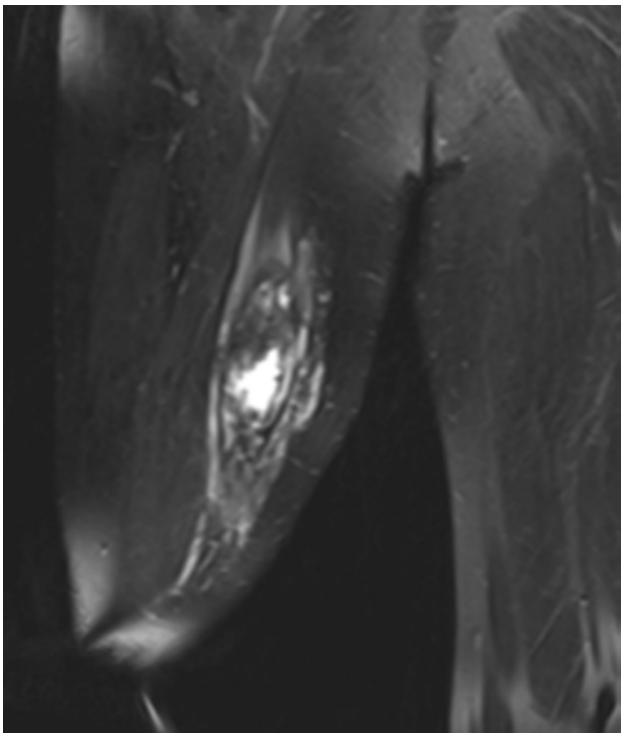

Figure 2. T2 Coronal FS of initial MRI prior to biopsy and procedure demonstrates the long, enhancing mass (4.5 x 4.0 x 10.1 cm)

reaccumulation of the mass, now 6.1 × 4.1 × 12.6 cm with heterogenous signal intensity and peripheral T2 hypointense areas of debris/nodularity as well as a peripheral T2 hypointense rim. There was a new superficial component posteriorly measuring 2.9 × 1.8 cm. This prompted concern for malignancy, but a CNB at this time was again consistent with hematoma.

The patient was then seen by an orthopaedic oncologist. At that time, he had continued pain with knee extension and a 20-degree flexion contracture. Despite negative biopsy results, concern for a malignant process was high enough to prompt a repeat ultrasound-guided biopsy. Results were consistent with a spindled and epithelioid neoplasm with necrosis with the differential including sarcomatoid carcinoma versus high grade soft tissue sarcoma.

The patient the underwent wide excision of the posterior thigh mass with orthopaedic oncology. Final pathology showed high-grade spindle and epithelioid sarcomatoid tumor with perineural and arteriolar vascular invasion. Over the course of the next year, he developed metastases to the left deltoid and presumed metastases to the lung. The patient passed 19 months after initial diagnosis.

Discussion

Soft-tissue sarcomas can be difficult to diagnose and often present with minimal or non-specific findings. Misdiagnosis can occur even after workup with appropriate imaging and biopsy, as elucidated in this case report. Hematomas are a common culprit in the misdiagnosis of soft tissue sarcomas. Negative FNA of soft-tissue sarcomas with hemorrhage was reported in 87% in a small case series.[9] In this case, the history (no clear history of trauma) and physical examination (no presence of ecchymosis) were not consistent with hematoma, so sarcoma should have been suspected even giving the initial MRI and pathology findings.

The proportion of soft tissue sarcomas that are inadvertently excised by surgeons without subspecialized oncology training at the primary surgical intervention is reported as high as 40%.[10] Educating the surgical community as well as our primary care colleagues to appropriately evaluate any new soft tissue mass can help limit unplanned excisions and improve outcomes for patients.

References

1. Church DJ, Krumme J, Kotwal S. Evaluating Soft-Tissue Lumps and Bumps. *Mo Med*. 2017;114(4):289-294.

2. Mankin, H. J., & Hornicek, F. J. Diagnosis, classification, and management of soft tissue sarcomas. *Cancer Control* 2005, 12(1), 5-21.

3. Mayerson, J. L., Scharschmidt, T. J., Lewis, *et al.* Diagnosis and Management of Soft tissue Masses. *Instr Course Lect* 2015;64, 95-103.

4. Jernigan, E. W., & Esther, R. J. Soft tissue masses for the general orthopedic surgeon. *Orthop Clin North Am* 2015, 46(3), 417-428, xi.

5. Doyle AJ, Miller MV, French JG. Ultrasound of soft-tissue masses: pitfalls in interpretation. *Australas Radiol*. 2000;44(3):275-280.

6. Subhawong, T. K., Fishman, E. K., Swart, *et al.* (2010). Soft-tissue masses and masslike conditions: what does CT add to diagnosis and management? *AJR Am J Roentgenol*, 194(6), 1559-1567.

7. Verheijen, P., Witjes, H., van Gorp, J., *et al.* Current pathology work-up of extremity soft tissue sarcomas, evaluation of the validity of different techniques. *Eur J Surg Oncol* 2015, 36(1), 95-99.

8. Kiefer J, Mutschler M, Kurz P, *et al.* Accuracy of core needle biopsy for histologic diagnosis of soft tissue sarcoma. ***Sci Rep***. 2022;12(1):1886. Published 2022 Feb 3.

9. Qureshi, Y. A., Huddy, J. R., Miller, *et al.* Unplanned excision of soft tissue sarcoma results in increased rates of local recurrence despite full further oncological treatment. *Ann Surg Oncol* 2012, 19(3), 871-877.

10. Ward, W. G., Sr., Rougraff, B., Quinn, R., *et al.* Tumors masquerading as hematomas. *Clin Orthop Relat Res*, 465, 232-240.

Orthoplastics

U·P·O·J

Tips and Tricks: Latissimus Dorsi Free Flap for Tumor-related Soft Tissue defects: A Case Report

Tensae Assefa, MD
Sand Mastrangelo, MD
Caroline Granruth, MD
Scott Levin, MD FACS
Cara Cipriano, MD

Department of Orthopaedic Surgery
University of Pennsylvania

Introduction

Large soft tissue defects resulting from malignant tumor resection can pose significant challenges to orthopaedic and plastic surgeons. Soft tissue deficiencies caused by trauma, infection, and tumors can result in nonviability of vital skin structures. The goal of soft tissue reconstruction is to restore function while maintaining optimal cosmesis. Frequently, staged treatments are necessary to minimize post-operative infection, facilitate healing, and reduce complications.[1]

Free flap surgery, or microsurgical tissue transfer, refers to a microvascular reconstruction that involves the transfer of autologous skin, fat, bone, and/or muscle from one area of the body to another. The tissue that is transferred (donor tissue) maintains its vascular supply and is re-anastomosed to an area (recipient site) to provide soft tissue coverage or functional reconstruction.[1] Common free flap donor sites include the anterolateral thigh (ALT) flap, radial forearm (RF), lateral arm (LA), gracilis muscle, rectus abdominis (RA), and the latissimus dorsi (LD).[2,3] In this case study, we present the use of a latissimus dorsi myocutaneous free flap to cover a large soft tissue defect of the left hemipelvis.

Case Presentation

Our patient is a 64-year-old male with a history of undifferentiated pleomorphic sarcoma (UPS). He received his initial diagnosis in 2002 following a right axillary/chest wall mass biopsy and subsequently completed 4 cycles of neoadjuvant chemotherapy with etoposide, ifosfamide, doxorubicin, and mesna. Four months after his diagnosis, he underwent wide surgical excision of the chest wall mass. Secondary excision was indicated due to positive surgical margins, so he underwent a secondary tumor bed resection one month following his initial excision. During postoperative surveillance visits in 2007, an enlarging right parascapular axillary nodule was identified and biopsied; pathology was consistent with recurrent UPS. In 2007, the patient underwent radical resection of the right axillary tumor bed with rectus abdominus free flap reconstruction. UPS recurrence in the right axilla was again noted during postoperative surveillance visits in 2010, and the patient underwent a fourquarter radical upper extremity amputation.

In 2012, the patient was found to have metastatic UPS in his left thigh and buttocks which were treated initially with chemoradiation, but then ultimately with left buttock resection in 2014. A secondary metastatic UPS left thigh mass was detected in 2018, and the patient underwent radical resection 3 months later. The surgery was complicated by persistent wound drainage which was operatively managed with prompt irrigation and debridement. Given the dependent location of the patient's wound, he endured significant surrounding skin breakdown resulting in a large wound about his left hip. He was offered a hip disarticulation at an outside institution but returned to our care for limb salvage.

In 2019, the patient underwent anterolateral thigh free flap reconstruction from his right thigh to cover his large left hip wound. This was followed by skin grafting to the posterior aspect of the free flap. Intraoperative pathology was negative for malignancy. However, routine surveillance imaging in 2020 revealed a heterogenous enhancing mass in the left thigh and iliac wing. A biopsy was performed in 2021 and was consistent with MDM2 positive dedifferentiated liposarcoma (DD LPS) and the patient elected treatment with serial cryoablation and radiation therapy. In 2023, he enrolled in the SARC041 blinded trial (placebo vs abemaciclib); however, the fungating mass about his left thigh and ilium continued to grow. Shortly thereafter, he was unblinded from the clinical trial and elected to proceed with surgical resection and staged soft tissue reconstruction given the tumor's continued growth on abemaciclib.

On 1/24/2024, the patient underwent wide excision of the left hip fungating mass with Dr. Cipriano. Intraoperative pathology confirmed negative margins. A wound vac was applied over the 25 cm × 6 cm × 20 cm open left hip and flank wound while the patient awaited definitive soft tissue coverage (Figure 1).

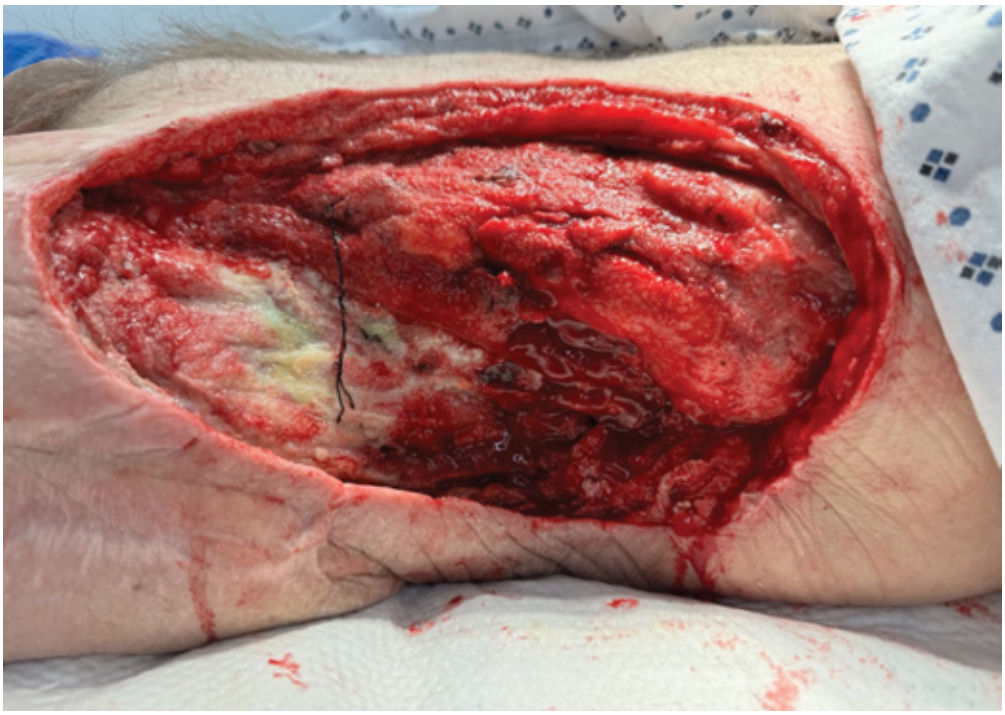

Figure 1. Open wound over the left hip and left flank following radical tumor resection.

Latissimus Dorsi Free Flap (LDFF)

On 2/1/2024, the patient underwent LDFF reconstruction of the open left hip wound with Dr. Levin—his third free flap in the treatment of this tumor. To ensure adequate vascularity, ultrasound dissection of the left thigh arteriovenous (AV) loop from his prior ALT free flap procedure was performed prior to the reconstruction. An oblique, myocutaneous latissimus dorsi flap measuring 22 cm × 12 cm was harvested from the patient's left chest wall (Figure 2). The serratus branch of the thoracodorsal artery was taken down with double hemoclips and the dissection proceeded to the level of the circumflex scapular artery. The flap was then divided and repositioned to cover the flank wound; it was inset over the transversalis and external oblique muscles to prevent herniation. Mesh was used to reinforce the abdominal wall. The flap was then anastomosed to the previous AV loop vessels using microsurgical technique, resulting in excellent inflow, outflow, and perfusion of the overlying skin pedicle (Figure 3). A skin graft was harvested from the patient's left thigh, meshed, and applied over the muscle of the myocutaneous latissimus dorsi free flap (Figure 4).

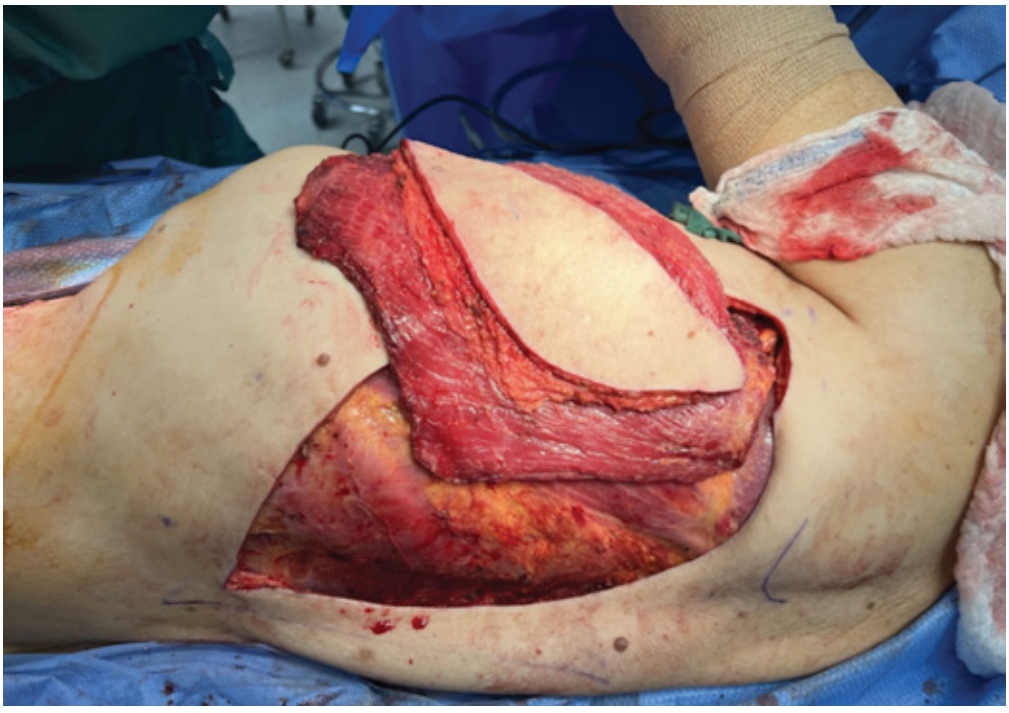

Figure 2. Donor site oblique skin paddle including the entire latissimus dorsi muscle.

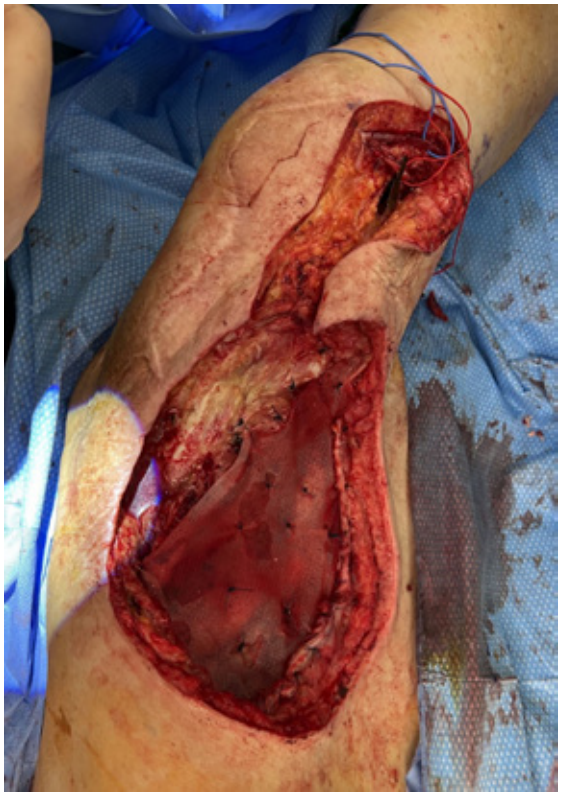

Figure 3. Preparation of flap anastomosis at the recipient site.

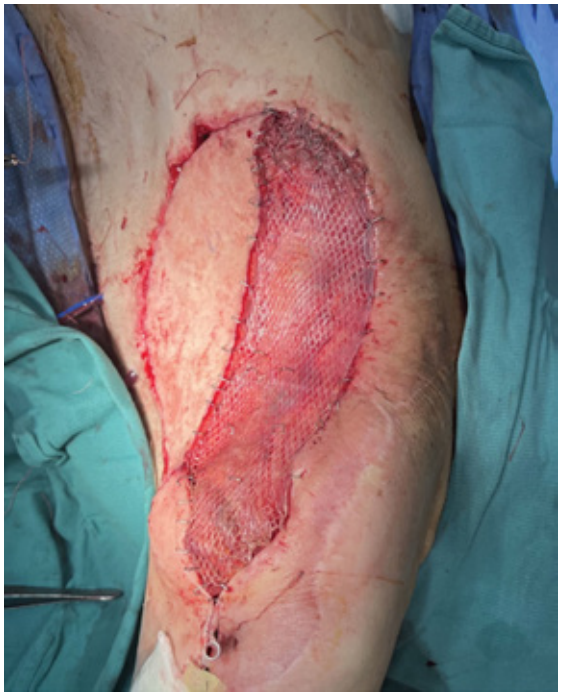

Figure 4. Latissimus dorsi free flap reconstruction with skin grafting.

Post-operatively, the patient was extubated and taken to the surgical intensive care unit (SICU) for hourly neurovascular flap checks. The patient remained in bed until post-operative day two to protect the anastomosis and facilitate adequate soft tissue rest. At this point, the patient was tolerating a regular diet and receiving oral pain medications with adequate pain control. His neurovascular checks were stable, and he was transferred to the floor on post-operative day three. Physical and occupational therapy were initiated, and the patient demonstrated the ability to perform assisted transfers with expected improvement in his strength and endurance. His hospital course was uncomplicated, and he was discharged to an acute rehab facility on post-operative day nine.

Discussion

Undifferentiated pleomorphic sarcoma (UPS) is a high-grade sarcoma that is especially challenging to treat. Despite a multidisciplinary approach to treatment, approximately 30% of patients experience distant metastasis within 5 years of initial diagnosis.[4,5] Patients with recurrent malignancies often require multiple surgeries for adequate tumor resection. Neoadjuvant radiation to the tumor is an important factor in local control that plays a critical role in limb salvage surgery for sarcoma; however, it does compromise wound healing and increase rates of soft tissue complication to approximately 30%.[6,7] This further contributes to the need for repeated operations and secondary soft tissue coverage.

In this article, we present a patient with a large soft tissue defect involving his left thigh and hemipelvis secondary to UPS successfully treated with LDFF. Microsurgical techniques were employed intraoperatively to maintain the donor tissue vascular supply and subsequently re-anastomose it to the recipient site. These microsurgical skills were particularly important in this case, as the anastomosis was to the prior AV loop vessel from his prior ALT flap. Thus, fastidious technical skill and microsurgical technique were necessary to ensure flap viability.

Postoperative care for free flaps includes strict adherence to a protocol designed to optimize soft tissue healing and patient function. This includes graduated neurovascular checks, positioning restrictions, and a carefully selected nutrition plan. Physical and occupational therapy sessions should be started early in the postoperative course to facilitate functional recovery.

The patient's flap continued to function during the patient's post-operative course. Clinical photos taken three weeks post-operatively demonstrate adequate wound healing and soft tissue recovery (Figure 5).

Two months post-operatively, the patient has continued to heal well. Both his LDFF and his skin graft recipient sites are healthy-appearing and progressing well.

Conclusion

Latissimus dorsi free flap reconstruction provides a versatile and technically suitable option for large soft tissue defects requiring staged reconstruction. The free myocutaneous tissue transfer can be used in a tension free fashion to provide coverage to larger areas of soft tissue defect and is a useful technique for orthopaedic and plastic reconstructive surgeons.

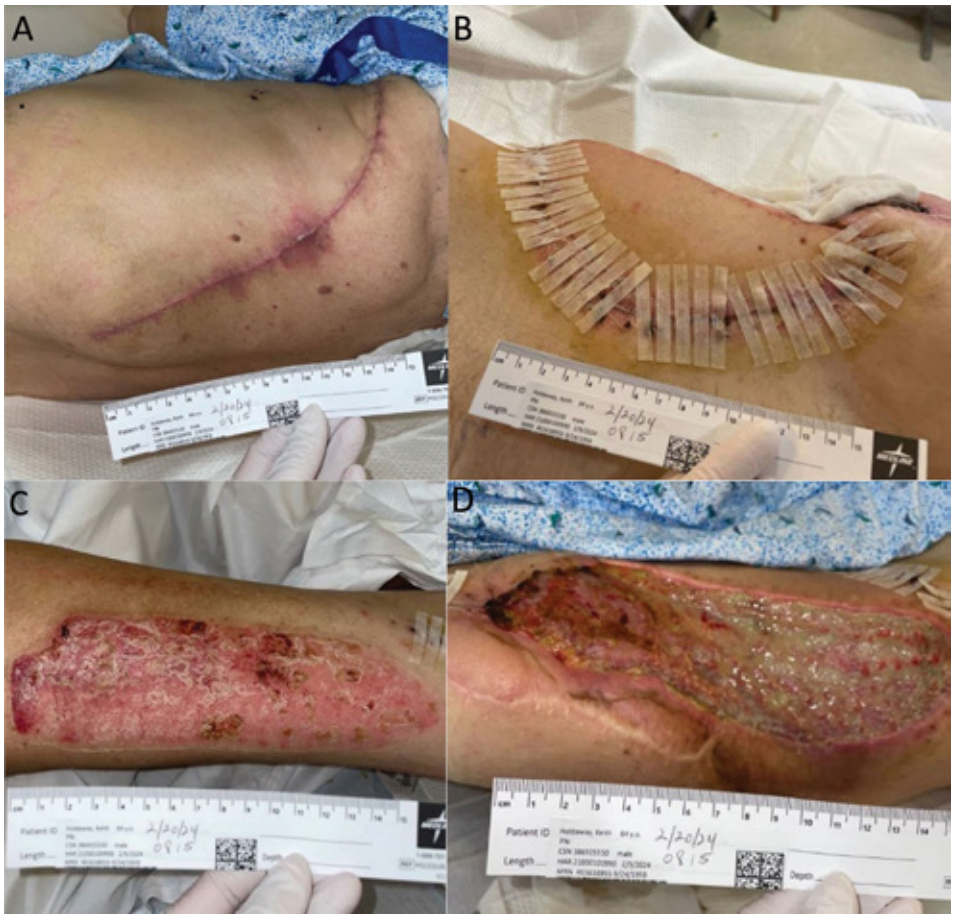

Figure 5. Post-operative day twenty-one (A) Latissimus dorsi free flap donor site incision; (B) LDFF recipient site; (C) Left thigh skin graft donor site; (D) Left thigh skin graft recipient site.

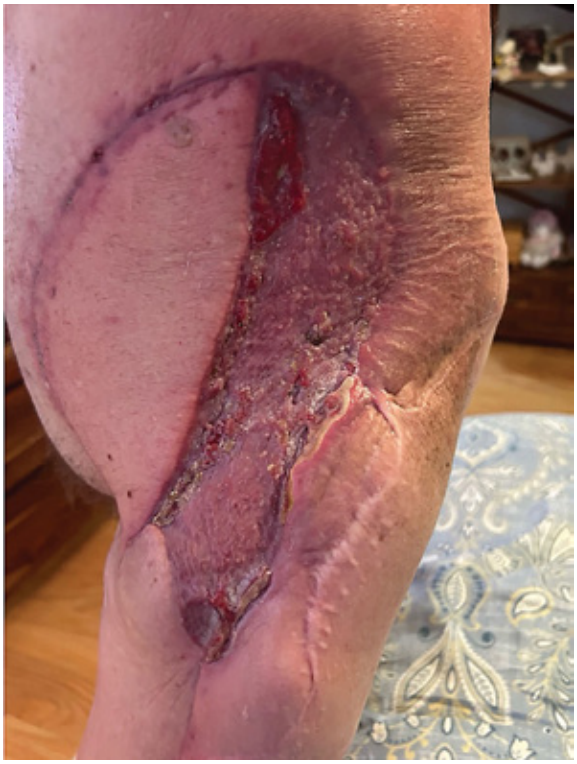

Figure 6. Post-operative week 8.

References

1. Tu YK, Yen CY, Ma CH, *et al.* Soft-tissue injury management and flap reconstruction for mangled lower extremities. *Injury*. 2008 Oct;39 Suppl 4:75-95.

2. Kozusko SD, Liu X, Riccio CA, *et al.* Selecting a free flap for soft tissue coverage in lower extremity reconstruction. *Injury*. 2019 Dec;50 Suppl 5:S32-S39

3. He J, Qing L, Wu P, *et al.* Variations of Extended Latissimus Dorsi Musculocutaneous Flap for Reconstruction of Large Wounds in the Extremity. *Orthop Surg*. 2022 Oct;14(10):2598-2606.

4. Fletcher CD. Diagnostic histopathology of the tumors. Vol. 2. New York: *Curchill Livingstone*; 1995. p 1049–52

5. Graves L, Jeck WR, Grilley-Olson JE. A League of Its Own? Established and Emerging Therapies in Undifferentiated Pleomorphic Sarcoma. *Curr Treat Options Oncol*. 2023 Mar;24(3):212-228.

6. Shoham Y, Koretz M, Kachko L, *et al.* Immediate reconstruction of the chest wall by latissimus dorsi and vertical rectus abdominis musculocutaneous flaps after radical mastectomy for a huge pleomorphic liposarcoma. *J Plast Surg Hand Surg*. 2013 Apr;47(2):152-4.

7. Tashiro K, Arikawa M, Fukunaga Y, *et al.* Free latissimus dorsi musculocutaneous flap for external hemipelvectomy reconstruction. *Microsurgery*. 2019 Feb;39(2):138-143.

A Tale of Perseverance—A Ukrainian Soldier's Fight to Keep His Arm After a Blast Injury

Bradley Osemwengie, MD
Chielozor Okafor, MD
Tyler Humphrey, MD
L. Scott Levin, MD

Department of Orthopaedic Surgery
University of Pennsylvania

Introduction

Blast injuries can have disastrous outcomes in soldiers during wartime. In addition to psychological effects, a significant portion of these injuries unfortunately end with amputation.[1,2] In cases where the affected extremity is still intact, limb salvage techniques have continued to advance to preserve the limb and functionality of patients who sustain traumatic injuries to their extremities. Vascularized osseous grafts are a good option to provide soft tissue coverage and support for large bony defects from blast injuries[3] When complications such as infection arise, the ultimate priority is to preserve the structural integrity of the bone to allow for functional use of the limb. We present a case of a Ukrainian soldier who sustained life altering injuries and still fights to keep his left arm despite multiple setbacks.

Case Presentation

The patient is a 43-year-old male Ukrainian military referral who suffered a blast injury in May 2022. Orthopedic injuries included a left comminuted humeral shaft fracture, and a left comminuted femoral shaft fracture, ruptures of the cruciate ligaments of the left knee, and gunshot wounds to both hands (right index finger, left thumb metacarpal). The patient underwent left humerus open reduction internal fixation in Ukraine. This was unfortunately complicated by an infection. The left humerus hardware was removed, and an external fixator was placed then placed. This was further complicated by another fracture while in the external fixator, so a revision external fixator was placed.

On presentation to clinic, the patient was noted to have intact hand and elbow function. He had minimal shoulder range of motion since this injury. The patient's left humerus external fixator pins were draining as well. X-rays of his left humerus showed an external fixator in place with segmental bone loss and areas of persistent fracture lines along the midshaft of the humerus (Figure 1). His left lower extremity x-rays demonstrated healing of his left femur fracture with callous formation along the shaft (Figure 2). The patient unfortunately developed a foot drop after his injury with an inability to evert his foot. He also endorsed numbness along the dorsal aspect of his foot for which he wore a brace.

On mid-September 2023, the patient underwent a right vascularized fibular graft

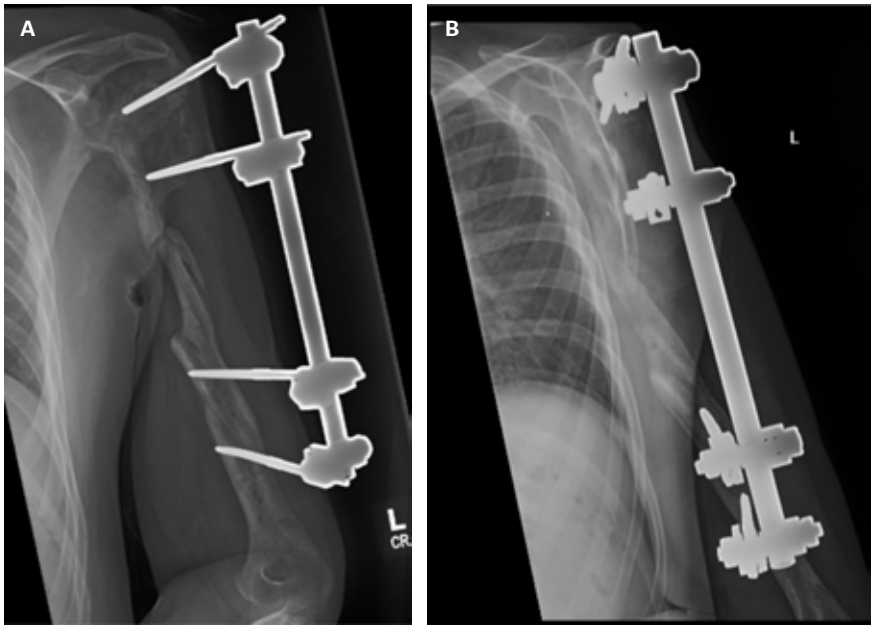

Figure 1. Left humerus x-rays. **(A)** AP **(B)** and lateral x-rays of the left humerus showing an external fixator in place. There is segmental bone loss and areas of persistent fracture lines along the midshaft of the humerus.

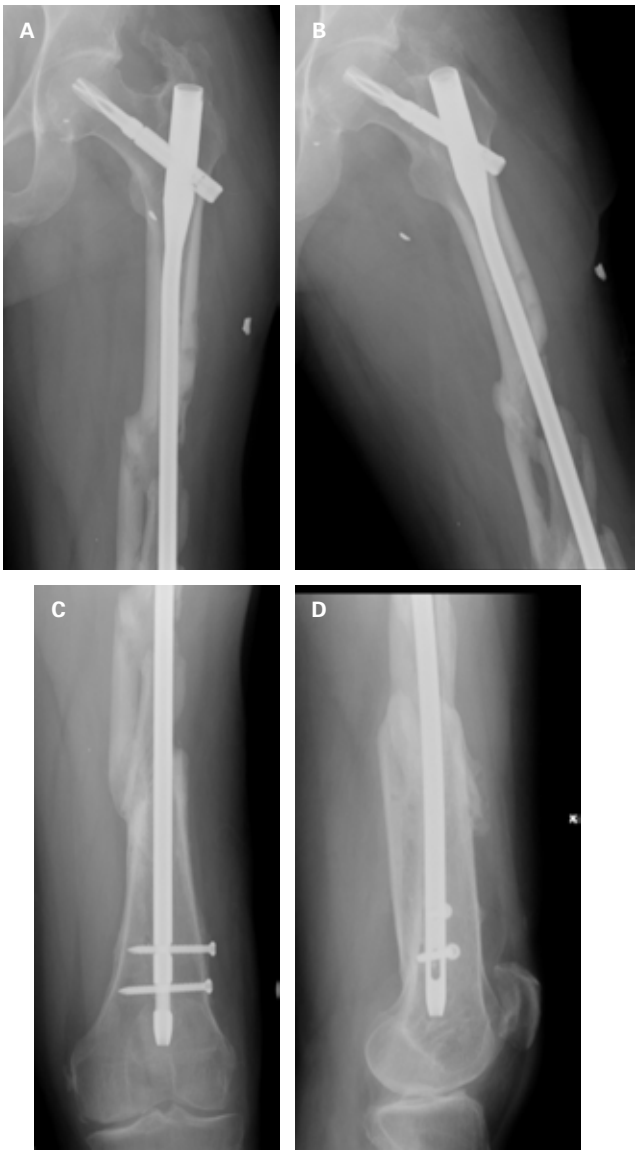

Figure 2. Left femur x-rays. **(A)** AP **(B)** Oblique proximal femur **(C)** and lateral of the distal femur showing LEFT femur showing callous formation along the midshaft of the femur. Multiple scattered metallic shrapnel/fragments about the thigh/proximal hip. Heterotopic ossification about the left hip is also noted.

with skin flap transfer to the left humerus due to the segmental bone loss (Figure 3). He also had a split thickness skin graft from his right thigh placed onto his right distal shin to cover the donor site. For further structural support to his left humerus, a bridge plate was placed as well. During the postoperative period, the left upper extremity flap became cool, signals grew faint, and an ecchymotic color change was noticed by the orthopedic team. On postoperative day 2 (POD2), he was taken back for left upper extremity flap exploration. A sizeable hematoma was found and evacuated. Thrombotic agents were applied to the flap site. Addition of a second venous outflow with the saphenous vein from the left leg was performed. A skin substitute was used for additional reinforcement. A clinical photo of the left upper extremity after this operation is shown in Figure 4.

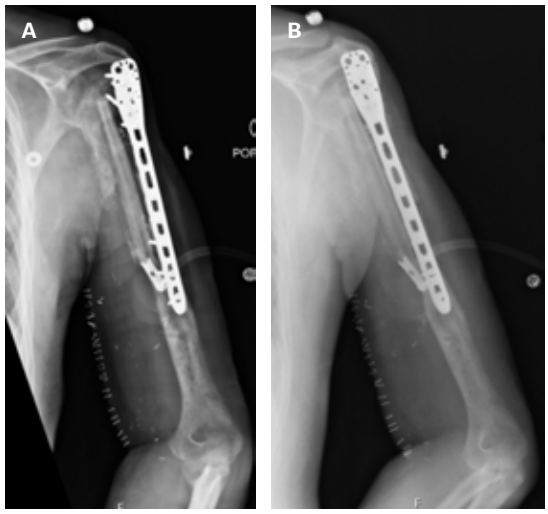

Figure 3. Left humerus x-rays after vascularized fibula graft. **(A)** AP and **(B)** lateral x-rays showing a lateral plate with screws. A large defect of the proximal humerus is filled with vascularized fibula graft. There is a plate remnant along the inferior margin of the bone graft. Severe glenohumeral arthritis is noted with evidence of remodeling.

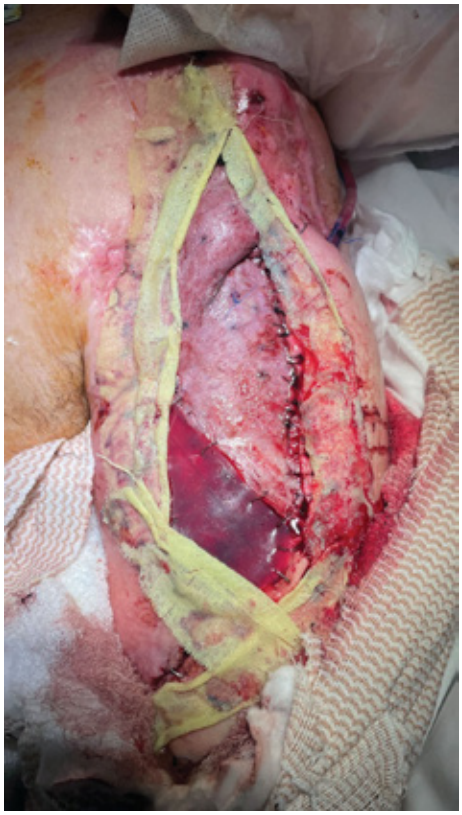

Figure 4. Clinical photo of the left humerus demonstrating the flap on POD1 from hematoma evacuation and skin substitute placement. There is slight ecchymosis over the proximal portion of the flap. Flap edges are covered with xeroform. A posterior slab splint is in place for support of the extremity.

On POD6, the patient was found to have an acute superficial vein thrombosis of his right upper extremity. This was treated with therapeutic low molecular weight heparin. The patient subsequently developed left upper extremity flap proximal wound dehiscence.

On POD9, the patient underwent a removal of the skin paddle with fasciocutaneous flap transposition via a thoracoacromial perforator from his left upper chest to his left arm. Right thigh skin graft was taken to cover his left chest and left distal arm. A negative pressure wound

therapy (NPWT) sponge bolster to his left chest was applied to help with granulation at his left chest wall site. Surgical pathology from this operation yielded no growth. The NPWT was removed a few days after the operation. A clinical photo of the LUE after this operation is depicted in Figure 5. Further into his hospital course, it was noted that his right lower extremity had exposed peroneal tendons (Figure 6). His left humerus flap site also expressed purulent drainage.

Figure 5. Clinical photo of the left humerus demonstrating the flap on POD4 from left chest thoracoacromial perforator flap transposition to the left arm. There is progression of the distal flap ecchymosis. A drain is in place adjacent to the lateral aspect of the flap.

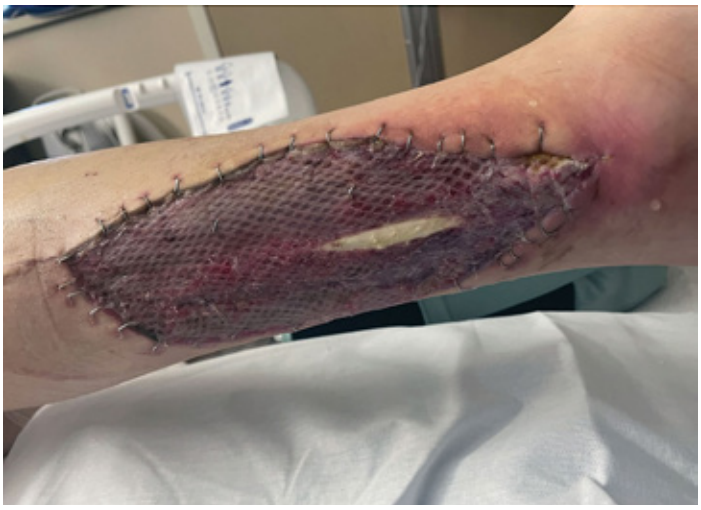

Figure 6. Clinical photo of the right lower extremity (lateral shin) demonstrating exposed peroneal tendon in the center of the skin graft recipient site.

On POD18, he underwent a left upper extremity irrigation and debridement and a right lower extremity irrigation and peroneal tendon debridement. Purulent drainage was encountered at the left upper extremity flap site. A NPWT sponge was applied to his left arm and right leg. On POD21, he underwent a left chest wall/left upper extremity (LUE) irrigation and debridement and a right lower extremity (RLE) irrigation and debridement with removal of the RLE NPWT. Skin substitute was used on his LUE and RLE at this time as well. OR Cultures from this operation grew Klebsiella pneumonia, Pseudomonas, Streptococcus mitis, Streptococcus oralis, Enterobacterales.

On POD29, the patient underwent a left chest wall, LUE, and RLE irrigation and debridement. A skin substitute was placed to his LUE and RLE. On POD30, a RUE ultrasound revealed a radial vein deep vein thrombosis (DVT) and basilic vein superficial vein thrombosis. The patient was started on a therapeutic heparin drip.

The patient developed an increase oxygen requirement and work of breathing. On POD36, sputum Cultures grew gram positive cocci, gram negative rods, and Klebsiella pneumonia.

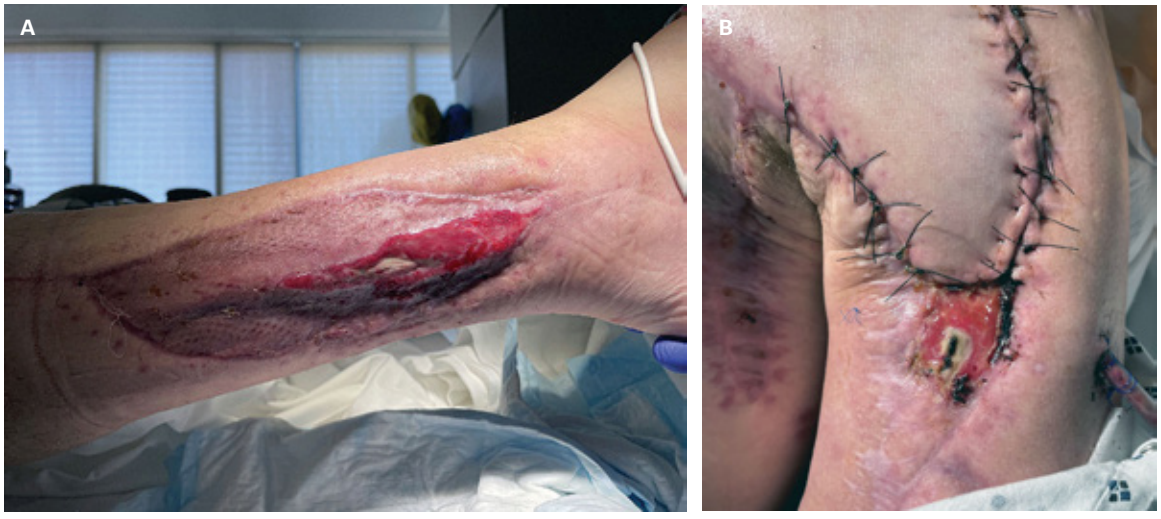

Figure 7. Clinical photos postop day ten from a repeat LUE and RLE irrigation and debridement. **(A)** Right leg (distal lateral shin) showing robust granulation tissue and only a minimal amount of exposed peroneal tendon; **(B)** LUE showing a healthy flap with a small amount of granulation tissue and eschar on its distal portion. Drain is present lateral to the flap.

On POD38, the patient underwent a repeat LUE and RLE irrigation and debridement. Gross purulence was noted around the LUE flap site. Intra-operative cultures grew Pseudomonas. Clinical photos ten days after this procedure are shown in Figure 7. On POD46, the patient also developed acute respiratory distress syndrome during this time and was treated conservatively with Lasix as he was already on antibiotics.

On POD57, the patient underwent a LUE and RLE irrigation and debridement as well as split thickness skin grafting from the right thigh to the LUE and RLE (distal lateral shin). On POD65, the patient underwent a left upper extremity irrigation and debridement with removal of the humerus bridge plate (Figure 8). On POD85, the patient sustained a fall onto his left upper extremity and developed wound dehiscence at his flap site. On POD86, the patient underwent a left upper extremity examination under anesthesia, irrigation and debridement, and revision closure of his wound dehiscence. The patient was placed into a coaptation splint at that time. He was eventually transitioned to a Sarmiento brace. During his clinical stay, the patient had frequent dressing changes to his operative sites with wet-to-wet dressings.

During this clinical course, the patient was followed by the infectious disease specialists. They placed him on cefiderocol and daptomycin during his stay. He was ultimately discharged without antibiotics due to the pan-resistant nature of his grown infectious organisms. For his RUE DVT, he was eventually discharge on apixaban. The patient was admitted for sixty-nine days consecutive days during his longest hospital stay. He was discharged to acute rehab. He was made weight bearing as tolerated to his RLE and non-weightbearing to his LUE in an abduction brace and sling.

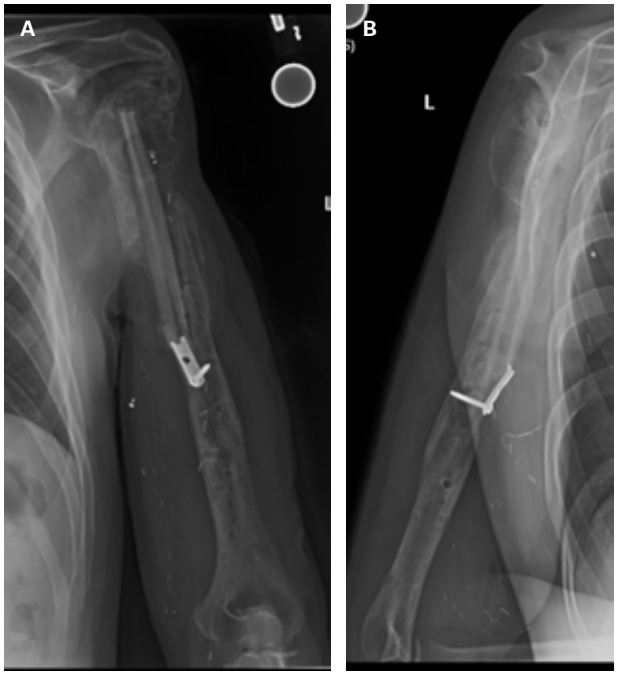

Figure 8. Left humerus x-rays. **(A)** AP and **(B)** lateral showing evidence of vascularized bone graft in the proximal femur. The bridge plate has been removed. Glenohumeral arthritis is noted.

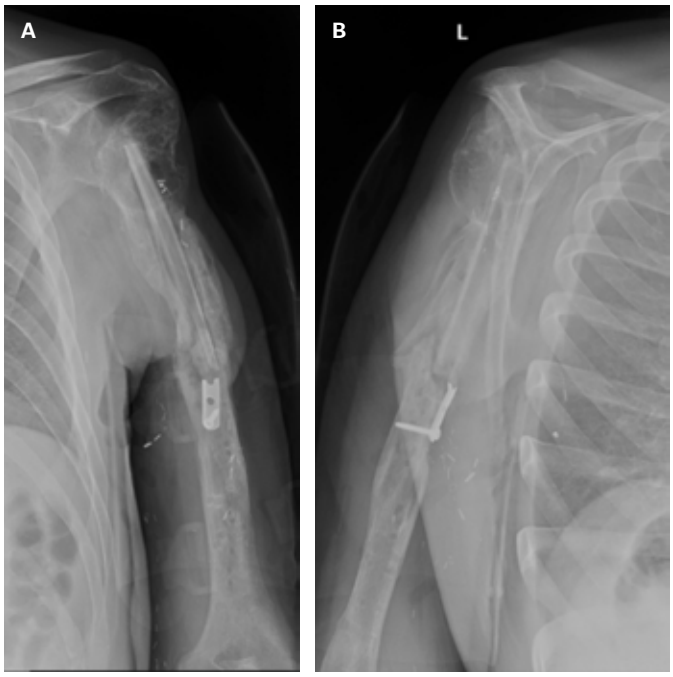

Figure 9. Left humerus x-rays from most recent follow up visit. **(A)** AP and **(B)** lateral showing evidence of vascularized bone graft in the proximal femur. The bridge plate has been removed. Fracture lines are still present but there is slightly more callus along the course of the humeral shaft compared to prior imaging. Glenohumeral arthritis is noted.

During his most recent clinic visit (six months postop), he noted to have no pain in his left upper extremity. There was no motion at the fracture site on clinical examination. X-rays at that time showed persistent fracture lines but slightly more callus along the course of the humeral shaft compared to prior imaging (Figure 9)

The patient followed with sports medicine for chronic left ACL/MCL sprain with arthrofibrosis in suprapatellar pouch for which a surgical arthroscopy with manipulation under anesthesia is recommended. He has also followed with foot and ankle specialists who recommend a tendon transfer versus an arthrodesis for his persistent foot drop. He is currently wearing an ankle-foot orthosis to manage this condition.

Discussion

Blast injuries can be life-altering injuries to soldiers during war time. To minimize the morbidity associated with these injuries, limb salvage is a viable option to preserve the injured limb. In the setting of significant bone loss or infection, vascularized fibula free flaps have been presented as an excellent source of bone to promote healing.[5,6] In the setting of severe proximal humerus bone loss, some have advocated for glenohumeral arthrodesis using a vascularized fibula bone graft.4 We did not elect for this procedure as the patient still had some shoulder range of motion which he wanted to preserve. Complications of vascularized osseous flaps include nonunion, infection,

and wound complications.[7] Flap hematomas can lead to flap failure because the increased pressure at the flap site makes it difficult for the tissues to get adequate perfusion. Infections of the flap should be treated promptly with irrigation and debridement and targeted antibiotics to have the best chance for flap viability and for osseous healing. Vigilance should be maintained by the inpatient team to ensure that changes in flap color, signal, or turgor are caught in a timely manner so that early interventions can minimize damage to the flap site. The importance of DVT prophylaxis and incentive spirometry should also be emphasized as DVTs/pulmonary embolisms and acute respiratory distress syndrome/pneumonia are complications that are associated with longer hospital stays and immobilization.

Conclusion

We present a case of a Ukrainian soldier with multiple devastating blast injuries. Despite many setbacks and complications along his clinical course, the patient was able to keep his left arm after a vascularized free fibula graft. In addition, the patient has reasonable functionality of that extremity and can perform his daily activities. The determination, resolve, and perseverance that this patient displayed along his clinical course is an inspiration to family, friends, and the medical staff who took care of him.

In the attachments (and with the patient's consent), there is a link to the patient's most recent clinical exam showing use of his left arm.

References

1. Smith SA, DaCambra MP, McAlister VC. Impact of traumatic upper-extremity amputation on the outcome of injury caused by an antipersonnel improvised explosive device. *Can J Surg*. 2018;61(6):S203-S207.

2. Mitchell SL, Hayda R, Chen AT, *et al.* The Military Extremity Trauma Amputation/Limb Salvage (METALS) Study: Outcomes of Amputation Compared with Limb Salvage Following Major Upper-Extremity Trauma. *J Bone Joint Surg Am*. 2019;101(16):1470-1478.

3. Taqi M, Raju S. Fibula Free Flaps. In: *Stat Pearls*. Treasure Island (FL): Stat Pearls

4. Armangil M, Bilgin SS. Reconstruction of Proximal Humeral Defects with Shoulder Arthrodesis Using Free Vascularized Fibular Graft: Surgical Technique. *JBJS Essent Surg Tech*. 2013;3(2):e8.

5. Bumbasirevic M, Stevanovic M, Bumbasirevic V, *et al.* Free vascularized fibular grafts in orthopaedics. *Int Orthop*. 2014;38(6):1277-1282.

6. Petrella G, Tosi D, Pantaleoni F, Adani R. Vascularized bone grafts for post-traumatic defects in the upper extremity. *Arch Plast Surg*. 2021;48(1):84-90.

7. Atilgan N. The Use of Free Fibula Flap in Different Extremities and Our Clinical Results. *Cureus*. 2023;15(10):e4745.

Arthroplasty

Tips and Tricks: Robotic-Assisted Total Knee Arthroplasty

Jaret M. Karnuta, MD, MS
Maxwell Cardwell, MD
Christopher Travers, MD

Department of Orthopaedic Surgery, University of Pennsylvania, Philadelphia, PA

Introduction

Total knee arthroplasty (TKA) surgical rate has been increasing in a monotonic fashion since the introduction of modern prosthesis designs in the 1970s.[1] TKA is now one of the most frequently performed operations by orthopaedic surgeons in the United States, with surgical volume expected to reach 3.48 million cases per annum in 2030.[2] Despite the introduction of advanced prosthesis designs, reproducible surgical technique, thoughtful pre-surgical optimization, and contemporary post-surgical rehabilitation, studies have demonstrated that patient outcomes have plateaued, with approximately 20% of patients are dissatisfied with their surgical outcome.[3] With the substantial increase in surgical volume comes a concomitant increase in the number of dissatisfied patients. This looming increase in suboptimal outcomes has lead surgeons to innovate methods for optimizing outcomes following TKA.

Successful TKA requires several critical components: restoration of knee biomechanics, precise tibial and femoral bone cuts, accurate alignment of articulating components, balancing of the soft tissues and knee stabilizers, and avoidance of patellar maltracking. Modern robotic total knee arthroplasty (rTKA) was introduced in 2015 to optimize the above surgical factors. The most studied rTKA system on the market utilizes a pre-operative computed tomography (CT) scan to understand the patient's preoperative bony anatomy and allows the surgeon to execute a pre-defined operative plan to accurately place implants and balance soft tissues.[4,5]

Despite the promise of technology-aided "precision surgery" offered by rTKA, these systems have a large upfront capital investment.4 rTKA also requires learning a new surgical system and offers a surmountable albeit present learning curve for surgeons, with operative times decreasing as surgeons become more comfortable with the system.[6] This learning curve is steeper for surgeons without arthroplasty-specific fellowship training.[7] While an ongoing area of research, there are significant positives to using rTKA technology. In a propensity-score matched cohort of 255 patients, prior researchers have demonstrated that total knee replacement performed with robotic assistance leads to lower length of stay and an increased odds of discharge to home over manual total knee arthroplasty.[8] In the appropriately indicated patient, robotic total knee replacement is a powerful addition to the surgeon's toolbox.

In this review, we present a systematic and reproducible method for performing rTKA with a semiactive, closed robotic system (Mako, MAKO Surgical Corporation, Ft. Lauderdale, FL).

Indications

In patients who are indicated for TKA (e.g., end-stage arthritis recalcitrant to nonoperative measures without systemic factors that may pose an unacceptable anesthesia or infection risk), the surgeon must then consider if the patient is able to undergo rTKA. The surgeon must consider the following patient factors:

- Sufficient range of motion of the hip joint to allow for bony registration at time of surgery.
- Absence of metal in the proximity of the knee joint. Metal in close proximity to the planned surgery may result in photon starvation and beam hardening artifacts within the pre-operative CT scan,[9] which may limit the ability of rTKA software to map the patient's anatomy.
- Absence of infection within the host at time of surgery. Acute and chronic infection, both local and systemic, should be ruled out prior to surgery.
- Poor bone quality which may affect implant stability.
- Patient size. Large patients may limit the ability of the rTKA arm to assist in bone resection.
- Poor ligamentous integrity which may prevent the restoration of a stable knee joint.
- The type and significance of the patient's present deformity, which may limit the

ability for registration and restoration of normal biomechanics.

Surgical Technique

Positioning

The patient is placed in a supine position on a regular surgical table. A bump consisting of a single rolled blanket is placed under the patient's ipsilateral hip. A nonsterile tourniquet is placed and secured around the patient's thigh.

Ensure the MAKO system is in the appropriate location prior to scrubbing. The body of the system should be on the patient's operative side, with the long axis of the system perpendicular to the surgical table centered at the level of the patient's hip. The camera system should be on the patient's contralateral side with an unobstructed view of the patient.

The patient is then prepped and draped in standard fashion for a TKA by the surgical team, all of which should be wearing standard surgical personal protective equipment.

The patient's incision is then marked using a sterile marker while the knee is on a sterile bump in approximately 70 degrees of flexion, starting from three fingerbreadths proximal to the superior pole of the patella and extending distally to the patellar tendon insertion on the tibial tubercle (Figure 1). Once marked, the patient's limb is exsanguinated and tourniquet is inflated to 100 mmHg above the patient's systolic blood pressure.

Exposure

Exposure down to the knee joint is similar to that of a manual TKA. An anterior midline surgical incision is made down to the patella using a #10 surgical blade. A medial parapatellar arthrotomy is made down to bone, leaving a cuff of medial retinacular tissue attached to the patella for later closure. A distal femur synovectomy is performed and the infrapatellar fat pad is resected to define the anterolateral aspect of the tibia. The patella is then subluxed laterally to expose the medial femoral condyle and the ACL is resected.

Anatomic Registration

Prior to bone cuts, the femoral and tibial arrays must be placed. First, the distal femoral pin footprint is marked with bovie cautery one fingerbreadth proximal to the most superomedial aspect of trochlea (Figure 2). After placement of the 4.5mm diameter bone pin, the array stabilizer is placed on the pin and a second pin is placed proximally to the first slightly off angle. Similarly, the tibial pin is then placed three fingerbreadths distal to the tibial plateau at the medial aspect of the incision. A stabilizer is inserted over the pin and another pin is inserted proximally to the first 30 degrees off center laterally from the anatomic axis of the leg. It is critical to ensure the array stabilizer barrels are firmly on bone prior to securing them to their respective pins. Two navigational arrays are placed on the connector jigs such that they are facing the infrared camera. The pins are placed in such a way to give as much clearance for the robotic cutting arm as possible and to avoid interference with the final implants (Figure 3).

A right angle retractor is placed between the lateral tibial plateau and patella to retract the patella laterally and protect the lateral collateral ligament (LCL), whereas a Z retractor is placed medially to protect the medial collateral ligament (MCL).

Bone checkpoint pins are then placed. The femoral checkpoint is placed as medial as possible at the level of the distal-most femoral pin, approximately 1 fingerbreadth posterior to the distal-most femoral pin to ensure it is clear of the anterior chamfer cut. The tibial checkpoint is placed

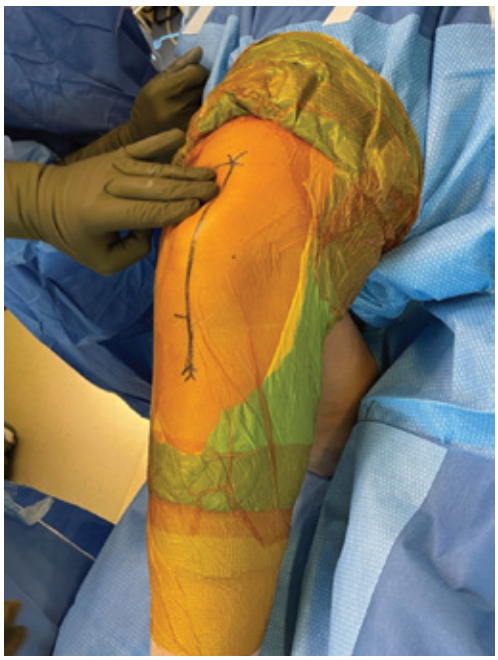

Figure 1. Incision placement allowing adequate exposure and respect of soft tissues.

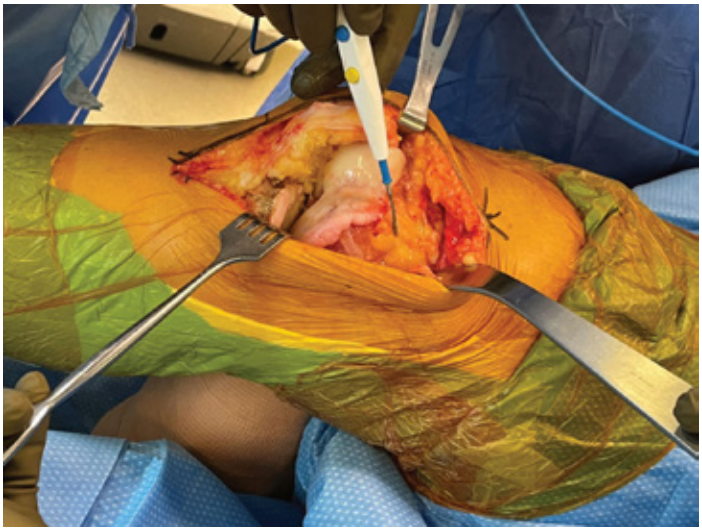

Figure 2. Bovie electrocautery marking of first (distal) pin for the femoral array.

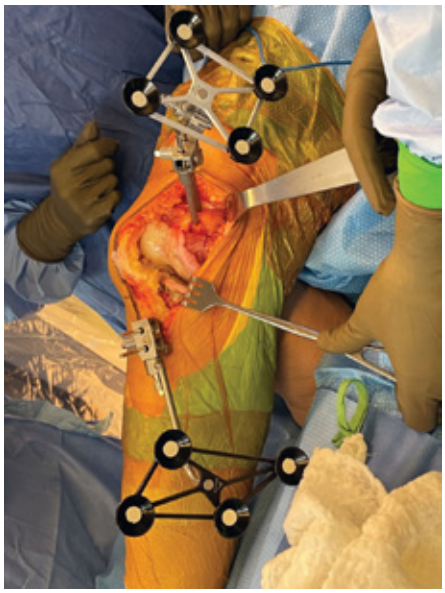

Figure 3. Final array placement. Note the array stabilizer barrels are on bone and are slightly off axis to allow unobstructed movement of the robotic arm and saw blade.

Figure 5. MAKO registration software screen during femoral registration demonstrating previous joint line (blue dots) and proposed joint line (grey shading) with planned implant position.

just proximal to the tibial array outside of the planned tibial cuts, approximately 1 fingerbreadth distal to the tibial plateau (Figure 4).

Next, the surgeon must undergo checkpoint registration using the MAKO software. Registration involves three steps: patient landmarks, bone checkpoints, and bone registration.

First, the hip center of rotation is calculated by circumducting the hip with the pelvis stabilized until verified by the MAKO software. The medial and lateral malleoli positions are then collected using blunt, green probe on each malleolus.

Second, the checkpoints are registered on the MAKO software using the blunt, green probe.

Third, bone registration is performed. Bone registration is completed by following the prompts on the MAKO screen (Figure 5) using the sharp probe to penetrate cartilage down to subchondral bone. The exact location of these points is not critical to successful registration, but the surgeon should ensure points are accurately registered on the surface of the subchondral and cortical bone, with care taken to have the probe sit precisely on top of the native cortical surface. Driving the probe deep into bone or superficially resting on cartilage will result in incorrect registration landmarks.

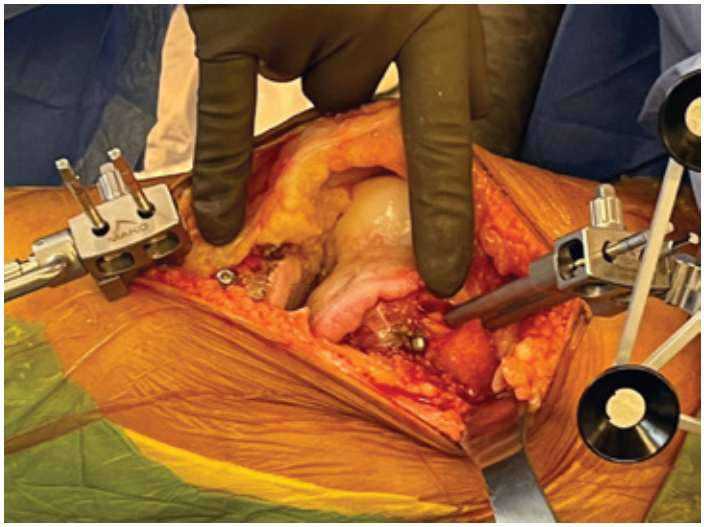

Figure 4. Location of femoral and tibial checkpoint pins.

Once registration is complete, the joint space can be evaluated throughout the range of motion, with particular attention paid to balance just short of full extension and at 90 degrees of flexion. Varus and valgus stress is applied to assess the predicted extension gap and a Chandler or Cobb elevator is used to assess the predicted flexion gap. Component position can be adjusted and soft tissue releases completed to ensure balanced flexion and extension gaps as predicted by the MAKO implant positioning software. Once component positioning is complete, proposed cuts should be reviewed to confirm appropriate bony resection and acceptable TKA parameters.

Bone Cuts

Bone cuts are performed using the MAKO robotic arm with the handle rotated laterally to allow quick transitions between the surgeons left and right hand for cutting and soft tissue retraction. The saw blade is controlled using an underhand grip with the ring finger or index finger actuating the saw as the surgeon transitions between hands as needed. At risk structures during cutting include the MCL, patellar tendon, and posterior structures. The haptic boundary drawn and enforced by the MAKO software/robotic arm provides some protection but diligent retractor placement is also critical, especially for the patellar tendon which is not protected by a haptic boundary.

Prior to performing any resections, the saw blade and femoral checkpoints are verified with the blunt probe to

confirm the infrared arrays have remained stable. Cuts are performed using the MAKO haptic boundaries and the previously determined surgical plan. The femur is cut first, starting with the distal femoral cut (starting with this cut is the authors preference as performing the distal femoral cut first allows for easier conversion to a traditional 4-in-1 cutting guide in the event that robotic equipment problems arise prior to completion of all femoral bony resections). Next the posterior femoral chamfer cut is performed followed by the posterior femoral cut, anterior femoral cut, and ending with the anterior chamfer cut (Figure 6).

Following the femoral cuts, the saw blade and tibial checkpoints are verified with the blunt probe. The tibial cut is performed again using the haptic boundaries defined by the MAKO software. Of note, patellar resurfacing, if indicated, is performed freehand without assistance of the robotic arm.

Gap balancing and Prosthesis Implantation

Following bone cuts, the surgery proceeds similar to a manual TKA procedure with some key differences. Once trial components are placed, varus and valgus stress is applied to the knee throughout the range of motion. The MAKO software and manual feedback are used to confirm stability and range of motion of the knee joint. Following this check, the trials, both arrays, and both checkpoints are removed. The tibia is prepared in typical fashion and final implants are placed. Of note, the increased precision of robotic bony resections facilitates the use of press-fit implants if this is the surgeons preference. Once implants are placed, the tourniquet is let down, hemostasis achieved with electrocautery, an analgesic cocktail is instilled into the soft tissues, and the surgical wound is closed in a layered fashion.

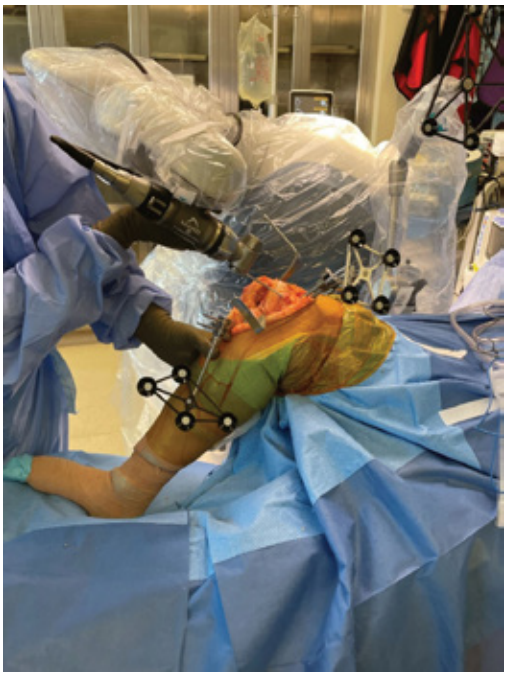

Figure 6. Anterior femoral cut.

Case Report

A 66-year-old female initially presented to our clinic with an 18 month history of anterior and posterior right knee pain. She had a history of prior left knee osteoarthritis status post manual total knee replacement over 10 years prior to her presentation. She failed conservative treatment including physical therapy, anti-inflammatory medications, corticosteroid injections, and two different courses of viscosupplementation injections. On physical exam, the patient has a moderate effusion and is tender to palpation at the medial and lateral joint lines with range of motion of 0-120 degrees. She is stable to varus and valgus stress with good range of motion of the hip. Pre-operative radiographs demonstrate moderate degenerative changes with osteophyte formation, subchondral sclerosis, and joint space narrowing (figure 7).

After a thorough discussion of risks, benefits, and alternatives, the patient elected to proceed with a total knee arthroplasty using the MAKO robotic system. At the latest two year follow-up, she was "thrilled" with her recovery and her pain had completely resolved. Radiographs at this appointment demonstrate a well-fixed, press-fit total knee prosthesis without component loosening, subsidence, or migration (figure 8).

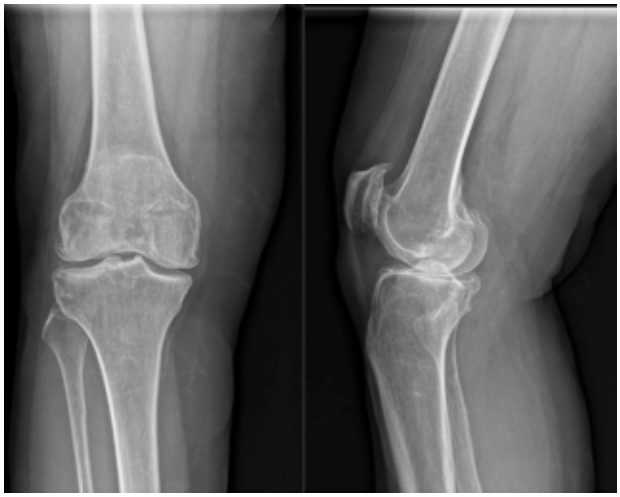

Figure 7. Pre-operative right knee radiographs demonstrating Kellgren-Lawrence stage 3 osteoarthritis.

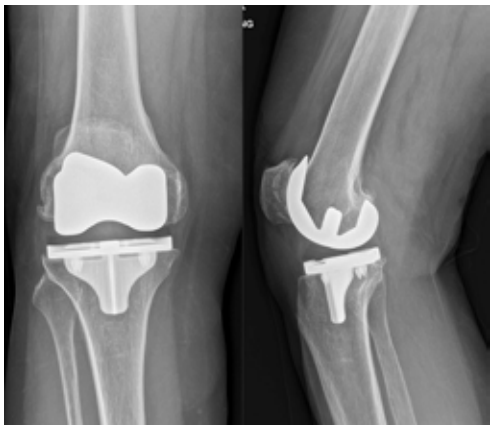

Figure 8. Post-operative right knee radiographs demonstrating a right knee total knee prosthesis in normal alignment without evidence of loosening, subsidence, or migration.

References

1. Robinson RP. The early innovators of today's resurfacing condylar knees. *J Arthroplasty* 2005;20:2–26.

2. Sloan M, Premkumar A, Sheth NP. Projected Volume of Primary Total Joint Arthroplasty in the U.S., 2014 to 2030. *J Bone Jt Surg* 2018;100:1455–60.

3. Bourne R, Chesworth B, Davis A, *et al.* Patient satisfaction after total knee arthroplasty: who is satisfied and who is not? *Clin Orthop*;468. Epub ahead of print January 2010. DOI: 10.1007/s11999-009-1119-9.

4. Walgrave S, Oussedik S. Comparative assessment of current robotic-assisted systems in primary total knee arthroplasty. *Bone Jt Open* 2023;4:13.

5. Siddiqi A, Mont MA, Krebs VE, *et al.* Not All Robotic-assisted Total Knee Arthroplasty Are the Same. *J Am Acad Orthop Surg* 2021;29:45–59.

6. Chen Z, Bhowmik-Stoker M, Palmer M, *et al.* Time-Based Learning Curve for Robotic-Assisted Total Knee Arthroplasty: A Multicenter Study. *J Knee Surg* 2023;36:873–7.

7. Stegelmann SD, Butler J, Eaddy SG, *et al.* Learning curve for imageless robotic-assisted total knee arthroplasty in non-fellowship trained joint replacement surgeons. *J Orthop* 2023;45:72–7.

8. Samuel LT, Karnuta JM, Banerjee A, *et al.* Robotic arm-assisted versus manual total knee arthroplasty: a propensity score-matched analysis. *J Knee Surg* 2023;36:105–14.

9. Katsura M, Sato J, Akahane M, *et al.* Current and Novel Techniques for Metal Artifact Reduction at CT: Practical Guide for Radiologists. *Radiogr Rev Publ Radiol Soc N Am Inc* 2018;38:450–61.

Medicare Payments May Inappropriately Favor Hemiarthroplasty Over Total Hip Arthroplasty for Geriatric Hip Fracture Treatment

Pranav Kodali, BA[1]
Eric Hume, MD[1, 2]
Joseph Bernstein, MD[1, 2]

[1]Perelman School of Medicine at the University of Pennsylvania, Philadelphia, PA

[2]Corporal Michael J. Crescenz Department of Veterans Affairs Medical Center, Philadelphia, PA

Introduction

Displaced fractures of the femoral neck in geriatric patients are typically not treated with open reduction and internal fixation (ORIF) procedures. That is sensible. For one thing, patients who had ORIF surgery might have to delay their full rehabilitation while waiting for their fractures to unite. Also, because the blood supply to the femoral head ascends the femoral neck and could be disrupted by the fracture, there is a risk for osteonecrosis of the head even if the fracture were to heal uneventfully. Taken together, there is a consensus in the orthopaedic surgery community that displaced femoral neck fractures in geriatric patients should be treated with joint replacement. With joint replacement, physical therapy can begin expeditiously and the risks of osteonecrosis are avoided.

There are two types of joint replacements that can be used for displaced geriatric femoral neck fractures: hemiarthroplasty and total hip arthroplasty. In hemiarthroplasty, a femoral stem and a prosthetic head are inserted. In a total hip arthroplasty, an acetabular cup is inserted as well. In brief, total hip arthroplasty is said to give better long term results but at the price of greater surgical complexity and an increased risk for short term complications such as dislocation.[1–3]

There is reason to believe that there is a shortage of total hip arthroplasty relative to the true appropriate demand.[4] Hochfelder et al.[5] reported on the treatment of femoral neck fractures in New York and noted that among 33,226 elderly patients treated with arthroplasty, 30,763 (93%) received hemiarthroplasty (HA). By contrast, when Bhandari's group[6] surveyed patients at risk for hip fracture, they found that 93% of patients preferred total hip arthroplasty.

This putative shortage of total hip arthroplasty procedures may be due to improper financial incentives built into the Medicare fee schedules. If reimbursement for total hip arthroplasty is the same as that for hemiarthroplasty, despite increased costs associated with total hip arthroplasty, the proper equilibrium at which supply matches demand cannot be achieved. Along those lines, if there is a shortage caused by inadequate reimbursement, the obvious solution would be to pay more for the appropriate procedure.

In this study, we review some common reasons to suggest why total hip arthroplasty should be compensated at a higher level than it currently is. We further detail several potential payment reforms that might help rectify this imbalance. We conclude with a discussion of why reform may not succeed—and indeed may not be necessary.

Background

Ordinarily, for patients with medical insurance (and most geriatric hip fracture patients are Medical-eligible) there are two separate payments for surgical treatment of hip fracture. There is a payment to the physician based on the CPT code, and there is a payment to the hospital based on the diagnosis code.

Although there are three distinct operations for hip fracture, there is a single CPT code that covers all of them: CPT code 27236. This code is defined as "open treatment of femoral fracture, proximal end, neck, internal fixation or prosthetic replacement." Although separate CPT codes exist for hemiarthroplasty and total hip arthroplasty, 27125 and 27130, respectively, these codes are reserved–according to the letter of law[7] at least –for degenerative, non-trauma indications.[8]

Because payments to the orthopaedic surgeon are based on the CPT code, the existence of a single code for all three operations ensures that payment for both total hip arthroplasty and hemiarthroplasty will be the same. And needless to say, if there is a single, similar payment for the two operations, despite one them incurring greater costs, this structure creates perverse incentives for potentially choosing the cheaper one (hemiarthroplasty) in settings where the more expensive one (total hip arthroplasty) is better.

Total hip arthroplasty incurs greater costs. First, total hip arthroplasty takes more time, if nothing else because the additional task of cup insertion[9] is required. In addition, there are potential complications associated with this additional step, notably fracturing the acetabulum while inserting the cup. (Most surgeons are familiar with inserting a cup into arthritic, sclerotic bone; patients with fracture, by contrast, are typically osteoporotic.) This can add operative time and perhaps increase the length of stay.

Beyond that, there is the issue of postoperative complications—and who may be blamed for them. When a hemiarthroplasty fails, it typically fails years after the index operation, either by loosening of the implant or protrusion into the pelvis (protrusio acetabuli). In general, late complications will be blamed on nature taking its course. On the other hand, the most common unique complication of a total hip arthroplasty, dislocation, may occur within days to weeks after surgery. Dislocation is more likely to be deemed a "surgical complication." Reports of surgical complications may adversely affect surgeons' quality metrics or invite malpractice litigation.

In short, paying a surgeon the same fee for a hemiarthroplasty and a total hip arthroplasty assuredly underpays for total hip arthroplasty relative to hemiarthroplasty. This may lead to suboptimal treatment selection. Although we may wish to believe that orthopaedic surgeons are motivated by altruism alone and are thereby exempt from financial temptations, systems should not be built on this assumption. To the point, DeMik et al demonstrated how Medicare's transition to a bundled payment model for elective total joint replacement was built to improve care by altering financial incentives.[10] This program would make no sense if physicians were not swayed by incentives.

A second, separate payment made is to hospitals. Although it may be assumed that changing the incentives for hospitals will not affect the selection of treatments (as it is the surgeon, not the bureaucrat, who makes this decision), such an assumption ignores potential institutional influences on clinical decision making. Experience teaches that when physicians' behaviors markedly affect hospitals' margins, hospitals take action to modify physician behaviors. This may be done through individual "counseling" or by instituting pathways and treatment algorithms that nudge the physician in the desired direction. It is therefore reasonable to consider hospital incentives as well.

Similar to orthopedic surgeons, institutions are relatively underpaid for total hip arthroplasty, given that total hip arthroplasty is associated with greater institutional expenses (despite similar payments) relative to hemiarthroplasty. As noted, the operation is longer, and every additional minute in the operating room incurs both direct costs (i.e. staffing and material expenditures, etc.) and opportunity costs (in that the occupied OR cannot be used for another patient). The hospital must also purchase the acetabular implant (which may also be coupled to a more expensive stem) without additional reimbursement. For these reasons alone, at the margin, a hospital administrator would prefer that all patients receive a hemiarthroplasty.

The issue of hospital payments is made more complicated by the advent of so-called bundled payments. Traditionally, hospitals were reimbursed by Medicare using a Diagnosis Related Group (DRG), a single code for the diagnosis that yields a fixed reimbursement amount for the hospitalization. More recently though, Medicare introduced the Comprehensive Care for Joint (CJR) Model, which includes all associated expenses for the 90-day period following the completion of an outpatient procedure or discharge from an inpatient procedure. In this bundled payment model, each hospital is given a target price for each episode, and the actual spending at the end of each year is compared to this target price to determine a net bonus or penalty. The target price is also accordingly adjusted for the following year based on the previous year's performance and other factor.[11] Given the increased risk of complications for total hip arthroplasty over hemiarthroplasty, the CJR model further disincentives its use by creating an additional penalty for institutions with increased 90-day procedure-associated costs. Medicare also introduced the Bundled Payments for Care Improvement (BPCI) initiative, a voluntary bundle program. Since BPCIs are designed to favor the bundle owner, which can be a physician group instead of the actual hospital, BPCI fiscal pressure may be even more significant in influencing surgical decisions, overtly or subconsciously. With the greater emphasis on value-based healthcare through the use of bundled payments, more institutions will be increasingly affected by this double-penalty for using total hip arthroplasty.

Countervailing Arguments

It is of course possible that the perceived shortage of total hip arthroplasty for femoral neck fracture is illusory. To start, the subjects in the survey study asking about preferences may be confounded by a psychological bias: namely, subjects did not put sufficient weight on the possibility that they themselves would die too soon to reap any benefits from the bigger operation. In general, it is psychologically adaptive to not think about one's own mortality too much. In this instance, however, a life expectancy overconfidence bias may encourage patients to select the wrong treatment. Many geriatric hip fracture patients may die within one year,[12] and thereby not stand to benefit from total hip arthroplasty. All individuals in the survey study cited above may think that they are exempt from this fate, but not everyone can be above average. Thus, integrated across the entire population, overconfidence regarding one's life expectancy will produce an inappropriate preference for total hip arthroplasty.

Another factor to consider is that the differences between hemiarthroplasty and total hip arthroplasty are not properly understood. The most comprehensive information

to date comes from systematic reviews and meta-analyses, but a large randomized controlled trial[13] has suggested that at the two-year point, at least, the operations are not significantly different in outcome. One can criticize that study for conflating all additional surgical procedures into one category—the revision of a hemiarthroplasty counts as much as a closed reduction of a total hip arthroplasty—yet that study is ongoing, with additional endpoints under examination. In the near future, accordingly, we may have a revised understanding of the costs and benefits of the two procedures. With that, any putative shortage may disappear.

Still more, it is dubious to assume that if we were to perform more total hip replacements, the complication rates will remain as reported thus far. After all, the patients currently receiving total hip arthroplasty presumably represent the most ideal patients. Any additional (marginal) patient would be less ideal, even if only slightly. With that, surgical complication rates may be higher. This change might offset any improvement in long term outcomes.

In addition, a program that favors total hip arthroplasty might have an unintended consequence of causing treatment delays. Specifically, some surgeons may not feel comfortable inserting an acetabular cup in osteoporotic bone. They will therefore refer the patient who needs one to a colleague, but this second surgeon might not be available right away. The resulting treatment delay may increase mortality risk.[14]

Finally, there is the possibility that any "correction" of the hemiarthroplasty/total hip arthroplasty ratio will overshoot the optimal point. Given the high one-year mortality rate for femoral neck fracture in geriatric patients, total hip arthroplasty is certainly not the right answer for many patients. Yet one could imagine that if total hip arthroplasty fees were significantly higher than those for hemiarthroplasty too many of these procedures may be performed. That is, inversed incentives can create an inverse problem.

Proposed Solutions

The American humorist, H.L. Mencken, famously said, "For every complex problem, there's a solution that is simple, neat, and wrong." His analysis is a simple, neat, and correct. It would be naïve to assume that complex problems have easy answers. Nevertheless, with appropriate humility, we propose the following simple and neat reforms:

- There should be a new CPT code for the performance of a total hip arthroplasty for displaced geriatric femoral neck fracture. This operation is sufficiently different from hemiarthroplasty and internal fixation procedures that it deserves its own code. (Indeed, hemiarthroplasty should have a code distinct from internal fixation procedures too, if for no other reason than to facilitate research studies.)
- Along those lines, the payment for total hip arthroplasty for femoral neck fracture should be much higher than what is paid for hemiarthroplasty. This fee should be commensurate with the required skills and efforts and compensate the surgeon for the additional risks and responsibilities this operation brings with it.
- Additionally, there should be an amply rewarded CPT code for preoperative counseling and shared decision-making. This is similar to what is currently required by Medicare for the implantation of an implantable cardioverter-defibrillator.[15] Pre-operative counseling is normally bundled with the surgical fee and not compensated distinctly. That is a mistake in this instance. For geriatric hip fracture, such a session is often more time-consuming than the surgery itself. In some cases, a well-executed shared decision-making session might even provide more benefit than the surgery itself. Greater incentives are needed to ensure that counseling gets the time and attention it deserves.
- There should be an amply rewarded CPT code for CPT code for "nonoperative management, geriatric hip fracture." Currently, nearly all geriatric patients in the United States with a hip fracture are treated surgically. The high 30-day mortality rate suggests that perhaps some patients might be better off receiving nonoperative care.[16] Financial incentives should reflect that.

Conclusion

Femoral neck fracture has long been known as the "unsolved fracture."[17] More than 70 years ago, a "solution" was thought to be found,[18] but that prediction was at least a tad premature. It is certainly possible that the high mortality rates seen after this injury do not represent any inadequacies in our treatments, but rather reflect the underlying frailty, senescence, and decay that leads to both the fracture itself (through higher risks of falls, and decreased ability to prevent fracture given the fall) and the post-op mortality seen after treatment (poor physiological reserves). That said, it is possible that we can improve our care.[19] In the realm of treatment selection, we must ensure that we have the right operation, for the right patient, at the right time, performed by the right surgeon. Minor adjustments to the financial incentive structures may help us get there.

References

1. Zi-Sheng A, You-Shui G, Zhi-Zhen J, *et al.* Hemiarthroplasty vs primary total hip arthroplasty for displaced fractures of the femoral neck in the elderly: a meta-analysis. *J Arthroplasty* 2012;27:583–90.

2. Yu L, Wang Y, Chen J. Total hip arthroplasty versus hemiarthroplasty for displaced femoral neck fractures: meta-analysis of randomized trials. *Clin Orthop* 2012;470:2235–43.

3. Hopley C, Stengel D, Ekkernkamp A, *et al.* Primary total hip arthroplasty versus hemiarthroplasty for displaced intracapsular hip fractures in older patients: systematic review. *BMJ* 2010;340:c2332.

4. Bernstein J. Not the Last Word: Bhandari's Paradox. *Clin Orthop* 2018;476:674–7.

5. Hochfelder JP, Khatib ON, Glait SA, *et al.* Femoral neck fractures in New York State. Is the rate of THA increasing, and do race or payer influence decision making? *J Orthop Trauma* 2014;28:422–6.

6. Alolabi N, Alolabi B, Mundi R, *et al.* Surgical preferences of patients at risk of hip fractures: hemiarthroplasty versus total hip arthroplasty. *BMC Musculoskelet Disord* 2011;12:289.

7. Beck CM, Blair SE, Nana AD. Reimbursement for Hip Fractures: The Impact of Varied Current Procedural Terminology Coding Using Relative Value Units. *J Arthroplasty* 2020;35:3464–6.

8. CMS-1784-F | CMS. Available at https://www.cms.gov/medicare/medicare-fee-service-payment/physicianfeesched/pfs-federal-regulation-notices/cms-1784-f. Accessed May 2, 2024.

9. Blomfeldt R, Törnkvist H, Eriksson K, *et al.* A randomised controlled trial comparing bipolar hemiarthroplasty with total hip replacement for displaced intracapsular fractures of the femoral neck in elderly patients. *J Bone Joint Surg Br* 2007;89:160–5.

10. DeMik DE, Gold PA, Frisch NB, *et al.* A Cautionary Tale: Malaligned Incentives in Total Hip and Knee Arthroplasty Payment Model Reforms Threaten Promising Innovation and Access to Care. *J Arthroplasty* 2024;39:1125–30.

11. Medicare Program; Comprehensive Care for Joint Replacement Payment Model for Acute Care Hospitals Furnishing Lower Extremity Joint Replacement Services. Federal Register. Available at https://www.federalregister.gov/documents/2015/11/24/2015-29438/medicare-program-comprehensive-care-for-joint-replacement-payment-model-for-acute-care-hospitals. 2015, Accessed May 2, 2024.

12. Lee A, Xi IL, Ahn J, *et al.* Median survival following geriatric hip fracture among 17,868 males from the Veterans Health Administration. *Front Surg 2023*;10:1090680.

13. HEALTH Investigators, Bhandari M, Einhorn TA, *et al.* Total Hip Arthroplasty or Hemiarthroplasty for Hip Fracture. *N Engl J Med* 2019;381:2199–208.

14. McGuire KJ, Bernstein J, Polsky D, *et al.* The 2004 Marshall Urist award: delays until surgery after hip fracture increases mortality. *Clin Orthop* 2004;294–301.

15. Wallace BC, Allen LA, Knoepke CE, *et al.* A multicenter trial of a shared DECision Support Intervention for Patients offered implantable Cardioverter-DEfibrillators: DECIDE-ICD rationale, design, Medicare changes, and pilot data. *Am Heart J* 2020;226:161–73.

16. Parvizi J, Ereth MH, Lewallen DG. Thirty-day mortality following hip arthroplasty for acute fracture. *J Bone Joint Surg Am* 2004;86:1983–8.

17. Barnes R. The Unsolved Fracture. *Scott Med J* 1964;9:45–57.

18. McCarroll HR. Has a solution for the "unsolved fracture" been found?: Problems and complications of fractures of femoral neck. *J Am Med Asso*c 1953;153:536–40.

19. Bernstein J, Weintraub S, Hume E, *et al.* The New APGAR SCORE: A Checklist to Enhance Quality of Life in Geriatric Patients with Hip Fracture. *J Bone Joint Surg Am* 2017;99:e77.

Pediatrics

A Distal Humerus Fracture with a Proximal Medial Forearm Wound- Open or Closed?

Bradley O. Osemwengie, MD[1]
Chielozor I. Okafor, MD[1]
Jacob Jordan, BA/BS[2]
J. Todd R. Lawrence, MD/PhD[1,2,3]

[1]Department of Orthopaedic Surgery University of Pennsylvania

[2]Perelman School of Medicine at the University of Pennsylvania

[3]Children's Hospital of Philadelphia, Division of Orthopaedics

Introduction

Open fractures are associated with a higher risk of infection and if not identified and treated appropriately, can lead to limb- and life-altering consequences.[1] Prompt administration of intravenous antibiotics and tetanus treatment (if indicated) can help to significantly lower the rates of infection.[2] Because of the time sensitivity of treatment, a high level of clinical suspicion should be maintained when evaluating trauma patients to ensure that an open fracture is not missed. Traditional teaching is that any wound near a fracture site should be considered a potential conduit for communication of the fracture site with the environment. However, the distance between the fracture and the open wound raising the suspicion for an open fracture is not well studied. Conventionally, wounds associated with an open fracture are thought to at least be on the same limb segment as the fractured bone. Humeral shaft fractures are much less common than distal humerus fractures in the pediatric population and in many patients these fractures can be treated non-operatively.[3] Very few of these fractures are open on presentation, with only about 1% of pediatric supracondylar humerus fractures being open injuries.[4]

In this report, we present a case of a poly-trauma pediatric patient with a distal humeral shaft fracture with a traumatic wound in a different limb segment, the proximal forearm, that was eventually identified as being an open injury.

Case Presentation

The patient is a 12-year-old male who was involved in an automobile versus pedestrian accident. In the trauma bay, the patient was alert and oriented with no notable head, neck, or trunk trauma. He had gross deformities of his left upper arm and right lower leg. All his limbs were well perfused. He had a mixed neurological exam of his left upper extremity with weakness of thumb and wrist extension as well as finger abduction and flexion. He also endorsed global paresthesias of his left hand and right foot. On his left forearm roughly four centimeters distal to the medial epicondyle, there was a one-centimeter medial forearm wound that probed roughly six centimeters deep (Figure 1). On his right lower leg there was a two-centimeter stellate skin defect over the lateral portion of his mid-shin with consistent bloody drainage and visible bone. He also reported left ankle pain but there were no wounds or deformity noted. Preliminary imaging showed a transverse fracture of the left distal humerus shaft which was significantly displaced and angulated with a small butterfly fragment but no apparent fracture of the forearm (Figure 2). Air was also noted around the

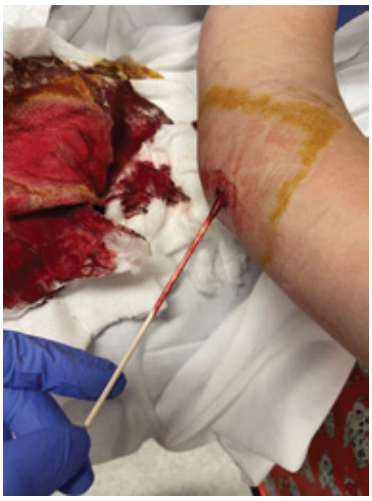

Figure 1. One centimeter wound over the proximal medial forearm. Cotton tip able to probe roughly six centimeters deep into the wound.

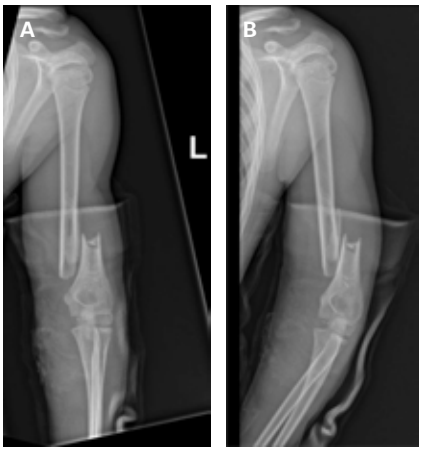

Figure 2. **(A)** AP and **(B)** oblique radiographs of the left humerus showing a displaced, comminuted transverse humeral shaft fracture.

distal humerus fracture site on CT (Figure 3). A right distal third transverse tibia and fibula fracture which was also significantly angulated and displaced was also identified (Figure 4). The patient was given a tetanus immunization booster and intravenous antibiotics (cefazolin and gentamicin) were administered for the open right tibia/fibula fracture. The open wounds of his left forearm and right shin were washed with betadine-diluted normal saline and dressed with soft dressings. The patient was administered conscious sedation and underwent closed reduction of his right tibia/fibula shaft fracture. The patient was temporarily stabilized in a right lower extremity short leg splint, a left upper extremity long arm splint, and a left lower extremity short leg splint. Secondary survey and additional imaging revealed additional injuries including a mandible fracture, a rib fracture, a left minimally displaced distal third clavicle fracture, and a left minimally displaced Salter Harris 2 fracture of the distal tibia.

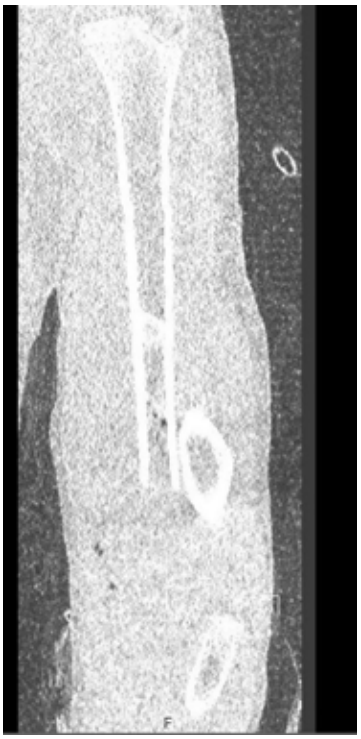

Figure 3. Coronal slice of CT of the left upper extremity showing distal humerus fracture with air around the fracture site.

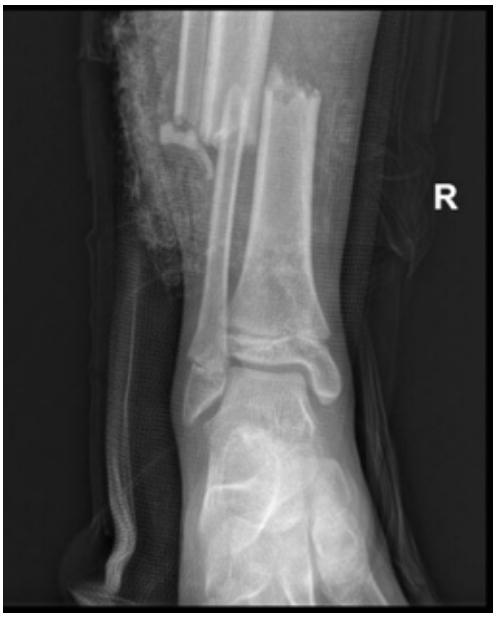

Figure 4. AP x-ray of the right distal tibia/fibula showing a displaced, transverse distal third tibia/fibula fracture.

Surgical Intervention

A few hours later, once medically cleared for surgery, the patient was taken to the operating room with the orthopedic surgery team to address his injuries. Initial attention was turned to the open right tibia/fibula fracture. The wound on his right lower leg was extended and an extensive sharp debridement with extensive irrigation procedure performed. Black gravel/stone-like material was encountered and removed from the wound. Devitalized soft tissue was sharply removed and the fracture edges were debrided. Once visibly clean, the area was extensively irrigated. His right tibia was then fixed with two flexible intramedullary nails. The open wound was closed loosely and the lower leg splinted.

Attention was then turned to his left upper extremity. The one-centimeter wound in the proximal medial forearm, about four centimeters distal to the medial epicondyle, was evaluated. This wound was extended proximally and distally by about one centimeter in each direction. Gently milking at the distal humerus then expressed a significant amount of dark sanguineous fluid from the wound. Gentle blunt finger dissection was performed through the zone of soft tissue injury which led across the antecubital fossa to the distal aspect of the proximal aspect of the humerus fracture. This finding was consistent with the distal humerus shaft fracture having created a large soft tissue zone of injury that extended from the distal third of the humerus all the way down to the proximal third of the forearm. Given the degree of contamination of the tibial wound, the decision was made to extend the humeral incision to explore this entire tract. The incision was extended proximally across the medial elbow to the fracture site and blunt dissection commenced. As expected, significant trauma was noted to the soft tissue and musculature about the antecubital fossa. The median nerve was explored through the zone of injury and was found to be intact. The proximal fragment of the humerus was found to be stripped of its periosteum and was contaminated with the similar black stone/gravel-like substance encountered in the right lower extremity. The soft tissues and bone were similarly debrided and irrigated. The fracture was fixed with flexible intramedullary nails. The wound was loosely closed and a posterior slab splint was placed.

His facial fracture was managed nonoperatively by the oral maxillofacial surgery team. Postoperatively, the patient was neurovascularly intact to all four limbs with resolution of all preoperative left hand/right foot paresthesias as well as left hand weakness. His humerus fracture went on to heal uneventfully with full return of arm/elbow function (Figures 5 and 6).

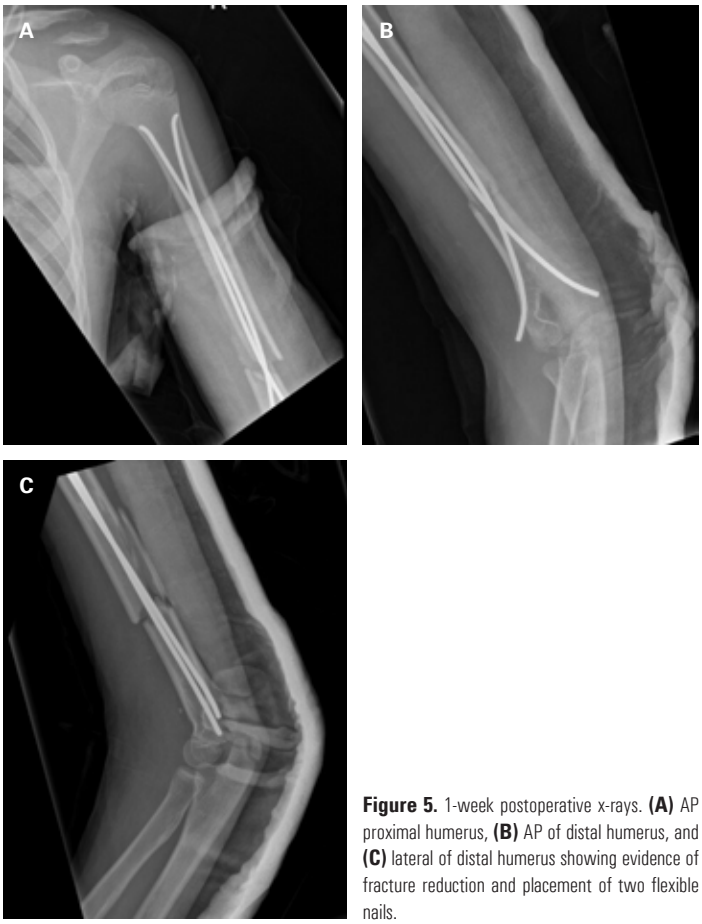

Figure 5. 1-week postoperative x-rays. **(A)** AP proximal humerus, **(B)** AP of distal humerus, and **(C)** lateral of distal humerus showing evidence of fracture reduction and placement of two flexible nails.

Discussion

A high index of clinical suspicion needs to be maintained by healthcare providers to ensure that open fractures are not missed. This includes a thorough inspection of the skin of an affected extremity to ensure the presence or lack of skin defects near the fracture site. To our knowledge, there has not been a report describing an open fracture where the open wound was found to only be present on a different limb segment than the fracture. In this case, we definitively found that a distal third humeral shaft fracture exited the skin through a laceration in the proximal forearm, leading to gross contamination of the bony segment and extensive soft tissue trauma through the zone of injury. This injury likely occurred as axial compression on the somewhat extended limb caused the proximal humeral segment to piston through the anterior medial soft tissues of the antecubital fossa and out of the proximal medial forearm prior to returning to its position in the upper arm.

Upon original primary survey evaluation of this patient, there was some question as to whether the left distal humerus fracture was open because the medial proximal forearm wound appeared to be far away from the fracture site. In this case, not initially declaring this an open injury did not seriously impact the management of this patient because treatment of his concomitant obviously open right distal tibia/fibula fracture necessitated prompt administration of intravenous antibiotics.[1,5] However, if this patient had not had the contralateral open tibia fracture, a clinical dilemma would have arisen as to whether to utilize the open fracture protocol for the left distal humerus fracture. In this case free air at the distal humeral shaft fracture site noted on the CT scan alerted the team of the strong possibility of the open injury, but had this study not been performed or had the wound not been thoroughly explored, this patient's clinical outcome may have been significantly different. Irrespective of the outcome, this case highlights that strong consideration should be given to administration of antibiotics in the setting of any open wound on the same extremity with a noted fracture or clinical deformity, even if it initially seems to be very distant or even on a different segment of the limb. In these cases,

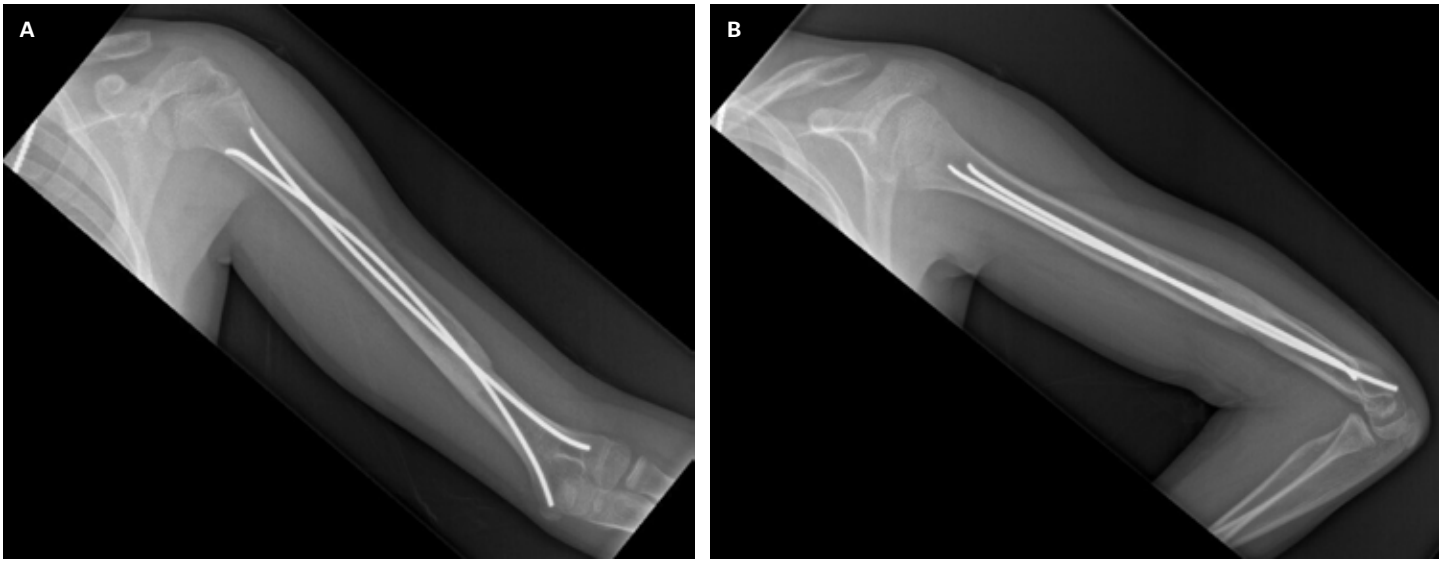

Figure 6. 10-month postoperative x-rays. **(A)** AP and **(B)** lateral humerus x-rays showing healing of the prior fracture site with evidence of callous formation. The 2 flexible nails are still in place.

the risks of missed treatment for an open fracture would seem to outweigh the risks of erroneously administering antibiotics if the wound turns out to only be superficial in nature.

Conclusion

Open fractures of long bones after a traumatic event can have significant ramifications if not identified and treated expeditiously. To mitigate the consequences of a missed open fracture, health care providers performing the original evaluation should be on high alert when skin defects are noted in the same extremity as a known or even suspected fracture, even if the site of the skin laceration does not appear close to the fracture site. As this case highlights, it is even possible for the fracture to create a zone of soft tissue injury that causes a skin defect in another portion of the limb.

References

1. Fraisse B, Marleix S, Lucas G, *et al.* Open fractures of the limbs in children and adolescents. *Orthop Traumatol Surg Res* 2024;110(1S):103771.

2. Sharma A, Gupta V, Shashikant K. Optimizing Management of Open Fractures in Children. *Indian J Orthop* 2018;52(5):470-480.

3. Qiu X, Deng H, Zhao Z, *et al.* Upper limb pediatric fractures in 22 tertiary children's hospitals, China: a multicenter epidemiological investigation and economic factor analysis of 32,832 hospitalized children. *J Orthop Surg Res* 2022;17(1):300.

4. Pan T, Widner MR, Chau MM, *et al.* Open Supracondylar Humerus Fractures in Children. *Cureus* 2021;13(3):e13903.

5. Annabell L, Shore BJ, Hedequist DJ, *et al.* Evaluation and Management of Pediatric Humeral Shaft Fractures. *Journal of the American Academy of Orthopaedic Surgeons* 2023; 31(6):265-273.

Management of Osteonecrosis of the Humeral Head in the Pediatric Population: A Systematic Review

Vineet Desai, BS[1,2]
Akbar N. Syed, MD[1]
Morgan Batley, BA[1]
Lawrence Wells, MD[1]
Brendan A. Williams, MD[1]

[1]Department of Orthopaedics, The Children's Hospital of Philadelphia

[2]Harvard Medical School

Corresponding author:
Brendan A. Williams, MD
Department of Orthopaedics
The Children's Hospital of Philadelphia
3401 Civic Center Blvd.
Philadelphia, PA 19104
Email: williamsba@chop.edu
Phone: (215)-590-152

Introduction

Osteonecrosis can present in the context of a variety of medical and iatrogenic abnormalities: trauma, hemoglobinopathies, and long term corticosteroid usage.[1-3] Although osteonecrosis of the proximal humerus is the second most common site after the femoral head, it is poorly understood and difficult to diagnose.[4, 5] Franceschi et al. (2017) conducted a systematic review of surgical management of osteonecrosis of the humeral head in the adult population, and found that whereas CD is effective for low-grade osteonecrosis, arthroplasty should be considered for high-grade osteonecrosis.[4] However, literature remains limited regarding the characteristics and management of humeral head AVN in younger populations.[4] The purpose of this study was to perform a systematic review to improve our understanding of the existing evidence regarding the prevalence and characteristics of proximal humeral AVN in young patients, the treatment modalities utilized, and the outcomes of these treatments in this population.

Methods

We searched PubMed, OVID Embase, and Scopus databases with terms "osteonecrosis", "pediatric", and "proximal humerus" on January 10, 2024. Two hundred and eighteen studies were screened, and 74 studies were evaluated for eligibility (Figure 1).

Studies that reported on the prevalence and/or management of pediatric humeral head osteonecrosis were included. The systematic review was conducted according to the Preferred Reporting Items for Systematic Review and Meta-Analyses (PRISMA) guidelines. Clinical characteristics (etiology of osteonecrosis, imaging, grade of osteonecrosis, symptoms) and management characteristics (conservative vs. operative management, reported interventions, outcome of intervention) were collected as well. Prevalence was calculated as the total number of patients/shoulders with osteonecrosis of the humeral head divided by the total number of patients/shoulders at risk. Two independent reviewers assessed the risk of bias within each study using the Cochrane Risk of Bias Assessment Tool: for Non-Randomized Studies of Interventions for cohort and case control studies as well as the Joanna Briggs Institute (JBI) critical appraisal tool for case series.[6, 7]

Results

After initial screening and eligibility review, 12 studies remained eligible for inclusion in this systematic review. These studies included three prospective case series,[8-10] four retrospective case series,[11-14] one retrospective case-control study,[15] one retrospective cohort study,[16] and three case reports[17-19] (Table 1).

Prevalence and Clinical Characteristics

Across eight studies that presented data for the number of patients with humeral head osteonecrosis within a greater at-risk population, there were 106 shoulders (77 patients) that developed osteonecrosis of the humeral head, and an overall at-risk population of 5,226 shoulders (3,608 patients). Thus, we calculated the overall prevalence of osteonecrosis of the humeral head within an at-risk pediatric population to be 2.0%.

Conservative Management

Six studies reported on conservative management. For example, Kaste et al. used the National Cancer Institute's Common Terminology Criteria for Adverse Events (CTCAE) scoring system to show an improvement in the impact of osteonecrosis on activities of daily living (ADL) (2.61 to 1.76), pain (2.69 to 1.23), and ROM (2.15 to 1.69) after intra-articular steroid injection11 (Table 2a).

Surgical Management

Three studies reported on surgical management. For example, Kaste et al. found that among 12 shoulders with osteonecrosis, nine experienced resolution after core decompression11. Additionally, the mean CTCAE scores improved for pain and impact on ADL (2.91 to 1.66), and slightly

worsened for ROM (2.00 to 2.08) after undergoing core decompression11. Mean CTCAE scores improved for impact on ADL (2.75 to 1.75), pain (2.87 to 0.85), and ROM (2.37 to 1.87) after undergoing resurfacing hemiarthroplasty[11] (Table 2b).

Risk of Bias

Overall, the one retrospective cohort study and one retrospective case-control study had a low risk of bias. The four retrospective and three prospective case series had good methodological quality.

Discussion

Literature regarding the most effective management strategies for osteonecrosis of the humeral head in the pediatric population is limited.[4] The goal of this systematic review was to summarize published studies and current evidence on the prevalence and clinical characteristics, conservative management, and surgical management of osteonecrosis of the humeral head within the pediatric population. The overall prevalence of osteonecrosis of the humeral head across eight studies was about 2%. Intra-articular steroid injections, physical therapy, and activity modification are effective conservative management strategies. Additionally, core decompression and hemiarthroplasty are surgical treatment options.

Few studies have published on the prevalence of humeral head osteonecrosis, likely due to both the rare nature of the condition and its often-asymptomatic presentation in comparison to osteonecrosis in greater weight-bearing joints like the hip. Chung et al. found in a population of forty sickle cell patients that the prevalence of humeral head osteonecrosis was 3.8%, which was slightly higher than the current study's prevalence of 2.0% across both chemotherapy and sickle cell etiologies20. Regarding management of humeral head osteonecrosis, Franceschi et al. conducted a systematic review comparing core decompression, hemiarthroplasty, and TSA in adults with humeral head osteonecrosis, and found that while core decompression is effective for low grade osteonecrosis, arthroplasty should be utilized for high grade osteonecrosis.[4] However, comparing the efficacy of both conservative and surgical interventions for pediatric humeral head osteonecrosis is challenging given the limited existing prospective or comparative studies.

There are several limitations to this study. First, we were restricted by the available evidence on this topic. Given the rarity of humeral head osteonecrosis, especially in the pediatric population, many of the included studies were limited in sample size and did not include rigorous and robust analyses for the included interventions. Second, it is important to note that when comparing the results of the included studies, the patients were not standardized in demographic characteristics, osteonecrosis grade, and treatment protocols. Thus, the data provided is susceptible to selection, indication, and surveillance bias. Third, some of the studies included were case reports or published before the year 2000. While this may limit their quality or relevance, given the rareness of this condition, they were included in the screening process.

Conclusions

The prevalence of osteonecrosis of the humeral head is low even among at-risk populations with associated medical conditions. A variety of conservative and surgical treatment options have been described but no comparative evaluations of these modalities has been conducted.

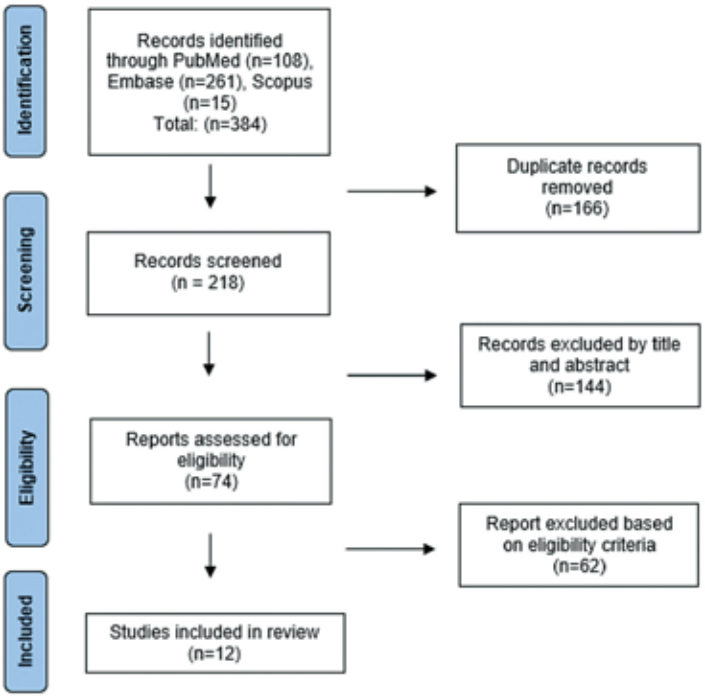

Figure 1. Study selection flowchart using PRISMA guidelines.

Table 1: Characteristics of Evaluated Studies included in Systematic Review (12)

Study	Level of Evidence and Study Type		Year	Study Period	Study Population	No. of patients		Median Age in years	Mean Length of Follow-Up in years
					Total (No. of shoulders)	Humeral Head Osteonecrosis (No. of shoulders)		(Range)	(Range)
Milner et al.*	IV	Prospective Case Series	1993	1979-1981	SCD	1,019 (2,038)	19 (NR)	NR (5-14)	5.6 (NR)
Inaba et al.	IV	Prospective Case Series	2020	2012-2017	ALL/L	15 (30)	8 (15)	14 (9-17)	NR
Kaste et al.	IV	Retrospective Case Series	2019	1996-2014	ALL/NHL	1,478 (2,956)	33 (62)	14.2 (4.3-19)	6.4 (0-12.7)
Mesleh Shayeb et al.	III	Retrospective Case-Control	2018	1998-2014	SCD	612 (1,224)	6 (8)	NR (6-18)	NR
Littooij, et al.	IV	Prospective Case Series	2017	2012-2015	HL	24 (48)	NR (2)	15.1 (10.1-17.9)	1.0 (0.48–3.6)
Heneghan et al.	III	Retrospective Cohort	2016	2004-2012	ALL	10,729 (21,458)	NR	7.04 (2.02 – 21.2)	NR
Kuhlen et al.	IV	Retrospective Case Series	2014	2003-2009	ALL	124 (248)	5 (8)	12.6 (2.4-19.9)	2.3 (0.1-6.2)
Miettunen et al.	IV	Retrospective Case Series	2012	2006-2008	ALL	32 (64)	5 (9)	5.4 (4.8–11.9)	NR
Riccio et al.	IV	Retrospective Case Series	2016	1982-2003	ALL	328 (656)	1 (2)	Mean: 7.2 SD: 0.1-14.3	NR
Wong et al.	IV	Case report	2022	-	SCD	1 (2)	1 (1)	12	0.2
Solarino et al.	IV	Case report	2008	-	ALL	1 (2)	1 (2)	12	5.3
Martin et al.	IV	Case report	1997	-	Salter-Harris II fracture	1 (2)	1 (1)	14	1
Total (of reported)**						3,608 (5,226)	77 (106)		

*Only information regarding patient group 5-14y included. **NR:** Not reported; **SCD:** Sickle Cell Disease; **ALL:** Acute Lymphoblastic Leukemia; **ALL/L:** Acute Lymphoblastic Leukemia/Lymphoma; **NHL:** Non-Hodgkin's Lymphoma; **HL:** Hodgkin's Lymphoma

**Does not include data from case reports or Heneghan et al.

Table 2: (A) Conservative Management of humeral head osteonecrosis in evaluated studies

Study	Shoulders	Reported Interventions	Outcome
Inaba et al.	NR	Reduction or cessation of chemotherapy	>30% epiphyseal involvement: 3/9 shoulder regressed <30% epiphyseal involvement: 1 shoulder resolved
Kaste et al.	13	Intra-articular steroid injections	7/13 shoulders resolved; Mean CTCAE score for ROM improved from 2.15 to 1.69; Mean CTCA score for pain improved from 2.69 to 1.23
	NR	Physical therapy; Anti-inflammatory agents	NR
Kuhlen et al.	8	Physiotherapy; Activity modification; Anti-inflammatory agents; bisphosphonates; Iloprost	NR
Riccio et al.	2	Activity modification; Physical therapy	Good ROM; residual humeral head deformity
Wong et al.	1	Physical therapy; Psychotherapy; Acupuncture; Intraarticular steroid injections; pain medication (pregabalin, meloxicam, methadone; hydrocodone as needed)	No improvement in pain
		Intra-articular Hyaluronic Acid injections	50% reduction in pain (6/10 to 0/10 at rest, 10/10 to 5/10 with activity); improvement in function
Martin et al.	1	Activity Modification	Asymptomatic

NR: Not reported; CTCAE: National Cancer Institute's Common Terminology Criteria for Adverse Events; ROM: range of motion

Table 2: (B) Surgical Management of humeral head osteonecrosis in evaluated studies

Study	Shoulders	Procedure	Outcome
Inaba et al.	3	Core Decompression: 2	No shoulders resolved
		Bone Resurfacing: 1	NR
Kaste et al.	20	Core Decompression: 12	9/12 shoulders resolved; Mean CTCAE score for ROM worsened from 2.00 to 2.08; Mean CTCAE score for pain improved from 2.75 to 1.00
		Hemiarthroplasty (Resurfacing): 8	Mean CTCAE score for ROM improved from 2.37 to 1.87; Mean CTCAE score for pain improved from 2.87 to 0.75
Heneghan et al.	8	NR	NR
		Total Shoulder Arthroplasty: 1	NR

NR: Not reported; CTCAE: National Cancer Institute's Common Terminology Criteria for Adverse Events; ROM: range of motion

References

1. Assouline-Dayan Y, Chang C, Greenspan A, *et al.* Pathogenesis and natural history of osteonecrosis. *Semin Arthritis Rheum*. 2002;32(2):94-124.

2. Chang CC, Greenspan A, Gershwin ME. Osteonecrosis: current perspectives on pathogenesis and treatment. *Semin Arthritis Rheum*. 1993;23(1):47-69.

3. Shah KN, Racine J, Jones LC, *et al.* Pathophysiology and risk factors for osteonecrosis. *Curr Rev Musculoskelet Med*. 2015;8(3):201-9.

4. Franceschi F, Franceschetti E, Paciotti M, *et al.* Surgical management of osteonecrosis of the humeral head: a systematic review. Knee surgery, sports traumatology, arthroscopy: *official journal of the ESSKA*. 2017;25(10):3270-8.

5. Hernigou P, Hernigou J, Scarlat M. Shoulder Osteonecrosis: Pathogenesis, Causes, Clinical Evaluation, Imaging, and Classification. *Orthopaedic Surgery*. 2020;12(5):1340-9.

6. Sterne JAC, Higgins JPT, Reeves BC. On behalf of the development group for ACROBAT-NRSI. A Cochrane risk of bias assessment tool: for non-randomized studies of interventions (ACROBAT-NRSI), Version 1.0.0, 24 September 2014.

7. Munn Z, Barker TH, Moola S, *et al.* Methodological quality of case series studies: an introduction to the JBI critical appraisal tool. *JBI Evid Synth*. 2020;18(10):2127-33.

8. Inaba H, Varechtchouk O, Neel MD, *et al.* Whole-joint magnetic resonance imaging to assess osteonecrosis in pediatric patients with acute lymphoblastic lymphoma. *Pediatric Blood & Cancer*. 2020;67(8):e28336.

9. Littooij AS, Kwee TC, Enríquez G, *et al.* Whole-body MRI reveals high incidence of osteonecrosis in children treated for Hodgkin lymphoma. *British Journal of Haematology*. 2017;176(4):637-42.

10. Milner PF, Kraus AP, Sebes JI, *et al.* Osteonecrosis of the humeral head in sickle cell disease. *Clinical Orthopaedics and Related Research*. 1993(289):136-43.

11. Kaste S, DeFeo B, Neel M, *et al.* Osteonecrosis of the Shoulders in Pediatric Patients Treated for Leukemia or Lymphoma: Single-Institutional Experience. *Journal of pediatric orthopedics*. 2019;39(2):104-10.

12. Kuhlen M, Moldovan A, Krull K, *et al.* Osteonecrosis in paediatric patients with acute lymphoblastic leukaemia treated on Co-ALL-07-03 trial: a single centre analysis. *Klinische Padiatrie*. 2014;226(3):154-60.

13. Miettunen PM, Lafay-Cousin L, Guilcher GMT, *et al.* Widespread Osteonecrosis in Children With Leukemia Revealed by Whole-body MRI. Clinical Orthopaedics and Related Research. 2012;470(12):3587-95.

14. Riccio I, Pota E, Marcarelli M, *et al.* Osteonecrosis as a complication in pediatric patients with acute lymphoblastic leukemia. La Pediatria Medica E Chirurgica: *Medical and Surgical Pediatrics*. 2016;38(3):118.

15. Mesleh Shayeb A, Smeltzer MP, Kaste SC, *et al.* Vaso-occlusive crisis as a predictor of symptomatic avascular necrosis in children with sickle cell disease. *Pediatric Blood & Cancer*. 2018;65(12):e27435.

16. Heneghan MB, Rheingold SR, Li Y, *et al.* Treatment of Osteonecrosis in Children and Adolescents With Acute Lymphoblastic Leukemia. *Clinical Lymphoma, Myeloma & Leukemia*. 2016;16(4):223-9.e2.

17. Martin RP, Parsons DL. Avascular necrosis of the proximal humeral epiphysis after physeal fracture. A case report. *The Journal of Bone and Joint Surgery American Volume*. 1997;79(5):760-2.

18. Solarino G, Scialpi L, Bruno M, *et al.* On a case of multifocal osteonecrosis in a patient suffering from acute lymphoblastic leukemia. *La Chirurgia Degli Organi Di Movimento*. 2008;92(2):119-22.

19. Wong JY-A, Le S, Lo C, *et al.* Hyaluronic acid injections for treatment of pediatric sickle cell avascular necrosis of the humeral head. *Regional Anesthesia and Pain Medicine*. 2022;47(2):136-8.

20. Chung SM, Ralston EL. Necrosis of the humeral head associated with sickle cell anemia and its genetic variants. *Clin Orthop Relat Res*. 1971;80:105-17.

Comparison between juvenile idiopathic arthritis and proliferative synovitis in children: Utility of contrast-enhanced MRI

Andressa Guariento MD, PhD[1]
Vandan Patel, BS[1,2]
David M. Biko, MD[1,3]
Alyssa Sze, BA[1]
Alexander Arkader, MD[2,3]
Theodore J. Ganley, MD[2,3]
Jie C. Nguyen, MD MS[1,3]

[1]Department of Radiology, Section of Musculoskeletal Imaging, Children's Hospital of Philadelphia

[2]Department of Orthopedic Surgery, Children's Hospital of Philadelphia

[3]Perelman School of Medicine, University of Pennsylvania

Introduction

Knee complaints are common among children, which can result from acute traumatic injury or more insidious causes. The latter includes non-infectious synovial diseases from inflammatory (i.e.: juvenile idiopathic arthritis, JIA) and proliferative (i.e.: intra-articular tenosynovial giant cell tumor, TGCT; and primary synovial chondromatosis, PSC) causes, which are often under-recognized, leading to diagnostic delay and additional interventions.[1-3] Although the diagnosis of JIA is typically established without advanced imaging, in some ambiguous cases, magnetic resonance imaging (MRI) is the recommended tool to complement the clinical assessment, exclude alternative diagnoses, and if necessary, guide synovial biopsy.[4-5]

Currently, the existing published literature lacks a systematic approach to characterize the synovium in children, with most existing studies predominantly including adult patients with signs not pertinent to children.[1-3,6-7] Thus, the purpose of our study was to characterize and compare patterns of synovitis on contrast-enhanced knee MRI between children with JIA and proliferative synovitis.

Methods

Following institutional review board approval, a retrospective chart and imaging review of pediatric patients with JIA, TGCT, and PSC was conducted. For patients with multiple examinations, only one contrast-enhanced MRI examination was included, either the first study during clinically active disease (for JIA) or the study that preceded surgical intervention (for TGCT and PSC). MRI examinations that lacked both axial and sagittal fluid-sensitive images (short tau inversion recovery, STIR, T2-weighted, or intermediate-weighted fat-suppressed pulse sequences) or contained non-diagnostic and motion-degraded images were excluded. Demographics, symptomology, surgical and pathological notes were recorded. All MRI were retrospectively reviewed by two board-certified radiologists, blinded to the patients' history and diagnosis, and after randomization. Additionally, the same radiologists independently measured semi-quantitative features including thickness of the synovium at 11 predetermined intra-articular sub-regions, according to previously published methodology.[8-9] Descriptive statistics were used to summarize the study variables.

Results

Twenty-three children (13 girls, 10 boys, mean age, 12.5±2.9 years) included 13 with JIA and 10 with histopathology-confirmed proliferative synovitis. Those with JIA were more likely to be girls ($p=0.04$), report morning stiffness ($p=0.02$), and have longer follow-ups ($p<0.001$) when compared to children with proliferative synovitis. Cohort characteristics are further summarized in Table 1. MRI findings of synovial susceptibility ($p=0.01$) and more severe Hoffa-synovitis ($p=0.003$) were more prevalent with proliferative synovitis whereas concomitant findings of bony changes ($p=0.045$) and larger popliteal nodes ($p=0.01$) were more prevalent with JIA. Additional MRI features noted are presented in Table 2. Finally, JIA had thinner synovium when compared to proliferative synovitis overall ($p<0.001$) and within most subregions (p-range: <0.001-0.03), except for lateral parapatellar, anterior to ACL, and posterior to PCL subregions (Table 3).

Corresponding author:
Jie C. Nguyen, MD, MS
3401 Civic Center Blvd.
Philadelphia, PA 19104
nguyenj6@chop.edu

Table 1. Demographics of children with proliferative synovitis and JIA and contrast-enhanced knee MRI

Characteristics	TGCT (n=7)	PSC (n=3)	p^d	Combined proliferative synovitis (n=10)	All JIA-subtypes[b] (n=13)	p^d
Age (years)	13.1±3.0	12.3±1.2	0.55	12.9±2.5	12.2±3.2	0.58
Sex (girls: boys)	3: 4	0: 3	**0.04**	3: 7	10: 3	**0.04**
Laterality (R: L)	4: 3	3: 0	0.48	7: 3	4: 9	0.10
BMI class (n=21)[a]			0.46			1
Underweight & normal	5 (83)	1 (33)		6 (67)	7 (58)	
Overweight & obese	1 (17)	2 (67)		3 (33)	5 (42)	
Symptoms:						0.25
Incidental	1 (14.5)	-		1 (10)	-	
Swelling	2 (28.5)	-		2 (20)	-	
Swelling & pain (S&P)	2 (28.5)	-		2 (20)	5 (38.5)	
S&P + Stiffness	-	-		-	6 (46)	
S&P + Biomechanical[c]	2 (28.5)	3 (100)		5 (50)	2 (15.5)	
Duration of symptoms (days):	13 (10-13.5)	9 (5-33)	0.70	12 (6-14)	31 (8-67)	0.18
Duration of follow-up (months):	11 (7-19)	16 (12-22)	0.83	14 (8-19)	54 (35-73)	<**0.001**

Note – With the exception of age (mean ± standard deviation), values are either number of patients (percentage) or median (IQR).
BMI = body mass index; IQR = interquartile range; JIA = juvenile idiopathic arthritis; MRI = magnetic resonance imaging; PSC = primary synovial chondromatosis; TGCT = tenosynovial giant cell tumor;
a BMI was not available for 2 children (1 JIA, 1 TGCT).
b JIA subtypes included 5 with oligoarticular, 3 children with enthesitis-related, 2 with polyarticular, rheumatoid-factor negative, 2 with undifferentiated, and 1 with psoriatic arthritis.
c Biomechanical symptoms include 2 children with limping (1 PSC, 1 JIA), 2 with buckling (1 TGCT, 1 PSC), 2 with locking (1 TGCT, 1 JIA), and 1 with mass (PSC).
d Student's t, Mann-Whitney U, or Fisher's exact tests were used.

Table 2. Qualitative assessment of MRI findings between children with proliferative synovitis and JIA

MRI findings	All synovitis (n=23)	Proliferative synovitis (n=10)	JIA (n=13)	p^c	Agreement (%)
Pre-contrast synovium					
GRE susceptibility (n=17)	7/17 (41)	6/7 (86)	1/10 (10)	**0.01**	83
Effusion-synovitis				0.18	91
Simple: Complex	6: 17	1: 9	5: 8		
Hoffa's synovitis				**0.006**	65
None-mild: Moderate-severe	11: 12	1: 9	10: 3		
Popliteus hiatus distention	17 (74)	9 (90)	8 (62)	0.18	100
Contrast-enhanced synovium					
Effusion size				0.41	74
Absent-small: Medium-large	12: 11	4: 6	8: 5		
Synovial enhancement				1	74
Linear-lamellar pattern	18 (78)	8 (80)	10(77)		
Nodular-frond-like pattern	5 (26)	2 (20)	3 (33)		
Distribution				0.11	74
Mostly effusion	7 (30.4)	5 (50)	2 (15)		
Mostly synovium	6 (26.1)	3 (30)	3 (23)		
Relatively equal	10 (43.5)	2 (20)	8 (35)		

Table 2. (Continued)

MRI findings	All synovitis (n=23)	Proliferative synovitis (n=10)	JIA (n=13)	p[c]	Agreement (%)
Other findings					
Extra-capsular edema	7 (30)	4 (40)	3 (23)	0.65	74
Juxta-capsular outpouching [a]	6 (26)	3 (30)	3 (23)	0.87	52
Osseous changes [b]	5 (22)	0	5 (38)	**0.045**	91
Popliteal lymph nodes	18 (78)	6 (60)		0.13	83
Number	-	1.0±0.6	12 (92) 2.0±0.9	0.43	
Short-axis dimension (mm)	-	2.8±1.3	5.1±2.5	**0.01**	
Chondromalacia	1 (4.3)	1 (10)	0	0.44	95

Note – Values are either mean± standard deviation or count (percentage).
GRE = gradient-recalled echo; JIA = juvenile idiopathic arthritis; MRI = magnetic resonance imaging; PSC = primary synovial chondromatosis; TGCT = tenosynovial giant cell tumor;
[a] Juxta-capsular outpouching included popliteal cyst (1 PSC and 2 JIA), tibiofibular joint (1 TGCT and 1 JIA), and around gastrocnemius (1 TGCT).
[b] All osseous changes involved bone marrow edema. No erosion, destruction or remodeling was observed.
[c] Fisher's exact or Mann-Whitney U tests were used.

Table 3. Semi-quantitative assessment of synovial disease using contrast-enhanced knee MRI

Synovial thickness	All synovitis (n=23)	Proliferative synovitis (n=10)	JIA (n=13)	pb
Overall thickness (mm)	2.2±0.9	2.6±0.6	1.9±1.0	**<0.001**
Anterior subregions:				
Suprapatellar	2.3±1.3	2.8±1.5	2.0±1.0	**0.002**
Infrapatellar	2.0±1.0	2.3±1.0	1.8±1.0	**0.02**
Medial parapatellar	1.9±0.9	2.3±0.8	1.7±0.9	**0.02**
Lateral parapatellar	1.8±1.0	2.1±0.9	1.6±1.1	0.12
Intercondylar subregions:				
Intercondylar	2.0±1.1	2.2±0.8	1.8±1.2	**0.03**
Anterior to ACL	1.7±1.6	1.8±1.7	1.6±1.6	0.74
Posterior to PCL	1.9±1.1	2.4±1.2	1.5±0.7	0.06
Posterior subregions:				
Medial perimeniscal	2.8±1.9	3.4±1.9	2.2±1.8	**0.003**
Lateral perimeniscal	3.4±2.2	3.6±1.6	3.3±2.6	**<0.001**
Others, if present [a]				
Popliteal cyst (n=3)	1.5±0.4	1.5±0	1.5±0.5	0.80
Around intra-articular body (n=4)	1.7±1.0	1.7±1.0	-	-
Synovial hypertrophy score				0.17
No synovitis (0-4)	9 (39)	2 (20)	7 (54)	
Mild synovitis (5-8)	8 (35)	4 (40)	4 (30)	
Moderate synovitis (9-12)	5 (22)	4 (40)	1 (8)	
Severe synovitis (>12)	1 (4)	0 (-)	1 (8)	

Note – Values are either mean± standard deviation or count (percentage).
ACL = anterior cruciate ligament; JIA = juvenile idiopathic arthritis; MRI = magnetic resonance imaging; PCL = posterior cruciate ligament; PSC = primary synovial chondromatosis; TGCT = tenosynovial giant cell tumor;
[a] Popliteal cysts were present in 2 children with JIA and 1 with PSC; intra-articular body was present in 2 children with PSC and 2 with TCGT.
[b] Student's t or Mann-Whitney U tests were used.

Discussion:

We investigated the synovial patterns on contrast-enhanced knee MRI examinations and found that the synovium is thinner with JIA than proliferative synovitis. Additionally, bony changes and larger popliteal lymph nodes are more common among children with JIA whereas synovial susceptibility and more severe Hoffa-synovitis are common with proliferative synovitis.

The synovium lines the deep layer of the articular capsule and is responsible for the production of joint fluid, which lubricates and facilitates low-friction loading and wear-resistant movement.[6,10] Synovial dysfunction, characterized by synovial thickening and effusion, is recognized as a precursor to premature and accelerated osteoarthritis, leading to progressive joint destruction.[10-11] Normal synovium is barely perceivable on MRI unless it is thickened;[12] synovial hypertrophy and certain MRI findings can reflect differences in the underlying pathophysiology. On histopathology, the diseased synovium in patients with TGCT contains giant cells and histiocytes that are laden with hemosiderin, which is most conspicuous on GRE images as susceptibility artifact.[7,13] However, this finding is neither sensitive or specific for TGCT and can be observed in inflammatory synovitis that contain blood products, post-traumatic hemarthrosis, and hemophilic arthropathy.[14-16] The latter may explain the single case of JIA with synovial susceptibility observed within our study.

In our study, children with JIA had thinner synovium when compared to those with proliferative synovitis. These findings emphasize the importance of properly distinguishing between joint effusion and synovium, which is only possible on contrast-enhanced images because fluid-sensitive images can over-estimate the total amount of intraarticular fluid.[4,8,17] Currently, the existing literature on the use of quantitative methods to assess synovial hypertrophy has predominantly focused on adults with osteoarthritis8-9 and children with JIA.[18-21] Our study utilized the former 11 subregion method,[9] which has not been previously applied to pediatric patients[18-21] or compared values between patients with JIA and proliferative synovitis, which is critically important as clinical distinction can be occasionally challenging. In our cohort, 53% of JIA patients had a normal synovial hypertrophy score, which is in concordance with Hemke and colleagues, who found that minimal and moderately active JIA patients had synovial hypertrophy in less than 50% of cases.19 In contrast, only 14% of children with proliferative synovitis had a normal score.

Bony changes and larger popliteal nodes were significantly more common among children with JIA than proliferative synovitis. While osteitis and pressure erosions can occur in patients with proliferative synovitis, these preferentially involve smaller (i.e.: ankle) and low capacity joints (i.e.: hip and shoulder),[1,22-26] which do not apply to the relatively capacious knee joint. In contrast, bony changes in JIA associate with disease status and reflect local inflammation. In skeletally-immature younger children with an abundance of cartilage, marginal erosions are uncommon and regional hyperemia and epiphyseal osteitis increase the risk for future growth disturbance and deformity.[27] Popliteal lymphadenopathy, preferential disease involvement among girls, and increase incidence of morning stiffness observed in our study group are well-established features of JIA.[12,19-20] Hoffa-synovitis were more severe with proliferative synovitis than JIA, which has not been previously reported in children, but the precise

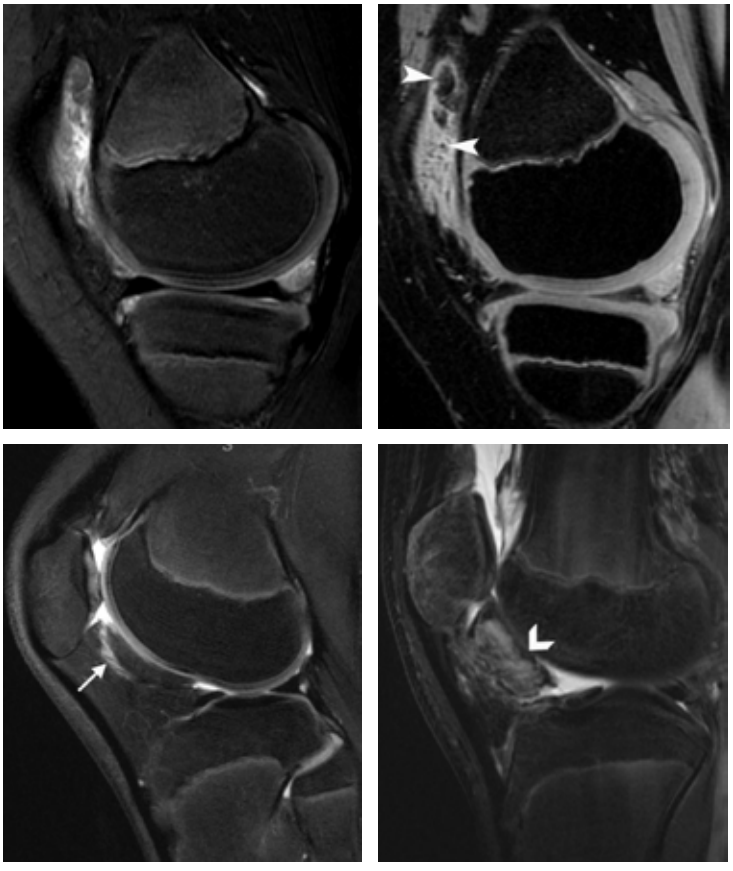

Figure 1. Synovial susceptibility and Hoffa synovitis. **(A)** Sagittal T2-weighted fat-suppressed and **(B)** gradient recalled echo (GRE) images from a 10-year-old girl show synovial susceptibility (arrowheads), an uncommon finding in JIA; **(C)** Sagittal T2-weighted fat-suppressed images from an 11-year-old girl with JIA and mild Hoffa synovitis, localized at the synovial cleft (arrow) and **(D)** from a 17-year-old boy with tenosynovial giant cell tumor (TGCT) and severe Hoffa synovitis with surface hemosiderin staining (chevron).

pathophysiology is unclear (Figure 1). Among adults with osteoarthritis, Hoffa-synovitis has been postulated to contribute to immune regulation and regional inflammation, directly impacting disease progression within the knee joint.[28-30]

Due to its retrospective nature, this study had inherent limitations. Diagnosis of JIA clinically often not requiring contrast-enhanced knee MRI examinations or tissue biopsy, thus, reducing our sample size. Second, inherent heterogeneity of the patient population may attenuate the comparison between groups but better reflects routine clinical practice and makes our results more generalizable. Finally, although the readers were blinded the clinical diagnosis, they were not blind to the findings on imaging findings, which may have biased their assessment.

Conclusion

In our study group of children with non-infectious synovitis, MRI findings of synovial susceptibility, more severe Hoffa-synovitis, and thicker synovium were significantly more prevalent with proliferative synovitis than JIA.

References

1. Kramer J, Recht M, Deely DM, *et al.* MR appearance of idiopathic synovial osteochondromatosis. *J Comput Assist Tomogr* 1993; 17:772–776.

2. Wittkop B, Davies AM, and Mangham DC. Primary synovial chondromatosis and synovial chondrosarcoma: a pictorial review. *Eur Radiol* 2002; 12:2112–2119.

3. Nadim B and Samet JD. Pediatric solid intra-articular masses of the knee: prevalence, imaging features and etiologies. *Pediatr Radiol* 2021; 51:1412–1420.

4. Malattia C, Tolend M, Mazzoni M, *et al.* Current status of MR imaging of juvenile idiopathic arthritis. *Best Pract Res Clin Rheumatol* 2020; 34:101629.

5. Murphey MD, Rhee JH, Lewis RB, *et al.* Pigmented villonodular synovitis: radiologic-pathologic correlation. *Radiographics* 2008; 28:1493–1518.

6. Wechalekar MD and Smith MD. Utility of arthroscopic guided synovial biopsy in understanding synovial tissue pathology in health and disease states. *World J Orthop* 2014; 5:566–573.

7. Eckhardt BP and Hernandez RJ. Pigmented villonodular synovitis: MR imaging in pediatric patients. *Pediatr Radiol* 2004; 34:943–947.

8. Roemer FW, Kassim Javaid M, Guermazi A, *et al.* Anatomical distribution of synovitis in knee osteoarthritis and its association with joint effusion assessed on non-enhanced and contrast-enhanced MRI. *Osteoarthr Cartil* 2010; 18:1269–1274.

9. Guermazi A, Roemer FW, Hayashi D, *et al.* Assessment of synovitis with contrast-enhanced MRI using a whole-joint semiquantitative scoring system in people with, or at high risk of, knee osteoarthritis: the MOST study. *Ann Rheum Dis* 2011; 70:805–811.

10. Hui AY, McCarty WJ, Masuda K, *et al.* A systems biology approach to synovial joint lubrication in health, injury, and disease. *Wiley Interdiscip Rev Syst Biol Med* 2012; 4:15–37.

11. Atukorala I, Kwoh CK, Guermazi A, *et al,* Synovitis in knee osteoarthritis: a precursor of disease? *Ann Rheum Dis* 2016; 75:390–395.

12. Frick MA, Wenger DE, and Adkins M MR imaging of synovial disorders of the knee: an update. *Radiol Clin North Am* 2007; 45:1017–31.

13. Kan JH, Hernanz-Schulman M, Damon BM, *et al.* MRI features of three paediatric intra-articular synovial lesions: a comparative study. *Clin Radiol* 2008; 63:805–812.

14. Hughes TH, Sartoris DJ, Schweitzer ME, *et al.* Pigmented villonodular synovitis: MRI characteristics. *Skeletal Radiol* 1995; 24:7–12.

15. Steinbach LS, Neumann CH, Stoller DW, *et al.* MRI of the knee in diffuse pigmented villonodular synovitis. *Clin Imaging* 1989; 13:305–316.

16. Cheng XG, You YH, Liu W, *et al.* MRI features of pigmented villonodular synovitis (PVNS). Clin Rheumatol 2004; 23:31–34.

17. Crema MD, Roemer FW, Li L, *et al.* Comparison between semiquantitative and quantitative methods for the assessment of knee synovitis in osteoarthritis using non-enhanced and gadolinium-enhanced MRI. *Osteoarthr Cartil* 2017; 25:267–271.

18. Hemke R, van Rossum MAJ, van Veenendaal M, *et al.* Reliability and responsiveness of the Juvenile Arthritis MRI Scoring (JAMRIS) system for the knee. *Eur Radiol* 2013; 23:1075–1083.

19. Hemke R, Maas M, van Veenendaal M, *et al.* Contrast-enhanced MRI compared with the physical examination in the evaluation of disease activity in juvenile idiopathic arthritis. *Eur Radiol* 2014; 24:327–334

20. Hemke R, Kuijpers TW, Nusman CM, *et al.* Contrast-enhanced MRI features in the early diagnosis of Juvenile Idiopathic Arthritis. *Eur Radiol* 2015; 25:3222–3229.

21. van Gulik EC, Hemke R, Welsink-Karssies MM, *et al.* Normal MRI findings of the knee in patients with clinically active juvenile idiopathic arthritis. *Eur J Radiol* 2018; 102:36–40.

22. Sviland L and Malcolm AJ. Synovial chondromatosis presenting as painless soft tissue mass--a report of 19 cases. *Histopathology* 1995; 27:275–279.

23. Norman A and Steiner GC. Bone erosion in synovial chondromatosis. Radiology 1986; 161:749–752

24. Nguyen JC, Biko DM, Nguyen MK, *et al.* Magnetic resonance imaging features of intra-articular tenosynovial giant cell tumor in children. *Pediatr Radiol* 2021; 51:441–449.

25. Cheng XG, You YH, Liu W, *et al.* MRI features of pigmented villonodular synovitis (PVNS). *Clin Rheumatol* 2004; 23:31–34.

26. Hao D-P, Zhang J-Z, Xu W-J, *et al.* Pigmented villonodular synovitis of the ankle: radiologic characteristics. *J Am Podiatr Med Assoc* 2011; 101:252–258.

27. Gylys-Morin VM, Graham TB, Blebea JS, *et al.* Knee in early juvenile rheumatoid arthritis: MR imaging findings. *Radiology* 2001; 220:696–706.

28. Yun SJ, Lim Y, Jin W, *et al.* Validity of Radiograph-Based Infrapatellar Fat Pad Opacity Grading for Assessing Knee Synovitis: Correlation With Contrast-Enhanced MRI. *Am J Roentgenol* 2017; 209:1321–1330.

29. Ballegaard C, Riis RGC, Bliddal H, *et al.* Knee pain and inflammation in the infrapatellar fat pad estimated by conventional and dynamic contrast-enhanced magnetic resonance imaging in obese patients with osteoarthritis: a cross-sectional study. *Osteoarthr Cartil* 2014; 22:933–940.

30. Clockaerts S, Bastiaansen-Jenniskens YM, Runhaar J, *et al.* The infrapatellar fat pad should be considered as an active osteoarthritic joint tissue: a narrative review. *Osteoarthr Cartil* 2010; 18:876–882.

Systematic Review of the Impact of Pelvic Obliquity in Patients with Neuromuscular Scoliosis

Joshua T. Bram, MD[1]
Christopher J. DeFrancesco, MD[2]
Tiffany C. Liu, MD[1]
Waleed Al-Mahdi, MD[2]
Keith D. Baldwin, MD, MPH, MSPT[2]
David A. Spiegel, MD[2]

[1]Department of Orthopaedic Surgery, Hospital for Special Surgery, New York, New York

[2]Division of Orthopaedics, Children's Hospital of Philadelphia, Philadelphia, PA

Corresponding author:
Apurva S. Shah, MD MBA
Assistant Professor of Orthopaedic Surgery
The Children's Hospital of Philadelphia
Division of Orthopaedics
3500 Civic Center Boulevard
4th Floor, The HUB for Clinical Collaboration
Philadelphia, PA 19104
Email: shaha6@chop.edu

Introduction

Scoliosis is common in patients with neuromuscular diseases—especially those with impaired trunk strength and/or control who are unable to ambulate. This scoliosis may impact seating, ease of care, pulmonary function, and quality of life. The typical long, sweeping thoracolumbar or lumbar curve patterns of these patients are often associated with pelvic obliquity (PO, tilt of the pelvis in the coronal plane).[1] While PO may be driven by scoliosis (a supra-pelvic cause), infra-pelvic causes of PO such as hip abduction/adduction contractures may also contribute.[2-7] As a result, the relationship between supra- and infra-pelvic deformities and PO is complex and unpredictable.[2,5,6,8-11]

PO in the patient with neuromuscular disease may interfere with seating balance and tolerance and may even lead to pressure sores.[7,12,13] However, it remains unclear what magnitude of PO can be reliably tolerated with external seating modifications alone.[14,15] Similarly, when surgical correction of neuromuscular scoliosis (NMS) is indicated, it is not known what degree of residual pelvic obliquity is acceptable and can be accommodated easily with seating modifications for non-ambulatory patients.

This concept is important because correction of significant supra-pelvic-driven PO in the setting of neuromuscular scoliosis in non-ambulatory patients is generally thought to require extending the spinal fusion construct to the pelvis, which comes with increased risk of complications such as infection and implant failure.[16] With this in mind, ending the spinal fusion construct in the lower lumbar spine (rather than the pelvis) has been considered in selected cases of NMS in non-ambulatory patients, even though it is expected to leave a larger residual PO. Thus, the goal of this systematic review is to compile and assess the available literature detailing the impact of PO on seating, function, ease of care, risk of ulceration, and/or quality of life in patients with NMS to better understand what degree of PO may be acceptable.

Methods

Data Sources

We performed a literature search for articles detailing NMS and PO in May of 2018. Studies from PubMed, Embase, and CINAHL were queried. Our search structure is detailed in Figure 1. We searched for the terms pelvic obliquity and scoliosis in combination with each of the following words or phrases: neuromuscular, spinal fusion, cerebral palsy, spina bifida, myelodysplasia, muscular dystrophy, spinal muscular atrophy, seating, and sitting balance. This search strategy was modified for each of the databases used. No specific date restriction was used, though articles were only searchable for the years covered by the databases (PubMed 1966 – present, Embase 1947 – present, CINAHL 1937 – present).

Study Selection

Studies were subsequently screened to identify those detailing untreated NMS and PO and their relationship to any one of seating, skin breakdown or pressure sores, patient/caregiver-reported pain, quality of life, or ease of care. After removal of duplicates, the initial search returned a total of 2,021 articles or abstracts (Figure 1). Titles were screened independently by two authors (TL, CD) and any study receiving 1 or 2 votes was advanced for abstract review. Only peer-reviewed studies published in English were included, while reviews and chapters were excluded. 1,442 studies were excluded based on title irrelevance. Abstract review was conducted in a similar fashion, after which another 318 studies were excluded. This left 293 studies for full-text review. After full text review (TL, CD), the final set of studies was examined, and data was compiled. Additionally, the references of each included study were

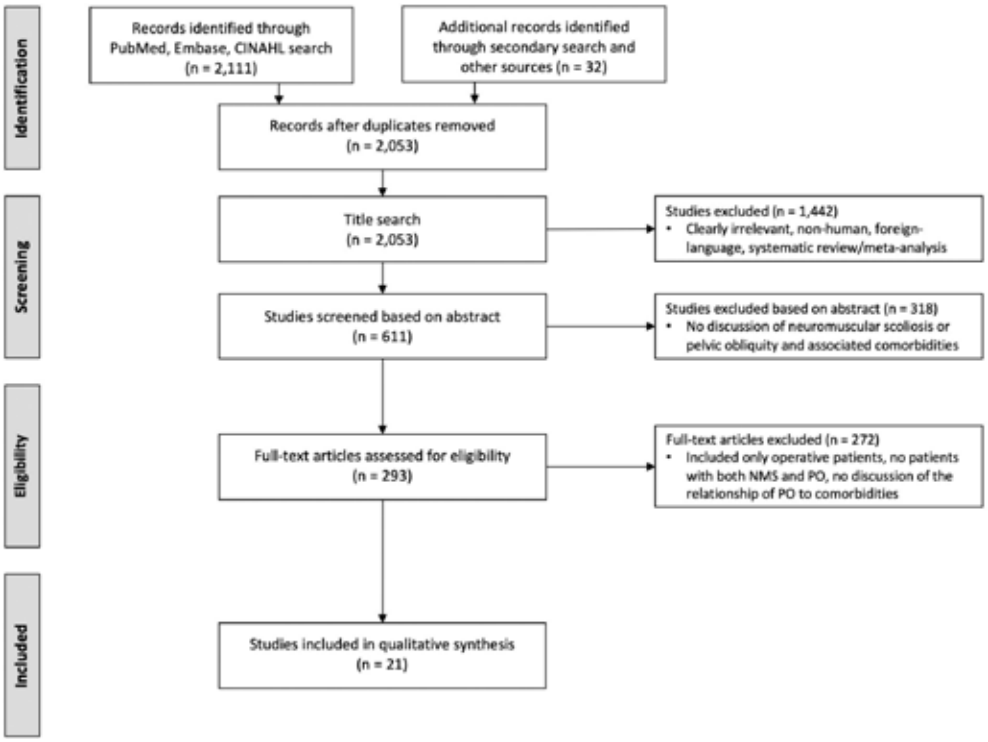

Figure 1. PRISMA diagram.

reviewed to identify articles that did not appear in the original search, yielding an additional 32 relevant studies. These were independently reviewed and included in the final data synthesis.

During review, only studies of the natural history (non-operative scoliosis management) of patients with neuromuscular disorders were advanced for consideration. These studies included patients both NMS and PO, some with a mixture of operative and non-operatively managed scoliosis patients that detailed PO and its relationship to the aforementioned comorbidities. Study level of evidence (LoE) was determined and consensus reached by three authors (JB, KB, DS) based on the criteria established by the Oxford Centre for Evidence-Based Medicine.[17] Conclusions were then drawn and grades of recommendation assigned based on established criteria again by three authors (JB, KB, DS), with disagreements resolved through discussion.[18] Using this system, a grade A = good evidence (level-I studies with consistent findings) for or against recommending intervention, grade B = fair evidence (level-II or III studies with consistent findings) for or against recommending intervention, grade C = conflicting or poor-quality evidence (Level-IV or V studies) not allowing a recommendation for or against intervention, and grade I = there is insufficient evidence to make a recommendation.

Data Extraction

Twenty-one studies were included in the final review (Table 1). Information was catalogued through manual review and kept in a spreadsheet (Excel, Microsoft, Redmond, WA). Data was extracted primarily by three authors (CD, JB, WA). Extracted data included study design, population demographics, quality of life and other associated findings, scoliosis or PO progression history, and any author conclusions.

Results

Pelvic obliquity has a deleterious effect on seating balance (grade B)

The most commonly cited problem arising from PO is "sitting imbalance", which has not been defined. Fourteen studies discussed sitting imbalance and its relationship to PO (Table 2) usinþain upright with push, or unstable = cannot sit without support) was associated with deterioration in spinopelvic angle and PO (PO of 0.7˚, 4.3˚, and 7.3˚, respectively for each group).27 Several other studies–4 level II, 2 level III, and 1 level IV–similarly noted that worsened sitting function (typically assessed using a subjective binary scale of balanced vs unbalanced) and functional status are associated with higher magnitudes of PO and resulting coronal imbalance.[4,19-21,23,25,28] One level IV article specifically noted mean PO 41˚ vs 22˚ for unbalanced and balanced sitters, respectively.[19] Another level 2 study showed higher pelvic obliquity in poor sitters versus good sitters.[20] In contrast, patients determined to be good or stable sitters more often have a level pelvis compared to those who require propping or who are bedridden (1 level III and 1 level IV paper).[5,9] It remains unclear whether PO drives sitting imbalance, as associated hip flexion contractures have also been shown to increase the odds of concomitant PO, trunk asymmetry, scoliosis,

Table 1. Study Characteristics

Author	Patients	LOE	Diagnosis	Operative *	Scoliosis†	Pelvic Obliquity†	Quality of Life	Function
Ágústsson[26]	714	3	CP	NR	286 (40%)	672 (94%)	-	PPAS
Bartnicki[20]	19	2	Myelomeningocele	0 (0%)	19 (100%)	17 (80%)	QOL-SBQ, HSDI-C, HSPPA, SBSQ, ASKp	Hoffer, ASKp
Drummond[12]	16	4	Neuromuscular Scoliosis	9 (56%)	12 (75%)	9 (90%) patients with high ischial loading	-	-
Kahanovitz[19]	39	4	Myelomeningocele	23 (59%)	39 (100%)	NR	-	Hoffer
Kalen[28]	56	3	CP	0 (0%)	14 (25%) curves ³45˚, 42 (75%) curves <45˚	8 (57%) of patients with curves ³45˚	-	Other
Khoshbin[24]	11	3	Spina Bifida	0 (0%)	11 (100%)	NR (mean 12.9˚)	SBSQ, SF-36	Hoffer, SBS
Knapp[10]	29	4	CP (Hip Dislocation)	NR	21 (72%)	12 (41%)	-	
Majd[13]	56	4	CP	0 (0%)	51 (91%)	NR (mean >10˚)	-	Hoffer
Moreau[14]	30	4	CP	NR	14 (47%)	14 (47%)	-	Hoffer
Murans[31]	14	3	Neuromuscular Scoliosis	0 (0%)	14 (100%)	10 (71%)	-	Other
Nielsen[32]	13	3	Neuromuscular Scoliosis (54%)	7 (54%)	13 (100%)	11 (85%)	-	-
Patel[30]	32	4	Myelodysplasia	7 (22%)	32 (100%)	NR (mean 15˚)	-	-
Pritchett[9]	50	3	CP (Unstable Hips)	NR	43 (86%)	30 (60%)	-	Other
Pritchett[5]	80	4	CP (Unstable Hips)	NR	68 (85%)	45 (56%)	-	Other
Sewell[29]	15	3	CP	0 (0%)	15 (100%)	NR (mean 12˚)	CP-CHILD	CP-CHILD
Sewell[34]	36	3	CP	0 (0%)	36 (100%)	NR (mean 14˚)	ASKp	ASKp
Shoham[33]	15	4	Neuromuscular Scoliosis	0 (0%)	15 (100%)	15 (100%)	-	-
Sibinski[21]	19	2	Myelomeningocele	0 (0%)	19 (100%)	17 (89%)	QOL-SBQ, HSDI-C, HSPPA, SBSQ, ASKp	Hoffer, ASKp
Smith[27]	39	3	Myelodysplasia	6 (15%)	23 (60%)	15 (39%)	-	Other
Suk[25]	26	2	Duchenne Muscular Dystrophy	0 (0%)	26 (100%)	NR (mean 29˚)	MDSQ	Modified Rancho Scale
Wai[23]	80	2	Myelodysplasia	24 (30%)	80 (100%)	NR (mean 9˚)	HSDI-C, HSPPA, SBSQ, ASKp	Hoffer, ASKp, SBS, Other

*Number (percentage) of patients who had undergone attempted spinal fusion at time of evaluation. Studies that did not state the specific number of operatively managed patients (NR = not reported) primarily described patients

uneven weight distribution, and windswept hip distortion, the combination of which leads to poor seating posture (level III).[26] From the 14 studies discussing the relationship of PO to sitting balance (4 level II, 8 level III, 2 level IV), the overall consensus is that PO likely contributes to but is not an isolated cause of sitting imbalance, earning a grade of B for relatively consistent findings with a fair level of evidence.

A threshold of pelvic obliquity exists past which sitting imbalance is likely (grade I)

One level IV article by Kahanovitz et al suggested that maintenance of ambulation and prevention of spine imbalance appeared to correlate with a major curve angle below 40˚ and PO less than 25˚.[19] While PO may impact sitting balance, a threshold or "tipping point" after which this causes symptoms such as seating intolerance remains unclear and may vary somewhat by patient. As only one level IV study specifically addressed the threshold at which PO may become problematic for sitting imbalance, there is grade I (insufficient) evidence to answer this question.

Pelvic Obliquity is associated with difficulty with perineal care (grade I)

Five studies discussed positioning or perineal care, though none described PO thresholds above which positioning and/or perineal care becomes particularly difficult (Table 3). Difficulties in perineal care were noted in 3-38% (2 level III and 2 level IV studies) of patients, but in some cases this was attributed to concomitant hip contractures or subluxation/dislocation (concomitant infra-pelvic causes of PO).[4,5,9,10] One level III study found that

Table 2. Studies Discussing Sitting Imbalance

Author	Sitting Imbalance
Ágústsson[26]	Asymmetric limited hip flexion <90° increased odds of PO, trunk asymmetry (i.e. poor sitting posture) – both items from the PPAS – scoliosis, and windswept hip distortion.
Bartnicki[20]	Poor sitters as evaluated by the article authors on a 3-point sitting stability scale had significantly greater PO (15° vs 9°) than good sitters, concluding that improved sitting stability correlated with decreased PO. Additionally, the odds of community ambulatory status was 2.5 times higher for stable sitters.
Kahanovitz[19]	Of 11 unbalanced sitters, 10 had scoliosis >35° and PO >25° whereas all ambulators (balanced sitters per the authors' definition) had PO <25°. Nine non-ambulatory but balanced sitters had mean PO of 22° vs 41° for unbalanced sitters.
Kalen[28]	Patients with higher major curve severity (>45°) and PO were more frequently lower functioning (e.g. less ambulatory) and required wheelchair modification to help with sitting function (81% vs 46%).
Khoshbin[24]	Of 9 non-operatively treated patients with available follow-up assessment, 3 (33%) required arms for sitting support on the SBS with a mean PO of 12.9°.
Moreau[4]	The authors concluded that a combination of PO and scoliosis led to loss of sitting balance in 9 of 14 (64%) of patients with either hip subluxation or hip dislocation.
Pritchett[9]	All self-propped sitters had a level pelvis (compared to propped or bedridden patients).
Pritchett[5]	All self-propped sitters had a level pelvis (compared to propped or bedridden patients).
Sewell[29]	Decreased CP-CHILD scores over 2 years were attributed to worse sitting balance and pain with a noted 4° increase in PO, though these results were not specifically correlated to final PO.
Sewell[34]	Decreased ASKp scores over 2 years were attributed to worse sitting balance and pain with an observed 4° increase in PO, though these results were not specifically correlated to final PO.
Sibinski[21]	While eight patients (42%) had poor sitting, there was no relationship between PO and any QoL metric evaluated. However, there was an observed correlation between PO and major curve magnitude as well as between sitting stability and QoL on the SBSQ. The authors concluded that severe scoliosis affects QoL and is associated with higher magnitude PO.
Smith[27]	Sitting stability was most closely associated with spinopelvic angle as well as intra-pelvic PO (mean values of 0.7°, 4.3°, and 7.3° for stable, poor, unstable sitters, respectively).
Suk[25]	MDSQ sitting scores for questions relevant to sitting – scores of 0 indicating the inability to perform a task and 4 indicating independence – were all below a mean 1.5 in a population with mean PO 29° at follow-up. However, the specific correlation between sitting scores and PO was not explored.
Wai[23]	Coronal imbalance, not major curve magnitude or PO, was the only factor found to correlate with the sitting balance, though the inclusion of operative and non-operatively managed patients in the regressions is unclear. Further the authors suggest that specific attention should be paid to correction of coronal balance through curve correction and leveling of PO.

Table 3. Studies Discussing Sitting Positioning, Perineal Care, and Pain

Author	Positioning, Perineal Care, and Pain
Knapp[10]	Eleven of 29 patients (38%) had difficulty with perineal care, which was more frequently attributed to severe adduction contractures in this cohort of patients with hip subluxation/dislocation.
Moreau[4]	In a subset of 30 patients with hip subluxation or dislocation - 14 of whom had PO and scoliosis - 11 were reported to have difficulty with perineal care.
Pritchett[9]	Two patients had perineal care difficulty, and 21 had minor/moderate pain attributed primarily to hip subluxation.
Pritchett[5]	Two patients had perineal care difficulty, and 30 had minor/moderate pain attributed primarily to hip subluxation.
Sewell[29]	Twelve patients (83%) initially reported no spinal-related pain, while at 2-year follow-up 66% reported mild or moderate spinal-related pain. However, this not specifically correlated with final PO, and there was no noted change in positioning or transferring despite the increase in PO.

caregivers did not observe any change in the positioning, transferring, or mobility of patients on the Caregiver Priorities & Child Health Index of Life with Disabilities questionnaire (CP-CHILD) despite an increase in mean PO from 8° to 12° over 2 years.[29] With only five lower-quality studies on this topic, it is difficult to assess the contribution of PO to these outcomes, and therefore we assign a grade of I for insufficient evidence that PO is associated with perineal care and positioning difficulties.

Pelvic Obliquity is associated with decubitus ulcers and skin breakdown (grade C)

The association between PO and skin breakdown is likely multifactorial and has been discussed in thirteen studies (Table 4). The lifetime incidence of decubitus ulcers in the neuromuscular population (e.g. CP, myelodysplasia, muscular dystrophy) ranged from 5-69% across 1 level II, 4 level III, and 5 level IV studies,[4,5,9,10,12,13,20,24,28,30] with the majority of ulcers in these patients tending to be sacral[13,28] or trochanteric.[5,9] A level IV study by Drummond et al suggested that risks of ulceration include >55% posterior weight distribution, >30% weight distributed over one ischium, >11% weight over sacro-coccygeal region, and non-ambulation; the risk was highest when 3 or more criteria were met.[12] Two level III studies consistently found greater seat load asymmetry with higher magnitude PO, though one of these showed a non-significant difference in PO compared to controls.[31,32] A level II study by Shoham

Table 4. Studies Discussing Decubitus Ulcers

Author	Decubitus Ulcers
Bartnicki[20]	25% of poor sitters had a history of decubitus ulcer (defined as major or minor) vs 18% of good sitters (non-significant results).
Drummond[12]	A total 10 of 16 paraplegic patients evaluated had history of ulcer, 9 of whom were noted to have asymmetric seating loads, which the authors concluded was associated with unbalanced scoliosis and PO.
Kalen[28]	Decubiti were noted in 22% of patients with major curves >45˚ (57% of whom had PO) vs 15% of patients with curves <45˚ (0% with PO). Authors concluded no correlation between PO or scoliosis and decubiti.
Khoshbin[24]	Only 1 patient (9%) had a decubitus ulcer at baseline assessment.
Knapp[10]	A total of 9 patients (31%) had a history of decubitus ulcers.
Majd[13]	Three patients evaluated with history of decubitus ulcer had mean PO of 45˚ and major curve of 106˚ in comparison to mean PO and major curve of 12˚ and 57˚ in non-ulcer patients, respectively. The authors concluded that a relationship exists between larger deformity (PO and major curve) and the risk of ulcer development.
Moreau[4]	Nine of 30 patients (30%) with hip subluxation or dislocation decubitus ulcers, all of whom were bedridden. The authors concluded that the ability to sit is greatly reduces the risk of decubiti, which they stated is impacted by PO and scoliosis.
Murans[31]	NMS patients have greater seat load asymmetry vs controls (30% vs 7%). However, PO in the NMS cohort (mean 13.5˚) was not significantly greater than controls.
Nielsen[32]	Evaluation of seat load characteristics in 13 children (mean PO 19.1˚) able to independently sit showed higher peak pressure (331.3 g/cm^3 vs 219.6 g/cm^3) and percent of body weight (61.6% vs 51.2%) on the side carrying the larger load vs controls. The top 25% of pressure was distributed over smaller area (10.2 cm^2 vs 27.0 cm^2) in NMS.
Patel[30]	Twenty-two of 32 patients (69%) had a history of at least one ulcer. The authors noted greater PO correlated with higher average and peak seated pressures as well as larger proportion of areas with high pressure. However, the magnitude of curve, PO, and seated pressures were similar in patients without history of ulcer.
Pritchett[9]	Twelve patients (24%) had a history of ulcer, which were noted to mostly be trochanteric or sacral (60% had PO).
Pritchett[5]	Nineteen patients (21%) had a history of ulcer (13 trochanteric, 6 sacral) in a population where 56% had PO.
Shoham[33]	There was no observed correlation between PO and seating pressure at baseline, but use of a TLSO improved seating pressure in patients with PO elevation contralateral to the convexity of the major curve.

et al also showed that TLSO bracing significantly improved seating pressure in patients with NMS and PO, and therefore recommended bracing treatment in this subset of NMS patients to reduce localized interface pressure and prevent decubitus ulcers.[33] The most commonly cited positive association is a level IV study of non-ambulatory adults with CP by Majd et al., which found that 3 patients with decubitus ulcers had significantly larger PO (45˚ vs 12˚) and major curve angles (106˚ vs 57˚) compared to the remaining 53 individuals.[13] In contrast, several other studies (1 each of level II, III, and IV) have found no difference in PO between patients with and without a history of ulcer development.[20,28,30] Despite an intuitively increased risk of decubitus ulcers relating to significant PO given increased seating pressures over small areas seen in these patients, there is conflicting, grade C evidence that higher magnitude PO contributes to the development of decubitus ulcers.

Untreated pelvic obliquity in NMS is associated with decreased HRQOL (grade C)

Regardless of the contributions of PO to sitting imbalance, ulcer development, or difficulty positioning patients, it is perhaps most important to understand its impact on quality of life (QoL). Seven studies reported or discussed PO in NMS patients with recorded QoL metrics, including: CP-CHILD29, Quality of Life in Spina Bifida Questionnaire (QoL-SBQ),[20,21] Spina Bifida Spine Questionnaire (SBSQ),[20,21,23,24] Muscular Dystrophy Spine Questionnaire (MDSQ)25, Short Form Health Survey (SF-36)24, Activities Scale for Kids (ASKp),[20,21,23,34] Health Self-Determinism Index for Children (HSDI-C),[20,21,23] and Harter's Self-Perception Profile for Adolescents (HSPPA).[20,21,23] While non-operatively managed patients tend to experience overall decreases in QoL as their scoliotic and pelvic deformities worsen—often attributed to impairments in sitting balance and pain[21,24,25]—3 studies (1 level II, 2 level III) did not find a correlation between QoL and PO.[21,29,34] Sibinski et al (level II) specifically demonstrated a significant correlation between sitting balance and SBSQ score, but failed to identify a correlation for PO with any index of HRQoL.[21] Suk et al. (level II) showed lower subsection scores related to sitting balance on the MDSQ for patients with high mean major curve angles of 106˚ and PO of 29˚, but did not report on the relationship of QoL and PO specifically.[25] A single level II paper identified better sitting stability (good vs poor sitters) and increased quality of life (QoL-SBQ) in patients with decreased PO (9˚ vs 15˚; not affected by major curve angle).20 There is conflicting evidence (grade C) that PO—which is often used as an indication for surgical intervention—is associated with decreased QOL in NMS.

Untreated pelvic obliquity in NMS is associated with increased pain (grade I)

There is also some evidence of an association between PO and pain, particularly as it relates to sitting imbalance. Patients with cerebral palsy (CP) showed significant

increases in pain over a 2-year period in one level III study with a concomitant increase in PO in one study from 8° to 12°, attributed primarily to worsened sitting balance.[29] While not explicitly comparing PO and pain, three other studies (1 level III, 1 level IV) reported rates of mild to major pain in patients with NMS and PO ranging from 33-60%.[5,9,10] Therefore, there is grade I (insufficient) evidence that PO is associated with higher pain.

Discussion

Pelvic obliquity—tilting of the pelvis in the coronal plane—may be driven by supra-pelvic (thoracolumbar/lumbar scoliosis) and/or infra-pelvic (contracture or subluxation/dislocation of hips) deformities. The finding is most commonly observed in non-ambulatory patients with neuromuscular disease, trunk weakness, and abnormalities in muscle tone and control that impair sitting balance. Many of these patients are unable to maintain an upright posture even in the absence of deformities above or below the pelvis. Previous studies have failed to define any consistent or predictable relationships between PO and supra- and/or infra-pelvic deformities. It is generally assumed that "significant" PO may be associated with pain, risk of skin breakdown, and impaired seating. While it has also been assumed that the goal of spine surgery in neuromuscular disease patients is a straight spine over a level pelvis, it remains unclear just what degree of pelvic obliquity can be tolerated given innovations in the design of current seating systems. To better understand this, we undertook this study of PO and its impact in the natural history of patients with NMS and PO. Our goal was to evaluate the relationship between PO and seating, attempting to determine the degree of obliquity that leads to symptoms, impairments, or alterations in quality of life.

The results of this review highlight the paucity of literature in this subject area. The first challenge is simply quantifying PO, and a variety of measurements have been described (Table 5). Further, only a subset of studies that did report PO (8/21) even stated which method was utilized. And the studies that did report what method was used reported a variety of methods. One can assess the degree of tilt relative to the horizontal plane, or for example the relationship of the spine to the pelvis which also assesses coronal balance (e.g. Maloney method). Schrader et al concluded that the Maloney method was most reliable with ICC ranges for inter- and intra-rater reliability of 0.964-0.965 and 0.845-0.962, respectively.[35] The Maloney method also has the advantage of relating the pelvis to the upper thoracic spine and overall spinal balance. Many studies use the Osebold or O'Brien methods which do not relate PO to the upper thoracic spine or overall spinal balance.[36] As such, we recommend future study standardize the method of PO measurement, preferably with Maloney as it has technical advantages as well as being shown to be the method with the most inter-rater reliability.

We also recognize that there are multiple variables that impact symptoms, function, and ease of care in non-ambulatory patients with neuromuscular conditions, such as weakness, challenges with controlling movement and balance, fixed supra- and infra-pelvic deformities, nutritional status and skin condition, and others, and our results suggest that it is impossible to disaggregate the impact of pelvic obliquity as an isolated variable. Many patients simply have weakness and poor trunk control and therefore have sitting imbalance and/or intolerance. This makes assessing the impact of PO very difficult. So while there seems to be an association between PO, sitting imbalance, and the development of skin breakdown, we were unable to identify a PO threshold that allows for reliable symptom/complication risk stratification. A single study found that maintenance of ambulation and prevention of spine imbalance was associated with a major curve angle below 40° and PO less than 25°.[19] Rates of decubitus ulcers varied significantly across neuromuscular

Table 5. Common Methods of Measuring Pelvic Obliquity[36]

Method	Description of Measurement Technique	Number
Not discussed	-	13
Osebold	One line is drawn between the most proximal points on the iliac crests and a second line intersecting the first is drawn parallel to the lower edge of the radiograph. The angle of intersection between these lines is the PO angle.	6
O'Brien	The pelvic coronal reference line is drawn using one of three methods depending on radiograph quality (in order: across tips of sacral alae, the iliac crests, greater sciatic notch). The angle formed by the intersection of this line and a line parallel to the lower edge of the radiograph is the PO.	1
Other	Intra-pelvic obliquity, defined as the angle formed between lines drawn across the iliac crests and across the base of the ischial tuberosities	1
Maloney	One line is drawn across the superior aspect of the iliac crests and a second line is drawn from the center of T1 to the center of S1. The angle of PO is then determined by measuring the angle between the second line and a line perpendicular to the first line.	0
Allen and Ferguson	A line is drawn across the iliac crests as in the Osebold method, with a corresponding perpendicular line drawn. A third line is then drawn intersecting the spinous processes of both the L4 and L5 vertebrae. The angle formed by the intersection of this third line with the perpendicular line is the PO.	0
Lindseth	A line is drawn perpendicular to the superior aspect of the top vertebra of a lumbosacral curve, with a second line drawn perpendicular to a line through the superior acetabular or inferior ischial tuberosity margins. The angle created by the intersection of these lines is the PO.	0

patients with differing degrees of PO. Patel et al. noted that ulcer location is often not described and seating modifications are not documented.[3]0

PO has not been specifically linked with any functional measure given that the few available measures of QoL and seating in the neuromuscular population do not specifically assess the contribution of PO. Several studies have noted that sitting balance correlates with the desires of caregivers and patient positioning rather than the actual deformity.[5,10] The limited existing metrics on QoL are unable to isolate the impact of a tilted pelvis, except those that specifically look at sitting (such as the Posture and Postural Ability scale or the Sitting Balance Scale). Motor strength and control and/or other variables are likely important, and wheelchair modifications may lead to adequate compensation for deformity.[23] From a measurement standpoint, it is unclear if any of these measures can detect the necessary change to identify improvements following surgery. Although this study focused on the experience in non-surgical treatment of patients with NMS, at least one study showed that parents viewed spinal fusion as one of the most helpful procedures for their child, edged out only by gastrostomy tube placement.[37]

Several limitations to this review should be noted. First, many of the studies were older studies, with all the methodologic flaws attendant with older literature. While we included any study that described the relationship of NMS to PO, few described their definition of PO, making it difficult to assess the correlation of PO magnitude to associated symptoms. Additionally, while we excluded studies primarily focused on surgical treatment outcomes, we opted to include older studies discussing populations of patients with both surgically and non-surgically; in some cases, the authors did not separate out these groups for analysis. This was done as many landmark papers for our understanding of PO natural history were among these studies. Without including several of these older, important articles, a thorough review of the impact of PO on NMS would not be possible given a lack of natural history studies in the modern era.

In summary, the pelvis serves as a linkage between the spine and the lower extremities, and tilting or obliquity of the pelvis is commonly observed in the neuromuscular population. While neutralizing PO is classically considered a major technical goal of spinal fusion for NMS, critical review of the literature reveals a lack of sound evidence showing that mild PO is not tolerable in the natural history of the disease. We found that any issues exist surrounding the measurement of PO. This review shows some support in the literature for the notion of increasing PO as a factor in seating difficulty in this population. While it may seem intuitive that having a straight spine and a level pelvis is preferable to severe scoliosis in patients with NMS, further studies with clearly defined endpoints and measures are needed to address these questions. "Seating" is a multidimensional concept that depends on motor strength and control, upper extremity function, balance, and the magnitude and flexibility of both infra- and supra-pelvic deformities which impact global positioning. We were unable to draw any solid conclusions regarding the magnitude of PO that impacts seating or function, perhaps due to the complex relationships noted above, the inability to define PO clinically or radiographically, and limitations in the number of functional outcome measures which evaluating seating. Future studies should focus on redefining PO within the context of global positioning, and newer outcome measures should be developed to assess seating.

References

1. Hart DA and McDonald CM. Spinal deformity in progressive neuromuscular disease. Natural history and management. **Phys Med Rehabil Clin N Am.** 1998;9(1):213-viii.

2. Porter D, Michael S, and Kirkwood C. Patterns of postural deformity in non-ambulant people with cerebral palsy: what is the relationship between the direction of scoliosis, direction of pelvic obliquity, direction of windswept hip deformity and side of hip dislocation?. **Clin Rehabil.** 2007;21(12):1087-1096. doi:10.1177/0269215507080121

3. Carr C and Gage JR. The fate of the nonoperated hip in cerebral palsy. **J Pediatr Orthop**. 1987;7(3):262-267. doi:10.1097/01241398-198705000-00004

4. Moreau M, Drummond DS, Rogala E, et al. Natural history of the dislocated hip in spastic cerebral palsy. **Dev Med Child Neurol.** 1979;21(6):749-753. doi:10.1111/j.1469-8749.1979.tb01696.x

5. Pritchett JW. The untreated unstable hip in severe cerebral palsy. **Clin Orthop Relat Res.** 1983;(173): 169-172.

6. Lonstein, JE and Beck K. Hip dislocation and subluxation in cerebral palsy. **J Pediatr Orthop.** 1986; 6(5): 521-526.

7. Gaine WJ, Lim J, Stephenson W, et al. Progression of scoliosis after spinal fusion in Duchenne's muscular dystrophy. J Bone Joint Surg Br. 2004; 86(4):550-555.

8. Senaran H, Shah SA, Glutting JJ, et al. The associated effects of untreated unilateral hip dislocation in cerebral palsy scoliosis. *J Pediatr Orthop.* 2006; 26(6):769-772. doi:10.1097/01.bpo.0000242426.60995.29

9. Pritchett JW. Treated and untreated unstable hips in severe cerebral palsy. *Dev Med Child Neurol.* 1990; 32(1): 3-6.

10. Knapp DR, and Cortes H. Untreated hip dislocation in cerebral palsy. *J Pediatr Orthop.* 2002; 22(5): 668-671.

11. Letts M, Shapiro L, Mulder K, *et al.* The windblown hip syndrome in total body cerebral palsy. *J Pediatr Orthop.* 1984; 4(1):55-62. doi:10.1097/01241398-198401000-00013

12. Drummond D, Breed AL, and Narechania R. Relationship of spine deformity and pelvic obliquity on sitting pressure distributions and decubitus ulceration. *J Pediatr Orthop.*1985; 5(4): 396-402.

13. Majd ME, Muldowny DS, and Holt RT. Natural history of scoliosis in the institutionalized adult cerebral palsy population. *Spine* (Phila Pa 1976). 1997; 22(13): 1461-1466.

14. Heller KD, Wirtz DC, Siebert CH, *et al.* Spinal stabilization in Duchenne muscular dystrophy: principles of treatment and record of 31 operative treated cases. *J Pediatr Orthop B.* 2001; 10(1):18-24.

15. Sussman MD, Little D, Alley RM, *et al.* Posterior instrumentation and fusion of the thoracolumbar spine for treatment of neuromuscular scoliosis. *J Pediatr Orthop.* 1996; 16(3):304-313. doi:10.1097/00004694-199605000-00004

16. Alman BA and Kim HK. Pelvic obliquity after fusion of the spine in Duchenne muscular dystrophy. *J Bone Joint Surg Br.* 1999; 81(5): 821-824.

17. Medicine, O.C.f.E.-B., *Oxford Centre for Evidence-Based Medicine 2011 Levels of Evidence.* 2011.

18. Wright JG, Einhorn TA, and Heckman JD. Grades of recommendation. *J Bone Joint Surg Am.* 2005; 87(9): 1909-1910.

19. Kahanovitz N. and Duncan JW. The role of scoliosis and pelvic obliquity on functional disability in myelomeningocele. *Spine* (Phila Pa 1976).1981; 6(5): 494-497.

20. Bartnicki B, Synder M, Kujawa J, *et al.* Siting stability in skeletally mature patients with scoliosis and myelomeningocele. *Ortop Traumatol Rehabil.* 2012; 14(4):383-389. doi:10.5604/15093492.1005086

21. Sibinski M, Synder M, Higgs ZC, *et al.* Quality of life and functional disability in skeletally mature patients with myelomeningocele-related spinal deformity. *J Pediatr Orthop B.* 2013; 22(2):106-109. doi:10.1097/BPB.0b013e32835c2a65

22. Hoffer MM, Feiwell E, Perry R, *et al.* Functional ambulation in patients with myelomeningocele. *J Bone Joint Surg Am*. 1973; 55(1):137-148.

23. Wai EK, Young NL, Feldman BM, *et al.* The relationship between function, self-perception, and spinal deformity: Implications for treatment of scoliosis in children with spina bifida. *J Pediatr Orthop*. 2005; 25(1):64-69. doi:10.1097/00004694-200501000-00015

24. Khoshbin A, Vivas L, Law PW, *et al.* The long-term outcome of patients treated operatively and non-operatively for scoliosis deformity secondary to spina bifida. *Bone Joint J*. 2014; 96-B(9):1244-1251. doi:10.1302/0301-620X.96B9.33857

25. Suk KS, Lee BH, Lee HM, *et al.* Functional outcomes in Duchenne muscular dystrophy scoliosis: comparison of the differences between surgical and nonsurgical treatment. *J Bone Joint Surg Am*. 2014; 96(5):409-415. doi:10.2106/JBJS.M.00777

26. Agustsson A, Sveinsson T, and Rodby-Bousquet E. The effect of asymmetrical limited hip flexion on seating posture, scoliosis and windswept hip distortion. *Res Dev Disabil*. 2017; 71: 18-23.

27. Smith, R.M. and J.B. Emans. Sitting balance in spinal deformity. *Spine* (Phila Pa 1976). 1992; 17(9): 1103-1109.

28. Kalen V, Conklin MM, and Sherman FC. Untreated scoliosis in severe cerebral palsy. *J Pediatr Orthop*. 1992; 12(3): 337-340.

29. Sewell MD, Malagelada F, Wallace C, *et al.* A Preliminary Study to Assess Whether Spinal Fusion for Scoliosis Improves Carer-assessed Quality of Life for Children With GMFCS Level IV or V Cerebral Palsy. *J Pediatr Orthop*. 2016; 36(3):299-304. doi:10.1097/BPO.0000000000000447

30. Patel J, Walker JL, Talwalkar VR, *et al.* Correlation of spine deformity, lung function, and seat pressure in spina bifida. *Clin Orthop Relat Res*. 2011; 469(5):1302-1307. doi:10.1007/s11999-010-1687-8

31. Murans G, Gutierrez-Farewik EM, and Saraste H. Kinematic and kinetic analysis of static sitting of patients with neuropathic spine deformity. *Gait Posture*. 2011; 34(4): 533-538.

32. Nielsen C, Gutierrez-Farewik EM, Hirschfeld H, *et al.* Seat load characteristics in children with neuromuscular and syndrome-related scoliosis: effects of pathology and treatment. *J Pediatr Orthop B*. 2008; 17(3):139-144. doi:10.1097/BPB.0b013e3282fde471

33. Shoham Y, Meyer S, Katz-Leurer M, *et al.* The influence of seat adjustment and a thoraco-lumbar-sacral orthosis on the distribution of body-seat pressure in children with scoliosis and pelvic obliquity. *Disabil Rehabil*. 2004; 26(1):21-26. doi:10.1080/09638280410001645940

34. Sewell MD, Wallace C, Malagelada F, *et al.* Does Spinal Fusion and Scoliosis Correction Improve Activity and Participation for Children With GMFCS level 4 and 5 Cerebral Palsy?. *Medicine* (Baltimore). 2015; 94(49):e1907. doi:10.1097/MD.0000000000001907

35. Shrader MW, Andrisevic EM, Belthur MV, *et al*. Inter- and Intraobserver Reliability of Pelvic Obliquity Measurement Methods in Patients With Cerebral Palsy. *Spine Deform*. 2018; 6(3):257-262. doi:10.1016/j.jspd.2017.10.001

36. Karkenny AJ, Magee LC, Landrum MR, *et al.* The Variability of Pelvic Obliquity Measurements in Patients with Neuromuscular Scoliosis. *JBJS Open Access*. 2021; 6(1):e20.00143. doi:10.2106/JBJS.OA.20.00143

37. Baldwin KD, Cahill PJ, Sponseller PD, *et al.* BMI change following spinal fusion for neuromuscular scoliosis surgery. *Spine Deform*. 2020; 8(5):1081-1087. doi:10.1007/s43390-020-00109-1

Bone and Development

Exploring the Efficacy of Additively Manufactured PLGA Implants for Fracture Repair at Early Time Points

Kathryn S. Strand, BS
Anna N. Smith, BS
Joseph B. Ulsh, MS
Trent J. Levy, BS
Michael W. Hast, PhD

McKay Orthopaedic Research Lab, Department of Orthopaedic Surgery, University of Pennsylvania, Philadelphia, PA

Introduction

Bone fractures can result in significant physical disabilities, chronic pain, increased healthcare costs, and an overall lower quality of life.[1] It has been established that micromotion at the fracture site can improve healing outcomes, so there is new interest in developing less rigid implants such as non-metallic plates.[2] Poly-lactic-co-glycolic acid (PLGA) is an attractive candidate material for bone plates due to its relatively high mechanical strength, biocompatibility, and controllable degradation kinetics, all of which make it suitable for fracture repair.[3] Additionally, its degradation products have been shown to promote osteogenesis and angiogenesis.[4] PLGA has been used in a variety of bone healing applications via additive manufacturing (AM).[5] However, we still do not know if AM PLGA can be used to create effective fracture implants. The purpose of this in vitro and in vivo study was to explore the potential for AM PLGA implants as devices for fracture repair at early healing time points. We hypothesized that AM PLGA implants would have decreased mechanical strength in comparison to non-degradable control implants, and that the bone healing response between groups would be similar.

Methods

In an IACUC-approved study, 19 male Sprague-Dawley rats underwent bilateral osteotomies of the femora (Figure 1). Each femur was fixed with either a PLGA (Lattice Medical) or BioMed Clear Resin (Formlabs) implant. PLGA implants were fabricated on a fused deposition 3-D printer with 85:15 PLGA filament (Prusa i3 MK3 3-D), and the resin implants were synthesized via photocuring (Formlabs Form 3). Because PLGA could not be sterilized in an autoclave, PLGA implants were soaked in 70% ethanol for 30 minutes. Resin implants were autoclaved. The polymer plates (193535 mm) were held in place with 4 non-locking screws (0-42 3 3/8"). The rats were allowed to weight-bear immediately after surgery. Rats were sacrificed at 3 and 6 weeks. Histology (n56) and micro-CT analyses (n56) were conducted at 3 and 6 weeks post-surgery. Torsional testing of healing femora was conducted at 6 weeks by performing a 90 ° internal rotation of the femur at 3°/sec (n57). Micro-CT outcome measures of the fracture callus included bone volume (BV) mean density, total volume (TV) mean density, and the BV/TV fraction. Histological analysis included Safrinin-O/FastGreen, hemotoxylin and eosin (H&E), and Picrosirius Red staining. Implants were harvested from all sacrificed animals and kept frozen at 220°C. To assess differences between in vitro and in vivo degradation of PLGA implants, additional PLGA and resin implants were manufactured (n510 per group) and incubated. Specimens were kept at 37°C on a rocker in a solution of 30% fetal bovine serum, 69% PBS, and 1% v/v Penicillin-Streptomycin-Fungizone.

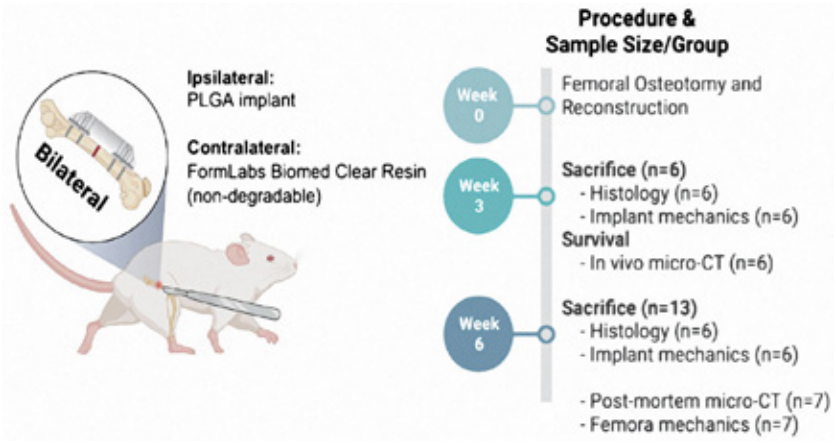

Figure 1. Left: Schematic of surgical procedure. Right: Relevant study timepoints including micro-CT, histology, and mechanical testing.

Serum changes were completed every 3-4 days. Harvested implants from the in vivo study and in vitro implants were subjected to torsional testing at 0, 3, and 6 weeks (90° rotation at 1°/sec). The primary mechanical testing outcome measure was virtual torsional rigidity (VTR). T-tests were used to make comparisons between groups at each time point. Paired t-tests were used to compare bones within each rat. A one-way ANOVA with a Holm-Sidak post-hoc test was conducted to compare outcomes from each implant type across all time points. Kruskal-Wallis tests with Dunn's post-hoc were used on nonparametric data sets. Significance was set to p,0.05.

Results

Micro-CT analysis revealed that PLGA significantly increased callus bone volume mean density from 3 to 6 weeks, but resin did not (Figure 2A). Significant increases in total volume mean density (Figure 2B) and BV/TV fraction (Figure 2C) existed for both implants between timepoints, but there were no differences between groups. Torsional testing of the femora at 6 weeks revealed no differences in VTR (Figure 2D). Histology results were still pending at the time of writing this abstract. In vitro degradation demonstrated significantly stiffer PLGA implants than resin at 0 and 3 weeks, but not 6 weeks (Figure 3A). PLGA implants retrieved from the in vivo study were different at all time points, and there were no significant differences between groups at 3 and 6 weeks (Figure 3B).

Discussion

To our knowledge, this is the first study to investigate

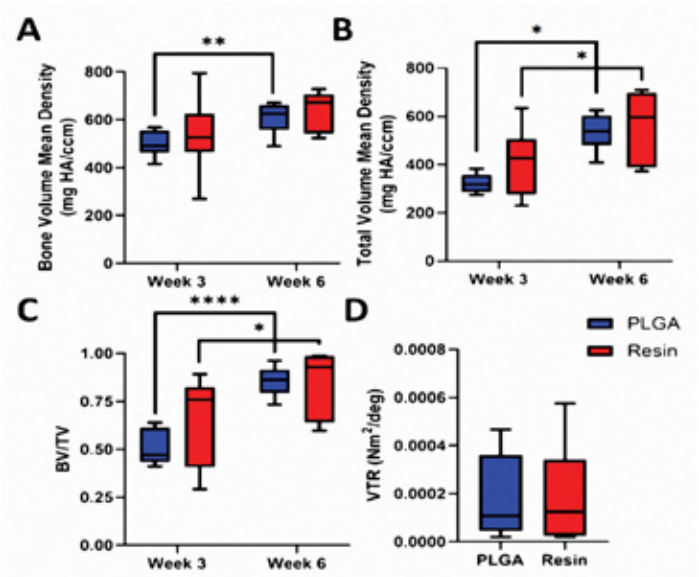

Figure 2. (A-C) Quantitative assessment of bone callus healing via micro-CT and **(D)** mechanical testing. *p<0.05, **p<0.01, ****p<0.0001.

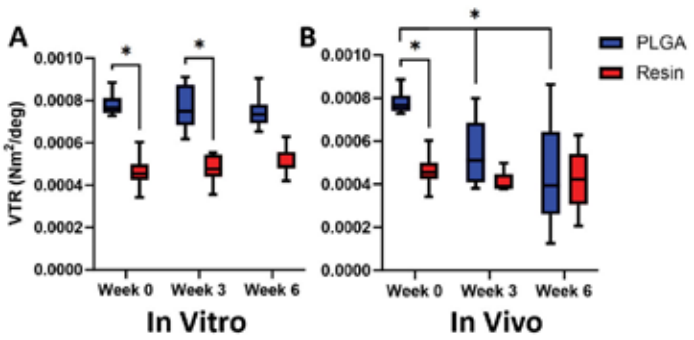

Figure 3. Mechanical testing results from in vitro **(A)** and in vivo **(B)** PLGA and resin implants. *p<0.05.

the effects of AM PLGA implants at early time points in fracture repair. At 3 and 6 weeks, we observed fracture healing, as indicated by the increase in BV mean density, TV mean density, and BV/TV. Notably, use of PLGA and resin implants led to similar bone healing responses. In vitro and in vivo analysis of the implant degradation demonstrates that mechanical loading in vivo significantly increased the degradation rate of the PLGA implants. These results reveal that unloaded in vitro degradation assays do not accurately reflect the degradation kinetics of AM PLGA, which is important for future experiments that will focus on PLGA implant form and function. Importantly, we found that PLGA implants did not have any detrimental effects on fracture healing progression at short time points (3-6 weeks). Further analyses at longer time points, when the strength of PLGA implants begins to go to zero, are necessary to determine the long-term relationships between AM PLGA implant degradation on mechanotransduction during bone healing.

Significance/Clinical Relevance

At early time points in the fracture healing process, the mechanical properties of biodegradable PLGA fracture implants were similar to matched non-degradable resin devices. Bone healing responses were similar between the two groups. We are encouraged by this finding, and we believe that the benefits of implant degradation at longer time points will lead to accelerated and improved bone repair.

References

1. Wu AM, Bisignano C, James SL, *et al.* Global, regional, and national burden of bone fractures in 204 countries and territories, 1990–2019: a systematic analysis from the Global Burden of Disease Study 2019. *Lancet Healthy Longev.* 2021;2(9):e580-e592.

2.Goodship AE, Kenwright J. The influence of induced micromovement upon the healing of experimental tibial fractures. *J Bone Joint Surg Br.* 1985;67-B(4):650-655.

3.Zhao D, Zhu T, Li J, *et al.* Poly(lactic-co-glycolic acid)-based composite bone-substitute materials. *Bioact Mater.* 2020;6(2):346-360.

4.Hu XF, Feng YF, Xiang G, *et al.* Lactic acid of PLGA coating promotes angiogenesis on the interface between porous titanium and diabetic bone. *J Mater Chem B.* 2018;6(15):2274-2288.

5.Jin S, Xia X, Huang J, *et al.* Recent advances in PLGA-based biomaterials for bone tissueregeneration. *Acta Biomater.* 2021;127:56-79.

U·P·O·J

Imaging mass cytometry reveals distinct cellular phenotypes in CD14 deficient mouse synovium

Kevin G. Burt[1,2]
Sanique M. South[3]
Vu Nguyen[1,2]
Lance A. Murphy[1,2]
Robert L Mauck[1,2]
Tim Griffin[4,5]
Carla Scanzello[1,2,6]

[1]Department of Orthopaedic Surgery
Perelman School of Medicine
University of Pennsylvania
Philadelphia, PA

[2]Translational Musculoskeletal Research Center
Corp. Crescenz VA Medical Center
Philadelphia, PA

[3]University of Oregon
Eugene OR

[4]Veterans Affairs Medical Center
Oklahoma City, OK

[5]Oklahoma Medical Research Foundation
Oklahoma City, OK

[6]Division of Rheumatology
Perelman School of Medicine
University of Pennsylvania
Philadelphia, PA.

Disclosures

KGB (N)—kevin.burt@pennmedicine.upenn.edu, VN (N), LAM (N), SMS (N), RLM (4,5,8), TG (8), CRS (8)

Introduction

Growing evidence has revealed that inflammation is a major driver of osteoarthritis (OA). However, previous consideration of OA as a noninflammatory disease placed early focus on mechanical and structural characterization. As a consequence, there is a knowledge gap with respect to the full description of the inflammatory state across tissues within the knee joint (synovium, meniscus, cruciate ligaments, etc.) during OA progression. Of these tissues, the synovium has been identified as a reservoir of not only inflammatory mediators but also innate (monocyte/macrophages) and adaptive (T- and B-cells) immune cells.[1] Both the diverse cell populations and unique structure of the synovium, including the lining and sublining layers, undergo unique inflammatory-mediated degenerative changes. CD14, a co-receptor to inflammatory toll-like receptor (TLR) signaling and subsequent macrophage activation, has also been identified as being upregulated in OA synovium and, in our prior work, we showed that global genetic CD14 deficiency in mice is protective against PTOA related bone-remodeling and mobility dysfunction.[2,3] Imaging mass cytometry (IMC) is an emerging technology that allows for the spatial localization of molecular species across tissue samples, facilitating investigation of cellular subtypes throughout diverse tissue structures, such as the synovium, as they change with disease. Utilizing this technology, we hypothesized that CD14 deficiency would modulate the innate immune cell profiles within the synovium during OA progression.

Methods

CD14 knockout (CD14-KO) mice: Global CD14 deficient mice of C57BL/6 background were obtained from Jackson Laboratories (#003726).[4] OA model (n = 5): Destabilization of the medial meniscus (DMM) surgery was performed to induce OA in skeletally mature (10-12 wk old) CD14-KO or C57BL/6 (WT) mice.[5] Flow cytometry analysis (n=5): Synovial and fat-pad tissue from 4 knees were pooled for each biological replicate, collected at 0- (preop), 4-, 8- or 16-wks post-surgery, and cells were isolated enzymatically. Cell suspensions were split in half and stained with antibodies for monocyte (CD45, Ly6C), and macrophage (CD45, CD64) cell markers or T cell (CD45, CD3) and T-helper cell (CD45, CD3, CD4) markers. Multicolor flow cytometry was performed (BD LSR II), and data was analyzed with FlowJo software (Version 10). Monocyte/macrophage populations were expressed as percent of the CD45+ population, T cell populations were expressed as percent of the CD45+ or CD3+ populations. IMC (n = 3, 4wks-post DMM): Whole knee joints were fixed, decalcified, paraffin embedded, and sectioned. Sagittal sections underwent heat-mediated antigen retrieval, and overnight incubation with a 22-marker multiplex panel of metal-conjugated antibodies, followed by incubation with Intercalator-Ir nuclear stain, and imaging using a Hyperion Imaging System (Standard Biotools). Spatial protein expression and cellular phenotype analysis (n = 3): Single cell masks were created using the nuclear stain (deepcell.org). IMACytE software was used to create t-distributed stochastic neighbor embedding (t-SNE) dimensionality reduction analysis with arcsin transformation to produce data normalization and cluster analysis.[6] Cell counts per cluster were exported for comparison between experimental groups. Statistical analysis: Student's t-test or two-way ANOVA (indicated in figure legends), with $p < 0.05$ considered significant.

Results

Initial analysis of immune cell populations via flow cytometry revealed general leukocyte (Ly6C−CD64−), monocyte (Ly6C+CD64−), and macrophage (Ly6C+CD64+) populations to be significantly increased compared to baseline following DMM in both WT and CD14−KO synovium (Figure 1A). Comparing

strains, the macrophage (Ly6C−CD64+) cell population was significantly decreased in CD14−KO mice compared to WT at 8-wks post DMM (Figure 1A). Further evaluations revealed T-helper cells (CD3+CD4+CD8−) to be increased in both WT and CD14-KO mice at 4wks post DMM (Figure 1B), however at 8wks post DMM the T-helper cell population in CD14-KO mice was significantly lower than in WT synovium (Figure 1B). IMC spatial protein analysis of synovial sections at 4-wks post DMM revealed notable differences in monocyte/macrophage marker expression (Ly6C, F480) within the synovial lining and sublining layers between WT and CD14-KO groups (Figure 2C,D). Dimensionality reduction analysis (t-SNE) revealed 12 unique cell populations across combined experimental synovial regions, with clustering by differential expression of vasculature (CD31), nerve (PGP9.5), monocyte/macrophage (Ly6C, F4/80, CD64, MHC-II, CX3CR1), T-cell (CD3), fibroblast, and other immune cell markers (Fig. 3A,B). The identified clusters could be localized throughout synovial lining and sublining layers (Figure 3C), and evaluation of cells within unique phenotype clusters revealed significant decreases in Cluster 2 ($p = 0.021$) and Cluster 8 ($p = 0.033$), and an increase in cluster 5 ($p = 0.026$) in CD14−KO synovium compared to WT at 4wks post DMM (Figure 3D).

Discussion

Flow cytometry analysis revealed significant changes within the synovium following DMM to innate (monocyte/macrophage) and adaptive (T-cells) immune cell populations that persist until at least 8-wks. In contrast, CD14 deficiency reduced the persistence of post-DMM elevations in CD64+ macrophages and CD3+CD4+ T helper populations by 8-wks (to near baseline), compared to WT controls at 8-wks. IMC further supported these results via spatial visualization of monocyte/macrophage and T cell markers across the two strains post DMM. Further, t-SNE analysis of the 22-marker IMC multiplex identified differences in cell cluster populations within CD14 deficient synovium compared to WT, with decreases in two distinct cell populations containing several immune cell markers (CD45, Ly6C, Ly6G, CD56), and fibrosis markers

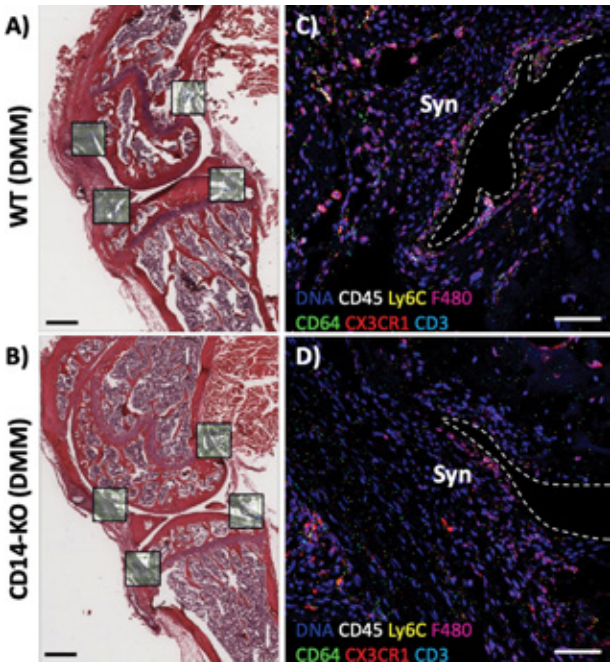

Figure 2. IMC staining of synovium post DMM. **(A,B)** H&E images of WT and CD14-KO knees 4wks post DMM, with ROIs indicating IMC spatial protein analysis (grey inset). **(C,D)** Subset of select monocyte/macrophage (Ly6C, F480, CD64, CX3CR1) and T-cell (CD3) marker expression within synovial ROIs. Synovial lining = dashed white line. Scale bars = 50μm.

(vimentin: VIM, tenascin C: TNC), and accompanied by an increased cell cluster expressing lining resident (CX3CR1) and general macrophage (F4/80) markers. As CD14 is commonly studied for TLR4-mediated inflammatory signaling, which can influence monocyte/macrophage phenotypic differentiation, it is possible that a global knockout of CD14 is mitigating this.2 Future work will further identify cell types within differential clusters, their spatial localization within the membrane, and temporal changes with disease.

Significance

These results reveal that CD14 deficiency produces distinct immune cell clusters with distinguishable spatial organization within the synovium following injury, providing mechanistic support for how CD14 deficiency may be protective against PTOA-associated pathology and mobility dysfunction.

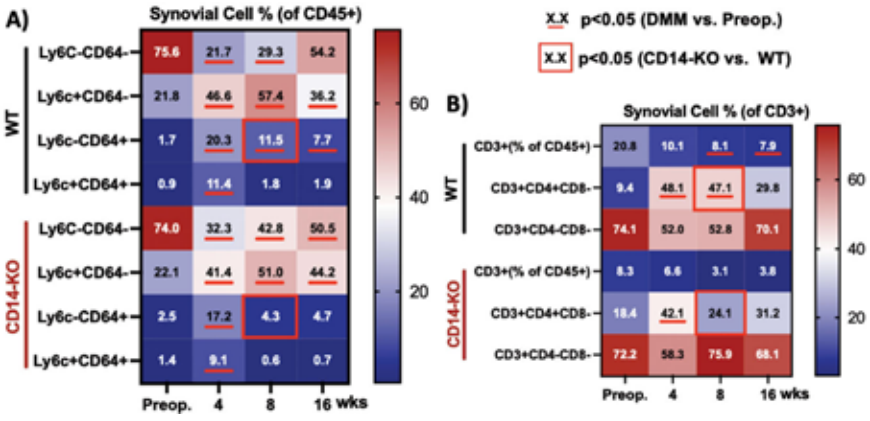

Figure 1. Flow cytometry analysis of synovial immune cell infiltration following DMM. **(A)** Heatmap of synovial CD45+ leukocyte (Ly6C-CD64-), monocyte (Ly6C+CD64-), and macrophage (Ly6C-CD64+, Ly6C+CD64+) cell populations (% of CD45+ synovial cells) and **(B)** T Cell (CD3+, CD3+CD4-CD8-), and helper T Cell (CD3+CD4+CD8-) populations (% of CD3+ synovial cells). $p<0.05$ significance by Student's T-test comparing groups (CD14-KO vs. WT) and 2-way ANOVA comparing time post DMM.

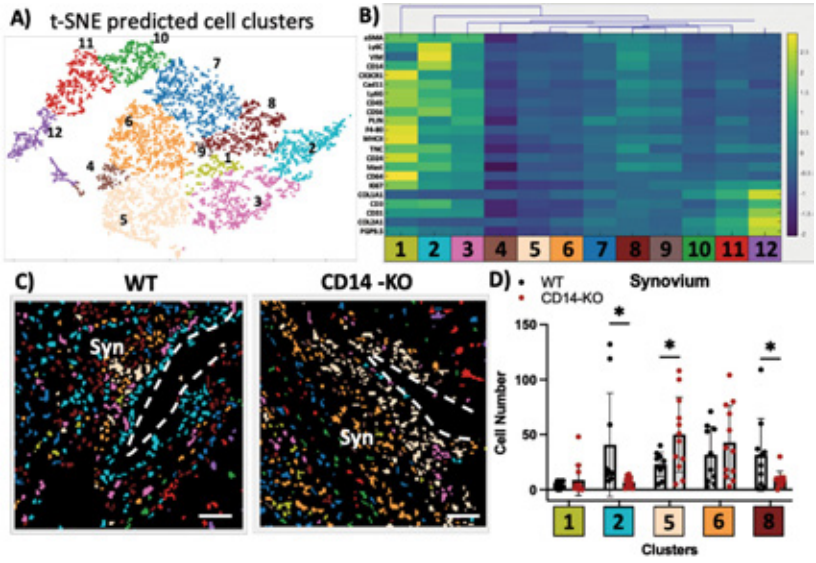

Figure 3. IMC analysis of synovial cell phenotypes post DMM. **(A)** Unique cell cluster analysis using t-SNE dimensionality reduction with IMC marker expression data. Data points represent individual cell masks from synovial ROIs across experimental groups. **(B)** Marker expression heatmap with cluster labels. **(C)** Single-cell unique phenotype cluster assignment within synovial ROIs. Synovial lining = white-dashed line. Scale bar = 50μm. **(D)** Cell number analysis within clusters between WT and CD14-KO DMM synovial ROIs. *p<0.05.

Acknowledgements

Caleb Marlin (OMRF) for IMC technical support. Funding, VA BLR&D (I01BX004912) and NIAMS (R01AR075737).

References

1. Loeser RF, Goldring SR, Scanzello CR, *et al.* Osteoarthritis: a disease of the joint as an organ. *Arthritis Rheum* 2012 Jun;64(6):1697-707.

2. Sanchez-Lopez E, Coras R, Torres A, *et al.* Synovial inflammation in osteoarthritis progression. *Nat Rev Rheumatol* 2022 May;18(5):258-275.

3. Sambamurthy N, Zhou C, Nguyen V, *et al.* Deficiency of the pattern-recognition receptor CD14 protects against joint pathology and functional decline in a murine model of osteoarthritis. *PLoS One* 2018 Nov 28;13(11):e0206217.

4. Moore KJ, Andersson LP, Ingalls RR, *et al.* Divergent response to LPS and bacteria in CD14-deficient murine macrophages. *J Immunol* 2000 Oct 15;165(8):4272-80.

5. Mobasheri A, Im GI, Katz JN, *et al.* Osteoarthritis Research Society International (OARSI): Past, present and future. *Osteoarthr Cartil Open* 2021 Feb 24;3(2):100146.

6. Somarakis A, Van Unen V, Koning F, *et al.* ImaCytE: Visual Exploration of Cellular Micro-Environments for Imaging Mass Cytometry Data. *IEEE Trans Vis Comput Graph* 2021 Jan;27(1):98-110.

Conditional Deletion of PTH/PTHrP Receptor 1 in Osteocytes Abolishes Lactation-induced Alterations in Canalicular Pericellular Space and Increases Bone Microstructure Deterioration

Xiaoyu Xu, PhD[1]
Yilu Zhou, PhD[1]
Rosa M. Guerra, BS[2]
Yongqiang Vincent Jin, MS[1]
Yuanhang Li, MS [1]
Wonsae Lee, PhD [1]
Tala Azar, PhD [1]
Kira Lu[1]
Liyun Wang, PhD[2]
X. Sherry Liu, PhD[1]

[1]McKay Orthopaedic Research Laboratory
University of Pennsylvania

[2]Center for Biomechanical Engineering Research
University of Delaware

Introduction

Pregnancy and lactation are unique physiological events for women that induce significant changes in maternal calcium and bone metabolism. Due to the demands of infant growth and milk production, the maternal skeleton experiences substantial mineral loss and structural deterioration during lactation, followed by partial recovery after weaning[1,2]. Osteocytes, the orchestrators of bone mass maintenance, have been considered to play a key role in lactation-induced maternal mineral metabolism by resorbing their surrounding bone matrix through perilacunar/canalicular remodeling (PLR)[3], resulting in a transient increase in dimensions of the lacunar canalicular system (LCS) in maternal bone during lactation. Moreover, our previous study suggested that increased dimensions of osteocyte LCS driven by PLR would amplify the transductions of mechanical and biochemical signals to osteocytes, leading to increased osteocyte mechanosensitivity, which in turn enhances the mechanical adaptation of the maternal skeleton to maintain its load-bearing function[4,5] (Figure 1A). However, the exact role of PLR in regulating maternal bone adaptations during lactation is still unclear. Therefore, the objective of this study was to investigate the impact of PLR on lactation-induced changes in the ultrastructure of the LCS and microstructure of the maternal bone. We hypothesized that abolishing osteocyte PLR would prevent changes in the pericellular matrix and LCS dimensions, leading to more significant bone loss and bone microstructure deterioration during lactation. In order to abolish lactation-induced PLR, PTH/PTHrP Receptor 1 (PPR) was conditionally deleted in osteocytes using a Dmp1-Cre; PPRfl/fl mouse model. Skeletal morphology, osteocyte LCS dimension, and pericellular ultrastructure were examined at different stages of reproduction to elucidate the role of osteocyte PLR in lactation-induced maternal alternations.

Methods

All animal experiments were IACUC approved. Animals: Female C57BL6 mice with osteocyte deletion of PPR (cKO: 14kb-Dmp1-Cre; PPRfl/fl) and the matched wildtype controls (WT: PPRfl/fl littermates) were both randomly assigned to three groups: Virgin, Lactation, and Post-weaning (n = 4-6 per group for both cKO and WT). Lactation and Post-weaning mice were mated at 11 and 9 weeks old, respectively, and underwent 3 weeks of pregnancy followed by 12 days of lactation. To ensure consistent suckling intensity, litter sizes were normalized to 5-6 pups per mother within 48 hours after birth. Post-weaning mice were allowed to recover for 14 days after 12 days of lactation. At 16 weeks old, Lactation and Post-weaning mice were euthanized with the age-matched Virgin mice. Histomorphometry: Longitudinal sections (6-μm) were prepared from the paraffin-embedded tibia (right) and subjected to Photon silver nitrate staining to evaluate the LCS dimensions in all groups (n = 3-4 per group; n = 30-35 lacunae per sample). Transmission electronic microscope (TEM): Bone marrow was washed out from the tibia (left) immediately after dissection. After fixation, the tibial midshaft was transversely cut into 1mm thick sections using a low-speed saw and processed for TEM imaging to analyze the ultrastructure of canaliculi (290-300 canaliculi per group). A Matlab program was developed to evaluate the pericellular area and cell process area of the osteocyte dendrites and the total canalicular area. μCT imaging: The trabecular bone of the lumbar vertebra L4 was scanned and analyzed using a microCT 45 (Scanco; 7.5 μm voxel size). Microstructural parameters, including bone volume fraction (BV/TV), trabecular thickness (Tb.Th), SMI, and connectivity density (Conn. D) were acquired. Statistics: One-way ANOVA with Bonferroni correction was used to detect the difference in relevant parameters across

Virgin, Lactation, and Post-weaning groups. Significant differences were considered when $p < 0.05$.

Results

In WT mice, 12-day lactation resulted in 20% and 9% greater lacunar area and perimeter, respectively, which returned to baseline levels as in Virgin mice 14 days after weaning (Figure 1B&C). These lactation-induced alternations were not found in mice lacking osteocyte PPR (Figure 1B-D). Although the number of canaliculi per lacuna remained consistent across Virgin, Lactation, or Post-weaning for both WT and cKO mice (Figure 1D), the ultrastructure of canaliculi adapted differently between WT and cKO mice during lactation. The pericellular area around osteocyte dendrites increased by 48% in WT lactating mice (Figure 1E), resulting in a 30% increase in total canalicular area compared to Virgin mice (Figure 1G). Following the weaning period, the recovery of canaliculi ultrastructure in WT mice was evidenced by the significant reduction in the pericellular area 14 days after weaning (Figure 1E). Unlike the alternation in WT mice, deleting PPR in osteocytes mitigated lactation-induced increases in pericellular and canalicular areas (Figure 1E&G). Moreover, the post-weaning recovery observed in WT did not appear in cKO mice, as both pericellular and canaliculi areas remained elevated after 14 days post weaning (Figure 1E&G). The dendrite process area remained at similar levels at different reproductive stages in WT and cKO mice (Figure 1F). At the tissue level, cKO mice displayed greater bone loss and microstructure deterioration during lactation than WT mice, demonstrated by significant reductions in BV/TV (−48%), Tb.Th (-26%), Conn.D (-34%), and a higher SMI (2.5 in cKO vs. 2.23 in WT) in cKO relative to WT (Figure 1H-K). Nevertheless, both WT and cKO mice fully recovered in bone microstructure post weaning (Figure 1H-K).

Discussion

Our results demonstrated the important role of osteocyte PLR in mediating alternations of the LCS ultrastructure and maternal bone microstructure in response to lactation. By deleting PPR in osteocytes, lactation-induced osteocyte PLR activities were abolished in the mouse maternal skeleton, demonstrated by the unchanged lacunar area and perimeter across different reproductive statuses in the cKO mice. TEM results provided further evidence of the functions of osteocyte PLR in altering the pericellular matrix of osteocyte dendrites and dimensions of canaliculi during lactation. According to the LCS fluid flow model established by Weinbaum et al.,[6] the enlarged LCS and pericellular fluid space could contribute to increased flow-mediated mechanical stimulation and enhanced mechano-signals on osteocytes and their processes when subjected to loading, thus enhancing bone's mechano-responsiveness during lactation. This may partially explain the accelerated

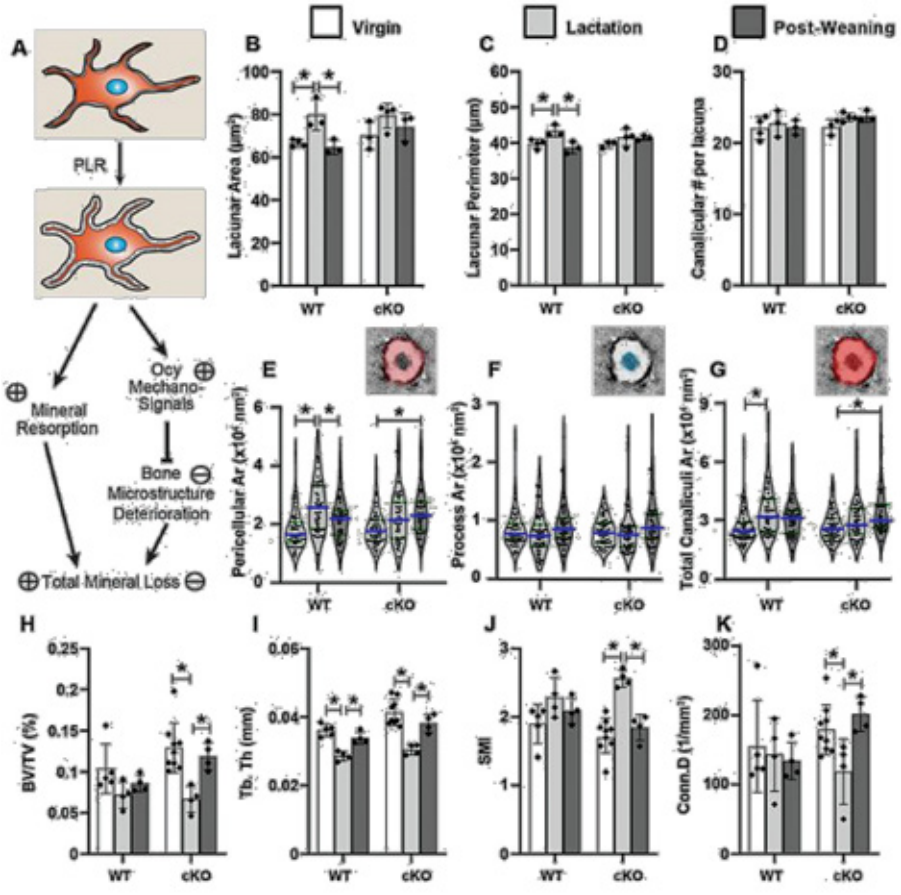

Figure 1. (A) Schematic diagram of osteocyte PLR regulation of mineral resorption and bone mechanical integrity. **(B)** Lacunar area, **(C)** lacuna perimeter, and **(D)** canaliculi number per lacuna derived from Ploton silver nitrate staining images of cKO and WT mice with different reproductive statues. **(E)** Pericellular area of Ocy dendrite processes (area between the two red dashed lines), **(F)** process area (central area highlighted in blue), and **(G)** total canaliculi area (the area highlighted in red). **(H-K)** L4 trabecular bone morphology in cKO and WT Virgin, Lactation, and Post-weaning mice. Asterisk (*) indicates a significant difference among Virgin, Lactation, and Post-weaning of cKO and WT mice by one-way ANOVA ($p<0.05$).

bone loss in lactating cKO mice with lactation-induced osteocyte PLR significantly inhibited.

Significance

This is the first study that quantified the lactation-induced alterations in canaliculi ultrastructure and demonstrated active remodeling of the pericellular matrix surrounding osteocyte dendrites during lactation and post-weaning. Future studies will continue to elucidate the critical roles of osteocyte PLR in regulating the balance between mineral resorption and mechanical integrity of the maternal skeleton.

References

1. Kovacs C. Maternal Mineral and Bone Metabolism During Pregnancy, Lactation, and Post-Weaning Recovery. *Physiol Rev*, 2015; 96(2): 449-547.

2. Liu XS, Wang L, de Bakker C, *et al.* Mechanical Regulation of the Maternal Skeleton during Reproduction and Lactation. *Biomech*, 2019; 17(6): 375-386.

3. Hai Q, Ardeshirpour L, Pajevic P, *et al.* Demonstration of osteocytic perilacunar/canalicular remodeling in mice during lactation. *JBMR*, 2012; 27(5): 1018-1029.

4. Lai X, Chung R, Li Y, *et al.* Lactation alters fluid flow and solute transport in maternal skeleton: A multiscale modeling study on the effects of microstructural changes and loading frequency. *Bone*, 2021; 151.

5. Li Y, de Bakker C, Lai X, *et al.* Maternal bone adaptation to mechanical loading during pregnancy, lactation, and post-weaning recovery. *Bone*, 2021; 151

6. Weinbaum S, Cowin S, and Zeng Y. A model for the excitation of osteocytes by mechanical loading-induced bone fluid shear stresses. *J Biomech*, 1994; 27(3): 339-360.

Mechanical Properties of 3D Printed Clavicles are Closer to Cadaveric Bones than 4th Generation Sawbones

Kathryn S. Strand, BS
Elizabeth Silvestro, MS
Iman Naqvi
Michael W. Hast, PhD

McKay Orthopaedic Research Lab, Department of Orthopaedic Surgery, University of Pennsylvania, Philadelphia, PA

Introduction

Synthetic bone models have increasing utility in experimental research and education.[1] Their benefits include lower costs, less variability than cadaveric bone, no institutional oversight, and no ethical considerations. Commercially available synthetic bones (4th Generation Sawbones) are created with injection molding techniques and have been validated to be equivalent to human bones in a variety of way.[2,3] The rise in additive manufacturing (AM) presents an opportunity for synthetic bone models to be custom-made for mechanical testing purposes. Little is known about the efficacy of these custom 3D printed models. Prior studies have examined the mechanical properties of AM bones, but they only tested small segments of bone and did not evaluate 3D prints under varied loading conditions.[4,5] The clavicle is an attractive testbed for such testing for several reasons. First, clavicular fractures are difficult to repair surgically, and implant design testing could benefit from an improved model. Second, the clavicle is the only horizontal long bone and undergoes a wide variety of loading paradigms during activities of daily living.[6] Applying different and physiologically relevant loading paradigms allows for a thorough analysis. Thus, the purpose of this study was to directly compare the mechanical properties of 3D printed, commercially available, and human cadaveric clavicles under variable loading scenarios. We hypothesized that 3D printed clavicles would better mimic the human condition in axial compression and bending, but not in torsion due to the layered structure of the AM specimens.

Methods

Four different experimental groups (n = 6) were analyzed for this study; fresh-frozen human cadaveric clavicles (3 left, 3 right, from 3 donors, 2 M, 1F, aged between 65-68 years), two groups of 3D printed clavicles printed in Verowhite (VW) and a composite of TissueMatrix and BoneMatrix (TB), and commercially available 4th generation Sawbones (SB) composite clavicles (Model 3408-1; Pacific Research Laboratories, Vashon, WA). Custom models were fabricated with a Stratasys (Eden Prairie, MN) J850 Digital Anatomy Printer. All samples were oriented to print layers along the long axis of the bone. Mechanical tests included nondestructive 4-point bending, torsion, and axial compression in a randomized order, followed by a final compressive test to failure. Testing protocols were based on previous studies and utilized triangular waveforms.[7] All specimens were potted in poly(methyl methacrylate) (PMMA) and loaded on a universal test frame (Electroforce 3550, TA Instruments, Eden Prairie, MN) with a 15 kN load cell. For 4-point bending, the upper anvils were displaced a total of 1 mm at 0.25 Hz for 10 cycles [7]. Bending was applied in both the anterior-posterior (AP) and superior-inferior (SI) directions and bending rigidity was calculated. For compressive and torsional testing, specimens were oriented vertically with the lateral end positioned upwards. Compressive testing loaded specimens between 10 and 315 N for 10 cycles 8. Torsional testing rotated specimens to $\pm 3°$ at 0.25 Hz for 500 cycles, and torsional rigidity was averaged across cycles 10, 100, 200, 300, 400, and 500 for anterior and posterior rotation of the sternal end [8]. For compressive testing to failure, specimens were compressed at a rate of 0.63 mm/sec.[9] Significant differences between groups were tested with a one-way ANOVA with Holm-Sidak post-hoc tests ($p < 0.05$). When tests for normality and equal variances failed ($p < 0.05$), Kruskal-Wallis tests with a Dunn's post-hoc was used.

Results

Results from torsional testing indicated that the SB group was significantly stiffer than Cadaveric and TB groups, respectively (Figure 1). Bending tests also showed that the SB group had higher bending rigidity than all groups in the SI direction (Figure 2A), but these findings were not as clear in AP bending. Notably, cadaveric samples had higher bending rigidity than the TB group during both bend tests, and higher bending rigidity

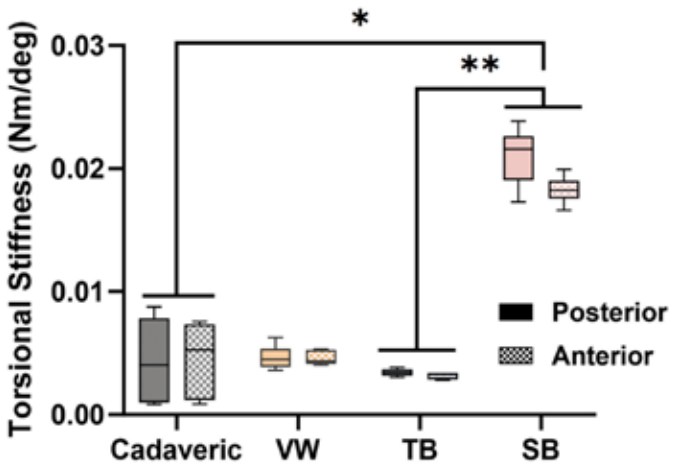

Figure 1. Average torsional stiffness **p<0.01.

than the VW group in the SI bend tests (Figure 2A&B). The axial stiffness of the SB group was significantly higher than the Cadaveric, VW, and TB groups, but there were no differences between the cadaveric specimens and either 3D printed group (Figure 3A). The compressive failure loads for Cadaveric, SB, VW, and TB groups were 3350 ± 1999 N, 4670 ± 969 N, 2611 ± 321 N, and 1883 ± 282 N, respectively, with significant differences between SB and TB groups (Figure 3B).

Discussion

We observed no differences between the Cadaveric and VW groups in any testing condition except for SI 4-point bending. Additionally, the SB group was significantly different from the cadaveric specimens in every outcome measure except for AP 4-point bending. These results demonstrate that commercially available synthetic models may be too rigid to accurately emulate the mechanical behavior of cadaveric clavicles. These findings partially disprove our original hypothesis that the layered materials in AM specimens would fail easily in torsional testing. As expected, the cadaveric group had the most variability across all outcome measures. However, the variances within the 3D oriented groups (TB and VW) were much lower, demonstrating consistency within this printing method which may lead to less noisy mechanical testing outcomes. Taken together, these results demonstrate that AM bone models can effectively mimic the mechanical behavior of human bones under a variety of physiological conditions. In particular, our findings suggest that the VW materials and printing protocol may be an attractive option for 3D printed complete synthetic bone models in both torsion and axial/transverse loading conditions.

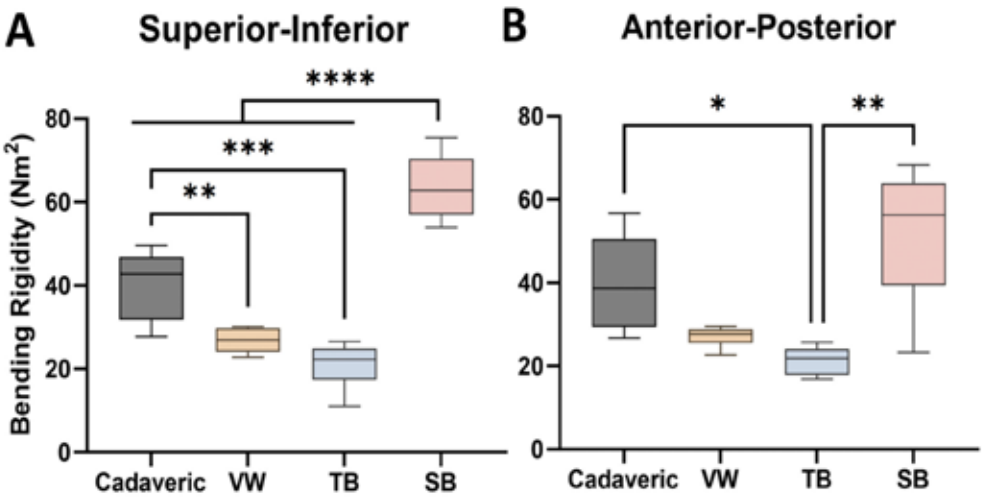

Figure 2. Average bending rigidity across 10 cycles in the **(A)** SI and **(B)** AP directions. *p<0.05, **p<0.01, ***p<0.001, ****p<0.0001.

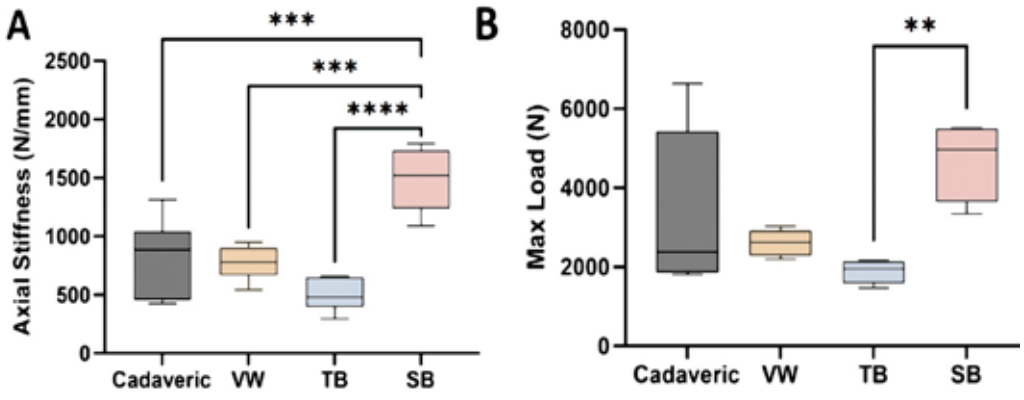

Figure 3. Axial compression testing results. **(A)** Average axial stiffness across 10 cycles; **(B)** Maximum loads during compressive failure tests. **p<0.01, ***p<0.001, ****p<0.0001.

Significance/Clinical Relevance

The results of this study suggest that AM specimens created with VW material are the most comparable to human cadaveric tissues under varied mechanical loading conditions. These findings present AM bone models as an accessible and physiologically relevant option, opening doors to utilize AM in developing patient-specific bone models for more wholistic and clinically relevant mechanical testing applications.

References

1. Elfar J, Stanbury S, Menorca RMG, *et al.* Composite Bone Models in Orthopaedic Surgery Research and Education. J Am Acad Orthop Surg. 2014;22(2):111-120.

2. Chong ACM, Miller F, Buxton M, *et al.* Fracture Toughness and Fatigue Crack Propagation Rate of Short Fiber Reinforced Epoxy Composites for Analogue Cortical Bone. J Biomech Eng. 2007;129(4):487-493.

3. Chong ACM, Friis EA, Ballard GP, *et al.* Fatigue Performance of Composite Analogue Femur Constructs under High Activity Loading. Ann Biomed Eng. 2007;35(7):1196-1205.

4. Husemoglu RB, Baysan G, Ertugruloglu P, *et al.* The Mechanical Comparison of Artificial Bone and 3D Printed Bone Segments. J Med Innov Technol. 2020;2(2):127-130.

5. Nägl K, Reisinger A, Pahr DH. The biomechanical behavior of 3D printed human femoral bones based on generic and patient-specific geometries. 3D Print Med. 2022;8(1):35.

6. Iannolo M, Werner FW, Sutton LG, *et al.* Forces across the middle of the intact clavicle during shoulder motion. J Shoulder Elbow Surg. 2010;19(7):1013-1017.

7. Schmidt EC, Dear KA, Hendow C, *et al.* Examining the novel use of continuous compression implants in clavicle reconstruction: A biomechanical study. *Clin Biomech.* 2021;88:105437.

8. Uzer G, Yildiz F, Batar S, *et al.* Biomechanical comparison of three different plate configurations for comminuted clavicle midshaft fracture fixation. *J Shoulder Elbow Surg.* 2017;26(12):2200-2205.

9. Sánchez-Molina D, García-Vilana S, Velázquez-Ameijide J, *et al.* Probabilistic assessment for clavicle fracture under compression loading: rate-dependent behavior. *Biomed Eng Appl Basis Commun.* 2020;32(05):2050040.

Cartilage, Meniscus and Disc

In Situ and *In Vivo* Mechanoactivation of Anti-Inflammatory Tension-Activated Repair Patches

Mohammed S. Abdullah[1,2]
Bijan Dehghani[1,2]
Caitlin Barrett[1,2]
Kevin G. Burt[1,2]
Robert L Mauck[1,2]
Thomas P. Schaer[1,2]
Harvey E. Smith[1,2]
Sarah E. Gulbrand[1,2]

[1]Department of Orthopaedic Surgery
Perelman School of Medicine
University of Pennsylvania
Philadelphia, PA

[2]Translational Musculoskeletal Research Center
Corp. Crescenz VA Medical Center
Philadelphia, PA

Disclosures: MA mohammed.abdullah@pennmedicine.upenn.edu—(N), BD (N), CB (N), KGB (N), RLM (4,5,8), HES (N), SEG (6)

Introduction

Two percent of the world is affected by disc herniations, which are associated with tears the annulus fibrosus (AF) due to injury or advanced intervertebral disc degeneration. The management of disc herniations through microdiscectomy surgery can alleviate symptoms but leaves the annulus unrepaired. Due to the poor capacity of the AF to heal following injury, 10-30% of patients experience recurrent disc herniation.[1] The lack of repair and the acute inflammation that arise after injury further compromises the disc and can result in disc-wide degeneration in the long term. To address this clinical need, we developed tension-activated repair patches (TARPs) for annular repair. TARPs transmit physiologic strains to mechanically-activated microcapsules (MAMCs) embedded within, which activate and release encapsulated biomolecules in response to physiologic loading.[2,3] In this study, we assessed in vitro and in situ activation thresholds for the MAMCs within the TARPs. Furthermore, we evaluated in vivo expression of physiologically relevant proinflammatory cytokines and neurofilament proteins in the anterior and posterior AF after TARP repair to determine if TARP- mediated delivery of an anti-inflammatory drug (IL-1Ra, Anakinra) improved repair.

Methods

In Vitro and In Situ TARP Mechanoactivation: TARPs were fabricated by melt-stamping MAMCs between two hydrated PCL-PEO scaffold strips, 10 mm in length and 3.5 mm in width. Mechano-activation strain thresholds for MAMCs were established in vitro via 1,800 cycles of tensile loading at varying strain levels (0%, 2%, 4%, 6%, 8%, n = 5 samples/strain level, Figure 1A). For in situ testing, a 5 mm × 2.5 mm cruciate laceration was created in the anterior annulus of goat cervical vertebra-disc-vertebra motion segments, with full thickness needle puncture (2.1 mm diameter) to the nucleus. TARPs were sutured to the AF overlying the defect using 6-0 Gortex suture. Seven motion segments were then subjected to 1,800 cycles of cyclic compression from 0 to 300N at 1Hz (Figure 1E-F). Four additional motion segments were utilized as unloaded controls. Following in situ and in vitro mechanical loading, each TARP was gently peeled apart and fluorescent microscopy was utilized to image the outer shell (580nm) and the inner contents (AlexaFluor 488nm) to quantify the number of full versus empty MAMCs. In Vivo TARP Annular

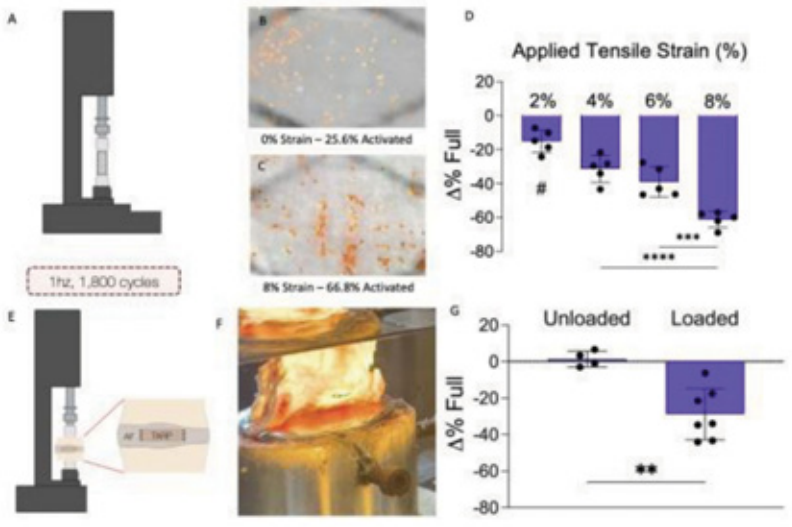

Figure 1. (A) Schematic of uniaxial tension loading of the TARPs. **(B-D).** Image and quantification of MAMC activation across a range of applied tensile strains. **(E-F).** Schematic and photograph of in situ testing of the TARP and **(G).** Quantification of MAMC activation. * $p<0.05$, # $p<0.05$ compared to all other groups.

Repair: To study the physiologic consequences of TARP mechanoactivation and local release of Anakinra (IL-1Ra), BSA-loaded TARPs (E-TARPs) and Anakinra loaded TARPs (A-TARPs) were implanted in a large animal cervical disc annular injury model.[2] Following IACUC approval, eight female goats underwent annular injury of the cervical intervertebral discs, as described above, followed by repair with either the E-TARP (n = 4) or A-TARP (n = 4) over the injury site at either C2-3. C3-C4 served as an injury-only control. Four weeks post-repair, animals were euthanized and isolated motion segments were processed for histology, sectioned in the sagittal plane at 10μm, and stained with picrosirius red and imaged with polarized light microscopy. Immunofluorescence was performed on additional sections to assess protein expression levels of inflammatory cytokines (TNF-α and IL-6) along with expression of Neurofilament Heavy Chain (NFH) and Protein Gene Product (PGP 9.5). Mean fluorescent intensity (MFI) and % fluorescent area were quantified in the anterior and posterior AF for each level using Image J. Statistical analysis was performed via one-way ANOVA with a Tukey's post-hoc test.

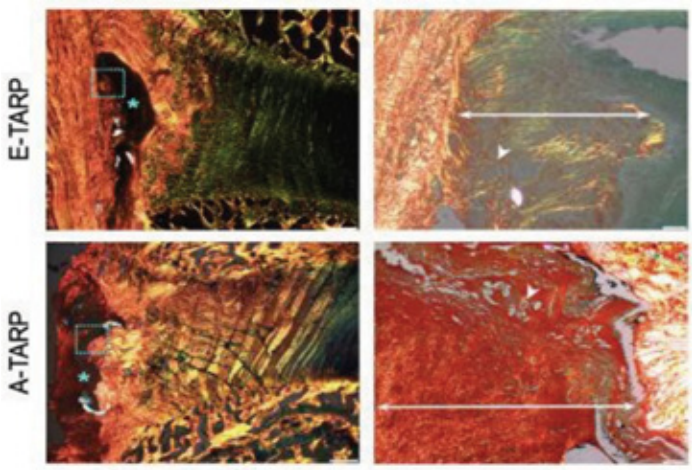

Figure 2. Polarized light microscopy of the anterior annulus of TARP repaired discs. The * denotes location of TARP, the right panel is a higher magnification (scale=100μm) of the area denoted in the dashed box on the left panel (scale=1mm).

Results

In vitro and in situ TARP mechanoactivation: Tensile loading of the TARP in vitro resulted in increasing MAMC activation with increasing levels of applied strain (Figure 1B-C). Compressive loading of spinal motion segments resulted in circumferential strain transfer through the disc to the TARP, significantly increasing MAMC rupture compared to TARPs sutured to the AF but not loaded (Figure 1G). In Vivo TARP Repair: Polarized light microscopy revealed increased collagenous matrix accumulation in the anterior annulus of the A-TARP group, compared to the E-TARP group, at 4 weeks post-repair (Figure 2). Post hoc analysis demonstrated a substantial reduction in the % area and MFI of inflammatory and nerve markers between the injury and E-TARP repaired levels, averaging 96% and 76%, respectively ($p < 0.05$). When comparing the A-TARP repair to the injury model, there was an 82% reduction in inflammation ($p = 0.053$) and a 76% decrease in nerve markers ($p = 0.24$), as assessed via MFI (Figure 3).

Discussion

Our studies demonstrated that MAMC rupture within the TARPS occurs in response to directly applied tensile strain and under tensile strains translated to the TARP in situ during compressive loading of the disc. In vivo, we observed an increase in collagenous matrix deposition in the anterior annulus of the A-TARP group, suggesting that the Anakinra released from the TARPS may have contributed towards enhanced AF repair. Furthermore, TARP repair demonstrated a significant attenuation of innervation and inflammation in the annulus compared to the unrepaired injury in both TARP groups. Interestingly, we observed a trend towards increased innervation and inflammation in the A-TARP group compared to the E-TARP group. Our prior studies in other joints suggest the most MAMC cargo is released over 2 weeks,[4] so it may be that the time course of inflammation and repair is shifted in the A-TARP group. Amid limited clinical alternatives, this work advances a novel annular repair strategy, bringing it closer

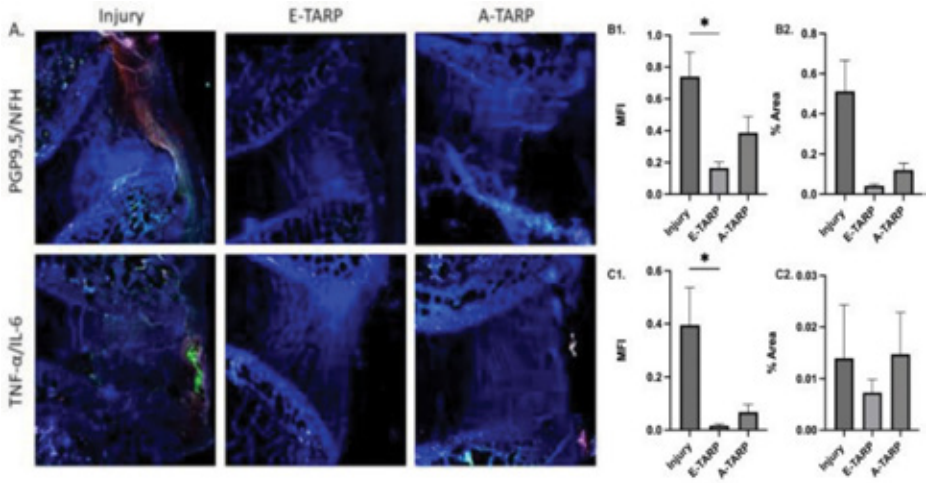

Figure 3. (A) Immunofluorescence microscopy of the annulus across Injury, E-TARP, and A-TARP groups (red = NFH & TNF-α, green = PGP 9.5 & IL-6). Quantification of MFI and % area in the anterior and posterior annulus for **(B)** PGP 9.5 & NFH and **(C)** TNF-α and IL-6. *p<0.05.

to clinical implementation for patients grappling with back pain resulting from disc herniation.

Acknowledgements

This study was supported by the Department of Veterans' Affairs.

References

1. Peredo AP, Jo YK, Duan G, Dodge GR, Lee D, Mauck RL. Mechano-activated biomolecule release in regenerating load-bearing tissue microenvironments. *Biomaterials*. 2021

2. Mohanraj B, Duan G, Peredo A, Kim M, Tu F, Lee D, Dodge GR, Mauck RL. Mechanically-Activated Microcapsules for 'On-Demand' Drug Delivery in Dynamically Loaded Musculoskeletal Tissues. *Adv Funct Mater*. 2019

3. Zlotnick HM, Locke RC, Hemdev S, Stoeckl BD, Gupta S, Peredo AP, Steinberg DR, Carey JL, Lee D, Dodge GR, Mauck RL. Gravity-based patterning of osteogenic factors to preserve bone structure after osteochondral injury in a large animal model. *Biofabrication*. 2022

4. Peredo AP, Gullbrand SE, Mauck RL, Smith HE. A challenging playing field: Identifying the endogenous impediments to annulus fibrosus repair. *JOR Spine*. 2021 Feb 11;4(1):e1133.

Viscous Hyaluronic Acid Carriers Enhance the Stability of Therapeutic Mechanically-Activated Microcapsules

Austin C. Jenk, BS[1,2,3]
Eric A. Schweppe, MD[2]
Elisabeth A. Lemmon, BS[1,2,3]
Sarah E. Gullbrand, PhD[1,2,3]
Robert L. Mauck, PhD[1,2,3]

[1]Departments of Bioengineering
University of Pennsylvania

[2]Department of Orthopaedic Surgery
University of Pennsylvania

[3]Translational Musculoskeletal Research Center
Corporal Michael J. Crescenz Veterans Affairs Medical Center

Introduction

Acute knee injuries are common among accident victims, athletes, and military service members and induce diverse pathogenic cascades that often result in post-traumatic osteoarthritis (PTOA). Despite active research, there are still no FDA-approved disease modifying OA drugs that focus on early intervention to delay, attenuate, or altogether prevent PTOA. Furthermore, the efficacy of current drug delivery platforms is limited by short half-lives and rapid joint clearance.[1,2] To this end, we developed mechanically-activated microcapsules (MAMCs), which are capable of prolonging residence time within the joint while delivering an array of therapeutic factors.[3,4] However, the relatively short therapeutic "window of opportunity" following an acute knee injury necessitates an "off-the-shelf" solution.[5,6] End-users, such as first responders, emergency department providers, and military medical personnel will require ready access to these therapeutics. However, they must also follow stringent design criteria to enable use in austere environments.[7] Like any microcapsule-based drug delivery system, MAMCs are susceptible to degradation from physical agitation and temperature changes. Our objective was to determine the resilience of MAMCs under environmental stressors and identify a clinically relevant carrier capable of providing physical and thermal protection. We hypothesized that viscous, high molecular weight hyaluronic acid (HA) solutions (EUFLEXXA®) would provide both physical and thermal protection to MAMCs and increase their retention of therapeutic contents in environmental stress.

Methods

MAMCs

MAMCs containing IL-1Ra (anakinra, KINERET®) were fabricated as previously described and stored in PBS at 4° until use. Before testing, MAMCs were suspended in a microtube in either 50% v/v PBS +/− 10% w/v trehalose or 50% v/v HA. MAMC percent (%) full was determined by confocal microscopy (Figure 1). ImageJ was used to quantify the total number of MAMCs and the number of intact (full) MAMCs. The % of full MAMCs was normalized to the original % full for each group to account for differences in starting values. After each test, MAMCs were incubated overnight at 4° to allow complete diffusion of the inner contents after rupture.

Physical and Thermal Stress Tests

To identify a carrier system for MAMCs and to evaluate their clinical and commercial translatability, rigorous physical and thermal stress tests were conducted, with the primary outcome being MAMC % full. To evaluate MAMC physical stability and the protecting capabilities of the HA carrier, MAMCs were agitated using a benchtop vortex mixer on the most vigorous setting for 10-60 min. To assess injectability across a range of clinically relevant needle sizes, MAMCs were loaded

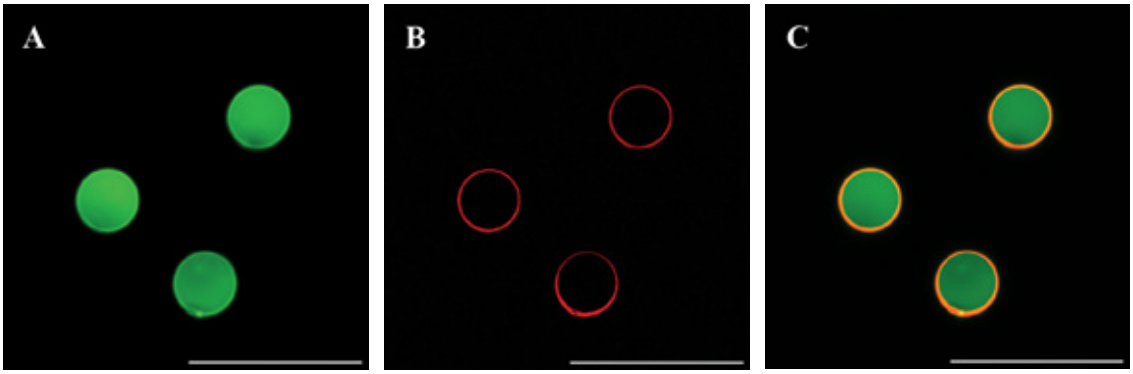

Figure 1. Mechanically-Activated Microcapsules (MAMCs). Fluorescent images of MAMCs showing their **(A)** inner therapeutic contents, **(B)** PLGA shell, and **(C)** merged composite. MAMC diameter: 38.2 μm, shell thickness: 2.3 μm, 60×, scale bar: 100 μm.

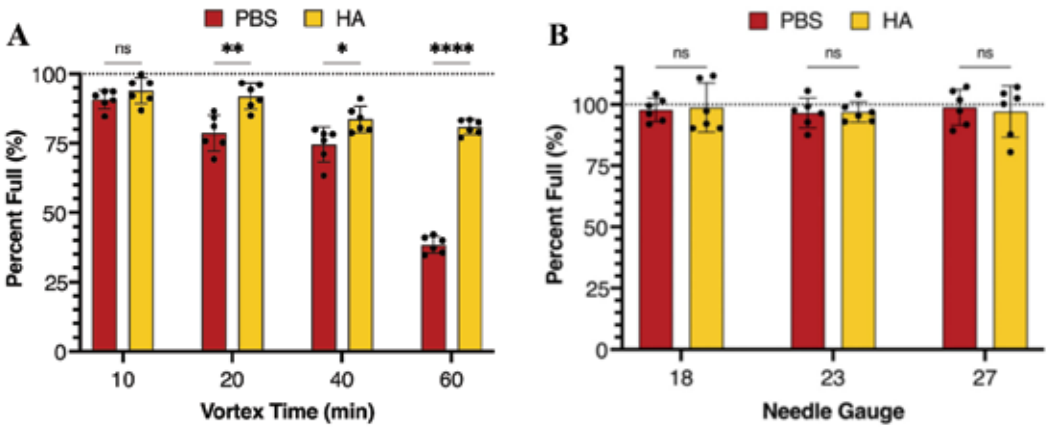

Figure 2. MAMC Physical Stability. **(A)** MAMC % full after physical agitation using a benchtop vortex mixer over 60 min; **(B)** MAMC % full after a single ejection at 10 mL/min through 18-, 23-, and 27-gauge needles. n=6, mean +/− SD, *p≤0.05, **p≤0.01, ****p≤0.0001.

into 3 mL syringes and ejected at 10 mL/min through 18-, 23-, and 27-gauge needles. To evaluate payload retention after freeze-thaw, an expected step in both the clinical and commercial cold chain, MAMCs were frozen at −20° for 30 min and thawed at 20° for 30 min over 1-5 freeze-thaw cycles. To assess the effect of temperature on payload retention, MAMCs were stored at −20, 4, 20, 37, and 50°, and % full was quantified on day 1, 3, and 7. Percent full was normalized to the 4° values on day 1.

Statistics

For all studies, n = 6/group with mean +/− SD shown. Two-way ANOVA with Fisher's LSD was used to compare carrier groups and treatment condition; $p \leq 0.05$.

Results

MAMCs suspended in HA were more resilient to physical agitation over longer durations compared to those

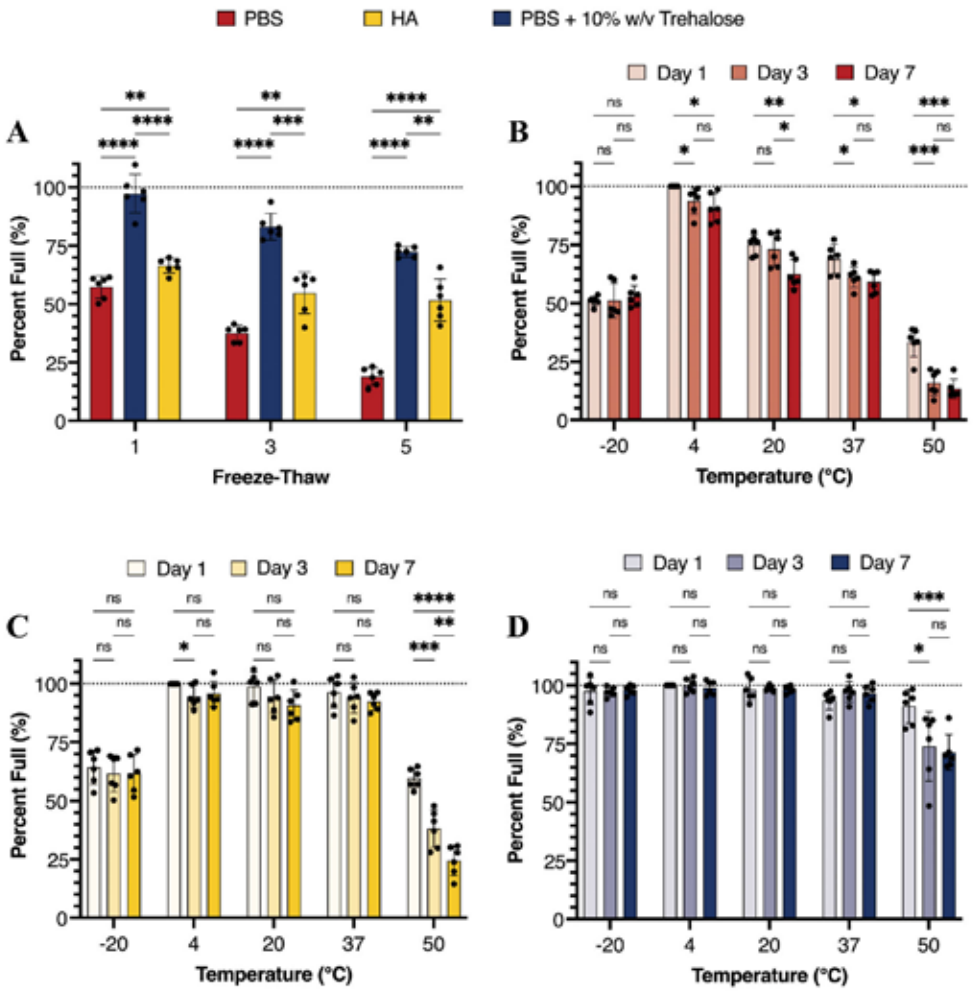

Figure 3. MAMC Thermal Stability. **(A)** MAMC % full after repetitive freeze-thaw cycles at −20° and 20°, respectively; MAMC % full after 1, 3, and 7 days of storage at −20 to 50° in **(B)** PBS, **(C)** HA, or **(D)** PBS+10% w/v trehalose. % full normalized to day 1, 4° values. n=6, mean +/− SD, *p≤0.05, **p≤0.01, ***p≤0.001, ****p≤0.0001.

suspended in PBS (Figure 2A). MAMCs ejected through 18-, 23-, and 27-gauge needles showed no difference in payload retention (Figure 2B). Subsequent freeze-thaw cycles ruptured MAMCs in a stepwise manner regardless of carrier, but the addition of 10% w/v trehalose or suspension in HA significantly increased cryoprotection at each cycle (Figure 3A). When suspended in PBS, MAMCs experienced significant loss of inner contents at 4, 20, 37, and 50° over 7 days (Figure 3B). In HA, MAMCs experienced no loss of inner contents at 4, 20, and 37° over 7 days (Figure 3C). In PBS+10% w/v trehalose, MAMCs did not experience any payload loss from -20 to 37° over 7 days (Figure 3D). In all carriers, the duration of storage at −20° with a single freeze-thaw cycle had no impact on MAMC payload retention (Figure 3B-D).

Discussion

Our findings show that suspension of MAMCs in HA confers significant physical and thermal protection to MAMCs and increases their payload retention when exposed to environmental stressors. HA increased MAMC physical stability after extended durations of high frequency agitation, circumstances that would be expected to be encountered in ambulances, MEDEVAC aircraft, or within the medical bags of first responders and military medical personnel. MAMCs withstood ejection from a wide range of needle gauges in both PBS or HA, facilitating use in small animal studies and patients with varying joint sizes. The use of trehalose, a common cryoprotectant, or suspension in HA, increased MAMC stability to repetitive freeze-thaw cycles. This finding diversifies and extends the shipping and storage parameters for these delivery systems. The use of HA and trehalose also maintained MAMC payload retention at 4, 20, and 37° over 7 days, which facilitates their "off-the-shelf" use where conventional refrigerated or frozen storage environments are not feasible, such as within resource-limited clinics or forward military bases. Future studies will assess the bioactivity of MAMC contents after exposure to physical and thermal stresses to ensure no loss of therapeutic efficacy and will assess how the HA carrier affects joint retention and localization of MAMCs after intra-articular injection. Overall, these data indicate the use of an HA carrier can prolong MAMC lifespan by retention of their inner contents, thus enabling the deployment of MAMCs in austere conditions and under physical and thermal environmental stress.

Significance and Clinical Relevance

This work establishes important storage and handling parameters for a novel drug delivery system and identified an FDA-approved, clinically available HA carrier that increases the physical and thermal stability of therapeutically loaded microcapsules. Our findings show that an HA carrier can be used to increase the therapeutic lifespan of microcapsules containing an anti-inflammatory factor, thus enabling their use in "off-the-shelf" applications, such as emergency or battlefield medicine.

References

1. **Burt HM, Tsallas A, Gilchrist S, *et al.***, *Expert Opin. Drug Deliv*, 2009.
2. **Rai MF and Pham CT,** *Pharmacol.*, 2018.
3. **Mohanraj B, Duan G, Peredo AP, *et al.***, *Adv. Funct. Mater.*, 2019.
4. **Peredo AP, Jo YK, Duan G, *et al.***, *Biomaterials*, 2021.
5. **Watt FE, Corp N, Kingsbury SR, *et al.***, *Osteoarthritis Cartilage*, 2019.
6. **Mason D, Englund M, and Watt FE,** *J. Orthop. Res.*, 2021.
7. **Dolan CP, Valerio MS, Childers WL, *et al.***, Npj Regen. *Med.*, 2021.

CD14 inhibition as a potential therapeutic for posttraumatic osteoarthritis.

Kevin G. Burt[1,2]
Vu Nguyen[1,2]
Lance A. Murphy[1,2]
Robert L. Mauck[1,2]
Anne-Marie Malfait[3]
Rachel E. Miller[3]
Carla R. Scanzello[1,2,4]

[1]Department of Orthopaedic Surgery, Perelman School of Medicine, University of Pennsylvania, Philadelphia, PA

[2]Translational Musculoskeletal Research Center, Corp. Crescenz VA Medical Center, Philadelphia, PA

[3]Department of Internal Medicine, Division of Rheumatology, Rush Medical College Chicago, IL

[4]Division of Rheumatology, Perelman School of Medicine, University of Pennsylvania, Philadelphia, PA

Disclosures

KGB (N)—kevin.burt@pennmedicine.upenn.edu, VN (N), LAM (N), REM (N), AMM (3,8), RLM (4,5,8), CRS (8)

Introduction

Osteoarthritis (OA) is the most common joint disorder, and growing evidence has identified inflammation as a major driver of disease progression. During progression, the synovium serves both as a source and reservoir for inflammatory mediators and immune cells, including monocyte/macrophages.[1] Though temporary pain relief is offered by non-steroidal anti-inflammatory therapeutics, no therapies have been able to halt or delay disease progression. One potential therapeutic target, soluble CD14, a co-receptor of inflammatory toll-like receptor signaling, produced primarily by activated macrophages, is present in synovial fluid in patients with OA and is positively associated with joint space narrowing and pain.[2] We previously reported that global genetic CD14 deficiency in mice protects against OA-associated bone-remodeling and pain-related joint dysfunction.[3] Towards translation, we hypothesize that an anti-CD14 therapeutic will attenuate inflammatory activation in the synovium during OA and mitigate disease progression and pain.

Methods

A model (n = 12 − 14): We performed destabilization of the medial meniscus (DMM) surgery to induce OA in skeletally mature (10-12 wk old) C57BL/6 mice.[4] Intervention: Mice were treated intra-articularly with either an anti-CD14 monoclonal antibody (mAb, clone biG53) or an IgG2a control (both 0.5mg/kg). Two dosing strategies were tested: 1) Prevention strategy: mice received anti-CD14 or IgG control 3 weekly doses, starting 48 hrs post DMM. 2) Treatment strategy: mice received 3 weekly injections beginning 4 wks post DMM. Behavioral analyses: At 4- and 8 wks-post DMM, evaluation of spontaneous cage behaviors was performed using the Laboratory Animal Behavior Observation Registration and Analysis System (LABORASTM, Metris).[3] Additionally, paw weight bearing distribution was measured via the Advanced Dynamic Weight Bearing (ADWB, Bioseb) system.[5] Histopathology analysis (n = 5): All mice were sacrificed at 8-wks post DMM, and knee joints were fixed, decalcified, paraffin embedded, and sectioned. Synovitis scoring was performed on H&E-stained coronal sections to assess lining hyperplasia (0-3), sub-lining cellularity (0-3), and fibrosis (0-1) across 4 synovial regions (medial-femoral and -tibial, lateral-femoral and -tibial gutters). Scores were averaged across 3 graders after determining acceptable inter-rater reliability. Cartilage degeneration scoring was performed by a board-certified veterinary pathologist on Toluidine blue stained coronal sections using the modified Osteoarthritis Research Society International (OARSI) score.[6] Scores (0-5) were summed across regions (medial and lateral tibial plateau or femoral condyle). Immunohistochemistry (n = 5, prevention strategy group): To evaluate innervation, coronal sections underwent antigen retrieval and overnight incubation with a primary antibody against PGP9.5, followed by incubation with fluorescent secondary antibody, and mounting medium containing DAPI nuclear dye, followed by imaging on a Zeiss Axio Scan.Z1. Immunofluorescent images were thresholded and expression of targets reported as percent fluorescent area across the entire knee joint (medial and lateral synovium, meniscus, intercondylar region, and cartilage). Statistical analysis: Student's t-test or one-way ANOVA with ***Šidák*** post-hoc were used with $p < 0.05$ considered significant, as indicated in figures.

Results

Prevention strategy: Early CD14 blockade significantly increased total distance traveled and rearing time at 4- and 8-wks post DMM, compared to control mice ($p < 0.05$) (Figure 1A). There was a decreasing trend ($p = 0.057$) in weight shifting from the rear to the front paws (front to rear paw weight ratio,

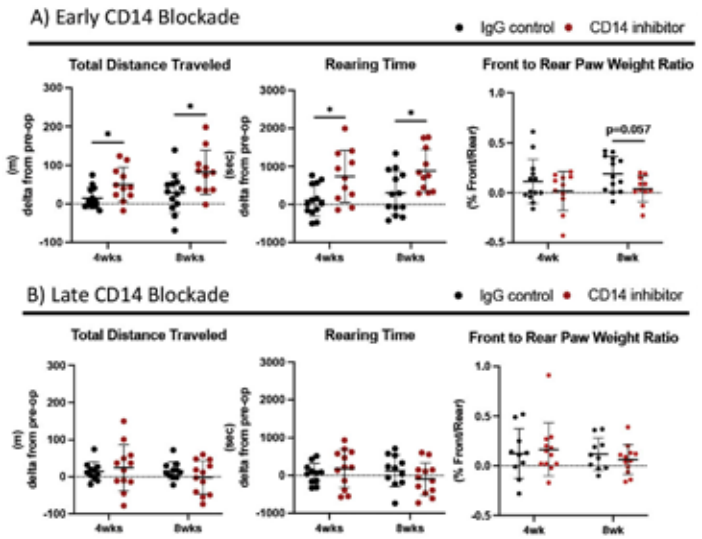

Figure 1. Spontaneous behavioral analysis. LABORAS behavioral analysis of the change from pre-op of Early **(A)** and Late **(B)** blockade groups. ADWB weight bearing analysis of the change from pre-op of front to rear paw & weight % ratio. *p<0.05 Student's T-test.

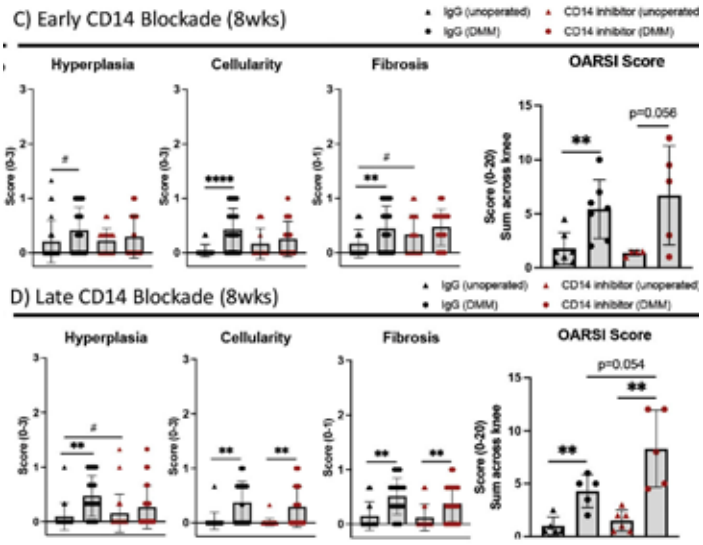

Figure 2. Histopathology analysis. Synovitis and OARSI scores across 4 knee compartments at 8-wks following DMM of Early **(C)** and Late **(D)** blockade groups. #p<0.1, *p<0.05, **p<0.01, ****p<0.0001 Student's T-test.

Figure 1A) 8-wks post DMM in the anti-CD14 treated mice compared to controls. At 8-wks post DMM differences were observed in synovial cellularity ($p < 0.0001$) and fibrosis ($p = 0.0078$) between control-treated DMM-operated knees compared to unoperated knees, however no significant differences in synovial pathology were observed between CD14 blockade- and control-treated DMM knees (Figure 2C). There was also no significant difference in cartilage pathology scoring in DMM-operated knees after early CD14 blockade compared to controls (Figure 2C). Treatment strategy: When treatment was delayed until 4-wks post DMM, no significant behavior or weight-bearing changes were observed between groups ((Figure 1B). 8-wks post DMM, synovial cellularity and fibrosis scores increased compared to unoperated knees similarly in both anti-CD14 and IgG treated mice (Figure 2D). Lining hyperplasia was significantly increased post DMM only in the IgG control group (Figure 2D). There was a trend ($p = 0.054$) towards increasing OARSI cartilage score in the anti-CD14 treated vs. IgG-treated DMM groups (Figure 2D), but no significant differences between early or late treatment groups (IgG vs. CD14 blockade) (Figure 2C,D). Immunofluorescent analysis of innervation in the early-dosed groups revealed significant increases in PGP9.5 expression in DMM-operated knees only in the IgG-control group, and a trend toward decreased staining in anti-CD14 treated DMM knees (Figure 3).

Discussion

Early intra-articular delivery of a CD14 blocking mAb after DMM injury was more effective at improving mobility, compared to delayed treatment, and reduced injury-related weight-bearing shifts towards the front paws. No significant impact of anti-CD14 treatment on cartilage degeneration or synovial histopathology was observed, despite the effects on weight bearing and mobility seen with early treatment. However, anti-CD14 attenuated post DMM increases in signal for the common nerve marker PGP9.5 across the joint, which may be one mechanism driving behavioral and weight-bearing differences. CD14 is known to facilitate inflammatory pathway activation via TLRs, which play important roles in both monocyte/macrophage differentiation and nociception. As such neuroinflammatory crosstalk has been implicated in OA, future work will focus on further elucidating effects of this treatment on the synovial neuroinflammatory milieu.[7]

Significance

These results explore the optimal timing of delivery of an anti-CD14 therapeutic to influence OA pain-related behaviors, ultimately supporting future work in utilizing

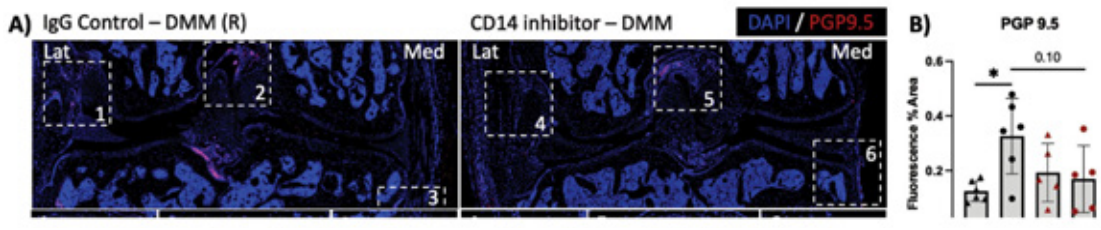

Figure 3. Innervation following DMM. **(A)** Fluorescent images of mice from IgG control and CD14 blockade treated mice (n=5) at 8 wks post DMM, stained for a general innervation marker (PGP9.5, white arrows). Medial and lateral regions are indicated; **(B)** PGP9.5 expression quantification via % fluorescent area across the knee (cartilage, meniscus, intercondylar region, medial- & lateral-synovium). *p<0.05 or as indicated, one-way ANOVA with Šídák's multiple comparison.

CD14 as a therapeutic target for post traumatic OA.

Acknowledgements

We would like to thank Inotiv Co for performing histopathology analysis for this study. Funding provided by VA BLR&D (I01 BX004912) and NIAMS (CRS: R01 AR075737) (AMM: P30AR079206).

References

1. Loeser RF, Goldring SR, Scanzello CR, *et al.* Osteoarthritis: a disease of the joint as an organ. *Arthritis Rheum* 2012; 64(6): 1697.

2. Sanchez-Lopez E, Coras R, Torres A, *et al.* Synovial inflammation in osteoarthritis progression. *Nat Rev Rheumatol* 2022; 18(5): 258-275.

3. Sambamurthy N, Englund K, Hanes MA, *et al.* Deficiency of the pattern-recognition receptor CD14 protects against joint pathology and functional decline in a murine model of osteoarthritis. *PLoS One* 2018; 13(11): e0206217.

4. Glasson SS, Blanchet TJ, Morris EA. The surgical destabilization of the medial meniscus (DMM) model of osteoarthritis in the 129/SvEv mouse. *Osteoarthr Cartil* 2007; 15(9): 1061-1069.

5. Krug HE, Dorman C, Blanshan N, *et al.* Spontaneous and evoked measures of pain in murine models of monoarticular knee pain. *JoVE* 2019; 144: e59024.

6. Glasson SS, Chambers MG, Van Den Berg WB, *et al.* The OARSI histopathology initiative–recommendations for histological assessments of osteoarthritis in the mouse. *Osteoarthr Cartil* 2010; 18: S17-S23.

7. Miller RE, Scanzello CR, Malfait AM. An emerging role for Toll-like receptors at the neuroimmune interface in osteoarthritis. *Semin Immunopathol* 2019; 41(5).

Healing Of Partial-Thickness Cartilage Injuries in the Immature Skeleton: Development of a Large Animal Model for Pediatric Cartilage Research

Brendan D. Stoeckl[1,2]
Elisabeth A. Lemmon[1,2]
Jie C. Nguyen[1,3]
Bijan Dehghani[1,2]
Vandan Patel[3]
Carlos Yaya[3]
Robert L. Mauck[1,2]
Theodore J. Ganley[1,3]
Soroush Baghdadi[3]

[1]University of Pennsylvania, Philadelphia PA

2CMC VA Medical Center, Philadelphia, PA.

3Children's Hospital of Philadelphia, Philadelphia PA

Introduction

Injuries to immature articular cartilage are uncommon in the pediatric population but can be a precursor to osteoarthritis and growth disturbance if not managed appropriately. Previous research on this topic has been limited to retrospective clinical cohorts, partly due to the lack of a reliable model for pediatric cartilage research. This study aimed to develop a large animal model for in vivo pediatric cartilage research by evaluating the healing potential of cartilage injuries in the developing knee.

Methods

Four 6-week-old Yucatan minipigs were utilized in this study, and all animal procedures were performed with IACUC approval. Under general anesthesia, a medial parapatellar arthrotomy was performed bilaterally to gain access to the medial femoral condyles. An 8mm-wide blade was guided by a 3D-printed jig to make a standardized cartilage defect on the weight-bearing surface of each medial femoral condyle at a 45-degree angle to the shaft of the femur (Figure 1A-B). For each animal, one flap was repaired with suture (Figure 1C), and the contralateral side left unrepaired (Figure 1D), and the knees were closed in layers in the usual fashion. Animals were euthanized 6 weeks post-operatively. Knees underwent MRI imaging, followed by dissection and gross assessment with India Ink staining to highlight areas of worn cartilage. Indentation creep tests were performed, both within and adjacent to each defect site, and the resulting deformation curves were fitted to a model that outputs compressive and tensile moduli and permeability. Condyles were then assessed via microCT after immersion in Lugol's solution (I2 and KI in water) to enhance cartilage radiopacity, and histologically with

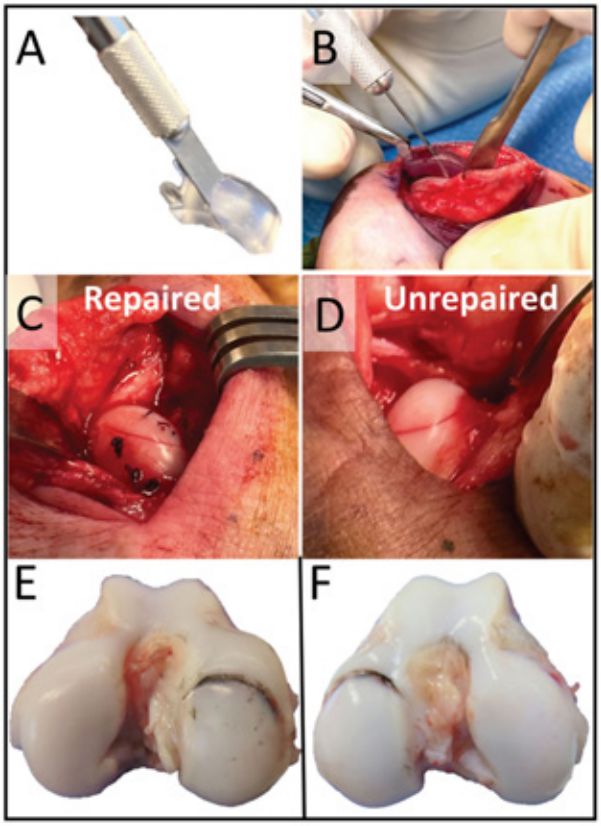

Figure 1. (A) 3D printed alignment jig and square blade used to create standardized femoral condyle defects. **(B)** Jig in use intraoperatively. **(C)** Medial femoral condyle defect after suture repair and **(D)** Defect left unrepaired. **(E)** Representative India Ink staining highlighting defect border after 6 weeks in vivo in a repaired specimen and an **(F)** unrepaired specimen.

Safranin-O/Fast Green staining. Comparisons were made between repaired and unrepaired specimens.

Results

On gross examination (Figure 1E-F), all flaps were stable, except for one unrepaired specimen where the flap detached and became an intra-articular cartilage fragment. On gross inspection, the cartilage injury was readily apparent as highlighted by India Ink staining. MRI examination showed normal cartilage signal intensity with varying degrees of subchondral marrow edema and localized endochondral ossification dysfunction. (Figure 2A-B) Contrast enhanced microCT showed a residual gap in all lesions (Figure 2C-D). Histologic examination confirmed these residual incisional gaps, with evidence of tissue bridging on the superficial edge of each defect and varying degrees of proteoglycan depletion (Figure 2E-F). With the exception of tensile modulus on the unrepaired side, there was a trend towards a reduction in cartilage moduli, and an increase in cartilage permeability, in the defect site in comparison to adjacent tissue, with no apparent difference between repaired and unrepaired specimens (Figure 3).

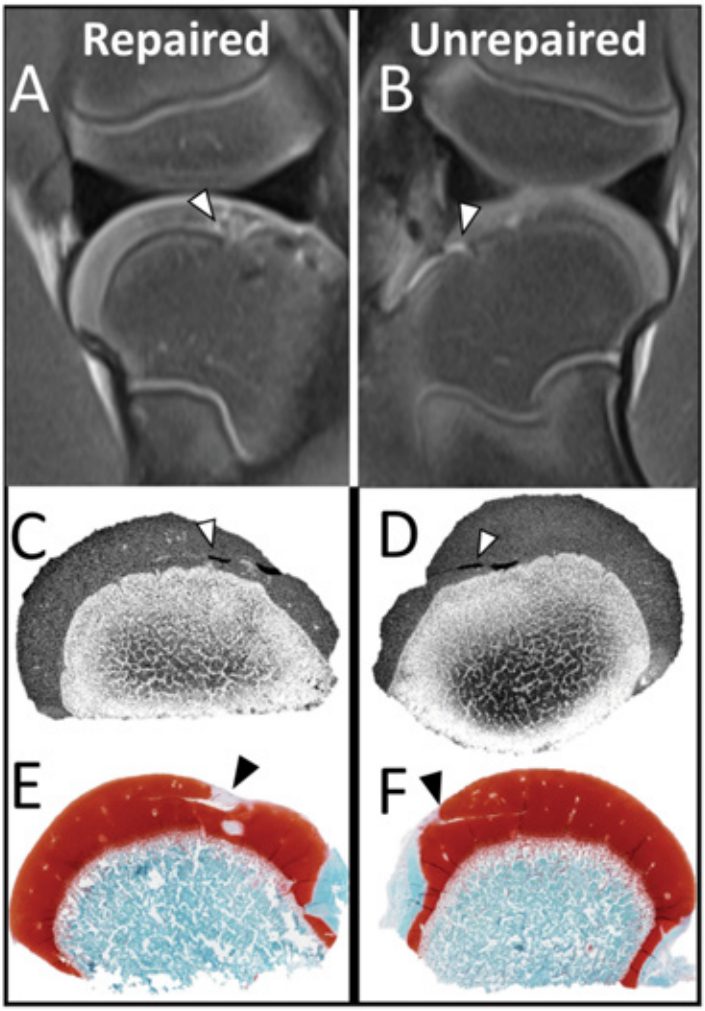

Figure 2. Representative MRI images, contrast enhanced mCT, and Safranin O-Fast Green stained osteochondral histology of repaired **(A, C, E)** and unrepaired; **(B, D, F)** specimens. Arrows emphasize residual cartilage gap.

Discussion

Young Yucatan minipigs can be used as an in vivo pediatric cartilage surgical defect model. The thick articular cartilage allows for the creation of partial- and full-thickness cartilage defects in a standardized manner and for clinically relevant repair. Clinically relevant MRI is feasible, and microCT, histology, and biomechanical tests allow for thorough assessment of tissue microstructure and quality. Our preliminary data on cartilage injury and repair suggests some healing potential, but with altered imaging and biomechanical properties. At this early (six week) timepoint, suture repair did not appear to result in superior healing when compared to defects left unrepaired, however it did prevent progression to a loose cartilage fragment. Future studies will focus on longer term timepoints to assess healing potential and growth alterations.

Significance

In this study, we developed an in vivo standardized surgical model for pediatric cartilage injury and repair that is safe, feasible, and easily reproducible, and can serve as a test bed to assess pediatric cartilage repair strategies.

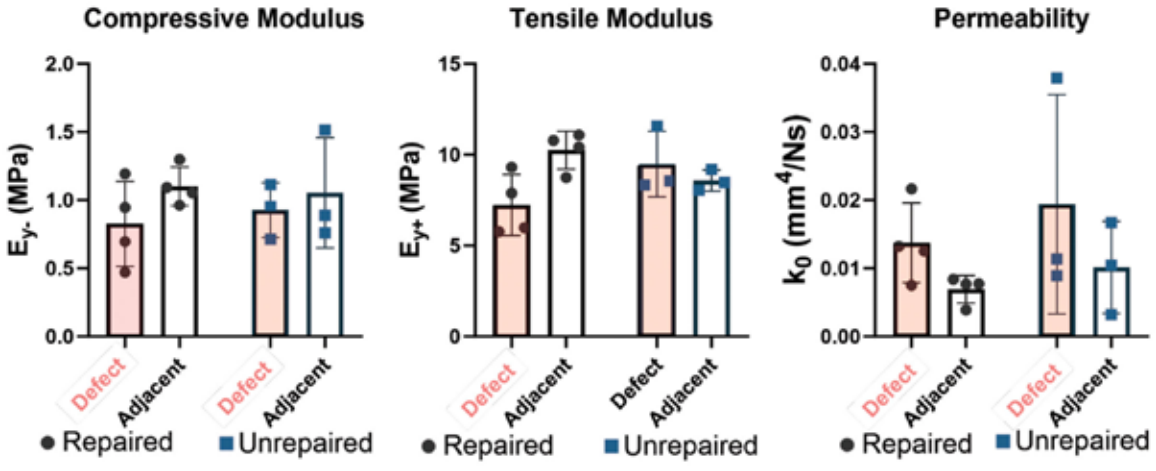

Figure 3: Compressive modulus, tensile modulus, and permeability as measured through creep indentation tests. Tests were performed in the middle of and adjacent to the defect created in each medial femoral condyle.

Osteochondral Defect Repair of Large Weight-Bearing Surfaces in a Porcine Model

Brendan D. Stoeckl[1,2]
Kendall M. Masada[1,2]
Axel C. Moore[3,4]
Natalie L. Fogarty[1,2]
Elisabeth A. Lemmon[1,2]
Bijan Dehghani[1,2]
Lorielle G. Laforest[1,2]
James L. Carey[1,2]
Robert L. Mauck[1,2]
Molly M. Stevens3
David R. Steinberg[1,2]

[1]University of Pennsylvania, Philadelphia, PA, USA

[2]CMC VA Medical Center, Philadelphia, PA, USA

[3]Imperial College London, London UK.

[4]Carnegie Mellon University, Pittsburgh, PA, USA.

Introduction

Knee osteoarthritis represents an enormous clinical burden, but treatment for end-stage disease is limited to total knee replacement.[1] While often effective at limiting pain and restoring function, these metal and plastic devices begin to wear immediately upon implantation, and many eventually require costly and invasive revision surgeries.[2] Given this, earlier intervention through biologic cartilage reconstruction may be an ideal solution. Indeed, several interventions exist for early-stage cartilage damage, including osteochondral autografting or allografting in which an osteochondral unit from a non-weightbearing portion of the knee (or from a donor) is implanted into a defect site.[3] However, as with all biologic repair solutions, this procedure is only indicated in near-ideal surgical conditions, excluding the vast majority of patients with cartilage damage.[4] Thus, there exists a need for a large animal model which realistically assesses osteochondral repair in a clinically relevant disease setting, not only to improve strategies for expanding indications for existing technology, but also as a testbed for evaluating emerging therapeutics. In this study, we developed a large animal model (Yucatan minipig) of osteochondral defect repair on the weightbearing surface of the medial femoral condyle and evaluated the outcomes from clinical repair and a novel implantable scaffold.

Methods

Surgery was performed unilaterally in skeletally mature Yucatan minipigs. A medial parapatellar arthrotomy was followed by patellar subluxation and hyperflexion of the stifle to allow for visualization of the medial femoral condyle. Next, a 6mm diameter x 10mm depth defect was created using a standard Arthrex OATS® kit. A second defect, 7mm diameter x 10mm depth was created, and the resulting osteochondral plug was press-fit into the first defect. The empty 7mm defect served as a negative empty control. Each defect was made on the weight-bearing midline of the medial femoral condyle, and their relative positions proximal or distal were alternated between subjects. Animals were sacrificed 5 weeks after surgery, and joints were assessed grossly with India Ink staining. Next, medial femoral condyles were isolated, potted, and indented with a 2mm diameter spherical indenter in the center of, and 5mm adjacent to, each defect. Fifteen-minute duration creep tests at a 0.1N load were fitted to a Hertzian biphasic creep model,[5] and values for compressive modulus, tensile modulus, and permeability were determined. Contralateral medial condyles were tested as a positive control. Next, osteochondral tissues were scanned via microCT before and after immersion in Lugol's solution to enhance the radiopacity of the cartilage. Finally, osteochondral units

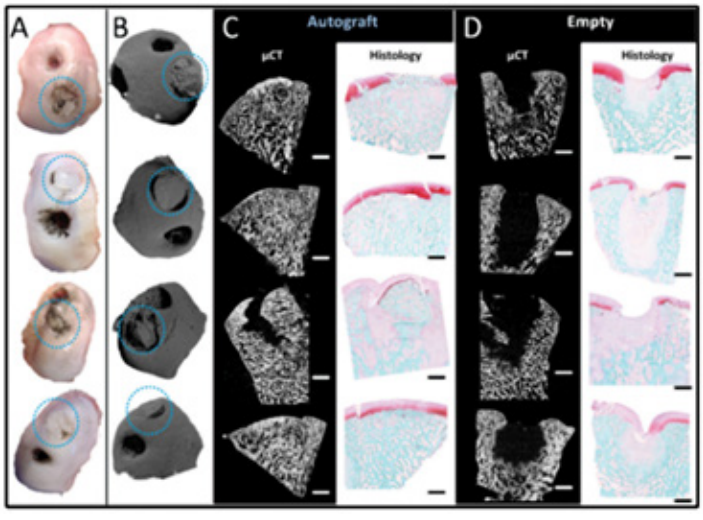

Figure 1. (A) Gross India ink-stained images of medial femoral condyles showing autograft repair (blue circles) and empty defects after 5 weeks in vivo. **(B)** 3D μCT reconstructions of condyles from 1A. **(C)** Sagittal 2D slices from μCT and Safranin-O/fast green stained sections of autograft repair and **(D)** empty defects. Scale = 1mm.

were decalcified, paraffin processed, embedded, sectioned, and stained with Safranin O/Fast Green to visualize matrix content. In follow-on studies, this same model was used in a second set of animals to test the efficacy of a synthetic, acellular, osteochondral construct. The osteochondral implant (Figure 3A) was composed of two components: (1) a poroelastic cartilage mimic and (2) an osseointegrating bone substitute. The poroelastic mimic, FiHy™, is described in.[6] The bone substitute was formed by direct printing of poly(e-caprolactone) onto FiHy™. This direct printing approach enabled a strong interfacial bond between the cartilage mimic and bone substitute and eliminated the need for adhesives for mechanical fixation. Eight mm diameter constructs were fabricated and press-fit into the 7mm osteochondral defect created while forming the autograft plug as described above. Scaffold-filled defects were analyzed as above at the 5-week time point. All quantitative data were compared with one-way ANOVA followed by Tukey's post hoc tests, with significance set at $p < 0.05$.

Results

Based on gross images (Figure 1A) and 3D reconstructions of μCT (Figure 1B), autograft implants remained in the defect at the 5-week timepoint and maintained congruence with the cartilage surface of the condyle. 2D μCT slices showed excellent implant integration with the surrounding bone in 3/4 specimens analyzed, while histology showed variable losses in proteoglycan content in the cartilage (Figure 1C). Empty defects showed persistent deficits in both bone and cartilage (Figure 1D). Both empty defect repair tissue and autograft cartilage were mechanically weaker than contralateral cartilage (Figure 2). However, autograft cartilage was significantly stronger than empty defect repair tissue and was not different from cartilage adjacent to the defect (Figure 2). Synthetic osteochondral constructs (Figure 3A) remained fully seated in the defect as evidenced grossly (Figure 3B) and via μCT (Figure 3C-E), with some evidence of bony integration (Figure 3D) at this early time point.

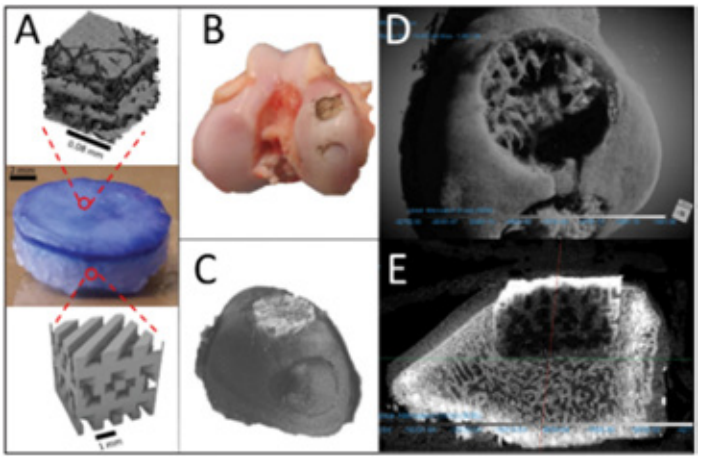

Figure 3. (A) Osteochondral implant consisting of a poroelasic cartilage mimic and a 3D printed PCL osseointegrating component. **(B)** Synthetic implant (top) and autograft (bottom) with India ink staining in the pig medial femoral condyle after 5 weeks in vivo. **(C)** 3D rendering of contrast-enhanced μCT. **(D)** Evidence of mineralized tissue within the implant. **(E)** 2D slice of contrast enhanced μCT showing implant remaining in and fully filling the defect.

Discussion

In this study, we developed a porcine model of large, osteochondral repair on the weightbearing surface of the medial femoral condyle. Most interestingly, it appears that even in the near ideal surgical conditions (healthy knee, fresh autograft implant) used here, implant tissue was mechanically weaker than native after only 5 weeks in vivo. This indicates that there may be room for adjuvant therapies to enhance the repair of large defects, even when fresh autograft tissue is available. This work also demonstrated the potential efficacy of an acellular biphasic poroelastic construct for osteochondral repair. Ongoing work includes quantitative analysis of μCT and scoring of histology, extending to longer time points and evaluating other engineered materials. Future work may further increase the usefulness of this model by inducing a degenerative phenotype in the knee [7] and assessing osteochondral repair in such a clinically typical, but rarely studied environment.

Significance

This study develops a clinically relevant model for assessing osteochondral repair in large weight-bearing defects.

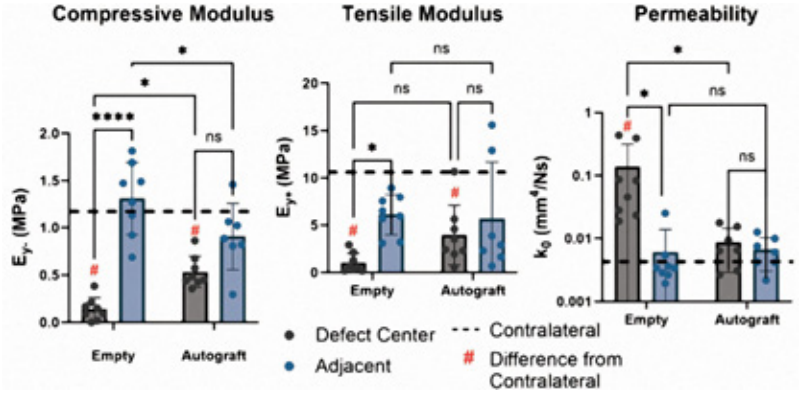

Figure 2. Results of creep indentation tests fitted to a hertzian biphasic model. * = p<.05; **** = p<.0001.

References

1. Devitt B, Bell S, Webster K *et al.* Surgical treatments of cartilage defects of the knee: Systematic review of randomised controlled trials. *Knee*. 2017 Jun;24(3):508-517

2. Bayliss L, Culliford D, Monk A *et al.* The effect of patient age at intervention on risk of implant revision after total replacement of the hip or knee: a population-based cohort study. *Lancet*. 2017 Apr 8;389(10077):1424-1430

3. Hangody L, Karpati G, Szerb I, *et al.* Arthroscopic autogenous osteochondral mosaicplasty for the treatment of femoral condylar articular defects. A preliminary report. *Knee Surgery*. 1997;5(4):262-7

4. Martin A, Patel J, Zlotnick H, *et al.* Emerging therapies for cartilage regeneration in currently excluded 'red knee' populations. *NPJ Regen Med*. 2019 May 30:4:12.

5. Moore A, DeLucca J, Elliott D, *et al.* Quantifying Cartilage Contact Modulus, Tension Modulus, and Permeability With Hertzian Biphasic Creep. *J Tribol*. 2016 Oct;138(4):0414051-414057

6. Moore A, Hennessy M, Nogueira L, *et al.* Fiber reinforced hydrated networks recapitulate the poroelastic mechanics of articular cartilage. *Acta Biomaterialia*. 2023 Sep 1:167:69-82

7. Stoeckl B, Meadows K, Bonnevie E *et al.* Surgical Reattachment of the Anterior Horn Slows OA Progression in a Large Animal Injury Model. *ORS*. 2022.

Sustained Structural and Functional Deficits in the Porcine Knee Six Months Following Meniscus Destabilization

Stoeckl BD[1,2]
Ching S1, Nadruz V[3]
McGroary O1, Boyes M[3]
Laforest L[1,2]
Teinturier T[1]
Zgonis MH[1,2]
Elliott DM[4]
Mauck RL[1,2]
Hast MW[1]
Schaer TP[3]
Steinberg DR1,[2]

[1]University of Pennsylvania, Philadelphia, PA

[2]CMC VA Medical Center, Philadelphia, PA

[3]University of Pennsylvania, School of Veterinary Medicine, Kennett Square, PA

[4]University of Delaware, Newark, DE

Introduction

To better understand the progression of OA pathology, and to establish a test bed for assessing interventions in the context of an OA phenotype, effective large animal, human scale models of joint injury are necessary. Our previous work developed a porcine destabilization of the medial meniscus (DMM) model, where transection of the anterior horn of the medial meniscus resulted in deleterious changes in the knee at an early time point. However, these changes resolved at later time points, as the anterior attachment scarred back into place and the knee resumed normal biomechanics.[1] In a second iteration of this model, a 6mm portion of the medial meniscus anterior horn was resected en bloc, resulting in more severe joint pathology at a six-week time point.[2] The aim of the current study was to assess the progression of this OA phenotype over a six-month period and to assess changes in gait.

Methods

Sixteen skeletally mature (12-month-old) Yucatan minipigs underwent mini-arthrotomy of the right stifle, and a 6mm portion of the medial meniscus anterior horn was resected en bloc. Animals were sacrificed at either 6 weeks or 6 months post-operatively (N = 8 for both), with contralateral limbs serving as intact controls. Four of the animals in the six-month group were used for gait analysis. Videos of walking pigs were captured at 30 fps both preoperatively and four months post-op. Using DeepLabCut markerless tracking software,[3] the hip, knee, ankle, and hind hoof of each pig were tracked across the gait cycle (Figure 3A). Landmark positions were used to compute knee flexion angles. Further analysis was conducted using the GAITFour® walkway system, six months post-operatively. The pigs walked across a sensor-embedded mat, and the contact pressure of each hoof-strike was recorded. A model which normalized by velocity and trial number was used to measure differences between left (intact) and right (DMM) limbs. After sacrifice, stifle joints were dissected, and osteochondral segments of both the medial femoral condyle and medial tibial plateau were isolated. Indentation creep tests were performed, and the resulting deformation curves fit to a model outputting compressive and tensile moduli and permeability.[4] Specimens were then scanned via microCT before and after contrast enhancement with Lugol's solution (I_2 and KI in water). Cylindrical regions of bone were defined superficial and deep to the cartilage interface, and bone volume fraction was calculated for each. For histologic analysis, osteochondral sections were stained with Safranin O/ Fast Green, and synovium sections were stained with Hematoxylin/ Eosin. Statistics were performed in Graphpad.

Results

Quantitative tissue analyses were performed at three regions per timepoint—on the medial tibial plateau in areas previously uncovered and covered by the meniscus, and on the medial femoral condyle (Figure 1). At 6 weeks, the cartilage was softer across regions of interest, with statistically significant differences in all regions, except for the uncovered tibial plateau. This mechanical weakening persisted at 6 months with statistical differences detected in the compressive modulus in the covered tibia and in the tensile modulus in the uncovered tibia region. Bone volume

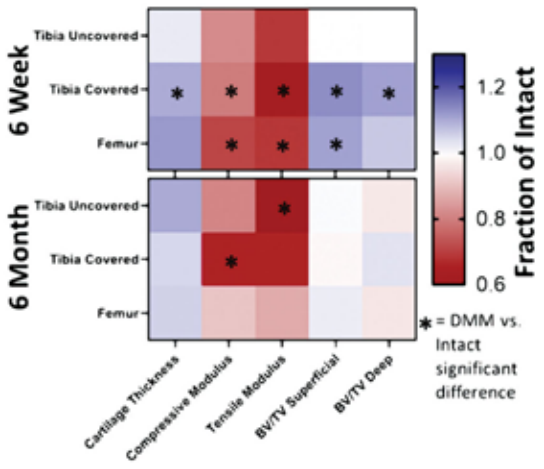

Figure 1. Tissue-scale quantitative outcomes of the operative limb after DMM for medial tibial plateau regions previously covered by the meniscus or uncovered, and for the medial femoral condyle, expressed as a fraction of intact control.

fraction increased in the covered tibia and superficial femoral condyle regions in DMM knees, but these subchondral changes were attenuated by the 6 month time point. (Figure 1). Histologically, osteochondral sections of DMM knees showed some degree of surface fibrillation and roughening at 6 weeks, and mild loss of proteoglycan by 6 months. (Figure 2A) At 6 weeks, the synovium of DMM knees showed hyperplasia and signs of fibrosis, but little difference was detectable by 6 months. Figure 2B). For gait analysis, graphical representations of post-op DMM knee flexion revealed a 'double-hump' signature during stance, which was not observed in the other groups (Figure 3B). Pigs exhibited greater maximal knee flexion in their post-op intact knee compared to pre-operative and post-op DMM knees (Figure 3C). Further, time spent in stance was shorter in both knees post-op compared to preoperatively (Figure 3D). When normalized for velocity and trial number, total pressure index percentage was significantly lower on the right hind limb when compared to the left hind limb (model adjusted effect: −0.5 , 95% CI: [−0.9, −0.1], p = 0.005; (Figure 3E) Similarly, the total scale pressure (the sum of peak pressure values recorded from each activated sensor by a hoof during mat contact) showed significantly less pressure in the right hind limb compared with the left hind limb (model adjusted effect: -1.4, 95% CI: [−2.4, −0.5], p = 0.004; (Figure 3F).

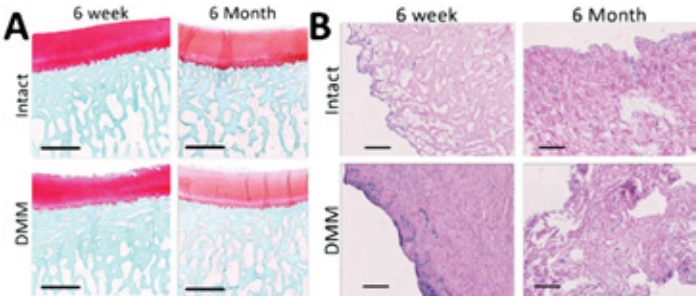

Figure 2. (A) Safranin O / Fast Green-stained osteochondral sections of the medial tibial plateau (scale =1mm) **(B)** Hematoxylin and Eosin stained synovium sections (scale = 100μm).

Discussion

This study showed that a more aggressive medial meniscus destabilization involving a partial anterior horn resection (as opposed to a simple transection) results in a durable osteoarthritic phenotype in a porcine model. We showed persistent cartilage weakening as well as histologic evidence of degenerative changes six months after surgery. Most importantly, functional assays of animal gait showed detectable abnormalities at four and six months after surgery. Animals displayed decreased range of motion during stride in the affected limb, as well as a reduction in time spent in the stance phase, indicating that animals were favoring the unoperated limb. Further, the kinematic parameters assayed during the gait analysis showed a significant and consistent decrease in weight distribution on the affected limb post-surgery. Joint pain alters normal function, particularly locomotion, and is one of the clinical signs of osteoarthritis. The alterations in gait and loadbearing in pigs 6 months postoperatively may reflect painful ambulation secondary to OA changes as a result of DMM.

Significance

This study developed a clinically relevant large animal model of OA leading to both structural and functional deficits of the knee and changes in pig gait patterns.

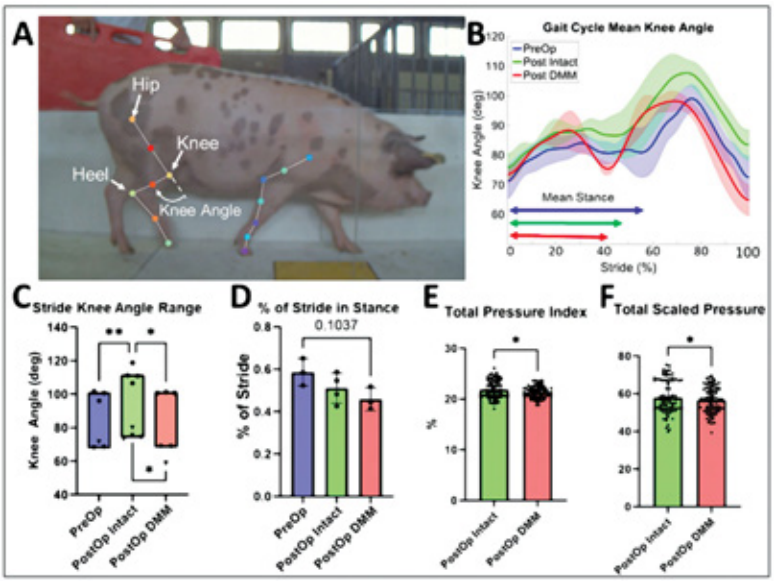

Figure 3. (A) Still from motion tracking showing tracked landmarks. **(B)** Average knee angle during gait cycle preoperatively, post-op on intact control limb, and post-op on DMM limb. **(C)** Average minimum and maximum knee angle during stride. D) Average % of each stride spent in the stance phase. **(E)** Total Pressure Index and F) Total Scaled Pressure, of each hoof strike as measured with the GAITFour system. *p<0.05, **p<0.01.

Acknowledgments

This work was supported by the Department of Veterans Affairs and the National Institutes of Health.

References

1. Bansal S, Meadows K, Miller L. *et al.* Six-Month Outcomes of Clinically Relevant Meniscal Injury in a Large-Animal Model. *Orthop J Sports Med*. 2021 Nov 12;9(11):23259671211035444

2. Stoeckl B, Meadows K, Bonnevie E *et al.* Surgical Reattachment of the Anterior Horn Slows OA Progression in a Large Animal Injury Model. *ORS*. 2022.

3. Moore A, DeLucca J, Elliott D, *et al.* Quantifying Cartilage Contact Modulus, Tension Modulus, and Permeability With Hertzian Biphasic Creep. *J Tribol*. 2016 Oct;138(4):0414051-414057

4. Mathis A, Mamidanna P, Cury K, *et al.* DeepLabCut: markerless pose estimation of user-defined body parts with deep learning. *Nature Neuroscience*. 2018 Sep;21(9):1281-1289.

Characterizing Discogenic Cell Based Tissue Engineered Disc Replacements

Matthew Fainor, BS[1,2]
Galina Dulatova, PhD[3]
Sage Frehner, MS[3]
Harvey E. Smith, MD[1,2]
Robert L. Mauck, PhD[1,2]
William L. Heaton, MS[3]
Sarah E. Gullbrand, PhD[1,2]

[1]Department of Orthopaedic Surgery
University of Pennsylvania,
Philadelphia, PA

[2]Translational Musculoskeletal Research Center,
Corporal Michael J. Crescenz VA Medical Center,
Philadelphia, PA

[3]DiscGenics, Salt Lake City, UT

Introduction

Current treatments for back pain associated with late-stage intervertebral disc (IVD) degeneration may temporarily relieve pain through fusion. However, they do not restore biological and mechanical function to the disc. The use of living tissue engineered constructs to replace degenerated discs has the potential to overcome these limitations and has been investigated in vitro by a number of groups.[1] Our group developed endplate-modified disc-like angle ply structures (eDAPS) that mimic the native structure and function of the disc.[2] Our previous work seeding eDAPS with either animal-derived mesenchymal stromal cells (MSCs) or animal-derived annulus fibrosus (AF) and nucleus pulposus (NP) cells revealed that both MSCs and native cells result in eDAPS that are compositionally and functionally similar to native, but only when produced at small size scales.[3,4] However, this comparison has not been validated at human size scales. This challenge of physically scaling the eDAPS is compounded by the challenges of working with human native disc cells, including the limited endogenous cell population and the difficulty of obtaining cells from healthy donors, which previously made translation of these findings insurmountable. DiscGenics has developed a manufacturing process utilizing intervertebral disc material obtained from human organ donors to produce Discogenic Cells.[5] This study sought to evaluate the compositional and functional maturation of eDAPS seeded with Discogenic AF and NP cells obtained via DiscGenics' manufacturing process, compared to eDAPS seeded with goat bone-marrow derived MSCs.

Methods

Adult IVD tissue was procured from a consented organ donor. The tissue was dissected into separate NP and AF regions followed by digestion with collagenase. The cells were expanded and passaged in attachment culture (Att.). Cells were then grown in a 3D suspension culture (Susp.) using a viscous media to allow growth of cell clusters. RNAs were isolated for gene expression, followed by real-time PCR. Protein expression was determined by seeding cells in a micromass-based assay for 5 days and measured in the supernatant by ELISA. Immunophenotyping was performed by incubating cells with fluorescently conjugated antibodies and determining positive cell expression via flow cytometry. eDAPS were seeded with Discogenic Cells as previously described.[6] The AF analog of the eDAPS was seeded with AF cells grown in attachment culture. NP analogs were seeded with NP cells grown in either attachment (Att. eDAPS) or suspension (Susp. eDAPS) culture. eDAPS were cultured for 10 weeks with constant mechanical agitation in a chemically defined chondrogenic medium containing TGF-b3. The AF and NP analogs of control eDAPS were seeded with goat MSCs and cultured for 12 weeks under the same conditions. Following culture, eDAPS were fixed, processed for paraffin histology, and stained with Alcian Blue, Picrosirius Red, and Hematoxylin/Eosin (n = 3/group). Remaining eDAPS (n = 3/group) were subjected to 20 cycles of 48N compression followed by a 10 minute 48N creep load. NP and AF components of these eDAPS were then separately digested in proteinase K for quantification of DNA, glycosaminoglycan (GAG), and collagen content.

Results

The ratio of gene expression for ACAN / COL1A2 was higher in NP cells from Att. or Susp. culture relative to that of AF cells from Att. culture (Figure 1A). Measurement of secreted protein showed that NP cells grown in suspension culture had a greater aggrecan / collagen 1 ratio than either AF or NP cells grown in attachment culture (Figure 1B). All cell surface markers tested showed similar expression between the AF and NP cells (Figure 1C). eDAPS cultured with attachment- or suspension-derived Discogenic NP cells were histologically, mechanically, and biochemically similar. Att. or Susp. NP cells deposited more proteoglycans in the NP region of the eDAPS than the goat MSCs (Figure 2A).

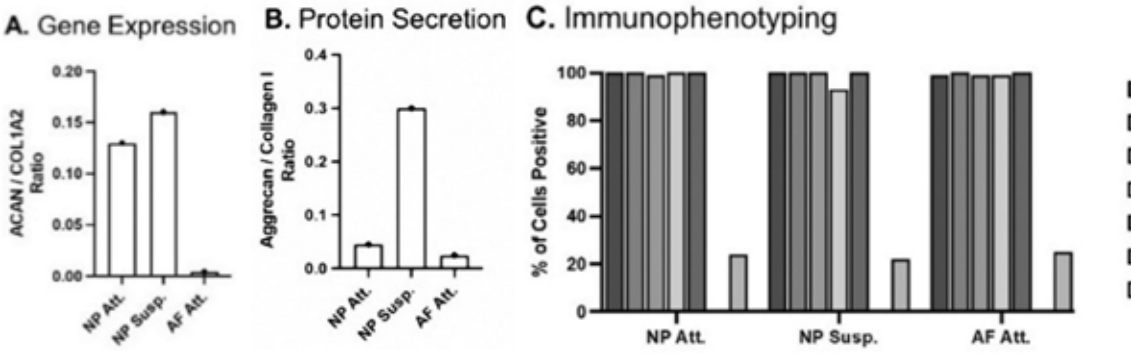

Figure 1. (A) Relative (normalized to HPRT1) gene expression for ACAN / COL1A2. **(B)** Ratio of protein secretion over a 5-day period for Aggrecan / Collagen IA2. **(C)** Cell surface expression of markers related to mesenchymal and intervertebral disc cell lineages

Disccogenic eDAPS were mechanically distinct from MSC eDAPS and had increased toe modulus (Figure 2B), increased linear modulus (Figure 2C), and decreased compressive strain (Figure 2D), when compared to goat MSC eDAPS. Both Discogenic eDAPS were mechanically similar, and both Discogenic NP cells produced the same amount of GAG (Figure 2E) and collagen (Figure 2F). Discogenic AF cells produced a minimal amount of GAG.

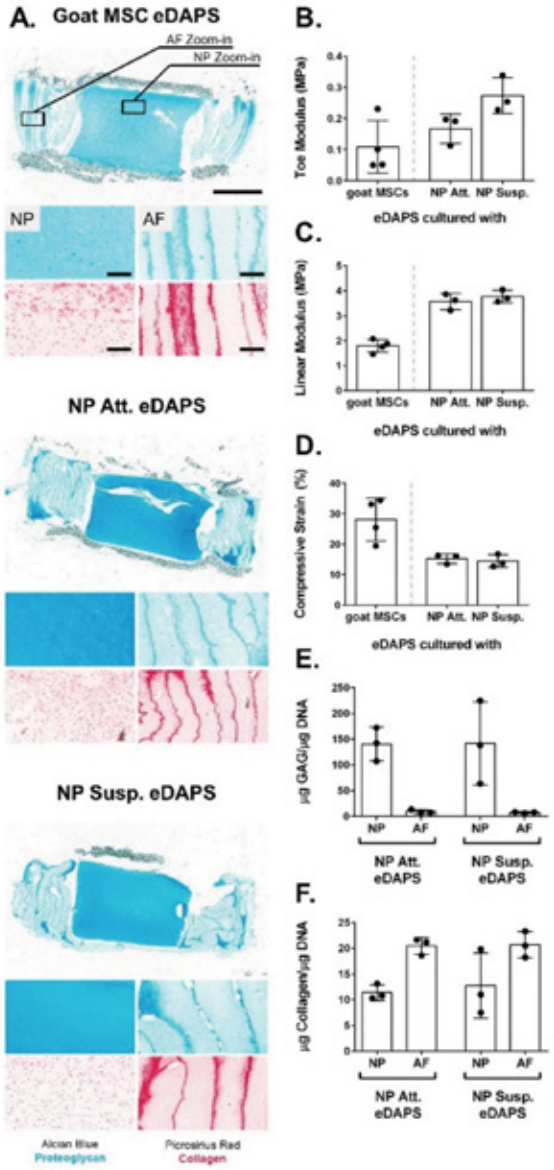

Figure 2. (A) Alcian Blue and Picrosirius Red histology staining (scale = 3mm for entire eDAPS, 300 μm for zoom-ins), **(B)** toe modulus, **(C)** linear modulus, and **(D)** compressive strain. (E) GAG content per DNA and **(F)** collagen content per DNA for the NP and AF regions of Discogenic eDAPS.

Discussion

Characterization of Discogenic Cells prior to seeding indicated that all cells embodied a progenitor phenotype, expressing extremely low levels of CD24.[7] Discogenic NP cells cultured in suspension initially produced greater amounts of aggrecan than NP cells cultured via attachment, but eDAPS cultured with both cell types were similar in every outcome measured. It is likely that both cell populations performed similarly once transitioned to 3D culture as NP cells expanded in monolayer have been shown to develop normal NP phenotypes following 3D culture.[8] Unfavorable diffusion gradients often create hostile environments for cells toward the center of large implants that result in heterogeneous matrix deposition,[9] as was observed in MSC-seeded eDAPS. Critically, the deposition of proteoglycans in the NP was more homogeneous in eDAPS seeded with Discogenic NP cells, indicating that Discogenic Cells more readily thrived in the unfavorable environment of a human-sized disc. Additionally, the NP and AF regions of Discogenic eDAPS were biochemically distinct, whereas goat MSC eDAPS regions were less defined with increased collagen deposited along the outer edges of the NP. Future work will involve the creation of human MSC eDAPS as well as in vivo evaluation of Discogenic eDAPS in our established large animal model.

Significance

Discogenic Cells are a promising development in the translation of tissue engineered therapies that remove the many hurdles of working with native human disc cells. Discogenic Cells were shown to be safe in clinical trials for patients with mild to moderate lumbar disc degeneration and produced clinically meaningful improvements in low back pain, function, and quality of life. This work further advances translation by culturing tissue engineered discs at a scale appropriate for human cervical disc replacement using a translatable human NP and AF cell source.

Acknowledgements

This work was supported by the Department of Veterans' Affairs and the Penn Center for Musculoskeletal Disorders. DiscGenics provided all Discogenic Cells at no cost according to established VA CRADA.

References

1. Gullbrand SE, Smith LJ, Smith HE, *et al.* Promise, progress, and problems in whole disc tissue engineering. *JOR Spine* 2018; 1(2): e1015.

2. Gullbrand SE, Ashinsky BG, Bonnevie ED, *et al.* Long-term mechanical function and integration of an implanted tissue-engineered intervertebral disc. Science *Translational Medicine* 2018; 10(468): eaau0670

3. Martin JT, Gullbrand SE, Kim DH, *et al.* In vitro maturation and in vivo integration and function of an engineered cell-seeded disc-like angle ply structure (DAPS) for total disc arthroplasty. *Scientific Reports* 2017; 7(1): 15765.

4. Kim DH, Martin JT, Gullbrand SE, *et al.* Fabrication, maturation, and implantation of composite tissue-engineered total discs formed from native and mesenchymal stem cell combinations. *Acta Biomaterialia* 2020; 114: 53-62.

5. Silverman LI, Dulatova G, Tandeski T, *et al.* In vitro and in vivo evaluation of discogenic cells, and investigational cell therapy for disc degeneration. *The Spine Journal* 2020; 20(1): 138-149.

6. Gullbrand SE, Kim DH, Bonnevie E, *et al.* Towards the scale up of tissue engineered intervertebral discs for clinical application. *Acta Biomaterialia* 2018; 70: 154-164.

7. Sakai D, Nakamura Y, Nakai T, *et al.* Exhaustion of nucleus pulposus progenitor cells with ageing and degeneration of the intervertebral disc. *Nature Communications* 2012; 3(1264).

8. Kim DH, Martin JT, Elliott DM, *et al.* Phenotypic stability, matrix elaboration and functional maturation of nucleus pulposus cells encapsulated in photocrosslinkable hyaluronic acid hydrogels. *Acta Biomaterialia* 2015; 12: 21-29.

9. Buckley CT, Meyer EG, & Kelly DJ. The influence of construct scale on the composition and functional properties of cartilaginous tissues engineered using bone marrow-derived mesenchymal stem cells. *Tissue Engineering Part A* 2012; 18(3-4).

Innervation and Inflammation Correlate with Structural and Mechanical Changes in a Large Animal Model of Intervertebral Disc Degeneration

Kevin G. Burt, PhD[1,2]
Caitlin Barrett, MD[2,3]
Thomas P. Schaer, VMD[4]
Harvey E. Smith, MD[1,2]
Robert L. Mauck, PhD[1,2]
Sarah E. Gullbrand, PhD[1,2]

[1]Department of Orthopaedic Surgery
University of Pennsylvania

[2]Translational Musculoskeletal Research Center
CMC Veterans Affairs Medical Center

[3]Drexel University College of Medicine

[4]School of Veterinary Medicine
University of Pennsylvania

Disclosures

KGB (N)—kevin.burt@pennmedicine.upenn.edu, CB (N), TPS (N), HES (N), RLM (6,8), SEG (6)

Introduction

Disc degeneration (DD) and associated lower back pain, a leading cause of chronic pain worldwide, is characterized by a cascade of structural and biological changes which ultimately compromise disc mechanical function and height, often resulting in discogenic pain.[1] Potential biological drivers of DD include inflammatory cytokines (IL6, IL1β, TNFα) and increased innate immune cell presence (phagocytic macrophages), which are persistently observed within the IVD during degeneration.[2,3] Current clinical treatments for DD, including spinal fusion, are limited in that they do not restore healthy disc structure or function, and further, do not target the inflammatory drivers that likely lead to symptomatic pain. Large animal models of DD are essential for translating new therapies to the clinical population, as they recapitulate the human IVD in morphology.[4] We previously developed a chondroitinase ABC (ChABC) model of goat lumbar and cervical disc degeneration, which enzymatically degrades the nucleus pulposus (NP), leading to decreased disc height, water content, histological evidence of degeneration, and increased NP inflammatory cytokine and catabolic enzyme expression.[5-7] However, innervation and presence of immune cell, commonly identified in human DD, has yet to be explored within this large animal model. ***We hypothesized that structural and functional changes observed in our large animal model of DD would correlate with increased innervation, inflammation, and immune cell presence.***

Methods

Induction of Disc Degeneration

Degeneration of the cervical C2-C3 or C4-C5 intervertebral discs of large frame goats (~3 years of age, equal distribution of male and female) was induced via intradiscal injection of 2U or 5U ChABC in 200 µL of buffer (sterile PBS, 0.1% BSA), following IACUC approval. Intradiscal injection of ChABC was performed percutaneously via an anterior approach using a 22G needle with fluoroscopic guidance.[5,6] C3-C4 discs were utilized as controls.

Immunohistochemical Analysis (n = 4-6)

Bone-disc-bone segments of cervical IVDs were prepared from explanted motion segments 12 weeks post-ChABC injection. Spine segments were fixed, decalcified, and paraffin embedded. Mid-sagittal sections were cut and used for immunohistochemical analysis of inflammatory cytokine (IL6, TNFα), nerve (PGP9.5, 1:1 phosphorylated & non-phosphorylated NFH), and monocyte (Ly6C) and macrophage (CD68) cell markers. Sections underwent antigen retrieval and overnight incubation with primary antibodies, followed by incubation with fluorescent secondary antibodies, and were cover-slipped with mounting medium containing DAPI nuclear dye before imaging (Zeiss Axio Scan.Z1).

Protein expression analysis (n=4-6)

Immunofluorescent images were thresholded and expression and localization of targets was assessed via percent of fluorescent area within hand drawn regions of interest (ROIs) containing the NP or annulus fibrosus (AF).

Statistical analysis

To assess relationships between inflammation, innervation, and IVD structure and function (NP T2 relaxation times, histology score, Toe and Linear Moduli), study outcomes were analyzed using a Pearson correlation test. Pearson r correlation values (rp) between measured variables were interpreted as either low ($rp < 0.29$), medium ($0.3 < rp < 0.49$), or high ($rp > 0.5$) effect size between measured variables. Significance was defined as correlations with $p < 0.05$ (GraphPad Prism).

Results

Analysis of neuroinflammation revealed a notable presence of innervation along the outer and inner AF and NP regions of degenerated IVDs (T2 < 60ms), as indicated by positive PGP9.5 and NFH staining (Figure 1). Further, increased presence of inflammatory cytokines, IL6 and TNFα, and naïve monocyte (Ly6C) and mature macrophage (CD68) markers was also observed within the NP and AF regions of degenerated discs (Figure 1). Evaluating relationships between structural and functional IVD outcomes revealed a high correlation ($r_p = -0.7138$, $p = 0.0091$) between increased disc histology score and decreased T2 (Figure 2). Neuroinflammation analysis revealed significant high positive correlations between innervation markers PGP9.5 and NFH with each other (NP & AF) and with degenerative structural and functional changes. This included increasing NFH (NP) presence with lower T2 ($r_p = -0.817$, $p = 0.0039$) and increasing AF PGP9.5 and NFH presence with increasing Toe and higher Linear moduli ($r_p = 0.749$, $p = 0.0127$)(Figure 2). Comparing correlations between innervation, inflammatory, and immune cell markers revealed significant high correlations between increased PGP9.5 and NFH expression with IL6, and CD68 (Figure 2).

Discussion

This study sought to determine whether biological drivers of human inflammation and pain commonly associated with DD are observed in a large animal model of ChABC-induced DD. Innervation was identified throughout the AF and NP of degenerated IVDs, as indicated by colocalization of PGP9.5 and NFH. These nerve markers were highly associated with both reduced NP T2, indicative of a loss of NP water and proteoglycan content, and increased Toe and Linear moduli. High positive correlations between inflammatory cytokine expression (IL6, TNFα) with both innervation markers (PGP9.5,

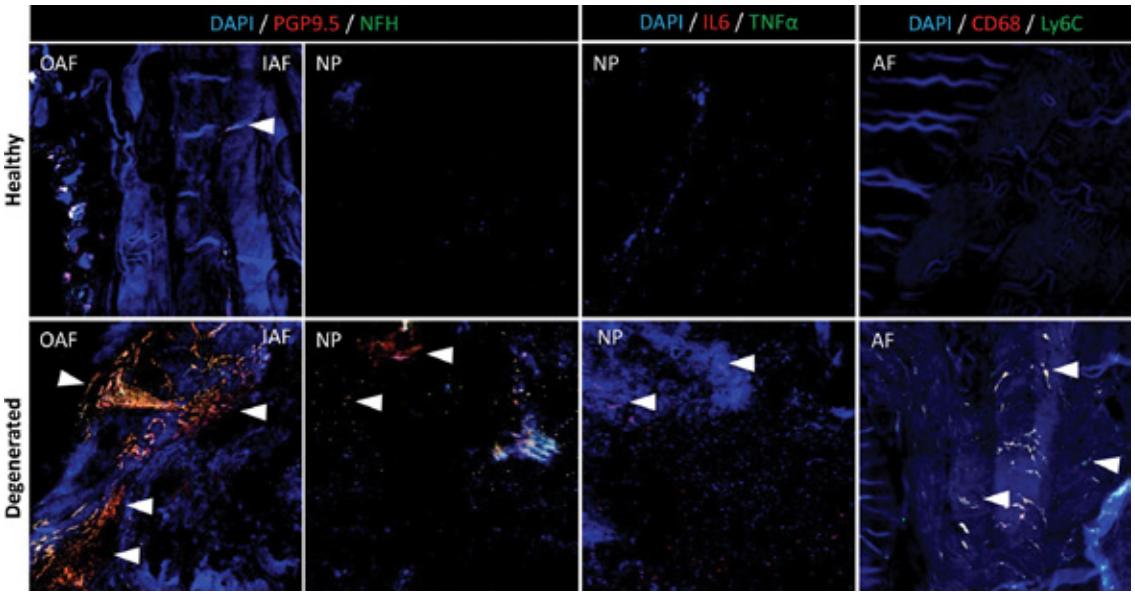

Figure 1. Innervation and inflammation with chABC induced DD. Fluorescent images of healthy (T2>60) and degenerated (T2<60) IVDs stained for nerve, inflammation, and immune cell markers. Positive staining is indicated by white arrows. IVD region is indicated (outer annulus fibrosis AF (OAF), inner AF (IAF), and nucleus pulposus (NP).

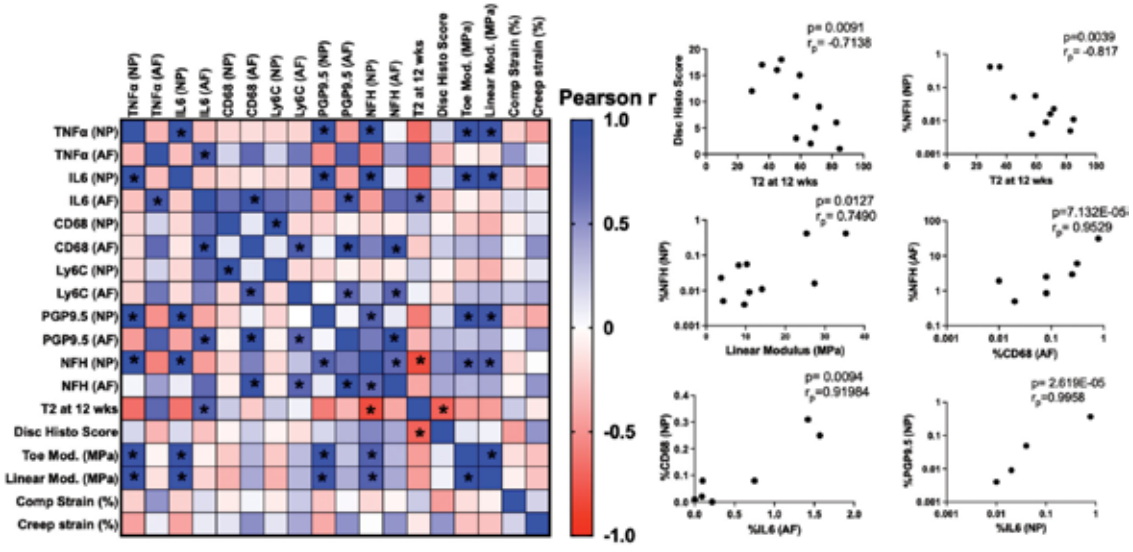

Figure 2. IVD innervation, inflammation, and structure and mechanics correlation matrix. Correlation matrix across study outcomes using Pearson r (rp) statistical analysis. Significance was observed in correlation data by *p<0.05.

NFH) and a mature macrophage marker (CD68) provide a possible mechanism through which local inflammation may be initiating or synergistically promoting immune cell infiltration and innervation to degenerated IVDs, suggesting neuroinflammatory pathways, which have been identified in other chronic inflammatory joint diseases (e.g. OA).[8] Ultimately, these results provide new evidence of immune cell presence and innervation within a large animal DD model, supporting the use of such a model in evaluating both structural and neuroinflammatory therapies.

Significance

This work improves our understanding of the nociceptive and inflammatory responses within a large animal model of disc degeneration, allowing for the rationale design and application of therapeutics targeting these pathways to reduce disc inflammation and pain.

Acknowledgements

This study was supported by the Department of Veterans Affairs and the Penn Center for Musculoskeletal Disorders.

References

1. Gopal, (2012)
2. Shamji, *Art. & Rheum.* (2010)
3. Nakazawa, *Spine J.* (2018)
4. O'Connell, *Spine* (2007)
5. Gullbrand, *OAC* (2017)
6. Gullbrand, *ORS Conf.* (2022)
7. Zhang, J. *Orthop Res* (2020)
8. Guida, *Biomolecules* (2022)

Micromechanics and Mechanoresponsivity of the Developing Porcine Meniscus

Meghan E. Kupratis, PhD[1]
Yuqi Zhang, BS[1]
Jiaqi Xiang, BS[2]
Bryan Kwok, B[S]2
Elisabeth A. Lemmon, VMD[1]
Karen L. Xu, BS[1]
Nathaniel A. Dyment, PhD[1]
Lin Han, PhD[2]
Eiki Koyama, PhD[3]
Robert L. Mauck, PhD[1]

[1]University of Pennsylvania

[2]Drexel University

The Children's Hospital of Philadelphia

Introduction

The meniscus is critical for knee joint stability and load distribution. Unfortunately, its limited endogenous cell-mediated repair capacity means that meniscus injuries often fail to heal in adults.1 Given the superior repair capacity of juvenile meniscus tissues, understanding their initial formation and specialization mechanisms during embryonic development may provide insights that could be harnessed for tissue regeneration in the adult. Our group previously examined the embryonic formation and postnatal maturation of the murine meniscus, revealing that its region-specific matrix composition and cellular phenotypes are established prenatally.[2-3] Furthermore, we showed that mechanical forces that arise from muscle loading and cellular contraction are essential for meniscus formation and specialization, while reduced postnatal weightbearing has little effect on meniscus morphology and micromechanics.[4,5] While these studies provide critical insight to the mechanoregulation of meniscus morphogenesis, translatability of the murine model is limited by its small size and mechanical and morphological distinctions relative to humans. To overcome these limitations, the goal of the present study was to establish a more translationally relevant model of meniscus development using the Yorkshire pig. Here, we established the timeline for key events in knee joint formation in early gestation (28-45 days after fertilization, E28-45) and evaluated matrix micromechanics and emergent mechanoresponsivity of meniscus cells in pigs from early gestation (E45), mid-gestation (E84), and newborn (P1) stages.

Methods

Timed Pregnancies and Embryo Collection

Adult female Yorkshire pigs were artificially inseminated at the National Swine Research Center (NSRRC, Columbia, MO). Pregnancy was confirmed via ultrasound, and sows were euthanized on embryonic day 45 or 84, or on postnatal day 1.

Micromechanics

Freshly dissected left knee joints were embedded in OCT and cryo-sectioned into 10µm coronal sections. AFM nanoindentation was performed in 1X PBS using polystyrene microspherical tips (Ø25µm, k~0.6N/m) at ≥10 different locations within the inner and outer meniscus per specimen. The effective indentation modulus (Eind) was calculated from the finite thickness-corrected Hertz model.[3]

Histology

Left hindlimbs were fixed in 4% paraformaldehyde, embedded in paraffin, and sectioned to 5µm (sagittal and coronal orientations). Cellularity and proteoglycan distribution were assessed from Safranin O/Fast Green staining.

Cell Isolation

Menisci from the right hindlimbs were identified and isolated under a dissecting microscope. At E84 and P0, menisci were segmented into inner and outer regions. All tissues were minced into ~1mm3 pieces and cultured in basal medium (DMEM, 10% FBS, 1% anti-anti) to allow for cell egress from the tissue fragments.

Mechanoresponse Assay

Isolated cells were cultured on fibronectin-coated polyacrylamide (PA) hydrogels (5 or 55kPa) or glass for one day in basal medium. Cells were fixed and stained for YAP (AF-488), actin (phalloidin AF-555), and nuclei (Hoechst 33342, excitation 350nm). Confocal z-stack images were obtained at 10X magnification and processed in Cell Profiler to quantify cell area and YAP localization.

Results

Histological assessments of hindlimb development across early gestation timepoints (E28-42) were used to establish the timing of knee joint formation in the Yorkshire pig. Skeletal rudiments were apparent at E28, as indicated by cartilaginous condensations at the prospective femur and tibia locations (Figure 1a).

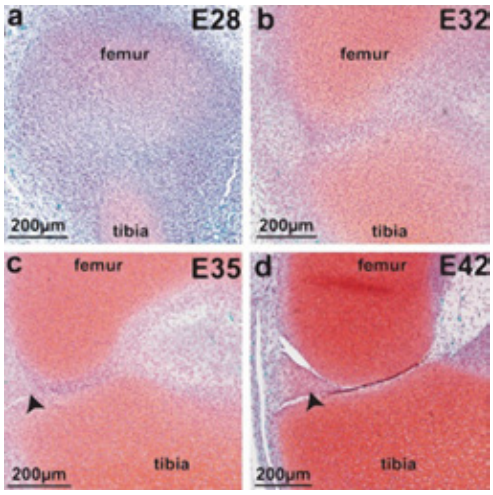

Figure 1. Knee joint formation during early embryonic development in the pig.

The future joint line was established by E32 (Figure 1b), and primitive menisci were visible, but not yet separated from the adjacent cartilaginous structures at E35 (Fig. 1c, arrowhead). The menisci were fully formed and separated from the articular cartilage at E42 (Figure 1d, arrowhead). Subsequent tissue and cellular analyses were performed from E45 onwards, at which point the menisci were readily isolated (Figure 2). Safranin O/fast green staining of menisci from these later timepoints showed that regional matrix specification, namely, proteoglycan enrichment within the inner meniscus, was evident in these tissues (Figure 3).

AFM nanoindentation revealed rapid stiffening of the meniscus primitive matrix throughout gestation (Figure 4) The microscale modulus of the outer zone was significantly greater than the inner zone at all three timepoints (#$p < 0.03$). In the inner meniscus, Eind increased from 3.5 ± 1.4 kPa (mean ± SD) at E42 to 18.2 ± 4.3 kPa at P1, while Eind of the outer meniscus increased from 6.5 ± 2.5 kPa to 26.1 ± 8.0 kPa. Together with our histological observations, these data indicate that the inner and outer meniscus develop distinct compositional and mechanical

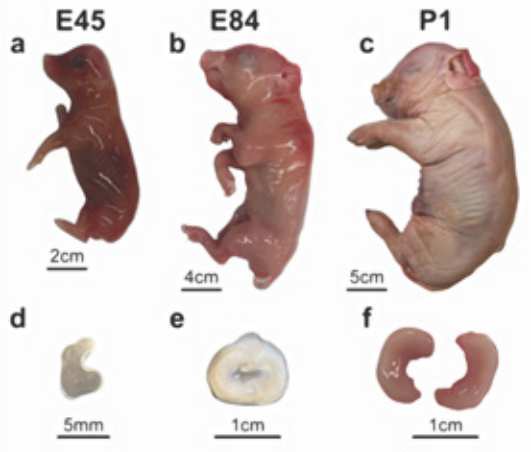

Figure 2. Gross anatomy **(A-C)** and isolated menisci **(D-F)** of embryonic newborn pigs.

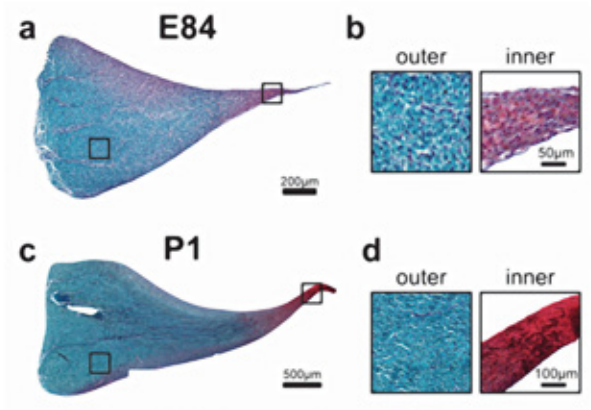

Figure 3. Regional specification is apparent in the developing pig meniscus.

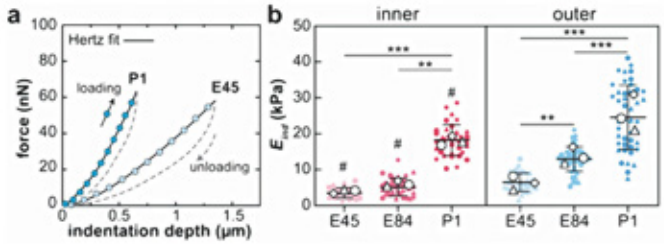

Figure 4. (A) Representative indentation force vs. depth curves for early embryonic and newborn outer meniscus; **(Bb)** Nanoindentation moduli (Eind) of inner (left) and outer (right) meniscus increase throughout gestation (**$p<0.001$, ***$p<0.0001$), and Eind of the inner region was less than that of the outer region (#$p<0.05$). For each animal ($n=3$), ≥10 indentation locations were tested in each region. White points represent the average Eind from one animal, and colored points of the same shape correspond to multiple indentations from the same animal.

microenvironments early in prenatal development that undergo continued specialization through the end of gestation, and these changes appear to initiate earlier in the outer zone.

Meniscus progenitor cells migrated from isolated meniscus segments onto tissue culture polystyrene over 5-7 days Figure 5). These cells were allowed to proliferate for an additional 7-10 days, then were passaged and seeded onto PA hydrogels or glass slides. Meniscus progenitors isolated at all three gestational timepoints exhibited increased mechanoactivation (i.e., greater cell area and increased YAP nuclear localization) with increasing substrate stiffness (Figure 5). Interestingly, P1 outer zone cells exhibited higher YAP nuclear localization than P1 inner zone or E42 cells, even on soft substrates.

Discussion

In the present work, we begin to establish a detailed, multiscale timeline of the coordinated morphological and mechanobiological changes that govern knee joint development in a translationally relevant porcine model. Consistent with prior investigations in the mouse, we show that meniscus formation and knee joint cavitation proceed rapidly following skeletal rudiment condensation and establishment of the interzone at the prospective joint

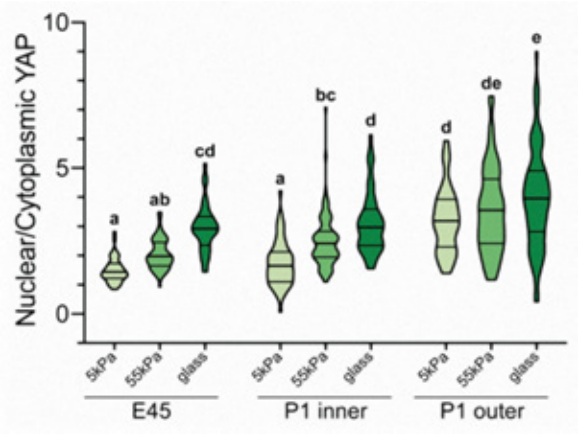

Figure 5. YAP nuclear: cytoplasmic ratio on substrates of different stiffnesses. Groups not sharing a common letter are significantly different ($p<0.05$).

line.[4,5] Histological and micromechanical assessments revealed that microenvironmental distinctions between the proteoglycan-rich inner meniscus and type I collagen-rich outer meniscus are apparent as early as E45 in the pig. At this point, embryos and hindlimbs are sufficiently large to allow meniscal tissue isolation with the aid of a dissection microscope. The differing regional matrix composition and micromechanics at this timepoint suggests resident cell identity and matrix synthesis are determined early in embryonic development. Furthermore, cells from E45 exhibited a characteristic mechanosensitive response (e.g., increased cell spreading as a function of substrate stiffness, indicating that resident meniscal cells are able to sense and respond to their mechanical microenvironment as soon as cavitation is complete. Interestingly, P1 outer zone cells showed a distinct mechanoresponse from P1 inner zone and E45 cells, wherein nuclear YAP localization was greater on all substrate stiffnesses, suggesting exposure to a stiffer microenvironment in vivo may enhance mechanosensitivity.

Future work will continue probing the phenotypic and mechanosensitive attributes of the developing meniscus, for example, by examining the heterogeneity of these cells and the matrix they synthesize via single cell RNAseq and immunohistochemistry, to establish the spatiotemporal characteristics of meniscus specialization throughout development. By uncovering the mechanisms by which emergent meniscus cells respond to biophysical cues to establish a mature, functional meniscus in the pig, we aim to shed light on mechanobiologic mechanisms that could be harnessed for injury repair and regeneration in adult fibrous tissues.

Acknowledgements

This work was supported by the NIH (R01AR075418, P30AR069619) and NSF (CCMI-2047073).

References

1. Makris EA, Hadidi P, and Athanasiou KA. The knee meniscus: Structure-function, pathophysiology, current repair techniques, and prospects for regeneration. *Biomaterials* 2011; 32(30): 7411-7431.

2. Tsinman TK, Jiang X, Han L, *et al.* Intrinsic and growth-mediated cell and matrix specialization during murine meniscus tissue assembly. *FASEBJ* 2021; 35:e21779.

3. Kwok B, Chandrasekaran P, Wang C, *et al.* Rapid specialization and stiffening of the primitive matrix in developing articular cartilage and meniscus. *Acta Biomater* 2023; 168: 235-251.

4. Tsinman TK, Huang Y, Ahmed S, *et al.* Lack of skeletal muscle contraction disrupts fibrous tissue morphogenesis in the developing murine knee. *J Orthop Res* 2023; 41(10): 2305-2314.

5. Fogarty NL, Johnson T, Kwok B, *et al.* Reduction in postnatal weight-bearing does not alter the trajectory of murine meniscus growth and maturation. *J Orthop Res* 2023: Epub ahead of print.

Muscle, Tendon, and Ligament

An Automated Tracking Algorithm Characterizing Deformation of Fatigue-Induced Achilles Tendons

Sittinon Nuethong, MS[1,2,3]
Todd J. Hullfish, BME[1,2,3]
Josh R. Baxter, PhD[1,2,3]

[1]Department of Orthopaedic Surgery
University of Pennsylvania

[2]Department of Bioengineering
University of Pennsylvania

[3]McKay Orthopaedic Laboratory
University of Pennsylvania

Introduction

Ultrasound is widely used in clinical research as a non-invasive and effective modality for imaging the Achilles tendon. Our recent work developed an ultrasound stress imaging approach to predict Achilles tendon failure under fatigue loading in vitro[1]. However, these published findings did not characterize tendon mechanics to assess fatigue damage of the Achilles tendon mid-substance. Therefore, the purpose of this study was to develop an automated ultrasound tracking tool to characterize mid-substance strain mechanics across the fatigue life of human Achilles tendon. We then tested its efficacy by correlating the bulk strains measured using the tensile testing system and our automated ultrasound tracking tool. We hypothesized that the Achilles mid-substance bulk strain measurements would correlate with the tensile testing system across the fatigue life. Establishing this tool is a critical step towards longitudinally monitoring Achilles tendon fatigue damage *in vivo* to guide personalized rehabilitative care.

Methods

Ten cadaveric Achilles tendons (4M, 3F; Age: 60 ± 15) were dissected, cut into a dog-boned shape, and mounted onto a custom-built tank and pulley system as previously described (Figure 1A)[1]. The tendons were loaded up for 150,000 cycles or until rupture using a sine waveform that generated loading cycles between 10 and 20 MPa at 1 Hz. After every 500 cycles, continuous B-mode ultrasound images of the mid-substance of each specimen were acquired at 41 Hz during 2 loading cycles at 0.25 Hz to remove motion artifact[1]. After the experiment, a custom script (MATLAB 2022b.) was implemented to track the deformation of the tendon mid-substances through the acquired ultrasound images. A rectangular region of interest (ROI) was drawn over the mid-substance (yellow rectangle), in which a 11 x 3 grid of kernels (red rectangles) was formed inside to define the subregions of the mid-substance (Figure 1B). Each kernel was seeded with point trackers (white dots) generated by Kanade-Lucas-Tomasi point tracking algorithm that detects corner point eigenvalues, as we previously used in our

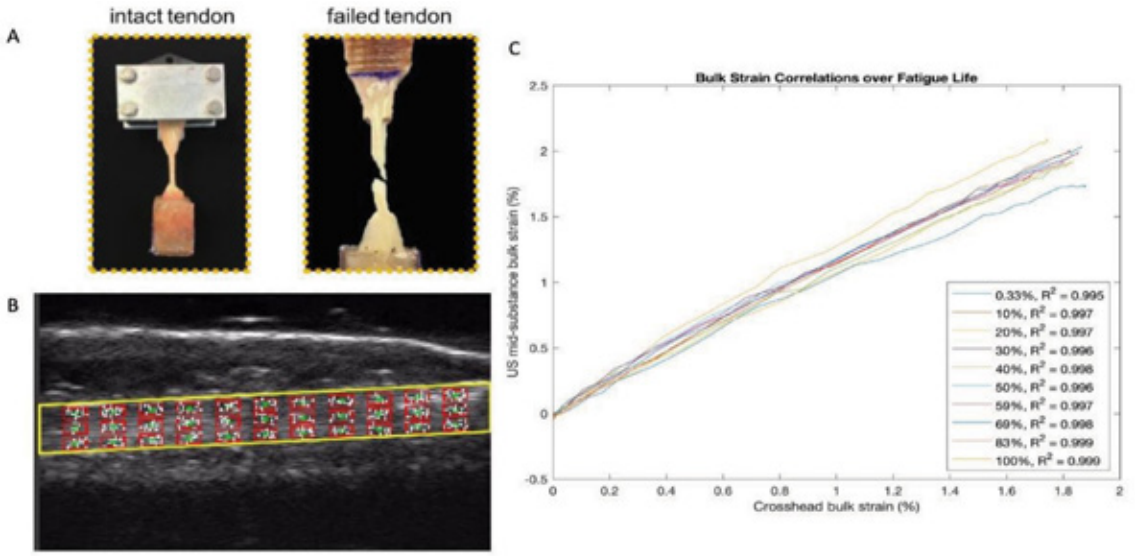

Figure 1. (A) Schematic of specimen preparation of a cadaveric Achilles tendon mounted on a moveable crosshead and fixed end excerpted from Schmidt et al.,2020; **(B)** A representative ultrasound image with an ROI (yellow rectangle), a 11 x 3 set of kernels (red rectangles), point trackers (white dots), and speckles (green dots) centered inside the kernels; **(C)** A representative correlation between mid-substance bulk strain and crosshead bulk strain over the 10 points of fatigue life, from the unstretched position to fully stretched position.

recent work, and a speckle inside was defined as the mid-point of the kernel[2]. The point trackers returned their x- and y-coordinates after tracking each frame of the ultrasound images. The x-displacement of the point tracker at a frame was calculated from subtracting its x-coordinate by its x-coordinate at the reference frame. Further, the x-displacement of the speckle in each kernel was calculated by averaging all point trackers' x-displacements in that kernel. The displacements of the three speckles in the furthest right/left three kernels were averaged and divided by the original gauge length determined from the distance between three speckles in the furthest right kernels and three speckles in the furthest left kernels to calculate the bulk strain of the mid-substance. We calculated the crosshead bulk strain of the whole specimen by dividing crosshead displacement by the measured gauge length. We correlated the bulk strains of both mid-substance and crosshead from the references to the first peaks every 10% of the fatigue life in the 6 specimens that ruptured and the 4 specimens that survived 150,000 cycles to determine whether mid-substance ultrasound tracking is robust in human tendon with differing magnitudes of mechanical fatigue damage (Figure 1C).

Results

Our automated ultrasound tracking tool accurately quantified bulk tendon strain across cadaveric tendons (Figure 1C). The average correlation between mid-substance bulk strain and crosshead bulk strain was 0.991 ± 0.004 in the ruptured group and 0.995 + 0.014 in the non-ruptured group. This very strong tracking fidelity was similarly strong at the 100% cycles (0.995 + 0.002) for the ruptured group. The average mid-substance bulk strain in the ruptured group (2.193% ± 0.316%) was 45% greater ($p < 0.001$) than the average mid-substance bulk strain in the survived group (1.508% ± 0.459%).

Discussion

In this study, we implemented our tracking algorithm over ultrasound continuous images to measure mid-substance bulk strains as well as validate its performance throughout the fatigue life. Regardless of ruptured and survived conditions or the numbers of applied cycles, the average correlations between both bulk strains remained very strong, beyond 0.990. This indicates that our automated tracking tool works effectively for all mechanically induced tendon fatigue damage. It is important to note that the mid-substance bulk strain values we report do not represent the failure strains because these stress-images were acquired at relatively low tendon stresses (10-20 MPa) compared to experimentally derived values of tendon rupture[3]. These low tendon stresses are clinically important because they are safe to apply in patients with symptomatic Achilles tendinopathy. Our tool uses a 11 x 3 tracking grid (and user customizable) that allows researchers to quantify regional strain mechanics. This is an important feature to evaluate local strains in the mid-substance and we are currently linking these mid-substance strain mechanics with altered neuromechanical profiles in patients with tendinopathy.

Conclusions

Our automated ultrasound tracking tool reliably quantifies mid-substance Achilles tendon strain across the fatigue life. Our future work will use this tool on different Achilles tendon injuries like tendinopathic tendons and ruptured tendons to assess tendon mechanical status throughout treatment and guide precision rehabilitation.

References

1.Schmidt EC, Hullfish TJ, O'Connor KM, *et al.* Ultrasound echogenicity is associated with fatigue-induced failure in a cadaveric Achilles tendon model. *Journal of biomechanics* 2020; 105: 109784.

2.Drazan JF, Hullfish TJ, Baxter JR. An automatic fascicle tracking algorithm quantifying gastrocnemius architecture during maximal effort contractions. *PeerJ* 2019: 7 ;e7120.

3.Maganaris CN, Narici MV, Maffulli N. Biomechanics of the Achilles tendon. *Disability and rehabilitation* 2008, 30(20-22): 1542–1547.

Comparing the Efficiency of Anterior Cruciate Ligament Reconstruction across Ambulatory Surgery Centers, a University Hospital, and a Hybrid Inpatient Hospital: A Prospective Study

Vineet Desai, BS[1]
Morgan Swanson, BA[1]
Divya Talwar, PhD[1]
Alexandra Stevens, BS[1]
Theodore J. Ganley, MD[1]

[1]Department of Orthopaedics
The Children's Hospital of Philadelphia

Introduction

The incidence of anterior cruciate ligament (ACL) injuries has been increasing among the pediatric and adolescent population in the last few decades, with an incidence of almost seven injuries per every 1000 hours of exposure in adolescent athletes.[1] Instead of traditional, large inpatient hospitals, orthopaedic surgeons are increasingly utilizing ambulatory surgery centers (ASCs).2 For example, the percent of knee arthroscopies performed at ASCs increased from 16% in 1996 to over 50% by 2006.[3] ASCs offer lower financial costs, increased patient convenience, and faster surgical times.[2,4] Kadhim et al. found in a retrospective review of 359 ACL reconstructions that surgeries performed at a traditional, university hospital had a greater median turnover time, longer workday, and reduced work efficiency than at an ASC.[5] Furthermore, Fabricant et al. found that performing surgery at ASCs instead of a traditional, university hospital can result in 17% to 43% cost savings for the hospital.[6]

The goal of this study was to prospectively determine if ACL reconstructions, performed by the same surgeon, differed in efficiency between a traditional, university hospital, ASCs, and a novel hybrid inpatient hybrid hospital. We hypothesized that both the ASCs and the hybrid inpatient hospital would be more surgically efficient than the university hospital.

Methods

Following Institutional Review Board (IRB) approval, patients aged 12 to 18 years at the time of ACL reconstruction were prospectively enrolled in this study. All ACL reconstructions were performed by a single, fellowship-trained pediatric sports surgeon. Patients requiring multiple ligament reconstruction other than anterolateral ligament (ALL) lateral extra-articular tenodesis (LET) or having had previous ipsilateral knee surgery were excluded. ACL reconstructions were performed at three types of sites: a traditional, tertiary-care university hospital, ASCs, and a new hybrid inpatient hospital. This hybrid hospital was initially an ASC and opened an inpatient wing in January 2022. Patients undergoing ACL reconstruction at this location before January 2022 were enrolled in the ASCs cohort, and those after January 2022 were enrolled in the new hybrid inpatient hospital cohort.

Preoperatively, we collected age, baseline pain score (NRS),[7] physical exam, physeal status, meniscal injuries, Pedi-FABS score,[8] and Pedi-IKDC score.[9] Surgical variables collected included: anesthesia time, concurrent procedures, regional anesthesia type, rate of opioids administered, type of ACL tear and type of graft used, surgery time, and in-room time. Postoperatively we collected postoperative pain scores (NRS) at post-op day one, three, and seven, and Pedi-FABS and Pedi-IKDC scores at three, six, nine, and twelve months post-op. Descriptive statistics, Pearson's Chi-squared test for independence, ANOVA, and Kruskall-Willis test were performed.

Results

Baseline Characteristics

98 patients (57.1% female, mean age 15.5 +/− 1.7 years) were enrolled. 29 patients (30.0%) received ACL reconstruction at the university hospital, 34 patients (35%) at ASCs, and 35 patients (36%) at the hybrid inpatient hospital. All patients underwent ACL reconstruction using quadriceps tendon autograft. There were no differences in age, sex, BMI, time from injury to surgery, and additional procedures between the three cohorts (Table 1).

Surgical Efficiency

The mean surgery duration for ACL reconstruction with ALL-LET (125.0 ± 28.0

Table 1. Demographic and Clinical Characteristics by Surgery Location

Characteristic	Total Cohort	University Hospital	ASCs	Hybrid Inpatient Hospital	p value
Male	42 (42.9%)	13 (44.8%)	17 (50%)	12 (34.3%)	0.406
Female	56 (57.1%)	16 (55.2%)	17 (50%)	23 (65.7%)	0.406
Age at Preoperative Visit (Years)	15.5 (±1.7)	15.8 (±1.9)	15.7 (±1.7)	15.0 (±1.6)	0.168
BMI	23.7 (±4.3)	25.6 (±4.8)	22.8 (±3.1)	23.6 (±4.7)	0.115
Time Between Injury and Surgery (Days)	69 (±73.7)	101 (±115.6)	53.7 (±37.6)	57.5 (±39.8)	0.198

*Data are presented as mean ± standard deviation or counts and percentage as appropriate.

min) did not exceed that of the overall study population. Mean ACL reconstruction surgery duration with a medial meniscus repair, lateral meniscus repair, and both menisci repair (155.5 ± 31.5, 146.7 ± 36.2, 162.1 ± 46.5 min) exceeded that of ACLR with no additional procedures (146.3 ± 30.9 min); however, these differences were not statistically significant ($p = 0.4034$). Length of surgery, time for anesthesia induction, duration of anesthesia, and overall time in the operative room were shorter in both the ASCs and the hybrid inpatient hospital in comparison to the university hospital (Table 2).

Pain Scores & Patient-Reported Outcomes

There were no differences in type of intra-operative opioid used, rate of intra-operative opioid, or postoperative pain scores between the three cohorts. Similarly, patient reported outcomes via the Pedi-FABS and Pedi-IKDC score did not differ at any time point post-operatively among the three cohorts (Table 3).

Discussion

Given the rising cost of healthcare, orthopaedic surgeons are increasingly utilizing ambulatory surgery centers (ASCs) for common, outpatient procedures.10 ASCs can increase cost savings and reduce hospital stay and postoperative complications.[10] In a previous retrospective analysis, Kadhim et al. found that performing ACL reconstructions at ASCs owned by the same institution as a traditional, university hospital could improve both surgical and workday efficiency.[5] The goal of this study was to prospectively compare the efficiency of ACL reconstructions at three types of sites: a university hospital, ASCs, and a novel hybrid inpatient hospital.

Our study found that patients undergoing ACL reconstruction at the ASCs or the novel hybrid inpatient hospital had lower length of surgery, anesthesia time, and overall operation time than patients who received the same surgery at a university hospital. Additionally, patients in the three cohorts did not demonstrate any significant differences in postoperative pain scores or patient-reported outcomes. Fabricant et al. similarly found that operating room time at ASCs was on average 64 minutes shorter than at the university hospital for common orthopaedic procedures.6 Kadhim et al. also found that the total operating room work time was shorter for hospital-owned ASCs in comparison to the inpatient hospital.[5]

There are several limitations to our study. First, the hybrid inpatient hospital was initially an ASC that was later converted to a hybrid inpatient hospital in 2022. In order to continue enrollment in our prospective study, we included patients receiving ACL reconstruction at this site after January 2022 in a separate cohort. Second, all ACL reconstructions were performed by a single surgeon, potentially limiting generalizability. However, by limiting our study to surgeries performed by one surgeon at sites all owned by the same institution, we were able to limit confounding in our findings. Lastly, the variables in our study do not capture all the surgical and patient-reported variables that characterize efficiency.

Table 2. Surgical Efficiency based on Surgery Location

Characteristic	Total Cohort	University Hospital	ASCs	Hybrid Inpatient Hospital	p value
Surgery Efficiency					
Time for Anesthesia Induction (Min)	13.7 (±8.8)	18.7 (±10.3)	9.9 (±6.4)	13.7 (±8.0)	0.0039*
Duration of Anesthesia (Min)	206 (±48.3)	262.4 (±39.5)	181.1 (±28.2)	185 (±28.6)	0.001*
Length of Surgery (Skin Open to Close) (Min)	149 (±36.0)	185.2 (±32.9)	132.8 (±23.2)	135.8 (±26.8)	0.001*
Time in Operative Room (Min)	200.3 (±46.4)	252.8 (±41.4)	178.1 (±28.3)	179.8 (±27.2)	0.001*
Continuous Peripheral Nerve Catheter	3 (3.1%)	3 (10.3%)	0 (0%)	0 (0%)	0.025*
Single-Injection Nerve Block	95 (96.9%)	26 (89.7%)	34 (100%)	35 (100%)	0.025*

*Data are presented as mean ± standard deviation or counts and percentage as appropriate.

Table 3. Pain Scores and Patient-Reported Outcomes by Surgery Location

Characteristic	Total Cohort	University Hospital	ASCs	Hybrid Inpatient Hospital	p value
Pedi-FABS	N				
Pre-Operative	99	19.4 ± 11.1	19.9 ± 9.2	17.0 ± 13.1	0.9439
3-Months Post-Op	91	2.7 ± 5.9	5.1 ± 11.3	2.1 ± 4.7	0.4550
6-Months Post-Op	86	5.3 ± 7.6	7.3 ± 8.1	10.1 ± 8.9	0.0554
9-Months Post-Op	72	10.7 ± 9.0	11.6 ± 11.13	13.1 ± 10.3	0.7549
1-Year Post-Op	45	10.3 ± 10.8	16.2 ± 12.3	11.2 ± 12.8	0.4416
Pedi-IKDC	N				
Pre-Operative	99	52.8 ± 39.4	62.61 ± 31.3	52.4 ± 39.4	0.8822
3-Months Post-Op	91	47.8 ± 31.1	61.3 ± 10.7	46.6 ± 31.1	0.5243
6-Months Post-Op	86	54.9 ± 34.1	43.4 ± 36.4	59.2 ± 33.3	0.11
9-Months Post-Op	72	49.6 ± 38.9	55.6 ± 39.5	52.2 ± 40.1	0.5007
1-Year Post-Op	45	56.3 ± 14.0	49.7 ± 21.6	53.8 ± 13.0	0.6309
Baseline Pain Scores at Preoperative Visit	2.2 ± 1.8				
Postoperative Pain Scores					
Maximum Pain Score: PACU	1.9 ± 2.8	2.1 ± 2.1	1.8 ± 1.4	2.6 ± 1.9	0.060
Median Pain Score: PACU	0 (0-2)	0 (0-3)	0 (0-2)	0 (0-0)	0.306
Maximum Pain Score: Day 1	5.8 ± 2.5	5.3 ± 2.9	5.8 ± 2.4	6.3 ± 2	0.636
Average Pain Score at Rest: Day 3	3.3 ± 2.1	4 ± 2.4	2.8 ± 2	3.2 ± 1.8	0.262
Average Pain Score at Rest: Day 7	1.8 ± 1.5	2.2 ± 1.4	0.9 ± 1.1	2.1 ± 1.6	0.023*
Rate of Intra-Operative Opioids Administered (Y/N)	34 (34.7%)	14 (48.3%)	11 (32.3%)	9 (25.7%)	0.158
Type of Intra-Operative Opioid Administered					
Morphine	7 (7.1%)	2 (6.9%)	2 (5.9%)	3 (8.6%)	0.909
Fentanyl	23 (23.5%)	9 (31%)	9 (26.5%)	5 (14.3%)	0.254

*Data are presented as mean ± standard deviation or counts and percentage as appropriate.

Conclusions

This prospective, multi-center study found that ACL reconstructions performed at either ASCs or a hybrid inpatient hospital can be more efficient than those performed at traditional, inpatient university hospitals. This information can help counsel both surgeons and families regarding both the financial and patient-centered benefits of undergoing outpatient surgeries at ambulatory centers.

References

1. Bram JT, Magee LC, Mehta NN, *et al.* Anterior Cruciate Ligament Injury Incidence in Adolescent Athletes: A Systematic Review and Meta-analysis. *Am J Sports Med*. 2021;49(7):1962-72.

2. Goldfarb CA, Bansal A, Brophy RH. Ambulatory Surgical Centers: A Review of Complications and Adverse Events. *J Am Acad Orthop Surg*. 2017;25(1):12-22.

3. Kim S, Bosque J, Meehan JP, *et al.* Increase in outpatient knee arthroscopy in the United States: a comparison of National Surveys of Ambulatory Surgery, 1996 and 2006. *J Bone Joint Surg Am*. 2011;93(11):994-1000.

4. Munnich EL, Parente ST. Procedures take less time at ambulatory surgery centers, keeping costs down and ability to meet demand up. *Health Aff (Millwood)*. 2014;33(5):764-9.

5. Kadhim M, Gans I, Baldwin K, *et al.* Do Surgical Times and Efficiency Differ Between Inpatient and Ambulatory Surgery Centers That are Both Hospital Owned? *J Pediatr Orthop*. 2016;36(4):423-8.

6. Fabricant PD, Seeley MA, Rozell JC, *et al.* Cost Savings From Utilization of an Ambulatory Surgery Center for Orthopaedic Day Surgery. *J Am Acad Orthop Surg*. 2016;24(12):865-71.

7. Breivik H, Borchgrevink PC, Allen SM, *et al.* Assessment of pain. *Br J Anaesth*. 2008;101(1):17-24.

8. Fabricant PD, Robles A, Downey-Zayas T, *et al.* Development and validation of a pediatric sports activity rating scale: the Hospital for Special Surgery Pediatric Functional Activity Brief Scale (HSS Pedi-FABS). *Am J Sports Med*. 2013;41(10):2421-9.

9. Nasreddine AY, Connell PL, Kalish LA, *et al.* The Pediatric International Knee Documentation Committee (Pedi-IKDC) Subjective Knee Evaluation Form: Normative Data. *Am J Sports Med*. 2017;45(3):527-34.

10. Lopez CD, Boddapati V, Schweppe EA, *et al.* Recent Trends in Medicare Utilization and Reimbursement for Orthopaedic Procedures Performed at Ambulatory Surgery Centers. *J Bone Joint Surg Am*. 2021;103(15):1383-91.

U·P·O·J

Strain-Induced Collagen Fibril Deformation is Diminished with Advanced Age in Mouse Supraspinatus Tendon

Jeremy D. Eekhoff
Stephanie N. Weiss
Louis J. Soslowsky

McKay Orthopaedic Research Laboratory, University of Pennsylvania, Philadelphia, PA

Introduction

Age-related tendon degeneration increases the risk of rotator cuff injuries which can lead to significant pain and disability.[1] The supraspinatus tendon, as part of the rotator cuff, exhibits region-dependent mechanical properties that change with advanced age which are likely a contributing factor to the increased risk of rupture in the elderly population.[2,3] While these age-related changes to bulk tissue properties in the supraspinatus tendon have been demonstrated,[2,4] tendon is a complex hierarchical tissue that dynamically responds to mechanical loading though changes in structural organization at multiple length scales. Despite this, it is unclear how aging affects the relationship between bulk tissue strain and collagen fibril deformation on the nanoscale level.[5] Therefore, the objective of this study was to determine how collagen fibrils deform with applied strain in different regions of the supraspinatus tendon at two distinct ages. We hypothesized that collagen fibrils would experience deformation earlier in older tendons because of a reduction in early strain attenuation mechanisms such as uncrimping and changes in fiber alignment.

Methods

Supraspinatus tendon-humerus complexes were harvested from p300 and p570 male wild-type C57BL/6 mice (IACUC approved). Tendon cross-sectional area was measured using a laser displacement sensor. After preparation for mechanical testing, samples were subjected to 10 cycles of preconditioning between 0.02 and 0.04 N followed by a one-minute rest and then a ramp to a randomly assigned strain (1%, 5%, or 9%; n = 5-6/group) at a rate of 0.1% strain per second. The tendon was immediately flash frozen after reaching the target strain, removed from the test fixture, and embedded in optimal cutting temperature compound while keeping the tissue frozen to maintain the applied strain.[6,7] Cryosections of the tendons were collected at 20 μm thickness and fixed in formalin. Nanoscale topographical images of the sections were acquired using tapping-mode atomic force microscopy (AFM) to visualize collagen fibrils. Five 2x2 μm images were acquired in both the insertion region (within 1 mm of humeral insertion) and midsubstance region (1-2mm away from humeral insertion) across multiple tissue sections for each sample (Figure 1). Collagen fibril d-period was measured using Fourier transform analysis.[8] The average d-period length, local variance (average variance in d-period length within individual images), and global variance (variance in d-period length across entire sample) were calculated for the insertion and midsubstance regions of each sample. Data for p300 and p570 samples were analyzed independently using two-way ANOVAs including the main effects of region, strain, and their interaction with Tukey-adjusted post-hoc testing within significant main effects.

Results

The applied strains of 1%, 5%, and 9% corresponded to the early toe, early linear, and early yield portions of the stress-strain curves, respectively, in both ages (Figure 2a,b,f,g). Average d-period length increased from 67.8 nm to 68.7 nm with applied strains of 1% to 5% in p300 samples, corresponding to a fibril strain of approximately 1.3% (Figure 2c). However, d-period length was not different between applied strains of 1% and 9%. In contrast with the p300 data, fibrils from p570 samples experienced no strain-induced changes in d-period length (Fig 2h). Moreover, local and global variance in d-period length

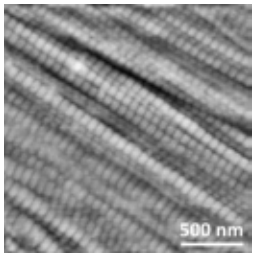

Figure 1. Representative image

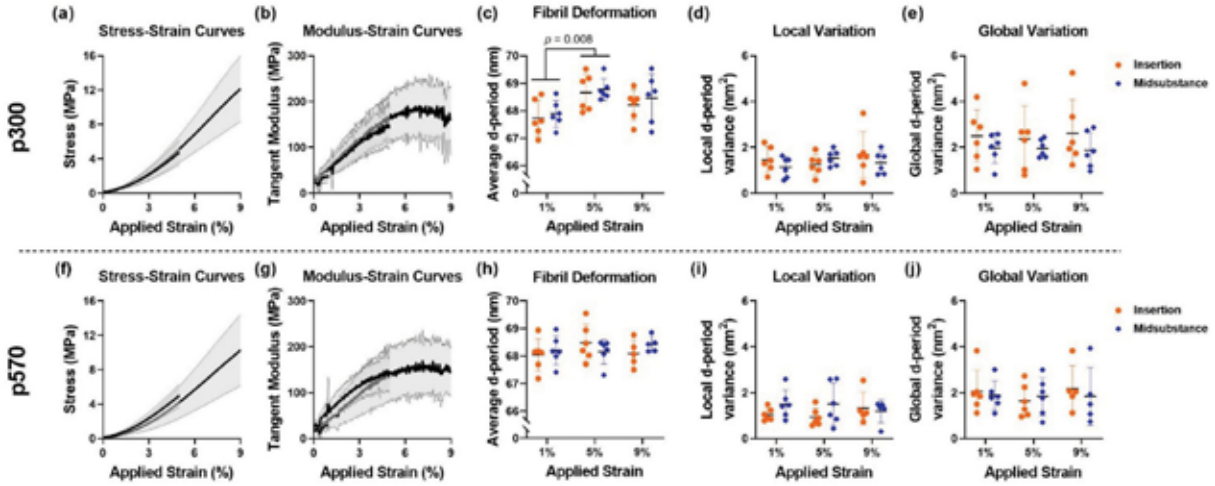

Figure 2. Average stress-strain curves **(A,F)** and modulus-strain curves **(B,G)** from p300 and p570 samples. Fibril deformation was significantly increased from 1% to 5% applied strain independently of region in p300 samples **(C)** but was unaffected by strain and region in p570 samples **(H).** Local and global variation were unaffected by strain and region in both p300 and p570 samples **(D,E,I,J)**.

showed no effect of strain or region in both p300 and p570 ages (Figure 2d,e,i,j).

Discussion

Significant deformation of collagen fibrils was observed in p300 supraspinatus tendons. Unexpectedly, this fibril deformation occurred at the lower applied strain of 5%. Therefore, some of the applied strain is transmitted from the bulk tissue level to the collagen fibrils between the early toe and early linear regions of the loading curve despite the uncrimping and reorganization that would be expected concurrently between these strains.[9] At the larger applied strain of 9%, the d-period length was no longer different than the 1% strain baseline value. Because the tissue exhibited early yield behavior (i.e., a reduction in modulus) at 9% strain, these data suggest that tissue yielding may result from early damage to the extracellular matrix that causes the collagen fibril d-period to begin to return to its initial length. Similar strain-dependent changes, with larger fibril deformations at intermediate applied strains, were found previously in supraspinatus tendons from younger p150 mice.[6,7] Contrary to our hypothesis, no fibril deformation was observed in supraspinatus tendons from p570 mice in this study. At this advanced age, the lack of strain transmission from the bulk tissue scale to the fibril scale indicates that smaller-scale mechanisms are likely dominated by structural reorganization such as uncrimping, sliding, and/or realignment rather than deformation of collagen fibrils.[9,10] Identifying the interplay between, and combination of, these mechanisms which become prominent with advanced age is a promising area for future study. In addition to measuring fibril deformation, this study also investigated the variation in d-period lengths. Even with changing d-period length in p300 samples, the variation remained similar for all strains. Therefore, the increase in d-period length was homogenous across all fibrils in the tissue, rather than the alternative where some fibrils would experience deformation while others would not. However, it should be noted that while fibril deformation was homogeneous in this controlled experiment, more complex mechanical loading of the supraspinatus tenon in situ could result in heterogenous fibril engagement.

Significance

Results from this study provide insights regarding nanoscale mechanisms that influence age-related degeneration and changes in mechanical properties of supraspinatus tendon.

Acknowledgment

This study was supported by NIH/NIAMS (AR070750) and the Penn Center for Musculoskeletal Disorders (NIH/NIAMS, P30 AR069619).

References

1. Zhao J, Luo M, Lian G, *et al.* Risk Factors for Supraspinatus Tears: A Meta-analysis of Observational Studies. *Orthop J Sports Med* 2021; 9(10): 23259671211042826.

2. DiStefano MS, Han B, Paglia PL, *et al.* Determining Region-Specific Mechanical and Structural Differences in Aging Mouse Supraspinatus Tendons. *ORS Annual Meeting*, 2022.

3. Johnson J, von Stade D, Gadomski B, *et al.* Biomechanical and histological changes secondary to aging in the human rotator cuff: A preliminary analysis. *J Orthop Res* 2023; 41(1):2221-31.

4. Connizzo BK, Sarver JJ, Birk DE, *et al.* Effect of age and proteoglycan deficiency on collagen fiber re-alignment and mechanical properties in mouse supraspinatus tendon. *J Biomech Eng* 2013; 135(2):021019.

5. Fang F, Lake SP. Experimental evaluation of multiscale tendon mechanics *J Orthop Res* 2017; 35(7);1353-65.

6. Connizzo BK, Sarver JJ, Han L, *et al.* In situ fibril stretch and sliding is location-dependent in mouse supraspinatus tendons *J Biomech* 2014; 47(16)3794-8.

7. Connizzo BK, Han L, Birk DE, *et al.* Collagen V-heterozygous and -null supraspinatus tendons exhibit altered dynamic mechanical behaviour at multiple hierarchical scales. *Interface Focus* 2016; 6(1): 20150043.

8. Rigozzi S, Stemmer A, Muller R, *et al.* Mechanical response of individual collagen fibrils in loaded tendon as measured by atomic force microscopy. J Struct Biol 2011. 176(1);9-15.

9. Miller KS, Connizzo BK, Feeny E, *et al.* Characterizing local collagen fiber re-alignment and crimp behavior throughout mechanical testing in a mature mouse supraspinatus tendon model. *J Biomech* 2012; 45(12):2061-5.

10. Szczesny SE, Elliott DM. Interfibrillar shear stress is the loading mechanism of collagen fibrils in tendon. *Acta Biomater* 2014; 10(6):2582-90.

Tendon-Targeted Collagen V Deficiency and Knockout Attenuate Mature Supraspinatus Tendon Mechanics

Michael S. DiStefano
Stephanie N. Weiss
Andrew F. Kuntz
Louis J. Soslowsky

McKay Orthopaedic Research Laboratory, University of Pennsylvania, Philadelphia, PA
micdis@seas.upenn.edu

Disclosures

AF Kuntz (5, Integra Lifesciences, Orthofix, Inc., FX Shoulder USA, Inc.; 9, American Shoulder and Elbow Surgeons, American Board of Orthopaedic Surgery, Inc.), no other disclosures

Introduction

Collagen V is a critical tendon matrix protein that regulates fibrillogenesis and is expressed throughout development and in mature tendons.[1] Clinical manifestation of collagen V deficiency is the classic form of Ehlers-Danlos syndrome (EDS), a connective tissue disorder with greater than 50% of patients being haploinsufficient for COL5A1, characterized by hyperextensible skin, joint hypermobility and instability, and abnormal wound healing.[2] Recent data from mouse supraspinatus tendon, which experiences a complex, region-dependent (insertion and midsubstance) loading environment within the rotator cuff of the shoulder, demonstrated that deficiency of collagen V during development resulted in severely altered collagen fibril structure, biomechanical properties, and dynamic responses to load.[3] However, the region-specific roles of collagen V tendon-targeted deficiency and knockout on mature supraspinatus tendons remain unknown. The objective of this study is to elucidate the regulatory role of collagen V on supraspinatus tendon whole-tissue and regional mechanics in mature mice using tendon-targeted (Scleraxis-Cre) collagen V heterozygous and knockout mice. Due to the role of collagen V in the regulation of tendon structure during development, we hypothesized that collagen V heterozygous and knockout supraspinatus tendons would have inferior whole-tissue and regional elastic mechanical properties, whole-tissue viscoelastic mechanical properties and reduced regional collagen fiber realignment compared to wild type control tendons.

Methods

Animals

Supraspinatus tendons (n = 10/genotype) from tendon-targeted collagen V heterozygous (TEN-HET) mice (ScxCre;Col5a1f/wt), knockout (TEN-KO) mice (ScxCre;Col5a1f/f), and wild-type (WT) control mice (Cre-littermates) were used (IACUC approved).

Mechanics and Collagen Fiber Realignment

All mice were sacrificed at 150 days old and were subjected to our mechanical testing and collagen fiber realignment protocol: stress relaxations at 3%, 5%, and 7% strain each with subsequent frequency sweeps at 0.1, 1, 5, and 10 Hz, followed by a quasistatic ramp-to-failure.[3] Throughout the ramp-to-failure, dynamic collagen fiber realignment was quantified using cross-polarization imaging, and regional fiber alignment data was interpolated with a polynomial fit as a function of strain from the load-displacement data. Images were acquired during the ramp-to-failure for optical strain tracking of stain lines demarcating the insertion and midsubstance regions of the tendon.

Statistics

Comparisons between genotypes were conducted using one-way ANOVAs followed by Bonferroni post-hoc tests. Significance was set at $p \leq 0.05$ and trends at $p \leq 0.1$.

Results

Whole-tendon cross-sectional area was reduced in the TEN-KO group compared to the TEN-HET and WT groups (Figure 1A). Consistent with our hypothesis, collagen V deficiency and knockout resulted in dose-dependent reductions in elastic mechanical properties (e.g., failure load and linear stiffness (Figure 1B, C)). Viscoelastic differences were also observed. Percent relaxation was increased in TEN-KO tendons compared with TEN-HET and WT tendons at all strain levels (7% strain shown in (Figure 2A). Additionally, collagen V TEN-HET and TEN-KO resulted in dose-dependent reductions in dynamic modulus, while phase shift was increased in TEN-KO tendons relative to TEN-HET and WT across all strain levels and frequencies (7% strain at 1 Hz shown in Figure 2B and 2C). As hypothesized, collagen V TEN-HET

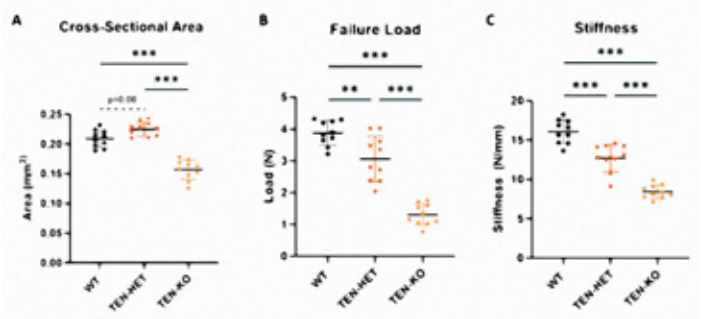

Figure 1. TEN-KO tendons demonstrated reduced cross-sectional area relative to TEN-HET and WT tendons **(A).** Tendon-targeted deficiency and knockout of collagen V resulted in significant reductions in elastic mechanical properties failure load and stiffness in a dose-dependent manner **(B-C).** Data as mean ± standard deviation (--p≤0.1, *p≤0.05, **p≤0.01, ***p≤0.001).

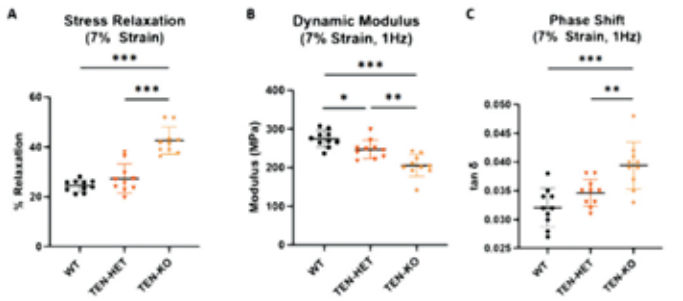

Figure 2. TEN-KO tendons had increased percent relaxation relative to TEN-HET and WT tendons **(A).** Tendon-targeted collagen V deficiency and knockout resulted in significant reductions in dynamic modulus in a dose-dependent manner **(B),** while phase shift was significantly increased in TEN-KO tendons relative to TEN-HET and WT tendons **(C).** Data as mean ± standard deviation (*p≤0.05, **p≤0.01, ***p≤0.001).

and TEN-KO resulted in dose-dependent reductions in insertion modulus, while midsubstance modulus was reduced in TEN-KO tendons relative to TEN-HET and WT tendons (Figure 3A, B). These results are supported by reductions in collagen fiber realignment in TEN-HET and TEN-KO tendons across region, as demonstrated by greater normalized circular variance values for insertion and midsubstance regions from 3-7% strain (Figure 3C-D), encompassing the toe and linear elastic regions of these tendons.

Discussion

This study investigated the role of collagen V on supraspinatus tendon elastic and viscoelastic mechanics using TEN-HET and TEN-KO mice. Consistent with previous data, we demonstrated that tendon-targeted collagen V TEN-HET and TEN-KO 5esulted in reductions in regional and whole-tissue elastic and viscoelastic mechanical properties.[3] Further, reductions in these properties in our collagen V TEN-HET tendons highlight the allele-dependency of collagen V on tendon elastic and viscoelastic mechanical function and collagen fiber realignment. These functional deficits could be attributed to the improper hierarchical assemblies of TEN-HET and TEN-KO tendons resulting in disorganized tendon matrices with an inferior ability to respond to load.[4] This was evidenced by marked

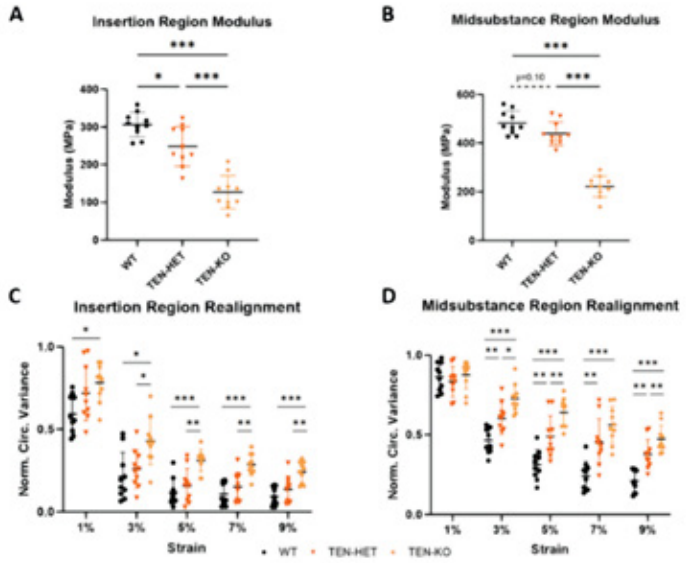

Figure 3. TEN-HET and TEN-KO tendons demonstrated reduced moduli and collagen fiber realignment in the insertion **(A, C)** and midsubstance **(B, D)** regions. Decreased normalized circular variance is indicative of increased collagen fiber realignment. Data as mean ± standard deviation (--p≤0.1, *p≤0.05, **p≤0.01, ***p≤0.001).

reductions in the TEN-HET and TEN-KO tendons' responses to realign resulting in inferior whole-tissue and regional elastic and viscoelastic mechanical properties. Overall, results demonstrate that decreased collagen V expression detrimentally affects supraspinatus whole-tissue and regional elastic and viscoelastic mechanical properties and collagen fiber realignment.

Significance/Clinical Relevance

This study elucidates the critical role of collagen V in regulating supraspinatus tendon function. Future studies will evaluate the structural and compositional mechanisms that contribute to these mechanical results. Understanding the effects of collagen V in tendon can be used to develop potential treatments modalities for classic Ehlers-Danlos syndrome.

Acknowledgement

This study was supported by NIH/NIAMS (AR070750) and the Penn Center for Musculoskeletal Disorders (NIH/NIAMS, P30 AR069619).

References

1 Wenstrup RJ, Smith SM, Florer JB, *et al.* Regulation of collagen fibril nucleation and initial fibril assembly involves coordinate interactions with collagens V and XI in developing tendon. *J Biol Chem.* 2011;286(23):20455-20465.

2 Royce PM, Steinmann BU. *Connective Tissue and It Heritable Disorders : Molecular, Genetic, and Medical Aspects.* Wiley-Liss; 2002.

3 Connizzo BK, Han L, Birk DE, *et al.* Collagen V-heterozygous and -null supraspinatus tendons exhibit altered dynamic mechanical behaviour at multiple hierarchical scales. *Interface Focus.* 2016;6(1):20150043.

4 Connizzo BK, Adams SM, Adams TH, *et al.* Collagen V expression is crucial in regional development of the supraspinatus tendon. *J Orthop Res.* 2016;34(12):2154-2161.

U·P·O·J

Tendon-Targeted Collagen V Knockout Influences Mechanical Properties of Aged Supraspinatus Tendon

Mitchell J. Hallman
Michael S. DiStefano
Stephanie N. Weiss
Jeremy D. Eekhoff
Louis J. Soslowsky

McKay Orthopaedic Research Laboratory, University of Pennsylvania, Philadelphia, PA

Introduction

Collagen V is one of the minor collagens in tendon, yet it plays a critical role in collagen fibrillogenesis by influencing the hierarchal assembly of collagen I into fibrils, fibers, and fascicles.[1] Clinical manifestations of reduced collagen V expression are present in patients with classic Ehlers-Danlos syndrome (EDS), a heritable connective tissue disorder with generalized connective tissue fragility as well as joint hypermobility and instability.[2] In addition to the altered tissue properties caused by reduced collagen V expression in EDS, the supraspinatus tendon is at high risk for injury with increased age and exhibits region-specific properties due to its complex leading environment.[3-4] Previous work has demonstrated that collagen V deficiency during development resulted in severely altered collagen fibril structure, biomechanical properties, and dynamic responses to load in the mouse supraspinatus tendon.[5] However, little remains known regarding the region-specific roles of collagen V in mouse supraspinatus tendon with more advanced age. Therefore, the objective of this study was to elucidate the region-specific role of collagen V in supraspinatus tendon mechanical properties of aged mice. We hypothesized that reduction in collagen V would result in inferior mechanical properties of the supraspinatus tendon, and that the mechanical changes would be greater in the insertion region than in the midsubstance region.

Methods

Supraspinatus tendons (n = 10/group) from male, 300 day old tendon-targeted collagen V heterozygous (Ten-Het) (ScxCre;Col5a1$^{f/wt}$), knockout (Ten-Null) (ScxCre;Col5a1f/f), and Cre-littermate controls (control) were used in this IACUC approved study. Supraspinatus tendon-humerus complexes were finely dissected, and the cross-sectional area was measured using a laser displacement sensor. Lines were applied to the tendon using Verhoeff's stain at 0, 1, 2, and 2.5mm from the humeral insertion to demarcate the insertion region (0-1mm) and midsubstance region (1-2mm) for optical strain tracking and to establish the gauge length (2.5mm). After potting the humerus and securing the free end of the tendon between sandpaper using cyanoacrylate glue, the samples were subjected to mechanical testing: after preloading to 0.05N and performing 10 cycles of preconditioning, stress relaxations were conducted at 3%, 5%, and 7% strain each with subsequent frequency sweeps at 0.1, 1, 5, and 10 Hz, followed by a quasistatic ramp-to-failure at a rate of 0.1% strain/second. Failure load and linear stiffness were quantified from the ramp to failure. Percent relaxation was calculated for each stress relaxation, and dynamic modulus and phase shift (tan δ) were quantified for each frequency sweep. Images were acquired during the ramp-to-failure for optical strain tracking of stain lines to calculate the modulus of the insertion and midsubstance regions. Comparisons between genotypes were conducted using one-way ANOVAs followed by Bonferroni post-hoc tests.

Results

Whole tendon cross-sectional area did not differ between groups (Figure 1A). Significant differences were seen in tendon elastic and viscoelastic mechanical properties. Ten-Null tendons failed at a significantly lower loads compared to both control and Ten-Het tendons and demonstrated a lower stiffness than controls (Figure 1B-C). Additionally, Ten-Null tendons exhibited increased percent relaxation at 7% strain compared to control tendons (Figure 1D). There were no differences in percent relaxation between groups at 3% or 5% strain (data not shown). Ten-Null tendons demonstrated a decreased dynamic modulus and increased phase shift across all strain levels and frequencies (7% strain at 1 Hz shown in Figure 1E-F). Ten-Null tendons demonstrated a decreased elastic modulus in the insertion region compared to control and Ten-Het tendons, while the Ten-Null tendons had a lower modulus only compared to controls in the midsubstance region Figure 2A-B).

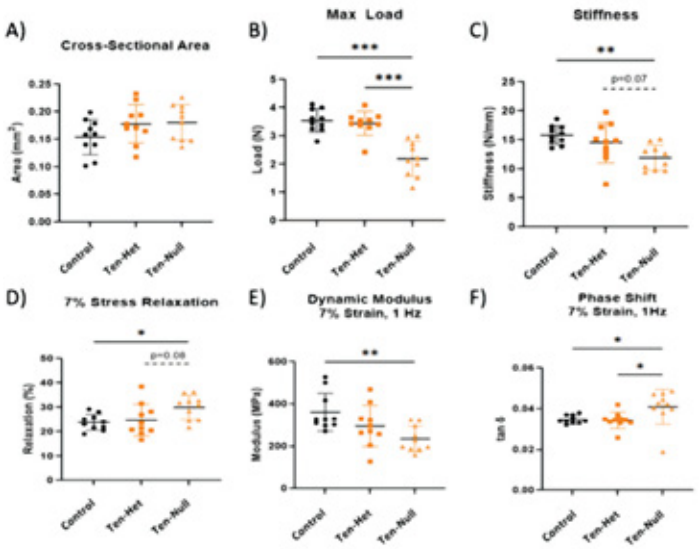

Figure 1. (A) No differences were seen in whole-tendon cross-sectional area. Ten-Null tendons demonstrated decreased in **(B)** max load and **(C)** stiffness. Within viscoelastic properties, Ten-Null tendons had **(D)** increased percent relaxation, **(E)** decreased dynamic modulus, and **(F)** increased phase shift. Data shown as mean ± standard deviation. (--p≤0.1, *p≤0.05, **p≤0.01, ***p≤0.001).

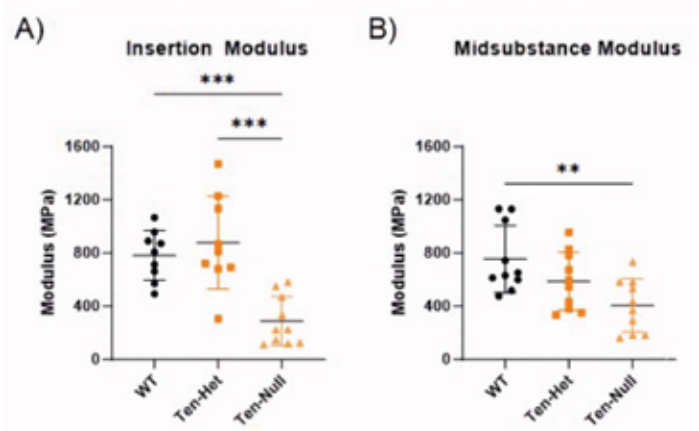

Figure 2. Ten-Null tendons demonstrated reduced modulus in the **(A)** insertion region, compared to control and Ten-Het samples, and in the **(B)** midsubstance, compared to controls. Data shown as mean ± standard deviation. (**p≤0.01, ***p≤0.001).

Discussion

This study investigated the role of collagen V on aged supraspinatus tendon elastic and viscoelastic mechanical properties. Results demonstrate that collagen V plays a critical role in regulating the extracellular matrix of supraspinatus tendon that has lasting effects into advanced age. Both the insertion and midsubstance regions were affected by collagen V knockout, yet its influence caused a greater decrease in modulus in the insertion region where the supraspinatus tendon is the least organized and experiences the highest strains.[6] Previous work investigating the regional influence of collagen V on fibril morphology in the supraspinatus tendon has shown that collagen V knockout mice demonstrate a significant disruption of fibril assembly with an increase in structurally aberrant fibrils at the insertion region compared to controls.[7] This regional variation in how collagen V influences collagen fibril structure could contribute to the respective mechanical responses of the insertion and midsubstance regions. This is the first study to evaluate the role of collagen V in tendons from mice aged 300 days as previous work evaluated tendons from younger mice (60-120 days).[5-7] Evaluating tendons at this age allows us to gain an understanding of the influence of collagen V on tendon properties after maturation into more advanced age. Future studies will investigate the underlying structural and compositional properties of the tendon extracellular matrix caused by knockout of collagen V that give rise to these mechanical findings. Moreover, continued work will investigate the varied effect of collagen V knockout at different ages to gain a better understanding of the distinct roles of collagen V in tendon properties during development, maturation, and aging.

Clinical Relevance

EDS is a clinical syndrome with limited treatment options. Furthering our understanding of collagen V in tendon under different conditions will aid the development of therapeutic targets for EDS.

Acknowledgement:

This study was supported by NIH/NIAMS (AR070750) and the Penn Center for Musculoskeletal Disorders (NIH/NIAMS, P30 AR069619).

References

1. Wenstrup RJ, Smith SM, Florer SM, *et al.* Regulation of collagen fibril nucleation and initial fibril assembly involves coordinate interactions with collagens V and XI in developing tendon. *J Biol Chem* 2011; 286(23):20455-65.

2. Steinmann B, Royce PM, Superti-Furga A. The Ehlers-Danlos Syndrome in *Connective Tissue and Its Heritable Disorders: Molecular, Genetic, and Medical Aspects*. 2002.

3. Minagawa *et al.* *J Orthop.* 2013.

4. DiStefano MS, Han B, Paglia PL, *et al.* Determining Region-Specific Mechanical and Structural Differences in Aging Mouse Supraspinatus Tendons. *ORS Annual Meeting*, 2022.

5. Connizzo BK, Han L, Birk DE, *et al.* Collagen V-heterozygous and -null supraspinatus tendons exhibit altered dynamic mechanical behaviour at multiple hierarchical scales. *Interface Focus* 2016; 6(1): 20150043.

6. Connizzo BK, Adams SM, Adams TH, *et al.* Multiscale regression modeling in mouse supraspinatus tendons reveals that dynamic processes act as mediators in structure-function relationships. *J Biomech* 2016; 49(9):1649-57.

7. Connizzo BK, Adams SM, Adams TH, *et al.* Collagen V expression is crucial in regional development of the supraspinatus tendon. *J Orthop Res.* 2017; 34(12):2154-61.

Collagens V and XI Jointly Regulate Fibril Assembly and Elastic Mechanical Properties during Tendon Maturation

Nat A. Thurlow
Jeremy D. Eekhoff
Ashley K. Fung
Courtney A. Nuss
Stephanie N. Weiss
Nathaniel A. Dyment
Louis J. Soslowsky

McKay Orthopaedic Research Laboratory, University of Pennsylvania, Philadelphia, PA
nthurlow@seas.upenn.edu

Disclosures

None

Introduction

Tendon hierarchical structure is established during development through the coordinated assembly of matrix proteins, including minor fibril-forming collagens such as collagens V and XI. Collagen V influences collagen fibrillogenesis through nucleating fibril formation and co-assembling with collagens I and II[1], and lack of Col5a1 expression leads to larger fibrils, reduced fibril density, and smaller tendon cross-sectional area2. Collagen XI has a similar role in fibril regulation during development3 and co-assembles with collagen V to form heterotypic fibrils.[1] The expression of genes for collagen V and XI is similar in developing tendons, but the expression of collagen XI encoding genes is decreased in mature tendons compared to collagen V genes. Moreover, in global knockdown mouse models, haploinsufficiency of both Col5a1 and Col11a1 in tandem yielded more irregular fibril shapes and greater heterogeneity of fibril diameters in developing tendons than Col5a1 haploinsufficiency alone1. Together, these findings suggest interactive roles between collagens V and XI during development. However, the structural and functional deficits associated with coordinated knockdown of Col5a1 and Col11a1 remain unknown. Since the tendon-specific compound Col5a1, Col11a1 knockout is postnatally unviable, the objective of this work was to assess the cooperative roles of collagens V and XI during fibril growth and assembly using a tendon-specific (ScxCre) compound Col5a1 null, Col11a1 heterozygous mouse model. Based on prior work in tendons lacking Col5a1 expression, we hypothesized that ScxCre;Col5a1flox/flox;Col11a1flox/+ (VKO-XIHet) tendons would demonstrate structural changes consistent with aberrant fibril growth.

Methods

Animals

Male and female postnatal day 30 VKO-XIHet mice (n = 10) and ScxCre- littermate controls (Ctrl, n = 10) were used (IACUC approved).

Transmission Electron Microscopy

Immediately after sacrifice, Achilles tendons (ATs) (n = 4/genotype) were isolated, fixed, embedded, sectioned, stained, and imaged as described4. Fibril diameters were measured using a custom MATLAB script (n = 10 images/sample).

Mechanics

AT-calcaneus complexes were harvested, finely dissected, and cross-sectional area was measured using a custom laser device. The free end of the tendon was secured in sandpaper with cyanoacrylate glue, and the calcaneus and sandpaper were gripped in custom fixtures. Tendons were tested in a PBS bath at 37°C using a protocol of preloading to 0.03N, preconditioning for 10 cycles, stress relaxations at 3% and 5% strain, and quasistatic ramp-to-failure at 0.1% strain/sec (Instron 5848). Each stress relaxation was followed by a frequency sweep of 10 cycles at 0.1, 1, 5, and 10 Hz.

Statistics

Fibril diameter distributions were compared between genotypes using a Kolmogorov-Smirnov test. Cross-sectional area and mechanical properties were compared across genotypes using a two-sample t-test. Significance was set at $p \leq 0.05$, and all data visualization and statistics were conducted in R (v4.3.1).

Results

VKO-XIHet ATs demonstrated substantial changes in fibril structure and mechanical properties. The collagen fibril distribution in

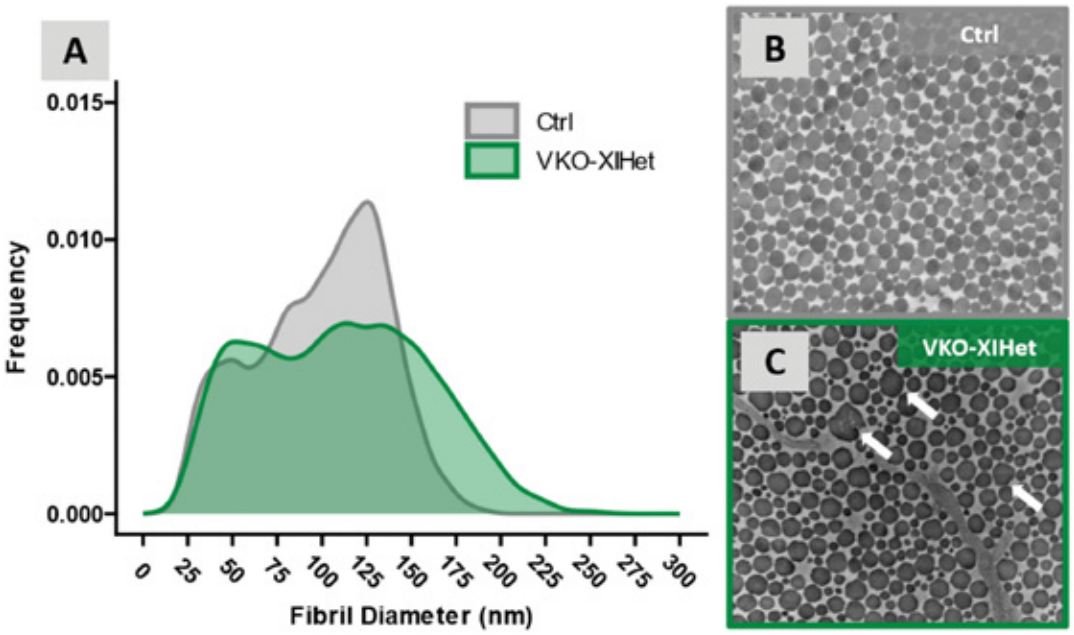

Figure 1. (A) VKO-XIHet fibril distributions demonstrate statistical differences with a population of larger diameter fibrils. Fibril distributions were compared using a Kolmogorov-Smirnov test. **(B-C)** Fibril boundaries are irregularly shaped in VKO-XIHet tendons (white arrows), especially in larger fibrils.

VKO-XIHet tendons was different than Ctrl with a distinct population of larger (>175 nm) fibrils (Figure 1A). While fibrils in Ctrl tendons had circular cross-sections, many fibrils in VKO-XIHet tendons had irregularly shaped cross-sections with these irregularities most apparent and severe in the population of larger fibrils (Figure 1B-C). Despite larger fibril diameters, overall tendon cross-sectional area was smaller in VKO-XIHet tendons (Figure 2A). Maximum load, stiffness, and maximum stress were also lower in VKO-XIHet tendons compared to Ctrl (Figure 2B-D). Viscoelastic properties showed minimal differences between genotypes (data not shown).

Discussion

We studied the combined roles of collagens V and XI in establishing structural and mechanical properties of the AT during postnatal growth. Supporting our hypothesis, VKO-XIHet tendons showed fibril-level structural and tissue-level mechanical changes consistent with altered fibril assembly. The shift towards larger diameter fibrils and irregularity of fibril boundaries in VKO-XIHet tendons suggest that these collagen types work in concert to regulate lateral growth of fibrils. This finding is consistent with previous work where the absence of Col5a1 expression led to larger fibril dimeters[3,5] and irregular fibril boundaries.[5] Additionally, we previously found a 39% decrease in maximum load and a 19% decrease in maximum stress in post-natal day 60 ScxCre;Col5a1flox/flox ATs2. In comparison, the post-natal day 30 ScxCre;Col5a1floxflox;Col11a1flox/+ tendons in this study showed 75% and 45% decreases in the same parameters, respectively. These markedly reduced mechanical properties coupled with increased lateral

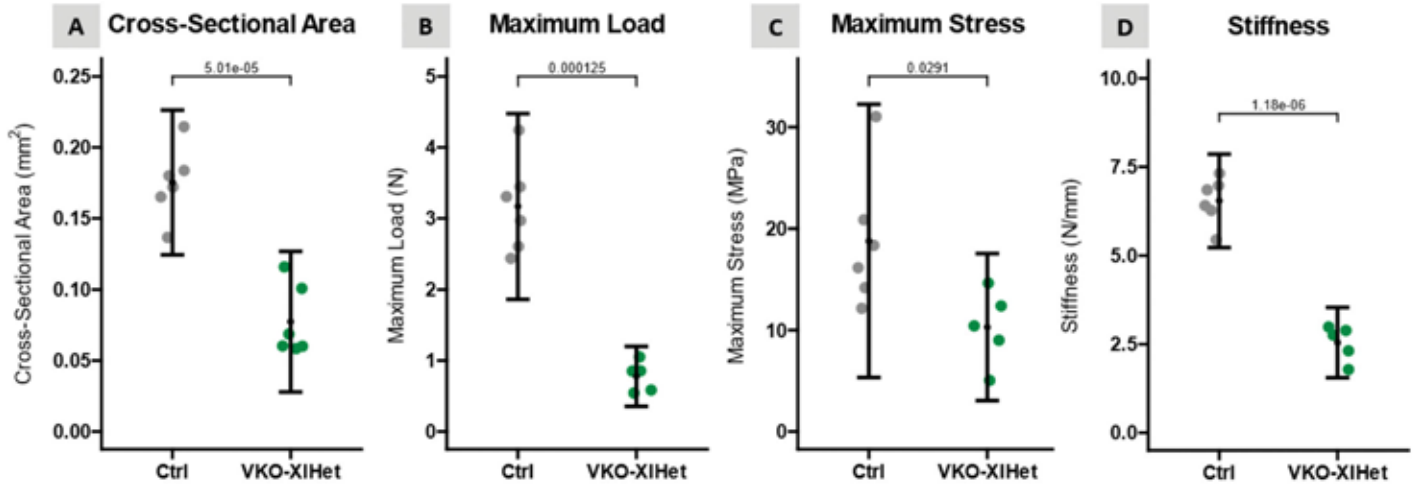

Figure 2. Cross-sectional area **(A)**, maximum load **(B)**, maximum stress **(C)**, and stiffness **(D)** were significantly decreased in VKO-XIHet tendons. Properties were compared between genotypes using t-tests; p-values are listed above significance bars. Data shown as mean ± SD.

growth in a sizable portion of fibrils demonstrate that ablation of 1 allele of Col11a1 in addition to both alleles of Col5a1 further exacerbates the phenotype during tendon development. Future work will focus on delineating possible compensatory mechanisms between collagens V and XI and understanding interactions at early stages of development.

Significance

Collagens V and XI have known roles in fibrillogenesis and the acquisition of tendon structure during development. Due to their coordinated roles and structural similarities, defining the interactions between collagens V and XI in tendon is essential to understanding mechanisms underlying collagen fibril formation.

Acknowledgements

This study was supported by NIH/NIAMS (R01AR073231) and Penn Center for Musculoskeletal Disorders (P30AR069619).

References

1. Wenstrup RJ, Smith SM, Florer JB, *et al.* Regulation of collagen fibril nucleation and initial fibril assembly involves coordinate interactions with collagens V and XI in developing tendon. *J Biol Chem.* 2011;286(23):20455-20465.

2. Connizzo BK, Freedman BR, Fried JH, *et al.* Regulatory role of collagen V in establishing mechanical properties of tendons and ligaments is tissue dependent. *J Orthop Res.* 2015;33(6):882-888.

3. Sun M, Luo EY, Adams SM, *et al.* Collagen XI regulates the acquisition of collagen fibril structure, organization and functional properties in tendon. *Matrix Biol.* 2020;94:77-94.

4. Dunkman AA, Buckley MR, Mienaltowski MJ, *et al.* The injury response of aged tendons in the absence of biglycan and decorin. *Matrix Biol.* 2014;35:232-238.

5. Connizzo BK, Adams SM, Adams TH, *et al.* Collagen V expression is crucial in regional development of the supraspinatus tendon. *J Orthop Res.* 2016;34(12):2154-2161.

Type III Collagen Expression Decreases During Neonatal Tendon Development and is Unchanged in Early Neonatal Tendon Healing

Margaret K. Tamburro, MS[1]
Jaclyn A. Carlson, PhD[1,2]
Miranda K. Doro[1]
Stephanie N. Weiss[1]
Susan W. Volk, VMD, PhD[2]
Louis J. Soslowsky, PhD[1]

[1]McKay Orthopaedic Research Laboratory
University of Pennsylvania

[2]School of Veterinary Medicine
University of Pennsylvania

Introduction

After tendon injury, fibrovascular scarring leads to inferior tendon function and high re-injury risk. Specifically, poor and insufficient remodeling of the provisional, type III collagen (Col3)-rich matrix to a highly aligned, type I collagen (Col1)-rich matrix results in a disorganized and weak matrix throughout healing. Much like the early healing matrix in adult tendon, developing embryonic tendon contains high levels of Col3.[1] However, the magnitude and timing of *Col3a1* gene expression in the developing and healing neonatal tendon have not been elucidated; this information may provide crucial foundation for investigations of neonatal development and healing as potential mechanisms of superior tendon remodeling from a Col3- to Col1-rich matrix. Therefore, the objective of this study was to define the expression profile of the *Col3a1* gene throughout early neonatal development and healing. We hypothesized that *Col3a1* expression would be highest immediately post-partum and decrease throughout neonatal development. Additionally, we expected healing neonatal tendons to mount a quick and robust Col3 response with increased *Col3a1* expression during early healing timepoints.

Methods

For investigations of neonatal development, thirty-five right knees from C57/B6 wild-type (WT) mice were harvested at postnatal days 0, 3, 7, 10, and 14 (p0, p3, p7, p10, p14; $n \geq 6$/group mixed sex). For investigations of neonatal healing, twelve WT mice received right patellar tendon biopsy punch injury (0.3 mm diameter, performed under 10X magnification; Fig 1A-B) at 7 days of age. Right knees were harvested at 3- and 7-days post-injury, corresponding to p10 and p14 of the mice, respectively (n = 6/group mixed sex). All studies were IACUC approved. For all groups, patella-patellar tendon-tibia complexes were fixed for 4 hours in 4% paraformaldehyde, dissected, and cryo-embedded. Tendons were sectioned coronally (40 μm) and micro-dissected with a 25G needle to ensure proper isolation of the neonatal tendon for developmental ages (p0, p3, p7, p10, p14) or injured matrix for healing timepoints (3 days post-injury/p10, 7 days

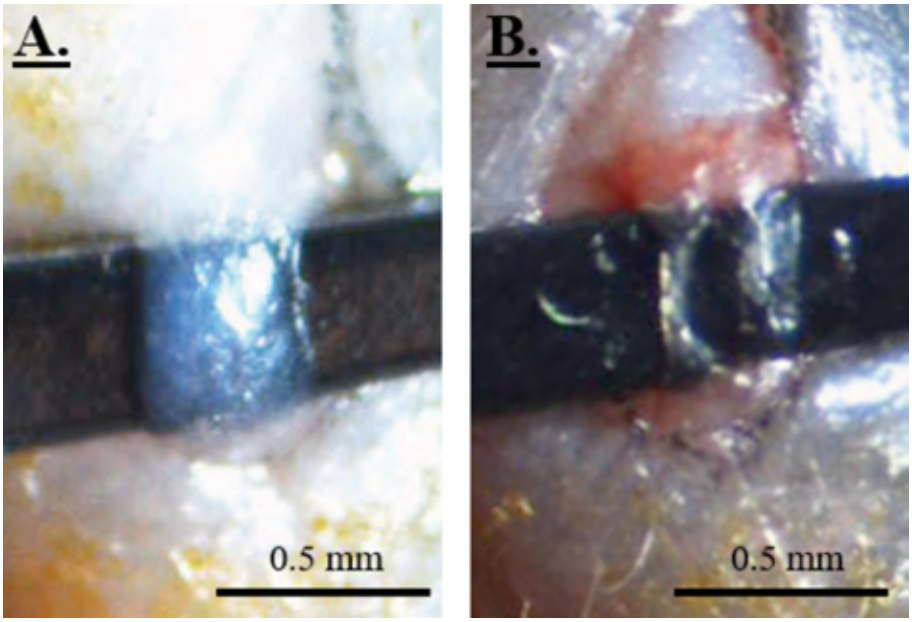

Figure 1. (A) Uninjured p7 patellar tendon; **(B)** p7 patellar tendon after biopsy punch (0.3 mm diameter) injury.

post-injury/p14). Dissected tendon tissue was digested, and RNA was isolated as described.[2] qPCR for *Col3a1* and *Abl1* (housekeeper) was performed. ΔCt values were calculated with reference to Abl1 expression ($\Delta Ct = Ct_{Abl1} - Ct_{Col3a1}$). A one-way ANOVA was used to assess differences in *Col3a1* expression between developmental ages and healing timepoints. Significance was set at $p < 0.05$.

Results

Supporting our hypothesis in the developing neonatal tendon, *Col3a1* expression was highest at p0 and decreased through p14, representing a 76% decrease in average *Col3a1* expression throughout this period (Fig 2A). Interestingly, *Col3a1* expression was not increased with neonatal injury throughout early healing timepoints. *Col3a1* expression 3 and 7 days after injury was not different from the uninjured baseline at p7 (Fig 2B) or from *Col3a1* expression at corresponding, uninjured developmental timepoints (p10 and p14; Fig 2B).

Discussion

In this study, we defined the expression profile of the *Col3a1* gene throughout early neonatal development and healing to provide crucial foundation for investigations of neonatal development and healing as potential mechanisms of superior tendon remodeling.

Development is regarded as the ideal physiologic process for tendon matrix formation. Many regenerative approaches seek to recapitulate development, making the study of a key component of the developing tendon matrix, Col3, an important foundational step. *Col3a1* expression was previously known to be high *in utero*,[1] and the current study is the first to measure the decrease in Col3a1 expression in early neonatal development. Given the importance of temporally coordinated *Col3a1* expression in other developing, fibroblast-rich tissues,[3] this *Col3a1* expression decrease may implicate Col3 in regulation of neonatal tendon development. Moreover, the temporal profile of Col3a1 expression during neonatal development follows the same temporal profile of *Col3a1* expression during mature tendon healing[4] where expression is high after injury and decreases as healing progresses. Encouragingly, this highlights commonalities between neonatal development and mature healing which may be leverageable in approaches that seek to improve mature healing through biomimicry of neonatal development. Further research is evaluating additional developmental timepoints to identify when homeostatic *Col3a1* expression is achieved.

Neonatal tendon healing is another model of improved tendon matrix formation as neonatal healing is superior in speed and quality5,[6] to mature healing. Given the similarities between healing in neonatal and mature contexts, neonatal tendon healing has become a favorable model for investigations of improved healing. Interestingly in the current study, neonatal injury did not affect overall *Col3a1* expression during early healing. This indicates a significant deviation from mechanisms of mature tendon healing where dramatically increased *Col3a1* expression is considered a hallmark of the healing response. Our previous investigations of mature mice (same C57/B6 strain) demonstrate increased *Col3a1* expression in early healing (Fig 3) [7, unpublished]. Given the improved healing observed in neonatal tendon, this finding may reveal potential for *Col3a1* modulation as a therapeutic method for improved tendon healing. Additional earlier and later healing timepoints are being explored to understand the complete temporal profile of *Col3a1* expression after neonatal tendon injury. Furthermore, immunostaining for

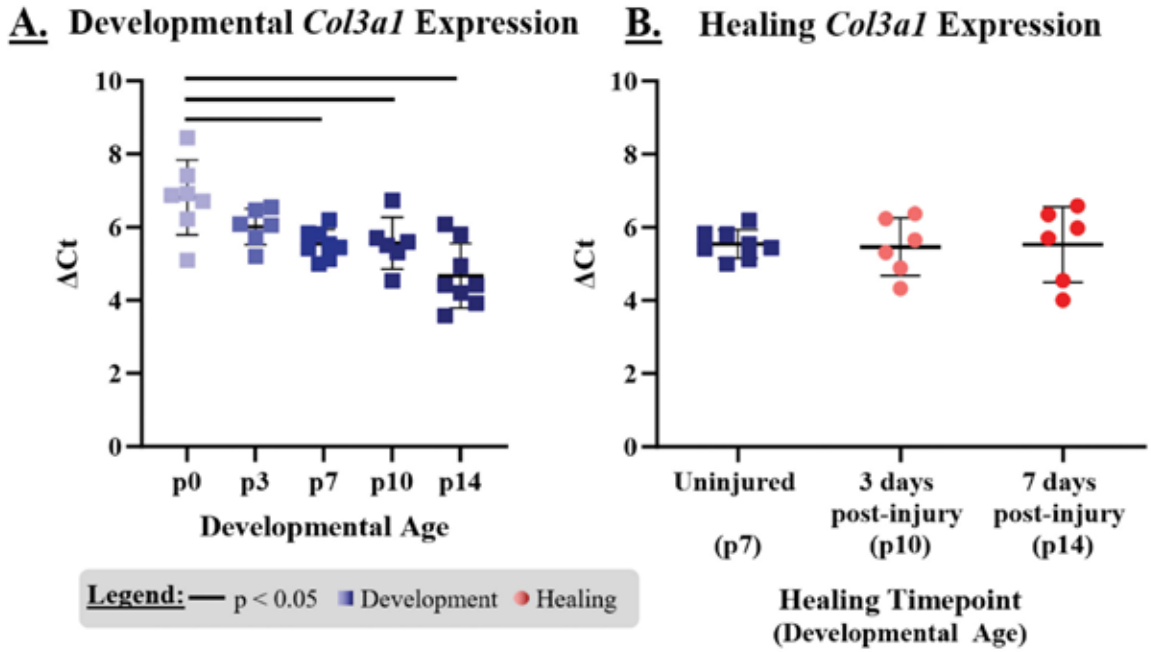

Figure 2. (A) Throughout postnatal development, *Col3a1* expression decreases; **(B)** after injury induced at p7, *Col3a1* expression is not increased 3 or 7 days after injury.

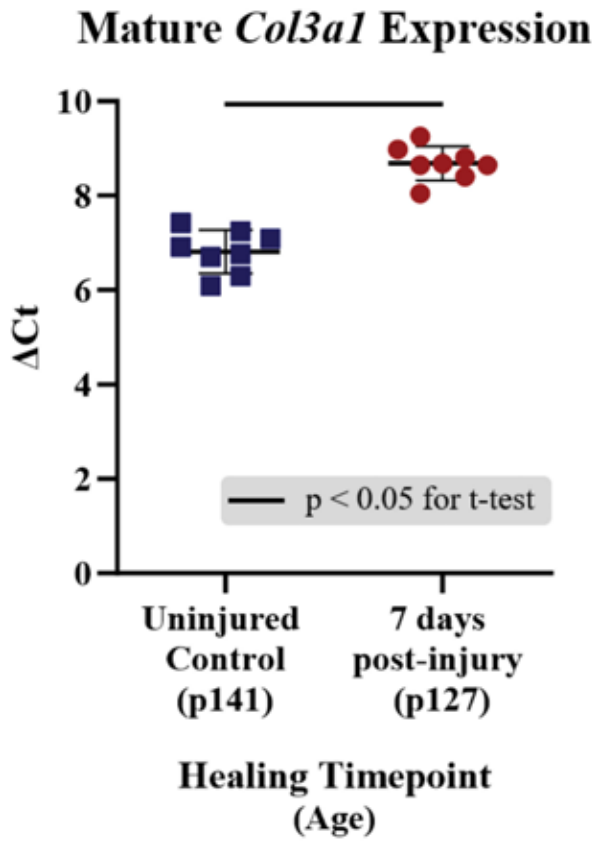

Figure 3. *Col3a1* expression during early tendon healing increases in mature mice [7, unpublished].

Col3 will be completed for all developmental and healing timepoints to evaluate protein translation to add to the gene expression findings from the current study.

Acknowledgements

This study was funded by NIH R01GM124091, R01AR080029, F31AR082282 and the Penn Center for Musculoskeletal Disorders (P30AR069619). The authors thank Nat Thurlow and Ashley Fung for their assistance.

References

1. Birk DE, Mayne R. Localization of collagen types I, III and V during tendon development. Changes in collagen types I and III are correlated with changes in fibril diameter. *Eur J Cell Biol* 1997; 72(4), 352-361.

2. Leiphart RJ, Weiss SN, Soslowsky LJ, *et al.* Collagen V knockdown in mature murine tendons causes sex-dependent expression changes. *ORS*, 2022.

3. Niederreither K, D'Souza R, Metsäranta M, *et al.* Coordinate patterns of expression of type I and III collagens during mouse development. *Matrix Biol* 1995; 14(9), 705-713.

4. Dyment NA, Liu CF, Kazemi N, *et al.* The paratenon contributes to scleraxis-expressing cells during patellar tendon healing. *PLOS ONE* 2013; 8(3), e59944.

5. Ansorge HL, Hsu JE, Edelstein L, *et al.* Recapitulation of the Achilles tendon mechanical properties during neonatal development: A Study of differential healing during two stages of development in a mouse model. *J of Orthop Res* 2012; 30(3), 448-456.

6. Howell K, Chien C, Rebecca B, *et al.* Novel Model of Tendon Regeneration Reveals Distinct Cell Mechanisms Underlying Regenerative and Fibrotic Tendon Healing. *Sci Rep* 2017; 23(7), 45238.

7. Leahy TP, Fung AK, Weiss SN, *et al.* Investigating the temporal roles of decorin and biglycan in tendon healing. *J Orthop Res* 2023; 41(10); 2238-2249.

Focal Adhesion Kinase Regulates Physiological Tendon Development and Growth

Thomas P. Leahy[1,2]
Srish S. Chenna[1]
Louis J. Soslowsky[1]
Nathaniel A. Dyment[1]

[1]McKay Orthopaedic Research Laboratory and Department of Bioengineering, University of Pennsylvania, Philadelphia, PA

[2]Department of Mechanical Engineering and Institute for Stem Cells and Regenerative Medicine, University of Washington, Seattle, WA

Introduction

Mechanical stimuli are known to impact tendon formation and homeostasis via cell mechanotransductive signaling. Focal adhesion kinase (FAK, gene: Ptk2) is an intracellular protein kinase that regulates cytoskeletal dynamics and transmission of mechanical strain to the cell nucleus from its surrounding extracellular matrix (ECM).1 Pharmacological FAK inhibition alters cell morphology and tenogenic gene expression in monolayer cell culture and attenuates ECM to nuclei strain transmission and mechanotransductive gene expression in explant tendon culture.2-7 Despite these known roles for FAK in tendon cells, the mechanism by which FAK regulates tendon physiology and the cell mechano-response throughout tendon development and postnatal growth remains unknown. Therefore, the objective of this study was to define the role of FAK in promoting cell proliferation and ECM deposition during the stage of rapid postnatal growth. We hypothesized that tendon-targeted FAK conditional knockout will reduce cell proliferation and impair matrix assembly, resulting in mechanically inferior tendons.

Methods

To attenuate FAK expression in vivo, we utilized tendon-targeted FAK knockout (Scx-Cre;FAKF/F; FAK-KO) mice,8 in which we have previously validated reduced Ptk2 expression.6 Achilles tendons (ATs), flexor digitorum longus (FDL) tendons, and patellar tendons (PTs) from P10, P30, and P60 FAK-KO and WT littermate controls were used for viscoelastic mechanical testing, histology, and collagen fibril structure measures. In addition, we performed an EdU labeling experiment to quantify cell proliferation in P10 mice.

Viscoelastic Mechanics

Tendon cross-sectional areas (CSAs) were measured, and tendons were subjected to a viscoelastic mechanical testing protocol (preconditioning, viscoelastic stress relaxation and dynamic frequency sweep, and a quasi-static ramp to failure).

Histology

Whole knee joints from P10 mice were fixed, decalcified, paraffin embedded, and sectioned in the transverse plane to visualize the PT cross-section. Overall tissue morphology was visualized via toluidine blue staining.

Cell Proliferation Analysis

Mice were injected with EdU (3g/g bodyweight; Invitrogen A10044) at P0 and P2 and euthanized at P10. Knees joints were cut into sagittal sections and stained with Click-iT™ Cell Reaction Buffer Kit (Invitrogen C10269) to quantify EdU-positive nuclei within the PT.

Collagen Fibril Structure

To quantify collagen fibril diameter distributions, PTs from all timepoints were fixed, embedded, sectioned at 85 nm, and imaged with transmission electron microscopy at 60,000x.

Results

In our mechanical assessment, FAK-KO ATs and PTs exhibited reduced CSAs at P10 (Figure 1). Despite this, there were

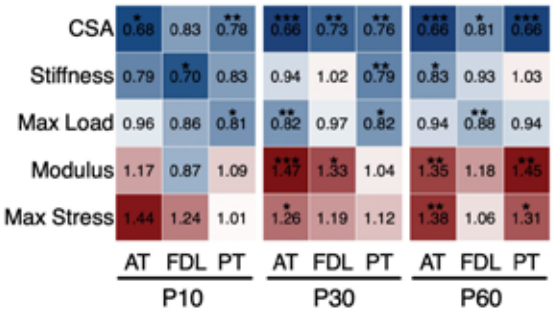

Figure 1. Viscoelastic mechanical testing datasets for all tendons evaluated in this study. Color and numbers within the cells indicate the ratio of the FAK-KO group mean relative to the WT group mean for that parameter. n=7−16/genotype/timepoint. Asterisks represent significant differences between WT and FAK-KO groups, which were compared with t-tests (*p<0.05; **p<0.01; ***p<0.001).

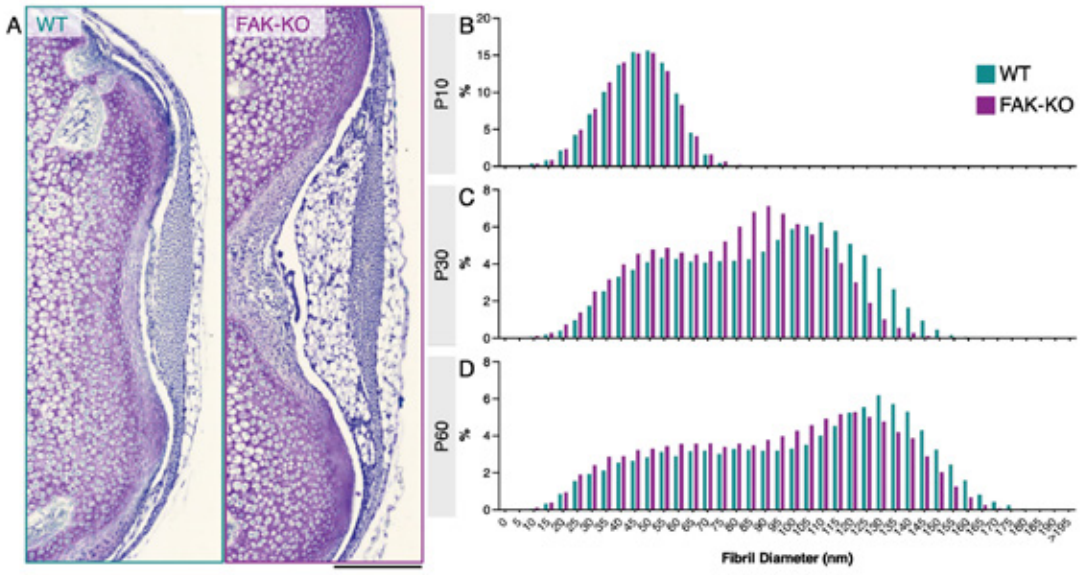

Figure 2. (A) Representative images of transverse sections of P10 WT and FAK-KO tendons demonstrating reduced tendon CSA (n=4-5/genotype). **(B)** P10, **(C)** P30, and **(D)** P60 collagen fibril diameter distribution quantifications (n=5-6/genotype/timepoint). Fibril diameter distributions were compared between groups using Kolmogorov-Smirnov tests, which demonstrated statistical significance ($p<0.001$) between groups at all experimental timepoints.

few mechanical differences in structural or material properties in FAK-KO tendons at P10. This contrasts with tendons at P30 and P60 ages, in which FAK-KO tendons exhibited reduced size and structural properties (i.e., stiffness and max load) yet increased material properties (i.e., modulus and max stress) relative to WT tendons. Viscoelastic dynamic modulus values followed a similar trend to the other material properties (data not shown). Interestingly, while the reduced size of FAK-KO tendons was visible histologically at P10 (Figure 2A), EdU labeling did not demonstrate a difference between proliferative cell behavior at this age (percent EdU-positive nuclei (MeanSD); WT:7.02.5; FAK-KO:8.92.2). Finally, while the collagen fibril diameter distribution was not robustly altered between groups at P10 (Figure 2B), the FAK-KO tendons demonstrated markedly s maller fibril diameters compared to WT tendons at both P30 and P60 (Figure 2C-D).

Discussion

This study investigated the regulatory roles of FAK signaling on tendon physiology during postnatal growth. Consistent with our hypothesis, we observed reduced tissue size in FAK-KO tendons at all experimental timepoints. Interestingly, the differences in tissue mechanical properties were more drastic at the P30 and P60 timepoints compared to P10. Overall, these findings suggest that FAK regulates the generation of tendon size early in development, while altered ECM mechanical properties develop later during postnatal growth in FAK-KO mice. Given this finding, we hypothesized that FAK-KO led to altered tendon physiology by controlling cell proliferation and matrix deposition. While we did not observe a difference in EdU labeling or collagenous matrix deposition at P10, FAK ablation markedly reduced the size of collagen fibrils at P30 and P60, which suggests altered ECM deposition and remodeling behavior in FAK-KO tendons. Ongoing studies will further identify the effect of FAK-KO on the ECM structure by evaluating ECM-related gene expression and protein content. In addition, our future work will explore the effect of in vivo mechanical loading paradigms on FAK-dependent mechanotransduction and the tendon physiological response.

Significance

Mechanical stimuli are essential for regulating tendon physiology, and defining the key signaling pathways that control tendon cell mechanotransduction will improve our understanding of disease and enable the development of improved therapies. Our results indicate that FAK signaling is important for tendon growth and the establishment of native structure/function.

Acknowledge

We acknowledge support from NIH/NIAMS (T32AR007132 and P30AR069619).

References

1 Stephan Huveneers, Erik H. J. Danen. Adhesion signaling—crosstalk between integrins, Src and Rho. *J Cell Sci* 2009, 122 (8): 1059–1069.
2. Xiaoning Li, Suphannee Pongkitwitoon, Hongbin Lu, *et al.*, *J Orthop Res* 2019; 37(3): 574-582.
3. Liu *et al.*, *Stem Cells Int*, 2018;
4.Xu *et al.*, *J Cell Physiol*, 2012;
5. Leahy *et al.*, *ORS Annual Meeting*, 2022;
6. Leahy *et al.*, *ORS Annual Meeting*, 2023
7. Leahy *et al.*, SB3C, 2023
8. Hilary E. Beggs, Dorreyah Schahin-Reed, Keling Zang *et al.*, FAK Deficiency in Cells Contributing to the Basal Lamina Results in Cortical Abnormalities Resembling Congenital Muscular Dystrophies. *Neuron* 2003, 40(3); 501-514.

Non-Muscle Myosin II Knockdown Disrupts Tenocyte Morphology and Contractility

Elizabeth R. Bernstein
Mary Kate Evans
Xi Jiang
Timur B. Kamalitdinov
Robert L. Mauck
Nathaniel A. Dyment

Department of Bioengineering
University of Pennsylvania

Introduction

Mechanical loading at physiologic levels is essential to the normal development, homeostasis, and repair of tendon.[1] It is well established that resident tenocytes are mechanoresponsive, but the mechanisms by which these cells sense, transmit, and respond to mechanical stimuli are still unclear.[2] The interaction between actin fibers and non-muscle myosin II (NM-II) is essential for force generation within cells.[3,4] Non-muscle myosin IIA and IIB, encoded by the genes *Myh9* and *Myh10*, are known to drive morphological changes in epithelial force-generating tissues.[5,6] Within tendon cells, we recently found that acto-myosin contractility mediates extracellular matrix remodeling through Yap/Taz/TEAD-mediated transcriptional activity.[7] The purpose of this study was to clarify the role of non-muscle myosin in tendon cell morphology and contractility using cells isolated from *Myh9/Myh10* double-floxed mice. The toxicity and variability of adenoviral vectors are a common pitfall of *in vitro* knockdown models. To address this challenge, we utilized a novel method of *in vitro* recombination, employing recombinant Cre protein modified to include a TAT cell-penetrating peptide in addition to a nuclear localization sequence.

Methods

All animal work was IACUC approved. Cell isolation: Tail tendons were dissected from Ai9 Rosa-tdTomato Cre reporter mice (n = 3) or *Myh9$^{f/f}$;Myh10$^{f/f}$* mice (n = 4) and digested in 2% collagenase IV/1.5% dispase II. Cell culture: Tendon cells were expanded and passaged in growth media. TAT-Cre treatment: Cells were treated with TAT-Cre at 0.5μM or 3μM for 5 hours in basal media without FBS. Adeno-Cre treatment: Cells were transduced with adeno-Cre (Ad5-CMV-Cre) at an MOI of 50 or 300 for 24 hours. To maximize infection efficiency, basal media was supplemented with 5μM polybrene. Recombination rate quantification: Twenty-four hours after treatment, tdTomato signal was assessed_in live Ai9+ cells using inverted fluorescence microscopy. Immunofluorescence: *Myh9$^{f/f}$;Myh10$^{f/f}$* cells were seeded on fibronectin-coated glass coverslips. Two days after treatment, cells were fixed in 4% PFA, permeabilized with 0.1%Triton-X/PBS, stained with anti-paxillin (1:200) and phalloidin (1:100) then counterstained with DAPI. Morphology analysis: Cell area and solidity were quantified using CellProfiler. Explant model: Individual tendon fascicles were isolated from *Myh9$^{f/f}$;Myh10$^{f/f}$* mice (n = 4) and cut to a length of approximately 15mm. Free floating explants were cultured in growth media supplemented with 50μg/mL ascorbic acid in 12-well plates. Explants were treated with TAT-Cre, blebbistatin, or nothing. The TAT-Cre group was incubated with 3μM TAT-Cre for 5 hours on days 1, 4, and 7. The blebbistatin group received fresh media with 10μM blebbistatin every 3 days for the duration of the experiment. Live/Dead assay: After 16 days, explants were incubated with 2μM calcein AM and 4μM EthD-1 for 30 minutes and imaged using inverted fluorescence microscopy. Statistics: Treatment groups for monolayer experiments and the live/dead assay were compared using a one-way ANOVA with Tukey post-hoc tests ($\alpha = 0.05$). Explant groups were compared using a repeated measures two-way ANOVA with Tukey post-hoc tests ($\alpha = 0.05$).

Results

TAT-Cre induces recombination of tendon cells in monolayer. Incubation with 3μM TAT-Cre resulted in significantly higher Ai9 recombination than control cells ($p = 0.02$) (Figure 1A-C). The average recombination rate of cells treated with 3μM TAT-Cre was 26.32% (SD = 11.03%) compared to 7.79% (SD = 6.72%) among control cells. Neither concentration of Adeno-Cre resulted in effective recombination, even with previous concentrations used successfully by our group (Figure 1C). NM-II knockdown disrupts stress fiber and focal adhesion formation. Based on the recombination rates seen in Ai9 cells, only

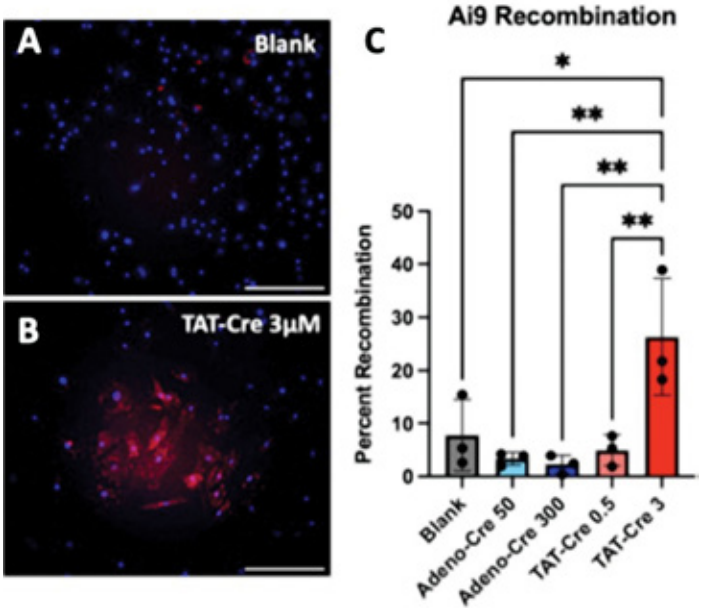

Figure 1. Representative images of **(A)** control cells and **(B)** TAT-Cre treated cells. Scale bars = 200mm; (C) Percent Ai9 recombination. * $p \leq 0.05$. ** $p \leq 0.01$.

the higher doses of Adeno-Cre and TAT-Cre were used for NM-II knockdown. *Myh9*$^{f/f}$;*Myh10*$^{f/f}$ cells treated with TAT-Cre had disrupted morphology compared to control cells (Figure 2A). NM-II knockdown resulted in decreased cell area ($p < 0.0001$) and cell solidity ($p < 0.0001$) (Figure 2B,C). Additionally, TAT-Cre treatment disrupted focal adhesions (Figure 2A). NM-II knockdown impairs tendon contractility. Given the lack of response to Adeno-Cre, functional outcomes were tested in an explant model using only TAT-Cre and the NM-II inhibitor, blebbistatin. Similar to blebbistatin, treatment with TAT-Cre disrupted the ability of tendon cells to contract the free-floating fascicle compared to control tendons ($p = 0.05$). (Figure 3A,B). Live/dead staining showed increased cell death in TAT-Cre-treated explants relative to control and blebbistatin groups, but these differences did not reach significance ($p > 0.05$) (Figure 3C,D).

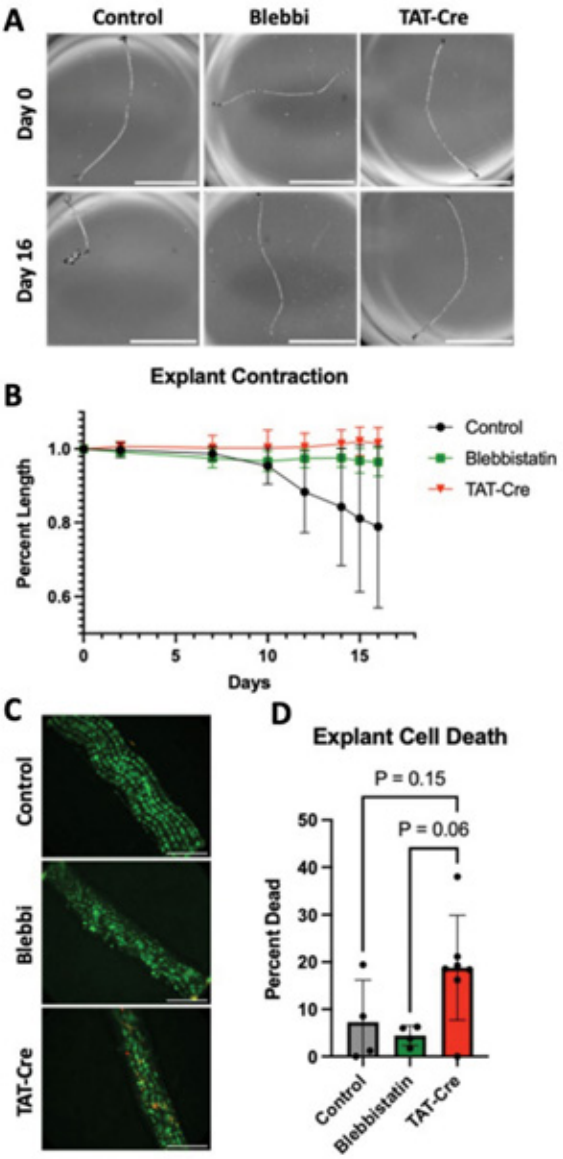

Figure 3. (A) Representative images of explants. Scale bars = 5mm; **(B)** Explant percent of initial length; **(C)** Representative images of live/dead staining of explants. Scale bars = 200μm; **(D)** Percent dead cells at day 16.

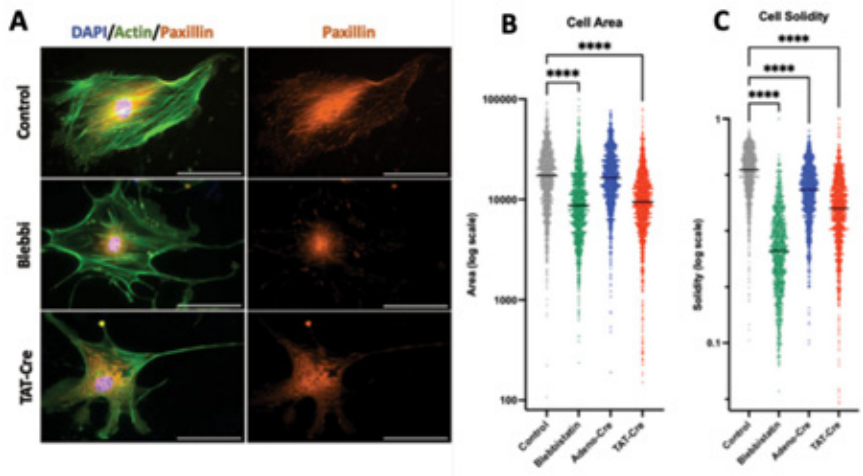

Figure 2. (A) Representative images of Myh9f/f;Myh10f/f cells. Scale bars = 100μm; **(B)** Cell area and **(C)** solidity. **** $p \leq 0.0001$.

Discussion

This study demonstrates that TAT-Cre is an effective tool for inducing *in vitro* and *in situ* recombination of tendon cells. A concentration of 3μM was sufficient to induce Ai9 recombination in over 25% of cells without noticeable effects on cell morphology or viability. After confirming its efficacy, we used TAT-Cre to illustrate the vital role of NM-II in directing tendon cell morphology through stress fiber and focal adhesion formation. Within 48 hours of knockdown, cells showed altered morphology with decreased cell spreading and solidity. Furthermore, these data establish the necessity of *Myh9* and *Myh10* in tendon contractility as TAT-Cre-mediated gene excision in our explant model was equal to blebbistatin-mediated NM-II inhibition, although we are investigating the impact of the increased cell death in this finding. Future work will further tune treatment dose and duration, in order to minimize cell death, as well as confirm NM-II knockdown via qPCR and western blotting.

References

1. Galloway MT, Lalley AL, and Shearn JT. The role of mechanical loading in tendon development, maintenance, injury, and repair. *J Bone Joint Surg* 2013; 95(17):1620-8.

2. Lavagnino M, Wall ME, Little D, *et al.* Tendon mechanobiology: Current knowledge and future research opportunities. *J Orthop Res* 2015;33(6):813-22.

3. Murrell M, Oakes PW, Lenz M, *et al.* Forcing cells into shape: the mechanics of actomyosin contractility. *Nat Rev Mol Cell Biol* 2015;16(8):486-98.

4. Vicente-Manzanares M, Ma X, Adelstein RS, *et al.* Non-muscle myosin II takes centre stage in cell adhesion and migration. *Nat Rev Mol Cell Biol* 2009;10(11):778-90.

5. Pecci A, Ma X, Savoia A, *et al.* MYH9: Structure, functions and role of non-muscle myosin IIA in human disease. *Gene* 2018; 664:152-167.

6. Franke JD, Montague RA, and Kiehart DP. Nonmuscle myosin II generates forces that transmit tension and drive contraction in multiple tissues during dorsal closure. *Curr Biol* 2005;15(24):2208-21.

7. Jones DL, Hallström GF, Jiang X, *et al.* Mechanoepigenetic regulation of extracellular matrix homeostasis via Yap and Taz. *Proc Natl Acad Sci U S A* 2023; 120(22):e2211947120.

Col1a1 Expression Decreases while *Col3a1* Expression Increases after Neonatal Tendon Injury

Miranda K Doro[1]
Margaret K Tamburro, MS[1]
Jaclyn A Carlson, PhD[1, 2]
Susan W Volk, VMD, PhD[2]
Louis J Soslowsky, PhD[1]

[1]McKay Orthopaedic Laboratory
University of Pennsylvania

[2]School of Veterinary Medicine
University of Pennsylvania

Introduction

Injured tendons in adult mammals heal with collagen III (Col3)-rich fibrovascular scarring. Col3 fibrils organize as a meshwork to resist low levels of multiaxial tensile strain.[1] In contrast, type I collagen (Col1) fibrils, the primary component of healthy tendon, align in parallel in uninjured tendons to resist high levels of uniaxial tensile strain. Consequently, healed tendons have compromised function and higher re-injury risk. Unlike injured adult tendons, neonatal tendons heal quickly with full recovery of functional properties.[2] Contributions of Col3 to the enhanced neonatal healing response are beginning to be explored; given the recently demonstrated dynamic nature of *Col3a1* expression throughout development,[3] *Col3a1* expression during neonatal healing must be assessed relative to appropriately matched developmental controls. Furthermore, given the significance of coordinated *Col1a1* and *Col3a1* expression in matrix development,[4] *Col3a1* expression dynamics should be contextualized in terms of Col1a1 expression dynamics to better understand regulation of matrix formation during neonatal development and healing. Therefore, the objective of this study was to define the dynamics of *Col1a1* and *Col3a1* expression following neonatal tendon injury. We hypothesized that, compared to physiologic developmental baseline, both *Col1a1* and *Col3a1* expression would increase in early neonatal tendon healing and return to developmental baseline by 21 days-post injury, reflecting a healing response that is more efficient and complete than adult healing.

Methods

C57/B6 wild-type mice (n = 9, mixed sex) received left patellar tendon biopsy punch injury (0.3mm diameter, performed under 10X magnification) at postnatal day 7 (p7). Right patellar tendons served as uninjured developmental controls. Mice were sacrificed at 7-days post injury (p14, n = 5) and 21-days post injury (p28, n = 4). At the time of sacrifice, left and right patellar tendons were isolated and homogenized in TRIzolTM (Invitrogen, Thermo, Waltham, MA). RNA was extracted, converted to cDNA, and pre-amplified (14 cycles) with TaqMan assays for *Col3a1* and *Abl1* as described.[5] qPCR was performed for Col1a1, Col3a1, and *Abl1* (housekeeper). ΔCt values were calculated with reference to *Abl1* expression, and fold change (FC) was calculated relative to uninjured developmental controls ($2^{\Delta\Delta Ct}$). Repeated measures two-way ANOVAs (injury status, timepoint) with multiple comparisons were used to assess differences in gene expression ($\alpha = 0.05$).

Results

Col1a1 expression increased while *Col3a1* expression was unchanged throughout physiologic development from p14 to p28 (Fig. 1A-B). Early after neonatal injury, at 7 days post-injury, *Col1a1* expression was decreased while *Col3a1* expression was increased compared to physiologic baseline (Fig. 1A-C). As healing progressed through 21 days-post injury, *Col1a1* expression increased but remained below physiologic baseline while *Col3a1* expression decreased but remained above physiologic baseline (Fig. 1A-C).

Discussion

We defined *Col1a1* and *Col3a1* expression dynamics during early and late healing to better understand matrix regulation during neonatal healing. In development, from p14 to p28, we observed an increase in *Col1a1* expression while *Col3a1* expression remained consistent. This complements previous work showing *Col3a1* expression decreases from p0 to p143 and suggests that expression may plateau at p14, remaining consistent through p28.3 Dynamic *Col1a1* expression in the context of stable *Col3a1* expression from p14 to p28 may implicate a changing Col3:Col1 ratio as important in physiologic tendon development.

Injury disrupts physiologic *Col1a1* and *Col3a1* expression in the healing neonatal tendon, with no return to baseline in late healing; *Col1a1* expression decreases while *Col3a1* expression increases. This *Col3a1*

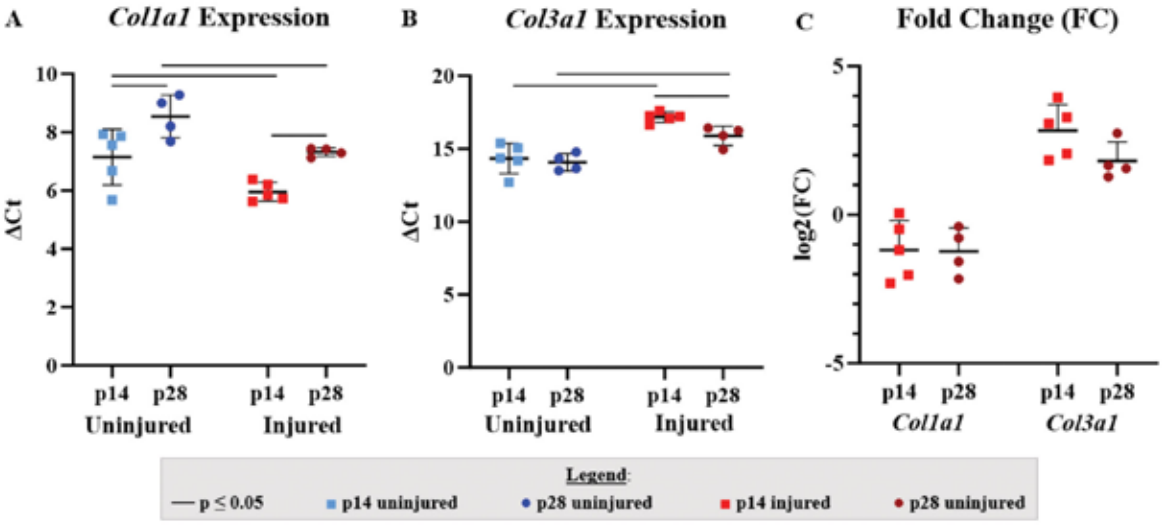

Figure 1. (A) *Col1a1* expression increases from p14 to p28 in uninjured development and is decreased at 7- and 14-days post-injury; **(B)** *Col3a1* expression is unchanged from p14 to p28 in uninjured development and is increased at 7- and 14-days post-injury; **(C)** Compared to uninjured, developmental baseline, injured tendons have a reduced *Col1a1* FC and increased Col3a1 FC at early and late healing timepoints.

expression increase parallels mature tendon healing, implying that neonatal injury may serve as a model of superior healing which is translatable to the adult condition.[6] Moreover, these expression dynamics may indicate that the neonatal healing process is ongoing at 21 days post-injury. Notably, in healing neonatal Achilles tendons, mechanical properties are recovered by 21 days post-injury.[2] As such, neonatal healing may restore mechanical properties despite persistent gene expression changes, or alternatively, this study may highlight differences in patellar and Achilles tendon healing. Mechanical assessment of healing neonatal patellar tendons should be pursued to further understand these possibilities.

Results from this study should be interpreted with consideration of the limitations of comparing injured and uninjured contralateral limbs. Systemic effects of injury on the contralateral limb have the capacity to influence tendon gene expression.[7] Additionally, as this investigation focused gene expression, future work will assess Col1 and Col3 protein amounts, offering a more comprehensive understanding of tissue healing. Nevertheless, this investigation demonstrates similarities in the *Col3a1* expression response in neonatal and adult tendon healing, highlighting the importance of continued study of mechanisms of improved healing in neonates and contributions of Col3 to superior neonatal healing to ultimately identify translatable targets for improving mature healing.

References

1. Williams IF, McCullagh KG, Silver IA, *et al.* The distribution of types I and III collagen and fibronectin in the healing equine tendon. *Connect Tissue Res* 1984; 12(3-4): 211-227.

2. Ansorge HL, Hsu JE, Edelstein L, *et al.* Recapitulation of the Achilles tendon mechanical properties during neonatal development: A Study of differential healing during two stages of development in a mouse model. *J Orthop Res* 2012; 30(3): 448-456.

3. Tamburro MK, Carlson JA, Doro MK, *et al.* Type III collagen expression decreases during neonatal tendon development and is unchanged in early neonatal tendon healing. *ORS* 2023.

4. Niederreither K, D'Souza R, Metsäranta M, *et al.* Coordinate patterns of expression of type I and III collagens during mouse development. *Matrix Biol* 1995; 14(9): 705-713.

5. Leiphart RJ, Weiss SN, Soslowsky LJ, *et al.* Collagen V knockdown in mature murine tendons causes sex-dependent expression changes. *ORS* 2022.

6. Dyment NA, Liu CF, Kazemi N, *et al.* The paratenon contributes to scleraxis-expressing cells during patellar tendon healing. *PLoS One* 2013; 8(3): e59944.

7. Moran TE, Ignozzi AJ, Burnett Z, *et al.* Deficits in contralateral limb strength can overestimate limb symmetry index after anterior cruciate ligament reconstruction. *Arthrosc Sports Med Rehabil* 2022; 4(5): e1713-1719.

High-Speed Treadmill Running Does Not Induce a Tendinopathic Phenotype in Rat Achilles Tendon

Snehal S. Shetye,* PhD[1]
Margaret K. Tamburro,* MS[1]
Ashley K. Fung, PhD[1]
Thomas P. Leahy, PhD1
Madison N. Magee[1]
Harina A. Raja, MS[1]
Stephanie N. Weiss, BS[1]
Courtney A. Nuss, BS[1]
Alexander J. Bein[1]
Daniel C. Farber, MD[1]
Louis J. Soslowsky, PhD[1]

* co-first authors

1McKay Orthopaedic Research Laboratory
University of Pennsylvania

Introduction

Achilles tendon pathology comprises an increasing and consequential clinical burden,[1,2] but robust and reproducible preclinical animal models of Achilles tendinopathy are lacking. Overuse is a common etiology of tendon pathology, and exercise-induced overuse has been considered a promising mechanism for creating a clinically relevant tendinopathy model. In rat Achilles tendon, treadmill running at moderate speed (17-20 m/min) results in variable structural and functional outcomes,[3-7] failing to induce a consistent tendinopathy phenotype. Effects of running at higher speeds (> 25 m/min) on Achilles tendon structure and function have not been thoroughly investigated, though early results have shown potential for a tendinopathic phenotype.[7,8] Therefore, the objective of this study was to rigorously assess the structural and biomechanical impacts of high-speed treadmill running on rat Achilles tendon. We hypothesized that 16 weeks of high-speed treadmill running would induce an overuse tendinopathy phenotype characterized by matrix disorganization, rounded cell morphology, and reduced tensile mechanical properties.

Methods

Sprague-Dawley rats (~400 g) were randomized into two groups: cage activity (n = 12) and running (n = 9). The running group underwent a 3-week acclimation protocol followed by 16 weeks of high-speed treadmill running (27 m/min, 10° incline, 1 hour/day, 5 days/week); mild electrical shock was used at the back of the treadmill to encourage running. After 16 weeks, Achilles tendons were harvested bilaterally for histological and mechanical assessment. For histology, ankles were prepared for paraffin histology with standard techniques,[9] sectioned sagittally (7 mm thickness), stained serially with DRAQ5TM (abcam, Waltham, MA, USA) then 0.1 % toluidine blue, and imaged (10X magnification). Midsubstance regions (~1.3 × 0.65 mm) from two sections per tendon were analyzed (CellProfilerTM[10]) for cell count and nuclear shape. Tendons designated for mechanical testing were first μCT imaged (10 μm resolution, μCT35, Scanco Medical, Brüttisellen, Switzerland) to identify heterotopic ossification (HO). Images were segmented and HO volume was quantified with Amira 6.7 (Thermo Fisher Scientific, Waltham, MA). After scanning, tendons were prepared[9] and tested with a viscoelastic testing protocol (preconditioning; stress relaxation at 9% strain; sinusoidal frequency sweeps at 0.1, 1, 5, and 10 Hz) followed by a quasi-static ramp (0.3% strain/s) to failure with image capture for optical strain measurement. Digital image correlation software (Vic2D, Correlated Solutions, Irmo, SC) was used to determine strain distributions along the length of the tendon at the transition point, mid-linear region (2 × transition strain), and

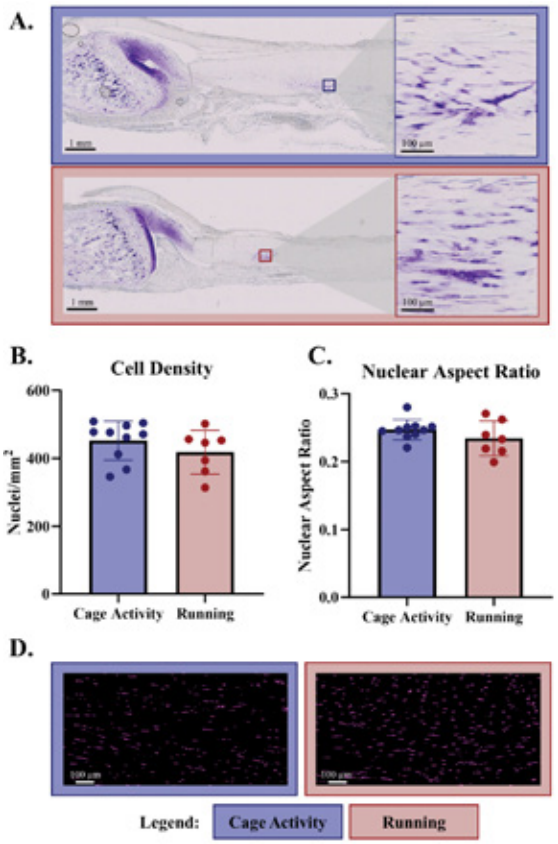

Figure 1. Both cage activity (blue) and running (red) tendons contain discrete regions of disorganization with rounded cells, indicative of HO **(A)**; running did not impact cell density **(B)** or nuclear aspect ratio **(C)** in the midsubstance (representative images shown in **D)**.

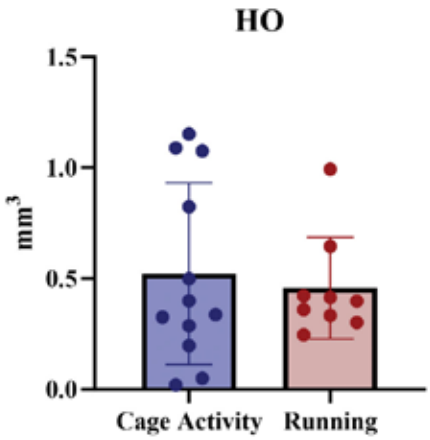

Figure 2. Tendons from both activity groups demonstrated HO by μCT. Running did not influence HO volume.

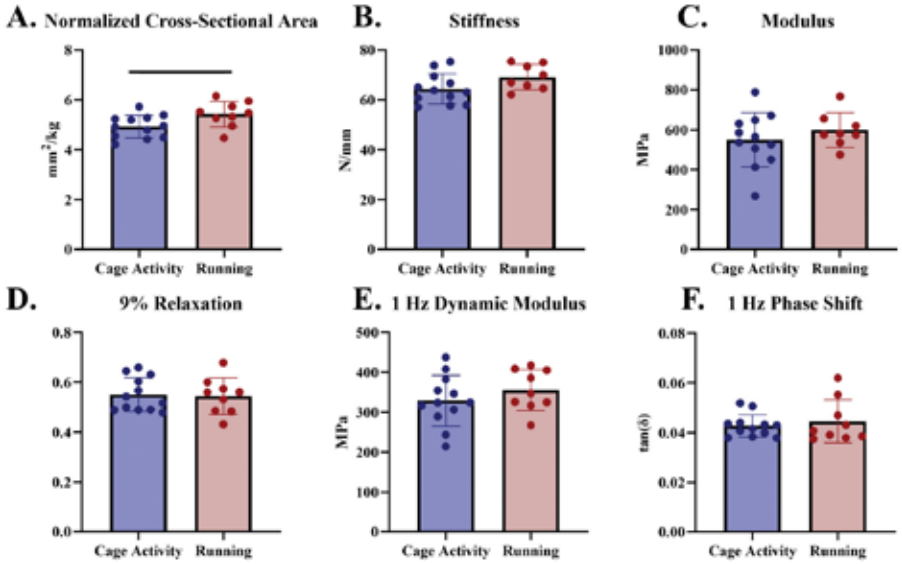

Figure 3. Running increased Achilles tendon CSA normalized to body weight **(A)**; neither stiffness **(B)** nor optical modulus **(C)** were influenced by treadmill running. Similarly, percent relaxation **(D)**; dynamic modulus **(E)**; and phase shift **(F)** were unaffected by treadmill running (data shown for 1 Hz, consistent across frequencies).

failure. T-tests were used to compare histological and mechanical properties between cage activity and running groups, and 2-way repeated measures ANOVAs with Šídák's multiple comparison tests were used to assess differences in regional strain and modulus between activity groups. Significance was set at $p < 0.05$.

Results

All histology samples demonstrated varying amounts of discrete pockets of matrix disorganization, increased staining intensity, and rounded cell morphology, demonstrating an HO phenotype (Figure 1A). In regions of interest, chosen to exclude regions of suspected HO, cell density and nuclear shape were unaffected by treadmill running (Figure 1B-D). In contralateral limbs, we consistently detected the presence of HO on µCT, though HO volume (Figure 2) and mineral density (data not shown) were unaffected by activity level. While running was associated with a decrease in cross-sectional area (CSA, $p = 0.04$), when normalized to body weight, runners demonstrated increased normalized CSA ($p = 0.02$). Despite this, no differences were detected between groups in viscoelastic(relaxation at 9% strain, dynamic modulus, phase shift) or elastic (stiffness, modulus) mechanical properties (Figure 3A-F). Local strain and modulus varied along the tendon length as expected ($p < 0.05$) but were unaffected by activity group (data not shown).

Discussion

Contrary to our hypothesis, 16 weeks of high-speed treadmill running did not induce an overuse tendinopathy phenotype. While rat Achilles tendon is a well-established model for investigations of HO,[11] previous studies of impacts of treadmill running on rat Achilles tendon have not considered potential impacts of HO on tendon structure and biomechanics. We speculate that the high incidence of HO may impact the consistency of both histological and mechanical findings from previous rat Achilles tendon tendinopathy models. Future methods for inducing Achilles tendinopathy should consider alternative approaches to achieve a reproducible phenotype.

Acknowledgements

Dedicated to the memory of Madison Magee. We thank Miranda Doro for her assistance. Funding support provided by the Penn Center for Musculoskeletal Disorders (NIH/NIAMS, P30 AR069619) and F31AR082282.

References

1. **Longo UG, Ronga M, Maffulli N *et al.*** *Sports Med Arthrosc Rev* 2009; 17(2), 112-126.
2. **Lanto I, Heikkinen J, Flinkkilä T *et al.*** *Scand J Med Sci Sports*, 2015; 25(1), e133-138.
3. **Huang TF, Perry SM, Soslowsky LJ *et al.*** *Ann Biomed Eng*, 2004; 32(3), 336-341.
4. **Glazebrook MA, Wright Jr JR, Langman M, *et al.*** *J Orthop Res*, 2008; 26(6), 840-846.
5. **Abraham TP, Fong GH, Scott AM, *et al.*** *BMC Musculoskelet Disord*, 2011; 12(26).
6. **Heinemeier KM, Skovgaard D, Bayer ML, *et al.*** *J Appl Physiol*, 2012; 113(5), 827-836.
7. **Xu SY, He YB, Deng SY, *et al.*** *Exp Ther Med*, 2018; 15(6), 5377-5383.
8. **Xu SY, Li SF, Ni GX, *et al.*** *Med Sci Monit*, 2016; 15(22), 3705-3712.
9. **Leahy TP, Nuss CA, Evans MK, *et al.*** *Am J Sports Med*, 2022; 50(1), 170-181.
10. **Stirling DR, Swain-Bowden MJ, Lucas AM, *et al.*** *BMC Bioinform*, 2021; 22, 433.
11. **Pierantoni M, Hammerman M, Barreto IS, *et al.*** *FASEB J*, 2023; 37(6).

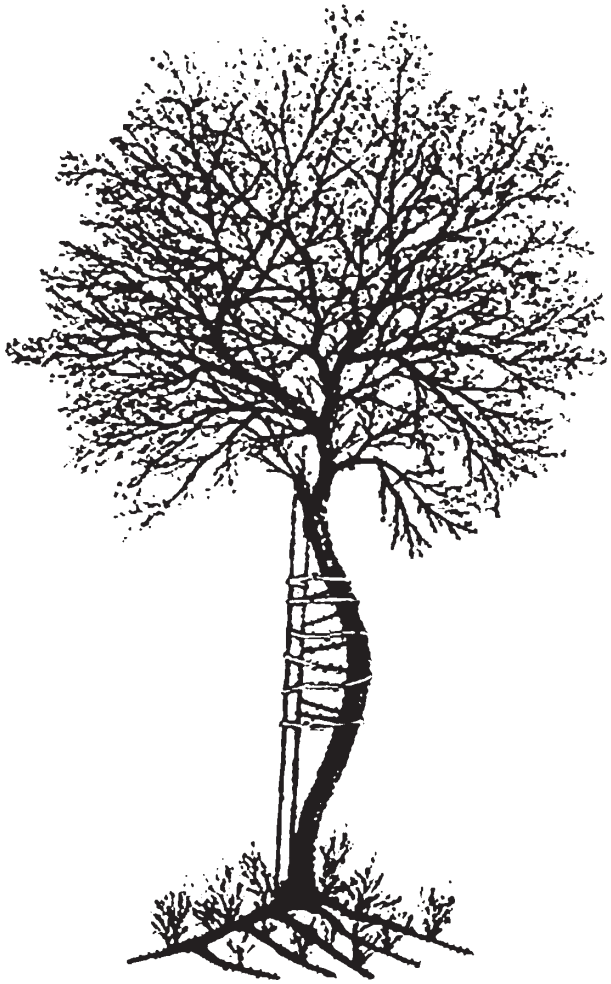

GEMINUS®

volar plating system

skeletal dynamics®

THE UNIVERSITY OF PENNSYLVANIA ORTHOPAEDIC JOURNAL VOLUME 34